ABSTRACT

Efforts Toward an Enantioselective Total Synthesis of (–)-Oxazolomycin B and Simplified Chemical Probes for Proteomics Studies; Pharmacophore-Directed Retrosynthesis Applied to Gracilin A: Simplified Bioactive Derivatives

Christian M. Chaheine, Ph.D.

Mentor: Daniel Romo, Ph.D.

The oxazolomycins are bioactive peptide-polyketide hybrid natural products first isolated in 1985 by Uemura and co-workers from *Streptomyces* bacteria. Their complex structure and wide-ranging bioactivity against various human cancer cell lines, gram-positive bacteria, and viruses like HIV, herpes, and vaccinia has enthralled organic chemists for three and a half decades. Many chiral pool-based, asymmetric synthetic approaches to the unique spiro- or fused-lactone γ-lactam core structure of these natural products have been reported. To the best of our knowledge no catalytic enantioselective strategies for the synthesis of the densely functionalized oxazolomycin γ-lactam exist in the literature.

We have extended the utility of our previously developed enantioselective nucleophile-catalyzed Michael-proton transfer lactamization organocascade to the decagram scale production of a γ-lactam applicable to the total synthesis of the oxazolomycins and analogs thereof. An exhaustive experimental procedure is described for the synthesis of this γ-lactam starting material and a synthetic route utilizing this

scalable procedure enabled access to the complete carbon skeleton of (–)-oxazolomycin B, with all seven stereogenic centers set. Issues encountered in the penultimate step of our total synthesis are discussed as well as early efforts to circumvent known redox/protecting group steps in accessing the particular γ-methoxy ester arrangement of the core of oxazolomycin. A formal synthesis of (+)-neooxazolomycin serves to support our assignment of the absolute stereochemistry in our intermediates, in addition to two X-ray crystal structures.

While oxazolomycin bioactivity and biosynthesis has been studied extensively, there is a dearth of studies into their cellular mode of action and protein target identification. Aligned with our interest in the total synthesis of bioactive, spiro-β-lactone-containing natural products and the recent adoption of a pharmacophore-directed retrosynthesis strategy, we sought an efficient, modular synthesis of the intricate spiro-β-lactone γ-lactam core of the oxazolomycins that would allow the construction of simplified derivatives bearing terminal alkynes. A small series spiro-β-lactones were made by our route and several proved to be too hydrolytically unstable for the proposed proteomics investigations, prompting computational studies in collaboration with Prof. Dean Tantillo's group at UC Davis to understand relative spiro-β-lactone stabilities. This revealed the essential nature of the C4-OMe group of the oxazolomycins, which sterically shields the C17-carbonyl from hydrolysis. Future simplified spiro-β-lactone γ-lactams will include this and other structural features to impart enhanced stability.

Our published work on the application of pharmacophore-directed retrosynthesis to the gracilin natural products is also enumerated here by virtue of the level of my personal contribution to the synthesis and the preparation of the manuscript.

Efforts Toward an Enantioselective Total Synthesis of (–)-Oxazolomycin B and Simplified Chemical Probes for Proteomics Studies; Pharmacophore-Directed Retrosynthesis Applied to Gracilin A: Simplified Bioactive Derivatives

by

Christian M. Chaheine, B.S.

A Dissertation

Approved by the Department of Chemistry and Biochemistry

_____

Patrick Farmer, Ph.D., Chairperson

Submitted to the Graduate Faculty of
Baylor University in Partial Fulfillment of the
Requirements for the Degree
of

Doctor of Philosophy

Approved by Dissertation Committee

_____

Daniel Romo, Ph.D., Chairperson

_____

John L. Wood, Ph.D.

_____

Bryan F. Shaw, Ph.D.

_____

Robert R. Kane, Ph.D.

_____

Joseph Taube, Ph.D.

Accepted by the Graduate School

December 2020

_____

J. Larry Lyon, Ph.D., Dean

Page bearing signatures is kept on file in the Graduate School.

TABLE OF CONTENTS

LIST OF FIGURES

LIST OF SCHEMES

LIST OF TABLES

ACKNOWLEDGMENTS

Without the unyielding love and support of my parents, Ezdine and Letitia Chaheine, I would not have had the privilege of a good education and would not have learned the resolve that was necessary to overcome the challenges of the last six years. I love you, Mom and Dad. Thank you for the life you have made possible.

To my sisters Alex and Roxy, I love you guys and thanks for all of your encouragement. I consider myself extremely fortunate to have such intelligent, creative, and talented younger siblings.

I have been blessed to have met many amazing people throughout my years in this doctoral program: Alex J. Kosanovich, you were one of the first people I met at TAMU when I began my journey into Chemistry, and we immediately recognized our kinship in intellect and spirit. You have really become my brother from another principle investigator. I wish for you and Josephine a beautiful adventure in life and I know it will be punctuated by memories we'll share in the future.

Many thanks to my other TAMU family: Molinski, Smith, Komatsu, Hogancamp, Fleer, Cardenal, Washburn, Watson. I cherished our interactions and hope we cross paths again. Sorry for being a "turncoat".

Zach Hulsey, since we met in our freshman year at UTA living in the Arlington Hall dormitory you have been a great friend. Your ability to think outside of the box and the perspective you bring to our conversations on science are things I treasure. I wish you and your family the best. I thank you and Christina for your enduring friendship.

Ryan and Haley Manning, thank you for keeping me sane, being steadfast friends, and always incredible hosts. Inviting me to your parties and outings has brought me joy and kept me tethered to earth. Thank you for everything and all the good times we have to look forward to.

Will McCullick, your words have kept me motivated and grounded; always very reasonable but also bearing that unique brand of humor. Thank you for being you.

My Lake Travis family, those I have known since middle school and high school: Ian Steigmeyer, Tate Meehan, Chris Pham, Ryan Manning, Will McCullick. I couldn't ask for a better collection of brothers I never had. I know we will remain friends always.

To my fellow Romo group family, you all are remarkable human beings, scientists, and friends: Nate Truax, Conner Song, Patrick Sutter, Evan Wood, Yongfeng Tao, Guowei Kang, Weixu Kong, Sreekumar Vellalath, Ragha Kovvuri, Sigrid Killedal, Khoi Van, Natalie Harvey, Mikail Abbasov, Paul Gladen, Michael Conner, Haoran Xue, Tammy Sailer. Thank you for making the lab and the world a better place to be.

Roxane Jourdain, you are tremendously creative, intelligent, and highly capable. You have been a constant source of support in the face of both personal and scientific challenges and you should know you are greatly valued by all those fortunate enough to call themselves your friend.

Cindy and Nina, the time we got to spend together I will always hold dear to my heart. Though our paths had to stray, I will love you both and remember you always.

Dr. Romo, thank you for taking me in and supporting me in my development as a professional, an experimentalist, a chemist, a mentor, and a leader. Under your guidance I have learned far more than I imagined possible. My gratitude is undying.

DEDICATION

To Remi a.k.a XIV Karat Willing Heart, my dissertation puppy. I picked you up on October 16th, 2020. Here is to our new adventure. Let's see what we can do with the next ten years.

ATTRIBUTIONS

i. The content of Chapter 2 has been submitted for publication as Christian M. Chaheine, Conner J. Song, Paul T. Gladen, Daniel Romo. Enantioselective Michael-Proton Transfer-Lactamization for Pyroglutamic Acid Derivatives: Synthesis of dimethyl-(*S,E*)-5-oxo-3-styryl-1-tosylpyrrolidine-2,2-dicarboxylate. *Organic Syntheses* (2020):

I, Christian M. Chaheine, wrote the majority of the experimental procedure as it was submitted and was responsible for optimization of the nucleophile-catalyzed Michael-proton Lactamization (NCMPL) reaction. Paul Gladen was the first to apply this reaction to 5-phenyl-2,4,-pentadienoyl chloride and performed initial optimization and wrote the first iteration of the procedure. Conner J. Song optimized the procedure for the synthesis of the sulfonamidomalonate starting material and helped to refine the procedure for the NCMPL to the level of detail required for publication in *Organic Syntheses*. Dr. Romo supervised the study and edited/submitted the manuscript.

ii. The content of Chapter 3 has been accepted for publication as Christian M. Chaheine, Paul T. Gladen, Mikail E. Abbasov, Daniel Romo. Enantioselective, Organocatalytic Strategy to the Oxazolomycin Core: Formal Total Synthesis of (+)-Neooxazolomycin. *Organic Letters* (2020):

I developed the entirety of the synthesis starting from dimethyl γ-lactam **3.9**, and also optimized the NCMPL and desulfonylation reactions preceding this intermediate. I also wrote the manuscript and all experimental procedures. Paul Gladen was the first to synthesize the *N*-Ts-γ-lactam starting material and did early studies into C4-C5 bond

formation via organometal addition. Mikail Abbasov showed that a high degree of diastereoselectivity can be obtained in the Evan's anti aldol reaction of β-substituted acrolein using stoichiometric Lewis Acid toward the synthesis of the middle fragment (C5-C9) of oxazolomycin. Dr. Romo supervised the study and edited/submitted the manuscript.

iii. The content of Chapter 5 was published as Abbasov, M. E.; Alvariño, R.; Chaheine, C. M.; Alonso, E. A.; Sánchez, J. A.; Conner, M. L; Alfonso, A; Jaspars, M.; Botana, L. M.; Romo, D. Simplified Neuroprotective and Immunosuppressive Agents Based on Gracilin A. *Nature Chemistry* **2019**, *11*, 342:

I was responsible for the synthesis of the simple bicyclic derivative as well as the synthesis and completion of the spectroscopic characterization of the most complex derivatives that showed potent immunosuppressive activity. I was also heavily involved in proofing/editing of the manuscript as well as writing, development, proofing, and editing of all synthetic procedures. Mikail Abbasov, was the first to synthesize the most complex derivatives of gracilin A and all other bioactive derivatives bearing the pendant cyclohexyl ring. Mikail wrote the first draft of the manuscript and the supplemental information. Michael Conner synthesized some derivatives, studied the contrasteric Zincate addition and wrote related experimental procedures. Alvariño, Alonso, Sánchez, Alfonso, and Botana performed all bioactivity assays and resulting data analysis. Jaspars isolated gracilin A. Dr. Romo supervised the study and edited/submitted the manuscript.

CHAPTER ONE

Total Synthesis of the Oxazolomycins

1.1 Introduction

The oxazolomycins[1] are bioactive polyene peptide-polyketide natural products that bear a densely functionalized and stereochemically complex spiro-β-lactone γ-lactam core, excluding neooxazolomycin (**1.4**), which bears a fused-γ-lactone γ-lactam core (Figure 1.1).[2-13] All oxazolomycins were isolated from marine or terrestrial species of *Streptomyces* bacteria with the first congeners, oxazolomycin A (**1.1**) and neooxazolomycin (**1.4**), isolated in 1985 by Uemura and co-workers.[3, 6]

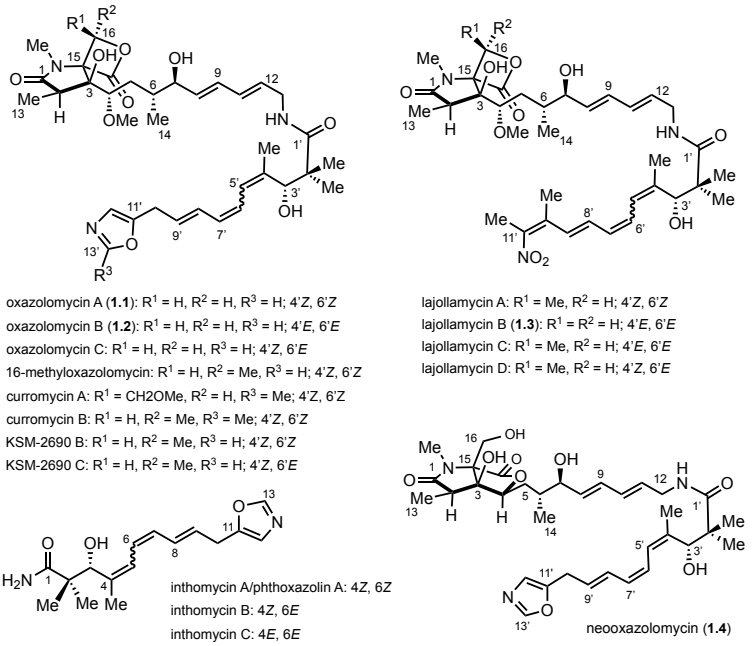

Figure 1.1. Structures of oxazolomycin and inthomycin natural products.

The truncated amido trienyloxazole fragment of the oxazolomycins, known as inthomycins A-C, are also natural products that were isolated[14-18] primarily from *Streptomyces* sp. The inthomycins exhibit bioactivity seemingly unrelated to that of the oxazolomycins, inhibiting cellulose biosynthesis in *Phytophthora* sp. of plant-pathogenic[14-16, 18] fungi, prostate cancer cell growth, through their interference with tumor-stromal cell interactions,[19] and bacterial DNA supercoiling.[20]

Over the last three and a half decades twelve additional oxazolomycin congeners have been isolated, with the only variations in structure occurring as substitution and relative stereochemistry at C16 of the spiro-β-lactone, the geometry of the conjugated triene, and the oxazole or vinyl nitro moiety (*i.e.* lajollamycin A-D) terminating the side chain. Additionally, oxazolomycin A2 and bis-oxazolomycin A, a dimeric ester of parent oxazolomycin A (structures not shown), were isolated recently, though these compounds seem likely to result as artifacts from the isolation procedure.[21] Researchers across the globe have studied the bioactivity[22-26] and biosynthesis[27-31] of the various oxazolomycin natural products and the bioactivity results are summarized in Table 1.1.[1] While in the majority of cases, only modest, single to double digit μM IC_{50}, EC_{50}, or minimum inhibitory concentrations (MIC) were observed, the most intriguing aspect is the wide range of organisms affected (*i.e.* gram-positive bacteria, human cancer, and viruses). The scope of this activity may reflect the oxazolomycin structure as a general strategy of *Streptomyces* bacteria against competing organisms, which can potentially be leveraged in the identification of a novel therapeutic chemotype to combat infectious disease. The most potent activity known to date is associated with C16-substituted spiro-β-lactones like 16-methyloxazolomycin and curromycins A and B. This could be due to enhanced hydrolytic

stability of the strained spiro-β-lactone (see Chapter Four for a discussion on oxazolomycin spiro-β-lactone stability).

Table 1.1. Bioactivities reported for the oxazolomycins

Activity (μM)	oxazoA	oxazoB	oxazoC	16-MeOxo	KSM-2690B	KSM-2690C	curroA	curroB	lajolla[2]
crown gall formation, MID (μg/disc)	0.8	0.8	0.8						
Agrobacterium tumefaciens IFO 13263, MIC	4.9	>152.5	>152.5						
Agrobacterium tumefaciens EHA101, MIC	9.6	>152.5	>152.5						
Agrobacterium rhizogenes IFO 13257, MIC	76.2	>152.5	>152.5						
Micrococcus luteus FDA16, MIC					76.2[1]		35	37	
Pseudomonas aurugenosa A3, MIC							70	74	
Bacillus subtilis 1069, MIC				7.5	76.2		active		
Staphylococcus aureus smith, MIC					76.2				
murine melanoma B16-F10, EC_{50}							active	3.7	9.6
murine leukemia P388, IC_{50}	active			0.35			0.084	0.28	
human lung adenocarcinoma A-549, IC_{50}				7.0					
human bladder carcinoma T24, IC_{50}	15.2				15.2	15.2			
influenza A, MIC	23.8								
herpes simplex type I, MIC	23.8								
vaccinia, MIC	23.8								
human immunodefficiency virus, EC_{50}							3.5	7.3	

MIC: Minimum Inhibitory Concentration, MID: Minimum Inhibitory Dose

[1]KSM-2690B displayed activity against Micrococcus luteus ATCC 9341

[2]lajollamycin also displayed antibiotic activity against: resistant and sensitive *S. aureus* (MIC = 5.8, 7.3 μM); *S. pneumoniae* (MIC = 2.9, 2.2 μM); *E. faecalis* (MIC = 20.4 μM); *E. faecium* (MIC = 29.1 μM); *E. coli* (MIC = 17.5 μM)

Coupled with this variety of bioactivity, its intricate chemical structure, which consists of a strained and reactive spiro-β-lactone, seven stereogenic centers, amino diene and a quaternary center-containing conjugated polyene tail, has attracted global attention from synthetic organic chemists. Since 1985, however, there have only been five successful total syntheses of the oxazolomycins (*i.e.* neooxazolomycin **1.4**, oxazolomycin A **1.1**, and lajollamycin B **1.3**). Being that the most synthetically challenging facet of any of the oxazolomycins is the core *fused* or *spiro*-lactone γ-lactam, the discussion below regarding successful total syntheses of these natural products centers on a detailed overview of approaches to this core structure.

1.2.1 Kende's Total Synthesis of Neooxazolomycin

In 1990, Kende and co-workers reported the first total synthesis of the fused-γ-lactone γ-lactam member of the oxazolomycins, neooxazolomycin **1.4**.[32] The synthesis utilized chiral pool starting material α-*D*-glucose, which, over 14 steps, was elaborated to ester **1.6** (Scheme 1.1). Ester **1.6** was condensed with the dianion of an amido dimethyl malonate in a key Dieckmann cyclization, intramolecular aldol cascade reaction, generating a complex γ-lactam tetrahydropyran **1.7** that bears five of the seven stereogenic centers found in neooxazolomycin, albeit with the undesired diastereoselectivity.[33]

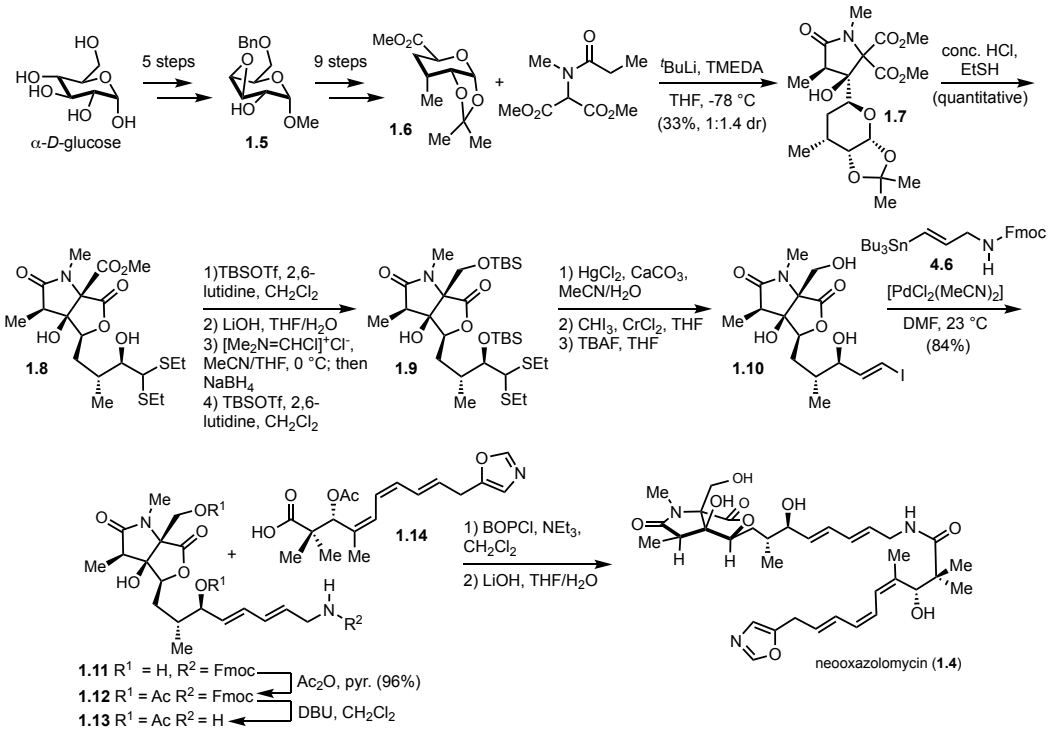

Scheme 1.1. Kende's total synthesis of neooxazolomycin.

Brønsted acid-promoted opening of the carbohydrate-derived ring with ethanethiol led to *fused*-γ-lactone γ-lactam ester **1.8**. The secondary alcohol was silylated and the axial methyl ester was saponified and reduced with $NaBH_4$ via its acylchloride, establishing the core of neooxazolomycin. Following silylation of the primary alcohol, the terminal thioacetal was hydrolyzed to the aldehyde which was then homologated and desilylated to the *E*-vinyliodide **1.10**. The bis-silylether of vinyliodide **1.10** was accessed by our enantioselective, organocatalytic synthetic route illustrated in detail in Chapter Three in only 10 steps (longest linear sequence, LLS) from known compounds, whereas, by Kende's route vinyliodide **1.10** is accessed in 25 steps from α-*D*-glucose. In a footnote in the publication on this total synthesis Kende et. al. mention the importance of C7 hydroxyl protection, briefly stating that desilylation at the vinyliodide stage was necessary because desilylation on later silyl ether intermediates proceeded poorly with conventional methods. This footnote is the only portent of the issues with C7 hydroxyl deprotection that we would encounter in our own synthetic campaign toward oxazolomycin B (see Chapter Four).

The vinyliodide **1.10** was coupled with vinylstannane **4.6** via the Stille reaction[34, 35] to generate the C1-C14 core of neooxazolomycin with a terminal Fmoc-protected primary amine poised for amide coupling to the triene oxazole acid fragment **1.14**. *In situ* Fmoc deprotection with DBU produced an intermediate primary amine that was condensed with the activated ester of oxazole acid **1.14**. The first total synthesis of neooxazolomycin was completed following removal of the acetate protecting groups, which occurred without isomerization of the conjugated triene. Many methods applied in this seminal total synthesis of the oxazolomycin natural products have been repurposed in the later syntheses discussed below as well as in our own synthetic efforts.

1.2.2 Hatakeyama's Total Synthesis of Neooxazolomycin

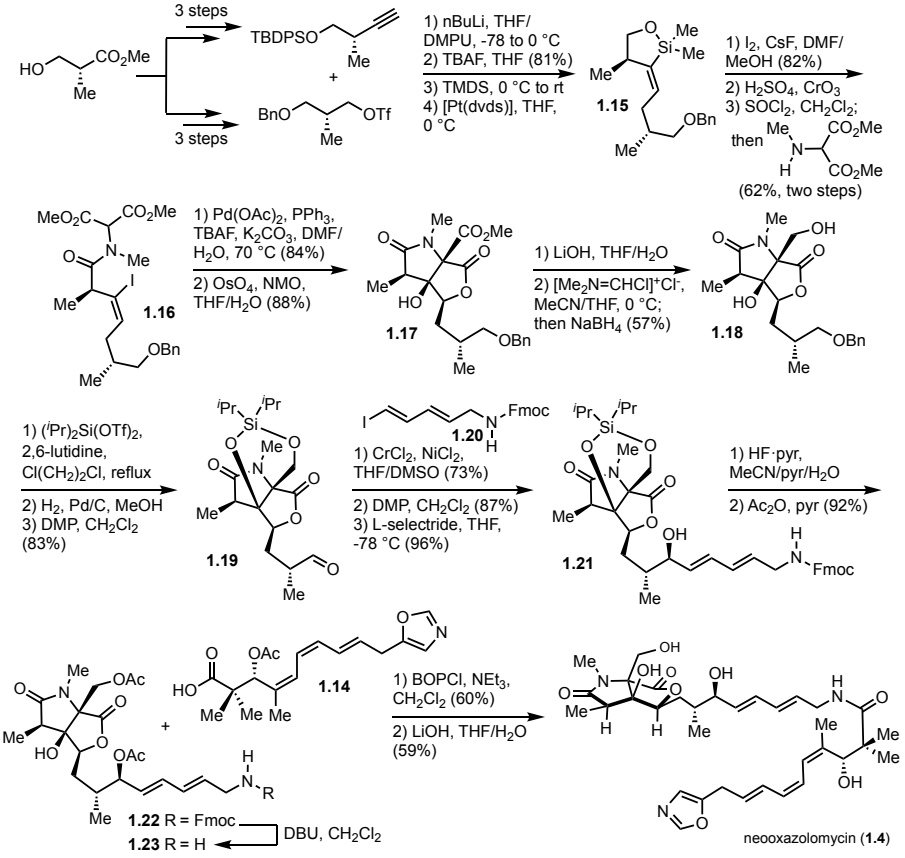

Scheme 1.2. Hatakeyama's total synthesis of neooxazolomycin.

In 2007, the Hatakeyama group reported their total synthesis of neooxazolomycin using a chiral pool approach and substrate-controlled stereoselective transformations.[36] Starting from (*S*)-3-hydroxy-2-methylpropanoate ($592/25 g, Sigma-Aldrich), terminal alkyne and primary triflate fragments were synthesized and coupled by alkyne alkylation (Scheme 1.2). A Pt-catalyzed, intramolecular hydrosilylation generated siloxane **1.15** that was opened to a vinyliodide amidomalonate **1.16** that was, in turn, cyclized with a Pd-catalysis to a γ-lactam diester with an exocyclic, tri-substituted alkene. The exocyclic alkene was dihydroxylated with complete diastereofacial selectivity to generate the desired

fused-γ-lactone γ-lactam **1.17**. NOESY studies and molecular mechanics calculations of the exocyclic alkene intermediate (not shown) suggest that the preferred conformation of the side chain places the benzyl ether moiety on the α-face of the γ-lactam, leading to the observed β-face selectivity.

The axial ester of γ-lactone γ-lactam **1.17** was selectively reduced by the same method as used by Kende and the resulting 1,3-diol was protected as a dioxasilane. Protection of the tertiary alcohol was found to be essential to prevent hemiacetal formation that would hinder the following key C7-C8 bond forming Nozaki-Hiyama-Kishi reaction. This key coupling reaction proceeded with no diastereoselectivity and so the secondary alcohol had to be oxidized to a ketone and reduced with L-selectride to generate the desired C7 stereochemistry. These concession steps highlight a major shortcoming in the known syntheses of the C1-C14 core of the oxazolomycins, and that is, the excessive need for redox and protecting group manipulations to construct precisely the core of the natural products; a need that arises from the high degree of oxygenation and unsaturation decorating their carbon skeleton and becomes more taxing with spiro-β-lactone-containing oxazolomycin targets.

Desilylation and acetylation of the primary and secondary alcohols of **1.21** produced Kende's C1-C14 neooxazolomycin core intermediate **1.22**/**1.12**. Kende's amide coupling protocol was likewise used here and, after, saponification of the acetate groups, finalized the second total synthesis of neooxazolomycin.

1.2.3 Hatakeyama's Total Synthesis of Oxazolomycin A

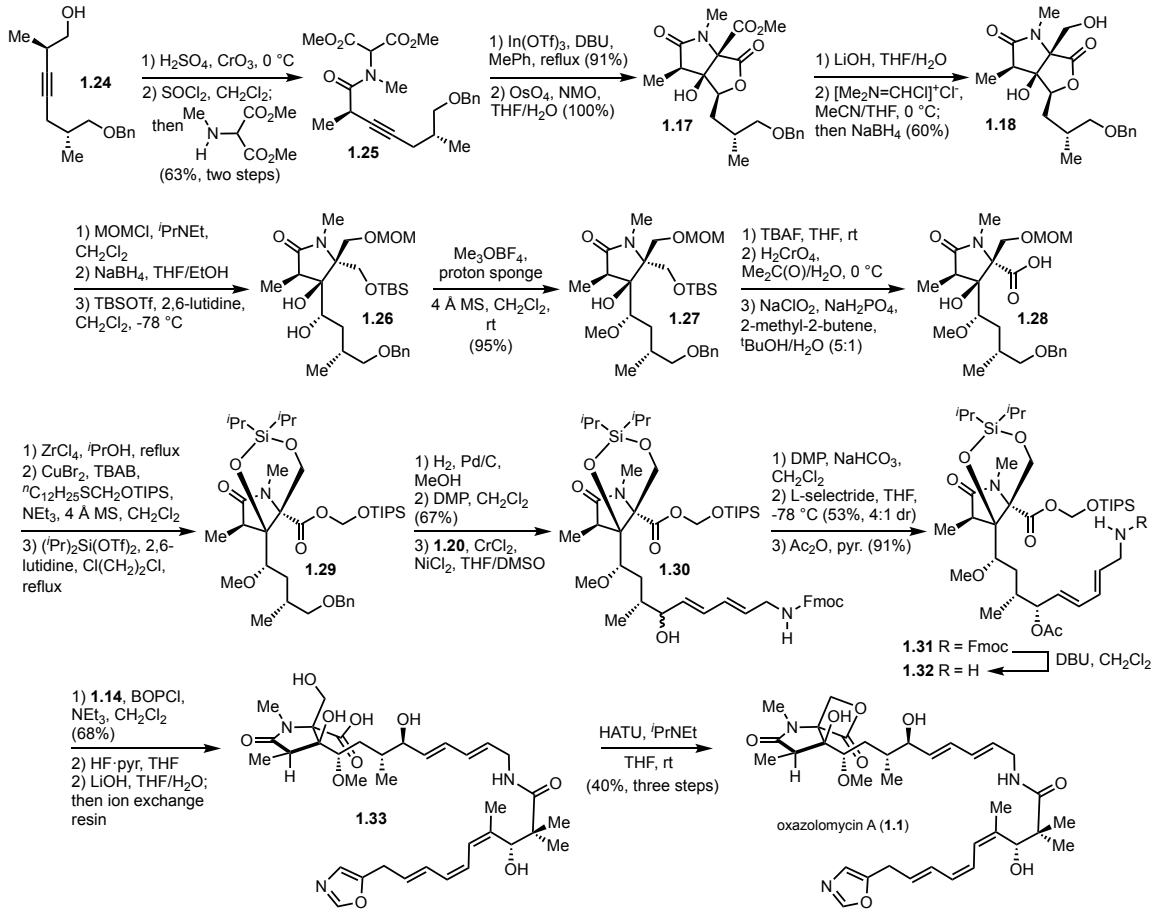

Scheme 1.3. Hatakeyama's total synthesis of oxazolomycin A.

Four years after their synthesis of neooxazolomycin, in 2011, the Hatakeyama group disclosed the first total synthesis of oxazolomycin A,[37] synthetically a much more formidable target owing to its strained, reactive spiro-β-lactone. Jones oxidation the same alkyne alcohol intermediate used in their synthesis of neooxazolomycin, and condensation of the resulting acid with the same *N*-methyl aminomalonate led to an alkynyl amidomalonate **1.25** (Scheme 1.3). Alkynyl amidomalonate **1.25** was cyclized with a Pd-catalyzed intramolecular Conia-ene reaction to generate an exocyclic alkene γ-lactam that

was dihydroxylated as previously to γ-lactone y-lactam **1.17**. Reduction to the neooxazolomycin core **1.18** was followed by a lengthy sequence of concession steps that Hatakeyama et. al. found necessary to convert the γ-lactone to the γ-methoxy ester **1.29**; all in order to install the C7-OMe functionality. Efforts were made in our own synthesis of oxazolomycin to circumvent these steps, which are detailed in Section 4.4. The silyloxymethyl protection of the C17-carboxylic acid group was essential as late stage ester saponification was found to be impossible due to the sterically hindered environment surrounding C17.[38]

Benzyl ether **1.29** was converted to the aldehyde and exposed to the same Nozaki-Hiyama-Kishi reaction conditions used previously, again generating a mixture of epimeric alcohols that was oxidized to the corresponding ketone and diastereoselectively reduced with L-selectride. Kende's amide coupling protocol was again used to merge the C1-C14 oxazolomycin core **1.31** to the triene oxazole acid fragment **1.14** and the spiro-β-lactone was installed with the use of hydroxybenzotriazole tetramethyluronium (HBTU) from the β-hydroxy acid following global deprotection, yielding the first total synthesis of oxazolomycin A. Overall, Hatakeyama's approach to the oxazolomycin natural products represents one of the more efficient to date, in particular, in its construction of the core of neooxazolomycin **1.18**.

1.2.4 Hatakeyama's Total Synthesis of Lajollamycin B

Most recently, in 2019, Hatakeyama and co-workers extended their approach to the oxazolomycins to the synthesis of lajollamycin B,[39] a congener of oxazolomycin that possesses a conjugated tetraene terminating in a rare vinylnitro moiety. From their C1-C14

oxazolomycin core **1.31**. Amide coupling with dienyliodide carboxylic acid 1.34 and formation of the spiro-β-lactone by their previously employed conditions led to a very interesting vinyliodide spiro-β-lactone intermediate (Scheme 1.4). Notably, the formation of the spiro-β-lactone was incomplete under the HBTU-mediated conditions and the activated ester intermediate was isolated and had to be re-exposed to base to effect lactonization (inset, Scheme 1.4). This same issue was encountered in our synthesis of oxazolomycin B (see Chapter Four). The Hatakeyama group then demonstrated the possibility of a Stille cross-coupling in the presence the oxazolomycin spiro-β-lactone and produced two geometric isomers of the desired product. On the basis of NOESY experiments and comparison of ^{1}H-NMR and ^{13}C-NMR spectra, the originally proposed structure of lajollamycin B[13] was revised to that of **1.3** with the *Z*-configuration of the terminal olefin.

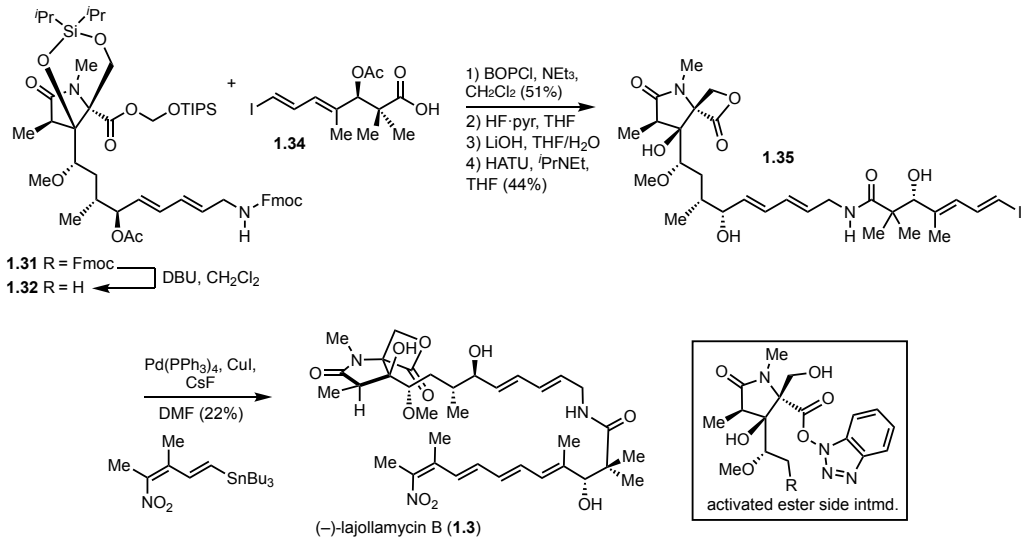

Scheme 1.4. Hatakeyama's total synthesis of lajollamycin B from a common intermediate **1.31**.

1.2.5 Kim's Total Synthesis of Neooxazolomycin

Also, in 2019, Kim et. al. published their total synthesis of neooxazolomycin based on a memory of chirality approach using *D*-serine as a chirality source (Scheme 1.5). Protection of *D*-serine with formaldehyde to form oxazolidine ester **1.36** initiated the synthetic route and amide coupling with benzyloxy acetoacetate gave the β-ketoamide ester **1.37**. Very similarly to Moloney's biomimetic intramolecular aldol reactions (Scheme 1.6),[40] β-ketoamide ester **1.37** was treated with alkoxide base at low temperature for 12 h, leading to the desired, functionalized γ-lactam with the correct stereochemistry relative to the natural oxazolomycin γ-lactam.

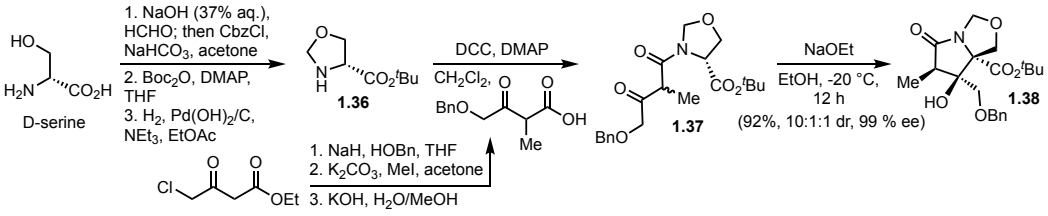

Scheme 1.5. Kim's memory of chirality approach to the γ-lactam core of oxazolomycin.

In contrast to this result, Moloney, in using *L*-serine as starting material and Seebach-type enolate intermediates has only reported the synthesis of analogues of the oxazolomycin core that bear differing relative stereochemistry to the natural products (inset, Scheme 1.6), which underscores Kim's deft use of the property of chiral memory in producing the desired relative configuration in γ-lactam **1.39** with high diastereoselectivity and enantioselectivity.

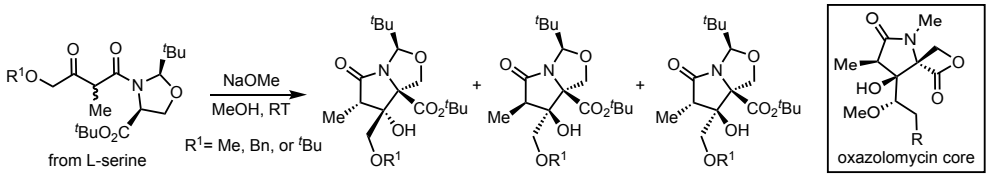

Scheme 1.6. Moloney's biomimetic intramolecular aldol toward oxazolomycin-like γ-lactones with alternate relative stereochemistry.

From γ-lactam **1.38** two step conversion of the benzyl ether to an α-hydroxyaldehyde intermediate of similar to that used as a key intermediate in our synthesis (see Chapters Three and Four). The authors mention briefly their struggles in forming the C4-C5 bond, which we also found to be surprisingly difficult to forge by more widely applied methods. Grignard addition and Nozaki-Hiyama-Kishi conditions led to no desired reaction, presumably owing to steric hindrance about the *pseudo*neopental α-hydroxyaldehyde. Likewise to Kim et. al. we found that allylations are possible on this type of system (see Section 4.4). $In^{(0)}$ metal, *tert*-butylammonium iodide and allylic bromide ester **1.39** was employed in a Barbier reaction in water, forming in 12:1 dr, the undesired epimer at C4 (Scheme 1.7). However, this stereochemical outcome played a role in forming the desired relative configuration of C6 in the subsequent alkene hydrogenation. Opening the pendant γ-lactone with to the Weinreb amide **1.41** was followed by oxidation of the C4-carbinol to an α-hydroxyketone that was diastereoselectively reduced under Luche conditions to achieve the desired C4 stereochemistry in **1.42**. Despite our own efforts to prevent cyclization of γ-hydroxy esters like **1.42**, we were unable. Thus, we found it interesting that the C4 hydroxyl in **1.42** could be protected as its TMS ether, though the authors do mention that competing γ-lactone formation was problematic and conditions for

silylation were carefully selected. The use of a *tert*-butyl ester at C17 undoubtedly serves to inhibit this thermodynamically favored vexation (see Section 4.4).

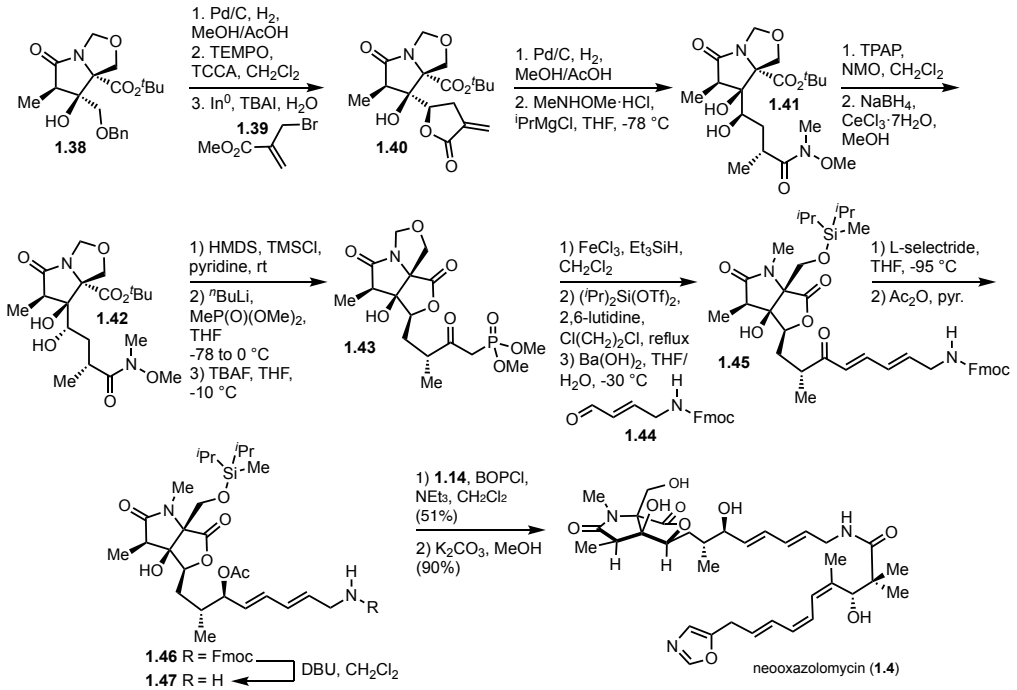

Scheme 1.7. Completion of Kim's total synthesis of neooxazolomycin from γ-lactam **1.39**.

Intermediate silyl protection of the C4-hydroxyl allowed the Weinreb ketone synthesis to proceed smoothly and the resulting β-ketophosphonic ester was treated with $Fe^{(III)}$ and triethylsilane to effect *N*-methylation of the γ-lactam. Dioxasilane protection of the 1,3-diol, as employed by Hatakeyama, preceded Horner-Wadsworth-Emmons olefination with amino enal **1.44**. The C1-C14 neooxazolomycin core was thus prepared for the indispensable Kende amide coupling with triene oxazole acid **1.14**. Simple saponification delivered the natural product.

1.3 Conclusion

That, to this day, there are organic synthesis research groups around the world with programs centered around the oxazolomycins and that the only successful total syntheses of spiro-β-lactone containing congeners are two and emanate from the same chiral pool-based synthetic strategy and the same laboratory (i.e. the Hatakeyama lab), demonstrates the challenges that arise from these highly oxidized, and nitrogenated natural products of hybrid biosynthetic lineage. Their breadth of bioactivity also speaks to the value of synthetic pursuits toward these natural products. It is a great hope that my own toil, which has conveyed some small measure of triumph will guide well future endeavors toward the total synthesis of oxazolomycin natural products and their analogues undertaken in our own research group as well as others.

1.4 References

1. Moloney, M. G.; Trippier, P., C.; Yaqoob, M.; Wang, Z., The Oxazolomycins: A Structurally Novel Class of Bioactive Compounds. *Curr. Drug Disc. Technol.* **2004,** *1* (3), 181-199.

2. Aizawa, S.; Shibuya, M.; Shirato, S., Resistaphilin, A New Antibiotic. I, Production, Isolation and Properties. *J. Antibiot.* **1971,** *24* (6), 393-396.

3. Mori, T.; Takahashi, K.; Kashiwabara, M.; Uemura, D.; Katayama, C.; Iwadare, S.; Shizuri, Y.; Mitomo, R.; Nakano, F.; Matsuzaki, A., Structure of Oxazolomycin, a Novel Beta-Lactone Antibiotic. *Tetrahedron Lett.* **1985,** *26* (8), 1073-1076.

4. Ogura, M.; Nakayama, H.; Furihata, K.; Shimazu, A.; Seto, H.; Otake, N., Structure of a New Antibiotic Curromycin A Produced by a Genetically Modified Strain of *Streptomyces Hygroscopicus* a Polyether Antibiotic Producing Organism. *J. Antibiot.* **1985,** *38* (5), 669-673.

5. Ogura, M.; Nakayama, H.; Furihata, K.; Shimazu, A.; Seto, H.; Otake, N., Isolation and Structural Determination of a New Antibiotic Curromycin-B. *Agric. Biol. Chem.* **1985,** *49* (6), 1909-1910.

6. Takahashi, K.; Kawabata, M.; Uemura, D.; Iwadare, S.; Mitomo, R.; Nakano, F.; Matsuzaki, A., Structure of Neooxazolomycin, an Antitumor Antibiotic. *Tetrahedron Lett.* **1985,** *26* (8), 1077-1078.

7. Ikeda, Y.; Kondo, S.; Naganawa, H.; Hattori, S.; Hamada, M.; Takeuchi, T., New Triene-β-lactone Antibiotics, Triedimycins A and B. *J. Antibiot.* **1991,** *44* (4), 453-455.

8. Ryu, G.; Hwang, S.; Kim, S. K., 16-methyloxazolomycin, a new antimicrobial and cytotoxic substance produced by a Streptomyces sp. *J. Antibiot.* **1997,** *50* (12), 1064-1066.

9. Kanzaki, H.; Wada, K.-i.; Nitoda, T.; Kawazu, K., Novel Bioactive Oxazolomycin Isomers Produced by Streptomyces albus JA3453. *Biosci., Biotechnol., Biochem.* **1998,** *62* (3), 438-442.

10. Ryu, G. S.; Kim, S. K., Absolute stereochemistry determination of 16-methyloxazolomycin produced by a Streptomyces sp. *J. Antibiot.* **1999,** *52* (2), 193-197.

11. Otani, T.; Yoshida, K. I.; Kubota, H.; Kawai, S.; Ito, S.; Hori, H.; Ishiyama, T.; Oki, T., Novel Triene-β-lactone Antibiotics, Oxazolomycin Derivative and Its Isomer, Produced by *Streptomyces* sp. KSM-2690. *J. Antibiot.* **2000,** *53* (12), 1397-1400.

12. Manam, R. R.; Teisan, S.; White, D. J.; Nicholson, B.; Grodberg, J.; Neuteboom, S. T. C.; Lam, K. S.; Mosca, D. A.; Lloyd, G. K.; Potts, B. C. M., Lajollamycin, a nitro-tetraene spiro-beta-lactone-gamma-iactam antibiotic from the marine actinomycete Streptomyces nodosus. *J. Nat. Prod.* **2005,** *68* (2), 240-243.

13. Ko, K.; Lee, S. H.; Kim, S. H.; Kim, E. H.; Oh, K. B.; Shin, J.; Oh, D. C., Lajollamycins, Nitro Group-Bearing Spiro-β-lactone-γ-lactams Obtained from a Marine-Derived Streptomyces sp. *J. Nat. Prod.* **2014,** *77* (9), 2099-2104.

14. Shiomi, K.; Arai, N.; Shinose, M.; Takahashi, Y.; Yoshida, H.; Iwabuchi, J.; Tanaka, Y.; Omura, S., New Antibiotics Phthoxazolins B, C and D Produced by *Streptomyces* sp. KO-7888. *J. Antibiot.* **1995,** *48* (7), 714-719.

15. Tanaka, Y.; Kanaya, I.; Takahashi, Y.; Shinose, M.; Tanaka, H.; Omura, S., Phthoxazolin A, A Specific Inhibitor of Cellulose Biosynthesis from Microbial Origin, II. Isolation, Physio-chemical Properties, and Structural Elucidation. *J. Antibiot.* **1993,** *46* (8), 1208-1213.

16. Tanaka, Y.; Kanaya, I.; Shiomi, K.; Tanaka, H.; Omura, S., Phthoxazolin A, A Specific Inhibitor of Cellulose Biosynthesis from Microbial Origin, I. Discovery, Taxonomy of Producing Microorganism, Fermentation, and Biological Activity. *J. Antibiot.* **1993,** *46* (8), 1214-1218.

17. Henkel, T.; Zeeck, A., Secondary Metabolites by Chemical-Screening .16. Inthomycins, New Oxazole-Trienes from Streptomyces-Sp. *Liebigs Ann. Chem.* **1991,** (4), 367-373.

18. Omura, S.; Tanaka, Y.; Kanaya, I.; Shinose, M.; Takahashi, Y., Phthoxazolin, A Specific Inhibitor of Cellulose Biosynthesis, Produced by a Strain of *Sreptomyces* sp. *J. Antibiot.* **1990,** *43* (8), 1034-1036.

19. Kawada, M.; Inoue, H.; Usami, I.; Ikeda, D., Phthoxazolin A inhibits prostate cancer growth by modulating tumor-stromal cell interactions. *Cancer Sci.* **2009,** *100* (1), 150-157.

20. Kreiss, W.; Frode, R.; Mohrle, V.; Eberz, G., Chromatography-bioluminescence coupling reveals surprising bioactivity of inthomycin A. *Anal. Bioanal. Chem.* **2010,** *398* (5), 2081-2088.

21. Koomsiri, W.; Inahashi, Y.; Kimura, T.; Shiomi, K.; Takahashi, Y.; Ōmura, S.; Thamchaipenet, A.; Nakashima, T., Bisoxazolomycin A: a new natural product from 'Streptomyces subflavus subsp. irumaensis' AM-3603. *J. Antibiot.* **2017,** *70* (12), 1142-1145.

22. Kawai, S.; Kawabata, G.; Kobayashi, A.; Kawazu, K., Inhibitory Effect of Oxazolomycin on Crown Gall Formation. *Agric. Biol. Chem.* **1989,** *53* (4), 1127-1133.

23. Grigorjev, P. A.; Schlegel, R.; Gräfe, U., On the Protonophoric Activity of Oxazolomycin. *Pharmazie* **1992,** *47* (9), 707-709.

24. Kawazu, K.; Kanzaki, H.; Kawabata, G.; Kawai, S.; Kobayashi, A., Oxazolomycin Esters, Specific Inhibitors of Plant Transformation. *Biosci., Biotechnol., Biochem.* **1992,** *56* (9), 1382-1385.

25. Tonew, E.; Tonew, M.; Grafe, U.; Zopel, P., On the Antiviral Activity of Diffusomycin (Oxazolomycin). *Acta Virol.* **1992,** *36* (2), 166-172.

26. Nakamura, M.; Honma, H.; Kamada, M.; Ohno, T.; Kunimoto, S.; Ikeda, Y.; Kondo, S.; Takeuchi, T., Inhibitory Effect of Curromycin-a and Curromycin-B on Human-Immunodeficiency-Virus Replication. *J. Antibiot.* **1994,** *47* (5), 616-618.

27. Grafe, U.; Kluge, H.; Thiericke, R., Biogenetic Studies on Oxazolomycin, a Metabolite of Streptomyces-Albus (Strain Ja-3453). *Liebigs Ann. Chem.* **1992,** (5), 429-432.

28. Zhao, C. H.; Ju, J. H.; Christenson, S. D.; Smith, W. C.; Song, D. F.; Zhou, X. F.; Shen, B.; Deng, Z. X., Utilization of the methoxymalonyl-acyl carrier protein biosynthesis locus for cloning the oxazolomycin biosynthetic gene cluster from Streptomyces albus JA3453. *J. Bacteriol.* **2006,** *188* (11), 4142-4147.

29. Song, D. F.; Coughlin, J.; Ju, J. H.; Zhou, X. F.; Shen, B.; Zhao, C. H.; Deng, Z. X., Alternative method for site-directed mutagenesis of complex polyketide synthase in Streptomyces albus JA3453. *Acta Biochim. Biophys. Sin.* **2008,** *40* (4), 319-326.

30. Zhao, C. H.; Coughlin, J. M.; Ju, J. H.; Zhu, D. Q.; Wendt-Pienkowski, E.; Zhou, X. F.; Wang, Z. J.; Shen, B.; Deng, Z. X., Oxazolomycin Biosynthesis in Streptomyces albus JA3453 Featuring an "Acyltransferase-less" Type I Polyketide Synthase That Incorporates Two Distinct Extender Units. *J. Biol. Chem.* **2010,** *285* (26), 20097-20108.

31. Xie, X.; Cane, D. E., Stereospecific Formation of Z-Trisubstituted Double Bonds by the Successive Action of Ketoreductase and Dehydratase Domains from trans-AT Polyketide Synthases. *Biochemistry* **2018,** *57* (22), 3126-3129.

32. Kende, A. S.; Kawamura, K.; Devita, R. J., Enantioselective Total Synthesis of Neooxazolomycin. *J. Am. Chem. Soc.* **1990,** *112* (10), 4070-4072.

33. Kende, A. S.; Devita, R. J., Synthesis of the Fused Bicyclic Lactam-Lactone Terminus of Neooxazolomycin by a Novel Dianion Cyclocondensation. *Tetrahedron Lett.* **1988,** *29* (21), 2521-2524.

34. Stille, J. K., The Palladium-Catalyzed Cross-Coupling Reactions of Organotin Reagents with Organic Electrophiles [New Synthetic Methods (58)]. *Angew. Chem. Int. Ed.* **1986,** *25* (6), 508-524.

35. Kende, A. S.; DeVita, R. J., A mild four-carbon homologation of aldehydes to E,E-dienamines. *Tetrahedron Lett.* **1990,** *31* (3), 307-310.

36. Onyango, E. O.; Tsurumoto, J.; Imai, N.; Takahashi, K.; Ishihara, J.; Hatakeyama, S., Total synthesis of neooxazolomycin. *Angew. Chem. Int. Ed.* **2007,** *46* (35), 6703-6705.

37. Eto, K.; Yoshino, M.; Takahashi, K.; Ishihara, J.; Hatakeyama, S., Total Synthesis of Oxazolomycin A. *Org. Lett.* **2011,** *13* (19), 5398-5401.

38. Ishihara, J.; Hatakeyama, S., Total Synthesis of Oxazolomycins. *Chem. Rec.* **2014,** *14* (4), 663-677.

39. Nishimaru, T.; Eto, K.; Komine, K.; Ishihara, J.; Hatakeyama, S., Total Synthesis of Lajollamycin B. *Chem. Eur. J.* **2019,** *25* (33), 7927-7934.

40. Andrews, M. D.; Brewster, A. G.; Moloney, M. G., Highly functionalised pyroglutamates by intramolecular aldol reactions: Towards the pyroglutamate skeleton of oxazolomycin. *Synlett* **1996,** (7), 612-&.

CHAPTER TWO

Scalable, Enantioselective, Nucleophile-Catalyzed, Michael-Proton Transfer-γ-Lactamization: Concise Route to a Functionalized γ-Lactam Applicable to Oxazolomycin Synthesis

This chapter was published with modifications as: Christian M. Chaheine, Conner J. Song, Paul T. Gladen, Daniel Romo. Enantioselective Michael-Proton Transfer-Lactamization for Pyroglutamic Acid Derivatives: Synthesis of dimethyl-(S,E)-5-oxo-3-styryl-1-tosylpyrrolidine-2,2-dicarboxylate. *Organic Syntheses* (2020). *Submitted*

2.1 Introduction

The development of synthetic methods for enantioselective access to functionalized pyroglutamate,[41, 42] and, more generally, γ-lactam (aka pyrrolidine-2-one, γ-butyrolactam, azolidine-2-one, 2-oxopyrrolidine) containing compounds remains a highly active topic in the field of organic synthesis. This is due to their versatility as synthetic intermediates and their presence in many natural products, metabolites, and pharmaceuticals with broad-ranging and potent biological activities (Figure 2.1).[1, 32, 36, 37, 39, 43-55]

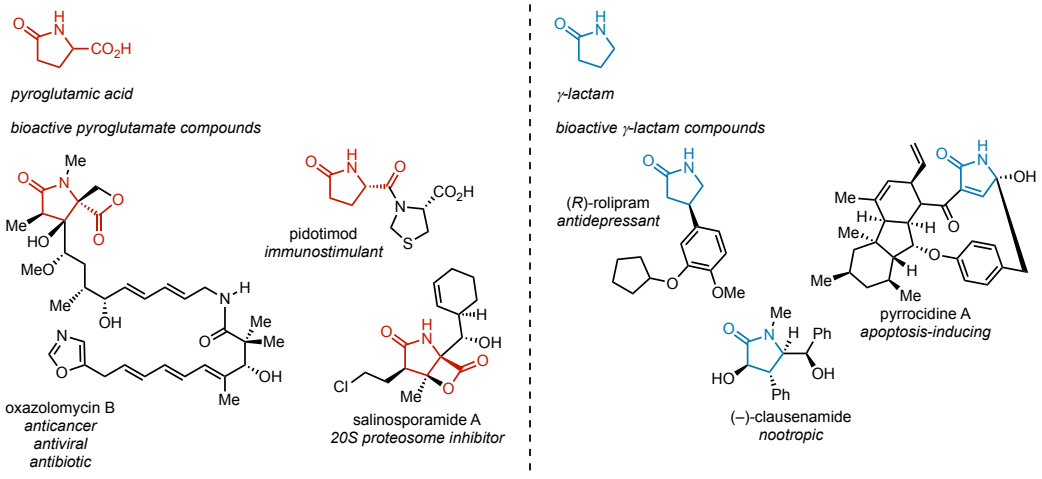

Figure 2.1. A selection of bioactive γ-lactam/pyroglutamate-containing natural products and pharmaceutical drugs.

There are an abundance of chemical methods for the synthesis of γ-lactams in racemic form, primarily through intramolecular cyclizations of functionalized linear substrates via C-N as well as C-C bond formation.[45, 54, 56-60] In only the last three years, several methods for the construction of racemic γ-lactams have been reported– tandem addition/cyclization,[61-64] multi-component,[65-68] intramolecular C-H activation[69-73], photoredox-catalyzed,[74-76] transition metal-catalyzed cyclizations,[77, 78] rearrangement,[79] direct α-alkylation of primary amines with acrylates,[80] ring contraction/expansion,[81, 82] and flow chemistry.[83] Chemoenzymatic,[84] enzymatic resolution,[85] and chiral pool synthesis[86, 87] have also been reported recently as asymmetric strategies. While these myriad, powerful methods are now available for the synthesis of γ-lactams, fewer examples illustrate a robust means of *enantioselective* construction of this key *N*-heterocycle from achiral starting materials. Even fewer methods have demonstrated scalability while maintaining a high degree of enantiopurity in the product.

2.1.1 Enantioselective Synthesis of γ-Lactams

The following will briefly highlight recent (within the last three years) advances in synthetic methods to access chiral γ-lactams in an enantioselective fashion from achiral starting materials. This will be followed by a discussion of our group's research activity in the area of unsaturated acylammonium catalysis, centering on the nucleophile-catalyzed Michael-proton transfer lactamization (NCMPL) used in the described procedure.

Asymmetric organocatalytic routes to γ-lactams primarily employ chiral *N*-heterocyclic carbenes (NHCs),[88] which is a complementary strategy to the NCMPL methodology in its use of α,β-unsaturated carbonyl derivatives as substrates in a cascade

process. In addition to multiple NHC-based organocatalytic methods, chiral phosphoric acids,[89] phase-transfer,[90] and hydrogen bond donor catalysts,[91] and multi-component reactions[92, 93] have also appeared recently as alternate avenues to optically active γ-lactams. Huang disclosed a Michael-addition/cyclization reaction using chiral NHC **2.1** as a precatalyst, α-bromo-α,β-enals and α-sulfonamidoketones as substrates, and an excess of alkylamine base (Scheme 2.1A).[94] High-enantioselectivities and diastereoselectivites are obtained, and the reaction was performed on gram scale without significant loss of yield or enantiopurity. Notably, heteroaryl and cycloalkyl substituted ketones are efficient reactants in this process, delivering functionalized *trans*-γ-lactams that are aptly suited to the synthesis of clausenamide analogues.

A chiral NHC-catalyzed homoenolate addition/cyclization was reported by Li.[95] Utilizing the same precatalyst **2.1** and various α,β-enals as homoenolate precursors, the Li group demonstrated a formal (3+2) annulation occurs with α-sulfonamidoacrylates (Scheme 2.1B). Mechanistic investigations revealed that, rather than the anticipated homoenolate Michael-addition/cyclization sequence, a tautomerization of the sulfonamidoacrylate to an α-iminoester precedes homoenolate addition and cyclization, yielding pyroglutamate derivatives that bear an *aza*-quaternary center in good yield and enantioselectivity.

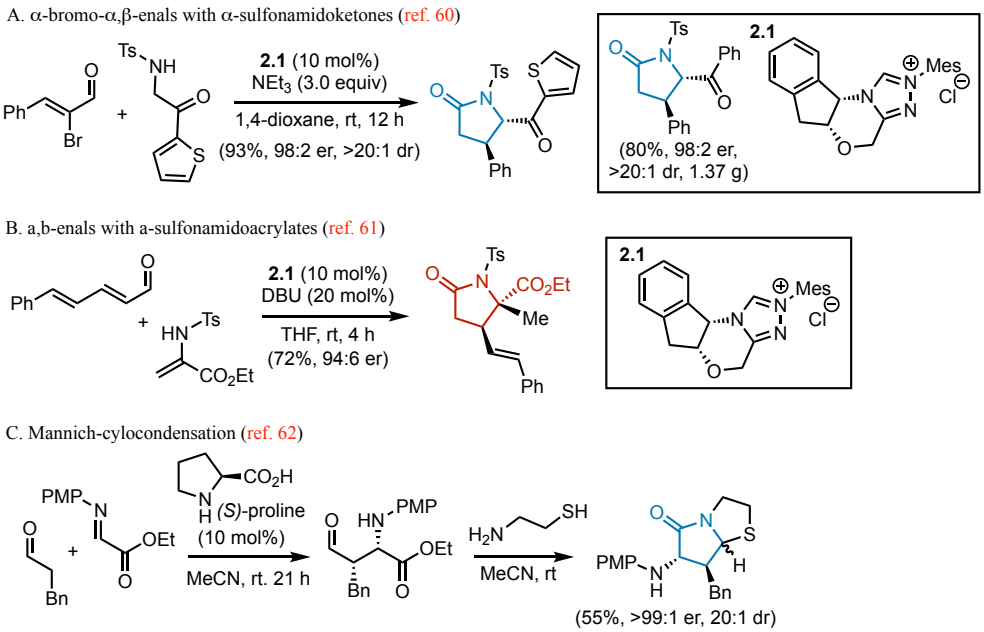

Scheme 2.1. organocatalytic, enantioselective γ-lactam synthesis.

In contrast, Córdova developed an asymmetric cascade processes to construct bicyclic γ- and δ-lactam *N,S*-acetals through chiral amine catalysis (Scheme 2.1C).[96] The bicyclic products are intriguing scaffolds that occur in 5-membered ring analogs of penicillin antibiotics. In this reaction, Mannich-addition of an enolizable aldehyde onto an α-iminoester is catalyzed by (*S*)-proline, forming a Mannich-base intermediate that is then treated with an aminothiol to afford bicyclic α-amino as well as α-hydroxy-γ-lactam *N,S*-acetals with excellent enantioselectivity.

More prevalent in the literature are methods based on transition metal catalysis. The asymmetric reductive amination of γ-ketoesters for the synthesis of enantioenriched *N*-unprotected-γ-lactams was realized by the Yin group.[97] A chiral bidentate phosphine ligand **L1** in combination with $Ru(OAc)_2$ under an atmosphere of H_2 was identified as an efficient catalytic system for the reductive amination to NH-γ-lactams (Scheme 2.2A). Only aryl-substituted ketone substrates led to high enantioselectivities, however. This method was

used on up to a gram-scale to build a pyrrolidine intermediate toward an anti-cancer therapeutic, Larotrectinib, as well as a benzolactam intermediate toward a quinolone antibiotic drug, Garenoxacin.

An enantioselective cobalt-catalyzed hydroboration cyclization of linear N-allyl-propiolamides was recently reported by Ge.[98] Borylated γ-lactams bearing stereogenic all-carbon quaternary centers were constructed in high yield and enantioselectivity with the application of chiral bidentate phosphine ligand **L2** and $Co(acac)_2$ (Scheme 2.2B). This reaction was conducted on a gram-scale and the versatility of the boryl functionality was demonstrated through a variety of known transformations.

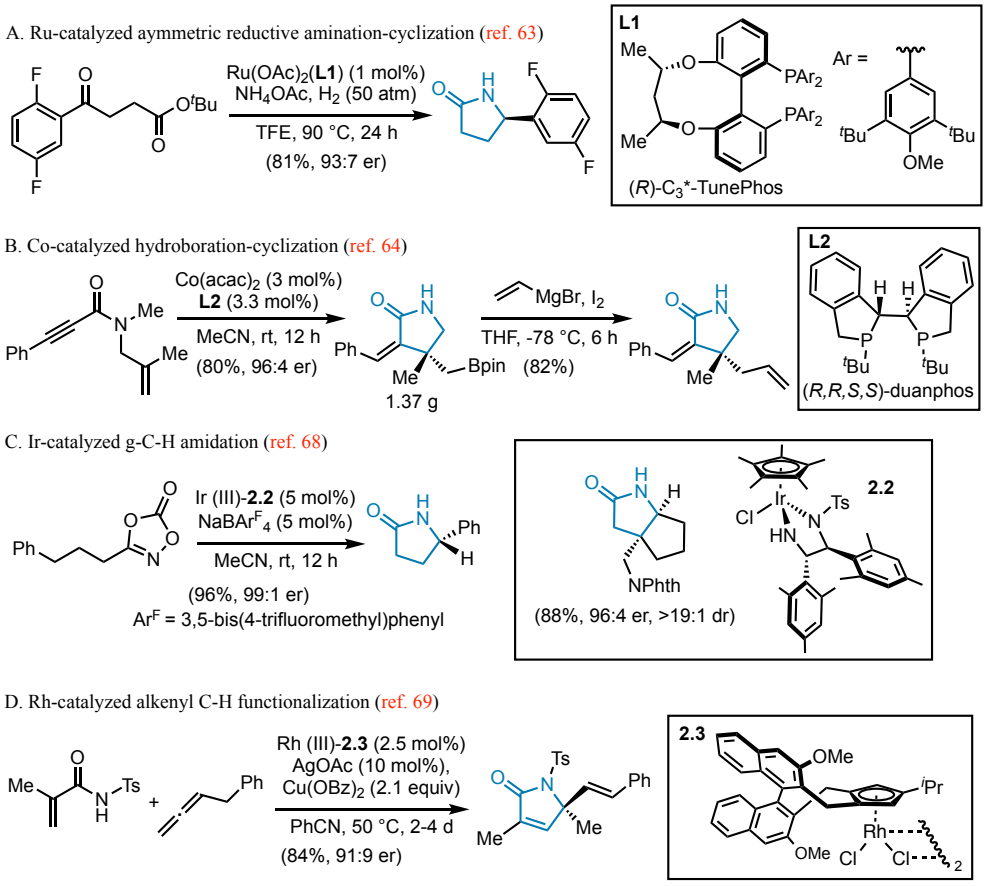

Scheme 2.2. Enantioselective, transitionmetal-catalyzed γ-lactam synthesis.

Activation of sp^3 C-H bonds by transition metal catalysts is an important and fertile subfield in organometallic chemistry and recently has enabled the enantioselective synthesis of NH-γ-lactams from readily-available carboxylic acid derivatives like 1,4,2-dioxazol-5-ones.[99-101] Chang optimized the intramolecular, Ir (III)-catalyzed γ-C-H amidation using a chiral diamine ligand and 1,4,2-dioxazol-5-ones as acylnitrenoid precursors (Scheme 2.2C).[102] The Curtius rearrangement pathway that commonly impedes the desired CH-amidation through the formation of isocyanate side-products is completely suppressed with Ir catalyst **2.2** under their established conditions. An impressive substrate scope is demonstrated using a variety of aliphatic sp^3 C-H containing dioxazolones, leading to functionalized γ-stereogenic-γ-lactams in good yields and high enantioselectivities. The reaction can be carried out in air and has been demonstrated on half-gram scale without erosion of product enantiopurity.

Alkenyl C-H-activation has also been employed recently in the enantioselective synthesis of γ-lactams by Cramer.[103] Acrylamides and allenes are reacted in a (4+1) annulation to γ-stereogenic-α,β-unsaturated-γ-lactams via chiral cyclopentadienyl Rh (III) catalyst **2.3** (Scheme 2.2D). AgOAc is used to generate the active Rh (III) catalyst by ligand substitution and $Cu(OBz)_2$ was found to be the optimal source of terminal oxidant to regenerate the catalyst. Mild heating and extended reaction times (2-4 days) lead to chiral α,β-unsaturated-γ-lactams in good yields and high enantioselectivities, although the scalability of this method is unaddressed. Other methods of note for the enantioselective construction and reactions of γ-lactams include hydrogenation,[104, 105] C-H functionalization,[106, 107] desaturation,[108] and cyclopropanations.[109]

2.1.2 Synthetic Utility of α,β-Unsaturated Acylammonium Salts

Initial reports of acylammonium salts as reactive intermediates emerged as early as the 1930s with Wegler's description of an asymmetric acyl-transfer process.[110] The synthetic potential of acylammonium salts has since expanded to include a multitude of asymmetric organocascade processes initiated by different types of chiral acylammonium intermediates (Figure 2.2), leading to mono- and polycyclic frameworks of varying complexity. Developments in this area have been recently reviewed.[111, 112] In the last four years additional examples of asymmetric organocascade reactions using α,β-unsaturated acylammonium salts have been reported.

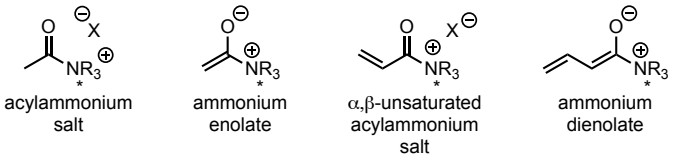

Figure 2.2. Chiral acylammonium salt intermediates

In 2016, Birman disclosed an asymmetric thio-Michael addition/aldol/β-lactonization/decarboxylation cascade process toward the synthesis of thiochromenes and thiochromanes (Scheme 2.3).[113] Catalyzed by HBTM-2.0[114] (**2.4**) or H-PIP[115] (**2.5**), highly enantioselective generation of these heterocycles starting from readily available α,β-unsaturated thioesters was demonstrated.

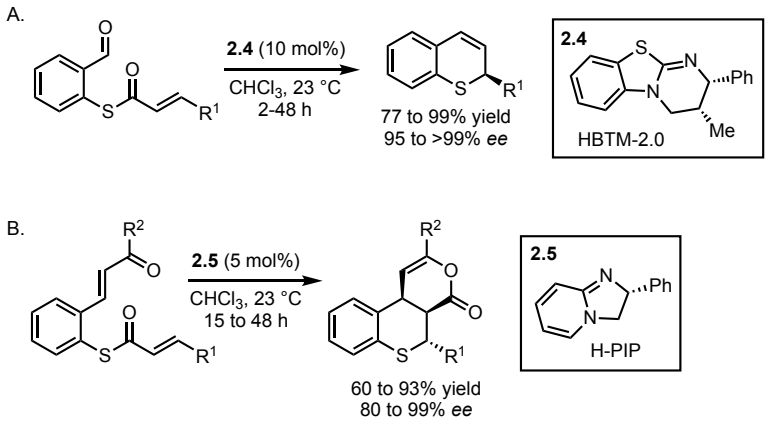

Scheme 2.3. Thiocromane and thiochromene synthesis via α,β-unsaturated acylammonium salts.

In the same year, Smith reported chemo- and enantioselective, benzazole annulations catalyzed by HBTM-2.1 (**2.6**) that employ α,β-unsaturated homoanhydride electrophiles and afford benzazole δ-lactams and lactones from acylbenzothiazole and acylbenzoxazole nucleophiles (Scheme 2.4).[116] Computational studies suggested that the presence of two 1,5-S–O *n*-σ* interactions following the initial Michael-addition step dictate the chemoselectivity of δ-lactone vs δ-lactam formation.

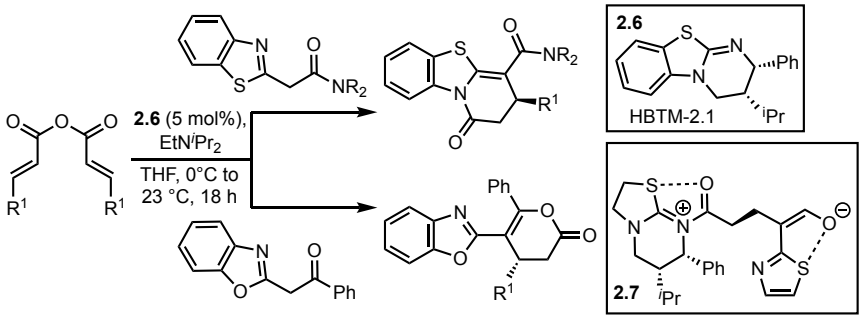

Scheme 2.4. Isothiourea-catalyzed annulation of benzazoles with unsaturated homoanhydrides.

Until recently, catalytic turnover of the chiral Lewis-base in acylammonium organocascades was driven by acyl substitution with a pendant, *in situ* generated

nucleophile. In 2017, Smith showed that catalyst regeneration can be facilitated by an aryloxide counterion that is produced following the formation of the acylammonium intermediate from α,β-unsaturated aryl esters, expanding the scope of potential nucleophiles applicable in these types of organocascades (Scheme 2.5).[117] The Smith group demonstrated the utility of this approach with an enantioselective isothiourea-catalyzed Michael-addition of nitroalkanes to the α,β-unsaturated aryl esters in up to 79% yield and 99:1 er. The branched nitroalkane products could be elaborated to optically active γ-lactams following chemoselective reduction of the nitro moiety. Smith quite recently described the use of aryloxide-facilitated turnover toward the enantioselective Michael-addition of *N*-heterocyclic pronucleophiles[118] and silylnitronates[119] to α,β-unsaturated aryl esters.

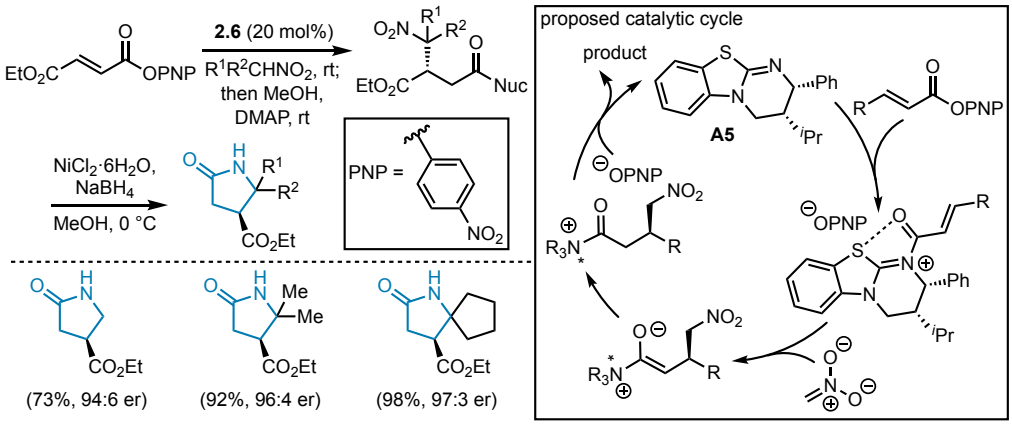

Scheme 2.5. Catalyst turnover driven by an aryloxide anion in enantioselective Michael-addition leading to γ-lactams.

A long-standing research focus of our group has been the application of chiral acylammonium salts in the organocatalytic, asymmetric synthesis of heterocycles. Since 2001, we developed a nucleophile-catalyzed/aldol/lactonization (NCAL),[120, 121]

nucleophile-catalyzed Michael/aldol/β-lactonization (NCMAL),[122] Diels-Alder/lactonization (DAL),[123, 124] and a nucleophile-catalyzed Michael/proton transfer/lactamization (NCMPL),[125] the basis of the procedure discussed below.

2.2 Discussion

In 2013, we disclosed an enantioselective, organocatalytic nucleophile-catalyzed Michael/proton transfer/lactamization (NCMPL) cascade. Using α,β-unsaturated acylammonium salts generated from commercially available α,β-unsaturated acid chlorides, readily accessible *O*-trimethylsilylquinidine (TMSQD, **2.8**) or *O*-trimethylsilylquinine catalysts (TMSQN), and *N*-protected aminomalonates as bis-nucleophilic reaction partners. The substrate scope from the original publication as well as the product of the current procedure (a new entry in the table) is illustrated below (Table 2.1).

During optimization of this method, the importance of 1,8-diazabicyclo[5.4.0]undec-7-ene (DBU) as an acid scavenger was noted, omitting this amine base resulting in <5% yield. The use of cinchona alkaloid derived, as opposed to isothiourea Lewis-bases, led to superior enantioselectivities. Additionally, substitution of LiHMDS with sodium bis(trimethylsilyl)amide (NaHMDS) also drastically reduced enantioselectivity, implicating the lithium cation as a crucial coordinating Lewis acid in the transition-state arrangement. This method was also applicable to the enantioselective synthesis of enol lactones when β-ketoesters are used as bis-nucleophilic reactants. The following procedure represents another example of the robustness of the NCMPL wherein a functionalized lactam is produced as virtually a single enantiomer on a decagram scale.

We have been able to scale the reaction up to 20 g of sulfonamidomalonate starting material without detriment to yield or enantiopurity. The above procedure can also be conducted using *diethyl*aminomalonate hydrochloride, which is significantly less costly, however, we were unable to find conditions for the recrystallization of the product γ-lactam from the crude reaction mixture. The exclusion of column chromatography following the NCMPL to obtain the desired γ-lactam product, as is possible in the case of *diemthyl*aminomalonate, significantly simplifies the purification and was chosen for this reason.

Table 2.1. A new addition to the substrate scope of the NCMPL (red).

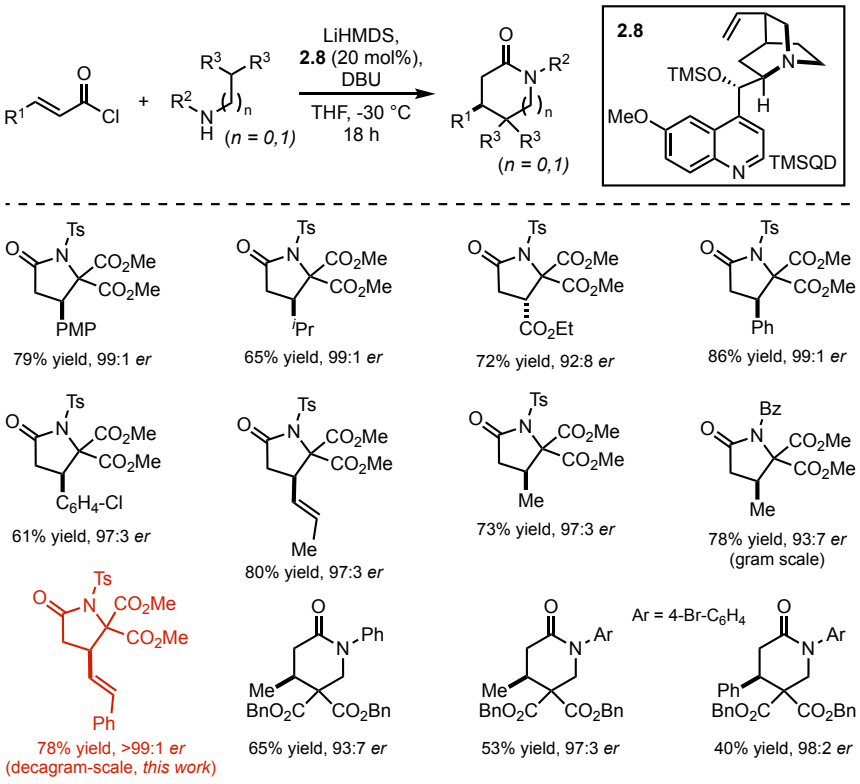

Further expanding on the utility of chiral, α,β-unsaturated acylammonium salts, we also adapted the NCMPL to the synthesis of medium-sized lactams.[126] The resulting azepanones, benzazepinones, azocanones, and benzazocinones were generated in high enantiopurity and synthetically useful yield.

2.3 Conclusion

In summary, the NCMPL organocascade provides a convenient route for functionalized, small to medium-sized lactams, including pyroglutamic acid derivatives, in optically active form often with high enantiopurity. The utility of the derived lactams and established manipulations can be found in the published work from our group in this area.[91,92] The following synthetic procedure represents a convenient, highly detailed and optimized example of the NCMPL that has been applied in our lab to the synthesis of oxazolomycin natural products and analogous, simplified derivatives toward protein target identification studies in collaboration with the Sieber lab at the Technical University of Munich.

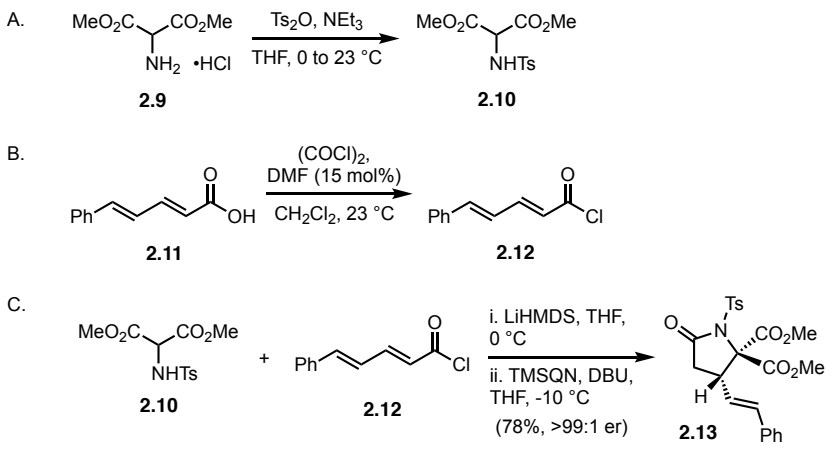

Scheme 2.6. NCMPL reaction of dienoyl chloride **2.12** with sulfonamidomalonate **2.10** and synthesis of substrates.

*2.4.1 Synthesis of Sulfonamidomalonate **2.10***

Dimethyl 2-((4-methylphenyl)sulfonamido)malonate (2.10, Scheme 2.6A): To a single-necked, 500 mL round-bottomed flask containing a football-shaped, teflon-coated stir bar (5 cm) and fitted with a 24/40 glass, threaded gas-inlet adapter with a silicone/PTFE septa (Figure 2.3A, Note 2), in-turn connected via chemical resistant tubing to a vacuum/nitrogen manifold was added commercially available dimethyl aminomalonate hydrochloride (**2.9**, 12.5 g, 68.1 mmol, 1.00 equiv) and *p*-toluenesulfonic anhydride (27.2 g of 90 wt. % purity, 74.9 mmol, 1.10 equiv; Note 3) as solids. The atmosphere in the flask was replaced with nitrogen by three cycles of vacuum (Note 4) and nitrogen back-filling via the vacuum/nitrogen manifold. The glass adapter was briefly removed and tetrahydrofuran (272 mL) was then added from a polyethylene graduated cylinder under a stream of nitrogen from the manifold. The resulting beige suspension was stirred vigorously and cooled to 0 °C in an ice/water bath (Figure 2.3B) for 15 min before adding freshly distilled

triethylamine (28.5 mL, 204 mmol, 3.00 equiv; Note 5) by rapid dropwise addition via a 60 mL, plastic, luer-lock syringe fitted with a stainless steel 18-gauge needle over ~5 min. A yellow-orange suspension formed within 1 h (Figure 2.3C) and gradually became a light-yellow color as it was stirred over 24 h (Note 6, Figure 2.3D) and allowed to slowly warm to ambient temperature (23 °C).

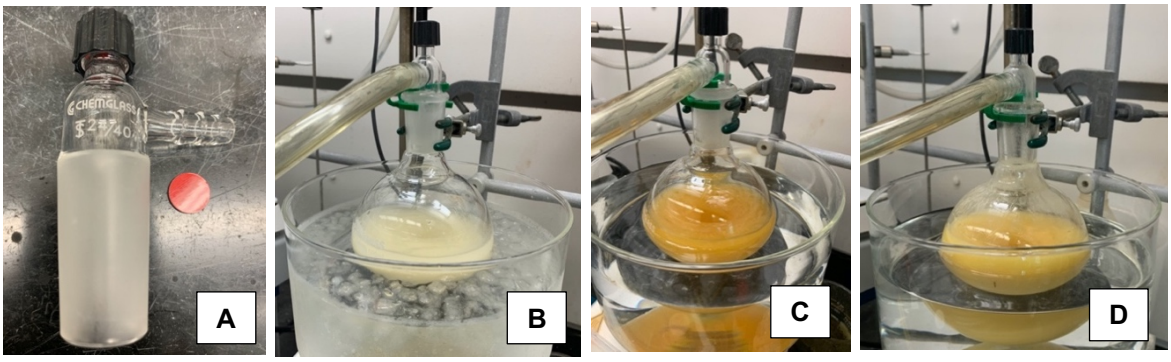

Figure 2.3. *N*-tosylation of dimethylaminomalonate hydrochloride: A) Threaded gas-inlet adapter, 24/40 joint size, fitted with a red/white PTFE/silicone septa in an open-top screw cap. B) Prior to addition of triethylamine. C) 1 hour after addition of triethylamine. D) 16 h after addition of triethylamine.

The yellow-orange suspension was then vacuum-filtered through a pad of celite (Note 7, Figure 2.4A) into a 1 L, heavy-walled vacuum Erlenmeyer flask to remove the white precipitate by-product, triethylammonium *p*-toluenesulfonate. Quantitative transfer of the crude material to the filter funnel was carried out by rinsing with ethyl acetate from a polyethylene squirt bottle (~25 mL). The filter cake was rinsed with ethyl acetate (250 mL) and the filtrate was transferred to a 1 L recovery flask and concentrated by rotary evaporation (~150 to 75 mmHg) to a yellow oil that was dry-loaded onto 70 g of silica gel (Note 8 and 9). The resulting fine yellow powder was loaded onto a pre-packed flash chromatography column for purification (Figure 2.4B-C, Note 10), yielding 14.2 g (69%)

of dimethyl 2-((4-methylphenyl)sulfonamido)malonate (**2.10**) as an off-white grainy powder (97% purity by q1H-NMR, Note 11, Figure 2.4D).

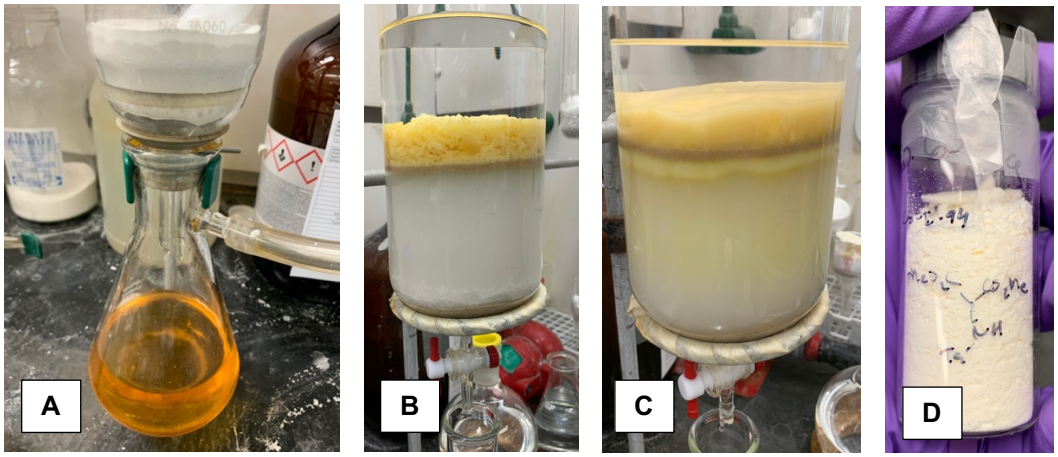

Figure 2.4. *N*-tosylation reaction monitoring, work-up, and column chromatography: A) Crude reaction solution after filtering through Celite. B) Flash column prior to fraction collection with crude mixture pre-absorped onto silica gel. C) Flash column following product collection; yellow color that progresses through column is not collected. D) Appearance of *N*-tosyl-2-aminomalonate.

*2.4.2 Synthesis of Dienoyl Chloride **2.12***

(2*E*,4*E*)-5-phenylpenta-2,4-dienoyl chloride (2.12, Scheme 2.6B): To an oven-dried (Note 12), 500 mL, single-necked, round-bottomed flask containing a football-shaped, teflon-coated stir bar (4 cm) and fitted with a 24/40 glass, threaded gas-inlet adapter with a silicone/PTFE septa (Figure 2.3A, Note 2), in-turn attached via chemical resistant tubing to a vacuum/nitrogen manifold was added commercially available 5-phenyl-2,4-pentadienoic acid (**2.11**, 10.0 g, 57.4 mmol, 1.00 equiv; Note 13). The atmosphere in the vessel was replaced with nitrogen by three cycles of evacuation (Note 4) and back-filling with nitrogen via the vacuum/nitrogen manifold. The hose connection to the manifold was then quickly replaced with tygon tubing connected in sequence to a mineral oil bubbler followed by a solution of saturated, aqueous sodium bicarbonate (150 mL) in a 250 mL Erlenmeyer flask (Figure 2.5A). CH_2Cl_2 (230 mL) was then added in four portions via a

60 mL plastic syringe fitted with an 18-gauge stainless steel needle, forming a beige-colored suspension that was stirred at ambient temperature (23 °C). *N,N*-dimethylformamide (670 mL, 8.6 mmol, 15 mol%) was added via a plastic 1 mL syringe, and was followed by dropwise addition of oxalyl chloride (14.8 mL, 172 mmol, 3.00 equiv) over 15 min via a 30 mL plastic luer-lock syringe fitted with a 20-gauge stainless-steel needle connected to a syringe pump (59 mL/h flow rate). The reaction mixture was stirred at ambient temperature (23 °C) while venting gaseous by-products through the mineral oil bubbler/sodium bicarbonate solution (caution! Note 14) until it became a homogenous, gold-colored solution and had ceased gas evolution (~3-4 h).

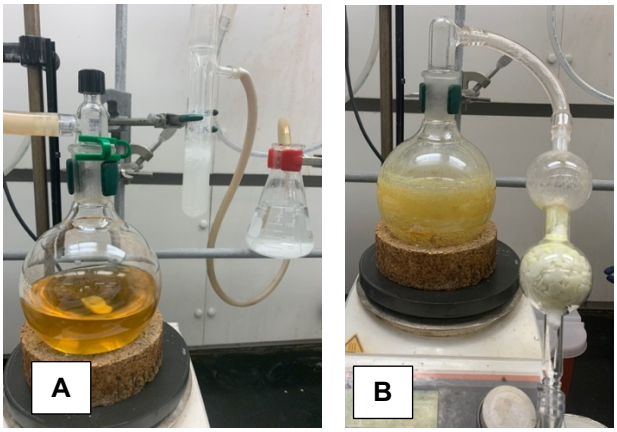

Figure 2.5. Acid chloride synthesis: A) Reaction set up with mineral oil bubbler and sodium bicarbonate solution in sequence to control and quench exhaust gases. B) Crude acid chloride used in the next reaction after drying on high vacuum with an attached acid scrubber (KOH pellets).

The stir bar was then removed and the crude reaction mixture was concentrated by rotary evaporation (150 to 75 mmHg, ~1 h) to a light-brown, amorphous solid that was further dried under high vacuum (~3 mm Hg; Note 15, Figure 2.5B) with an intervening acid scrubber column for at least 3 h to provide (2*E*,4*E*)-5-phenylpenta-2,4-dienoyl chloride (**2.12**). The atmosphere in the flask was charged with nitrogen via the Schlenk

manifold and the crude acid chloride was used directly in the next reaction without purification (Note 16).

*2.4.3 Synthesis of N-Ts Pyroglutamate NCMPL Product **2.13***

Dimethyl-(*S*,*E*)-5-oxo-3-styryl-1-tosylpyrrolidine-2,2-dicarboxylate (2.13, Scheme 2.6C): To an oven-dried (Note 12), 1 L, single-necked, round-bottomed flask containing a football-shaped, teflon-coated stir bar (5 cm) was added dimethyl sulfonamidomalonate (12.4 g, 41.2 mmol, 1.00 equiv). The reaction vessel was fitted with a T-bore Schlenk adapter attached to both vacuum and an argon balloon (Note 17 and 18, Figure 2.6A). The atmosphere in the flask was replaced with argon by three cycles of vacuum/back-filling via the Schlenk adapter, which was then quickly replaced with a rubber septum and an argon balloon. Tetrahydrofuran was added (206 mL, 0.20 M initial concentration of sulfonamidomalonate; Note 19 and 20) in four portions via a plastic 60 mL syringe fitted with an 18-gauge stainless steel needle and the resulting clear solution was stirred vigorously and cooled to 0 °C in an ice bath over 15 min. A newly opened 100 mL bottle of lithium hexamethyldisilazide (LiHMDS, 1.0 M in tetrahydrofuran, 47.2 mL, 47.2 mmol, 1.15 equiv; Note 21) was then added dropwise from a 60 mL plastic luer-lock syringe fitted with an 18-gauge stainless-steel needle connected to a syringe pump over 15 min (189 mL/h flow rate, Figure 2.6B).

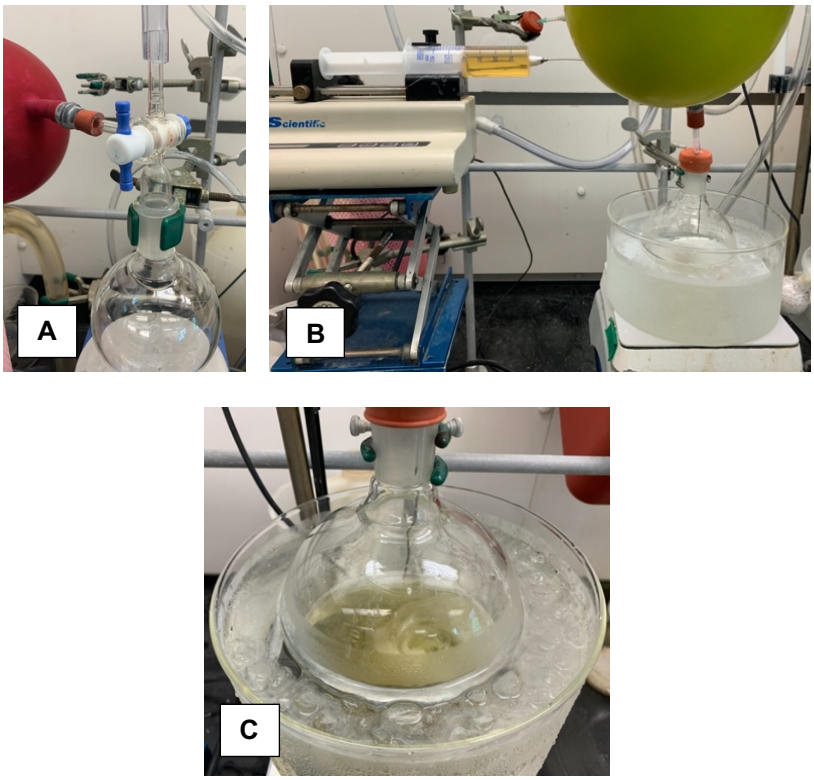

Figure 2.6. NCMPL deprotonation of sulfonamidomalonate: A) T-bore Schlenk adapter attached to 1 L, single-necked round-bottomed flask. B) Addition of LiHMDS solution via syringe pump. C) Following complete addition of LiHMDS.

The resulting clear yellow (and sometimes cloudy yellow; Figure 2.6C) solution was further cooled in a cryobath set to -10 °C for 15 min (Note 22). 1,8-diazobyciclo[5.4.0]undec-7-ene (DBU, 6.72 mL, 45.0 mmol, 1.10 equiv) and *O*-trimethylsilylquinine (TMSQN; Note 23), prepared as a solution in tetrahydrofuran (1.0 M, 3.26 g, 8.24 mmol, 0.20 equiv in 8.2 mL THF) in an oven-dried (Note 12) 25 mL pear-shaped flask fitted with a glass, threaded gas-inlet adapter with a silicone/PTFE septa (Note 2), were added each in one portion sequentially within 5 min. A solution of crude, (2*E*,4*E*)-5-phenylpenta-2,4-dienoyl chloride (**2.12**, 1.0 M in tetrahydrofuran, 57.4 mmol, 1.39 equiv in 57.4 mL; Note 24, Figure 2.7A) was then set to add dropwise over 3 h from a 60 mL

luer-lock plastic syringe fitted with a 16-gauge stainless-steel needle connected to a syringe pump (19 mL/h flow rate; Figure 2.7B-C).

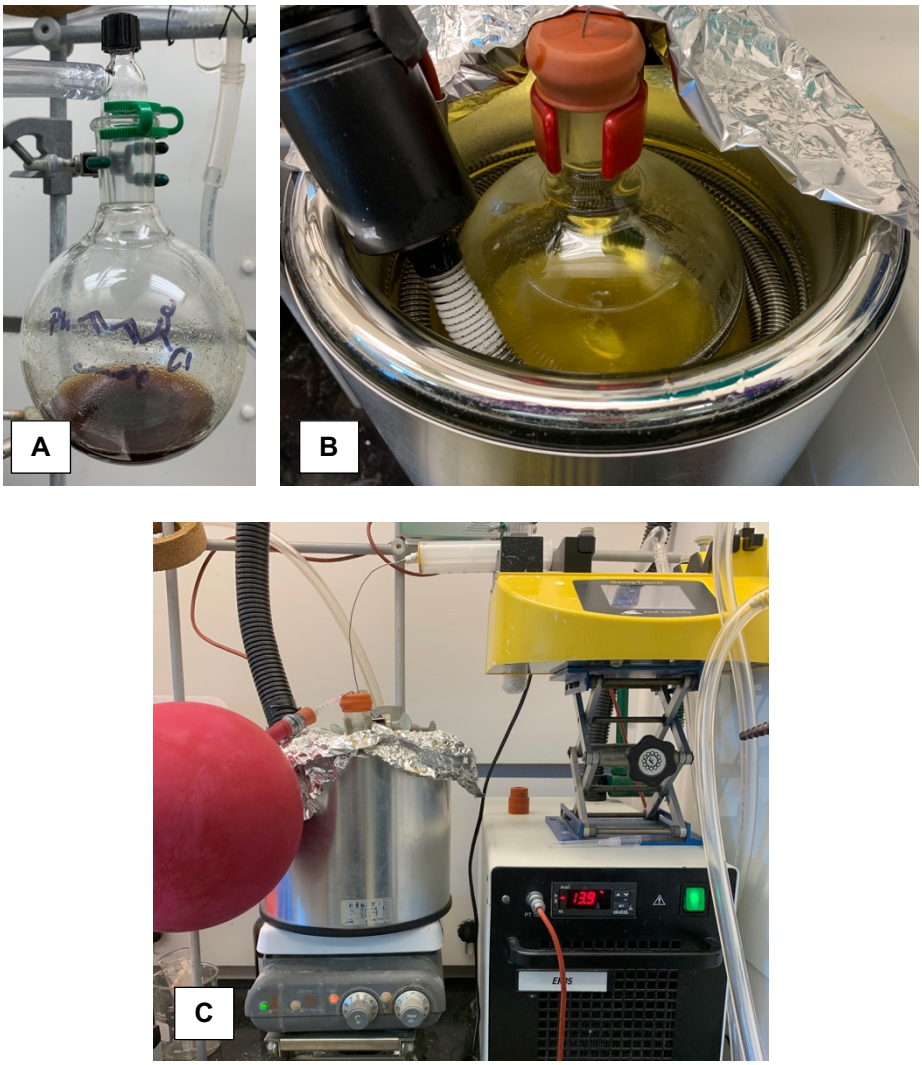

Figure 2.7. NCMPL Organocascade: A) Appearance of crude unsaturated acid chloride solution in THF. B) Reaction solution following addition of DBU and TMSQN. C) Addition of crude unsaturated acid chloride solution via syringe pump with cooling from a cryobath system.

The reaction mixture was stirred at -10 to -14 °C for an additional 3 h (total reaction time = 6h; Note 25) and was quenched by carefully pouring the cold orange-red solution into a 1 L separatory funnel containing aqueous hydrochloric acid (1M, 150 mL).

Quantitative transfer of the crude reaction mixture to the separatory funnel was carried out with ethyl acetate (150 mL). The layers were separated (Figure 2.8A) and the aqueous layer was extracted with ethyl acetate (4 x 125 mL; Figure 2.8B). The combined organic layers were washed with saturated, aqueous sodium chloride solution (150 mL) dried over magnesium sulfate, filtered through celite (Note 7, Figure 2.8C) into a 1 L Erlenmeyer flask, and the filter cake was rinsed with ethyl acetate (75 mL).

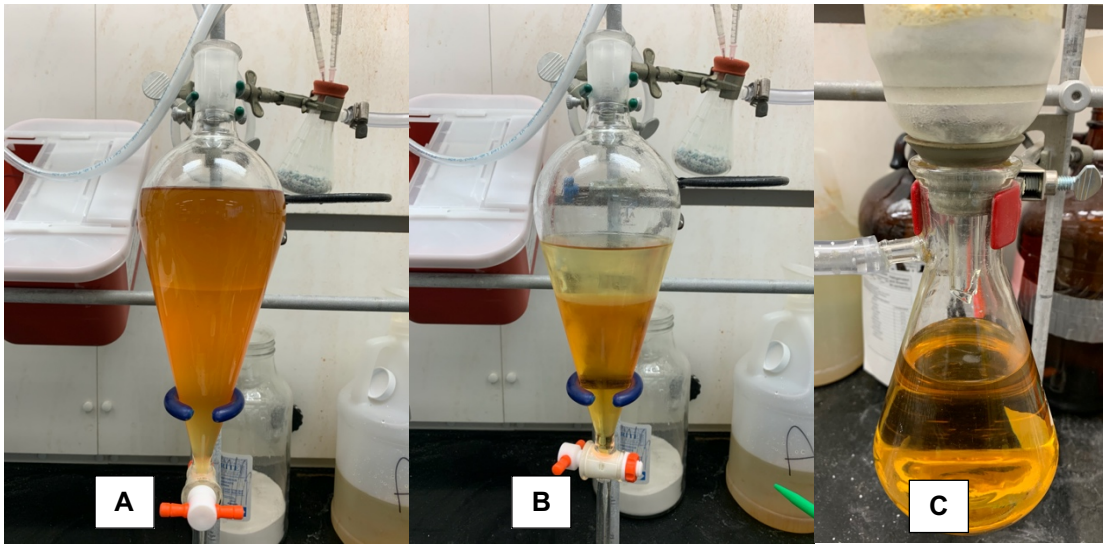

Figure 2.8. NCMPL reaction work up: A) Formation of layers in separation funnel upon first extraction with ethyl acetate. B) Appearance of layers in separation funnel following final extraction with ethyl acetate. C) Combined organic layers after drying and filtering through Celite.

The filtrate was transferred to a 2 L recovery flask and concentrated by rotary evaporation (~200 mm Hg, 30 °C bath temperature) until a yellow, amorphous solid formed (Figure 2.9A). This crude, yellow solid was transferred to a Büchner funnel (7 cm diameter) with a stainless-steel spatula and washed with a minimal methanol (~200 mL) from a polyethylene squirt bottle while carefully agitating the solid with the spatula under vacuum filtration (Note 26, Figure 2.9B). After transferring the now off-white solid to a two 6 dram

vials and removing the residual solvent under high vacuum for at least 4 h (Note 4 and 27), 14.7 g of dimethyl-(*S*,*E*)-5-oxo-3-styryl-1-tosylpyrrolidine-2,2-dicarboxylate (**2.13**, 78% isolated yield, >99:1 er) was obtained as an off-white crystalline powder that was of sufficient purity (97% by q^{1}H-NMR) for subsequent reactions. (Note 28).

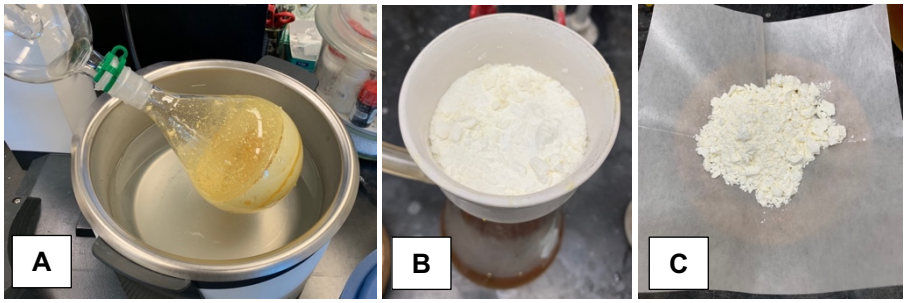

Figure 2.9. NCMPL product isolation: A) Crude solid following thorough removal of volatiles by rotary evaporation. B) Product after washing with methanol under gentle vacuum filtration in a Büchner funnel. C) Appearance of γ-lactam product as a powdery crystalline solid.

2.4.4 Notes

1. Prior to performing each reaction, a thorough hazard analysis and risk assessment should be carried out with regard to each chemical substance and experimental operation on the scale planned and in the context of the laboratory where the procedures will be carried out. Guidelines for carrying out risk assessments and for analyzing the hazards associated with chemicals can be found in references such as Chapter 4 of "Prudent Practices in the Laboratory" (The National Academies Press, Washington, D.C., 2011; the full text can be accessed free of charge at https://www.nap.edu/catalog/12654/prudent-practices-in-thelaboratory-handling-and-management-of-chemical. See also "Identifying and Evaluating Hazards in Research Laboratories" (American Chemical Society, 2015) which is available via

the associated website “Hazard Assessment in Research Laboratories” at https://www.acs.org/content/acs/en/about/governance/committees/chemicalsafety/hazard-assessment.html. In the case of this procedure, the risk assessment should include (but not necessarily be limited to) an evaluation of the potential hazards associated with Dimethyl aminomalonate hydrochloride, *p*-toluenesulfonic anhydride, triethylamine, 5-phenyl-2,4-pentadienoic acid, oxalyl chloride, methylene chloride, *N,N*-dimethylformamide, mineral oil, sodium bicarbonate, dihydrogen monoxide, carbon monoxide, carbon dioxide, hydrogen chloride, lithium hexamethyldisilazide, 1,8-diazobyciclo[5.4.0]undec-7-ene, methanol, tetrahydrofuran, ethyl acetate, hexanes, Celite, magnesium sulfate, and silica gel.

2. A rubber septum and needle connected to a nitrogen/vacuum manifold can also be used if the glass adapter shown in Figure 2.3A is unavailable.
3. Dimethyl aminomalonate hydrochloride (97%) was purchased from Sigma Aldrich, *p*-toluenesulfonic anhydride (90%) was purchased from Oakwood, triethylamine (99%), tetrahydrofuran (HPLC grade, unstabilized) ethyl acetate (ACS grade), and hexanes (ACS grade) were purchased from Fisher Scientific. All reagents and solvents, excluding triethylamine, were used as received.
4. A Welch Duo Seal 1400 rotary vane vacuum pump (~3 mm Hg) connected to the vacuum/nitrogen manifold through a cold-trap was used for high-vacuum throughout this procedure.
5. Triethylamine was distilled from calcium hydride (95%, purchased from Oakwood) under an atmosphere of dry nitrogen prior to use.

6. The formation of product can be monitored by thin-layer chromatography (TLC, 30% ethyl acetate/hexanes, sulfonamidomalonate product R_f = 0.40, visualized under a 254 nm UV-lamp). Glass-backed, 250 mm-thickness TLC plates were purchased from Silicycle inc.

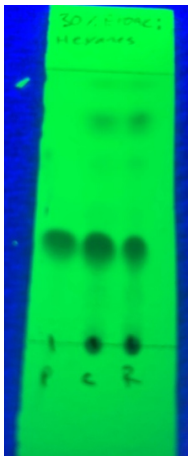

7. Celite 545 filter aid was purchased from Fisher Scientific. A pad of celite (1.5 cm tall) was used in a 150 mL funnel (6.5 cm height x 7 cm inner diameter) with a glass frit of porosity M.
8. Silica Gel (Silicycle Ultrapure SilicaFlash silica gel, 60 Å pore size, particle size distribution 40-63 microns) was purchased from Fisher Scientific.
9. 70 g of silica gel was added to the crude yellow oil following rotary evaporation. Ethyl acetate was used to rinse the walls of the 1 L recovery flask to ensure complete and uniform absorption onto the silica. Solvent that could interfere with chromatographic separation was thoroughly removed by rotary evaporation until the yellow powder thus formed was dry and free-flowing.
10. A heavy-walled, glass flash chromatography column 10 cm in diameter was used. The free-flowing fine yellow powder silica with the absorbed crude material was carefully loaded into the column, which, beforehand, was wet-packed with 250 g

of fresh silica gel using hexanes and topped with a layer of sand. A step-wise gradient was used (500 mL each of hexanes, then 20% ethyl acetate/hexanes, then 40% ethyl acetate/hexanes, then 2500 mL 60% ethyl acetate/hexanes). The eluent from 0% to 20% ethyl acetate/hexanes was collected in 1 L Erlenmeyer flasks. The product was collected in 250 mL fractions using Erlenmeyer flasks starting at 40% and ending at 60% ethyl acetate/hexanes. A light-yellow color that slowly progresses through the column indicates the position of impurities that were not collected.

11. Characterization data for dimethyl 2-((4-methylphenyl)sulfonamido)malonate (**2.10**): IR (thin film) 3235, 1750, 1596 cm^{-1}; **^{1}H-NMR** (600 MHz, $CDCl_3$) δ 7.73 (d, *J* = 8.3 Hz, 1H), 7.30 (d, *J* = 8.3 Hz, 1H), 5.62 (d, *J* = 8.5 Hz, 1H), 4.69 (d, *J* = 8.5 Hz, 1H), 3.67 (s, 3H), 2.42 (s, 2H); **^{13}C-NMR** (150 MHz, $CDCl_3$) δ 166.1, 144.2, 136.4, 129.9, 127.4, 58.6, 53.7, 21.7; Melting Temperature = 124 °C; **MS (APCI+)** *m/z* = 302.7 $[M + H]^+$; This compound can be stored at ambient temperature (23 °C) indefinitely without decomposition.
12. Reaction flasks were dried in an oven at 125 °C for at least 4 h prior to use.
13. 5-phenyl-2,4-pentadienoic acid (98%) was purchased from Combi-Blocks, oxalyl chloride (99% reagent plus) was purchased from Sigma Aldrich, *N,N*-dimethylformamide (99.8% extra dry, AcroSeal) was purchased from Acros and were used as received. Methylene chloride (HPLC grade, cyclohexane preservative) was purchased from Fisher Scientific and passed through a column of activated alumina under an atmosphere of ultra-high purity argon (JC Meyer Solvent Purification System) prior to use.

14. Caution! This reaction rapidly expels gaseous by-products: carbon dioxide, caustic hydrogen chloride, and toxic carbon monoxide. Thus, careful dropwise addition of neat oxalyl chloride is done in a uniform, controlled fashion using a syringe pump over ~15 min.
15. A column of potassium hydroxide pellets (Fisher Scientific) was connected in-line between the Schlenk manifold and the round-bottomed flask with a fritted gas outlet adapter and thick-walled tygon tubing to act as an acid scrubber and prevent HCl corrosion of the vacuum pump.
16. Characterization data for (2*E*,4*E*)-5-phenylpenta-2,4-dienoyl chloride (**2.12**): **^{1}H-NMR** (600 MHz, $CDCl_3$) δ 7.63 (ddd, *J* = 14.8, 11.2, 0.7 Hz, 1H), 7.55-7.46 (m, 2H), 7.45-7.33 (m, 3H), 7.11 (d, *J* = 15.5 Hz, 1H), 6.93 (ddd, *J* = 15.5, 11.1, 0.7 Hz, 1H), 6.20 (d, *J* = 14.8 Hz, 1H); **^{13}C-NMR** (125 MHz, $CDCl_3$) δ 166.0, 151.0, 145.4, 135.4, 130.3, 129.2 (2), 127.9 (2), 125.2, 124.9; **IR (thin film)** 1674, 1614 cm^{-1}; Melting Temperature = 46 °C; This compound could be stored for up to a week under inert atmosphere in a sealed vessel at -20 °C, but was usually used immediately.
17. The submitters found the use of an argon balloon was more convenient in providing an inert atmosphere for the nucleophile-catalyzed Michael-proton transfer lactamization, but a typical nitrogen line with a needle and rubber septum can also be used.
18. Thick-walled, natural latex rubber balloons were purchased from Sigma Aldrich (SKU-Z154997)

19. Tetrahydrofuran (HPLC grade, unstabilized) was purchased from Fisher Scientific and passed through a column of activated alumina under an atmosphere of ultra-high purity argon (JC Meyer Solvent Purification System). Methanol (ACS grade) was purchased from Fisher Scientific and used as received. Lithium hexamethyldisilazide (1.0 M in tetrahydrofuran) and 1,8-diazobyciclo[5.4.0]undec-7-ene (DBU, 98%) was purchased from Sigma Aldrich and used as received. Sodium chloride was purchased from Fisher Scientific and used as received. Magnesium sulfate (99%, anhydrous powder) was purchased from Oakwood and used as received.
20. The initial concentration of the dimethyl sulfonamidomalonate starting material is essential to the yield of this reaction as variations led to formation of insoluble salts as the base is added and greatly reduced yields.
21. The quality of the LiHMDS used is very important and a newly opened 100 mL bottle for this procedure is required to ensure titer of base is as close as possible to the nominal 1.0 M indicated. The appearance of the LiHMDS solution in the plastic syringe should be a very light yellow/orange in color and clear (not dark orange or cloudy). Complete formation of the enolate from the starting sulfonamidomalonate is essential to the yield of the product lactam.
22. Maintaining the reaction temperature between -10 to -14 °C temperature is critical to obtain high enantioselectivity in the initial Michael-addition step.
23. *O*-trimethylsilylquinine (TMSQN), an off-white, amorphous solid, was prepared according to the *Organic Syntheses* procedure previously reported by the submitters.[127]

24. A light-yellow solid may remain undissolved when forming the THF solution of the crude unsaturated acyl chloride and some solid may be pulled into the syringe prior to dropwise addition to the reaction mixture. This does not create an issue with the reaction. However, the syringe/syringe pump apparatus should be checked periodically to ensure the needle is not clogged and regular dropwise addition is proceeding.
25. The consumption of starting material and the formation of the product could be monitored by thin-layer chromatography (TLC, 30% ethyl acetate/hexanes, sulfonamidomalonate substrate R_f = 0.40, lactam product R_f = 0.50, visualized under a 254 nm UV-lamp) Glass-backed, 250 mm-thickness TLC plates were purchased from Silicycle inc.

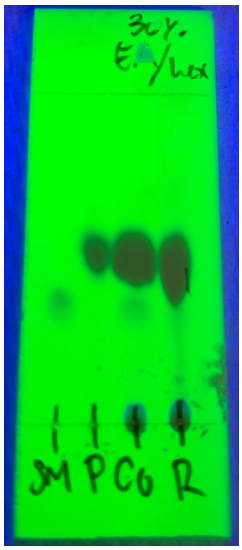

26. The methanol rinse using a squirt bottle under vacuum filtration removes the yellow color of the crude solid and should be done with caution to prevent the resulting fine crystalline powder from passing underneath the filter paper. The product is sparingly soluble in MeOH. Up to 200 mL of methanol is typically required to

completely remove the yellow impurity. A stainless steel spatula is used to break apart clumps of yellow solid to expose product surface for thorough rinsing.

27. Thorough removal of residual methanol from the product by high vacuum is necessary in order to avoid decomposition upon storage at ambient temperature.
28. Characterization data for dimethyl-(*S*,*E*)-5-oxo-3-styryl-1-tosylpyrrolidine-2,2-dicarboxylate: Absolute stereochemistry was assigned based on X-ray analysis using anomalous dispersion; $\mathbf{[\alpha]}_{D}^{20.0}$ +0.76 (*c* 10.5, $CHCl_3$); **IR (thin film)** 3061, 3027, 2955, 1749, 1597, cm^{-1}; **^{1}H-NMR** (500 MHz, $CDCl_3$) δ 8.05 (d, *J* = 8.4 Hz, 2H), 7.35-7.24 (m, 7H), 6.47 (d, *J* = 15.8 Hz, 1H), 6.07 (dd, *J* = 15.8, 8.0 Hz, 1H), 3.93 (s, 3H), 3.80 (s, 3H), 3.53 (app q, *J* = 8.5 Hz, 1H), 2.70 (dd, *J* = 17.1, 8.3 Hz, 1H), 2.65 (dd, *J* = 16.9, 9.4 Hz, 1H), 2.44 (s, 3H); **^{13}C-NMR** (125 MHz, $CDCl_3$) δ 171.7, 167.6, 166.0, 145.5, 135.9, 135.2, 134.6, 130.0 (2), 129.1 (2), 128.8 (2), 128.4, 126.6 (2), 123.4, 76.2, 53.8, 53.5, 45.1, 35.9, 21.8; **HRMS (ESI+)** *m/*z calcd. for $C_{23}H_{24}NO_7S$: $[M+H]^+$: 458.1268, found: 458.1274; This compound can be stored at ambient temperature (23 °C) on the benchtop indefinitely without decomposition. Enantiomeric ratio was determined by chiral-HPLC analysis in comparison with an authentic racemic sample of the product using a Chiralcel AD-H column: hexanes/^{i}PrOH = 80:20, flow rate of 0.5 mL/min, λ = 254 nm: t_{minor} = 75.3 min, t_{major} = 80.1 min:

2.4.5 Determination of Enantiopurity of NCMPL Product

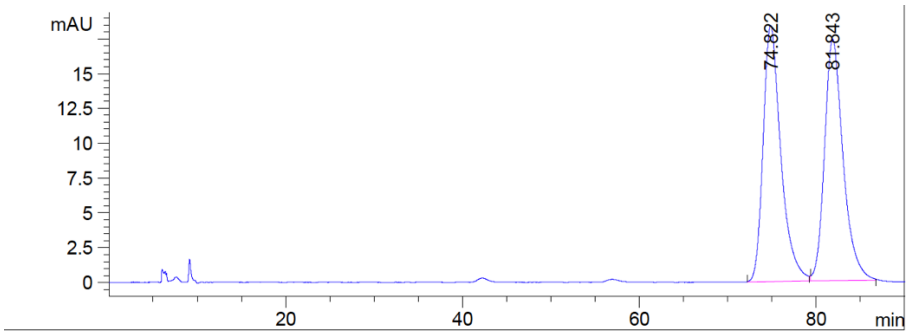

Peak #	RetTime [min]	Type	Width [min]	Area [mAU*s]	Height [mAU]	Area %
1	74.822	BB	2.0150	2560.09033	18.40271	50.1912
2	81.843	BB	2.0723	2540.58325	17.35113	49.8088

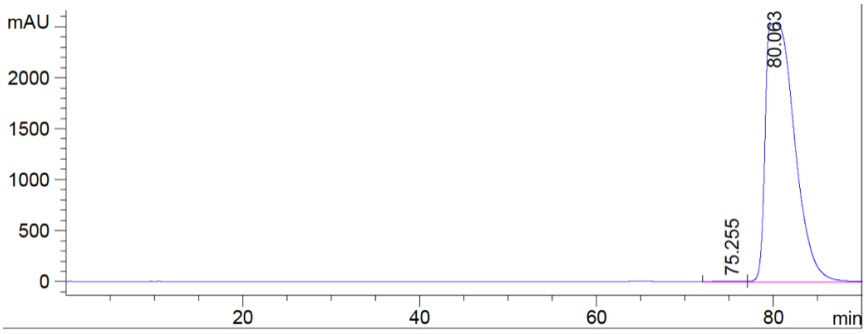

Peak #	RetTime [min]	Type	Width [min]	Area [mAU*s]	Height [mAU]	Area %
1	75.255	BV	2.0678	995.64697	5.67231	0.1723
2	80.063	VBA	2.6702	5.76937e5	2535.95020	99.8277

Figure 2.10. Chiral HPLC Analysis. A) an authentic racemic sample of the product using a Chiralcel AD-H column: hexanes/^{i}PrOH = 80:20, flow rate of 0.5 mL/min, λ = 254 nm: t_{minor} = 75.3 min, t_{major} = 80.1 min:. (b) desired γ-lactam (*S*)-enantiomer

2.4.6 Determination of Product Purity by q^{1}H-NMR

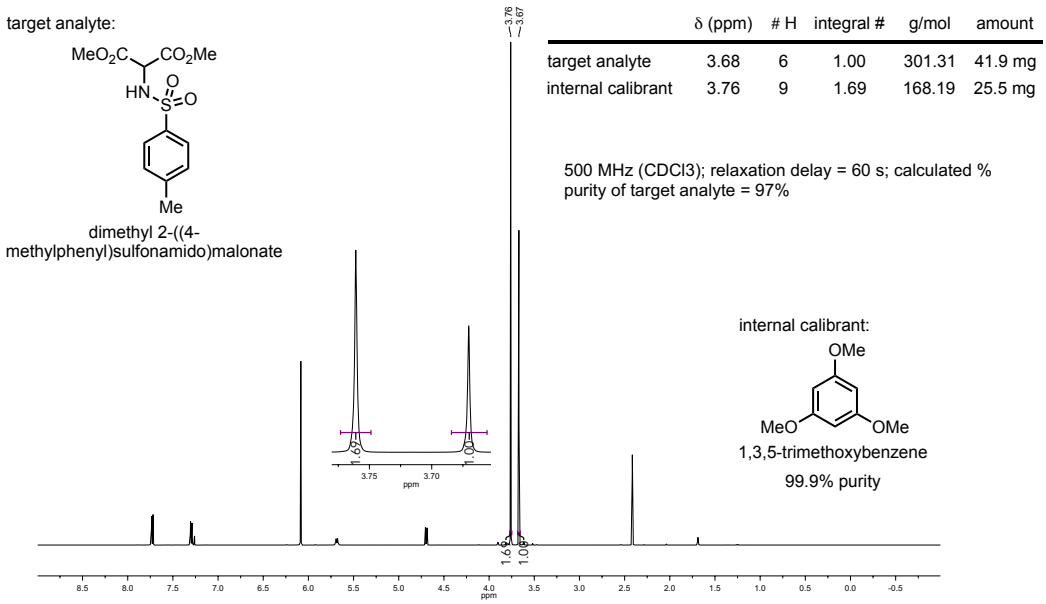

Figure 2.11. q^{1}H-NMR of sulfonamidomalonate **2.10** using 1,3,5-trimethoxybenzene as internal standard.

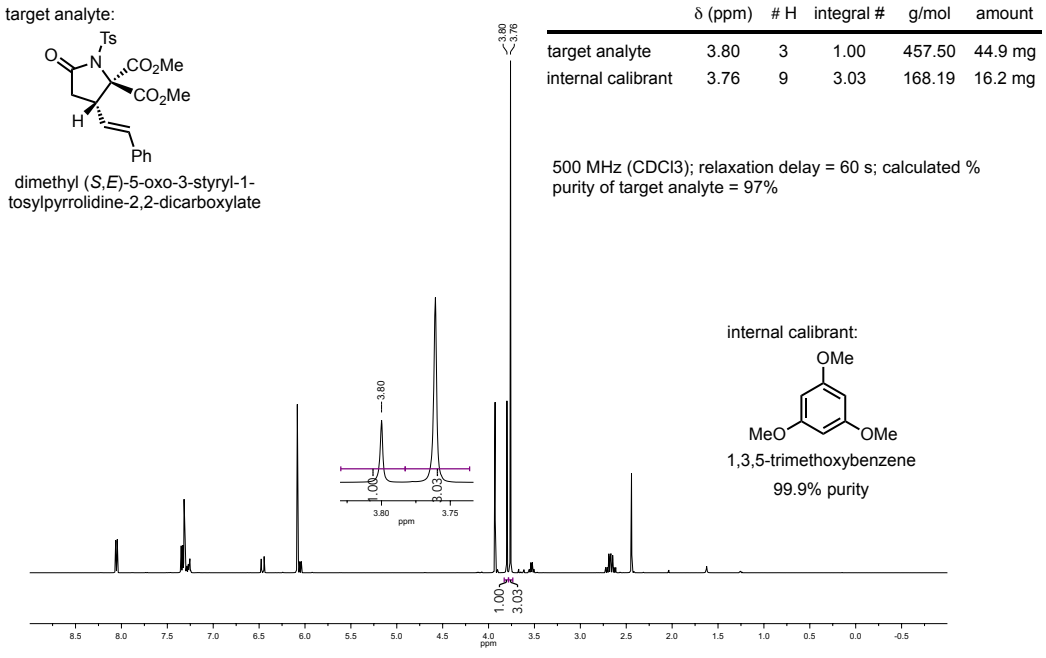

Figure 2.12. q^{1}H-NMR of NCMPL product **2.13** using 1,3,5-trimethoxybenzene as internal standard.

2.5 References

1. Moloney, M. G.; Trippier, P., C.; Yaqoob, M.; Wang, Z., The Oxazolomycins: A Structurally Novel Class of Bioactive Compounds. *Curr. Drug Disc. Technol.* **2004,** *1* (3), 181-199.

32. Kende, A. S.; Kawamura, K.; Devita, R. J., Enantioselective Total Synthesis of Neooxazolomycin. *J. Am. Chem. Soc.* **1990,** *112* (10), 4070-4072.

36. Onyango, E. O.; Tsurumoto, J.; Imai, N.; Takahashi, K.; Ishihara, J.; Hatakeyama, S., Total synthesis of neooxazolomycin. *Angew. Chem. Int. Ed.* **2007,** *46* (35), 6703-6705.

37. Eto, K.; Yoshino, M.; Takahashi, K.; Ishihara, J.; Hatakeyama, S., Total Synthesis of Oxazolomycin A. *Org. Lett.* **2011,** *13* (19), 5398-5401.

39. Nishimaru, T.; Eto, K.; Komine, K.; Ishihara, J.; Hatakeyama, S., Total Synthesis of Lajollamycin B. *Chem. Eur. J.* **2019,** *25* (33), 7927-7934.

41. Panday, S. K.; Prasad, J.; Dikshit, D. K., Pyroglutamic acid: a unique chiral synthon. *Tetrahedron: Asymmetry* **2009,** *20* (14), 1581-1632.

42. Nájera, C.; Yus, M., Pyroglutamic acid: a versatile building block in asymmetric synthesis. *Tetrahedron: Asymmetry* **1999,** *10* (12), 2245-2303.

43. Saldívar-González, F. I.; Lenci, E.; Trabocchi, A.; Medina-Franco, J. L., Exploring the chemical space and the bioactivity profile of lactams: A chemoinformatic study. *RSC Advances* **2019,** *9* (46), 27105-27116.

44. Khan, M. K.; Wang, D.; Moloney, M. G., Functionalised Nitrogen Heterocycles and the Search for New Antibacterials and Bioactives. *Synthesis (Germany)* **2020,** *52* (11), 1602-1616.

45. Nay, B.; Riache, N.; Evanno, L., Chemistry and biology of non-tetramic γ-hydroxy-γ-lactams and γ-alkylidene-γ-lactams from natural sources. *Nat. Prod. Rep.* **2009,** *26* (8), 1044-1062.

46. Kim, J. H.; Kim, I.; Song, Y.; Kim, M. J.; Kim, S., Asymmetric Total Synthesis of (+)-Neooxazolomycin Using a Chirality-Transfer Strategy. *Angew. Chem. Int. Ed.* **2019,** *58* (32), 11018-11022.

47. Mahashur, A.; Thomas, P. K.; Mehta, P.; Nivangune, K.; Muchhala, S.; Jain, R., Pidotimod: In-depth review of current evidence. *Lung India : official organ of Indian Chest Society* **2019,** *36* (5), 422-433.

48. Gulder, T. A. M.; Moore, B. S., Salinosporamide Natural Products: Potent 20 S Proteasome Inhibitors as Promising Cancer Chemotherapeutics. *Angew. Chem. Int. Ed.* **2010,** *49* (49), 9346-9367.

49. Shibasaki, M.; Kanai, M.; Fukuda, N., Total Synthesis of Lactacystin and Salinosporamide A. *Chemistry – An Asian Journal* **2007,** *2* (1), 20-38.

50. Uesugi, S.; Fujisawa, N.; Yoshida, J.; Watanabe, M.; Dan, S.; Yamori, T.; Shiono, Y.; Kimura, K.-i., Pyrrocidine A, a metabolite of endophytic fungi, has a potent apoptosis-inducing activity against HL60 cells through caspase activation via the Michael addition. *The Journal of Antibiotics* **2016,** *69* (3), 133-140.

51. Chu, S.; Liu, S.; Duan, W.; Cheng, Y.; Jiang, X.; Zhu, C.; Tang, K.; Wang, R.; Xu, L.; Wang, X.; Yu, X.; Wu, K.; Wang, Y.; Wang, M.; Huang, H.; Zhang, J., The anti-dementia drug candidate, (−)-clausenamide, improves memory impairment through its multi-target effect. *Pharmacol. Ther.* **2016,** *162*, 179-187.

52. Chu, S.-f.; Zhang, J.-t., Recent advances in the study of (–)clausenamide: chemistry, biological activities and mechanism of action. *Acta Pharmaceutica Sinica B* **2014,** *4* (6), 417-423.

53. He, H.; Yang, H. Y.; Bigelis, R.; Solum, E. H.; Greenstein, M.; Carter, G. T., Pyrrocidines A and B, new antibiotics produced by a filamentous fungus. *Tetrahedron Lett.* **2002,** *43* (9), 1633-1636.

54. Caruano, J.; Muccioli, G. G.; Robiette, R., Biologically active γ-lactams: synthesis and natural sources. *Org. Biomol. Chem.* **2016,** *14* (43), 10134-10156.

55. Shorvon, S., Pyrrolidone derivatives. *The Lancet* **2001,** *358* (9296), 1885-1892.

56. Varvounis, G.; Gerontitis, I. E.; Gkalpinos, V., Metal-catalyzed synthesis of five-membered ring N-heterocycles. A recent update. *Chemistry of Heterocyclic Compounds* **2018,** *54* (3), 249-268.

57. Rivas, F.; Ling, T., Advances toward the Synthesis of Functionalized γ-Lactams. *Org. Prep. Proced. Int.* **2016,** *48* (3), 254-295.

58. Ye, L.-W.; Shu, C.; Gagosz, F., Recent progress towards transition metal-catalyzed synthesis of γ-lactams. *Org. Biomol. Chem.* **2014,** *12* (12), 1833-1845.

59. Ordóñez, M.; Cativiela, C., Stereoselective synthesis of γ-amino acids. *Tetrahedron: Asymmetry* **2007,** *18* (1), 3-99.

60. Soleimani-Amiri, S.; Vessally, E.; Babazadeh, M.; Hosseinian, A.; Edjlali, L., Intramolecular cyclization of: N-allyl propiolamides: A facile synthetic route to highly substituted γ-lactams (a review). *RSC Advances* **2017,** *7* (45), 28407-28418.

61. Deng, B.; Rao, C. B.; Zhang, R.; Li, J.; Liang, Y.; Zhao, Y.; Gao, M.; Dong, D., A Formal [3+2] Annulation of β-Oxoamides and 3-Alkyl- or 3-Aryl-Substituted Prop-2-Ynyl Sulfonium Salts: Substrate-Controlled Chemoselective Synthesis of Substituted γ-Lactams and Furans. *Adv. Synth. Catal.* **2019,** *361* (19), 4549-4557.

62. Zhu, X. Q.; Yuan, H.; Sun, Q.; Zhou, B.; Han, X. Q.; Zhang, Z. X.; Lu, X.; Ye, L. W., Benign catalysis with zinc: Atom-economical and divergent synthesis of nitrogen heterocycles by formal [3 + 2] annulation of isoxazoles with ynol ethers. *Green Chem.* **2018,** *20* (18), 4287-4291.

63. Zhmurov, P. A.; Ushakov, P. Y.; Novikov, R. A.; Sukhorukov, A. Y.; Ioffe, S. L., A Novel Entry to 3,4,5-Trisubstituted 2-Pyrrolidones from Isoxazoline-N-oxides. *Synlett* **2018,** *29* (14), 1871-1874.

64. Çinar, S.; Ünaleroglu, C., Facile synthesis of heteroaryl substituted γ-lactams from nitrovinyl arenes. *Turkish Journal of Chemistry* **2018,** *42* (1), 29-35.

65. Mardjan, M. I. D.; Mayooufi, A.; Parrain, J.-L.; Thibonnet, J.; Commeiras, L., Straightforward Access to a Great Diversity of Complex Biorelevant γ-Lactams Thanks to a Tunable Cascade Multicomponent Process. *Org. Process Res. Dev.* **2020,** *24* (5), 606-614.

66. Borja-Miranda, A.; Sánchez-Chávez, A. C.; Polindara-García, L. A., Ammonium Persulfate Promotes Radical Cyclization of 1,3-Dicarbonyl-Ugi 4-CR Adducts: Synthesis of Polysubstituted γ-Lactams in Aqueous Media. *Eur. J. Org. Chem.* **2019,** *2019* (14), 2453-2471.

67. Gockel, S. N.; Buchanan, T. L.; Hull, K. L., Cu-Catalyzed Three-Component Carboamination of Alkenes. *J. Am. Chem. Soc.* **2018,** *140* (1), 58-61.

68. De Marigorta, E. M.; De Los Santos, J. M.; De Retana, A. M. O.; Vicario, J.; Palacios, F., Multicomponent reactions in the synthesis of γ-Lactams. *Synthesis (Germany)* **2018,** *50* (23), 4539-4554.

69. Audic, B.; Cramer, N., Rhodium(III)-Catalyzed Cyclopropane C-H/C-C Activation Sequence Provides Diastereoselective Access to α-Alkoxylated γ-Lactams. *Org. Lett.* **2020**.

70. Jung, H.; Schrader, M.; Kim, D.; Baik, M. H.; Park, Y.; Chang, S., Harnessing Secondary Coordination Sphere Interactions That Enable the Selective Amidation of Benzylic C-H Bonds. *J. Am. Chem. Soc.* **2019,** *141* (38), 15356-15366.

71. Huh, S.; Hong, S. Y.; Chang, S., Synthetic Utility of N-Benzoyloxyamides as an Alternative Precursor of Acylnitrenoids for γ-Lactam Formation. *Org. Lett.* **2019,** *21* (8), 2808-2812.

72. Zhou, D.; Wang, C.; Li, M.; Long, Z.; Lan, J., Palladium-catalyzed 2-pyridylmethyl-directed β-C(sp3)–H activation and cyclization of aliphatic amides with gem-dibromoolefins: A rapid access to γ-lactams. *Chin. Chem. Lett.* **2018,** *29* (1), 191-193.

73. Png, Z. M.; Cabrera-Pardo, J. R.; Peiró Cadahía, J.; Gaunt, M. J., Diastereoselective C-H carbonylative annulation of aliphatic amines: A rapid route to functionalized γ-lactams. *Chemical Science* **2018,** *9* (39), 7628-7633.

74. Zheng, S.; Gutiérrez-Bonet, Á.; Molander, G. A., Merging Photoredox PCET with Ni-Catalyzed Cross-Coupling: Cascade Amidoarylation of Unactivated Olefins. *Chem* **2019,** *5* (2), 339-352.

75. Koleoso, O. K.; Elsegood, M. R. J.; Teat, S. J.; Kimber, M. C., Photoredox Approach to N-Acyl-N′-aryl-N,N′-aminals Using Enamides and Their Conversion to γ-Lactams. *Org. Lett.* **2018,** *20* (4), 1003-1006.

76. Jia, J.; Ho, Y. A.; Bülow, R. F.; Rueping, M., Brønsted Base Assisted Photoredox Catalysis: Proton Coupled Electron Transfer for Remote C−C Bond Formation via Amidyl Radicals. *Chem. Eur. J.* **2018,** *24* (53), 14054-14058.

77. Rao, W. H.; Jiang, L. L.; Liu, X. M.; Chen, M. J.; Chen, F. Y.; Jiang, X.; Zhao, J. X.; Zou, G. D.; Zhou, Y. Q.; Tang, L., Copper(II)-Catalyzed Alkene Aminosulfonylation with Sodium Sulfinates for the Synthesis of Sulfonylated Pyrrolidones. *Org. Lett.* **2019,** *21* (8), 2890-2893.

78. Fukuyama, T.; Okada, T.; Nakashima, N.; Ryu, I., Radical Mediated Aza-Pauson-Khand Reaction of Acetylenes, Imines, and CO Leading to Five-Membered Unsaturated Lactams. *Helv. Chim. Acta* **2019,** *102* (10).

79. Ganesh Kumar, M.; Veeresh, K.; Nalawade, S. A.; Nithun, R. V.; Gopi, H. N., Direct Transformation of N-Protected α,β-Unsaturated γ-Amino Amides into γ-Lactams through a Base-Mediated Molecular Rearrangement. *J. Org. Chem.* **2019,** *84* (23), 15145-15153.

80. Ye, J.; Kalvet, I.; Schoenebeck, F.; Rovis, T., Direct α-alkylation of primary aliphatic amines enabled by CO<inf>2</inf> and electrostatics. *Nat. Chem.* **2018,** *10* (10), 1037-1041.

81. Wang, F.; Zhang, X.; He, Y.; Fan, X., Selective synthesis of pyrrolidin-2-ones and 3-iodopyrroles: Via the ring contraction and deformylative functionalization of piperidine derivatives. *Organic and Biomolecular Chemistry* **2019,** *17* (1), 156-164.

82. Dražić, T.; Roje, M., β-Lactam rearrangements into five-membered heterocycles. *Chemistry of Heterocyclic Compounds* **2017,** *53* (9), 953-962.

83. Schröder, F.; Erdmann, N.; Noël, T.; Luque, R.; Van der Eycken, E. V., Leaching-Free Supported Gold Nanoparticles Catalyzing Cycloisomerizations under Microflow Conditions. *Adv. Synth. Catal.* **2015,** *357* (14-15), 3141-3147.

84. Mourelle-Insua, Á.; Zampieri, L. A.; Lavandera, I.; Gotor-Fernández, V., Conversion of γ- and δ-Keto Esters into Optically Active Lactams. Transaminases in Cascade Processes. *Adv. Synth. Catal.* **2018,** *360* (4), 686-695.

85. Su, Y.; Gao, S.; Li, H.; Zheng, G., Enantioselective resolution of γ-lactam utilizing a novel (+)-γ-lactamase from Bacillus thuringiensis. *Process Biochem.* **2018,** *72*, 96-104.

86. Bagum, H.; Christensen, K. E.; Genov, M.; Pretsch, A.; Pretsch, D.; Moloney, M. G., Synthetic access to 3,4-disubstituted pyroglutamates from tetramate derivatives from serine, allo-threonine and cysteine. *Tetrahedron* **2019,** *75* (40).

87. Verho, O.; Maetani, M.; Melillo, B.; Zoller, J.; Schreiber, S. L., Stereospecific Palladium-Catalyzed C–H Arylation of Pyroglutamic Acid Derivatives at the C3 Position Enabled by 8-Aminoquinoline as a Directing Group. *Org. Lett.* **2017,** *19* (17), 4424-4427.

88. Enders, D.; Niemeier, O.; Henseler, A., Organocatalysis by N-Heterocyclic Carbenes. *Chem. Rev.* **2007,** *107* (12), 5606-5655.

89. del Corte, X.; Maestro, A.; Vicario, J.; Martinez de Marigorta, E.; Palacios, F., Brönsted-Acid-Catalyzed Asymmetric Three-Component Reaction of Amines, Aldehydes, and Pyruvate Derivatives. Enantioselective Synthesis of Highly Functionalized γ-Lactam Derivatives. *Org. Lett.* **2018,** *20* (2), 317-320.

90. Hu, B.; Deng, L., Catalytic Asymmetric Synthesis of Trifluoromethylated γ-Amino Acids through the Umpolung Addition of Trifluoromethyl Imines to Carboxylic Acid Derivatives. *Angewandte Chemie - International Edition* **2018,** *57* (8), 2233-2237.

91. Collar, A. G.; Trujillo, C.; Lockett-Walters, B.; Twamley, B.; Connon, S. J., Catalytic Asymmetric γ-Lactam Synthesis from Enolisable Anhydrides and Imines. *Chem. Eur. J.* **2019,** *25* (30), 7275-7279.

92. Sućˊ Sajko, J.; Ljoljić Bilić, V.; Kosalec, I.; Jerić, I., Multicomponent Approach to a Library of N-Substituted γ-Lactams. *ACS Combinatorial Science* **2019,** *21* (1), 28-34.

93. de Gracia Retamosa, M.; Ruiz-Olalla, A.; Bello, T.; de Cozar, A.; Cossio, F. P., A Three-Component Enantioselective Cyclization Reaction Catalyzed by an Unnatural Amino Acid Derivative. *Angew Chem Int Ed Engl* **2018,** *57* (3), 668-672.

94. Hu, Z.; Zhu, Y.; Fu, Z.; Huang, W., Asymmetric Synthesis of Enantioenriched 6-Hydroxyl Butyrolactams Promoted by N-Heterocyclic Carbene. *J. Org. Chem.* **2019,** *84* (16), 10328-10337.

95. Li, X. S.; Zhao, L. L.; Wang, X. K.; Cao, L. L.; Shi, X. Q.; Zhang, R.; Qi, J., Enantioselective [3 + 2] Annulation of Enals with 2-Aminoacrylates Catalyzed by N-Heterocyclic Carbene. *Org. Lett.* **2017,** *19* (14), 3943-3946.

96. Zhang, K.; Deiana, L.; Grape, E. S.; Inge, A. K.; Córdova, A., Catalytic Enantioselective Synthesis of Bicyclic Lactam N,S-Acetals in One Pot by Cascade Transformations. *Eur. J. Org. Chem.* **2019,** *2019* (29), 4649-4657.

97. Shi, Y.; Tan, X.; Gao, S.; Zhang, Y.; Wang, J.; Zhang, X.; Yin, Q., Direct Synthesis of Chiral NH Lactams via Ru-Catalyzed Asymmetric Reductive Amination/Cyclization Cascade of Keto Acids/Esters. *Org. Lett.* **2020,** *22* (7), 2707-2713.

98. Wang, C.; Ge, S., Versatile Cobalt-Catalyzed Enantioselective Entry to Boryl-Functionalized All-Carbon Quaternary Stereogenic Centers. *J. Am. Chem. Soc.* **2018,** *140* (34), 10687-10690.

99. Zhou, Z.; Chen, S.; Hong, Y.; Winterling, E.; Tan, Y.; Hemming, M.; Harms, K.; Houk, K. N.; Meggers, E., Non-C2-Symmetric Chiral-at-Ruthenium Catalyst for Highly Efficient Enantioselective Intramolecular C(sp3)–H Amidation. *J. Am. Chem. Soc.* **2019,** *141* (48), 19048-19057.

100. Xing, Q.; Chan, C. M.; Yeung, Y. W.; Yu, W. Y., Ruthenium(II)-Catalyzed Enantioselective gamma-Lactams Formation by Intramolecular C-H Amidation of 1,4,2-Dioxazol-5-ones. *J. Am. Chem. Soc.* **2019,** *141* (9), 3849-3853.

101. Wang, H.; Park, Y.; Bai, Z.; Chang, S.; He, G.; Chen, G., Iridium-Catalyzed Enantioselective C(sp(3))-H Amidation Controlled by Attractive Noncovalent Interactions. *J. Am. Chem. Soc.* **2019,** *141* (17), 7194-7201.

102. Park, Y.; Chang, S., Asymmetric formation of γ-lactams via C–H amidation enabled by chiral hydrogen-bond-donor catalysts. *Nature Catalysis* **2019,** *2* (3), 219-227.

103. Wang, S. G.; Liu, Y.; Cramer, N., Asymmetric Alkenyl C−H Functionalization by CpxRhIII forms 2H-Pyrrol-2-ones through [4+1]-Annulation of Acryl Amides and Allenes. *Angewandte Chemie - International Edition* **2019,** *58* (50), 18136-18140.

104. Lang, Q.; Gu, G.; Cheng, Y.; Yin, Q.; Zhang, X., Highly Enantioselective Synthesis of Chiral γ-Lactams by Rh-Catalyzed Asymmetric Hydrogenation. *ACS Catalysis* **2018,** *8* (6), 4824-4828.

105. Yuan, Q.; Liu, D.; Zhang, W., Iridium-Catalyzed Asymmetric Hydrogenation of β,γ-Unsaturated γ-Lactams: Scope and Mechanistic Studies. *Org. Lett.* **2017,** *19* (5), 1144-1147.

106. Jette, C. I.; Geibel, I.; Bachman, S.; Hayashi, M.; Sakurai, S.; Shimizu, H.; Morgan, J. B.; Stoltz, B. M., Palladium-Catalyzed Construction of Quaternary Stereocenters by Enantioselective Arylation of γ-Lactams with Aryl Chlorides and Bromides. *Angewandte Chemie - International Edition* **2019,** *58* (13), 4297-4301.

107. Nanjo, T.; De Lucca, E. C.; White, M. C., Remote, Late-Stage Oxidation of Aliphatic C-H Bonds in Amide-Containing Molecules. *J. Am. Chem. Soc.* **2017,** *139* (41), 14586-14591.

108. Chen, M.; Dong, G., Direct Catalytic Desaturation of Lactams Enabled by Soft Enolization. *J. Am. Chem. Soc.* **2017,** *139* (23), 7757-7760.

109. Harris, L.; Gilpin, M.; Thompson, A. L.; Cowley, A. R.; Moloney, M. G., Uncatalysed diaryldiazo cyclopropanations on bicyclic lactams: access to annulated prolines. *Org. Biomol. Chem.* **2015,** *13* (23), 6522-6550.

110. Wegler, R., Über die mit verschiedener Reaktionsgeschwindigkeit erfolgende Veresterung der optischen Antipoden eines Racemates durch opt. akt. Katalysatoren. *Justus Liebigs Ann. Chem.* **1932,** *498* (1), 62-76.

111. Vellalath, S.; Romo, D., Asymmetric Organocatalysis: The Emerging Utility of α,β-Unsaturated Acylammonium Salts. *Angew Chem Int Ed Engl* **2016,** *55* (45), 13934-13943.

112. Biswas, A.; Mondal, H.; Maji, M. S., Synthesis of Heterocycles by Isothiourea Organocatalysis. *J. Heterocycl. Chem.* **2020**.

113. Ahlemeyer, N. A.; Streff, E. V.; Muthupandi, P.; Birman, V. B., Dramatic Acceleration of an Acyl Transfer-Initiated Cascade by Using Electron-Rich Amidine-Based Catalysts. *Org. Lett.* **2017,** *19* (24), 6486-6489.

114. Birman, V. B.; Li, X., Homobenzotetramisole: An Effective Catalyst for Kinetic Resolution of Aryl-Cycloalkanols. *Org. Lett.* **2008,** *10* (6), 1115-1118.

115. Birman, V. B.; Uffman, E. W.; Jiang, H.; Li, X.; Kilbane, C. J., 2,3-Dihydroimidazo[1,2-a]pyridines: A New Class of Enantioselective Acyl Transfer Catalysts and Their Use in Kinetic Resolution of Alcohols. *J. Am. Chem. Soc.* **2004,** *126* (39), 12226-12227.

116. Robinson, E. R. T.; Walden, D. M.; Fallan, C.; Greenhalgh, M. D.; Cheong, P. H.-Y.; Smith, A. D., Non-bonding 1,5-S···O interactions govern chemo- and enantioselectivity in isothiourea-catalyzed annulations of benzazoles. *Chemical Science* **2016,** *7* (12), 6919-6927.

117. Matviitsuk, A.; Greenhalgh, M. D.; Antúnez, D.-J. B.; Slawin, A. M. Z.; Smith, A. D., Aryloxide-Facilitated Catalyst Turnover in Enantioselective α,β-Unsaturated Acyl Ammonium Catalysis. *Angew. Chem. Int. Ed.* **2017,** *56* (40), 12282-12287.

118. Shu, C.; Liu, H.; Slawin, A. M. Z.; Carpenter-Warren, C.; Smith, A. D., Isothiourea-catalysed enantioselective Michael addition of N-heterocyclic pronucleophiles to α,β-unsaturated aryl esters. *Chemical Science* **2020,** *11* (1), 241-247.

119. Matviitsuk, A.; Greenhalgh, M. D.; Taylor, J. E.; Nguyen, X. B.; Cordes, D. B.; Slawin, A. M. Z.; Lupton, D. W.; Smith, A. D., Unanticipated Silyl Transfer in Enantioselective α,β-Unsaturated Acyl Ammonium Catalysis Using Silyl Nitronates. *Org. Lett.* **2020,** *22* (1), 335-339.

120. Morris, K. A.; Arendt, K. M.; Oh, S. H.; Romo, D., Double Diastereoselective, Nucleophile-Catalyzed Aldol Lactonizations (NCAL) Leading to β-Lactone Fused Carbocycles and Extensions to β-Lactone Fused Tetrahydrofurans. *Org. Lett.* **2010,** *12* (17), 3764-3767.

121. Cortez, G. S.; Tennyson, R. L.; Romo, D., Intramolecular, nucleophile-catalyzed aldol-lactonization (NCAL) reactions: catalytic, asymmetric synthesis of bicyclic beta-lactones. *J. Am. Chem. Soc.* **2001,** *123* (32), 7945-7946.

122. Liu, G.; Shirley, M. E.; Van, K. N.; McFarlin, R. L.; Romo, D., Rapid assembly of complex cyclopentanes employing chiral, α,β-unsaturated acylammonium intermediates. *Nat. Chem.* **2013,** *5* (12), 1049-1057.

123. Abbasov, M. E.; Hudson, B. M.; Tantillo, D. J.; Romo, D., Stereodivergent, Diels–Alder-initiated organocascades employing α,β-unsaturated acylammonium salts: scope, mechanism, and application. *Chem. Sci.* **2017,** *8* (2), 1511-1524.

124. Abbasov, M. E.; Hudson, B. M.; Tantillo, D. J.; Romo, D., Acylammonium salts as dienophiles in Diels-Alder/lactonization organocascades. *J. Am. Chem. Soc.* **2014,** *136* (12), 4492-5.

125. Vellalath, S.; Van, K. N.; Romo, D., Direct Catalytic Asymmetric Synthesis of N-Heterocycles from Commodity Acid Chlorides by Employing α,β-Unsaturated Acylammonium Salts. *Angew. Chem. Int. Ed.* **2013,** *52* (51), 13688-13693.

126. Kang, G.; Yamagami, M.; Vellalath, S.; Romo, D., Enantioselective Synthesis of Medium-Sized Lactams via Chiral α,β-Unsaturated Acylammonium Salts. *Angew. Chem. Int. Ed.* **2018,** *57* (22), 6527-6531.

127. Nguyen, H.; Oh, S.; Henry-Riyad, H.; Sepulveda, D.; Romo, D., Organocatalytic enantioselective synthesis of bicyclic β-lactones from aldehyde acids via nucleophile-catalyzed aldollactonization (NCAL). In *Organic Synth.*, 2011; Vol. 88, pp 121-137.

CHAPTER THREE

Formal Total Synthesis of (+)-Neooxazolomycin

This chapter was published with modifications as: Christian M. Chaheine, Paul T. Gladen, Mikail E. Abbasov, Daniel Romo. Enantioselective, Organocatalytic Strategy to the Oxazolomycin Core: Formal Total Synthesis of (+)-Neooxazolomycin. *Organic Letters* (2020). *Submitted*

3.1 Introduction

Since the isolation and structural assignment of the peptide-polyketide natural products, oxazolomycin A[2, 3] and neooxazolomycin[6] by Uemura and co-workers in 1985, several related congeners have been identified from both marine and terrestrial *Streptomyces* bacteria and are known collectively as the 'oxazolomycins' (Figure 3.1).[4, 5, 7-9, 11-13, 21]

Across the various congeners that have been identified to date, the main structural differences are substitution at C16 of the spiro-β-lactone, the geometry of the conjugated triene, and the terminal group of the sidechain. The stereochemically rich spiro-β-lactone pyroglutamate core is common to all oxazolomycin family members with the exception of neooxazolomycin, which instead possesses a fused-γ-lactone. The only reports regarding the bioactivity of neooxazolomycin, to the best of our knowledge, include: 1) the original isolation paper that gives no quantitative measurements of its *in vivo* activity against Ehrlic ascites tumor cells; 2) A study on the inhibition of plant tumorigenesis activity of oxazolomycin A, which states that neooxazolomycin did not display this activity.[22] In contrast, there are many reports of spiro-β-lactone-containing oxazolomycins that demonstrate wide-ranging bioactivities, including antiviral, anti-cancer, and antibacterial

activity.[1] Thus, an efficient, stereoselective synthetic route to access both spiro- β-lactone and fused-γ-lactone pyroglutamate core structures of the oxazolomycins and neoxazolomycins, respectively, is desirable for a more complete understanding of the structure-activity relationship of these natural products.

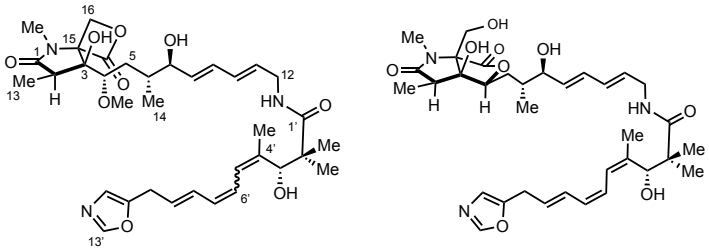

Figure 3.1. Structures of selected oxazolomycin natural products.

Numerous elegant synthetic strategies targeting the densely functionalized γ-lactam core have been described,[33, 38, 128-133] culminating in a formal synthesis of neooxazolmycin by Taylor,[134] total syntheses of oxazolomycin A[37] and lajollamycin[39] by Hatakeyama, and neoxazolomycin by Kim,[46] Hatakeyama,[36] and Kende.[32] Despite these various synthetic strategies only a few studies directed toward an understanding of the biological mode of action[23] of the oxazolomycin family have been reported.

Toward our goal of elucidating the cellular target(s) and delineating the minimal structural features required for the bioactivity of the oxazolomycin family, we report herein a scalable, organocatalytic, enantioselective approach to the pyroglutamate core of the oxazolomycins. A vinyliodide intermediate **3.2** utilized by Kende in the first total synthesis of neooxazolomycin was intercepted in 10 steps (longest linear sequence; previously obtained in 24 steps from glucose) from the known sulfonamido malonate **3.7**.[135] This

enabled correlation of the absolute stereochemistry of the C1-C9/C13-C17 core of the oxazolomycins obtained through the described synthetic route.

3.2 Results & Discussion

We adopted a common retrosynthetic disconnection for all oxazolomycins utilized to date, namely the side-chain amide bond that appends the core (C1-C17) to the conjugated triene oxazole fragment (C1'-C13'). With a goal of methodically increasing complexity of the side chain in a version of pharmacophore-directed retrosynthesis (PDR),[136-138] we next chose a C9-C10 disconnection of the diene,[35] leading to the initial synthetic target of our study, Kende's vinyliodide **3.2** that would enable correlation of the absolute and relative stereochemistry corresponding to that of neoxazolomycin and, by extension, oxazolomycin (Figure 3.2).

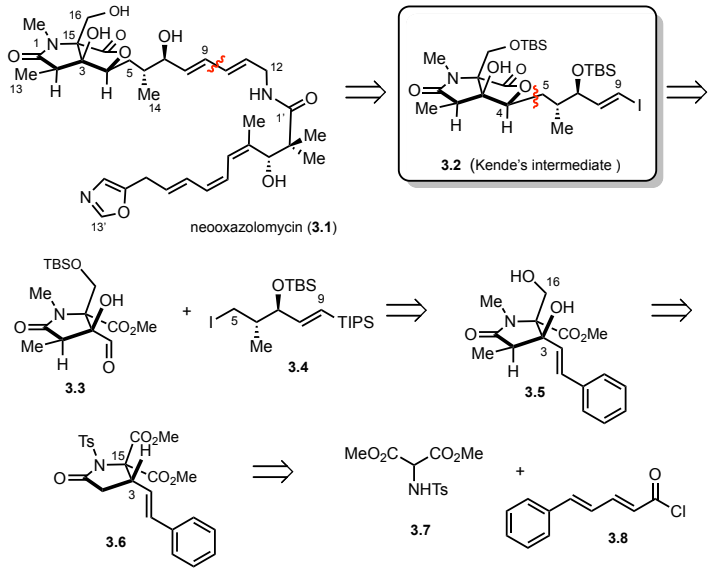

Figure 3.2. Retrosynthetic analysis of the pyroglutamate core of the oxazolomycins, intercepting Kende's vinyliodide intermediate **3.2**.

Disconnection of the C4-C5 bond through a facially selective addition to aldehyde **3.3** of an alkylmetal species derived from a C5-C9 bearing iodide **3.4**, builds on precedent from the Donohoe lab.[130] The appropriately functionalized aldehyde-bearing γ-lactam **3.3** would be derived from diol **3.5**, in turn derived from substrate-controlled alkylation and functional group manipulation of diester **3.6**. Finally, our previously described nucleophile-catalyzed Michael-proton transfer lactamization (NCMPL) organocascade[125, 139] would deliver diester lactam **3.6** in enantiopure form from aminomalonate **3.7**[135] and acid chloride **3.8**, each accessible in one step from commercial materials. The single C3-stereogenic center would impart diastereoselectivity during a-methylation at C2 and guide a diastereotopic group-selective reduction[140] of the geminal diester. The styryl moiety in the NCMPL was chosen to control regioselectivity for the allylic C-H hydroxylation at C3 and serve as a masked aldehyde.

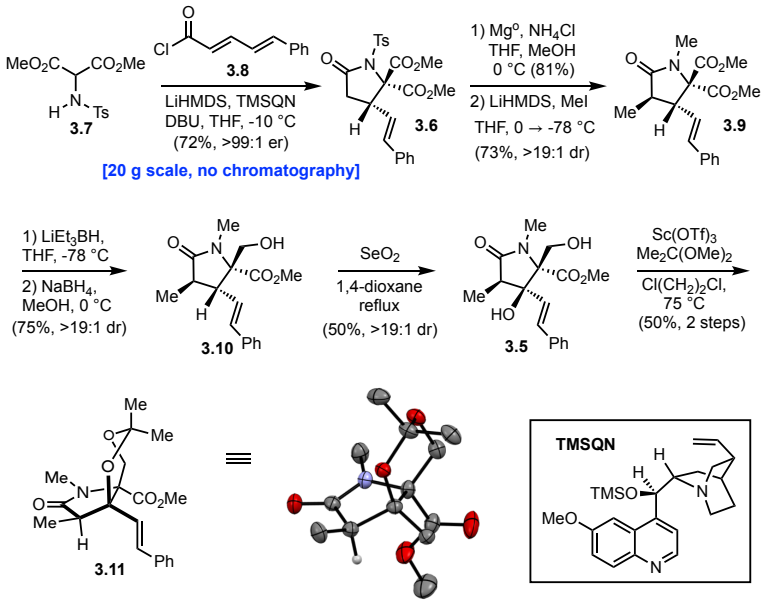

Scheme 3.1. Scalable, enantioselective synthesis of the pyroglutamate core diol **3.5** (inset: ORTEP representation of 11, 'PhCH=' omitted for clarity).

Our synthesis commenced with the NCMPL, employing acid chloride **3.8** and *N*-tosyl aminomalonate **3.7** as substrates with 20 mol% TMS-quinine (TMSQN) as chiral Lewis base, reliably delivering γ-lactam **3.6** on 20 g scale in 72% yield (>99:1 er, Scheme 3.1). Sufficiently pure, crystalline lactam **3.6** could be obtained by simple trituration (MeOH) of the crude solid following aqueous work up. The absolute stereochemistry was confirmed by X-ray analysis as recently described.[139] Desulfonylation of lactam **3.6** on decagram scale by stirring with Mg^0 turnings in cold MeOH/THF[141, 142] was followed by a one-pot *N*-methylation on the pyrrolidinone nitrogen and highly diastereoselective methylation at C2 to deliver dimethyl γ-lactam **3.9** on multigram scale in 73% yield (>19:1 dr).

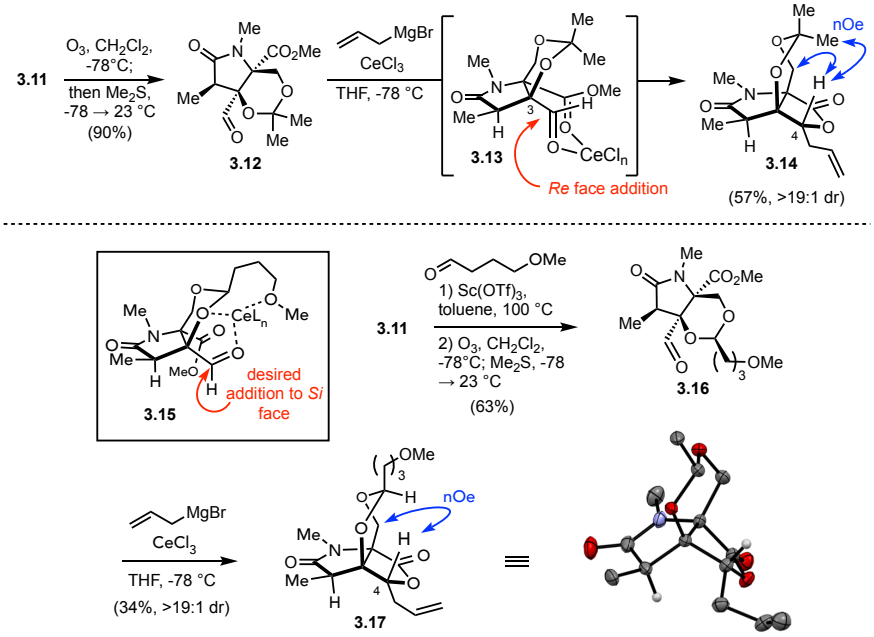

Scheme 3.2. Facially selective addition to aldehydes **3.12** and **3.16** (stereochemical assignments by nOe and X-ray (inset: ORTEP representation of lactone **3.17**, some groups omitted for clarity))

A diastereotopic group-selective monoreduction of the more sterically accessible methyl ester was possible through use of a bulky hydride source ($LiEt_3BH$, superhydride) at low temperature, giving an intermediate aldehyde which was directly reduced with $NaBH_4$ to the targeted β-hydroxy ester **3.10**. A subsequent allylic C-H hydroxylation with SeO_2, presumably directed by the adjacent primary alcohol,[143] provided multigram quantities of pyroglutamate diol **3.5** with the desired C3 configuration (confirmed by X-ray analysis of an acetonide derivative **3.11**, Scheme 3.1 inset). Notably, the diester **3.9**, when exposed to SeO_2 led to the desired stereochemistry at C3 but as a 4:1 mixture of epimers, supporting the directing effect of the C16 primary alcohol. Simple trituration of the crude diol **3.5** with CH_2Cl_2 provided sufficiently pure material for use in subsequent reactions.

With pyroglutamate diol **3.5** available in gram quantities, the stage was set for exploration of the key C4-C5 alkylmetal addition reaction, which required a careful choice of C3,C16 alcohol protection. Initially, we studied acetonide formation from **3.5** and the styrenyl moiety was oxidatively cleaved with ozone to yield aldehyde **3.12**. Exposure to several Grignard and organolithium reagents, led only to reduction or no reaction, respectively (Scheme 3.2). The sterically hindered nature of the C4 aldehyde presumably led to low reactivity, therefore we turned to the use of anhydrous lanthanide halides, known to assist in nucleophilic additions to hindered carbonyls through Lewis acid activation of the carbonyl oxygen and/or the *in situ* generation of an organolanthanide of enhanced nucleophilicity and reduced basicity.[144-146] A combination of excess allylmagnesium bromide[147] and anhydrous $CeCl_3$[148, 149] in THF led to a single diastereomer of γ-lactone **3.14** through a nucleophilic addition/γ-lactonization sequence (Scheme 3.2). Spectroscopic

analysis, including NOESY, unfortunately indicated that γ-lactone **3.14** had the undesired C4-configuration, presumably the product of addition to the *Re* face of aldehyde **3.13** induced by formation of the 7-membered chelate with the pendant ester. We speculated that the *gem*-dimethyl group in the acetonide of diol **3.5** sterically precluded the C3-ether oxygen from coordination to the cerium (III) ion that would induce the desired facial selectivity. An acetal protecting group bearing a pendant methoxy functionality was next considered with the aim of templating the chelation of cerium (III) ion onto aldehyde **3.16** via chelated intermediate **3.15**, Scheme 3.2) leading to *Si* face addition to the aldehyde, however this tactic did not override the competing 7-membered chelate. The NOESY spectra and X-ray single-crystal analysis of lactone **3.17** confirmed that the undesired C4-relative configuration was again formed in the allylation.

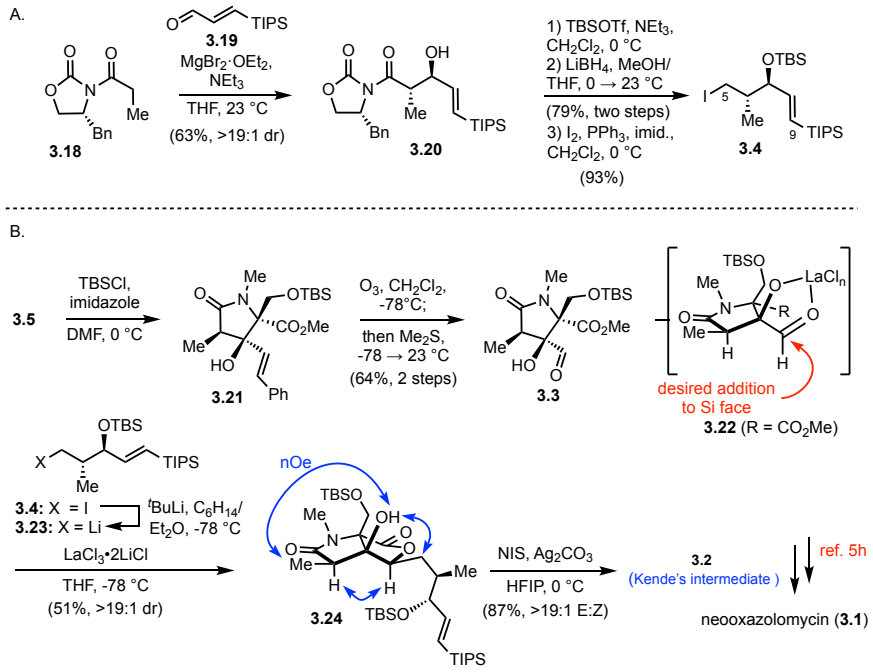

Scheme 3.3. A. Enantioselective synthesis of the C5-C9/C13-C17 fragment of the oxazolomycins. B. Formal total synthesis of (+)-neooxazolomycin (**3.1**).

Building on work by Donohoe, we considered the possibility that the C3-tertiary alcohol, once deprotonated, could enforce a chelated α-hydroxy aldehyde intermediate (*cf.* **3.22**, Scheme 3.3B), which would be expected to deliver the desired facial selectivity. This chelated α-alkoxy aldehyde was first proposed by Donohoe employing a similar α-hydroxy aldehyde and a primary alkylcerium reagent generated *in situ* by crushing pellets of anhydrous $CeCl_3$ in a solution of primary alkylithium with a metal rod under an atmosphere of argon.[130] We studied this tactic beginning with selective silyl protection of 1,3-diol **3.5**, yielding silyl ether **3.21**, followed by ozonolysis to afford the α-hydroxyaldehyde **3.3**. Initial studies with allymagnesium bromide were inconclusive regarding stereochemical outcome at C4 so we proceeded to correlate the stereochemical outcome by comparison to Kende's intermediate **3.2** through addition of the required side-chain as described below.

The required enantioenriched C5-C9 iodide **3.4** was synthesized through application of an Evans' anti-aldol reaction[150, 151] utilizing oxazolidinone[152] **3.18** and the β-triisopropylsilyl acrolein[153] **3.19** (63% yield, >19:1 dr, Scheme 2a). Silyl protection of the resulting secondary alcohol and reductive cleavage of the auxiliary gave a primary alcohol that was converted to iodide **3.4** under typical Appel conditions.[154]

The optimized procedure for this key fragment coupling involved lithium-halogen exchange of the primary iodide **3.4** at -78 °C in a mixture of dry hexanes/ether.[155, 156] The α-hydroxyaldehyde **3.3** was dissolved in a solution of $LaCl_3 \cdot 2LiCl$ in THF[157] and this mixture was then slowly added to the alkylithium solution maintained at -78 °C (Scheme 3.3B). The desired fused-pyroglutamate-γ-lactone **3.24** was generated through a highly diastereoselective nucleophilic addition/γ-lactonization sequence and the conformational rigidity of lactone **3.24** enabled initial determination of the C4 stereochemistry through

NOESY analysis. The relative and absolute stereochemical assignment of this fragment was further corroborated by intercepting Kende's vinyliodide intermediate **3.2**. Iododesilylation of the vinylsilane in **3.24** with NIS and Ag_2CO_3 in hexafluoroisopropanol[158, 159] (HFIP) at 0 °C delivered the (*E*)-vinyliodide **3.2** (87% yield, >19:1 *E*:*Z*) which was correlated spectroscopically to that previously reported (see Table 3.1).

3.3 Conclusion

In summary, we developed a scalable, enantioselective synthetic route to a versatile pyroglutamate diol **3.5** serviceable for the synthesis of oxazolomycin-based chemical probes toward bioactivity investigations. Diol **3.5** was converted in 4 steps to an advanced vinyliodide **3.2** synthesized by Kende in the first total synthesis of neooxazolomycin, confirming the relative and absolute stereochemistry of the C1-C17 fragment.[32] A simplified procedure involving a lanthanide-mediated alkylithium addition, building on work by Donohoe, provided a highly diastereoselective installation of the C4-C5 bond which initiates construction of the oxazolomycin side chain. Our modular synthetic route will enable synthesis of simplified oxazolomycin derivatives including derived proteomics probes to facilitate a more in-depth understanding of the structure-activity relationships and the various reported biological activities for this family of unique peptide-polyketide natural products.

3.4 Experimental

3.4.1 General Information

All reactions were carried out under an atmosphere of nitrogen passed through a column of Dri-Rite in oven-dried glassware (≥4 h at 125 °C), using a Teflon stir-bar, and a glass, threaded adapter with a septum cap and serrated hose connection unless stated otherwise. Liquid chemical reagents and solutions were transferred under inert atmosphere using air-tight, disposable, polypropylene/polyethylene syringes fitted with disposable/reusable stainless-steel needles unless stated otherwise. Dichloromethane (CH_2Cl_2), tetrahydrofuran (THF), diethyl ether (Et_2O), methanol (MeOH), acetonitrile (MeCN), and toluene (PhMe) were dried by filtration through a column of activated alumina or activated molecular sieves (J.C. Meyer Solvent System) prior to use. Triethylamine (Et_3N) was distilled from calcium hydride prior to use. Commercially available reagents were purchased from Sigma Aldrich, Combi-Blocks, or Oakwood Chemical and used as received. Compounds were dried of residual solvent under "high vacuum" with the use of a Welch 1400 Duo-Seal two stage vacuum pump operating at ~0.3-0.4 torr attached to a vacuum trap and Schlenk manifold. Deuterated solvents ($CDCl_3$) were purchased from Sigma Aldrich and used as received.^{1}H-NMR spectra were measured at 400, 500, or 600 MHz and chemical shifts are reported as δ values in ppm relative to residual chloroform signal (7.26 ppm). Coupling constants (*J*) were reported in Hertz (Hz) with multiplicity reported following the normal convention: s, singlet; d, doublet; t, triplet; q, quartet; m, multiplet; br s, broad singlet; dd, doublet of doublets; ddd, doublet of doublet of doublets; dt, doublet of triplets; ddt, doublet of doublet of triplets; dddt, doublet of doublet of doublet of triplets; td, triplet of doublets; dq, doublet of quartets; qd, quartet of

doublets; td, triplet of doublets; prefix 'app' indicates 'apparent'. ^{13}C-NMR spectra were measured at 100 or 150 MHz and chemical shifts are reported as δ values in ppm relative to residual chloroform signal (77.16 ppm). Chromatographic purifications were performed with 60 Å silica gel (Silicycle, 230-400 mesh) as stationary phase using a thick-walled, glass flash chromatography column with a positive pressure of air or on an automated flash chromatography system (Teledyne Isco, CombiFlash R$_f$). High-resolution mass spectra (HRMS) were obtained by electrospray ionization (ESI) time of flight mass spectrometry using a Thermo Orbitrap Discovery– pure compound was directly injected as a solution in HPLC-grade MeOH. Reactions were monitored by thin layer chromatography (TLC) using glass-backed 60 Å silica gel F-254 plates (Silicycle, 250 μm thickness). Visualization of developed TLC plates was done by fluorescence quenching with a 254 nm UV lamp or by immersion in $KMnO_4$, anisaldehyde, or dinitrophenylhydrazine (DNPH) staining solutions followed by heating with a heat gun. Fourier Transform Infrared (FTIR) spectra were obtained from a thin film of the pure compound on a NaCl plate. Specific rotations were recorded on a polarimeter at 589 nm employing a 25 mm quartz cell. X-ray diffraction data was collected and processed by Dr. Kevin Klausmeyer (Baylor University).

3.4.2 Abbreviation List

allylMgBr	allylmagnesium bromide
$(COCl)_2$	Oxalyl chloride
$Cl(CH_2)_2Cl$	1,2-dichloroethane
DBU	1,8-Diazabicyclo(5.4.0)undec-7-ene
DMF	*N,N*-Dimethylformamide

DNPH	2,4-dinitrophenylhydrazine
Et_3N	Triethylamine
EtOAc	Ethyl acetate
HFIP	1,1,1,3,3,3-hexafluoro-2-propanol
$LiEt_3BH$	Superhydride
LiHMDS	Lithium hexamethyldisilylazide
$Me_2C(OMe)_2$	2,2-dimethoxypropanest
MeI	Methyl iodide
Me_2S	Dimethyl sulfide
$MgBr_2 \cdot OEt_2$	Magnesium (II) bromide diethyl etherate
NIS	*N*-iodosuccinimide
PPh_3	Triphenylphosphine
$Sc(OTf)_3$	Scandium (III) trifluoromethanesulfonate
TBSCl	*tert*-butyldimethylsilyl chloride
TBSOTf	*tert*-butyldimethylsilyl trifluoromethanesulfonate
^{t}BuLi	*tert*-butyllithium
TMSQN	*O*-trimethylsilylquinine

3.4.3 Synthetic Procedures

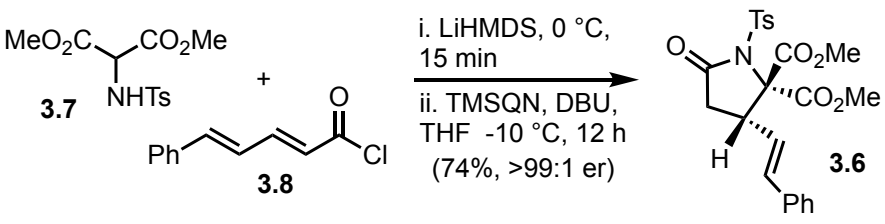

***N*-tosyl-g-lactam 3.6.** The optically enriched γ-lactam **3.6** was obtained via the NCMPL, employing unsaturated acid chloride **3.8** and *N*-tosyl aminomalonate **3.7** as substrates with 20 mol% *O*-trimethylsilylquinine (TMSQN) as chiral Lewis base. This procedure reliably delivered the required starting material for this study on 20 g scale in 72% yield (>99:1 er) of sufficient purity for subsequent steps by simple trituration (MeOH) of the crude solid following aqueous work up. The absolute stereochemistry was confirmed by X-ray analysis as recently described.[139]

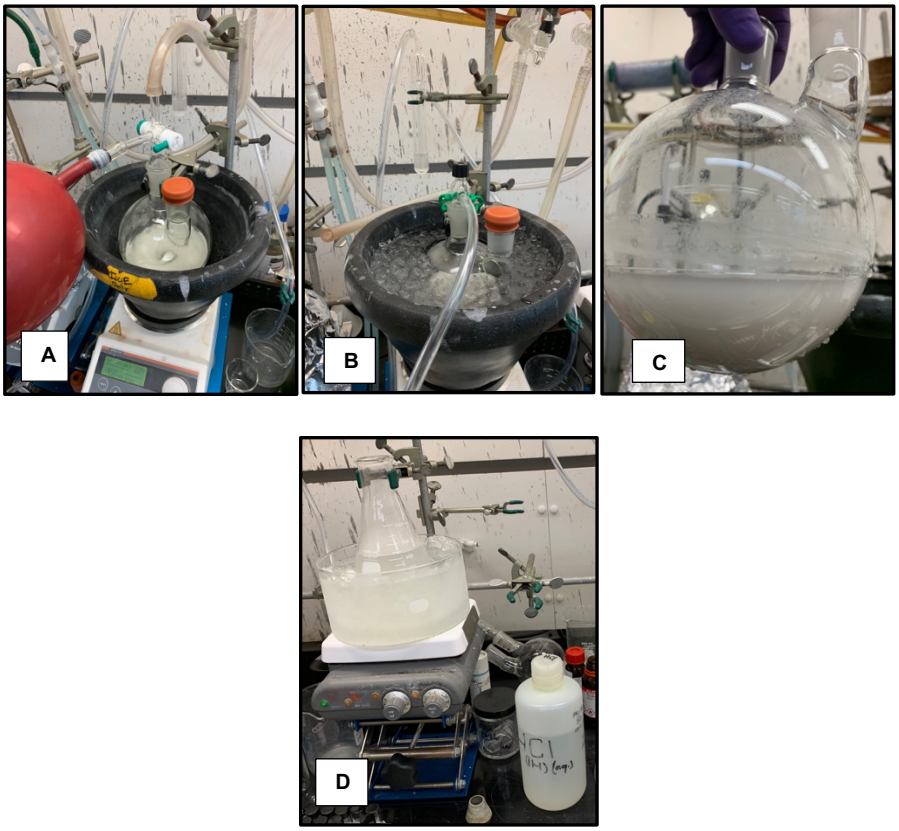

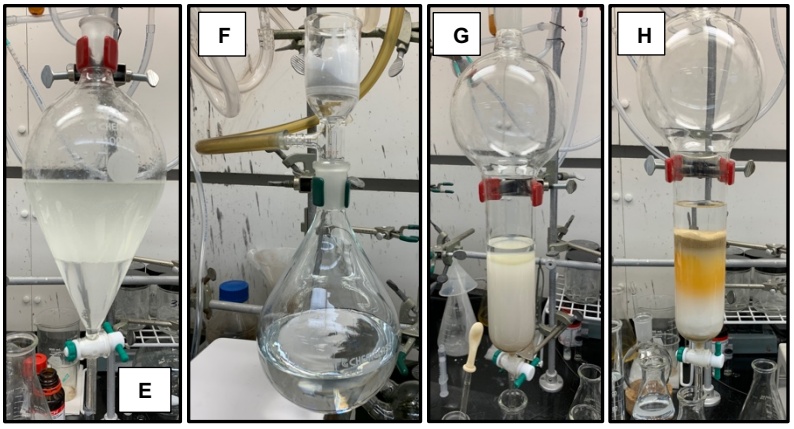

A. N-tosyl lactam and NH_4Cl stirring in THF under Ar-filled balloon. **B.** Following thorough cooling to 0 °C and addition of Mg^0 in one portion, gradual gas evolution is observed through mineral oil bubbler. **C.** Crude reaction mixture prior to quench. **D.** After careful addition of crude reaction mixture to a pre-cooled (0 °C) solution of aqueous HCl and dilution with CH_2Cl_2. **E.** Appearance of organic and aqueous layers in 1 L separatory funnel. **F.** Appearance of combined organic phase following $MgSO_4$ drying and filtration through celite. **G.** Appearance of silica gel chromatography column prior to fraction collection with crude material visible at top of column. **H.** Appearance of silica gel chromatography column after fraction collection.

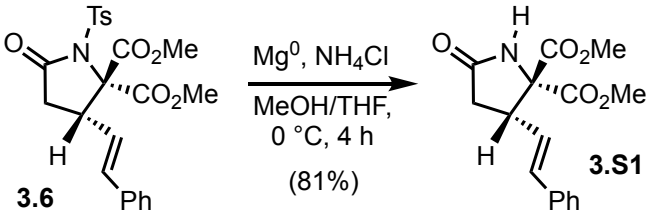

Dimethyl-(*S*,*E*)-5-oxo-3-styrylpyrrolidine-2,2-dicarboxylate (3.S1): To a two-necked, 1 L round-bottomed flask containing a Teflon-coated, football-shaped (5 cm) stir bar and a T-bore Schlenk adapter (connected to a high vacuum and an argon balloon). In the second neck, a rubber septum is used *N*-tosyl lactam **3.6**[139] (15.41 g, 33.7 mmol, 1.0 equiv) and NH_4Cl (45.1 g, 843 mmol, 25.0 equiv) were added as solids. The atmosphere in the flask was replaced with argon by three cycles of vacuum/back-filling. The solids were stirred (~250 rpm) for ~5 min neat and then MeOH (100 mL) and THF (125 mL) were added and the resulting suspension was stirred vigorously (~450 rpm) for 10 min at 23 °C (23 °C) and then cooled to 0 °C in an ice bath and stirred for an additional 20 min to ensure that internal temperature is close to 0 °C. Magnesium turnings (20.5 g, 843 mmol, 25.0 equiv) were then added under a positive pressure of argon in one portion. (**Safety Precaution**: This

reaction is highly exothermic with significant gas evolution. It is imperative to ensure that the internal temperature is close to 0 °C prior to addition of Mg^0 turnings. In addition, the use of Mg^0 turnings and NOT powder prevents rapid exotherms and was essential to achieve high yields in this reaction) The Schlenk adapter was then quickly replaced with a gas outlet adapter connected to a mineral oil bubbler. The resulting suspension was stirred at 0 °C for 3-4 h, venting H_2 through the mineral oil bubbler and allowing the reaction to slowly warm to 23 °C. The dark grey suspension was then poured slowly into a stirring solution of aqueous HCl (3 x 843 mmol Mg^0 = 2529 mmol HCl = 211 mL of conc. HCl dissolved in 300 mL H_2O) pre-cooled to 0 °C. The quenched reaction mixture was diluted with CH_2Cl_2 (300 mL). The layers were separated and the aqueous layer was extracted with CH_2Cl_2 (3 x 150 mL). The combined organic layers were dried over $MgSO_4$, filtered through celite, and concentrated by rotary evaporation to provide a yellow oil which was purified by flash column chromatography (0 → 100%, EtOAc/hexanes, 25% increments, 250 mL each; then 5% MeOH/EtOAc until product was no longer eluting; product elutes ~70% EtOAc/hexanes to 5% MeOH/EtOAc) to afford styrenyl lactam **3.S1** (8.32 g, 81%) as a sticky white foam upon drying under high vacuum:

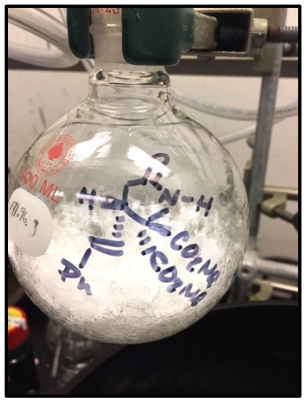

R_f = 0.12 (50% EtOAc/hexanes, UV-active); **$[\alpha]_D^{20}$** -34.4 (*c* 3.26, $CHCl_3$); **IR (thin film)**: 3443 (br), 2960, 1750, 1700, 1648 cm^{-1}; **^{1}H-NMR** (500 MHz, $CDCl_3$) δ 7.35-7.23 (m, 5H), 7.18 (br s, 1H), 6.58 (d, *J* = 15.8 Hz, 1H), 6.13 (dd, *J* = 15.8, 8.5 Hz, 1H), 3.88-3.83 (m, 1H), 3.82 (s, 3H), 3.68 (s, 3H), 2.74 (dd, *J* = 16.8, 8.2 Hz, 1H), 2.51 (dd, *J* = 16.8, 6.7 Hz, 1H); **^{13}C-NMR** (125 MHz, $CDCl_3$) δ 176.0, 168.3, 168.1, 136.3, 133.9, 128.7 (2), 128.1, 126.5 (2), 125.0, 72.2,

53.6, 53.3, 44.0, 35.6; **HRMS (ESI+)** *m/*z calcd. for $C_{16}H_{18}NO_5$ $[M+H]^+$: 304.1180, found: 304.1181.

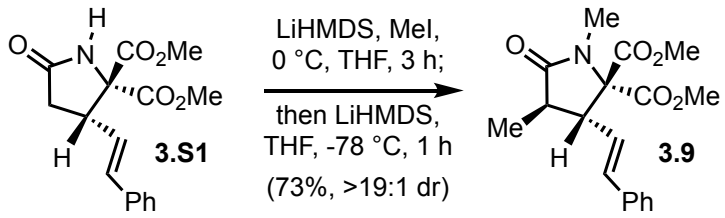

Dimethyl-(3*R*,4*R*)-1,4-dimethyl-5-oxo-3-((*E*)-styryl)pyrrolidine-2,2-dicarboxylate (3.9): To a 500 mL single-necked, round-bottomed flask containing styrenyl lactam **3.S1** (8.32 g, 27.4 mmol, 1.0 equiv) was added THF (110 mL) with stirring. The resulting colorless solution was cooled to 0 °C in an ice bath over ~10 min before adding a solution of LiHMDS (1.0 M in THF, 34.3 mL, 34.3 mmol, 1.25 equiv) dropwise via a 50 mL plastic syringe fitted with a stainless-steel needle over 15 min. The resulting solution was stirred at 0 °C for 5 min then MeI (6.9 mL, 110 mmol, 4.0 equiv) was added in one portion over ~2 min and stirred for an additional 5 min. The cooling bath was then removed, and the reaction mixture was allowed to warm to 23 °C and stirred for 3.0 h. The reaction mixture was cooled to -78 °C in a dry ice/acetone bath over 15 min before adding LiHMDS (1.0 M in THF, 34.3 mL, 34.3 mmol, 1.25 equiv) dropwise over 45 min using a syringe pump (46 mL/min) with a 50 mL syringe. Upon complete addition of base, the reaction was stirred at -78 °C for 1 h and was then quenched at this temperature by addition of saturated, aqueous $NaHCO_3$ (18 mL), warmed to 23 °C, and diluted with EtOAc (200 mL) and H_2O (120 mL). The layers were separated and the aqueous layer was extracted with EtOAc (3 x 150 mL). The combined organic layers were washed with brine, dried over $MgSO_4$, filtered through celite, and concentrated by rotary evaporation to provide an amber oil

which was purified by automated flash chromatography (0 → 70%, EtOAc/hexanes, continuous gradient; product elutes at 55-60% EtOAc) to afford bis-methyl lactam **3.9** as an off-white granular solid (6.63 g, 73%, >19:1 dr):

R_f = 0.65 (50% EtOAc/hexanes, UV-active); **$[\alpha]_D^{20}$** +26.4 (*c* 2.58, $CHCl_3$); **IR (thin film)**: 3046, 2985, 2954, 1751, 1732, 1710 cm^{-1}; **^{1}H-NMR** (500 MHz, $CDCl_3$) δ 7.36-7.23 (m, 5H), 6.55 (d, *J* = 15.8 Hz, 1H), 6.06 (dd, *J* = 15.8, 8.5 Hz, 1H), 3.86 (s, 3H), 3.74 (s, 3H), 3.21 (ddd, *J* = 10.4, 8.5, 1.0 Hz, 1H), 2.96 (s, 3H), 2.56 (dq, *J* = 10.4, 7.1 Hz, 1H), 1.23 (d, *J* = 7.1 Hz, 3H); **^{13}C-NMR** (125 MHz, $CDCl_3$) δ 177.1, 167.9, 167.7, 136.4, 134.4, 128.7 (2), 128.1, 126.5 (2), 124.4, 75.1, 53.2, 53.0, 51.4, 39.8, 29.1, 14.4; **HRMS** (ESI+) *m/z* calcd. for $C_{18}H_{22}NO_5$ $[M+H]^+$: 332.1492, found: 332.1502.

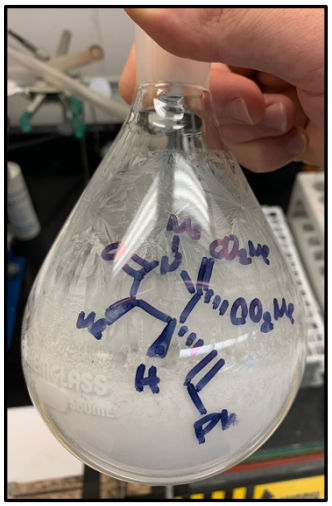

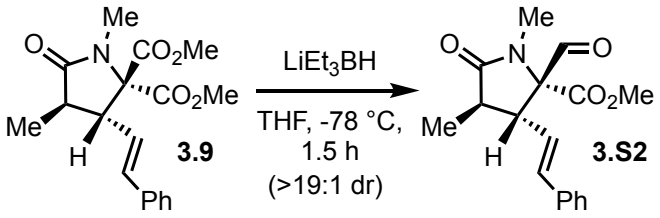

methyl-(2*R*,3*R*,4*R*)-2-formyl-1,4-dimethyl-5-oxo-3-((*E*)-styryl)pyrrolidine-2-carboxylate (3.S2): Bis-methyl lactam **3.9** (4.79 g, 14.5 mmol, 1.0 equiv) was azeotropically dried with dry xylenes (stored over 4 Å MS, 5 mL) under high vacuum and with vigorous stirring over 1 h in a single-necked 500 mL round-bottomed flask. The atmosphere in the flask was charged with N_2 (*g*) and dry THF (145 mL) was then added to the flask and the resulting solution was cooled to -78 °C in a dry ice/acetone bath over 30 min. A solution of $LiEt_3BH$ (1.0 M in THF, 21.8 mL, 21.8 mmol, 1.5 equiv) was then added

dropwise over 1 h via 30 mL plastic luer-lock syringe fitted with an 18-gauge stainless-steel needle via syringe pump (22 mL/h) after which the reaction mixture was stirred for an additional 1 h at -78 °C. The mixture was quenched at this temperature by dropwise addition of a saturated solution of $NaHCO_3$ (aq.) (50 mL), allowed to warm to 23 °C (23 °C), and diluted with EtOAc (150 mL). The resulting suspension was poured into a 1:1 (v/v) solution of H_2O/brine (150 mL), the layers were separated, and the aqueous layer was extracted with EtOAc (3x 75 mL). The combined organic layers were dried over $MgSO_4$, filtered through celite, concentrated by rotary evaporation, and dried further under high vacuum for 1 h to provide crude ester aldehyde **3.20** as a white sticky foam that was used in the next step without purification.

For purposes of characterization, ester aldehyde **3.S2** was isolated as a colorless crystalline solid by recrystallization from EtOAc/hexanes following filtration of the reaction mixture through SiO_2:

R_f = 0.23 (streaking spot, 50% EtOAc/hexanes, UV-active); $[\alpha]_D^{20}$ +32.4 (*c* 1.00, $CHCl_3$); **IR (thin film)**: 2959, 2877, 1749, 1722, 1700 cm^{-1}; **^{1}H-NMR** (600 MHz, $CDCl_3$) δ 10.0 (s, 1H), 7.36-7.27 (m, 5H), 6.58 (d, *J* = 15.7 Hz, 1H), 5.95 (dd, *J* = 15.7, 9.1 Hz, 1H), 3.84 (s, 3H), 2.86 (s, 3H), 2.76 (m, 1H), 2.58 (dq, *J* = 10.0, 7.1 Hz, 1H), 1.21 (d, *J* = 7.1 Hz, 3H); **^{13}C-NMR** (150 MHz, $CDCl_3$) δ 195.6, 176.8, 168.3, 135.83, 135.79, 128.9 (2), 128.6, 126.6 (2), 123.4, 77.2, 53.2, 52.5, 40.8, 28.7, 14.4; **HRMS (ESI+)** *m/*z calcd. for $C_{17}H_{20}NO_4$ $[M+H]^+$: 302.1387, found: 302.1389.

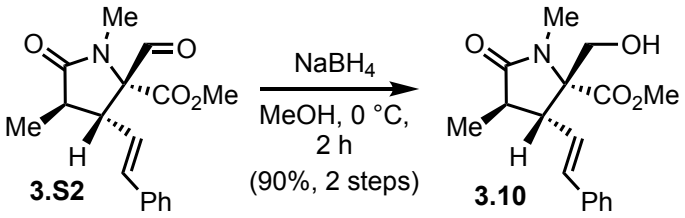

methyl-(2*R*,3*R*,4*R*)-2-(hydroxymethyl)-1,4-dimethyl-5-oxo-3-((*E*)-styryl)pyrrolidine-2-carboxylate (3.10): In an undried 1 L flask open to air, containing crude ester aldehyde **3.S2**, from the previous reaction was added MeOH (150 mL). The resulting solution was stirred vigorously and cooled to 0 °C in an ice bath and then $NaBH_4$ was added portion-wise (1.64 g, 43.5 mmol, 3.0 equiv) and was stirred at 0 °C until TLC indicated consumption of starting aldehyde **3.S2**. The reaction mixture was quenched by dropwise addition of 2 mL of AcOH at 0 °C. The ice bath was then removed, and the mixture was allowed to warm to 23 °C over 1 h; after which the solvent was removed by rotary evaporation to provide a viscous off-white oil. SiO_2 (silica gel, approx. 50 g) was added to the flask to absorb the oil and MeOH was used to rinse the sides of the flask and ensure all crude residue was absorbed onto the SiO_2. The silica gel was dried by careful rotary evaporation and the resulting free-flowing solid was subjected to flash column chromatography (0 → 100%, EtOAc/hexanes, 20% increments, 200 mL each; then 20% MeOH/EtOAc until product has finished eluting; product elutes at 90-100% EtOAc/hexanes to 20% MeOH/EtOAc) to afford β-hydroxy ester **3.10** as a white grainy solid (3.96 g, 90% over two steps):

R$_f$ = 0.51 (80% EtOAc/hexanes, UV-active); $[\alpha]_D^{23}$ +48.99 (*c* 1.09, MeOH); **IR** (thin film) 3385 (br), 2926, 2854, 1737, 1678 cm^{-1}; **^{1}H-NMR** (600 MHz, $CDCl_3$) δ 7.34-7.31 (m, 4H), 7.28-7.25 (m, 1H), 6.56 (d, *J* = 15.7 Hz, 1H), 5.85 (dd, *J* = 15.7, 8.9 Hz, 1H), 4.07 (dd, *J* = 12.4, 4.7 Hz, 1H), 3.88 (dd, *J* = 12.4, 8.7 Hz, 1H), 3.77 (s, 3H), 2.86 (s, 3H), 2.70-2.64 (m,

1H), 2.57 (dq, *J* = 10.8, 7.0 Hz, 1H), 2.05 (dd, *J* = 8.7, 4.7 Hz, 1H), 1.22 (d, *J* = 7.0 Hz, 3H); **^{13}C-NMR** (150 MHz, $CDCl_3$) δ 177.7, 171.3, 136.4, 135.2, 128.8 (2), 128.2, 126.5 (2), 124.6, 72.3, 63.2, 52.7, 50.4, 40.5, 27.6, 14.4; **HRMS (ESI+)** *m/*z calcd. for $C_{17}H_{21}NO_4Na$ $[M+Na]^+$: 326.1363, found: 326.1365.

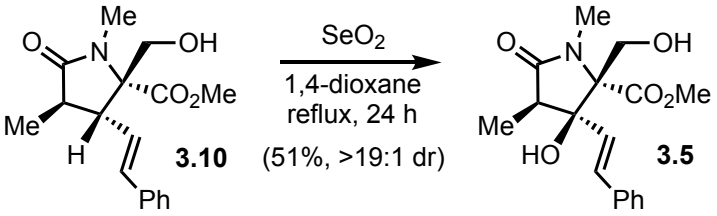

methyl-(2*S*,3*S*,4*R*)-3-hydroxy-2-(hydroxymethyl)-1,4-dimethyl-5-oxo-3-((*E*)-styryl)pyrrolidine-2-carboxylate (3.5): To an undried 250 mL, two-necked, round-bottomed flask fitted with a reflux condenser and a rubber septum was added β-hydroxy ester **3.10** (3.46 g, 11.4 mmol, 1.00 equiv) and SeO_2 (8.85 g, 79.8 mmol, 7.00 equiv) as solids under a positive pressure of N_2 (*g*), followed by anhydrous 1,4-dioxane (114 mL). The resulting suspension was vigorously stirred and heated to reflux (approx. 101 °C) for 24 h (the reflux condenser was connected in sequence to a water recirculation pump and a mechanical water chiller). The heat was then removed and the amber-colored solution with suspended grey selenium powder was allowed to cool to 23 °C. A saturated solution of $NaHCO_3$ (aq.) (150 mL) was carefully added to the reaction mixture with vigorous stirring (Safety note: Quenching is done carefully since gas evolution occurs!). The resulting mixture was poured into a separatory funnel containing EtOAc (100 mL). The layers were separated and the aqueous layer was extracted with EtOAc (4x 50 mL). The combined organic layers were washed with brine, dried over $MgSO_4$, filtered through celite, and concentrated by rotary evaporation to provide an orange-red paste. This paste was

transferred to a Büchner funnel and rinsed with CH_2Cl_2, resulting in diol lactam product **3.5**, an off-white, fine powder with traces of selenium red (1.86 g, 51%, >19:1 dr):

R_f = 0.55 (80% EtOAc/hexanes, UV-active); **$[\alpha]_D^{24}$** +119.55 (*c* 1.27, MeOH); **IR (thin film)**: 3126, 2992, 1733, 1685 cm^{-1}; **^{1}H-NMR** (600 MHz, $CDCl_3$) δ 7.36-7.28 (m, 5H), 6.76 (d, *J* = 15.9 Hz, 1H), 6.04 (d, *J* = 15.9 Hz, 1H), 4.34 (dd, *J* = 12.6, 3.3 Hz, 1H), 3.99 (dd, *J* = 12.5, 9.8 Hz, 1H), 3.73 (s, 3H), 2.92-2.85 (m, 3H), 2.86 (s, 3H), 1.17 (d, *J* = 7.3 Hz, 3H); **^{13}C-NMR** (150 MHz, $CDCl_3$) δ 176.0, 171.3, 135.7, 132.3, 129.0, 128.6(2), 127.8, 126.8(2), 81.3, 75.2, 61.4, 53.0, 44.5, 27.3, 7.3; **HRMS (ESI+)** *m/*z calcd. for $C_{17}H_{21}NO_5Na$ $[M+Na]^+$: 342.1312, found: 342.1314.

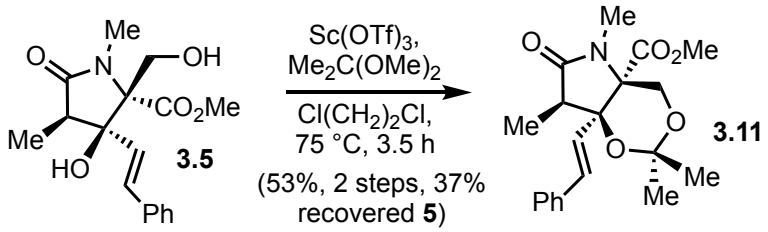

methyl-(4a*S*,7*R*,7a*S*)-2,2,5,7-tetramethyl-6-oxo-7a-((*E*)-styryl)tetrahydro-[1,3]dioxino[5,4-*b*]pyrrole-4a(4*H*)-carboxylate (3.11): A 250 mL, single-necked, pressure reaction vessel was charged with crude diol lactam **3.5** (5.50 mmol, 1.00 equiv; obtained from the previous allylic oxidation reaction without triturating with CH_2Cl_2), anhydrous $Cl(CH_2)_2Cl$ (75 mL), $Me_2C(OMe)_2$ (13.5 mL, 110 mmol, 20.0 equiv), and $Sc(OTf)_3$ (134.0 mg, 0.55 mmol, 0.10 equiv). The pressure vessel was tightly sealed, stirred vigorously, heated to 75 °C, and maintained at this temperature for 3.5 h. The heat was then removed and the resulting reaction mixture was allowed to cool to 23 °C. The mixture was concentrated by rotary evaporation to a crude, dark-brown oil that was purified by

automated flash chromatography (0 → 100%, EtOAc/hexanes, continuous gradient) to afford *fused*-acetonide lactam **3.11** as an amber oil (1.05 g, 53% over two steps, 37% recovered β-hydroxy ester **3.10**):

R_f = 0.44 (50% EtOAc/hexanes, UV-active); **[α]** $\overset{23}{D}$ +119.00 (*c* 0.57, $CHCl_3$); **IR** (thin film) 2994, 2940, 2360, 1737, 1706 cm^{-1}; **^{1}H-NMR** (600 MHz, $CDCl_3$) δ 7.35-7.27 (m, 5H), 6.75 (d, *J* = 15.9 Hz, 1H), 6.15 (d, *J* = 15.9 Hz, 1H), 4.49 (d, *J* = 13.7 Hz, 1H), 3.98 (d, *J* = 13.7 Hz, 1H), 3.77 (s, 3H), 2.84 (s, 3H), 2.72 (q, *J* = 7.1 Hz, 1H), 1.53 (s, 3H), 1.39 (s, 3H), 1.14 (d, *J* = 7.2 Hz, 3H); **^{13}C-NMR** (150 MHz, $CDCl_3$) δ 176.4, 170.5, 136.1, 133.8, 128.9(2), 128.4(2), 126.7, 126.0, 99.2, 79.4, 68.1, 57.1, 53.1, 46.7, 30.0, 26.1, 24.5, 6.3; **HRMS (ESI+)** *m/*z calcd. for $C_{20}H_{26}NO_5$ $[M+H]^+$: 360.1805, found: 360.1806.

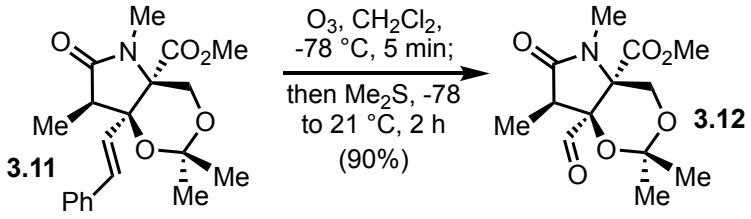

methyl-(4a*S*,7*R*,7a*S*)-7a-formyl-2,2,5,7-tetramethyl-6-oxotetrahydro-[1,3]dioxino[5,4-*b*]pyrrole-4a(4*H*)-carboxylate (3.12): To an undried 20 mL vial fitted with a septum cap was added *fused*-acetonide lactam **3.11** (112 mg, 0.310 mmol, 1.00 equiv) followed by CH_2Cl_2 (4 mL). The resulting dark-yellow solution was stirred and cooled to -78 °C in a dry ice/acetone bath under N_2 (*g*) atmosphere over 10 min. The septum was then removed and O_3 (*g*) was bubbled through the solution with a sparge tube for 5 min (until the reaction solution became a persistent light-blue color). The O_3 (g) was removed and the solution was purged with N_2 (*g*), producing a light-yellow solution. Me_2S was then added (115 μL, 1.56 mmol, 5.00 equiv) at -78 °C dropwise. The reaction mixture

was then allowed to warm slowly to 23 °C over 2 h under N_2 (*g*). The solvent was then removed by rotary evaporation leaving a crude yellow oil that was purified by automated flash chromatography (0 → 100%, EtOAc/hexanes, continuous gradient) to afford β-alkoxy aldehyde **3.12** as a light-yellow oil (79.6 mg, 90%):

R_f = 0.50 (streaked spot, 50% EtOAc/hexanes, stained yellow-orange with DNPH solution); **$[\alpha]_D^{23}$** +120.67 (*c* 0.60, $CHCl_3$); **IR (thin film)**: 2995, 2943, 1739, 1708 cm^{-1}; **^{1}H-NMR** (600 MHz, $CDCl_3$) δ 9.79 (s, 1H), 4.43 (d, *J* = 14.0 Hz, 1H), 4.00 (d, *J* = 14.0 Hz, 1H), 3.77 (s, 3H), 2.98 (qd, *J* = 7.3, 0.7 Hz, 1H), 2.79 (d, *J* = 0.7 Hz, 3H), 1.49 (s, 3H), 1.43 (s, 3H), 1.18 (d, *J* = 7.2 Hz, 3H); **^{13}C-NMR** (150 MHz, $CDCl_3$) δ 200.4, 174.7, 169.2, 99.3, 83.4, 63.7, 57.4, 53.2, 45.3, 29.2, 25.9, 22.8, 7.2; **HRMS (ESI+)** *m/*z calcd. for $C_{13}H_{20}NO_6$ $[M+H]^+$: 286.1285, found: 286.1286.

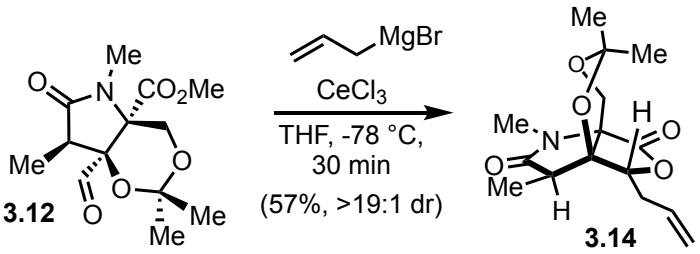

(7a*S*,8*S*)-8-allyl-2,2,5,7-tetramethyl-4*H*,5*H*-4a,7a-(methanooxymethano)[1,3]dioxino[5,4-*b*]pyrrole-6,10(7*H*)-dione (3.14): A flame-dried, 50 mL single-necked recovery flask fitted with a T-bore Schlenk adapter connected to an Ar (*g*) balloon and vacuum was charged with anhydrous $CeCl_3$ (211.8 mg, 0.860 mmol, 4.00 equiv) and placed under high vacuum, heated to 140 °C in an aluminum heating block, and stirred vigorously for 2.5 h. The atmosphere in the flask was purged with Ar by three cycles of vacuum/backfilling and heat was then removed, allowing the flask to cool

to 23 °C before quickly replacing the Schlenk adapter with a rubber septum and Ar balloon. THF was then added (4 mL) with vigorous stirring. The resulting milky-white suspension was sonicated for 30 min then cooled to -78 °C in a dry ice/acetone bath with vigorous stirring for 15 min. AllylMgBr solution (860 μL, 1.0 M in diethyl ether, 0.86 mmol, 4.0 equiv) was added to the cold suspension of $CeCl_3$ by dropwise addition from a plastic 1 mL luer-lock syringe. A dark-yellow suspension resulted and to this was added a solution of β-alkoxy aldehyde **3.12** (4.0 mL, 0.053 M in THF, 0.21 mmol, 1.0 equiv) by dropwise addition from a 6 mL plastic syringe over 10 min. The reaction mixture was stirred for an additional 30 min at -78 °C, after which it was quenched at this temperature by addition of a saturated solution of $NaHCO_3$ (aq.) (12 mL), allowed to warm slowly to 23 °C, and diluted with EtOAc (20 mL). The layers were separated, and the aqueous layer was extracted with EtOAc (2x 150 mL). The combined organic layers were dried over $MgSO_4$, filtered through celite, and concentrated by rotary evaporation to a solid that was purified by automated flash chromatography (0 → 80%, EtOAc/hexanes, continuous gradient) to afford bicyclic γ-lactone **3.14** as a colorless crystalline solid (35.6 mg, 57%, >19:1 dr):

R_f = 0.61 (50% EtOAc/hexanes, stained yellow with $KMnO_4$ solution); **[α]** $\overset{24}{D}$ -3.44 (*c* 1.63, $CHCl_3$); **IR (thin film)**: 2988, 2941, 1782, 1694 cm^{-1}; **^{1}H-NMR** (600 MHz, $CDCl_3$) δ 5.87 (ddt, *J* = 17.1, 10.2, 6.7 Hz, 1H), 5.23 (app dd, *J* = 17.1, 1.3 Hz, 1H), 5.19 (dd, *J* = 10.2, 1.0 Hz, 1H), 4.71 (dd, *J* = 9.4, 4.0 Hz, 1H), 4.14 (d, *J* = 13.2 Hz, 1H), 4.10 (d, *J* = 13.2 Hz, 1H), 3.04 (s, 3H), 2.66 (q, *J* = 7.2 Hz, 1H), 2.58-2.54 (m, 1H), 2.43-2.38 (m, 1H), 1.51 (s, 3H), 1.38 (s, 3H), 1.21 (d, *J* = 7.2 Hz, 3H); **^{13}C-NMR** (150 MHz, $CDCl_3$) δ 174.5, 171.9, 132.3, 119.1, 100.4, 83.1, 80.7, 61.9, 57.5, 41.6, 33.7, 28.4, 26.5, 26.1, 8.8; **HRMS (ESI+)** *m/*z calcd. for $C_{15}H_{22}NO_5$ $[M+H]^+$: 296.1492, found: 296.1493.

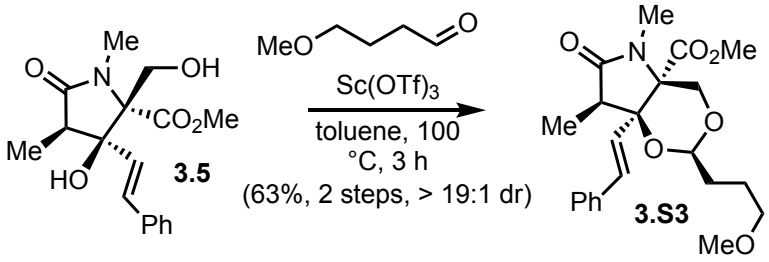

Methyl-(2*R*,4a*S*,7*R*,7a*S*)-2-(3-methoxypropyl)-5,7-dimethyl-6-oxo-7a-((*E*)-styryl)tetrahydro-[1,3]dioxino[5,4-*b*]pyrrole-4a(4*H*)-carboxylate (3.S3): A 15 mL, single-necked, pressure reaction vessel was charged with crude diol lactam **3.5** (0.500 mmol, 1.00 equiv; obtained from the previous allylic oxidation reaction but in this case without triturating with CH_2Cl_2), anhydrous toluene (5 mL), 4-methoxybutanal[160, 161] (454 mg, 5.00 mmol, 10.0 equiv), and $Sc(OTf)_3$ (14 mg, 0.028 mmol, 0.057 equiv). The pressure vessel was tightly sealed, stirred vigorously, heated to 100 °C in an oil bath, and maintained at this temperature for 3.5 h. Heating was stopped and the resulting reaction mixture was allowed to cool to 23 °C. The mixture was concentrated by rotary evaporation to a crude, dark-brown oil that was purified by automated flash chromatography (0 → 100%, EtOAc/hexanes, continuous gradient) to afford acetal **3.S3** as a yellow oil (126 mg, 63%, 2 steps, >19:1 dr):

R_f = 0.41 (50% EtOAc/hexanes, UV-active); **$[\alpha]_D^{23}$** +93.07 (*c* 1.50, $CHCl_3$); **IR (thin film)**: 2937, 2876, 2829, 1737, 1707 cm^{-1}; **^{1}H-NMR** (400 MHz, $CDCl_3$) δ 7.36-7.27 (m, 5H), 6.68 (d, *J* = 16.0 Hz, 1H), 5.97 (d, *J* = 16.0 Hz, 1H), 4.88 (m, 1H), 4.26 (d, *J* = 13.5 Hz, 1H), 4.19 (d, *J* = 13.5 Hz, 1H), 3.79 (s, 3H), 3.40-3.37 (m, 2H), 3.31 (s, 3H), 2.84 (s, 3H), 2.75 (q, *J* = 7.2 Hz, 1H), 1.73-1.68 (m, 4H), 1.11 (d, *J* = 7.2 Hz, 3H); **^{13}C-NMR** (150 MHz, $CDCl_3$) δ 176.4, 170.3, 135.9, 134.0, 128.9 (2), 128.6, 126.8 (2), 122.7, 97.0, 81.2, 72.5,

67.8, 63.7, 58.7, 53.2, 46.0, 31.4, 26.2, 23.9, 5.8; **HRMS (ESI+)** *m/*z calcd. for $C_{22}H_{30}NO_6$ $[M+H]^+$: 404.2068, found: 404.2068.

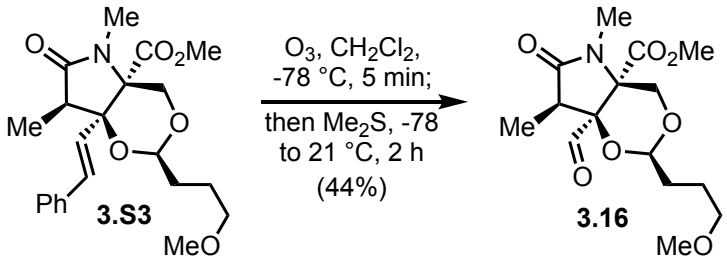

Methyl-(2*R*,4a*S*,7*R*,7a*S*)-7a-formyl-2-(3-methoxypropyl)-5,7-dimethyl-6-oxotetrahydro-[1,3]dioxino[5,4-*b*]pyrrole-4a(4*H*)-carboxylate (3.16): To an undried 15 mL vial fitted with a septum cap was added styryl acetal **3.S3** (111 mg, 0.270 mmol, 1.00 equiv) followed by CH_2Cl_2 (4 mL). The resulting yellow solution was stirred and cooled to -78 °C in a dry ice/acetone bath under N_2 (*g*) atmosphere over 10 min. The septum was then removed and O_3 (*g*) was bubbled through the solution with a sparge tube for 5 min (until the reaction solution became a persistent light-blue color). The O_3 (g) was removed and the solution was purged with N_2 (*g*), producing a light-yellow solution. Me_2S (101 μL, 1.37 mmol, 5.00 equiv) was then added dropwise at -78 °C. The reaction mixture was then allowed to warm slowly to 23 °C over 2 h under N_2 (*g*). The solvent was then removed by rotary evaporation to a crude yellow oil that was purified by automated flash chromatography (0 → 100%, EtOAc/hexanes, continuous gradient) to afford β-alkoxy aldehyde **3.16** as a pale yellow oil (38.8 mg, 44%):

$\mathbf{R_f}$ = 0.31 (streaked spot, 50% EtOAc/hexanes, stained yellow-orange with DNPH solution); $\mathbf{[\alpha]}_D^{20}$ +99.44 (*c* 1.44, $CHCl_3$); **IR (thin film)** 2940, 2879, 2833, 1738, 1709 cm^{-1}; **^{1}H-NMR** (400 MHz, $CDCl_3$) δ 9.75 (s, 1H), 4.90 (app t, *J* = 4.8 Hz, 1H), 4.27 (d, *J* =

13.6 Hz, 1H), 4.18 (d, *J* = 13.6 Hz, 1H), 3.76 (s, 3H), 3.37 (t, *J* = 6.1 Hz, 2H), 3.31 (s, 3H), 3.07 (q, *J* = 7.2 Hz, 1H), 2.82 (s, 3H), 1.76-1.66 (m, 4H), 1.15 (d, *J* = 7.2 Hz, 3H); **^{13}C-NMR** (100 MHz, $CDCl_3$) δ 198.3, 174.8, 168.9, 99.0, 84.4, 72.3, 64.8, 64.3, 58.7, 53.3, 43.8, 31.3, 26.0, 23.7, 6.9; **HRMS (ESI+)** *m/*z calcd. for $C_{15}H_{24}NO_7$ $[M+H]^+$: 330.1547, found: 330.1548.

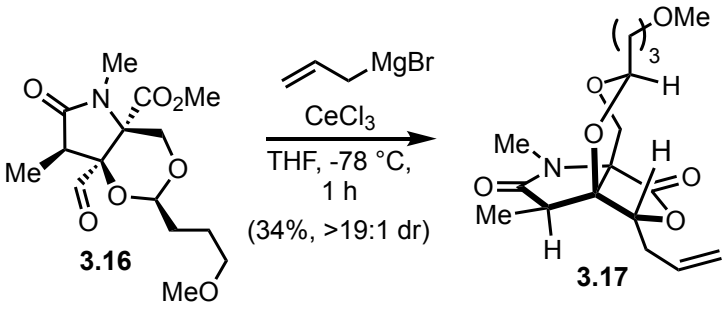

(2*S*,4a*R*,7a*S*,8*S*)-8-allyl-2-(3-methoxypropyl)-5,7-dimethyl-4*H*,5*H*-4a,7a-(methanooxymethano)[1,3]dioxino[5,4-*b*]pyrrole-6,10(7*H*)-dione (3.17): The same procedure for allylation-lactonization as applied toward the synthesis of **3.14** (*vide supra*) was employed. Reagent amounts: aldehyde **3.16** (27.0 mg, 0.082 mmol, 1.00 equiv); allylmagnesium bromide (1.0 M in THF, 86 mL, 0.086 mmol, 1.05 equiv); $CeCl_3$ (50.5 mg, 0.205 mmol, 2.50 equiv); THF (3 mL total). The crude material was purified by flash column chromatography (0 → 100%, EtOAc/hexanes, continuous gradient) to afford bicycle **3.17** as a colorless solid (9.6 mg, 34%, >19:1 dr):

R*f* = 0.69 (50% EtOAc/hexanes, stained yellow with $KMnO_4$ solution); $[\alpha]_D^{25}$ -14.72 (*c* 1.11, $CHCl_3$); **IR (thin film)**: 2926, 2874, 1784, 1707 cm^{-1}; **^{1}H-NMR** (600 MHz, $CDCl_3$) δ 5.87 (ddt, *J* = 17.0, 10.2, 6.7 Hz, 1H), 5.25 (app dq, *J* = 17.0, 1.3 Hz, 1H), 5.21 (app dq, *J* = 10.2, 1.3 Hz, 1H), 4.88 (app t, *J* = 4.9 Hz, 1H), 4.81 (dd, *J* = 9.3, 4.0 Hz, 1H), 4.47 (d,

J = 13.7 Hz, 1H), 3.84 (d, J = 13.7 Hz, 1H), 3.37 (t, J = 6.2 Hz, 2H), 3.31 (s, 3H), 3.08 (d, J = 0.74 Hz, 3H), 2.68 (dq, J = 7.2, 0.74 Hz, 1H), 2.56 (dddt, J = 14.9, 6.7, 4.0, 1.3 Hz, 1H), 2.45 (dddt, J = 14.9, 9.3, 6.7, 1.3 Hz, 1H), 1.75-1.71 (m, 2H), 1.67-1.62 (m, 2H), 1.23 (d, J = 7.2 Hz, 3H); **^{13}C-NMR** (150 MHz, $CDCl_3$) δ 174.3, 170.8, 132.0, 119.3, 97.3, 81.1, 77.1, 72.3, 62.3, 60.3, 58.7, 41.3, 33.8, 31.3, 26.1, 23.7, 7.8; **HRMS (ESI+)** *m/z* calcd. for $C_{17}H_{25}NO_6Na$ $[M+Na]^+$: 362.1574, found: 362.1576.

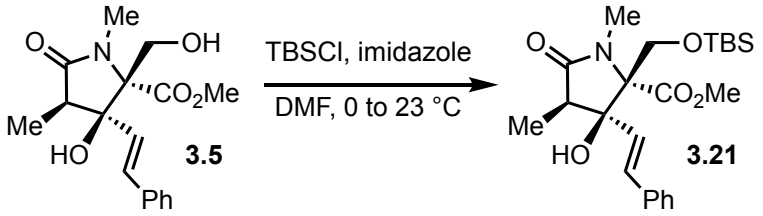

Methyl-(2*S*,3*S*,4*R*)-2-(((*tert*-butyldimethylsilyl)oxy)methyl)-3-hydroxy-1,4-dimethyl-5-oxo-3-((*E*)-styryl)pyrrolidine-2-carboxylate (3.21): To a 50 mL, single-necked, round-bottomed flask containing 1,3-diol lactam **3.5** (815 mg, 2.55 mmol, 1.00 equiv) was added DMF (4 mL) and the resulting solution was cooled to 0 °C with stirring in an ice bath. Imidazole (680 mg, 9.99 mmol, 5.14 equiv) was then added, followed by TBSCl (633 mg, 4.20 mmol, 2.16 equiv). The mixture was stirred for 1 h at 0 °C. The cooling bath was then removed and the mixture was stirred for 1 h (until TLC indicated complete consumption of starting 1,3-diol **3.5**). The reaction mixture was quenched by pouring into a separatory funnel containing a saturated solution of NH_4Cl (aq.) (25 mL), the reaction flask was rinsed with Et_2O (25 mL), and the layers were separated. The aqueous layer was extracted with Et_2O (3 x 12 mL). The combined organic layers were washed with H_2O (15 mL), brine (15 mL), dried over $MgSO_4$, filtered through celite, and concentrated by rotary evaporation. The resulting crude material was used in the next step without purification.

For purposes of characterization some of the crude material was purified by automated flash chromatography (0 → 65%, EtOAc/hexanes, continuous gradient; **3.21** elutes at ~50% EtOAc/hexanes), affording β-silyloxy ester **3.21** as a colorless sticky foam:

R_f = 0.80 (50% EtOAc/hexanes, UV-active); **[α]** $\overset{22}{D}$ +12.34 (*c* 1.88, $CHCl_3$); **IR (thin film)**: 3367, 2953, 2931, 2886, 2857, 1740, 1684 cm^{-1}; **^{1}H-NMR** (600 MHz, $CDCl_3$) δ 7.38-7.27 (m, 5H), 6.87 (d, *J* = 15.7 Hz, 1H), 5.94 (d, *J* = 15.7 Hz, 1H), 4.30 (d, *J* = 11.4 Hz, 1H), 4.24 (s, 1H), 4.03 (d, *J* = 11.4 Hz, 1H), 3.72 (s, 3H), 2.84 (s, 3H), 2.75 (q, *J* = 7.2 Hz, 1H), 1.14 (d, *J* = 7.2 Hz, 3H), 0.90 (s, 9H), 0.16 (s, 3H), 0.13 (s, 3H); **^{13}C-NMR** (150 MHz, $CDCl_3$) δ 176.7, 170.2, 136.4, 132.3, 128.8 (2), 128.2, 128.0, 126.8 (2), 81.0, 75.3, 60.9, 52.8, 45.5, 27.3, 25.8 (3), 18.1, 7.5, -5.65, -5.66; **HRMS (ESI+)** *m/*z calcd. for $C_{23}H_{35}NO_5SiNa$ $[M+Na]^+$: 456.2177, found: 456.2178.

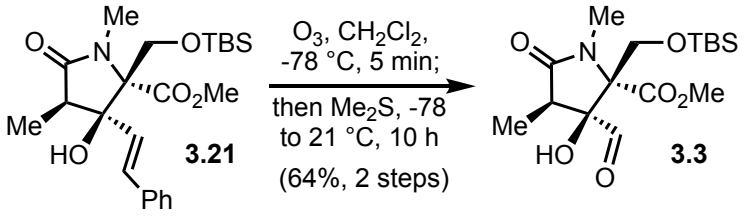

Methyl-(2*S*,3*S*,4*R*)-2-(((*tert*-butyldimethylsilyl)oxy)methyl)-3-formyl-3-hydroxy-1,4-dimethyl-5-oxopyrrolidine-2-carboxylate (3.3): To an undried 50 mL round-bottomed flask containing crude **3.21** (~5.63 mmol, 1.00 equiv) was added CH_2Cl_2 (15 mL). The resulting solution was stirred and cooled to -78 °C in a dry ice/acetone bath under N_2 (*g*) atmosphere over 10 min. The flask was then opened and the solution was perfused with O_3 (*g*) for 5 min (until the reaction solution became a persistent light-blue color). The O_3 (g) was removed and the solution was purged with N_2 (*g*), producing a light-yellow solution. Me_2S (2.10 mL, 23.2 mmol, 5.00 equiv) was then added dropwise at -78 °C. The reaction

mixture was then allowed to warm slowly to 23 °C over 10 h under N_2 (*g*). The solvent was then removed by rotary evaporation to provide a crude yellow oil that was purified by automated flash chromatography (0 → 75%, EtOAc/hexanes, continuous gradient; **3.3** elutes at ~60% EtOAc/hexanes) to afford □-alkoxy aldehyde **3.3** as a light-yellow oil (1.30 g, 64%, 2 steps):

R_f = 0.31 (streaked spot, 50% EtOAc/hexanes, stained yellow with DNPH solution); **$[\alpha]_D^{22.8}$** +99.44 (*c* 1.44, $CHCl_3$); **IR (thin film)**: 3320, 2957, 2934, 2888, 2860, 1740, 1689 cm^{-1}; **^{1}H-NMR** (600 MHz, $CDCl_3$) δ 9.57 (s, 1H), 4.09 (d, *J* = 10.5 Hz, 1H), 4.04 (br s, 1H), 3.99 (d, *J* = 10.5 Hz, 1H), 3.77 (s, 3H), 2.94 (s, 3H), 2.88 (q, *J* = 7.2 Hz, 1H), 1.04 (d, *J* = 7.2 Hz, 3H), 0.86 (s, 9H), 0.07 (s, 3H), 0.05 (s, 3H); **^{13}C-NMR** (150 MHz, $CDCl_3$) δ 198.4, 174.1, 169.6, 83.6, 75.1, 63.7, 53.0, 42.0, 27.8, 25.7 (3), 18.1, 7.3, -5.7, -5.8; **HRMS (ESI+)** *m/*z calcd. for $C_{16}H_{29}NO_6SiNa$ $[M+Na]^+$: 382.1656, found: 382.1655.

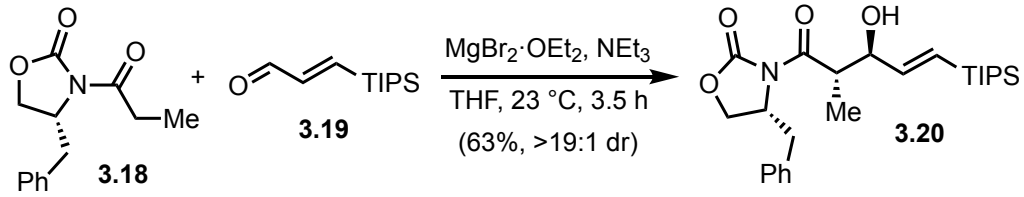

(*R*)-4-benzyl-3-((2*S*,3*R*,*E*)-3-hydroxy-2-methyl-5-(triisopropylsilyl)pent-4-enoyl)oxazolidin-2-one (3.20): The following is a modified procedure of the Evans *anti* aldol reaction.[150, 151] To a 50 mL, single-necked, round-bottomed flask fitted with a rubber septum was added crystalline priopionyloxazolidinone[152] **3.18** (1.50 g, 6.43 mmol, 1.00 equiv) followed by $MgBr_2 \cdot OEt_2$ (2.49 g, 9.65 mmol, 1.50 equiv) and THF (26 mL) (note: it was found that this reaction suffers from reduced yield when conducted on greater than 1.5 g scale, thus multiple batches were run in parallel and combined for work-up and

purification to maintain a decent yield of the desired aldolate product). To this orange solution was added freshly distilled NEt_3 (2.24 mL, 16.1 mmol, 2.50 equiv), resulting in a fine, beige suspension to which was added neat liquid silylacrolein[153] **3.19** (1.43 g, 6.75 mmol, 1.05 equiv). The mixture was stirred at 23 °C for ~3.5 h before being poured into aqueous HCl (1 M, 30 mL per batch). The reaction flask was rinsed with EtOAc (30 mL per batch) and the layers were separated. The aqueous layer was extracted with EtOAc (3 x 12 mL per batch). The combined organic layers were washed with brine (30 mL per batch), dried over $MgSO_4$, filtered through celite, and concentrated by rotary evaporation to a crude brown oil that was purified by automated flash chromatography (0 → 60%, EtOAc/hexanes, continuous gradient; **3.20** elutes at ~30% EtOAc/hexanes), affording aldolate **3.20** as a sticky yellow oil (3.61 g, 63%, >19:1 dr, two batches combined):

$\mathbf{R_f}$ = 0.23 (10% EtOAc/hexanes, stained dark-blue with anisaldehyde solution, slightly UV-active); $\mathbf{[\alpha]}_D^{22.0}$ -24.88 (*c* 3.73, $CHCl_3$); **IR (thin film)**: 3505, 2941, 2890, 2865, 1781, 1699, 1620 cm^{-1}; **^{1}H-NMR** (600 MHz, $CDCl_3$) δ 7.35-7.32 (m, 2H), 7.29-7.23 (m, 3H), 6.14 (dd, *J* = 18.9, 6.1 Hz, 1H), 5.88 (dd, *J* = 18.9, 1.3 Hz, 1H), 4.70–4.66 (m, 1H), 4.26 (m, 1H), 4.21-4.18 (m, 1H), 4.16 (dd, *J* = 9.1, 2.8 Hz, 1H), 3.99 (m, 1H), 3.32 (dd, *J* = 13.5, 3.4 Hz, 1H), 2.74 (dd, *J* = 13.5, 9.7 Hz, 1H), 2.69 (d, *J* = 7.2 Hz, 1H), 1.22 (d, *J* = 6.9 Hz, 3H), 1.12-1.07 (m, 3H), 1.06-1.03 (m, 18H); **^{13}C-NMR** (150 MHz, $CDCl_3$) δ 176.4, 153.7, 147.8, 135.4, 129.6 (2), 129.1 (2), 127.5, 127.2, 78.4, 66.2, 55.7, 43.1, 38.0, 18.78 (3), 18.76 (3), 14.7, 10.9 (3); **HRMS (ESI+)** *m/*z calcd. for $C_{25}H_{39}NO_4SiNa$ $[M+Na]^+$: 468.2541, found: 468.2542.

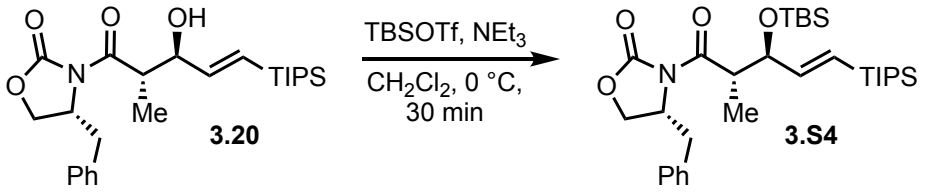

(*R*)-4-benzyl-3-((2*S*,3*R*,*E*)-3-((*tert*-butyldimethylsilyl)oxy)-2-methyl-5-(triisopropylsilyl)pent-4-enoyl)oxazolidin-2-one (3.S4): To a 50 mL, single-necked, round-bottomed flask charged with aldolate **3.20** (3.03 g, 6.80 mmol, 1.00 equiv) was added CH_2Cl_2 (15 mL). The resulting solution was cooled to 0 °C in an ice bath over 5 min and freshly distilled NEt_3 (1.90 mL, 13.6 mmol, 2.00 equiv) was then added followed by TBSOTf (1.87 mL, 8.16 mmol, 1.20 equiv) dropwise over ~2 min. The mixture was stirred at 0 °C for 30 min before being poured into saturated, aqueous $NaHCO_3$ (50 mL). The reaction flask was rinsed with Et_2O (40 mL) and the layers were separated. The aqueous layer was extracted with Et_2O (3 x 30 mL) and the combined organic layers were dried over $MgSO_4$, filtered through a plug of SiO_2 over celite. The filter cake was rinsed with Et_2O (25 mL) and the volatiles were removed by rotary evaporation and high vacuum. The resulting crude silyl aldolate **3.S4**, a yellow oil, was used in the next step without purification.

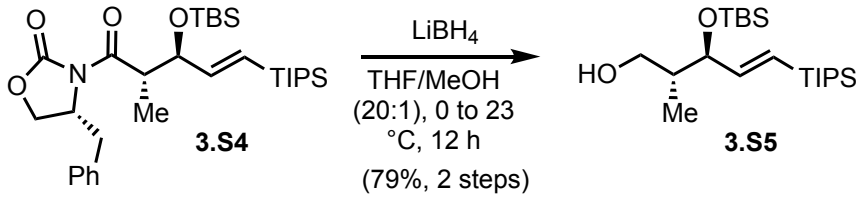

(2*R*,3*R*,*E*)-3-((*tert*-butyldimethylsilyl)oxy)-2-methyl-5-(triisopropylsilyl)pent-4-en-1-ol (3.S5): To a 50 mL, single-necked, round-bottomed flask charged with silyl aldolate **3.S4** was added THF (20 mL) followed by MeOH (1 mL). The mixture was cooled to 0 °C

in an ice bath over 5 min before adding a solution of $LiBH_4$ (2.0 M in THF, 6.80 mL, 13.6 mmol, 2.00 equiv) and was stirred, and allowed to warm overnight (~12 h). The reaction was quenched at 23 °C by careful dropwise addition (note: vigorous gas evolution) of saturated, aqueous NH_4Cl (30 mL) and then transferred to a separatory funnel with Et_2O (30 mL). The layers were separated and the aqueous layer was extracted with Et_2O (3 x 20 mL). The combined organic layers were dried over $MgSO_4$, filtered through, celite and concentrated by rotary evaporation to a colorless oil that was purified by automated flash chromatography (0 → 50%, EtOAc/hexanes, continuous gradient; **3.S5** elutes at 25-30% EtOAc/hexanes), affording primary alcohol **3.S5** as a colorless oil (2.08 g, 79% over two steps):

R_f = 0.85 (30% EtOAc/hexanes, stained dark-blue with anisaldehyde solution); **[α]** $_D^{24.2}$ +24.48 (*c* 2.32, $CHCl_3$); **IR (thin film)**: 3385 br, 2940, 2891, 2865, 1619 cm^{-1}; **^{1}H-NMR** (600 MHz, $CDCl_3$) δ 6.08 (dd, *J* = 19.0, 6.0 Hz, 1H), 5.73 (dd, *J* = 19.0, 1.2 Hz, 1H), 4.09 (td, *J* = 6.0, 1.2 Hz, 1H), 3.75 (ddd, *J* = 10.9, 5.5, 3.5 Hz, 1H), 3.56 (dt, *J* = 10.9, 5.8 Hz, 1H), 2.69 (td, *J* = 5.6, 1.7 Hz, 1H), 1.76-1.70 (m, 1H), 1.11-1.07 (m, 3H), 1.05-1.03 (m, 18H), 0.98 (d, *J* = 7.1 Hz, 3H), 0.91 (s, 9H), 0.10 (s, 3H), 0.05 (s, 3H); **^{13}C-NMR** (150 MHz, $CDCl_3$) δ 149.9, 124.8, 81.5, 66.0, 40.9, 26.0 (3), 18.78 (3), 18.77 (3), 18.2, 14.4, 11.0 (3), -4.0, -4.8; **HRMS (ESI+)** *m/*z calcd. for $C_{21}H_{46}O_2Si_2Na$ $[M+Na]^+$: 409.2929, found: 409.2931.

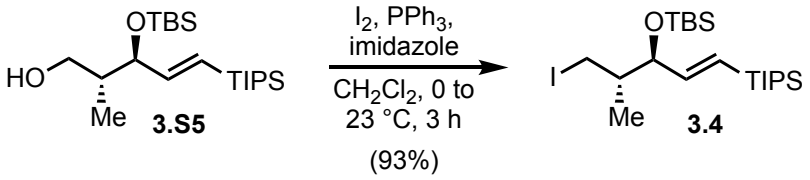

***tert*-butyl(((3*S*,4*S*,*E*)-5-iodo-4-methyl-1-(triisopropylsilyl)pent-1-en-3-yl)oxy)dimethylsilane (3.4):** To a 100 mL, single-necked, round-bottomed flask charged with primary alcohol **3.S5** (1.09 g, 2.81 mmol, 1.00 equiv) was added CH_2Cl_2 (18 mL). The resulting solution was cooled to 0 °C in an ice bath over 5 min before adding imidazole (478 mg, 7.03 mmol, 2.50 equiv), PPh_3 (1.11 g, 4.22 mmol, 1.50 equiv), and iodine (1.07 g, 4.22 mmol, 1.50 equiv) in that order. The mixture was stirred at 0 °C and allowed to warm over ~3 h before being diluted with hexanes (65 mL). The reaction flask was then capped and placed in a -20 °C freezer overnight (~10 h). Afterward, the reaction mixture was poured into saturated, aqueous $Na_2S_2O_3$ (60 mL), the flask was rinsed with hexanes (25 mL) and the layers were separated. The organic layer was washed with brine (60 mL), dried over $MgSO_4$, and filtered through a pad of basic Al_2O_3 over celite and the filter cake was rinsed with hexanes (100 mL). The combined organics were concentrated by rotary evaporation and residual solvent was removed under high vacuum, affording primary iodide **3.4** as a colorless liquid (1.29 g, 93%) that did not require further purification:

$\mathbf{R}_f$ = 0.87 (10% EtOAc/hexanes, stained with anisaldehyde solution, UV-active); $[\alpha]_D^{23.6}$ -5.60 (*c* 2.43, $CHCl_3$); **IR (thin film)**: 2957, 2940, 2891, 2864, 1617 cm^{-1}; **^{1}H-NMR** (600 MHz, $CDCl_3$) δ 5.99 (dd, *J* = 19.0, 6.6 Hz, 1H), 5.74 (dd, *J* = 19.0, 1.1 Hz, 1H), 3.95 (td, *J* = 6.6, 1.1 Hz, 1H), 3.30 (dd, *J* = 9.5, 4.7 Hz, 1H), 3.23 (dd, *J* = 9.5, 6.5 Hz, 1H), 1.64-1.57 (m, 1H), 1.10-1.07 (m, 3H), 1.07-1.04 (m, 18H), 0.96 (d, *J* = 6.7 Hz, 3H), 0.90 (s, 9H),

0.09 (s, 3H), 0.03 (s, 3H); **^{13}C-NMR** (150 MHz, $CDCl_3$) δ 148.6, 126.2, 79.6, 41.5, 26.1 (3), 18.8 (6), 18.3, 17.2, 13.8, 11.0 (3), -3.8, -4.6

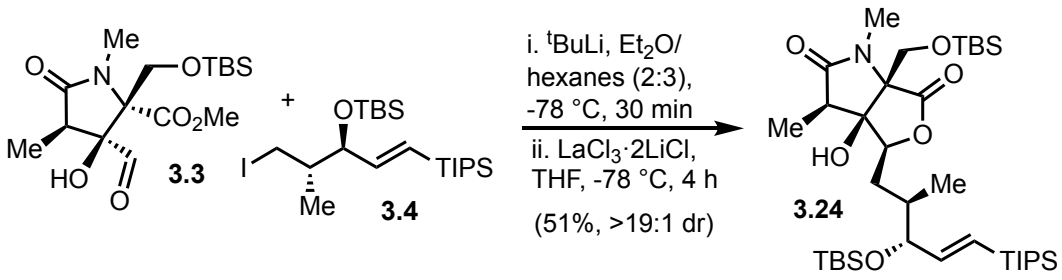

(3*R*,3a*S*,4*S*,6a*S*)-4-((2*R*,3*R*,*E*)-3-((*tert*-butyldimethylsilyl)oxy)-2-methyl-5-(triisopropylsilyl)pent-4-en-1-yl)-6a-(((*tert*-butyldimethylsilyl)oxy)methyl)-3a-hydroxy-1,3-dimethyltetrahydro-6*H*-furo[3,4-*b*]pyrrole-2,6(3*H*)-dione (3.24): A thick-walled 25 mL, single-necked, round-bottomed flask, fitted with a rubber septa and a teflon stir bar (51 x 19 mm, egg-shaped) and connected to a Schlenk manifold via a 16-guage needle and tubing and was carefully flame dried under high vacuum. A balloon of Ar (*g*) was then attached to the flask via a needle and the atmosphere in the flask was purged by three cycles of vacuum/Ar (*g*). Once the flask had cooled to 23 °C, primary iodide **3.4** was added via a plastic 1 mL syringe fitted with a disposable needle (297 mg, 0.60 mmol, 2.10 equiv). Dry hexanes was added (1.2 mL) followed by dry Et_2O (0.8 mL). The resulting clear solution was thoroughly cooled to -78 °C in a dry ice/acetone bath over 20 min. A solution of ^{t}BuLi (1.6 M in pentane, 738 μL, 1.18 mmol, 4.20 equiv, titrated with *N*-benzylbenzamide)[162] was added dropwise over 3 min via a glass, gas-tight 1 mL syringe fitted with a 22-guage stainless-steele (1.6 M in pentane, 738 μL, 1.18 mmol, 4.20 equiv) dropwise over ~3 min. The colorless solution was stirred at -78 °C for 15 min. During this time a solution of α-hydroxyaldehyde **3.22** (101 mg, 0.28 mmol, 1.00 equiv)

and $LaCl_3 \cdot 2LiCl$ (0.6 M in THF, 1.17 mL, 0.70 mmol, 2.50 equiv) in THF (0.8 mL) was prepared in a flame-dried 1.5-dram vial under N_2 (*g*) atmosphere. This homogenous yellow solution was then added slowly along the wall of the reaction vessel over ~3 min via a plastic 3 mL syringe. The vial was rinsed with an additional 1 mL of THF and transferred to the reaction mixture, which was allowed to stir at -78 °C for 4 h. The reaction mixture was quenched at -78 °C by slow addition of aqueous 0.5 M HCl (2.5 mL), diluted/transferred to a separatory funnel with EtOAc (15 mL). The layers were separated and the aqueous layer was extracted with EtOAc (3 x 7 mL). The combined organic layers were washed with brine (10 mL), dried over $MgSO_4$, filtered through celite and concentrated by rotary evaporation to a dark yellow oil that was purified by flash column chromatography (0 → 30%, EtOAc/hexanes, 10% increments, 30 mL each; **3.24** elutes at ~20% EtOAc/hexanes) affording vinylsilane **3.24** as a light-yellow oil that crystalized upon drying under high vacuum (100 mg, 51%, >19:1 dr). The stereochemical configuration at C4 was established by NOESY analysis in addition to the completion of the formal total synthesis of neooxazolomycin that is described below:

$\mathbf{R_f}$ = 0.78 (30% EtOAc/hexanes, stained dark blue with anisaldehyde solution); $\mathbf{[\alpha]}_D^{21.3}$ +21.78 (*c* 0.64, $CHCl_3$); **IR (thin film)**: 3406 br, 2956, 2937, 2889, 2863, 1771, 1676, 1619 cm^{-1};**^{1}H-NMR** (600 MHz, $CDCl_3$) δ 6.00 (dd, *J* = 19.0, 5.9 Hz, 1H), 5.71 (dd, *J* = 19.0, 1.2 Hz, 1H), 4.27 (dd, *J* = 7.9, 5.7 Hz, 1H), 4.03 (d, *J* = 11.0 Hz, 1H), 3.95 (d, *J* = 11.0 Hz, 1H), 3.95 (br s, 1H), 3.66 (s, 1H), 2.85 (s, 3H), 2.45 (q, *J* = 7.6 Hz, 1H), 2.07 (ddd, *J* = 14.3, 5.4, 4.1 Hz, 1H), 1.69-1.64 (m, 1H), 1.60-1.54 (m, 2H), 1.24 (d, *J* = 7.6 Hz, 3H), 1.10-1.02 (m, 21H), 0.90 (s, 9H), 0.89 (s, 9H), 0.13 (s, 3H), 0.12 (s, 3H), 0.06 (s, 3H), 0.02 (s, 3H); **^{13}C-NMR** (150 MHz, $CDCl_3$) δ 175.3, 171.3, 149.2, 125.2, 87.9, 80.6, 80.1, 71.6,

60.0, 45.5, 37.1, 30.6, 26.04, 26.02 (3), 25.9 (3), 18.8 (6), 18.4, 16.9, 11.7, 11.0 (3), -4.0, -4.7, -5.3, -5.6; **HRMS** (ESI+) *m/*z calcd. for $C_{36}H_{71}NO_6Si_3Na$ $[M+Na]^+$: 720.4481, found: 720.4477.

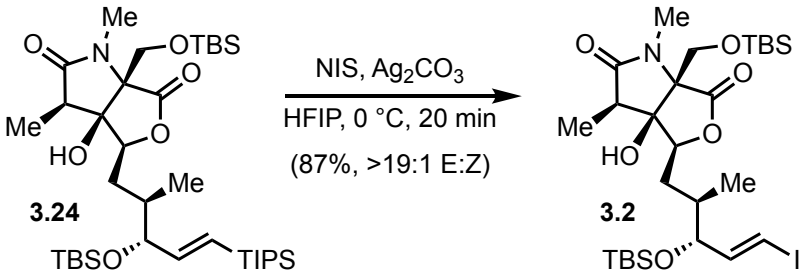

(3*R*,3a*S*,4*S*,6a*S*)-4-((2*R*,3*R*,*E*)-3-((*tert*-butyldimethylsilyl)oxy)-5-iodo-2-methylpent-4-en-1-yl)-6a-(((*tert*-butyldimethylsilyl)oxy)methyl)-3a-hydroxy-1,3-dimethyltetrahydro-6*H*-furo[3,4-*b*]pyrrole-2,6(3*H*)-dione (3.2): To a 10 mL, single-necked, round-bottomed flask charged with neooxazolomycin core vinylsilane **3.24** (18.6 mg, 0.027 mmol, 1.00 equiv) was added Ag_2CO_3 (3.7 mg, 0.013 mmol, 0.50 equiv) followed by HFIP (1 mL). The resulting green suspension was cooled to 0 °C in an ice bath and the reaction vessel was excluded from light with a sheet of aluminum foil. NIS (6.6 mg, 0.029 mmol, 1.10 equiv, excluded from light) was then added in one portion and the reaction mixture was stirred at 0 °C for 20 min before quenching at this temperature by addition of saturated, aqueous $Na_2S_2O_3$ (3 mL). The quenched reaction mixture was diluted with Et_2O (3 mL), the layers were separated and the aqueous layer was extracted with Et_2O (3 x 3 mL). The combined organic layers were washed with brine (4.5 mL), dried over $MgSO_4$, filtered through celite, and concentrated by rotary evaporation. The crude residue was purified by flash column chromatography (0 → 40%, EtOAc/hexanes, 10% increments, 20 mL each; **3.2** elutes at 20-30% EtOAc/hexanes), affording

neooxazolomycin core vinyliodide **3.2** as a white amorphous solid (15.5 mg, 87%, >19:1 *E*:*Z*). All spectroscopic data matched that previously reported. The relative and absolute stereochemistry of vinyliodide **3.2** is inferred by its comparison to the neooxazolomycin core vinyliodide prepared by Kende *et. al.* (*JACS* 1990) from glucose in ~24 steps: **R_f** = 0.82 (30% EtOAc/hexanes, stained violet with anisaldehyde solution, UV-active); **$[\alpha]_D^{23.4}$** +35.55 (*c* 1.64, $CHCl_3$); **IR (thin film)**: 3393 br, 2955, 2930, 2885, 2858, 1770, 1676, 1607 cm^{-1}; **^{1}H-NMR** (600 MHz, $CDCl_3$) δ 6.47 (dd, *J* = 14.4, 6.5 Hz, 1H), 6.24 (dd, *J* = 14.4, 1.1 Hz, 1H), 4.24 (dd, *J* = 7.9, 5.7 Hz, 1H), 4.06 (d, *J* = 11.0 Hz, 1H), 3.94 (d, *J* = 11.0 Hz, 1H), 3.92 (app t, *J* = 6.0 Hz, 1H), 3.81 (s, 1H), 2.85 (s, 3H), 2.45 (q, *J* = 7.6 Hz, 1H), 2.02 (ddd, *J* = 14.5, 5.7, 3.9 Hz, 1H), 1.69-1.64 (m, 1H), 1.59-1.54 (m, 1H), 1.26 (d, *J* = 7.6 Hz, 3H), 0.96 (d, *J* = 6.8 Hz, 3H), 0.90 (s, 9H), 0.89 (s, 9H), 0.14 (s, 3H), 0.13 (s, 3H), 0.05 (s, 3H), 0.02 (s, 3H); **^{13}C-NMR** (150 MHz, $CDCl_3$) δ 175.2, 171.1, 147.2, 87.5, 80.6, 79.3, 77.4, 71.3, 60.3, 45.5, 36.7, 30.6, 26.1, 25.95, 25.89, 18.36, 18.33, 16.3, 11.8, -4.2, -4.8, -5.4, -5.6; **HRMS** (ESI+) *m/z* calcd. for $C_{27}H_{50}INO_6Si_2Na$ $[M+Na]^+$: 690.2114, found: 690.2109.

Table 3.1. ^{1}H-NMR Comparison to Kende's vinyliodide (Compound **3.2**):

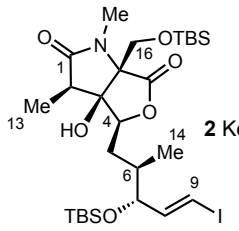

2 Kende's vinyliodide

	Kende et. al. *JACS* 1990 (400 MHz, $CDCl_3$) δ ppm	**This Work (600 MHz, $CDCl_3$) δ ppm**	Δ δ
H2	2.46 (q, 1H)	2.45 (q, *J* = 7.6 Hz, 1H)	0.01
H13	1.28 (d, *J* = 7.6 Hz, 3H)	1.26 (d, *J* = 7.6 Hz, 3H)	0.02
C3-OH	3.82 (s, 1H)	3.81 (s, 1H)	0.01
H16[a]	3.95 (d, *J* = 11.3 Hz, 1H)	3.94 (d, *J* = 11.0 Hz, 1H)	0.01
H16[b]	4.08 (d, *J* = 10.9 Hz, 1H)	4.06 (d, *J* = 11.0 Hz, 1H)	0.02
N-Me	2.87 (s, 3H)	2.85 (s, 3H)	0.02
H4	4.26 (dd, *J* = 7.5, 6.4 Hz, 1H)	4.24 (dd, *J* = 7.9, 5.7 Hz, 1H)	0.02
H5[a]	not given	1.59 - 1.54 (m, 1H)	-
H5[b]	2.03 (m, 1H)	2.02 (ddd, *J* = 14.5, 5.7, 3.9 Hz, 1H)	0.01
H6	1.65 (m, 1H)	1.69 - 1.64 (m, 1H)	0.02
H14	0.97 (d, *J* = 6.6 Hz, 3H)	0.96 (d, *J* = 6.8 Hz, 3H)	0.01
H7	3.93 (t, 1H)	3.92 (app t, *J* = 6.0 Hz, 1H)	0.01
H8	6.49 (dd, *J* = 14.4, 6.4 Hz, 1H)	6.47 (dd, *J* = 14.4, 6.5 Hz, 1H)	0.02
H9	6.25 (d, *J* = 14.4 Hz, 1H)	6.24 (dd, *J* = 14.4, 1.1 Hz, 1H)	0.01
C16 OTBS-Me[a]	0.14 (s, 3H)	0.13 (s, 3H)	0.01
C16 OTBS-Me[b]	0.15 (s, 3H)	0.14 (s, 3H)	0.01
C16 OTBS-^{t}Bu	0.91 (s, 9H)	0.90 (s, 9H)	0.01
C7 OTBS-Me[a]	0.04 (s, 3H)	0.02 (s, 3H)	0.02
C7 OTBS-Me[b]	0.06 (s, 3H)	0.05 (s, 3H)	0.01
C7 OTBS-^{t}Bu	0.90 (s, 9H)	0.89 (s, 9H)	0.01

3.5 References

1. Moloney, M. G.; Trippier, P., C.; Yaqoob, M.; Wang, Z., The Oxazolomycins: A Structurally Novel Class of Bioactive Compounds. *Curr. Drug Disc. Technol.* **2004,** *1* (3), 181-199.

2. Aizawa, S.; Shibuya, M.; Shirato, S., Resistaphilin, A New Antibiotic. I, Production, Isolation and Properties. *J. Antibiot.* **1971,** *24* (6), 393-396.

3. Mori, T.; Takahashi, K.; Kashiwabara, M.; Uemura, D.; Katayama, C.; Iwadare, S.; Shizuri, Y.; Mitomo, R.; Nakano, F.; Matsuzaki, A., Structure of Oxazolomycin, a Novel Beta-Lactone Antibiotic. *Tetrahedron Lett.* **1985,** *26* (8), 1073-1076.

4. Ogura, M.; Nakayama, H.; Furihata, K.; Shimazu, A.; Seto, H.; Otake, N., Structure of a New Antibiotic Curromycin A Produced by a Genetically Modified Strain of *Streptomyces Hygroscopicus* a Polyether Antibiotic Producing Organism. *J. Antibiot.* **1985,** *38* (5), 669-673.

5. Ogura, M.; Nakayama, H.; Furihata, K.; Shimazu, A.; Seto, H.; Otake, N., Isolation and Structural Determination of a New Antibiotic Curromycin-B. *Agric. Biol. Chem.* **1985,** *49* (6), 1909-1910.

6. Takahashi, K.; Kawabata, M.; Uemura, D.; Iwadare, S.; Mitomo, R.; Nakano, F.; Matsuzaki, A., Structure of Neooxazolomycin, an Antitumor Antibiotic. *Tetrahedron Lett.* **1985,** *26* (8), 1077-1078.

7. Ikeda, Y.; Kondo, S.; Naganawa, H.; Hattori, S.; Hamada, M.; Takeuchi, T., New Triene-β-lactone Antibiotics, Triedimycins A and B. *J. Antibiot.* **1991,** *44* (4), 453-455.

8. Ryu, G.; Hwang, S.; Kim, S. K., 16-methyloxazolomycin, a new antimicrobial and cytotoxic substance produced by a Streptomyces sp. *J. Antibiot.* **1997,** *50* (12), 1064-1066.

9. Kanzaki, H.; Wada, K.-i.; Nitoda, T.; Kawazu, K., Novel Bioactive Oxazolomycin Isomers Produced by Streptomyces albus JA3453. *Biosci., Biotechnol., Biochem.* **1998,** *62* (3), 438-442.

11. Otani, T.; Yoshida, K. I.; Kubota, H.; Kawai, S.; Ito, S.; Hori, H.; Ishiyama, T.; Oki, T., Novel Triene-β-lactone Antibiotics, Oxazolomycin Derivative and Its Isomer, Produced by *Streptomyces* sp. KSM-2690. *J. Antibiot.* **2000,** *53* (12), 1397-1400.

12. Manam, R. R.; Teisan, S.; White, D. J.; Nicholson, B.; Grodberg, J.; Neuteboom, S. T. C.; Lam, K. S.; Mosca, D. A.; Lloyd, G. K.; Potts, B. C. M., Lajollamycin, a nitro-tetraene spiro-beta-lactone-gamma-iactam antibiotic from the marine actinomycete Streptomyces nodosus. *J. Nat. Prod.* **2005,** *68* (2), 240-243.

13. Ko, K.; Lee, S. H.; Kim, S. H.; Kim, E. H.; Oh, K. B.; Shin, J.; Oh, D. C., Lajollamycins, Nitro Group-Bearing Spiro-β-lactone-γ-lactams Obtained from a Marine-Derived Streptomyces sp. *J. Nat. Prod.* **2014,** *77* (9), 2099-2104.

21. Koomsiri, W.; Inahashi, Y.; Kimura, T.; Shiomi, K.; Takahashi, Y.; Ōmura, S.; Thamchaipenet, A.; Nakashima, T., Bisoxazolomycin A: a new natural product from 'Streptomyces subflavus subsp. irumaensis' AM-3603. *J. Antibiot.* **2017,** *70* (12), 1142-1145.

22. Kawai, S.; Kawabata, G.; Kobayashi, A.; Kawazu, K., Inhibitory Effect of Oxazolomycin on Crown Gall Formation. *Agric. Biol. Chem.* **1989,** *53* (4), 1127-1133.

23. Grigorjev, P. A.; Schlegel, R.; Gräfe, U., On the Protonophoric Activity of Oxazolomycin. *Pharmazie* **1992,** *47* (9), 707-709.

32. Kende, A. S.; Kawamura, K.; Devita, R. J., Enantioselective Total Synthesis of Neooxazolomycin. *J. Am. Chem. Soc.* **1990,** *112* (10), 4070-4072.

33. Kende, A. S.; Devita, R. J., Synthesis of the Fused Bicyclic Lactam-Lactone Terminus of Neooxazolomycin by a Novel Dianion Cyclocondensation. *Tetrahedron Lett.* **1988,** *29* (21), 2521-2524.

35. Kende, A. S.; DeVita, R. J., A mild four-carbon homologation of aldehydes to E,E-dienamines. *Tetrahedron Lett.* **1990,** *31* (3), 307-310.

36. Onyango, E. O.; Tsurumoto, J.; Imai, N.; Takahashi, K.; Ishihara, J.; Hatakeyama, S., Total synthesis of neooxazolomycin. *Angew. Chem. Int. Ed.* **2007,** *46* (35), 6703-6705.

37. Eto, K.; Yoshino, M.; Takahashi, K.; Ishihara, J.; Hatakeyama, S., Total Synthesis of Oxazolomycin A. *Org. Lett.* **2011,** *13* (19), 5398-5401.

38. Ishihara, J.; Hatakeyama, S., Total Synthesis of Oxazolomycins. *Chem. Rec.* **2014,** *14* (4), 663-677.

39. Nishimaru, T.; Eto, K.; Komine, K.; Ishihara, J.; Hatakeyama, S., Total Synthesis of Lajollamycin B. *Chem. Eur. J.* **2019,** *25* (33), 7927-7934.

46. Kim, J. H.; Kim, I.; Song, Y.; Kim, M. J.; Kim, S., Asymmetric Total Synthesis of (+)-Neooxazolomycin Using a Chirality-Transfer Strategy. *Angew. Chem. Int. Ed.* **2019,** *58* (32), 11018-11022.

125. Vellalath, S.; Van, K. N.; Romo, D., Direct Catalytic Asymmetric Synthesis of N-Heterocycles from Commodity Acid Chlorides by Employing α,β-Unsaturated Acylammonium Salts. *Angew. Chem. Int. Ed.* **2013,** *52* (51), 13688-13693.

128. Papillon, J. P. B.; Taylor, R. J. K., The first syntheses of the 1-oxo-2-oxa-5-azaspiro[3.4]octane ring system found in oxazolomycin. *Org. Lett.* **2000,** *2* (14), 1987-1990.

129. Donohoe, T. J.; Chiu, J. Y. K.; Thomas, R. E., Synthesis of the Pyrrolidinone Core of KSM-2690 B. *Org. Lett.* **2007,** *9* (3), 421-424.

130. Donohoe, T. J.; O'Riordan, T. J. C.; Peifer, M.; Jones, C. R.; Miles, T. J., Asymmetric Synthesis of the Fully Elaborated Pyrrolidinone Core of Oxazolomycin A. *Org. Lett.* **2012,** *14* (21), 5460-5463.

131. Heaviside, E. A.; Moloney, M. G.; Thompson, A. L., Diastereoselective intramolecular aldol ring closures of threonine derivatives leading to densely functionalised pyroglutamates related to oxazolomycin. *RSC Adv.* **2014,** *4* (31), 16233-16249.

132. Josa-Culleré, L.; Towers, C.; Willenbrock, F.; Macaulay, V. M.; Christensen, K. E.; Moloney, M. G., Synthesis and bioactivity of fused- and spiro-β-lactone-lactam systems. *Org. Biomol. Chem.* **2017,** *15* (25), 5373-5379.

133. Eto, K.; Ishihara, J.; Hatakeyama, S., Stereoselective synthesis of the right-hand cores of 16-methylated oxazolomycins. *Tetrahedron* **2018,** *74* (7), 711-719.

134. Bastin, R.; Dale, J. W.; Edwards, M. G.; Papillon, J. P. N.; Webb, M. R.; Taylor, R. J. K., Formal synthesis of (+)-neooxazolomycin via a Stille cross-coupling/deconjugation route. *Tetrahedron* **2011,** *67* (51), 10026-10044.

135. Fritz, S. P.; Moya, J. F.; Unthank, M. G.; McGarrigle, E. M.; Aggarwal, V. K., An Efficient Synthesis of Azetidines with (2-Bromoethyl)sulfonium Triflate. *Synthesis* **2012,** *44* (10), 1584-1590.

136. Abbasov, M. E.; Alvariño, R.; Chaheine, C. M.; Alonso, E.; Sánchez, J. A.; Conner, M. L.; Alfonso, A.; Jaspars, M.; Botana, L. M.; Romo, D., Simplified immunosuppressive and neuroprotective agents based on gracilin A. *Nat. Chem.* **2019,** *11* (4), 342-350.

137. Tao, Y.; Reisenauer, K. N.; Masi, M.; Evidente, A.; Taube, J. H.; Romo, D., Pharmacophore-Directed Retrosynthesis Applied to Ophiobolin A: Simplified Bicyclic Derivatives Displaying Anticancer Activity. *Org. Lett.* **2020**, **Article ASAP**.

138. Truax, N. J. R., D., Bridging the Gap Between Natural Product Synthesis and Drug Discovery. *Nat. Prod. Rep.* **2020**, *accepted*.

139. Chaheine, C. M. S., Conner J.; Gladen, P. T.; Romo, D., Enantioselective Michael-Proton Transfer-Lactamization for Pyroglutamic Acid Derivatives: Synthesis of dimethyl-(S,E)-5-oxo-3-styryl-1-tosylpyrrolidine-2,2-dicarboxylate. *Org. Syn.* **2020**, submitted.

140. Horwitz, M. A.; Johnson, J. S., Local Desymmetrization through Diastereotopic Group Selection: An Enabling Strategy for Natural Product Synthesis. *Eur. J. Org. Chem.* **2017,** *2017* (11), 1381-1390.

141. Lee, G. H.; Youn, I. K.; Choi, E. B.; Lee, H. K.; Yon, G. H.; Yang, H. C.; Pak, C. S., Magnesium in Methanol (Mg / MeOH) in Organic Syntheses. *Curr. Org. Chem.* **2004,** *8* (13), 1263-1287.

142. Leduc, A. B.; Kerr, M. A., Total Synthesis of (±)-Decursivine. *Eur. J. Org. Chem.* **2007,** *2007* (2), 237-240.

143. Hoveyda, A. H.; Evans, D. A.; Fu, G. C., Substrate-directable chemical reactions. *Chem. Rev.* **1993,** *93* (4), 1307-1370.

144. Molander, G. A., Application of lanthanide reagents in organic synthesis. *Chem. Rev.* **1992,** *92* (1), 29-68.

145. Imamoto, T.; Sugiura, Y.; Takiyama, N., Organocerium reagents. Nucleophilic addition to easily enolizable ketones. *Tetrahedron Lett.* **1984,** *25* (38), 4233-4236.

146. Liu, H. J.; Shia, K. S.; Shang, X.; Zhu, B. Y., Organocerium Compounds in Synthesis. *Tetrahedron* **1999,** *55* (13), 3803-3830.

147. Duttwyler, S.; Chen, S.; Takase, M. K.; Wiberg, K. B.; Bergman, R. G.; Ellman, J. A., Proton Donor Acidity Controls Selectivity in Nonaromatic Nitrogen Heterocycle Synthesis. *Science* **2013,** *339* (6120), 678.

148. Dimitrov, V.; Kostova, K.; Genov, M., Anhydrous Cerium(III) Chloride — Effect of the Drying Process on Activity and Efficiency. *Tetrahedron Lett.* **1996,** *37* (37), 6787-6790.

149. Takeda, N.; Imamoto, T., Use of Cerium (III) Chloride in the Reactions of Carbonyl Compounds with Organolithiums or Grignard Reagents for the Suppression of Abnormal Reactions: 1-butyl-1,2,3,4-tetrahydro-1-napthol. *Org. Syn.* **1999,** *76*, 228.

150. Evans, D. A.; Downey, C. W.; Shaw, J. T.; Tedrow, J. S., Magnesium Halide-Catalyzed Anti-Aldol Reactions of Chiral N-Acylthiazolidinethiones. *Org. Lett.* **2002,** *4* (7), 1127-1130.

151. Evans, D. A.; Tedrow, J. S.; Shaw, J. T.; Downey, C. W., Diastereoselective Magnesium Halide-Catalyzed anti-Aldol Reactions of Chiral N-Acyloxazolidinones. *J. Am. Chem. Soc.* **2002,** *124* (3), 392-393.

152. Gage, J. R.; Evans, D. A., Diastereoselective Aldol Condensaiton Using a Chiral Oxazolidinone Auxiliary: (*2S,3S*)-3-hydroxy-3-phenyl-2methylpropanoic Acid. *Org. Syn.* **1990,** *68*, 83.

153. Ogasawara, M.; Okada, A.; Subbarayan, V.; Sorgel, S.; Takahashi, T., Palladium-Catalyzed Asymmetric Synthesis of Axially Chiral Allenylsilanes and Their Application to S(E)2 ' Chirality Transfer Reactions. *Org. Lett.* **2010,** *12* (24), 5736-5739.

154. Appel, R., Tertiary Phosphane/Tetrachloromethane, a Versatile Reagent for Chlorination, Dehydration, and P-N Linkage. *Angew. Chem. Int. Ed.* **1975,** *14* (12), 801-811.

155. Bailey, W. F.; Brubaker, J. D.; Jordan, K. P., Effect of solvent and temperature on the lithium-iodine exchange of primary alkyl iodides: reaction of t-butyllithium with 1-iodooctane in heptane-ether mixtures. *J. Organomet. Chem.* **2003,** *681* (1-2), 210-214.

156. Rathman, T.; Bailey, W. F., Optimization of Organolithium Reactions. *Org. Process Res. Dev.* **2009,** *13* (2), 144-151.

157. Krasovskiy, A.; Kopp, F.; Knochel, P., Soluble Lanthanide Salts (LnCl3·2 LiCl) for the Improved Addition of Organomagnesium Reagents to Carbonyl Compounds. *Angew. Chem. Int. Ed.* **2006,** *45* (3), 497-500.

158. Ilardi, E. A.; Stivala, C. E.; Zakarian, A., Hexafluoroisopropanol as a Unique Solvent for Stereoselective Iododesilylation of Vinylsilanes. *Org. Lett.* **2008,** *10* (9), 1727-1730.

159. Sidera, M.; Costa, A. M.; Vilarrasa, J., Iododesilylation of TIPS-, TBDPS-, and TBS-Substituted Alkenes in Connection with the Synthesis of Amphidinolides B/D. *Org. Lett.* **2011,** *13* (18), 4934-4937.

160. King, S. A., Orthoester-Dependent Alcoholysis of Lactones. Facile Preparation of 4-Alkoxybutanoates and 5-Alkoxypentanoates. *J. Org. Chem.* **1994,** *59* (8), 2253-2256.

161. Chau, S. T.; Hayakawa, Y.; Sulikowski, G. A., 18O Assisted Analysis of a γ,δ-Epoxyketone Cyclization: Synthesis of the C16−C28 Fragment of Ammocidin D. *Org. Lett.* **2011,** *13* (4), 756-759.

162. Burchat, A. F.; Chong, J. M.; Nielsen, N., Titration of alkyllithiums with a simple reagent to a blue endpoint. *J. Organomet. Chem.* **1997,** *542* (2), 281-283.

CHAPTER FOUR

Synthetic Efforts Toward (–)-Oxazolomycin B and Simplified Chemical Probes for Proteomics Studies

4.1 Introduction

Expanding on the introduction to the total synthesis of oxazolomycin natural products given in Sections 1.1 and 3.1 the following will give an overview of the literature regarding the synthesis of spiro-β-lactone γ-lactam analogues of the oxazolomycins.

Organic chemists have been invested in the synthesis of the core spiro-β-lactone γ-lactam of the oxazolomycins for over two decades now. This is due to, as mentioned previously, the wide-ranging bioactivity reported for the oxazolomycins (i.e. anticancer, antibiotic, antiviral) as well as the synthetic challenge posed by their unique and stereochemically dense core structure. While several approaches to γ-lactam systems related to that of the oxazolomycins are known, only a few have been able successfully install the strained/reactive spiro-β-lactone.

The first report of the synthesis of a spiro-β-lactone related to the oxazolomycins out of the Taylor lab demonstrated a racemic, tandem aldol-lactonization of proline-derived esters to obtain spiro-β-lactone pyrrolidines (Table 4.1).[128] They found that the *gem*-dialkyl substitution at the β-position of the β-lactone, resulting from the use of acetone as an electrophile in this tandem process, was essential to isolating stable spiro-β-lactone products (with variation in the *N*-protecting group) that could be functionalized to resemble the core of the oxazolomycins. The *gem*-dialkyl effect (Thorpe-Ingold effect)[163] in these cases enhances the rate of the cyclization step of the tandem aldol-lactonization as well as

the rate of cyclization via condensation of β-hydroxy carboxylic acid precursors. In addition, β-disubstitution provides steric shielding of both electrophilic positions of the strained spiro-β-lactone (C1 and C3, β-lactone numbering).

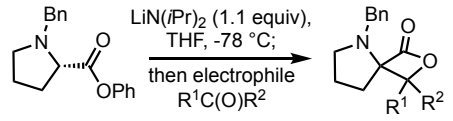

entry	electrophile		reaction time (h)	yield
	R^1	R^2		
1	Me	Me	0.25	62% (**4.a**)
2	H	Me	2	33%
3	H	TMS	2	65%
4	TMS	TMS	2	no product

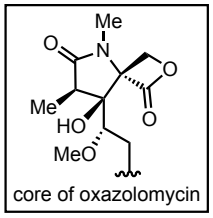

Table 4.1. Taylor's tandem aldol-lactonization using *N*-benzyl phenyl proline ester. Inset: the core spiro-β-lactone γ-lactam of oxazolomycin.

In the Romo group, we are perpetually fascinated by the question of: what reaction conditions can a β-lactone withstand? In this example by Taylor et. al., spiro-β-lactone pyrrolidine **4.a** was exposed to hydrogenolysis conditions (Pd/C, H_2, EtOAc), alkylation conditions (MeI, K_2CO_3, DMF, Scheme 4.1A), and a peruthinate oxidation ($RuCl_3$, $NaIO_4$, $MeCN/CCl_4/H_2O$; Scheme 4.1B,C). The β-unsubstituted spiro-β-lactone pyrrolidine **4.b**, which was synthesized in optically active form via *L*-proline, could only be oxidized under the aforementioned peruthinate oxidation conditions reported by Sharpless et. al.,[164] producing a 25% yield of a spiro-β-lactone γ-lactam **4.c** that represents a simplified oxazolomycin analogue (Scheme 4.1B). The low yield in the β-unsubstituted example (**4.b** to **4.c**) was said to be due to decomposition of the starting material under the reaction conditions. Owing to the lack of steric volume about the reactive spiro-β-lactone and the aqueous conditions employed, this instability can be expected.

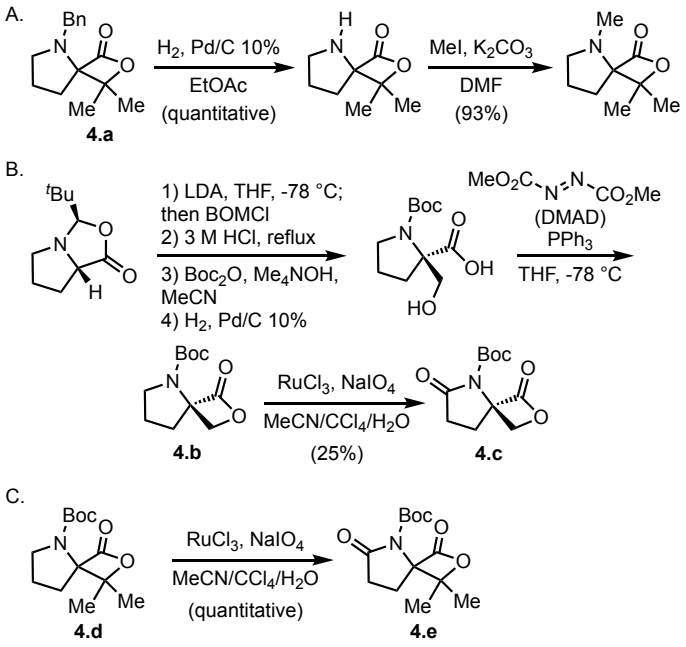

Scheme 4.1. A. Reactions in the presence of a spiro-β-lactone pyrrolidine. B. Synthesis of β-unsubstituted spiro-β-lactone pyrrolidine **4.b**. C. Peruthinate oxidation of **4.d** toward simplified analogues of the oxazolomycin core **4.c** and **4.e**, respectively.

In 2006[165] and later in 2010[166] Mondal et. al. published the synthesis of a more complex, functionalized spiro-β-lactone γ-lactam related to the oxazolomycin core. Their approach relied on double stereodifferentiating Crimmins' modified Evan's aldol reactions of propionyl oxazolidinone with Garner's aldehyde[167] in different enantiomeric combinations to form complex linear substates that could be cyclized to pyrrolidines like **4.g** that could be further functionalized to resemble the core of oxazolomycin. The relative stereochemistry of the Evan's aldol adducts like **4.f** are supported by X-ray crystallography. The synthesis that delivers the core spiro-β-lactone γ-lactam with the same relative stereochemistry as the natural product is illustrated below (Scheme 4.2).

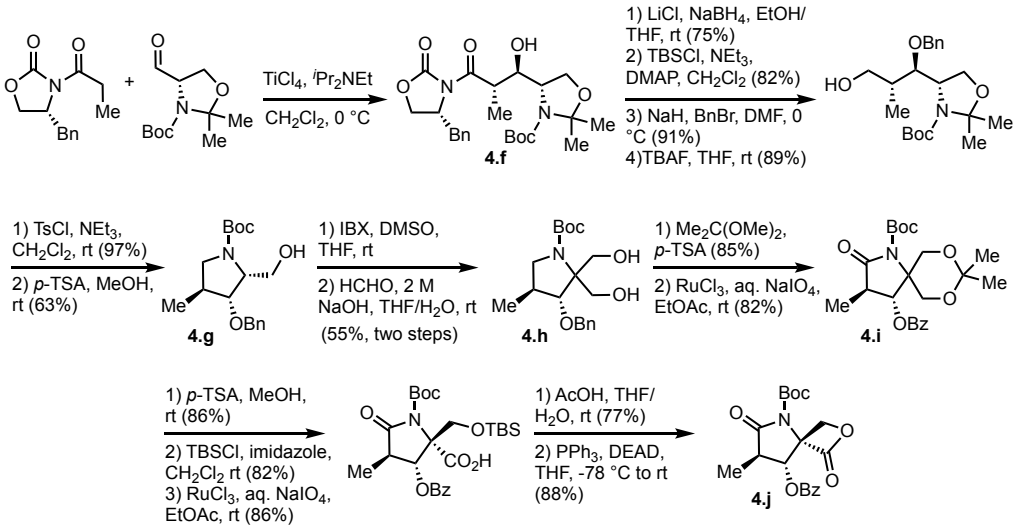

Scheme 4.2. Mondal et. al. synthesis of a more complex oxazolomycin related spiro-β-lactone γ-lactam **4.j**.

The primary alcohol in pyrrolidine **4.g** was oxidized to the aldehyde to allow another key reaction in this sequence to take place, namely, the cross Cannizzaro reaction to deliver a gem-hydroxymethyl pyrrolidine **4.h**. Protection of the 1,3-diol of **4.h** was followed by the peruthinate-catalyzed oxidation used by Taylor to install the lactam carbonyl oxygen atom. The product γ-lactam **4.i** was then manipulated with protecting group and redox chemistry to the spiro-β-lactone **4.j**. Detracting from the efficiency of this synthesis is the use of lengthy sequence of redox/protecting group concessions required to access the functionality of the central γ-lactam of the natural products from a linear starting material (15 steps from **4.f**).

In 2007 the Donohoe group disclosed the first synthesis of the core of an oxazolomycin congener called KSM-2690 B,[129] which was isolated in the year 2000 and possesses a methyl substituent at the spiro-β-lactone β-carbon (see inset Scheme 4.3) and (*R*)-C16 stereochemical configuration.[11] Their racemic approach to the core of KSM-2690 B commenced with an ammonia-free reductive aldol reaction of pyrrole **4.k** (Scheme 4.3).

Through a series of protecting group manipulations, functional group interconversions and alkylations, notably making use of a Ru-catalyzed terminal to internal olefin isomerization as well as substrate-directed diastereofacially selective dihydroxylation, enolate protonation, and nucleophilic addition, a densely functionalized pyrrolidine acetonide **4.l** intermediate was accessed.

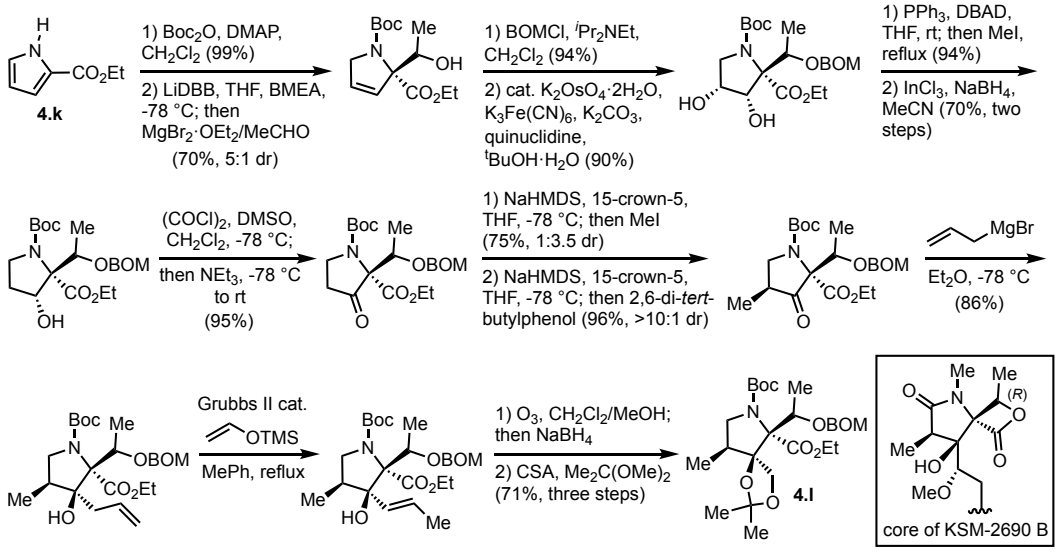

Scheme 4.3. Donohoe's synthesis of a complex pyrrolidine acetonide intermediate toward the core of KSM-2690 B.

From this pyrrolidine acetonide **4.l** Sharpless oxidation conditions[164] were also applied here to install the γ-lactam carbonyl oxygen atom (Scheme 4.4). Boc-protecting group removal with $ZnBr_2$ was followed by *N*-methylation and ester reduction with $LiBH_4$. Due to the hindered nature of the ethyl ester, hydrolysis to a β-hydroxy acid failed, and so a redox procedure had to be adopted to enable the construction of the spiro-β-lactone. Evidence suggesting the sterically hindered environment surrounding the carbonyl-C of the spiro-β-lactone (C17 by oxazolomycin numbering), is born out in this case. Indeed, the

low reactivity of this *pseudo*-neopental C17 ester recurs in related total syntheses across the last three decades. Oxidation of the primary alcohol **4.m** to the carboxylic acid was carried out over two steps and the spiro-β-lactone was formed through the use of classic β-lactonization conditions (TsCl, pyr.) first reported by Adam,[168] concluding the first synthesis of a complex spiro-β-lactone γ-lactam **4.n** with all of the relative stereochemistry and functionality of the oxazolomycin congener KSM-2690 B.

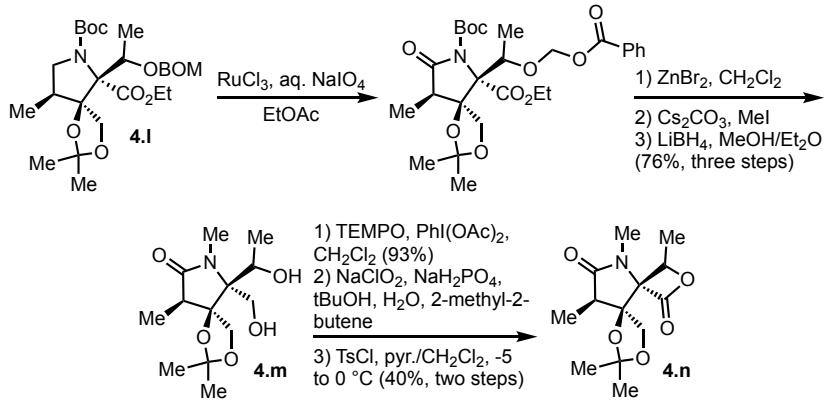

Scheme 4.4. Donohoe's synthesis of the core spiro-β-lactone of KSM-2690 B **4.i** from a complex pyrrolidine acetonide **4.g**.

The Donohoe group later, in 2012, published an asymmetric route to the oxazolomycin spiro-β-lactone γ-lactam.[130] They extended their partial Birch reduction methodology to the synthesis of an achiral *gem*-hydroxymethyl pyrroline **4.o**, which was desymmetrized by an enzymatic monoacetylation. The resulting monoacetate was manipulated to a protected 1,3-diol **4.p** with orthogonally cleavable protecting groups. An α-hydroxyaldehyde **4.q** was accessed by the same chemistry they used previously in the synthesis of the KSM-2690 B core. In the first example of a chelation-controlled 1,2-addition to an α-hydroxyaldehyde, the Donohoe group took advantage of anhydrous $CeCl_3$

to generate a primary organocerium reagent capable of adding to the sterically hindered *pseudo*-neopental C4-aldehyde **4.q**.[144-146, 148, 149, 169] A single diastereomer was produced and the relative stereochemistry is supported by NOESY analysis of an acetonide derived from *vicinal*-diol **4.r**, however, a glovebox is required to carry out their procedure and involves crushing pellets of anhydrous $CeCl_3$ into a solution of alkylithium with a metal rod and stirring for 13 h to generate the primary organocerium reagent. In contrast, the procedure described in this dissertation (see Sections 3.4.3 and 4.6.3) for a similar, chelation-controlled addition to an α-hydroxyaldehyde does not require a glovebox and boasts a significantly reduced reaction time (~3-4 h).

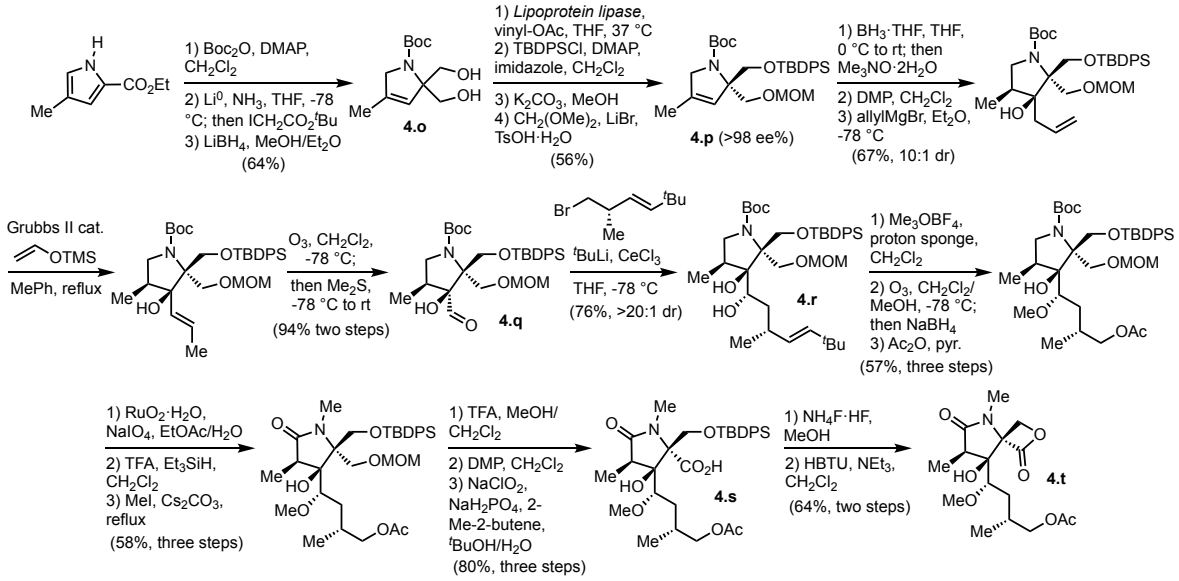

Scheme 4.5. Donohoe's synthesis of the fully functionalized spiro-β-lactone γ-lactam of oxazolomycin.

The secondary alcohol in **4.r** was selectively methylated using conditions first applied to the oxazolomycin system by Hatakeyama (see above). The γ-lactam carbonyl oxygen was again installed with Ru-catalysis, the γ-lactam nitrogen was methylated, and

the 1,3-diol functionality was manipulated to the desired β-hydroxy acid precursor **4.s**. The spiro-β-lactone **4.t** was formed in good yield using a hydroxybenzotriazole tetramethyluronium (HBTU) to activate the C17-carboxylic acid. No bioactivity studies of the KSM or oxazolomycin spiro-β-lactones **x** or **x** have been reported by the Donohoe group.

In 2014 Hatakeyama's synthesis of the simplified oxazolomycin spiro-β-lactone γ-lactam system **4.x** from a fused-γ-lactone γ-lactam **4.u** was published in *The Chemical Record*[38] and described detailed model studies carried out during their campaign toward the total synthesis of neooxazolomycin and oxazolomycin A. From the fused-γ-lactone γ-lactam intermediate **4.u** used in their total synthesis of neooxazolomycin, an orthogonally protected diol **4.v** was accessed (Scheme 4.6), which was selectively methylated at the C4-secondary alcohol with methyl Meerwein salt and proton sponge. Redox/protecting group chemistry led to a β-hydroxy acid **4.w** upon which the key β-lactonization could be studied. They found that Mitsunobu lactonizations deliver the desired spiro-β-lactone **4.x** but were found to be less effective than hydroxybenzotriazole tetramethyluronium reagent (HATU). Interestingly, when BOPCl/pyridine was used, the γ-lactone **4.u** was regenerated. This observation indicates the high propensity for five-membered ring formation versus 4-membered β-lactone formation and the reactivity of the C4-oxygen atom in its proximity to the C17-carbonyl carbon. Issues arising from this favored γ-lactone formation in our own work is described below.

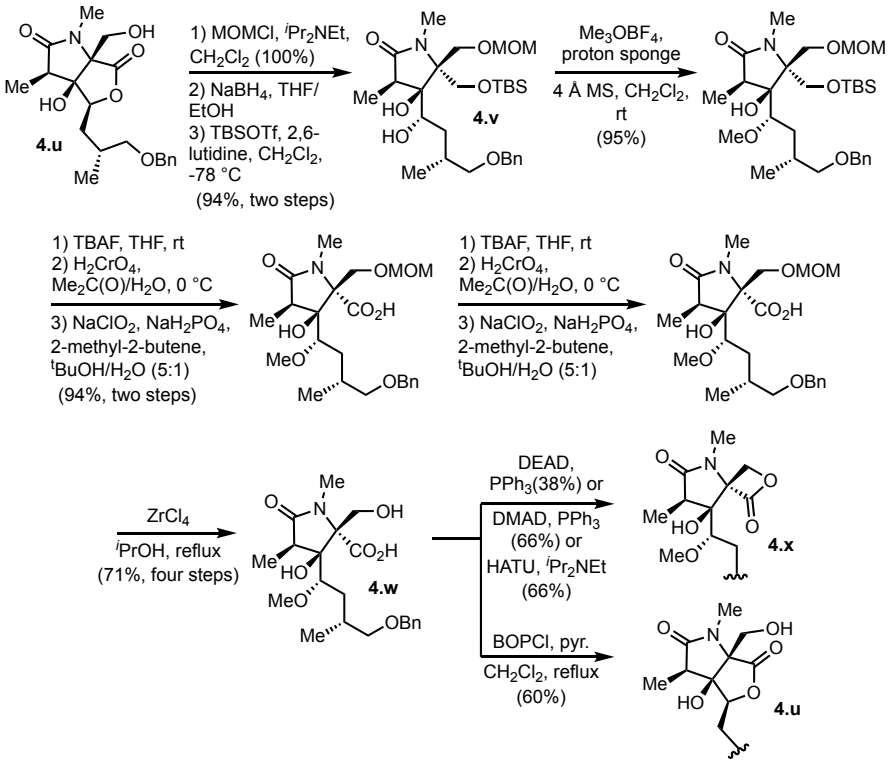

Scheme 4.6. Hatakeyama's study of spiro-β-lactone formation and synthesis of a simplified oxazolomycin analogue.

The Hatakeyama group, capitalizing on their established synthetic route to the neooxazolomycin γ-lactone γ-lactam intermediate **4.u**, reported syntheses of β-substituted oxazolomycin spiro-β-lactones bearing both C16 stereochemical configurations (Scheme 4.7 and 4.8). The primary alcohol in γ-lactone **4.u** was oxidized to an aldehyde and treated with methylmagnesium bromide at low temperature (Scheme 4.7). This led to a 3:1 mixture of epimers **4.y**, favoring the (*S*)-C16 configuration. The diastereoselectivity in this 1,2-addition is proposed to be controlled by a chelated intermediate via the C3-hydroxyl group. This C16-methylated compound **4.y** was taken through similar redox/protecting group chemistry as before to access the spiro-β-lactone γ-lactam system **4.z** of 16-methylated oxazolomycin congeners with the (*S*)-C16 configuration.

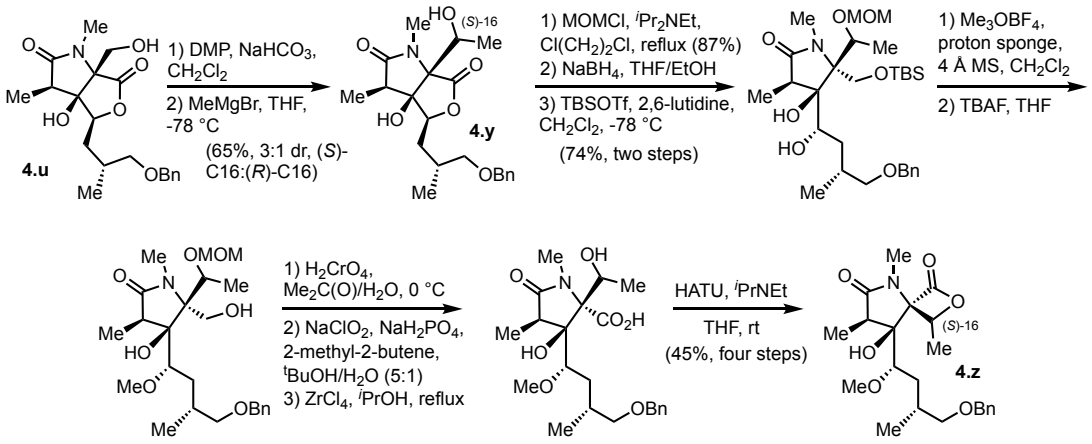

Scheme 4.7. Hatakeyama's synthesis of the core of 16-methyloxazolomycin with (*S*)-C16 stereochemical configuration.

Hatakeyama's synthesis of the (*R*)-C16 methyl-substituted oxazolomycin core involved TIPS-ether formation at C17 (Scheme 4.8). The β-silyloxy aldehyde stemming from the oxidation of 1,3-diol **4.aa** was exposed to methylmagnesium bromide and in this case the chelated intermediate thus generated exposes the opposing face of the aldehyde as the previous example and leads to the (*R*)-C16 configuration preferentially. Cyclization to the spiro-β-lactone **4.ab** was executed as before. Despite the great efforts put forth by the Hatakeyama group toward spiro-β-lactones related to the oxazolomycins as well as the only successful total syntheses of the natural products oxazolomycin A and lajollamycin B, no bioactivity studies, to the best of our knowledge, have emanated from their work.

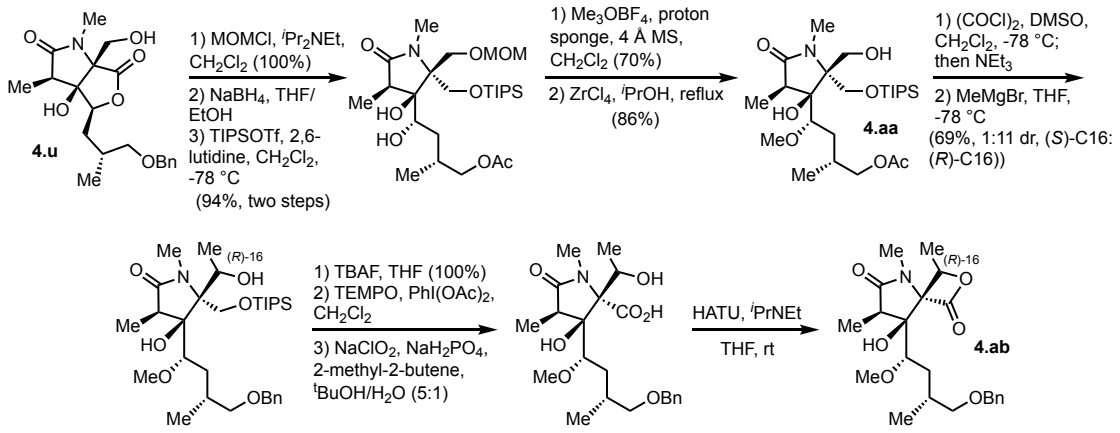

Scheme 4.8. Hatakeyama's synthesis of the 16-methyl-substituted spiro-β-lactone γ-lactam of the oxazolomycins with (*R*)-C16 configuration.

Recently, Fábian et. al. disclosed their synthesis of a simplified spiro-β-lactone γ-lactam resembling the core of oxazolomycin (**4.af**, Scheme 4.9). They access both enantiomers of derivative spiro-β-lactone **4.af** starting from both antipodes of xylose. A thioisocyanate intermediate **4.ac** was reduced to an amine and acylated with methacrolyloyl chloride yielding a precursor for ring-closing metathesis **4.ad**. Facially selective hydrogenation of the resulting olefin gave a 94:6 dr of γ-lactam **4.ae**. The carbohydrate backbone of γ-lactam **4.ae** was oxidatively cleaved with $NaIO_4$ following *N*-alkylation and removal of the acetonide protecting group. The spiro-β-lactone was forged in this case with the use of Adam's conditions (TsCl, pyridine)[168]. Both enantiomers of the simplified derivative spiro-β-lactones **4.af** were evaluated for their *in vitro* cytotoxic activity against three different human cancer cell lines (PaTu, pancreatic adenocarcinoma; Jurkat, acute T-lymphoblastic leukemia; HeLa, cervical adenocarcinoma) and a non-malignant cell line (MCF-10, human mammary epithelial cells). μM cytotoxic activity (IC_{50} = 5.1 – 14.8 mM) against these three cell lines was observed.

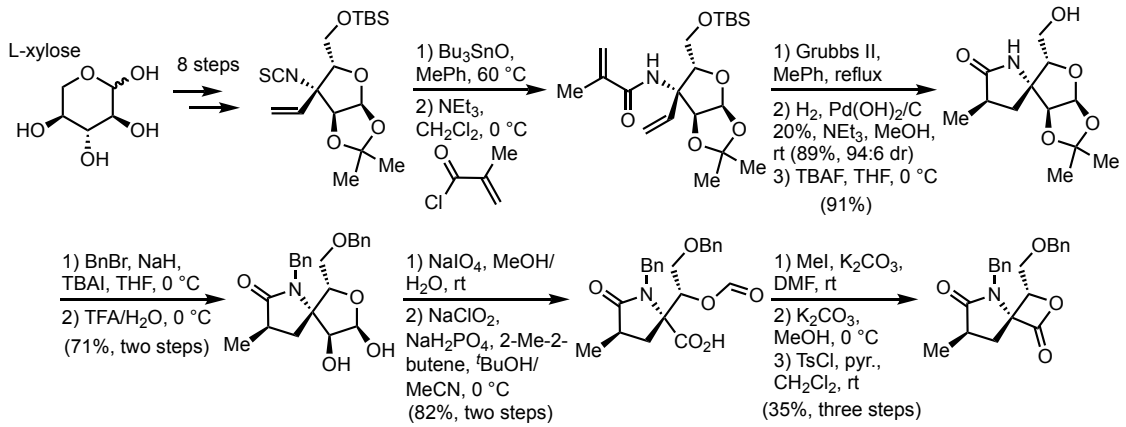

Scheme 4.9. Fábian's synthesis of a simplified C16-benzyloxymethyl-substituted oxazolomycin spiro-β-lactone γ-lactam.

While this handful of synthetic approaches to spiro-β-lactone γ-lactam systems related to the oxazolomycins have been established, very few have enabled detailed studies of the bioactivity and none toward the mode of action the natural products. The only investigation into the mode of action of the oxazolomycin was published in 1992 by Gräfe et. al. in which they utilized a synthetic lipid membrane model to show that oxazolomycin acts as a protonophore, shuttling protons and monovalent cations across the lipid bilayer via, as they propose, the nitrogen lone pair of the terminal oxazole.[23] Toward enabling further investigations into oxazolomycin bioactivity, our group has developed a modular, enantioselective synthetic route to the core of the oxazolomycins.

Described below are our efforts toward an enantioselective total synthesis of oxazolomycin B and pivalamide analogues thereof as well as the synthesis of simplified spiro-β-lactone γ-lactam systems related to the oxazolomycins and attempts to develop a streamlined conversion of the γ-lactone of neooxazolomycin to the core of oxazolomycin with minimal redox/protecting group transformations. These synthetic studies are primarily aimed at elucidating the mode of action of oxazolomycin natural products through the

design and synthesis of simplified chemical probes for proteomics studies[170] to be conducted in collaboration with the Sieber lab at the Technical University of Munich; work that is ongoing in our laboratory. To date, our efforts, in addition to the syntheses discussed above, have revealed the importance of steric shielding of the spiro-β-lactone C17 to the hydroliytic stability of the strained 4-membered ring and will be essential in developing chemical probes with the right balance of stability and reactivity to allow successful determination of cellular protein targets.

4.2 Toward a Total Synthesis of (–)-Oxazolomycin B

As an apex synthetic target, the all *E*-triene congener of oxazolomycin, oxazolomycin B[9] **4.1**, was chosen to guide our synthetic campaign (Figure 4.1).

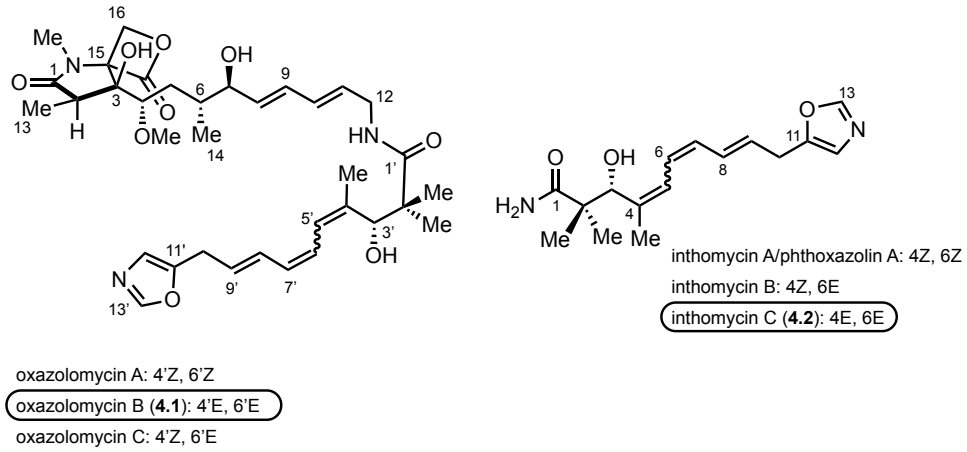

Figure 4.1. Structure of oxazolomycin A-C and inthomycin A-C.

Being that many β-lactone-containing natural products are known to covalently modify their protein targets ,[171-176] we hypothesize that the strained spiro-β-lactone serves as a reactive group that covalently modifies its protein target(s) (Figure 4.2) with the

remainder of the natural product structure serving to impart stability to the β-lactone as well as complex physiochemical properties and molecular topology/recognition elements for protein binding and cellular localization. Accessing simplified chemical probes along our synthetic route to oxazolomycin B **4.1**, in following with our group's pharmacophore-directed retrosynthesis (PDR) approach to natural product total synthesis,[136, 177-179] would divulge structure-activity relationship information as well as a comparative proteomic profile of protein binders within cancer cells.

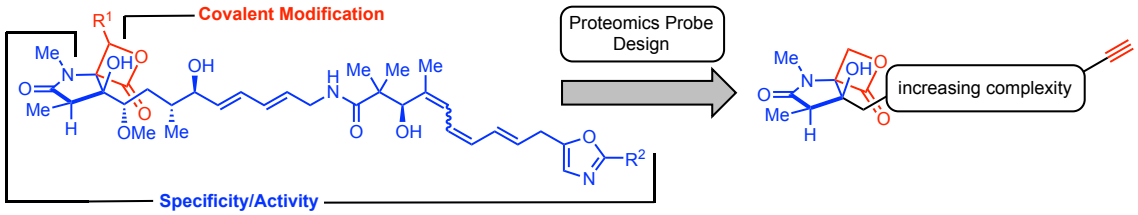

Figure 4.2. Chemical probe design based on oxazolomycin natural products toward proteomics studies.

A common retrosynthetic disconnection for all oxazolomycins utilized to date is the side-chain amide bond that appends the core (C1-C17) to the inthomycin moiety (C1'-C13'), which we also adopted as an initial disconnection (see Chapter One). With a goal of methodically increasing complexity of the side-chain, we next chose a C9-C10 disconnection of the diene enabled by a Stille cross-coupling with known vinyl stannane **4.6**.[35] Disconnection of the C4-C5 bond through a facially selective addition to aldehyde **4.7** of an alkylmetal species derived from a C5-C9 bearing iodide **4.8**, building on precedent from the Donohoe lab,[130] led to four principal fragments: the functionalized γ-lactam core **4.9**, the alkyliodide **4.8**, the activated ester **4.4**, a precursor to inthomycin C.[180-182] The appropriately functionalized α-hydroxyaldehyde γ-lactam **4.7** would be derived

from diol **4.9** in turn derived from a diastereotopic group-selective[183] reduction of the malonate group in **4.10**. Finally, our previously described nucleophile-catalyzed Michael-proton transfer lactamization (NCMPL) organocascade methodology[125] would deliver the *N*-tosyl γ-lactam **4.10** in enantiopure form employing sulfonamidomalonate **4.11** and unsaturated acid chloride **4.12** as substrates, each accessible in one step from commercial materials). The styryl moiety in the NCMPL was chosen to impart steric and electronic effects in the product to guide a diastereoselective α-methylation at C2 and diastereopic group selective reduction of the geminal diester, and to enable an allylic C-H hydroxylation at C3 (see Chapter Three).

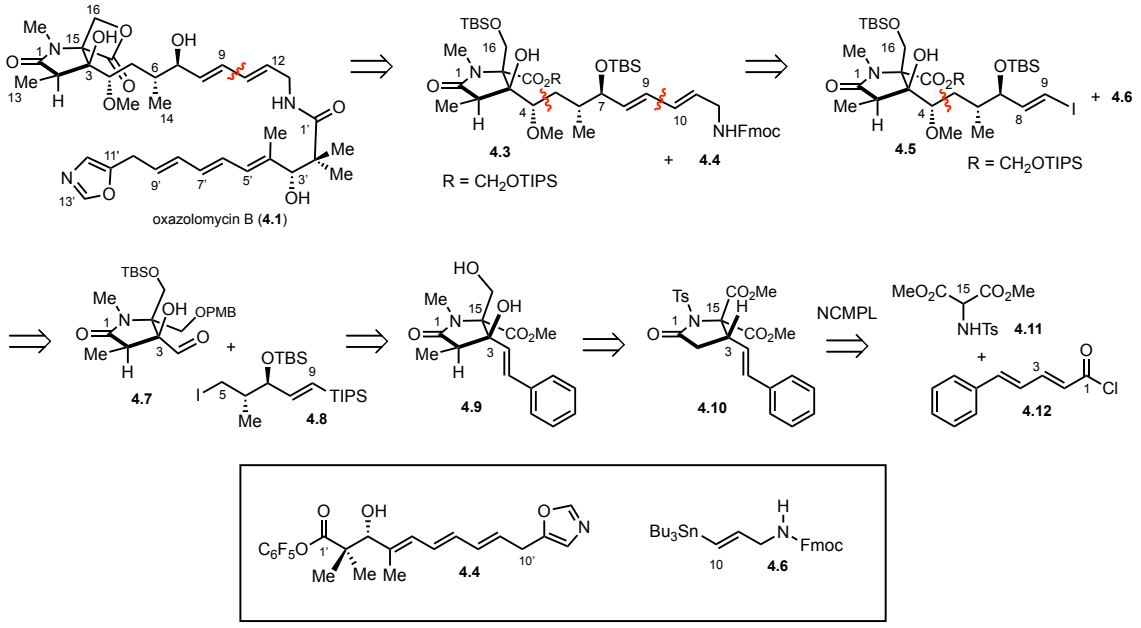

Figure 4.3. Retrosynthetic analysis of oxazolomycin B

Starting from an intermediate in our formal synthesis of neooxazolomycin (see Chapter Three), namely, β-silyloxy ester **3.21**, chemoselective reduction of the C17 methyl ester led to a primary alcohol that was protected as its *p*-methoxybenxyl ether in 72% yield

over two steps (Scheme 4.10). The styryl olefin in **4.13** was cleaved with ozone and the resulting α-hydroxyaldehyde was exposed to alkylithium **3.23** in the presence of $LaCl_3 \cdot 2LiCl$ as done previously (see Chapter Three), leading to a 13:1 isolated dr, favoring the desired (*S*)-C16 configuration. The mode of stereocontrol in this case is supported through correlation to neooxazolomycin core vinylsilane **3.24** by chemical derivatization. The hindered secondary alcohol of **4.15** was methylated,[37, 130] and the PMB-ether cleaved with DDQ. The resulting C17 primary alcohol was oxidized to the carboxylic acid and protected with a silyloxymethyl group.[37, 184, 185] The iododesilylation conditions used previously on neooxazolomycin core vinylsilane **3.24** gave the desired *E*-vinyliodide **4.19** in addition to a ketoiodide side product **4.20** (up to 33%). This side product presumably arises through a 1,2-hydride shift pathway of the iodonium intermediate. This unexpected issue notwithstanding, the desired vinyliodide **4.19** participated in a Stille cross-coupling [34, 186] with known stannane[32, 35] **4.6** to forge the C9-C10 bond and provide the C1-C17 core **4.21** of oxazolomycin primed for amide coupling to the triene oxazole tail fragment.

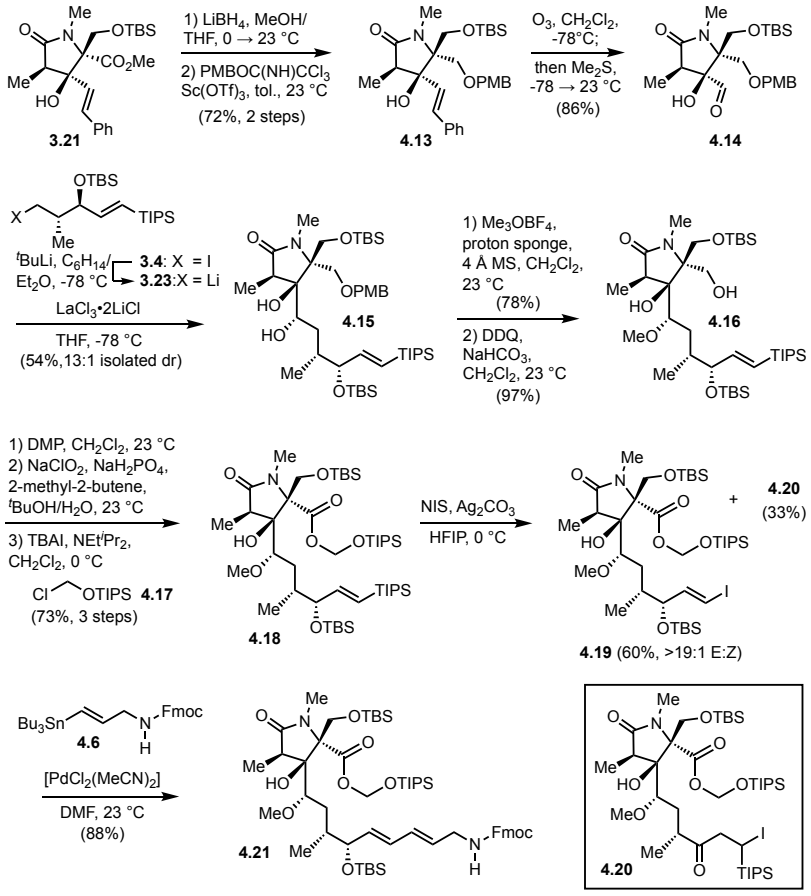

Scheme 4.10. Stereoselective synthesis of the oxazolomycin core **4.21** from a common intermediate in our formal synthesis of (+)-neooxazolomycin, **3.21**.

The synthesis of the known triene pentafluorophenyl (PFP) ester **4.4** commenced with a Horner-Wadsworth-Emmons olefination[187, 188] of the silyl acrolein[153] **3.19** used previously with the phosphonate ester **4.25**, delivering silyl dienoate **4.26** with high *E*-selectivity (97% 25:1 E:Z; Scheme 4.11B). The same iododesilylation conditions employed on vinylsilane **4.19** were successful here in producing the desired dienyliodide **4.27** with complete stereoretention. Stille cross coupling between dienyliodide **4.27** and vinylstannane oxazole **4.24**, itself derived from an allylation of silyloxazole **4.22** with allyl bromide **4.23**, proceeded smoothly (90% yield). Reduction to an intermediate primary alcohol with DIBAL-H and a subsequent Ley oxidation to known triene aldehyde[181] **4.28**

marked a point of interception in our synthesis of the required PFP ester **4.4** with the Burton[182] and Donohoe[181] group's syntheses of (–)-inthomycin C. Thus, the known enantioselective Kiyooka aldol reaction employed by Taylor[188] to form C3'-C4' bond was adopted here and likewise telescoped into a hydrolysis of the C13' oxazole silyl group. After ample consideration of which amide coupling method to apply in the combination of the oxazolomycin core **4.21** with the inthomycin C tail fragment we chose to adapt the Burton group's PFP ester intermediate **4.4** for the task. The Burton group reported recently their use of PFP ester **4.4** in the synthesis of (-)-inthomycin C; simple treatment of **4.4** with aqueous NH_4OH delivered the natural product without the need for C3' hydroxyl protection.

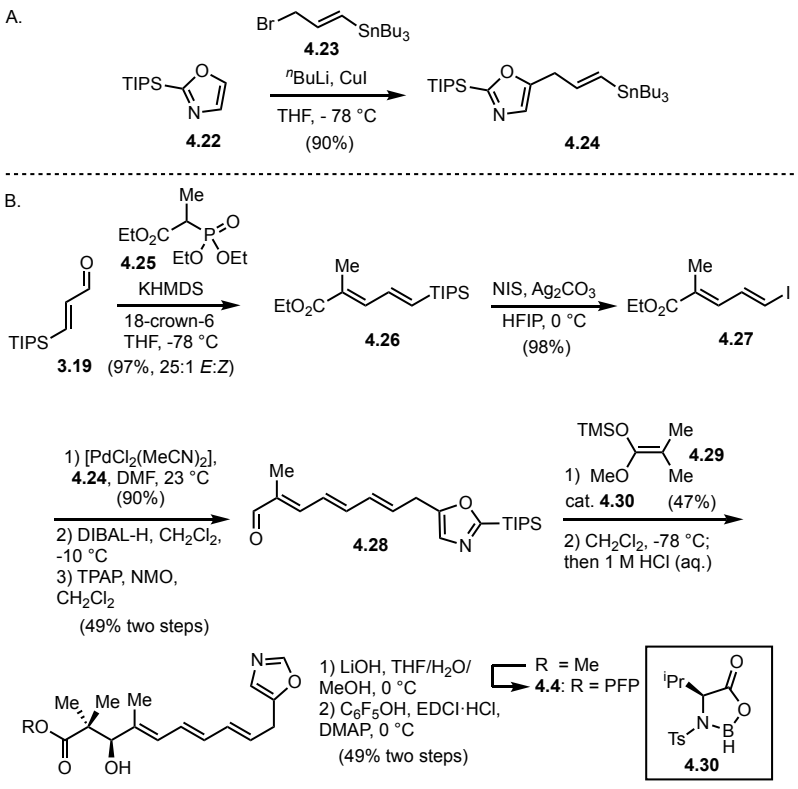

Scheme 4.11. A. Synthesis of vinylstannane oxazole, **4.24**. B. Enantioselective synthesis of the trieneacid oxazole fragment **4.4**. The synthetic route was executed with the help of Patrick J. Sutter.

Thus, the key amide coupling was initiated with *in-situ* Fmoc deprotection conditions first reported by Kende,[32, 35] followed by addition of the resulting primary amine **4.32** to a solution of the PFP ester **4.4** (Scheme 4.12). This led to efficient coupling, requiring only DBU as a reagent (79% yield). With the entire carbon framework of the natural product **4.33** assembled all that remained to complete the synthesis is a global desilylation, which proved to be non-trivial, requiring a large excess of HF·pyridine (~500 equiv) that was carefully quenched with silica gel to deliver what was believed to be the highly polar oxazolomycin B seco-acid based on crude ^{1}H-NMR. The crude seco-acid was immediately exposed to HATU and Hünig's base.[37] Surprisingly, the β-lactone was not secured from these conditions alone and instead the intermediate HOBt ester (proposed structure, Scheme 4.12 inset) was obtained as the major product. This could be due to the large amount of pyridinium fluorosilicate from the previous reaction buffering the lactonization medium. Redissolving the activated ester in THF and adding DMAP led to a spiro-β-lactone (1828 cm^{-1}) by crude IR. However, upon synthesizing 20 mg of the silyl-oxazolomycin B seco acid **4.33** and carrying this through the final desilylation and lactonization conditions thus developed, oxazolomycin B was not formed and an intractable mixture resulted. This unfortunate outcome is likely due to the amount of silica gel required in these final steps (silica gel quench of large excess of HF, prep-TLC of HOBt ester intermediate, and prep-TLC following treatment with DMAP). The only spectroscopic data available for oxazolomycin B is a ^{1}H-NMR line listing in the original isolation paper and this data did not align closely with that obtained following treatment with DMAP. Our efforts toward the synthesis of oxazolomycin B rest at this stage. We are

currently reconsidering our protecting group strategy to allow late stage deprotection of the C7-hydroxyl group.

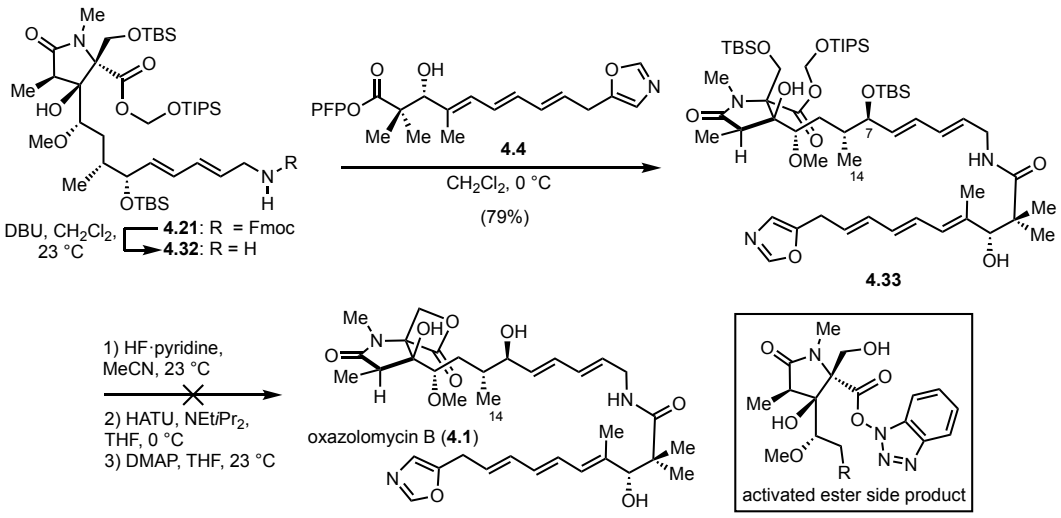

Scheme 4.12. Complications encountered in the endgame of our total synthesis of (–)-oxazolomycin B.

To investigate the issues we encountered in the endgame of our oxazolomycin B total synthesis efforts, we made simplified derivatives of neooxazolomycin and oxazolomycin that possess a pivaloyl terminus as opposed to the α,α-dimethyl triene oxazole (scheme 4.13). Stille cross coupling with vinylstannane pivalamide **4.34** and vinyliodide **4.19** delivered the silyl-oxazolomycin pivalamide derivative **4.35**. Treatment of this compound with TBAF over 3 days led to a complex mixture of products, with the major component being the corresponding C7-monoTBS ether.

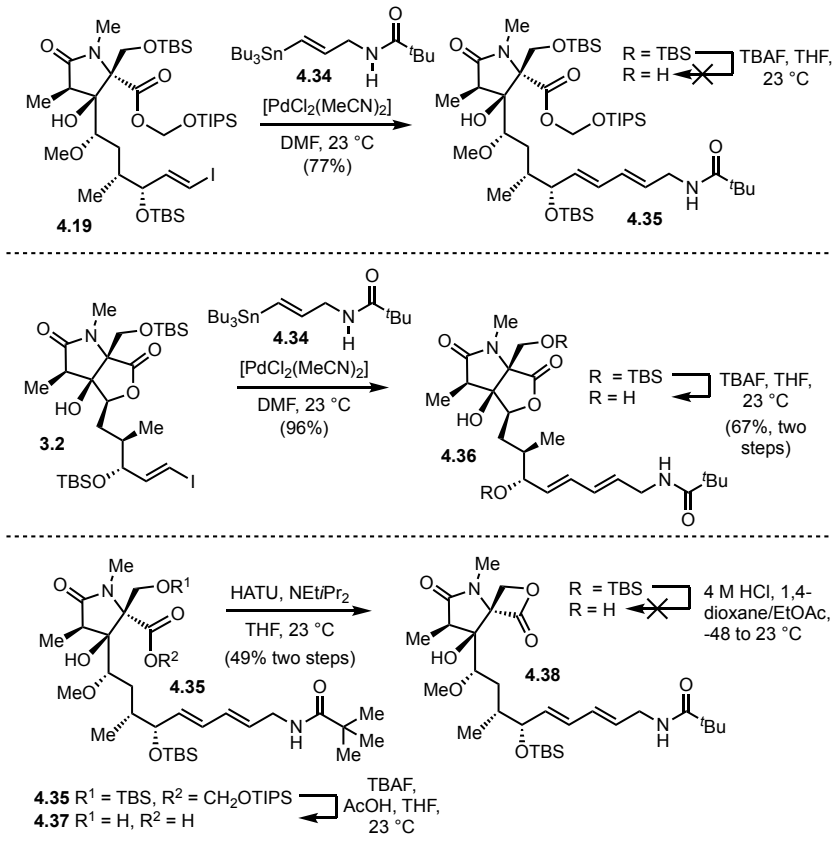

Scheme 4.13. Pivalamide derivatives of oxazolomycin and neooxazolomycin reveal differences in reactivity of C7 silyl ether toward deprotection.

In contrast, the silyl-neooxazolomycin pivalamide derivative **4.36** was deprotected within 6 h under the same conditions, suggesting the conformation of the side chains and steric environment surrounding the C7-silyl ether in these two systems is significantly different. The C7-mono TBS ether of oxazolomycin pivalamide **4.37** was isolated nonetheless following treatment with TBAF buffered by AcOH and was converted to the spiro-β-lactone **4.38**. As anticipated this spiro-β-lactone was found to be more stable than the simplified spiro-β-lactones discussed below, which lack the C3-hydroxyl and the C4-OMe group found in the oxazolomycins.

4.3 Synthesis of Simplified Spiro-β-lactone Chemical Probes Based on Oxazolomycin

Within five steps of our synthetic route toward the oxazolomycins a β-hydroxyester **3.10** is accessible (Scheme 3.1 and 4.14). Spiro-β-lactone formation from β-hydroxyester **3.10** was mediated by HBTU. Formation of the desired β-lactone was confirmed by crude IR (1823 cm^{-1}) however it proved too unstable to isolate by silica gel or basic alumina chromatography. However, hydrogenation of the styryl olefin and saponification led to β-hydroxy acid **4.39** whose corresponding β-lactone was sufficiently stable to isolate after silica gel chromatography. A brief screen of conditions to effect spiro-β-lactonization was carried out, identifying Adam's protocol[168] (TsCl, pyridine) and that applied by Hatakeyama (HBTU/HATU, amine base) as the most promising.

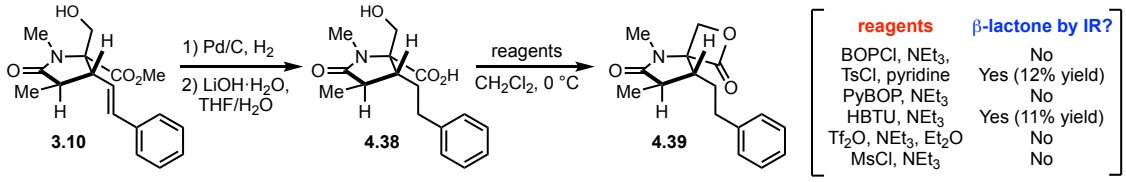

Scheme 4.14. Screening of reagents for spiro-β-lactone formation from β-hydroxyester **4.38**.

A simplified, terminal alkyne-bearing oxazolomycin spiro-β-lactone γ-lactam was synthesized from β-hydroxyester **3.10** by first protecting the primary alcohol as its TBS ether and hydrogenating the styryl olefin (Scheme 4.15). The resulting phenethyl compound was exposed to Sharpless Ru-catalyzed oxidation conditions[164] which was effective in cleaving the phenyl ring to a versatile carboxylic acid functional handle. Chemoselective reduction of the carboxylic acid **4.40** using BH_3·THF and Swern oxidation[189] produced aldehyde **4.41** that was homologated to terminal alkyne **4.42** using the Ohira-Bestmann reagent.[190] Desilylation and saponification of the C17-methyl ester

gave an intermediate β-hydroxy acid that was taken crude into the lactonization with HBTU. The terminal alkyne spiro-β-lactone **4.43** proved to by highly unstable, polymerizing when left as a neat oil in the fridge and decomposing (generating a complex mixture by ^{1}H-NMR) when exposed to $CDCl_3$ that was not first filtered through basic alumina. This instability, unfortunately, precluded the use of this spiro-β-lactone γ-lactam **4.43** from use in our proposed proteomic studies, and prompted the redesign of our most simple chemical probe as well as computational studies to help determine the source of the observed hydrolytic instability relative to the natural oxazolomycin spiro-β-lactone systems.

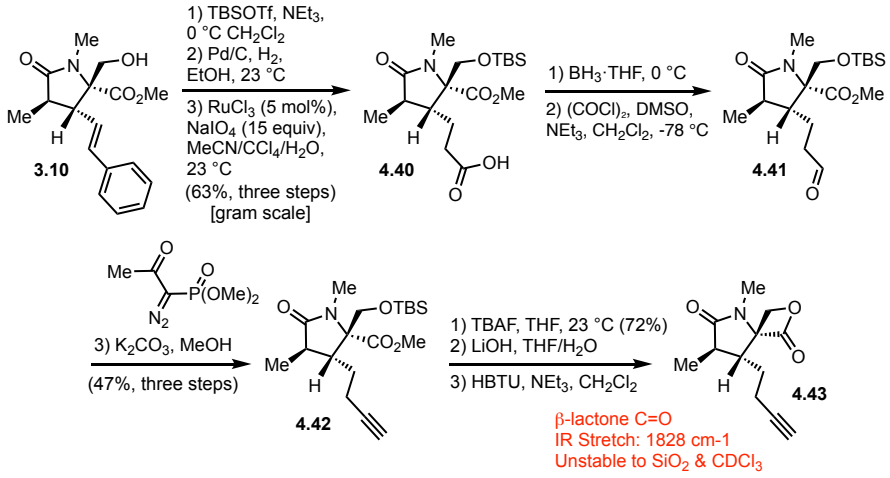

Scheme 4.15. Synthesis of a simplified, terminal alkyne-containing spiro-β-lactone based on oxazolomycin.

We hypothesized that a more sterically voluminous and hydrophobic side chain, might impart stability to a simple spiro-β-lactone γ-lactam derived from carboxylic acid **4.40**. To this end a symmetrical butynyl piperidine **4.47** was prepared from 4-piperidinone **4.44** by *N*-Boc protection and Wittig reaction with dioxolane phosphonium bromide **4.45** to give a piperidine dioxolane alkene **4.46** that was hydrogenated, the dioxolane

hydrolyzed, and the resulting aldehyde homologated to a terminal alkyne. This butynyl piperidine **4.47** was coupled to carboxylic acid **4.40** with HBTU and NEt_3 (Scheme 4.16A). The same desilylation/saponification/lactonization protocol as used above provided spiro-β-lactone terminal alkyne **4.50** that indeed proved to be reasonably more stable than β-lactone **4.43** (Scheme 4.16B). A brief ^{1}H-NMR stability study using wet d_6-DMSO showed piperidinyl spiro-β-lactone **4.50** decomposed with a half-life of approximately 4 h. An accurate yield for the four step sequence was not obtained as the β-lactone product could not be separated from tetramethylurea by-product of the lactonization with HBTU reagent. Unfortunately, this spiro-β-lactone was not stable enough for storage and shipment to our collaborator for bioactivity and proteomics applications.

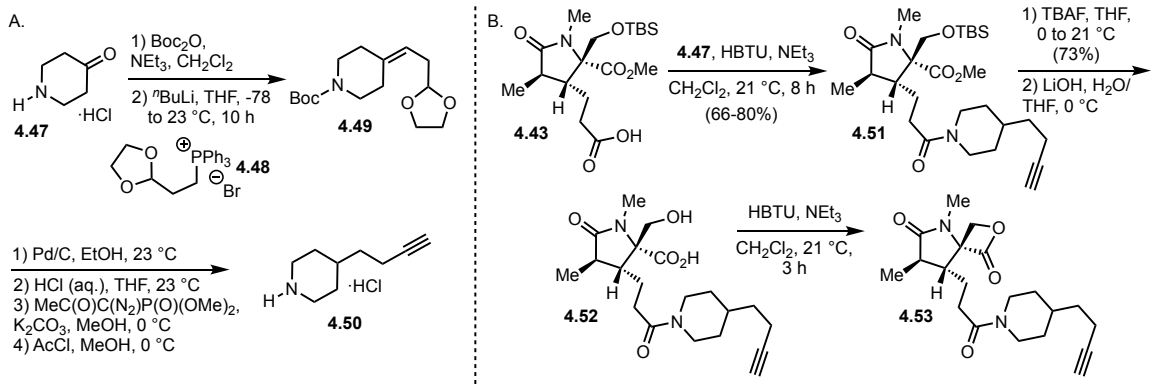

Scheme 4.16. Synthesis of a simplified, butynylpiperidine spiro-β-lactone toward a stable chemical proteomics probe.

In connection with our synthetic efforts toward the oxazolomycins, the Tantillo group calculated the relative hydrolysis and hydration propensities of various spiro-β-lactones (Table 4.2). This was prompted by an observed marked instability of synthesized spiro-β-lactones (*e.g.* **4.55**, **4.42**, **4.46**, **4.53**, Table 4.2) apparently related to their lack of

an adjacent C4-OMe group in comparison to the oxazolomycins. An unrelated spiro-β-lactone natural product, anistatin (**4.54**), also appears to be stable to harsh aqueous conditions, which we found surprising. Thus, hydrolysis and hydration propensity data was computed at the density functional theory (DFT) level for these spiro-β-lactone compounds to shed light on the observed stability differences. While lnK values reflect overall relative energies, conclusions about kinetic activation barriers can be made since transition states to hydrate must be at least as high as the relative energies to access the gem diol intermediates (lnK_{hydr}), assuming it is an intermediate. However, the current hydration propensity for **4.53** (-16.7) presents an apparent discrepancy with the experimental observations. The "stability" of **4.53** cannot be explained by the hydration propensity alone, as an lnK_{hyd} suggests an overall lower kinetic barrier to form the gem diol. Future computational work will investigate an alternative S_N2 ring opening pathway (vide infra). A Natural Bond Orbital analysis suggested that a potential donor-acceptor interaction, $n_{OMe} \longrightarrow C{=}O\ \pi^*$, is small (~0.8 kcal mol^{-1}), indicating that our hypothesis that this interaction might slow the rate of hydration/hydrolysis was found to be a minimal stabilizing effect. The 3D optimized structure suggests that the C4-OMe group primarily plays role in steric shielding.

When compared to the relatively stable natural product, anisatin, calculated lnK_{hydrol} data led us to conclude that all γ-lactam spiro-β-lactones related to the oxazolomycins devoid of an adjacent C4-OMe group (*i.e.* **4.57**) were more susceptible to hydrolysis (Table 4.2). However, DFT calculations revealed that hydration to the tetrahedral intermediate is energetically unfavorable and suggests an alternate mechanism for hydrolysis may be operative, namely S_N2 attack at the β-carbon known for β-

unsubstituted-β-lactones as observed by Vederas.[191, 192] Thus, this possibility is currently being explored. This hydrolysis lnK data gives an initial crude estimate of the barrier for hydrolysis and this data does in fact roughly correlate to experimentally observed "stabilities."

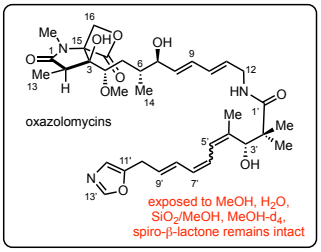

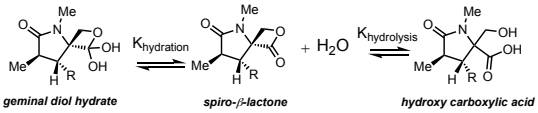

thermo-dynamic parameters \ spiro-β-lactones	anisatin (4.51)	4.52 not isolable (IR: 1823 cm^{-1})	4.39 isolable-unstable: (IR: 1827 cm^{-1} decomp. @ 23 °C)	4.43 isolable-more unstable (IR: 1829 cm^{-1} decomp. in $CDCl_3$)	4.50 isolable-more stable (IR: 1829 cm^{-1} $t_{1/2}$ ~4 h in d_6-DMSO)	not yet synthesized 4.53 (R = H)	not yet synthesized 4.54 (R = OMe)
lnK$_{hydr}$ (hydration rate to gem diol hydrate)	-14.4	-21.8 (- 22.2)	-20.5 (-20.7)	-16.7 (-16.8)	-16.7 (- 16.3)	-17.0 (-17.1)	-20.5 (-20.1)
lnK$_{hydrol}$ (to hydroxy carboxylic acid)	13.3	24.7	25.2	25.4	23.8	26.8	18.8

Table 4.2. Relative qualitative stability of spiro-β-lactones to hydrolysis as determined experimentally and computationally by hydration and hydrolysis propensities calculated by our collaborator Croix Laconsay from the Tantillo lab.

Our experimental observations in the pursuit of a stable spiro-β-lactone γ-lactam molecular probe based on the oxazolomycins in combination with the computational studies conducted by our collaborator Croix Laconsay in the Tantillo lab has led us to conclude that the C4-OMe group found in the natural products is indispensable to the hydrolytic stability of the spiro-β-lactone. B-unsubstituted spiro-β-lactone γ-lactams are exposed to nucleophilic addition at the C17 carbonyl carbon as well as the C16-β-carbon. New derivatives are being targeted currently that possess β-substitution, the C4-OMe, or both of these essential structural features. We expect the SAR information gathered to this

point will lead to the identification of simplified oxazolomycin-based spiro-β-lactones that will display enhanced hydrolytic stability and facilitate our proposed proteomic investigations.

4.4 Attempts at a Streamlined Synthesis of the Core of Oxazolomycin

Our early synthetic investigations into the construction of the γ-lactam system of the oxazolomycins, primarily the problem of efficient installation of the C4-OMe group paired with that of the carboxylic acid oxidation state at C17, focused on circumventing the need for redox/protecting group chemistry.[193, 194] Hasomi-Sakurai allylation of α-hydroxy dimethylacetals to directly form desired C4-OMe group were investigated (Scheme 4.17). Dr. Paul T. Gladen was the first to synthesize α-hydroxyaldehyde **4.58** via SeO_2 oxidation of dimethyl γ-lactam **3.9** (Scheme 3.1, Chapter Three) followed by ozonolysis. A-hydroxyaldehyde was then converted to its dimethylacetal **4.59** and exposed to typical allylation conditions with allyl-TMS and $TiCl_4$. Gratifyingly, a single product methyl ether **4.60** was generated with a 7:1 dr. The relative stereochemistry of the C4 stereocenter of the major product was never determined, however. We studied propargylations of this substrate to obtain a terminal alkyne probe in short order, but our attempts were unsuccessful. No desired reaction of dimethylacetal **4.59** was observed in these cases. We also attempted to advance homoallyl ether **4.60** to the γ-lactam system of oxazolomycin, but directed reductions of the C17-ester (*e.g.* $NMe_4BH(OAc)_3$, heat, not shown) and selective hydrolyses led to no desired reaction. We are currently considering a revisitation of intermediate **4.60** for advancement to spiro-β-lactone γ-lactams related to the oxazolomycins.

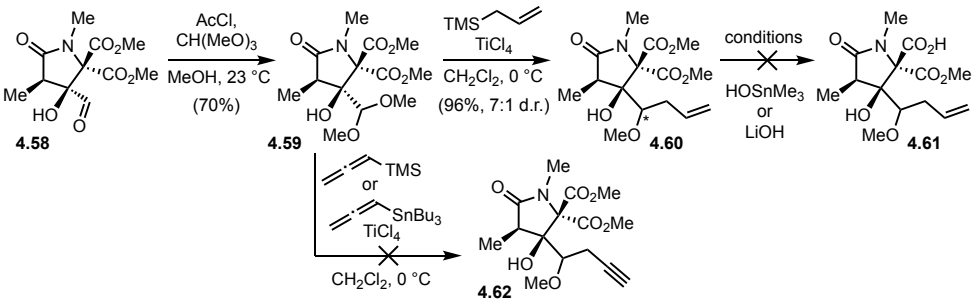

Scheme 4.17. Hasomi-Sakurai allylation and attempted propargylation of α-hydroxy dimethylacetal **4.56**. Work done with Dr. Paul T. Gladen.

From α-alkoxyaldehyde **3.12**, a similar dimethyl acetal **4.63**, this time bearing all of the functionality of the oxazolomycin core γ-lactam, specifically the C16-primary alcohol, was accessed (Scheme 4.18). Interestingly, despite the type of protecting group used for the C16-primary hydroxyl, no reaction was observed under the same allylation conditions used on diester dimethylacetal **4.59** (Scheme 4.17). Changing the Lewis acid or heating the mixture led to no reaction at all or, in cases of incomplete aqueous workup of the excess $TiCl_4$ employed, the dimethyl acetal was hydrolyzed and allylation of the resulting aldehyde led to an undesired γ-lactone product.

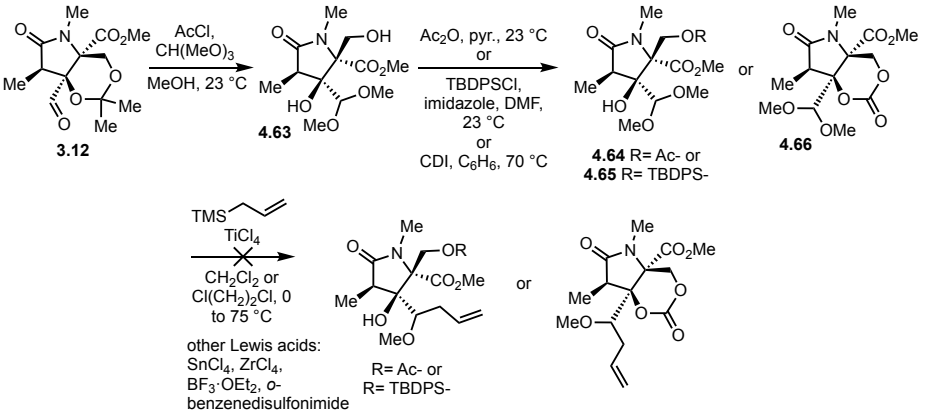

Scheme 4.18. Attempts at Hasomi-Sakurai allylation of α-hydroxy dimethyl acetals **4.63**-**4.66**.

Before we developed a route to the vinylsilane middle fragment of oxazolomycin **3.4** (Scheme 3.3A), we synthesized a silylalkyne middle fragment **4.72** (Scheme 4.19A), and set the two adjacent stereocenters by a cross-aldol reaction of a TIPS-propynal **4.68** with propanal catalyzed by the prolinol-derived secondary amine **4.69**. These conditions reported by Palomo et. al.[195, 196] delivered a serviceable yield of the desired *anti*-adduct as the 1,3-diol **4.70** with a 32:1 dr. Manipulation diol **4.70** by dioxasilane formation, followed by regioselective ring opening with MeLi[197] and Appel reaction[154] of the free primary alcohol led to primary iodide middle fragment **4.72**.

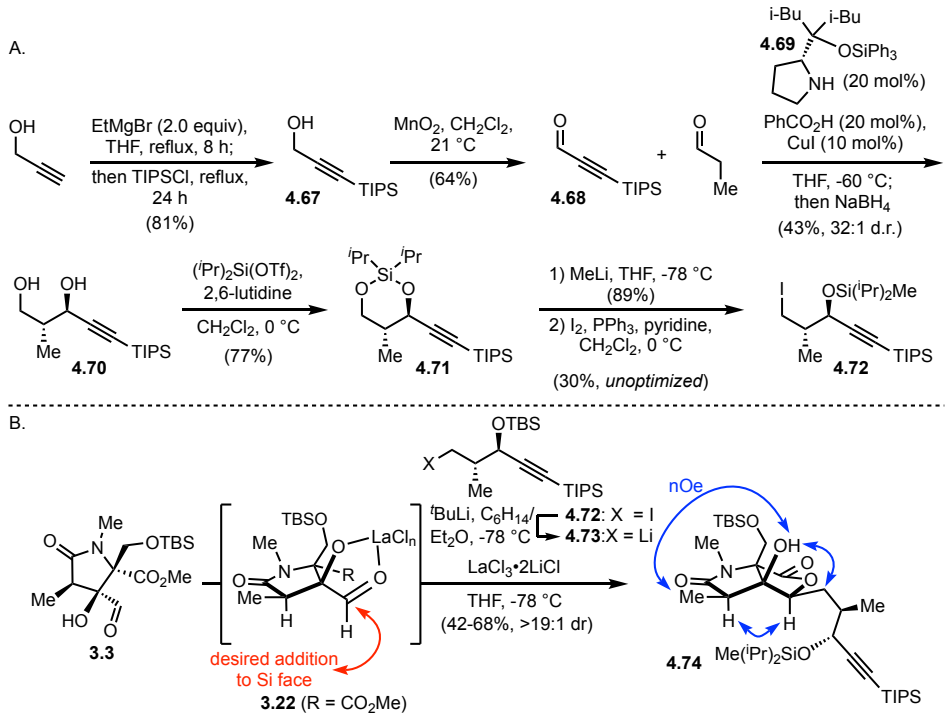

Scheme 4.19. A. Synthesis of alkynyl middle fragment (C5-C9) of oxazolomycin. B. Lithium/halogen exchange-1,2-addition of middle fragment to α-hydroxyaldehyde **3.3**.

The Li/halogen exchange conditions used to carry out the key, diastereofacially selective C4-C5 bond construction was first optimized on TIPS-alkyne primary iodide **4.72**

(Scheme 4.19B). It was found that a mixture of hydrocarbon and ether solvent was necessary to favor formation of the desired primary organolithium **4.73**.[155, 156] Reaction of this organolithium with the α-hydroxyaldehyde in the presence of $LaCl_3$ generated a single diastereomer of γ-lactone γ-lactam neooxaolomycin core **4.74**. The conformationally rigid nature of the *fused* bicycle allowed for determination of the relative stereochemistry by NOESY analysis.

Being that by this route six of seven stereogenic centers and all of the functionality of the natural products are set, we chose to focus efforts on an ideal transformation of the γ-lactone **4.74** to the γ-methoxy ester core found in oxazolomycin **4.75**. Ostensibly, this only requires the methylation of the C4-oxygen of the γ-lactone and ring-opening with MeOH (Scheme 4.20B). Undoubtedly, the Hatakeyama group in their synthetic campaign toward the oxazolomycins, attempted a similar circumvention of redox/protecting group concessions, however this work has not been published. Instead, Hatakeyama had to employ six steps to convert the γ-lactone of their key intermediate to the functional arrangement of oxazolomycin, involving reduction of the lactone, selective hydroxyl protection, methylation, deprotection and oxidation of C17 to the acid oxidation state to allow spiro-β-lactone formation (Scheme 4.20A).

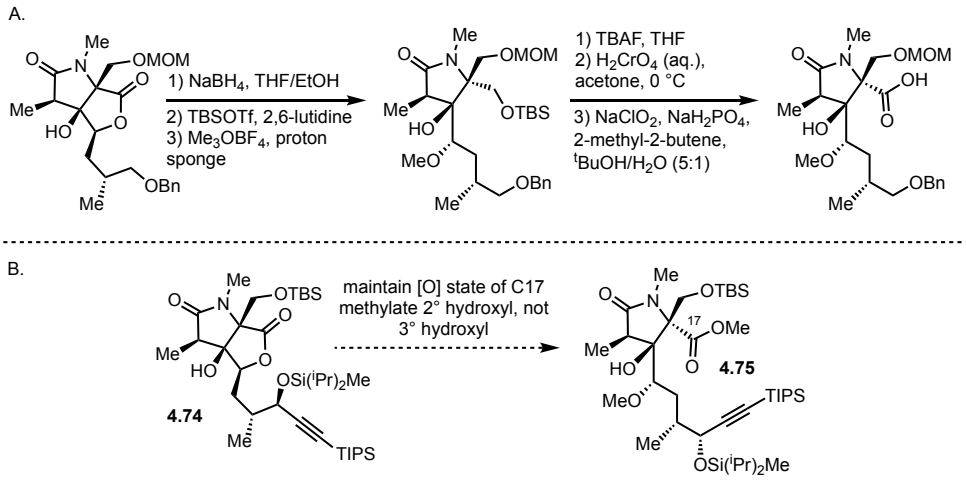

Scheme 4.20. A. Hatakeyamas redox/protection sequence to the core of oxazolomycin. B. An ideal conversion of the core of neooxazolomycin to the core of oxazolomycin.

Toward this ideal conversion we undertook a few different approaches, some of which are described below. We considered opening the γ-lactone with different nucleophiles to maintain the oxidation state at C17. Oxygen and sulfur nucleophiles would lead to no reaction likely to the propensity for five-membered ring formation, thus, amine nucleophiles were employed to generate amides that, we believed, would not recyclize and could, following selective secondary hydroxyl methylation at C4, could be hydrolyzed to the carboxylic acid ester (Scheme 4.21).

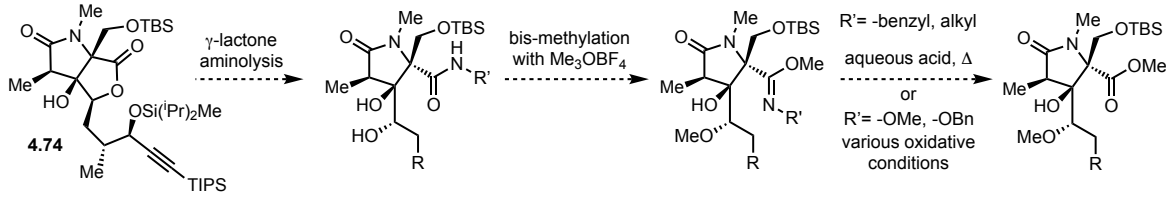

Scheme 4.21. γ-lactone amidolysis, methylation, hydrolysis sequence to the core of oxazolomycin.

We found that the γ-lactone **4.71** could be opened with Al[198] and Li amides derived from mehoxy- or benzyloxy- amine or *p*-methoxybenzylamine to give the γ-hydroxy amides **4.76**-**4.78** (Scheme 4.22). These γ-hydroxy amides proved to be unstable and would recyclize to γ-lactone **4.74** when exposed to silica gel chromatography or when left in solution.

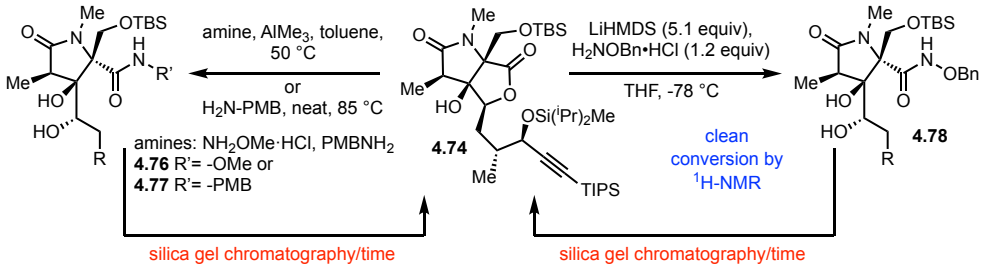

Scheme 4.22. Amidolysis of γ-lactone **4.74** leads to γ-hydroxyamides that spontaneously recyclize.

Since a stepwise amidolysis, methylation of a crude γ-hydroxy amide failed (Scheme 4.23), we chose to explore a one-pot method of γ-lactone amidolysis in the presence of excess base and quenching of the polyalkoxide intermediate with powerful methylating agents. When methyl iodide was used as the electrophile, an OTMS compound **4.76** was produced, presumably from *N* to *O*-silyl transfer from the amide base used in the reaction. When methyl triflate was used a methyl imidate **4.79** was formed that would recyclize on silica gel. At this point we realized that avoiding γ-lactone formation is the crux of the challenge in developing an efficient synthesis of the γ-methoxy ester arrangement of the oxazolomycins.

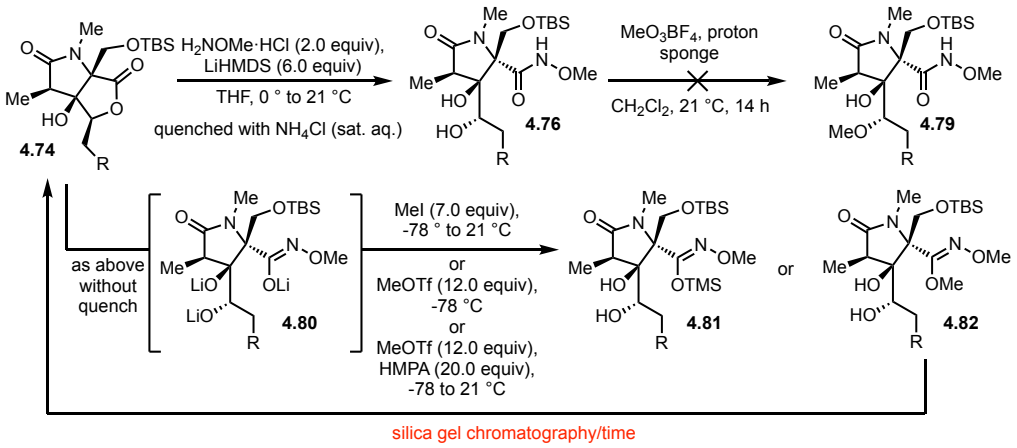

Scheme 4.23. Attempts at telescoped methylation of crude γ-hydroxyamide **4.76** and one pot methylation of *in situ* generated alkoxide intermediate **4.80**.

Another approach we considered was the *in situ* formation of a γ-hydroxy carboxylate salt that, once deprotonated by strong base, could perhaps be methylated selectively at the secondary hydroxyl of C4 and the C17 carboxylate to yield the desired γ-methoxy ester (Scheme 4.24).[199] In the event, γ-hydroxycarboxylate intermediate **4.83** was azeotropically dried following saponification and was exposed to an excess of LiHMDS. Quenching with methyl triflate led to a mixture of products, including γ-lactone **4.74**, C3-OMe γ-lactone **4.84**, and, notably, a tri-*O*-methylated compound **4.85**. None of the desired di-methylated compound was detected in the mixture.

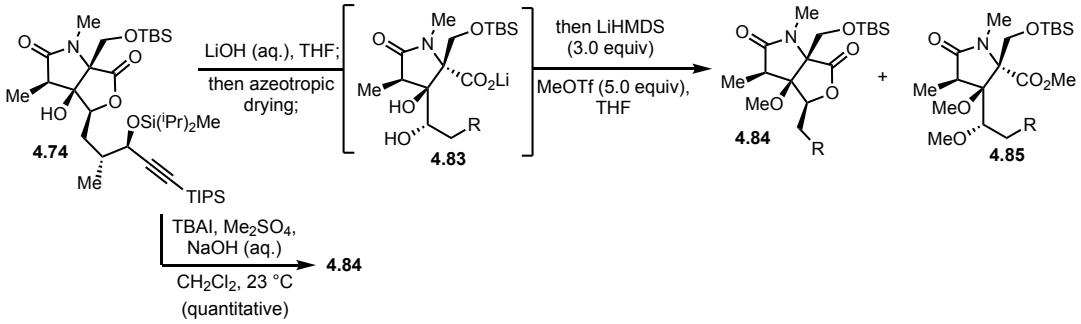

Scheme 4.24. Attempts at a one pot γ-lactone saponification, methylation.

After the above attempts at a streamlined conversion of the neooxazolomycin γ-lactone **4.74** proved unsuccessful, we chose to adopt a similar approach to Donohoe and Hatakeyama involving redox/protecting group chemistry that is described in detail above.

*4.5 Confirmation of Desired (S)-C4-Stereochemistry Following 1,2-Addition to α-Hydroxyaldehyde **4.14***

In the key Li/halogen exchange 1,2-addition to α-hydroxyaldehyde **4.14** of complex organolithium **3.23** two epimers were generated (Schemes 4.10 and 4.25A). In order to confirm that the predominant epimer possessed the desired (*S*)-C4 stereochemistry, as anticipated from considering the previous example (chelated intermediate **3.22**, Scheme 3.3, Chapter Three), the γ-lactone **3.24**, whose absolute stereochemistry is supported by single-crystal X-ray crystallography as well as spectroscopic correlation to Kende's vinyliodide intermediate **3.2** (accessed previously in ~24 steps from *D*-glucose, see Chapter Three),[32] was reduced to the corresponding triol with $LiBH_4$ (Scheme 4.25B). The primary alcohol was protected as its PMB ether in low yield, intercepting the 1,2-adduct under question **4.15**. The product of this two-step sequence from γ-lactone **3.24** was shown by comparison of its ^{1}H-NMR spectra to the two epimers isolated from the addition to α-hydroxyaldehyde **4.14**, to be identical to the major product of said 1,2-addition **4.15** (Figure 4.4). Thus, we concluded that the correct C4 stereoisomer was advanced through the rest of the synthetic route.

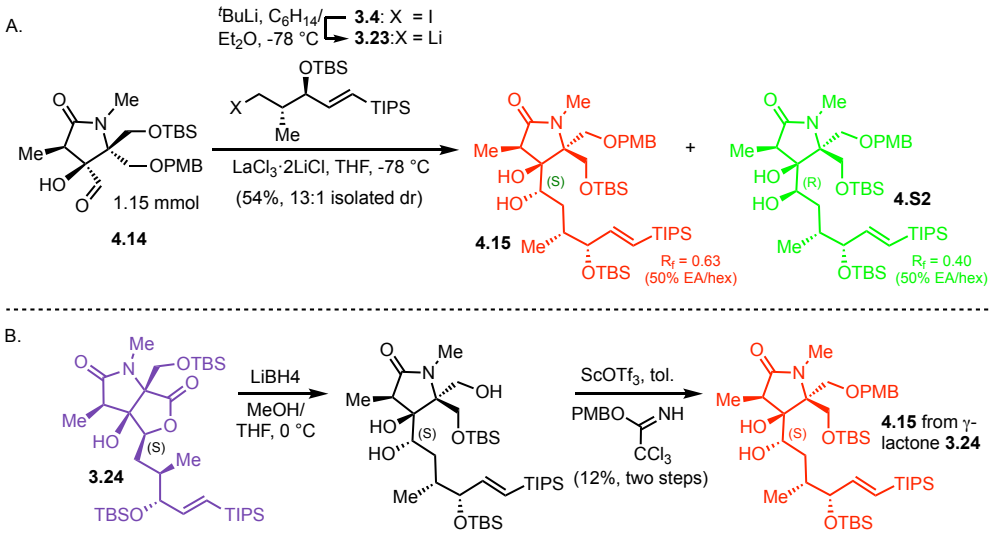

Scheme 4.25. A. The key 1,2-addition of organolithium **3.23** to α-hydroxyaldehyde **4.14** produces two epimers. B. Derivatization of γ-lactone **3.24** leads to a PMB ether that is identical with the 1,2-addition major product.

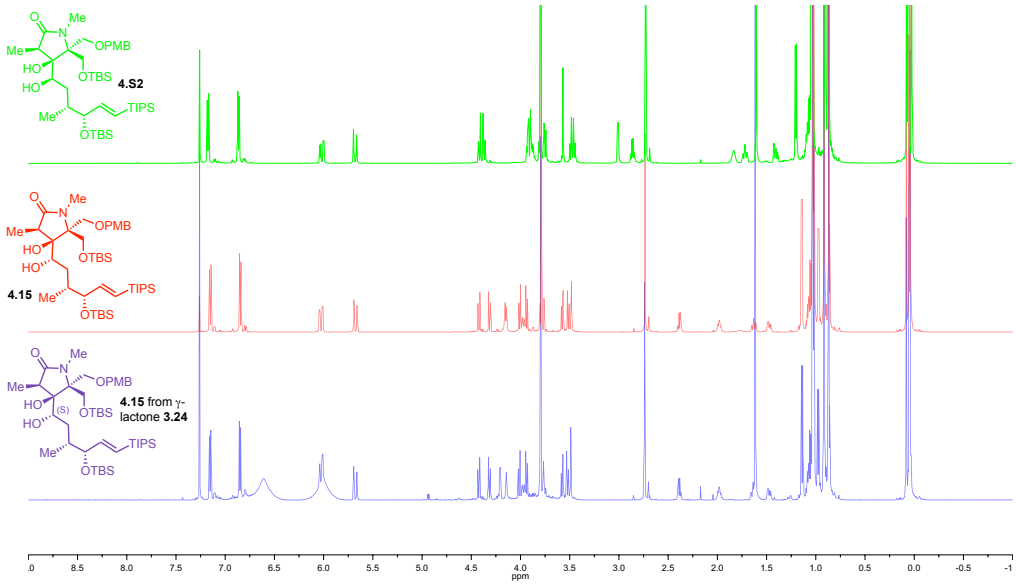

Figure 4.4. Superimposed 1H-NMR spectra (600 MHz, $CDCl_3$) of A. (R)-C4 epimer 4.S2, B. major (S)-C4 epimer addition product 4.15, and C. (S)-C4 epimer derived from γ-lactone 3.24.

4.6 Conclusion

In summary, our pursuit of the synthesis and biological evaluation of complex, bioactive β-lactone-containing natural products guided our efforts toward the oxazolomycins, and has led to a modular, and enantioselective synthesis of the silyl-seco acid of oxazolomycin B, an 11-step synthesis of inthomycin C from propargyl alcohol, and a concise formal synthesis of neooxazolomycin. With an adaptive synthetic approach in hand, our ongoing research is motivated by the potential to apply oxazolomycin-based chemical probes to putative cellular target identification studies. The inherent reactivity of the spiro-β-lactone present in these natural products suggests an ability to covalently modify nucleophilic amino acid residues on proteins (i.e. serine, threonine, cysteine) similar to other known β-lactones, including salinosporamide and tetrahdrolipstatin (Orlistat,® Allí®). Chemical proteomics studies implementing molecular probes based on the core's C1-C5/C15-C17 arrangement would be ideally suited for elucidation of the precise mechanistic effect of the oxazolomycins on cell biology. An array of terminal alkyne-containing probes constructed by modular attachment of the functional and stereochemical elements of the linear portion (C6-C13') will continue to allow simultaneous collection of SAR data and, eventually, the generation of a comprehensive protein binding profile. Future collaborative studies along these lines could result in identification of novel protein targets and lead compounds in the treatment of cancer, bacterial, and viral infections.

4.6 Experimental

4.6.1 General Information

Same as section 3.4.1

4.6.2 Abbreviation List

Same as section 3.4.2

4.6.3 Synthetic Procedures

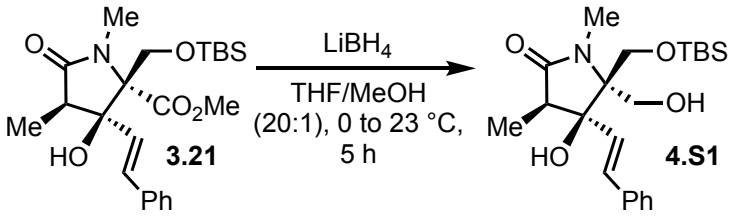

(3*R*,4*S*,5*S*)-5-(((*tert*-butyldimethylsilyl)oxy)methyl)-4-hydroxy-5-(hydroxymethyl)-1,3-dimethyl-4-((*E*)-styryl)pyrrolidin-2-one (4.S1): To an undried 50 mL, single-necked, round-bottomed flask charged with β-silyloxyester **3.21** (858 mg, 1.98 mmol, 1.00 equiv) was added THF (8.57 mL) and MeOH (0.430 mL) and the resulting colorless solution was stirred and cooled to 0 °C in an ice bath over ~10 min. $LiBH_4$ solution (2.0 M in THF, 1.98 mL, 3.96 mmol, 2.00 equiv) was then added via a plastic syringe over ~2 min (note: gas evolution) after which the reaction was allowed to warm to ambient temperature over 5 h and was then quenched by dropwise addition of saturated, aqueous NH_4Cl from a glass Pasteur pipet until no more gas was evolved (~5 mL). The mixture was diluted with EtOAc (10 mL) and an additional 20 mL of saturated, aqueous NH_4Cl and 20 mL EtOAc was used to transfer the mixture to a separatory funnel. The layers were separated, the

aqueous layer was extracted with EtOAc (3 x 10 mL) and the combined organic phase was washed with brine (25 mL), dried over $MgSO_4$, filtered through celite into a dry 100 mL round-bottomed flask, and concentrated by rotary evaporation. The resulting crude white solid 1,3-diol lactam **4.S1** was placed under high vacuum for 2 h and was then used in the next step without purification.

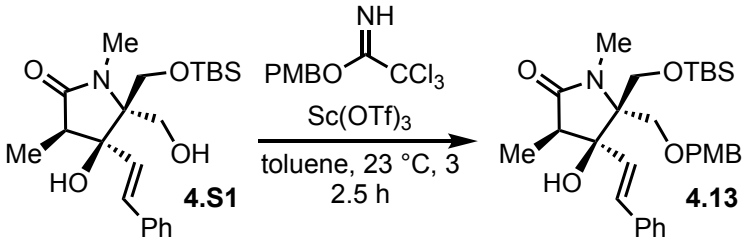

(3*R*,4*S*,5*S*)-5-(((*tert*-butyldimethylsilyl)oxy)methyl)-4-hydroxy-5-(((4-methoxybenzyl)oxy)methyl)-1,3-dimethyl-4-((*E*)-styryl)pyrrolidin-2-one (4.13): To the 100 mL, single-necked, round-bottomed flask containing crude 1,3-diol lactam **4.S1** from the previous reaction was added $Sc(OTf)_3$ (49.2 mg, 0.10 mmol, 0.05 equiv). These solids were suspended in toluene (20 mL, some of the crude substrate remained stuck to the wall of the flask) and stirred at ambient temperature (23 °C). Neat liquid trichloroacetimidate reagent, $PMBOC(NH)CCl_3$ (1.03 mL, 4.45 mmol, 2.50 equiv), was added via a plastic syringe fitted with a stainless-steel needle. The now yellow suspension was stirred for 10 min, while becoming gradually homogenous, and was swirled by hand to dissolve the substrate still adhered to the wall of the flask. A second portion of $PMBOC(NH)CCl_3$ (1.03 mL, 4.45 mmol, 2.50 equiv) was added and the reaction was allowed to stir for 3.5 h. The volatiles were removed by rotary evaporation to reduce the volume of the reaction solution by ~half and then silica gel was added to absorb the entire solution. The volatiles were again removed by rotary evaporation until a free-flowing

yellow powder resulted. This fine yellow powder was subjected to automated flash chromatography (0 → 70%, EtOAc/hexanes, continuous gradient; product elutes at 50-60% EtOAc) to afford orthogonally protected triol lactam **4.13** as a white solid with slight yellow impurity derived from trichloroacetimidate reagent (751 mg, 72% yield over two steps):

R_f = 0.52 (50% EtOAc/hexanes, UV-active); **[α]** $^{24.3}_{D}$ -4.72 (*c* 1.27, $CHCl_3$); **IR (thin film)**: 3386 br, 2953, 2930, 2857, 1678 cm^{-1}; **^{1}H-NMR** (600 MHz, $CDCl_3$) δ 7.34-7.27 (m, 5H), 7.20 (app d, *J* = 8.6 Hz, 2H), 6.88 (app d, *J* = 8.6 Hz, 2H), 6.85 (d, *J* = 15.9 Hz, 1H), 6.24 (d, *J* = 15.9 Hz, 1H), 4.44 (AB d, *J* = 11.8 Hz, 1H), 4.37 (AB d, *J* = 11.8 Hz, 1H), 3.87 (d, *J* = 10.8 Hz, 1H), 3.81 (s, 3H), 3.76-3.73 (m, 2H), 3.42 (AB d, *J* = 10.2 Hz, 1H), 3.38 (AB d, *J* = 10.2 Hz, 1H), 2.90 (q, *J* = 7.2 Hz, 1H), 2.81 (s, 3H), 1.09 (d, *J* = 7.2 Hz, 3H), 0.87 (s, 9H), 0.08 (s, 3H), 0.07 (s, 3H); **^{13}C-NMR** (150 MHz, $CDCl_3$) δ 176.6, 159.6, 136.8, 131.4, 129.7 (2), 129.52, 129.49, 128.7 (2), 127.8, 126.8 (2), 114.1 (2), 81.1, 73.5, 70.0, 68.7, 62.0, 55.4, 46.3, 26.3, 25.8 (3), 18.1, 7.3, -5.6, -5.7; **HRMS (ESI+)** *m/z* calcd. for $C_{30}H_{43}NO_5SiNa$ $[M+Na]^+$: 548.2803, found: 548.2802.

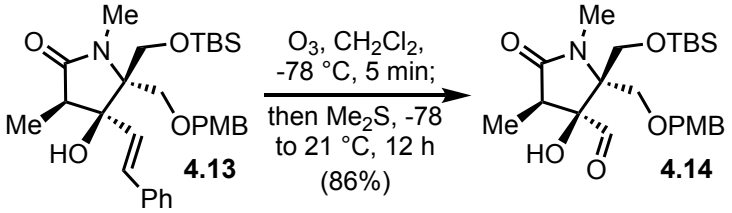

(2*S*,3*S*,4*R*)-2-(((*tert*-butyldimethylsilyl)oxy)methyl)-3-hydroxy-2-(((4-methoxybenzyl)oxy)methyl)-1,4-dimethyl-5-oxopyrrolidine-3-carbaldehyde (4.14): To an undried 50 mL, single-necked, round-bottomed flask containing **4.13** (751 mg, 1.43 mmol, 1.00 equiv) was added CH_2Cl_2 (15 mL). The resulting solution was stirred and

cooled to -78 °C in a dry ice/acetone bath under N_2 (*g*) atmosphere over 15 min (note: in this case the thorough cooling and duration of exposure to O_3 (*g*) is essential in avoiding undesired oxidation of the PMB protecting group). The flask was then opened and the solution was perfused with O_3 (*g*) for 5 min (until the reaction solution became a persistent light-blue color). The O_3 (g) was removed and the solution was purged with N_2 (*g*), producing a light-yellow solution. Me_2S (525 μL, 7.15mmol, 5.00 equiv) was then added dropwise at -78 °C. The reaction mixture was then allowed to warm slowly to ambient temperature (23 °C) over 12 h under N_2 (*g*). The solvent was then removed by rotary evaporation to provide a crude yellow oil that was purified by automated flash chromatography (0 → 70%, EtOAc/hexanes, continuous gradient; **4.14** elutes at 50-60% EtOAc/hexanes) to afford α-hydroxy aldehyde **4.14** as a light-yellow oil that would solidify upon storing at 8 °C into a light-yellow amorphous solid (555 mg, 86%):

[α] $\overset{24.4}{D}$ -9.95 (*c* 1.09, $CHCl_3$); **IR (thin film)**: 3331 br, 2953, 2931, 2857, 1722, 1695 cm^{-1}; **^{1}H-NMR** (600 MHz, $CDCl_3$) δ 9.65 (s, 1H), 7.19 (app d, *J* = 8.6 Hz, 2H), 6.88 (app d, *J* = 8.6 Hz, 2H), 4.45 (AB d, *J* = 11.6 Hz, 1H), 4.37 (AB d, *J* = 11.6 Hz, 1H), 3.81 (d, *J* = 9.9 Hz, 1H), 3.80 (s, 3H), 3.79 (br s, 1H), 3.72 (d, *J* = 9.9 Hz, 1H), 3.65 (AB d, *J* = 10.5 Hz, 1H), 3.58 (AB d, *J* = 10.5 Hz, 1H), 3.11 (q, *J* = 7.2 Hz, 1H), 2.73 (s, 3H), 1.00 (d, *J* = 7.2 Hz, 3H), 0.84 (s, 9H), 0.02 (s, 6H); **^{13}C-NMR** (150 MHz, $CDCl_3$) δ 200.2, 174.8, 159.7, 129.7 (2), 129.0, 114.1 (2), 83.7, 73.4, 70.1, 67.2, 63.1, 55.4, 41.8, 26.1, 25.8 (3), 18.2, 7.7, -5.6, -5.7; **HRMS (ESI+)** *m/*z calcd. for $C_{23}H_{38}NO_6Si$ $[M+H]^+$: 452.2463, found: 452.2464.

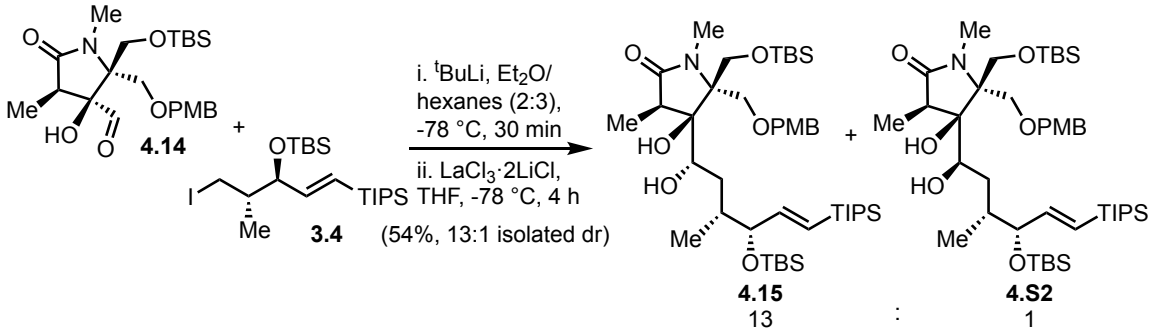

(3*R*,4*S*,5*S*)-4-((1*S*,3*R*,4*R*,*E*)-4-((*tert*-butyldimethylsilyl)oxy)-1-hydroxy-3-methyl-6-(triisopropylsilyl)hex-5-en-1-yl)-5-(((*tert*-butyldimethylsilyl)oxy)methyl)-4-hydroxy-5-(((4-methoxybenzyl)oxy)methyl)-1,3-dimethylpyrrolidin-2-one (4.15): A thick-walled 25 mL, single-necked, round-bottomed flask, fitted with a rubber septa and a teflon stir bar (51 x 19 mm, egg-shaped) and connected to a Schlenk manifold via a 16-guage needle and tubing and was carefully flame dried under high vacuum. A balloon of Ar (*g*) was then attached to the flask via a needle and the atmosphere in the flask was purged by three cycles of vacuum/Ar (*g*). Once the flask had cooled to ambient temperature, clear liquid primary iodide **3.4** was added via a plastic 1 mL syringe fitted with a disposable needle (675 mg, 1.36 mmol, 2.18 equiv). Dry hexanes was added (4.5 mL) followed by dry Et_2O (3 mL). The clear solution was thoroughly cooled to -78 °C in a dry ice/acetone bath over 20 min. A solution of ^{t}BuLi (1.7 M in pentane, 1.68 mL, titrated with *N*-benzylbenzamide)[162] was added slowly over 4 min via a plastic, luer-lock, 3 mL syringe fitted with a 20-guage stainless-steele needle secured at the luer-lock joint with Teflon tape. The colorless solution, which sometimes would occur as a suspension of fine white solid, presumably LiI salt, was stirred at -78 °C for 30 min. During this time a solution of α-hydroxy aldehyde **4.14** (282 mg, 0.625 mmol, 1.00 equiv) and $LaCl_3$·2LiCl (0.6 M in THF, 1.56 mL, 1.50 equiv, Aldrich) in THF (2.0 mL) was prepared in a flame-dried 1.5 dram

vial under N_2 (*g*) atmosphere. This homogenous yellow solution was then added slowly along the wall of the reaction vessel over ~4 min via a plastic 6 mL syringe. The vial was rinsed with an additional 2 mL of THF and transferred to the reaction mixture, which was allowed to stir at -78 °C for 2 h. The reaction mixture was quenched at -78 °C by slow addition of aqueous 0.5 M HCl (5.0 mL). The cooling bath was removed and the mixture was allowed to warm for 15 min before being diluted/transferred to a separatory funnel with EtOAc (15 mL). The layers were separated and the aqueous layer was extracted with EtOAc (3 x 10 mL). The combined organic layers were washed with brine (10 mL), dried over $MgSO_4$, filtered through celite and concentrated by rotary evaporation to a dark yellow oil that was purified by flash column chromatography (0 → 70%, EtOAc/hexanes, 100 mL of hexanes then 10% increments, 60 mL each; **4.15** elutes at 30-40% EtOAc, **4.S2** at 50-60% EtOAc) affording vicinal diol lactams **4.15** (277 mg, 54%) and **4.S2** (21 mg, 4%, 13:1 isolated dr). See **X** for our determination of the relative configuration at the newly formed stereocenter, C4:

4.15: white amorphous solid; $\mathbf{R_f}$ = 0.32 (20% EtOAc/hexanes, stains dark-blue with anisaldehyde solution, slightly UV-active); $\mathbf{[\alpha]}_D^{22.0}$ -3.04 (*c* 1.71, $CHCl_3$); **IR (thin film)** 3444 br, 2955, 2891, 2863, 1651, 1613 cm^{-1}; **^{1}H-NMR** (600 MHz, $CDCl_3$) δ 7.15 (app d, *J* = 8.7 Hz, 2H), 6.85 (app d, *J* = 8.7 Hz, 2H), 6.03 (dd, *J* = 19.1, 5.4 Hz, 1H), 5.67 (dd, *J* = 19.1, 1.4 Hz, 1H), 4.42 (AB d, *J* = 11.7 Hz, 1H), 4.31 (AB d, *J* = 11.7 Hz, 1H), 4.16-4.14 (m, 2H), 4.01 (AB d, *J* = 10.7 Hz, 1H), 3.99-3.96 (m, 1H), 3.94 (d, *J* = 10.7 Hz, 1H), 3.79 (s, 3H), 3.58 (AB d, *J* = 10.4 Hz, 1H), 3.51 (AB d, *J* = 10.4 Hz, 1H), 3.48 (s, 1H), 2.73 (s, 3H), 2.38 (q, *J* = 7.2 Hz, 1H), 1.98 (m, 1H) 1.63 (ddd, *J* = 14.5, 11.0, 3.9 Hz, 1H), 1.48 (ddd, *J* = 14.5, 7.3, 2.3 Hz, 1H), 1.14 (d, *J* = 7.2 Hz, 3H), 1.08-1.02 (m, 21H), 0.97 (d, *J* =

7.1 Hz, 3H), 0.92 (s, 9H), 0.87 (s, 9H), 0.08 (s, 3H), 0.06 (s, 3H), 0.04 (s, 3H), 0.04 (s, 3H); **^{13}C-NMR** (150 MHz, $CDCl_3$) δ 176.5, 159.5, 148.8, 129.6, 129.5 (2), 124.5, 114.0 (2), 81.1, 78.7, 73.3, 71.0, 70.3, 67.7, 63.8, 55.3, 43.1, 36.9, 33.5, 26.2, 25.94 (3), 25.86 (3), 18.7 (6), 18.4, 18.2, 16.4, 11.0 (3), 10.2, -4.3, -4.7, -5.6, -5.7; **HRMS (ESI+)** *m/*z calcd. for $C_{44}H_{83}NO_7Si_3Na$ $[M+Na]^+$: 844.5370, found: 844.5365.

4.S2: slight yellow oil; R_f = 0.12 (20% EtOAc/hexanes, stains dark-blue with anisaldehyde solution, slightly UV-active); **^{1}H-NMR** (600 MHz, $CDCl_3$) δ 7.18 (d, *J* = 8.5 Hz, 1H), 6.86 (d, *J* = 8.5 Hz, 1H), 6.02 (dd, *J* = 19.0, 5.9 Hz, 1H), 5.68 (d, *J* = 19.0 Hz, 1H), 4.42 (d, *J* = 11.6 Hz, 1H), 4.37 (d, *J* = 11.6 Hz, 1H), 3.94-3.87 (m, 3H), 3.80 (s, 3H), 3.75 (d, *J* = 11.1 Hz, 1H), 3.57 (s, 1H), 3.49 (d, *J* = 10.6 Hz, 1H), 3.45 (d, *J* = 10.6 Hz, 1H), 3.01 (d, *J* = 6.0 Hz, 1H), 2.86 (q, *J* = 7.4 Hz, 1H), 2.73 (s, 3H), 1.87-1.80 (m, 1H), 1.74-1.70 (m, 1H), 1.42-1.39 (m, 1H), 1.20 (d, *J* = 7.4 Hz, 3H), 0.90 (s, 9H), 0.88-0.87 (m, 12H), 0.08 (s, 3H), 0.06 (s, 3H), 0.06 (s, 3H), 0.03 (s, 3H); **^{13}C-NMR** (150 MHz, $CDCl_3$) δ 176.9, 159.7, 149.9, 129.8 (2), 128.9, 124.4, 114.1 (2), 81.7, 81.0, 73.6, 72.8, 69.6, 67.6, 63.1, 55.4, 43.2, 36.3, 34.2, 26.1 (3), 25.8 (3), 18.8 (6), 18.4, 18.2, 16.1, 11.0 (3), 10.5, -4.0, -4.6, -5.5, -5.7; **HRMS (ESI+)** *m/*z calcd. for $C_{44}H_{83}NO_7Si_3Na$ $[M+Na]^+$: 844.5370, found: 844.5365.

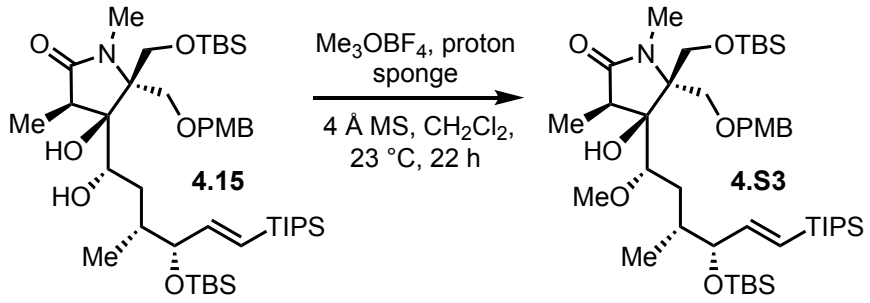

(3*R*,4*S*,5*S*)-4-((1*S*,3*R*,4*R*,*E*)-4-((*tert*-butyldimethylsilyl)oxy)-1-methoxy-3-methyl-6-(triisopropylsilyl)hex-5-en-1-yl)-5-(((*tert*-butyldimethylsilyl)oxy)methyl)-4-hydroxy-

5-(((4-methoxybenzyl)oxy)methyl)-1,3-dimethylpyrrolidin-2-one (4.S3): To a 25 mL, single-necked, round-bottomed flask fitted with a rubber septa and an Ar (*g*) balloon containing powered 4 Å MS (oven-dried at 125 °C for at least 8 h) was added a solution of vicinal diol lactam **4.15** (277 mg, 0.336 mmol, 1.00 equiv) in CH_2Cl_2 (8 mL, including rinse of substrate vessel). The resulting white suspension was stirred at ambient temperature (23 °C) and proton sponge (316 mg, 1.47 mmol, 4.39 equiv) was added by briefly uncapping the reaction vessel. Me_3OBF_4 was then added (161 mg, 1.09 mmol, 3.24 equiv; note: this white solid reagent is highly hydroscopic so to avoid significant generation of acid as the salt is hydrolyzed in air, 10 equiv of the reagent was weighed out into a dry vessel under N_2 (*g*) in a glovebox and was dispensed swiftly, portion-wise into the reaction vessel by briefly uncapping each. The amount of reagent added in each portion was determined by taring the reagent vessel). The atmosphere in the reaction flask was flushed with Ar (*g*) by attaching a gas outlet needle for ~2 min. The suspension was allowed to stir at ambient temperature (23 °C) for 2 h, during which time it gradually became a gold color. Proton sponge (294 mg, 1.37 mmol, 4.08 equiv) and Me_3OBF_4 (153 mg, 1.03 mmol, 3.08 equiv) was again added and the atmosphere in the flask again flushed for ~2 min. After stirring for 4 h a final portion of proton sponge (298 mg, 1.39 mmol, 4.14 equiv) and Me_3OBF_4 (150 mg, 0.101 mmol, 3.02 equiv) was added and the atmosphere flushed as done previously. The gold suspension was then allowed to stir for 16 h before being diluted with CH_2Cl_2 (10 mL) and filtered through celite. The filter cake was rinsed with an additional 15 mL of CH_2Cl_2. The filtrate was transferred to a separatory funnel and was shaken with 10 mL of 0.5 M aqueous HCl. The layers were separated and the aqueous layer was extracted with CH_2Cl_2 (3 x 10 mL). The combined organic layers were washed with

brine (10 mL), dried over $MgSO_4$, filtered through celite and concentrated by rotary evaporation to a yellow oil that was purified by flash column chromatography (0 → 50%, EtOAc/hexanes, 10% increments, 100 mL each to 30% EtOAc then 50 mL each to 50% EtOAc; **4.S3** elutes at ~30% EtOAc) to afford methyl ether **x** as an amorphous white solid (219 mg, 78%):

$\mathbf{R_f}$ = 0.67 (30% EtOAc/hexanes, stains dark-blue with anisaldehyde solution, slightly UV-active); $\mathbf{[\alpha]}_D^{23.7}$ +9.14 (*c* 0.88, $CHCl_3$); **IR (thin film)**: 3418 br, 2955, 2891, 2863, 1682, 1613 cm^{-1}; **^{1}H-NMR** (600 MHz, $CDCl_3$) δ 7.16 (app d, *J* = 8.7 Hz, 2H), 6.85 (app d, *J* = 8.7 Hz, 2H), 6.00 (dd, *J* = 19.0, 5.8 Hz, 1H), 5.70 (dd, *J* = 19.0, 1.2 Hz, 1H), 4.38 (AB d, *J* = 11.7 Hz, 1H), 4.36 (AB d, *J* = 11.7 Hz, 1H), 4.03 (AB d, *J* = 11.0 Hz, 1H), 4.00 (AB d, *J* = 11.0 Hz, 1H), 3.97 (app t, *J* = 5.4 Hz, 1H), 3.79 (s, 3H), 3.62 (dd, *J* = 7.6, 3.2 Hz, 1H), 3.58 (d, *J* = 10.7 Hz, 1H), 3.36 (d, *J* = 10.7 Hz, 1H), 3.33 (br s, 1H), 3.20 (s, 3H), 2.77 (s, 3H), 2.51 (q, *J* = 7.2 Hz, 1H), 2.07 (ddd, *J* = 14.9, 7.6, 3.9 Hz, 1H), 1.62-1.56 (m, 1H), 1.20-1.16 (m, 1H), 1.18 (d, *J* = 7.2 Hz, 3H), 1.08-1.02 (m, 21H), 0.91 (d, *J* = 6.7 Hz, 3H), 0.89 (s, 9H), 0.86 (s, 9H), 0.05 (s, 3H), 0.04 (s, 3H), 0.03 (s, 3H), 0.00 (s, 3H); **^{13}C-NMR** (150 MHz, $CDCl_3$) δ 176.4, 159.5, 148.3, 129.7 (2), 129.6, 125.1, 113.9 (2), 81.7, 81.0, 79.8, 73.4, 71.0, 67.8, 64.2, 55.6, 55.4, 43.1, 37.4, 31.0, 26.3, 26.0 (3), 25.9 (3), 18.8 (6), 18.3, 18.1, 14.7, 11.0 (3), 10.0, -4.1, -4.7, -5.5, -5.8; **HRMS (ESI+)** *m/*z calcd. for $C_{45}H_{85}NO_7Si_3Na$ $[M+Na]^+$: 858.5526, found: 858.5524.

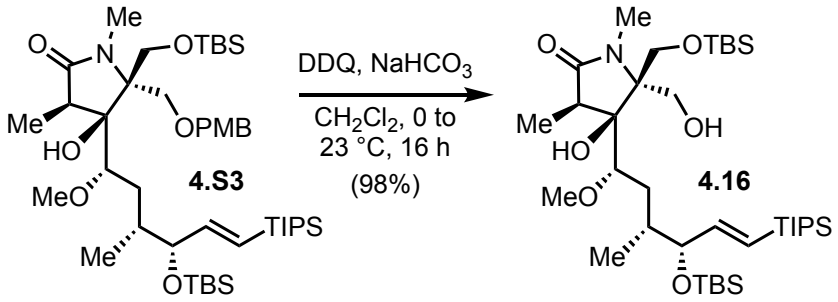

(3*R*,4*S*,5*S*)-4-((1*S*,3*R*,4*R*,*E*)-4-((*tert*-butyldimethylsilyl)oxy)-1-methoxy-3-methyl-6-(triisopropylsilyl)hex-5-en-1-yl)-5-(((*tert*-butyldimethylsilyl)oxy)methyl)-4-hydroxy-5-(hydroxymethyl)-1,3-dimethylpyrrolidin-2-one (4.16): To a 25 mL single-necked, round-bottomed flask containing PMB-ether **4.S3** (204 mg, 0.244 mmol, 1.00 equiv) was added CH_2Cl_2 (10 mL). The resulting colorless solution was cooled to 0 °C in an ice bath over 10 min before adding solid $NaHCO_3$ (820 mg, 9.76 mmol, 40.0 equiv). To this suspension was added 2,3-dichloro-5,6-dicyano-1,4-benzoquinone (DDQ, 553 mg, 2.44 mmol, 10.0 equiv) by briefly uncapping the reaction vessel, resulting immediately in a color change to a dark green. The reaction was allowed to stir and slowly warm to ambient temperature (23 °C) over 16 h before being quenched by pouring into a separatory funnel containing H_2O (5 mL). The reaction vessel was rinsed with CH_2Cl_2 (20 mL). The layers were separated and the aqueous layer was extracted with CH_2Cl_2 (3 x 7 mL). The combined organic layers were washed with brine (15 mL), dried over $MgSO_4$, filtered through celite and concentrated by rotary evaporation to an orange oil that was purified by flash column chromatography (0 → 50%, EtOAc/hexanes, 10% increments, 100 mL each; **4.16** elutes at ~40% EtOAc) to afford primary alcohol **4.16** as a white amorphous solid (171 mg, 98%): $\mathbf{R}_f$ = 0.39 (streaked spot, 40% EtOAc/hexanes, stains dark-blue with anisaldehyde solution); $[\alpha]_D^{23.7}$ +4.12 (*c* 0.49, $CHCl_3$); **IR (thin film)**: 3323 br, 2956, 2891, 2864, 1682, 1620 cm^{-1}; **^{1}H-NMR** (600 MHz, $CDCl_3$) δ 6.03 (dd, *J* = 19.0, 6.0 Hz, 1H), 5.72 (dd, *J* =

19.0, 1.2 Hz, 1H), 4.40 (br s, 1H), 4.22 (d, *J* = 11.5 Hz, 1H), 3.96 (app t, *J* = 5.8 Hz, 1H), 3.83 (d, *J* = 11.5 Hz, 1H), 3.60-3.52 (m, 3H), 3.47 (s, 3H), 3.42 (app t, *J* = 7.0 Hz, 1H), 2.82 (s, 3H), 2.70 (q, *J* = 7.2 Hz, 1H), 2.25 (dt, *J* = 14.3, 5.4 Hz, 1H), 1.86-1.80 (m, 1H), 1.43-1.38 (m, 1H), 1.16 (d, *J* = 7.2 Hz, 3H), 1.09-1.02 (m, 21H), 0.98 (d, *J* = 6.8 Hz, 3H), 0.90 (s, 9H), 0.88 (s, 9H), 0.12 (s, 3H), 0.10 (s, 3H), 0.05 (s, 3H), 0.02 (s, 3H); **^{13}C-NMR** (150 MHz, $CDCl_3$) δ 176.0, 148.7, 125.2, 82.8, 82.4, 80.3, 70.3, 63.9, 61.2, 59.1, 42.9, 37.9, 33.2, 26.1 (3), 25.8 (3), 25.4, 18.8 (6), 18.3, 18.0, 16.3, 11.1 (3), 8.2, -4.0, -4.5, -5.5, -5.8; **HRMS (ESI+)** *m/*z calcd. for $C_{37}H_{77}NO_6Si_3Na$ $[M+Na]^+$: 738.4951, found: 738.4948.

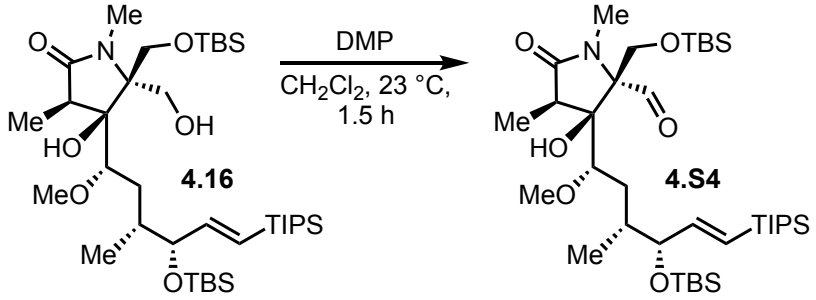

(2*S*,3*S*,4*R*)-3-((1*S*,3*R*,4*R*,*E*)-4-((*tert*-butyldimethylsilyl)oxy)-1-methoxy-3-methyl-6-(triisopropylsilyl)hex-5-en-1-yl)-2-(((*tert*-butyldimethylsilyl)oxy)methyl)-3-hydroxy-1,4-dimethyl-5-oxopyrrolidine-2-carbaldehyde (4.S4): To an undried 20 mL, 27 x 57 mm (OD x H) vial with a septum cap, containing primary alcohol **4.16** (171 mg, 0.239 mmol, 1.00 equiv) was added CH_2Cl_2 (3 mL). This colorless solution was stirred at ambient temperature (23 °C) for ~5 min before adding DMP (152 mg, 0.358 mmol, 1.50 equiv) in one portion by briefly uncapping the reaction vessel. A white suspension immediately results and is stirred for an additional 1.5 h (until TLC indicates complete consumption of starting primary alcohol **4.16**) before evaporating volatiles under a stream of N_2 (*g*). The white residue was transferred to a separatory funnel with Et_2O (15 mL) and saturated,

aqueous $NaHCO_3/Na_2S_2O_3$ (1:1, 10 mL). The layers were separated and the aqueous layer was extracted with Et_2O (3 x 8 mL). The organic layer was dried over $MgSO_4$, filtered through celite, and concentrated by rotary evaporation to a light-yellow oil that was used in the next reaction without purification.

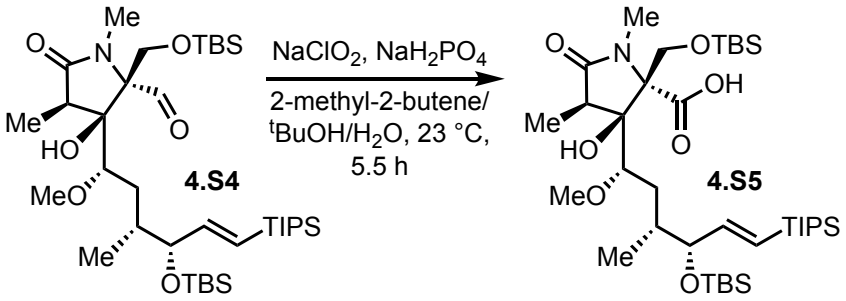

(2*S*,3*S*,4*R*)-3-((1*S*,3*R*,4*R*,*E*)-4-((*tert*-butyldimethylsilyl)oxy)-1-methoxy-3-methyl-6-(triisopropylsilyl)hex-5-en-1-yl)-2-(((*tert*-butyldimethylsilyl)oxy)methyl)-3-hydroxy-1,4-dimethyl-5-oxopyrrolidine-2-carboxylic acid (4.S5): To an undried 25 mL, single-necked, round-bottomed flask open to air, containing crude β-silyloxy aldehyde **4.S4** (0.239 mmol, 1.00 equiv) was added ^{t}BuOH (4 mL) and 2-methyl-2-butene (760 μL, 7.17 mmol, 30.0 equiv). This colorless solution was stirred at 23 °C while a separate solution of $NaClO_2$ (109 mg, 1.20 mmol, 5.00 equiv) and NaH_2PO_4 (229 mg, 1.91 mmol, 8.00 equiv) in H_2O (2 mL) was prepared in a glass test tube and was then added via glass pipet in one portion. The resulting mixture was stirred for 5 h (until TLC indicated complete consumption of starting β-silyloxy aldehyde **4.S4** before adding NaCl (*s*) to saturation and diluting with EtOAc (5 mL) and brine (3 mL). The layers were separated and the aqueous layer was extracted with EtOAc (3 x 5 mL). The combined organic layers were dried over $MgSO_4$, filtered through celite, and concentrated by rotary evaporation to a yellow oil that was used in the next step without purification.

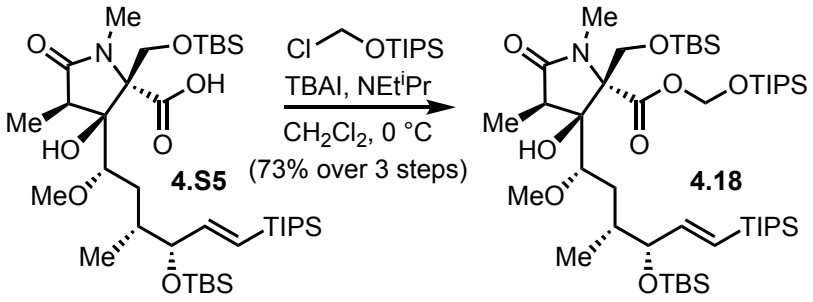

((triisopropylsilyl)oxy)methyl-(2*S*,3*S*,4*R*)-3-((1*S*,3*R*,4*R*,*E*)-4-((*tert*-butyldimethylsilyl)oxy)-1-methoxy-3-methyl-6-(triisopropylsilyl)hex-5-en-1-yl)-2-(((*tert*-butyldimethylsilyl)oxy)methyl)-3-hydroxy-1,4-dimethyl-5-oxopyrrolidine-2-carboxylate (4.18): To a 25 mL single-necked, round-bottomed flask containing crude β-silyloxy carboxylic acid **4.S5** (0.239 mmol, 1.00 equiv) was added TBAI (20.8 mg, 0.056 mmol, 0.240 equiv), followed by CH_2Cl_2 (4 mL). The resulting amber solution was stirred and cooled to 0 °C in an ice bath for 10 min before adding NEt^{i}Pr$_2$ (167 μL, 0.956 mmol, 4.00 equiv) in one portion followed by a solution of triisopropylsilyloxymethylchloride (80.0 mg, 0.359 mmol, 1.50 equiv) in CH_2Cl_2 (0.5 mL) and stirring was continued for 1 h. The reaction was diluted with EtOAc (5 mL) and quenched by addition of saturated, aqueous NH_4Cl (6 mL). The mixture was transferred to a separatory funnel with EtOAc (5 mL), the layers were separated, and the aqueous layer was extracted with EtOAc (3 x 6 mL). The combined organic layers were washed with brine (5 mL), dried over $MgSO_4$, filtered through celite, and concentrated by rotary evaporation to an amber oil that was purified by flash column chromatography (0 → 30%, EtOAc/hexanes, 10% increments, 75 mL each; **4.18** elutes at ~20% EtOAc) to afford silyloxymethyl ester **x** as a light yellow oil (159 mg, 73% over three steps):

$\mathbf{R}_f$ = 0.64 (20% EtOAc/hexanes, stains dark-blue with anisaldehyde solution); $[\alpha]_D^{22.6}$ +30.93 (*c* 1.91, $CHCl_3$; **IR (thin film)**: 3347 br, 2941, 2892, 2892, 2865, 1738, 1686, 1619 cm^{-1}; **^{1}H-NMR** (600 MHz, $CDCl_3$) 6.02 (dd, *J* = 19.0, 5.6 Hz, 1H), 5.73 (dd, *J* = 19.0, 1.1 Hz, 1H), 5.53 (d, *J* = 3.9 Hz, 1H), 5.44 (d, *J* = 3.9 Hz, 1H), 4.45 (d, *J* = 11.5 Hz, 1H), 4.42 (s, 1H), 4.08 (d, *J* = 11.5 Hz, 1H), 4.01 (app t, *J* = 5.2 Hz, 1H), 3.34 (t, *J* = 5.7 Hz, 1H), 3.25 (s, 3H), 2.75 (s, 3H), 2.61 (q, *J* = 7.3 Hz, 1H), 2.16 (dt, *J* = 14.6, 5.2 Hz, 1H), 1.69-1.65 (m, 1H), 1.41-1.36 (m, 1H), 1.18 (d, *J* = 7.3 Hz, 3H), 1.10-1.02 (m, 42H), 0.93 (d, *J* = 6.8 Hz, 3H), 0.90 (s, 9H), 0.87 (s, 9H), 0.13 (s, 3H), 0.10 (s, 3H), 0.04 (s, 3H), 0.01 (s, 3H); **^{13}C-NMR** (150 MHz, $CDCl_3$) δ 176.7, 169.1, 148.3, 124.8, 85.6, 83.5, 82.1, 79.4, 74.0, 62.1, 57.8, 42.8, 38.1, 31.5, 26.6, 26.0 (3), 25.8 (3), 18.8 (6), 18.3, 18.1, 17.8 (6), 15.7, 12.0 (3), 11.1 (3), 9.2, -4.1, -4.6, -5.5, -5.7; **HRMS (ESI+)** *m/*z calcd. for $C_{47}H_{97}NO_8Si_4Na$ $[M+Na]^+$: 938.6183, found: 938.6176.

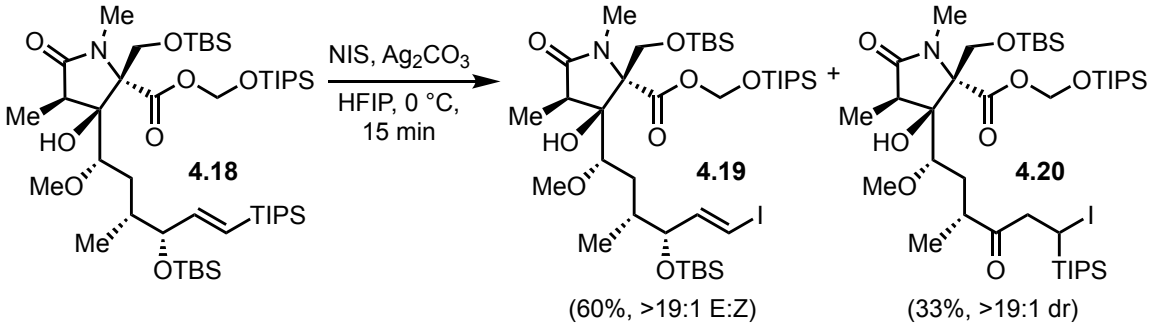

((triisopropylsilyl)oxy)methyl-(2*S*,3*S*,4*R*)-3-((1*S*,3*R*,4*R*,*E*)-4-((*tert*-butyldimethylsilyl)oxy)-6-iodo-1-methoxy-3-methylhex-5-en-1-yl)-2-(((*tert*-butyldimethylsilyl)oxy)methyl)-3-hydroxy-1,4-dimethyl-5-oxopyrrolidine-2-carboxylate (4.19): To an undried 1.5 dram vial (6 mL, 16 x 50 mm, OD x H) fitted with a septum cap, containing vinylsilane **4.18** (49.3 mg, 0.0538 mmol, 1.00 equiv), was added

Ag_2CO_3 (4.5 mg, 0.012 mmol, 0.30 equiv) followed by HFIP (300 μL). The resulting green suspension was stirred, cooled to 0 °C in an ice bath over 5 min, and was excluded from light with a sheet of aluminum foil. NIS (12.1 mg, 0.0538 mmol, 1.00 equiv, excluded from light) by briefly uncapping the reaction vessel (note: starting material is consumed in the time required to develop a TLC), and stirring is continued for 15 min. The reaction was diluted with Et_2O (4.5 mL) and quenched by the addition of saturated, aqueous $Na_2S_2O_3$ (1.5 mL). The layers were separated with a glass pipet and the aqueous layer was extracted with Et_2O (3 x 3 mL) and transferred to a separatory funnel. The combined organic layers were washed with brine (4.5 mL), dried over $MgSO_4$, filtered through celite, and concentrated by rotary evaporation to a colorless oil that was purified by flash chromatography (0 → 30%, EtOAc/hexanes, 10% increments, 40 mL each; **4.19** elutes at 20% EtOAc) to afford vinyliodide pyroglutamate **4.19** (28.6 mg, 60%) in addition to a β,β-silyliodoketone side product **4.20** (16.5 mg, 33%):

4.19: white foam; $\mathbf{R}_f$ = 0.69 (30% EtOAc/hexanes, stains purple with anisaldehyde solution, UV-active); $[\alpha]_D^{23.7}$ +39.53 (*c* 0.486, $CHCl_3$); **IR (thin film)**: 3356 br, 2950, 2931, 2894, 2866, 1739, 1686, 1606 cm^{-1}; **^{1}H-NMR** (600 MHz, $CDCl_3$) δ 6.51 (dd, *J* = 14.4, 6.3 Hz, 1H), 6.21 (dd, *J* = 14.4, 1.2 Hz, 1H), 5.51 (d, *J* = 3.9 Hz, 1H), 5.44 (d, *J* = 3.9 Hz, 1H), 4.63 (s, 1H), 4.47 (d, *J* = 11.7 Hz, 1H), 4.05 (d, *J* = 11.7 Hz, 1H), 4.06-4.03 (m, 1H), 3.31-3.30 (m, 1H), 3.29 (s, 3H), 2.75 (s, 3H), 2.66 (q, *J* = 7.4 Hz, 1H), 2.06 (ddd, *J* = 14.6, 6.1, 4.3 Hz, 1H), 1.72-1.68 (m, 1H), 1.45 (dt, *J* = 14.6, 7.2 Hz, 1H), 1.17 (d, *J* = 7.4 Hz, 3H), 1.14-1.05 (m, 21H), 0.94 (d, *J* = 6.8 Hz, 3H), 0.89 (s, 9H), 0.89 (s, 9H), 0.16 (s, 3H), 0.12 (s, 3H), 0.04 (s, 3H), 0.02 (s, 3H); **^{13}C-NMR** (150 MHz, $CDCl_3$) δ 176.7, 168.9, 146.5, 85.8, 83.7, 82.0, 78.4, 77.1, 73.1, 62.1, 58.8, 42.8, 38.2, 31.7, 26.4, 26.0 (3), 25.8

(3), 18.3, 18.1, 17.8 (6), 15.9, 12.0 (3), 8.7, -4.3, -4.7, -5.5, -5.6; **HRMS (ESI+)** *m/*z calcd. for $C_{38}H_{76}NO_8ISi_3Na$ $[M+Na]^+$: 908.3816, found: 908.3806.

4.20: white foam; R_f = 0.41 (30% EtOAc/hexanes, doesn't stain well, slightly UV-active); $[\alpha]_D^{23.7}$ -11.49 (*c* 0.56, $CHCl_3$); **IR (thin film)**: 3362 br, 2945, 2892, 2867, 1738, 1711, 1687 cm^{-1}; **^{1}H-NMR** (600 MHz, $CDCl_3$) δ 5.45 (AB d, *J* = 3.8 Hz, 1H), 5.43 (AB d, *J* = 3.8 Hz, 1H), 4.56 (s, 1H), 4.48 (d, *J* = 11.6 Hz, 1H), 4.07 (d, *J* = 11.6 Hz, 1H), 3.88 (dd, *J* = 12.0, 1.6 Hz, 1H), 3.38 (dd, *J* = 18.7, 12.0 Hz, 1H), 3.22 (dd, *J* = 7.1, 3.4 Hz, 1H), 3.15 (s, 3H), 3.11 (dd, *J* = 18.7, 1.6 Hz, 1H), 2.95 (ddq, *J* = 10.7, 6.9, 3.6 Hz, 1H), 2.75 (s, 3H), 2.63 (q, *J* = 7.2 Hz, 1H), 2.38 (ddd, *J* = 14.5, 9.4, 3.5 Hz, 1H), 1.82 (ddd, *J* = 14.5, 7.1, 3.3 Hz, 1H), 1.30 (dq, *J* = 14.7, 7.5 Hz, 1H), 1.18 (d, *J* = 7.3 Hz, 3H), 1.15-1.13 (m, 18H), 1.12 (d, *J* = 7.1 Hz, 3H), 1.10-1.08 (m, 3H), 1.05-1.04 (m, 18H), 0.89 (s, 9H), 0.14 (s, 3H), 0.11 (s, 3H); **^{13}C-NMR** (150 MHz, $CDCl_3$) δ 210.6, 176.5, 169.2, 85.5, 84.0, 81.0, 73.2, 62.2, 59.0, 46.6, 43.2, 43.0, 32.4, 26.6, 25.7 (3), 19.1 (3), 19.0 (3), 18.1, 17.8 (6), 16.6, 12.0 (3), 11.9 (3), 8.7, 4.6, -5.6, -5.7; **HRMS (ESI+)** *m/*z calcd. for $C_{41}H_{83}NO_8ISi_3$ $[M+H]^+$: 928.4466, found: 928.4459.

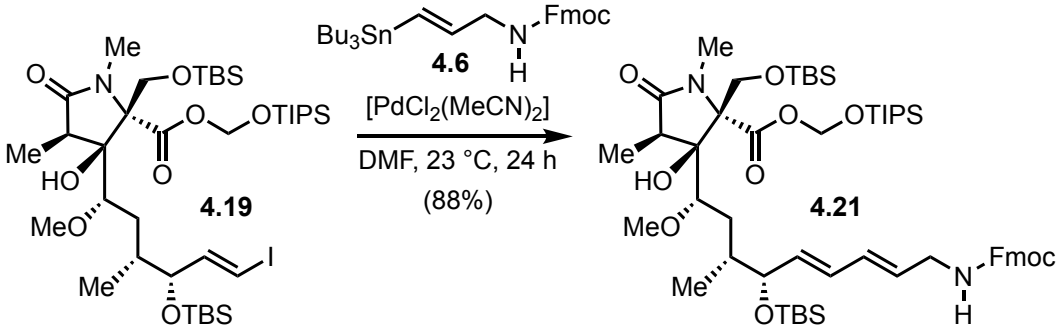

((triisopropylsilyl)oxy)methyl-(2*S*,3*S*,4*R*)-3-((1*S*,3*R*,4*R*,5*E*,7*E*)-9-((((9*H*-fluoren-9-yl)methoxy)carbonyl)amino)-4-((*tert*-butyldimethylsilyl)oxy)-1-methoxy-3-

methylnona-5,7-dien-1-yl)-2-(((*tert*-butyldimethylsilyl)oxy)methyl)-3-hydroxy-1,4-dimethyl-5-oxopyrrolidine-2-carboxylate (4.21): To an undried 1.5 dram (6 mL, 16 x 50 mm, OD x H) fitted with a septum cap, containing vinyliodide **4.19** (21.5 mg, 0.0242 mmol, 1.00 equiv) and vinylstannane **4.6** (24.1 mg, 0.0424 mmol, 1.77 equiv) was added DMF (700 μL) followed by a stock solution of $[PdCl_2(MeCN)_2]$ (0.051 M in DMF, 24 μL, 0.0012 mmol, 0.050 equiv). The colorless solution immediately became a dark-red/purple upon addition of the catalyst solution and was stirred for 24 h at 23 °C excluded from light with a sheet of aluminum foil. The reaction was then diluted with EtOAc (4.5 mL) and filtered through a short pad of SiO_2 over celite. The filter cake was rinsed with EtOAc (18 mL) and the volatiles were removed by rotary evaporation followed by high vacuum (to remove residual DMF) to give an orange oil that was purified by flash chromatography (0 → 40%, EtOAc/hexanes, 10% increments, 40 mL each; **4.21** elutes at ~30% EtOAc) to afford oxazolomycin core **4.21** as a white foam (21.8 mg, 88%):

$\mathbf{R_f}$ = 0.29 (30% EtOAc/hexanes, stains dark-blue with anisaldehyde solution, UV-active); $\mathbf{[\alpha]}_D^{22.4}$ +21.78 (*c* 0.514, $CHCl_3$); **IR (thin film)**: 3333 br, 2953, 2931, 2893, 2866, 1730, 1694 cm^{-1}; **^{1}H-NMR** (600 MHz, $CDCl_3$) δ 7.76 (d, *J* = 7.5 Hz, 2H), 7.62 (d, *J* = 7.4 Hz, 2H), 7.40 (t, *J* = 7.4 Hz, 2H), 7.31 (td, *J* = 7.5, 0.9 Hz, 2H), 6.17-6.12 (m, 2H), 5.66-5.60 (m, 2H), 5.54 (d, *J* = 3.9 Hz, 1H), 5.45 (d, *J* = 3.9 Hz, 1H), 5.09-5.05 (m, 1H), 4.50 (s, 1H), 4.45 (d, *J* = 11.6 Hz, 1H), 4.41 (d, *J* = 7.1 Hz, 2H), 4.24-4.21 (m, 1H), 4.10-4.07 (m, 1H), 4.06 (d, *J* = 11.6 Hz, 1H), 3.91-3.81 (m, 2H), 3.34 (dd, *J* = 6.5, 4.4 Hz, 1H), 3.28 (s, 3H), 2.75 (s, 3H), 2.60 (q, *J* = 7.2 Hz, 1H), 2.04 (dt, *J* = 13.8, 4.1 Hz, 1H), 1.74-1.69 (m, 1H), 1.42-1.38 (m, 1H), 1.17 (d, *J* = 7.3 Hz, 3H), 1.10-1.05 (m, 21H), 0.95 (d, *J* = 6.8 Hz, 3H), 0.90 (s, 9H), 0.87 (s, 9H), 0.12 (s, 3H), 0.09 (s, 3H), 0.04 (s, 3H), 0.00 (s, 3H); **^{13}C-NMR**

(150 MHz, $CDCl_3$) δ 176.8, 169.1, 156.4, 144.1 (2), 141.5 (2), 134.6, 131.8, 130.1, 129.0, 127.8 (2), 127.2 (2), 125.3 (2), 120.1 (2), 85.7, 83.8, 82.2, 76.4, 73.9, 66.9, 62.0, 58.0, 47.4, 43.0, 42.9, 38.5, 31.3, 26.5, 26.03 (3), 25.8 (3), 18.3, 18.1, 17.8 (6), 16.4, 12.0 (3), 9.23, -4.1, -4.7, -5.58, -5.62; **HRMS (ESI+)** *m/*z calcd. for $C_{56}H_{93}N_2O_{10}Si_3$ $[M+H]^+$: 1037.6133, found: 1037.6122.

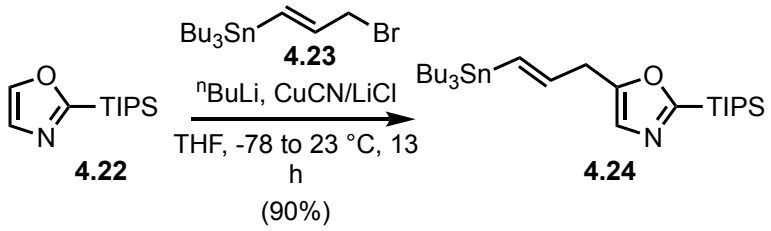

(*E*)-5-(3-(tributylstannyl)allyl)-2-(triisopropylsilyl)oxazole: To a 100 mL, single-necked, round-bottomed flask containing known 2-(triisopropylsilyl)oxazole (1.27 g, 5.63 mmol, 1.00 equiv) was added THF (10 mL). The solution was cooled to -78 °C in a dry ice/acetone bath over 10 min before adding ^{n}BuLi (2.5 M in hexanes, 2.5 mL, 6.19 mmol, 1.10 equiv) dropwise over ~3 min. The resulting solution was then stirred for 30 min, during which a separate 25 mL single-necked, round-bottomed flask containing CuCN (277 mg, 3.09, 0.55 equiv), LiCl (262 mg, 6.19 mmol, 1.10 equiv) and THF (10 mL) was sonicated for 30 min (until the salts, which were both oven-dried at 125 °C for at least 8 h, dissolved). This turquoise solution of CuCN/LiCl was added dropwise to the substrate solution over ~2 min and the resulting mixture was stirred for 1 h at -78 °C. A solution of vinylstannane allylic bromide **4.23** in THF (10 mL) was then added dropwise over ~3 min. The reaction mixture was allowed to warm slowly to 23 °C over 12 h before being quenched by careful addition of saturated, aqueous NH_4Cl (25 mL). The layers were separated and the aqueous layer was extracted with Et_2O (3 x 25 mL). The combined

organic layers were washed with brine (30 mL), dried over $MgSO_4$, filtered through celite, and concentrated by rotary evaporation. The crude residue was purified by flash chromatography (0 → 15%, EtOAc/hexanes, 5% increments, 100 mL each) to afford silyloxazole vinylstannane **4.24** (2.81 g, 90%):

R_f = 0.69 (10% EtOAc/hexanes, stains yellow with $KMnO_4$ solution, UV-active); **IR (thin film)**: 2956, 2867, 1463 cm^{-1}; **^{1}H-NMR** (600 MHz, $CDCl_3$) δ 6.83 (s, 1H), 6.09-5.97 (m, 2H), 3.52 (m, 2H), 1.50-1.45 (m, 6H), 1.41-1.36 (m, 4H), 1.32-1.26 (m, 8H), 1.14-1.12 (m, 21H), 0.89-0.86 (m, 9H); **^{13}C-NMR** (150 MHz, $CDCl_3$) δ 167.8, 152.9, 142.4, 131.7, 123.0, 77.4, 77.2, 76.9, 33.9, 29.2, 27.4, 18.5, 13.8, 11.1, 9.6; **HRMS (ESI+)** *m/*z calcd. for $C_{27}H_{54}NOSiSn$ $[M+H]^+$: 556.2992, found: 556.2996.

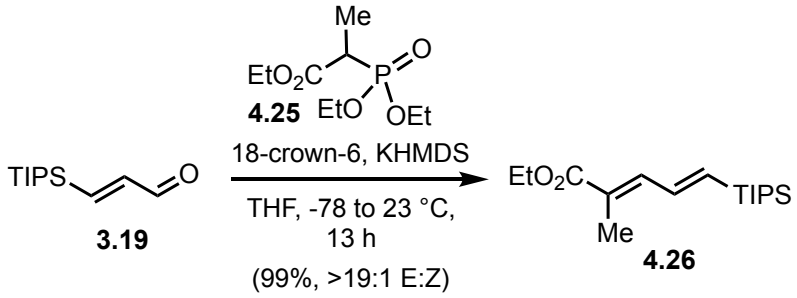

Ethyl-(2E,4E)-2-methyl-5-(triisopropylsilyl)penta-2,4-dienoate (4.26): To a 250 mL, single-necked, round-bottomed flask containing 18-crown-6 (11.0 g, 41.7 mmol, 4.10 equiv) and ethyl 2-(diethoxyphosphoryl)propanoate (2.64 mL, 12.1 mmol, 1.20 equiv) was added THF (200 mL). The solution was cooled to -78 °C in a dry ice/acetone bath over 15 min before adding KHMDS (1.0 M in THF, 12.6 mL, 12.6 mmol, 1.25 equiv) dropwise over ~3 min. The resulting suspension was stirred for 30 min at -78 °C before adding known yellow liquid (*E*)-3-(triisopropylsilyl)acrylaldehyde (2.15 g, 10.1 mmol, 1.00 equiv) dropwise over ~1 min via a plastic 3 mL syringe fitted with a stainless steel needle,

which was rinsed with THF (2 mL) into the reaction vessel. The reaction mixture was allowed to warm to 23 °C over 12 h before being quenched by careful addition of saturated, aqueous NH_4Cl (60 mL). THF was removed by rotary evaporation and the remaining aqueous phase was extracted with Et_2O (3 x 40 mL). The combined organic layers were washed with brine (50 mL), dried over $MgSO_4$, filtered through celite, and concentrated by rotary evaporation to an amber oil that was purified by automated flash chromatography (0 → 20%, EtOAc/hexanes, continuous gradient; product elutes at 15% EtOAc) to afford ethyl silyldieneoate **4.26** as a yellow liquid (2.96 g, 99%, >19:1 *E*:*Z*):

R_f = 0.93 (10% EtOAc/hexanes, UV-active)

IR (thin film): 2942, 2865, 1707, 1624, 1573, 1463 cm^{-1}; **^{1}H-NMR** (600 MHz, $CDCl_3$) δ 7.15 (app d, *J* = 10.8 Hz 1H), 6.89 (dd, *J* = 18.5, 10.8 Hz, 1H), 6.24 (d, *J* = 18.5 Hz, 1H), 4.22 (q, *J* = 7.1 Hz, 2H), 1.98 (d, *J* = 1.4 Hz, 3H), 1.31 (t, *J* = 7.1 Hz, 3H), 1.17-1.12 (m, 3H), 1.07-1.05 (m, 18H); **^{13}C-NMR** (150 MHz, $CDCl_3$) δ 168.8, 140.9, 140.5, 138.7, 127.1, 77.4, 77.2, 76.9, 60.8, 18.8, 14.5, 13.0, 11.0; **HRMS (ESI+)** *m/*z calcd. for $C_{17}H_{33}O_2Si$ $[M+H]^+$: 297.2245 found: 297.2246.

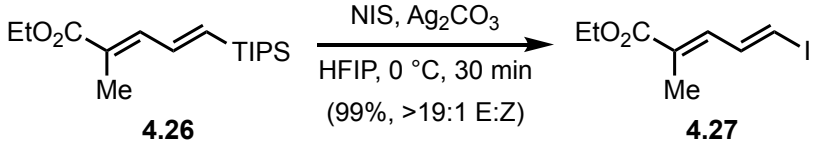

Ethyl-(2*E*,4*E*)-5-iodo-2-methylpenta-2,4-dienoate (4.27): To a 100 mL, single-necked, round-bottomed flask containing ethyl silyldieneoate **4.26** (2.43 g, 8.19 mmol, 1.00 equiv) was added HFIP (27 mL) and Ag_2CO_3 (676 mg, 2.45 mmol, 0.30 equiv) by briefly uncapping the reaction vessel. The atmosphere in the flask was flushed with a stream of N_2 (*g*) for ~1 min and cooled to 0 °C in an ice bath over ~10 min before adding NIS (3.13 g,

13.9 mmol, 1.70 equiv) in one portion by briefly uncapping the reaction vessel. The atmosphere in the flask was again flushed with a stream of N_2 for ~1 min. The reaction mixture was stirred for 30 min at 0 °C before being quenched (note: the work up was carried out with the lights off) by careful addition of saturated, aqueous $Na_2S_2O_3$ (30 mL). HFIP was removed by rotary evaporation and the remaining aqueous phase was extracted with Et_2O (3 x 40 mL). The combined organic layers were washed with brine (30 mL), dried over $MgSO_4$, filtered through celite, and concentrated by rotary evaporation to a red oil that was purified by automated flash chromatography (0 → 20%, EtOAc/hexanes, continuous gradient; product elutes at 15% EtOAc) to afford ethyl iododienoate **4.27** as an orange liquid (2.15 g, 99%, >19:1 *E*:*Z*):

R_f = 0.86 (10% EtOAc/hexanes, UV-active); **IR (thin film)**: 2944, 2866, 1622, 1464 cm^{-1}; **^{1}H-NMR** (600 MHz, $CDCl_3$) δ 7.36 (dd, *J* = 14.2, 11.6 Hz, 1H), 7.05 (ddd, *J* = 11.7, 1.5, 0.8 Hz, 1H), 6.83 (d, *J* = 14.3 Hz, 1H), 4.21 (q, *J* = 7.1 Hz, 2H), 1.91 (d, *J* = 1.0 Hz, 3H), 1.30 (t, *J* = 7.2 Hz, 3H); **^{13}C-NMR** (150 MHz, $CDCl_3$) δ 168.1, 141.2, 136.9, 127.9, 87.9, 77.4, 77.2, 76.9, 61.0, 14.4, 13.1; **HRMS (ESI+)** *m/z* calcd. for $C_8H_{12}O_2I$ $[M+H]^+$: 266.9877, found: 266.9876.

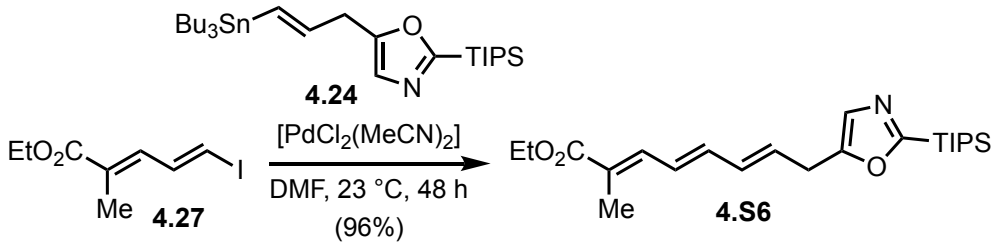

Ethyl-(2*E*,4*E*,6*E*)-2-methyl-8-(2-(triisopropylsilyl)oxazol-5-yl)octa-2,4,6-trienoate (4.S6): To a 50 mL, single-necked, round-bottomed flask fitted with a rubber septum and a balloon of argon was added $Pd(MeCN)_2Cl_2$ (15 mg, 0.058 mmol, 0.031 equiv). The

atmosphere in the flask was flushed with argon for ~3 min before adding a solution of ethyl iododienoate **4.27** (500 mg, 1.88 mmol, 1.00 equiv) in DMF (5 mL, degassed by bubbling argon for 30 min and stored over 4 Å MS). To the resulting amber solution was added silyloxazole vinylstannane **4.24** (1.20 g, 2.16 mmol, 1.15 equiv) in DMF (5 mL). The reaction mixture was stirred at 23 °C for 48 h before being diluted with Et_2O (30 mL) and filtered through a pad of celite. The filter cake was rinsed with Et_2O (20 mL) and the filtrate was washed with H_2O (3 x 50 mL), brine (25 mL), dried over $MgSO_4$, filtered through celite, and concentrated by rotary evaporation. The crude residue was purified by flash chromatography (0 → 15%, EtOAc/hexanes, 5% increments, 50 mL each) to afford ethyl oxazolyltrienoate **4.S6** (774 mg, 96%):

R_f = 0.48 (10% EtOAc/hexanes, UV-active); **IR (thin film)**: 2943, 2866, 1706, 1463 cm^{-1}; **^{1}H-NMR** (600 MHz, $CDCl_3$) δ 7.20 (d, *J* = 11.5 Hz, 1H), 6.85 (s, 1H), 6.52 (dd, *J* = 14.8, 10.7 Hz, 1H), 6.42 (dd, *J* = 14.8, 11.5 Hz, 1H), 6.25 (dd, *J* = 15.1, 10.7 Hz, 1H), 5.94 (dt, *J* = 14.4, 6.7 Hz, 1H), 4.21 (q, *J* = 7.1 Hz, 2H), 3.55 (d, *J* = 6.7 Hz, 2H), 1.95 (s, 3H), 1.39 (m, 3H), 1.30 (t, *J* = 7.1 Hz, 3H), 1.14-1.12 (m, 18H); **^{13}C-NMR** (150 MHz, $CDCl_3$) δ 168.5, 168.2, 152.0, 138.6, 138.0, 132.8, 131.8, 127.5, 127.4, 123.2, 60.7, 29.2, 18.5, 14.5, 12.8, 11.1; **HRMS (ESI+)** *m/*z calcd. for $C_{23}H_{38}NO_3Si$ $[M+H]^+$: 404.2616, found: 404.2889.

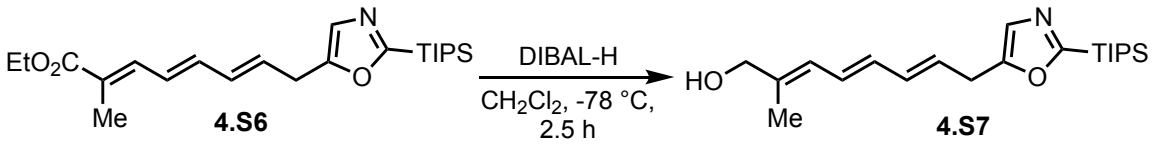

(2*E*,4*E*,6*E*)-2-methyl-8-(2-(triisopropylsilyl)oxazol-5-yl)octa-2,4,6-trien-1-ol (4.S7): To a 100 mL, single-necked, round-bottomed flask containing ethyl oxazolyltrienoate **4.S6**

(450 mg, 1.12 mmol, 1.00 equiv) was added CH_2Cl_2 (10 mL). The resulting solution was cooled to -78 °C in a dry ice/acetone bath over ~10 min before adding neat liquid DIBAL-H (600 μL, 3.36 mmol, 3.00 equiv) dropwise over ~2 min. The colorless solution was stirred at -78 °C for 2 h before quenching with EtOAc (10 mL) at this temperature followed by the addition of saturated, aqueous sodium potassium tartrate (10 mL). The biphasic mixture was stirred for 5 h after which the layers were separated and the aqueous layer was extracted with CH_2Cl_2 (3 x 15 mL). The combined organic layers were washed with brine (15 mL), dried over Na_2SO_4, filtered through celite, and concentrated by rotary evaporation to a colorless oil, oxazolyl trienyl alcohol **4.S7**, that was used in the next step without purification.

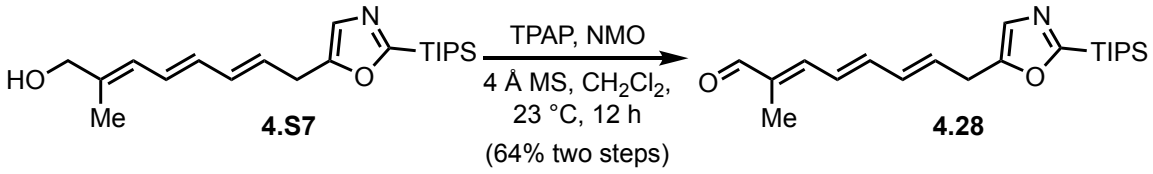

(2*E*,4*E*,6*E*)-2-methyl-8-(2-(triisopropylsilyl)oxazol-5-yl)octa-2,4,6-trienal (4.28): To a 100 mL, single-necked, round-bottomed flask containing 4 Å MS (~1 g), TPAP (20.0 mg, 0.0557 mmol, 0.050 equiv), and NMO (195 mg, 1.66 mmol, 1.48 equiv) was added CH_2Cl_2 (10 mL). The resulting mixture was stirred at 23 °C and a solution of crude oxazolyl trienyl alcohol **4.S7** (1.12 mmol, 1.00 equiv) in CH_2Cl_2 (5 mL) was added dropwise over ~2 min. The reaction mixture was stirred for ~12 h before diluting with CH_2Cl_2 (15 mL) and filtering through a short plug of SiO_2 over celite. The filter cake was rinsed with 50% EtOAc/hexanes (100 mL) and the filtrate was concentrated by rotary evaporation. The crude residue was purified by flash chromatography (0 → 30%, EtOAc/hexanes, 10%

increments, 50 mL each) to afford known oxazolyltrienal **4.28** (256 mg, 64% over two steps). All spectroscopic data matched that previously reported:[181]

R_f = 0.53 (30% EtOAc/hexanes, UV-active); **^{1}H-NMR** (600 MHz, $CDCl_3$) δ 9.44 (s, 1H), 6.86 (d, *J* = 11.8 Hz, 2H), 6.61 (ddd, *J* = 51.6, 15.2, 11.1, 4.4 Hz, 2H), 6.29 (dd, *J* = 15.1, 10.5 Hz, 1H), 6.05 (dt, *J* = 14.5, 6.7 Hz, 1H), 3.58 (d, *J* = 6.7 Hz, 2H), 1.85 (s, 3H), 1.39 (p, *J* = 7.7 Hz, 2H), 1.13 (d, *J* = 7.5 Hz, 18H); **^{13}C-NMR** (150 MHz, $CDCl_3$) δ 194.8, 168.3, 151.6, 148.3, 140.6, 137.8, 133.9, 132.5, 126.9, 123.3, 77.4, 77.2, 76.9, 29.3, 18.5, 11.1, 9.6.

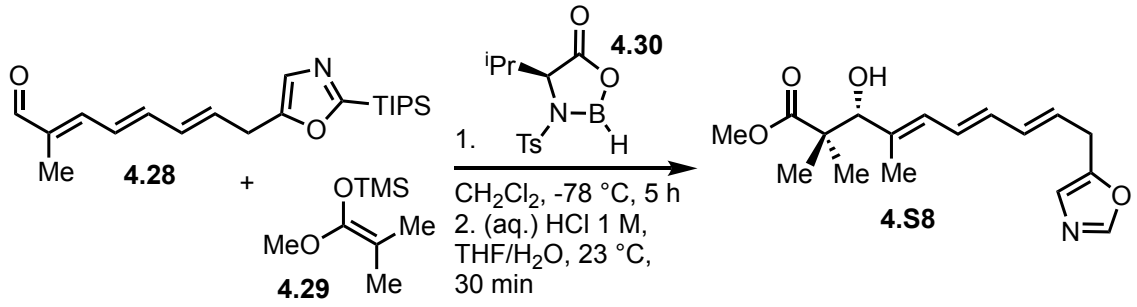

Methyl-(*R*,4*E*,6*E*,8*E*)-3-hydroxy-2,2,4-trimethyl-10-(oxazol-5-yl)deca-4,6,8-trienoate (4.S8): Oxazaborolidinone **4.30** was prepared *in situ* according to literature procedure.[181] Triene methyl ester **4.S8** was prepared according to procedure reported in the same article. All spectroscopic data matched that previously reported:[181]

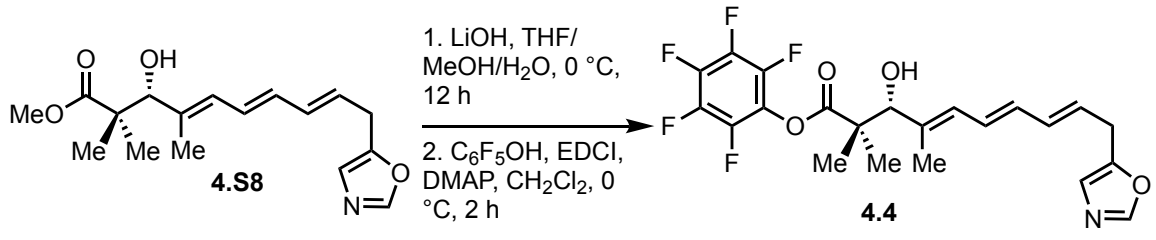

Perfluorophenyl-(*R*,4*E*,6*E*,8*E*)-3-hydroxy-2,2,4-trimethyl-10-(oxazol-5-yl)deca-4,6,8-trienoate (4.4): Pentafluorophenyl ester triene **4.4** was prepared according to literature procedure.

All spectroscopic data matched that previously reported:[182]

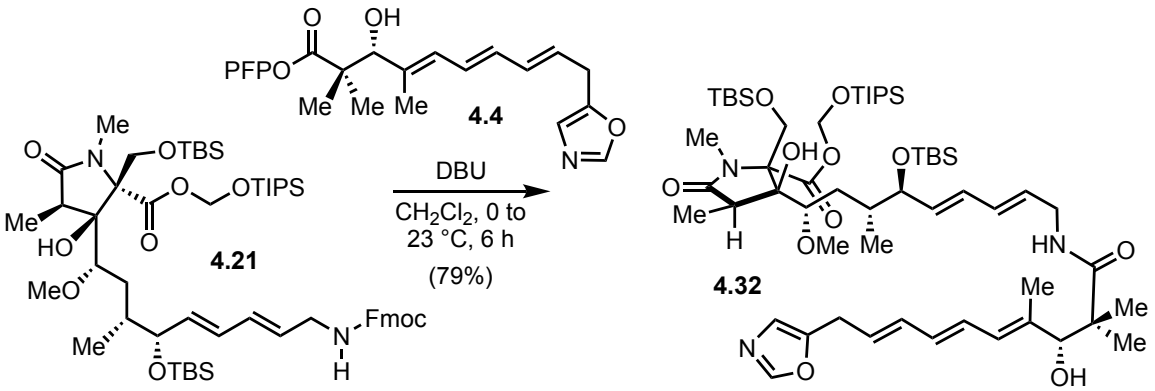

((triisopropylsilyl)oxy)methyl-(2*S*,3*S*,4*R*)-3-((1*S*,3*R*,4*R*,5*E*,7*E*)-4-((*tert*-butyldimethylsilyl)oxy)-9-((*R*,4*E*,6*E*,8*E*)-3-hydroxy-2,2,4-trimethyl-10-(oxazol-5-yl)deca-4,6,8-trienamido)-1-methoxy-3-methylnona-5,7-dien-1-yl)-2-(((*tert*-butyldimethylsilyl)oxy)methyl)-3-hydroxy-1,4-dimethyl-5-oxopyrrolidine-2-carboxylate (4.32): To a flame-dried 1.5 dram (6 mL, 16 x 50 mm, OD x H) vial fitted with a septum cap, containing dienyl allylic carbamate **4.21** (15 mg, 0.014 mmol, 1.00 equiv) was added CH_2Cl_2 (1 mL) followed by a stock solution of DBU (0.19 M in CH_2Cl_2, 110 μL, 0.021 mmol, 1.5 equiv). The resulting colorless solution was stirred at 23 °C for 1 h before turning the lights off, cooling to 0 °C in an ice bath over ~5 min, and adding a solution of pentafluorophenyl ester triene **4.4** (14 mg, 0.031 mmol, 2.20 equiv) in CH_2Cl_2 (600 μL). The syringe used to transfer pentafluorophenyl ester triene **4.4** was rinsed with CH_2Cl_2 (200 μL) and added to the reaction vessel. The reaction mixture was excluded from

light with a of sheet aluminum foil and allowed to stir and slowly warm to 23 °C over 5 h before being diluted with CH_2Cl_2 (3 mL) and washed with brine (2 mL). The layers were separated and the aqueous layer was extracted with CH_2Cl_2 (3 x 2 mL). The combined organic layers were dried over Na_2SO_4, filtered through celite, and concentrated by rotary evaporation to a yellow oil that was purified by flash chromatography (0 → 70%, EtOAc/hexanes, 10% increments, 15 mL each, product elutes at 40-60% EtOAc/hexanes), affording trisilyl oxazolomycin B ester **4.32** as a light yellow oil (12 mg, 79%):

$\mathbf{R_f}$ = 0.31 (50% EtOAc/hexanes, stains blue with anisaldehyde solution, UV-active); $\mathbf{[\alpha]}_D^{23.1}$ +4.67 (*c* 0.171, $CHCl_3$); **IR (thin film)**: 3346 br, 2954, 2931, 2894, 2866, 1736, 1686, 1648, 1532, 1510 cm^{-1}; **^{1}H-NMR** (600 MHz, $CDCl_3$) δ 7.78 (s, 1H, *H-13'*), 6.79 (s, 1H, *H-12'*), 6.47 (t, *J* = 5.1 Hz, 1H, *N-H*), 6.38 (dd, *J* = 13.7, 11.4 Hz, 1H, *H-6'*), 6.25-6.18 (m, 2H, *H-8'/7'*), 6.17-6.11 (m, 2H, *H-8/11*), 5.99 (d, *J* = 10.9 Hz, 1H, *H-5'*), 5.76-5.71 (m, 1H, *H-9'*), 5.66-5.59 (m, 2H, *H-10/9*), 5.55 (d, *J* = 3.9 Hz, 1H, *H^a-CH$_2$OTIPS*), 5.44 (d, *J* = 3.9 Hz, 1H, *H^b-CH$_2$OTIPS*), 4.50 (d, *J* = 5.5 Hz, 1H, *2°OH*), 4.43 (s, 1H, *3°OH*), 4.42 (d, *J* = 11.6 Hz, 1H, *H-16*), 4.11-4.09 (m, 1H, *H-7*), 4.04 (d, *J* = 11.6 Hz, 1H, *H-16*), 3.98 (d, *J* = 5.4 Hz, 1H, *H-3'*), 3.95 (dt, *J* = 14.7, 6.2 Hz, 1H, *H-12*), 3.85 (dt, *J* = 15.2, 5.9 Hz, 1H, *H-12*), 3.48 (d, *J* = 6.9 Hz, 2H, *H-10'*), 3.33 (dd, *J* = 6.7, 4.0 Hz, 1H, *H-4*), 3.28 (s, 3H, *-OCH$_3$*), 2.72 (s, 3H, *-NCH$_3$*), 2.55 (q, *J* = 7.2 Hz, 1H, *H-2*), 1.98 (ddd, *J* = 14.9, 5.5, 4.2 Hz, 1H, *H-5*), 1.74-1.69 (m, 1H, *H-6*), 1.73 (s, 3H, *4'- CH$_3$*), 1.43-1.38 (m, 1H, *H-5*), 1.29 (s, 3H, *2'-CH$_3$*), 1.13 (d, *J* = 7.3 Hz, 3H, *H-13*), 1.12-1.10 (m, 3H, *CH-TIPS*), 1.10 (s, 3H, *2'-CH$_3$*), 1.07-1.05 (m, 18H, *CH$_3$-TIPS*), 0.96 (d, *J* = 6.8 Hz, 3H, *H-14*), 0.90 (s, 9H, *^{t}Bu-TBS*), 0.87 (s, 9H, *^{t}Bus-TBS*), 0.12 (s, 3H, *CH$_3$-TBS*), 0.09 (s, 3H, *CH$_3$-TBS*), 0.03 (s, 3H, *CH$_3$-TBS*), 0.00 (s, 3H, *CH$_3$-TBS*); **^{13}C-NMR** (150 MHz, $CDCl_3$) δ 178.0 (*C-*

11), 176.7 (*C-1*), 169.2 (*C-17*), 151.0 (*C-11'*), 150.6 (*C-13'*), 138.4 (*C-4'*), 134.8 (*C-9*), 133.7 (*C-8'*), 132.3 (*C-8*), 132.2 (*C-7'*), 130.0 (*C-11*), 128.8 (*C-5'*), 128.5 (*C-10*), 128.4 (*C-6'*), 127.3 (*C-9'*), 122.7 (*C-12'*), 85.6 (*CH_2OTIPS*), 84.3 (*C-3'*), 83.8 (*C-3*), 82.2 (*C-4*), 76.2 (*C-7*), 74.2 (*C-15*), 61.9 (*C-16*), 57.7 (*-OCH_3*), 44.9 (*C-2'*), 42.9 (*C-2*), 41.6 (*C-12*), 38.4 (*C-6*), 31.1 (*C-5*), 29.0 (*C-*)10', 26.6 (*N-CH_3*), 26.0 (*^{t}Bu-CH_3-TBS*, 3), 25.9 (*2'-CH_3*), 25.8 (*^{t}Bu-CH_3-TBS*, 3), 21.7 (*2'-CH_3*), 18.3 (*^{t}Bu-quat-TBS*), 18.1 (*^{t}Bu-quat-TBS*), 17.8 (*^{i}Pr-CH_3-TBS*, 6), 16.7 (*C-14)*, 13.3 (*4'-CH_3)*, 12.0 (*^{i}Pr-CH-TBS*, 3), 9.4 (*C-13)*, -4.1 (*CH_3-TBS*), -4.7 (*CH_3-TBS*), -5.6 (*CH_3-TBS*), -5.6 (*CH_3-TBS*); **HRMS (ESI+)** *m/*z calcd. for $C_{57}H_{102}N_3O_{11}Si_3$ $[M+H]^+$: 1088.6817, found: 1088.6808.

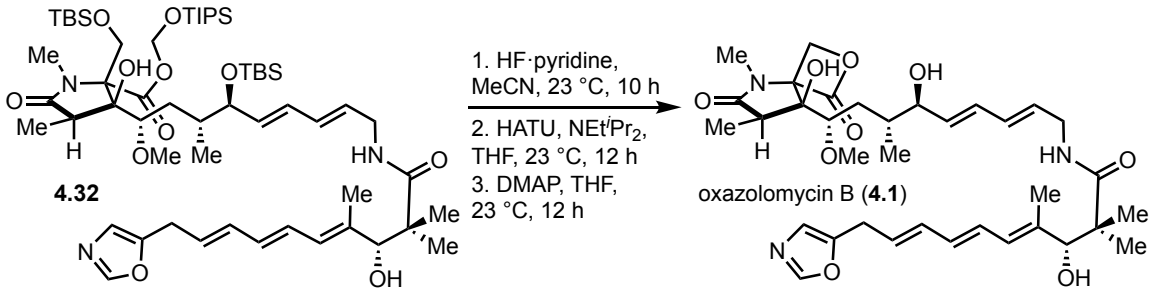

(*R*,4*E*,6*E*,8*E*)-3-hydroxy-*N*-((2*E*,4*E*,6*R*,7*R*,9*S*)-6-hydroxy-9-((4*S*,7*R*,8*S*)-8-hydroxy-5,7-dimethyl-1,6-dioxo-2-oxa-5-azaspiro[3.4]octan-8-yl)-9-methoxy-7-methylnona-2,4-dien-1-yl)-2,2,4-trimethyl-10-(oxazol-5-yl)deca-4,6,8-trienamide (4.1): Silyl oxazolomycin B **4.32** was transferred to a 45 mL plastic culture tube with CH_2Cl_2 (~2 mL). The solvent was evaporated under a stream of N_2 the tube was sealed with an inverted rubber septum secured with Teflon tape and copper wire. The tube was wrapped in foil and placed under high vacuum for 1 h. The tube was backfilled with N_2 and MeCN (4.0 mL) was added. The mixture was stirred at 23 °C shielded from light with aluminum foil. HF·pyridine (234 μL, ~9.0 mmol, ~500 equiv) was carefully added via 1 mL plastic

syringe. The reaction was stirred for 16 h before diluting with EtOAc (10 mL) and quenching by addition of SiO_2 (2.56 g) slowly over ~2 min. The slurry was stirred for 20 min before filtering through celite. The solid was rinsed with MeOH/EtOAc (1:10 v/v, 50 mL).

Volatiles were removed by rotary evaporation and the crude material was taken up in THF (2 mL) and cooled to 0 °C. Hünig's base was then added (16 μL, 0.090 mmol, 5.0 equiv), followed by HATU (10 mg, 0.027 mmol, 1.5 equiv). The mixture was stirred for 16 h and allowed to slowly warm to 23 °C while shielded from light with aluminum foil. Crude IR of the reaction mixture showed a small β-lactone absorbance (1828 cm^{-1}). Preparative TLC of the crude reaction mixture following aqueous workup with brine and EtOAc led to what is believed to be the HOBt ester of oxazolomycin B (based on crude ^{1}H-NMR doublet resonances in the aromatic region). This material was redissolved in THF (1.5 mL) and exposed to DMAP (1.8 mg). The crude IR showed a stronger β-lactone absorbance (1828 cm^{-1}). Preparative TLC led to re-isolation of what is believed to be the HOBt ester of oxazolomycin B.

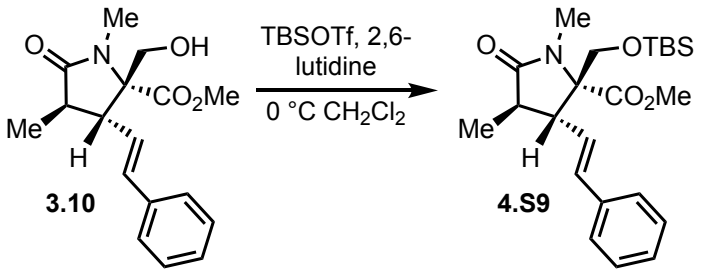

Methyl-(2*R*,3*R*,4*R*)-2-(((*tert*-butyldimethylsilyl)oxy)methyl)-1,4-dimethyl-5-oxo-3-((*E*)-styryl)pyrrolidine-2-carboxylate (4.S9): To a 50 mL, single-necked, round-bottomed flask charged with primary alcohol **3.10** (341 mg, 1.12 mmol, 1.00 equiv) was

added CH_2Cl_2 (11 mL). The resulting solution was cooled to 0 °C in an ice bath over 5 min and 2,6-lutidine (259 μL, 2.24 mmol, 2.00 equiv) was then added followed by TBSOTf (309 μL, 1.34 mmol, 1.20 equiv) dropwise over ~2 min. The mixture was stirred at 0 °C for 30 min before being poured into saturated, aqueous $NaHCO_3$ (50 mL). The reaction flask was rinsed with Et_2O (40 mL) and the layers were separated. The aqueous layer was extracted with Et_2O (3 x 30 mL) and the combined organic layers were dried over $MgSO_4$, filtered through a plug of SiO_2 over celite. The filter cake was rinsed with Et_2O (25 mL) and the volatiles were removed by rotary evaporation. The resulting yellow oil was used in the following steps without purification.

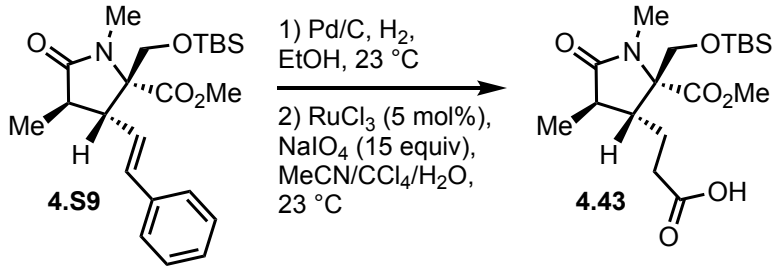

3-((2R,3R,4R)-2-(((tert-butyldimethylsilyl)oxy)methyl)-2-(methoxycarbonyl)-1,4-dimethyl-5-oxopyrrolidin-3-yl)propanoic acid (4.43): To a single-necked, 50 mL, round-bottomed, flask fitted with a rubber septum and needle connected to a N_2/vacuum manifold, and charged with crude silyl ether **4.S9** (3.26 mmol, 1.00 equiv), was added Pd/C (10% wt, 457 mg, 0.33 mmol Pd, 0.10 equiv). The atmosphere in the flask was replaced with N_2 by three cycles of vacuum and backfilling. EtOH was then added and the manifold connection was carefully replaced with a H_2 balloon. The black suspension was stirred at 23 °C overnight and was then diluted with EtOAc/hexanes (60% v/v) and filtered through a plug of SiO_2 over Celite. The filter cake was rinsed with additional EtOAc/hexanes (60%

v/v) and the volatiles were removed by rotary evaporation. The resulting crude off-white oil was used in the next step without purification.

To the above crude material in a single-necked, 250 mL round-bottomed flask open to air was added MeCN (18.6 mL), CCl_4 (18.6 mL), and H_2O (27.9 mL). To this solution was added $RuCl_3$ (34 mg, 0.16 mmol, 0.05 equiv) followed by NaIO4 (10.5 g, 48.9 mmol, 15.0 equiv). The resulting orange slurry was stirred at 23 °C for 52 h before being diluted with H_2O (90 mL) and CH_2Cl_2 (70 mL). The layers were separated, and the aqueous phase was extracted with CH_2Cl_2 (3 x 40 mL). The combined organic phases were dried over $MgSO_4$ and filtered through Celite. The volatiles were removed by rotary evaporation and the crude material was purified by automated flash chromatography (0 → 100%, EtOAc/hexanes, continuous gradient; product elutes at ~70% EtOAc/hexanes) affording carboxylic acid **4.43** (796 mg, 63% yield over three steps):

R_f = 0.17 (50% EtOAc/hexanes, stains faintly with $KMnO_4$ solution); $[\alpha]_D^{22.7}$ +84.13 (*c* 0.271, $CHCl_3$); **IR (thin film)**: 3124 br, 2955, 2931, 2885, 2858, 1738, 1702, 1664 cm^{-1}; **^{1}H-NMR** (600 MHz, $CDCl_3$) δ 3.96 (d, *J* = 11.3 Hz, 1H), 3.82 (d, *J* = 11.3 Hz, 1H), 3.73 (s, 3H), 2.74 (s, 3H), 2.49-2.49 (m, 2H), 2.26-2.20 (m, 1H), 2.12-2.07 (m, 1H), 1.81-1.75 (m, 1H), 1.66-1.60 (m, 1H), 1.23 (d, *J* = 7.0 Hz, 3H), 0.85 (s, 9H), 0.07 (s, 3H), 0.06 (s, 3H); **^{13}C-NMR** (150 MHz, $CDCl_3$) δ 177.6, 177.6, 171.3, 73.0, 61.5, 52.4, 43.8, 41.4, 32.4, 27.0, 25.8, 25.4, 18.2, 16.6, -5.5, -5.5; **HRMS (ESI+)** *m/*z calcd. for $C_{18}H_{33}NaNO_6Si$ $[M+Na]^+$: 410.1970, found: 410.1970.

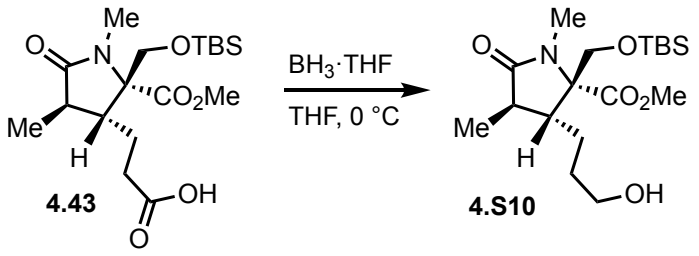

Methyl-(2R,3R,4R)-2-(((tert-butyldimethylsilyl)oxy)methyl)-3-(3-hydroxypropyl)-1,4-dimethyl-5-oxopyrrolidine-2-carboxylate (4.S10): To a single-necked, 50 mL, round-bottomed, flask containing carboxylic acid **4.43** (168 mg, 0.43 mmol, 1.00 equiv) was added THF (6 mL). The solution was cooled to 0 °C under N_2 and a solution of BH_3·THF (1.0 M in THF, 650 μL, 0.65 mmol, 1.50 equiv) was added dropwise over ~2 min. The reaction was stirred overnight and was then quenched by dropwise addition of H_2O (500 μL), diluted with EtOAc (25 mL) and filtered through Celite. The volatiles were removed by rotary evaporation and the crude material was used in the next step without purification.

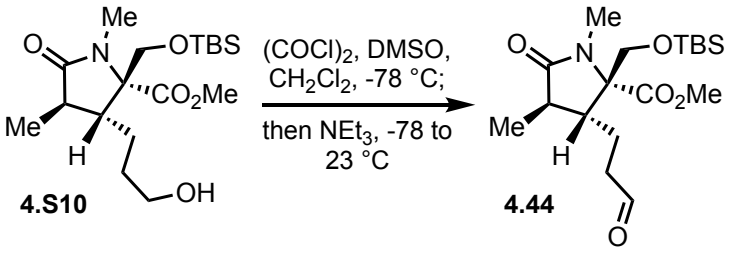

Methyl-(2R,3R,4R)-2-(((tert-butyldimethylsilyl)oxy)methyl)-1,4-dimethyl-5-oxo-3-(3-oxopropyl)pyrrolidine-2-carboxylate (4.44): To a single-necked, 50 mL, round-bottomed, flask containing $(COCl)_2$ (38 μL, 0.44 mmol, 2.00 equiv) in CH_2Cl_2 (1 mL) at -78 °C was added DMSO (62 μL, 0.88 mmol, 4.00 equiv) in CH_2Cl_2 (1 mL) dropwise down the wall of the vessel. After stirring the solution for 5 min, crude alcohol **4.S10** (0.22 mmol,

1.00 equiv) in CH_2Cl_2 (2 mL) was added dropwise down the wall of the vessel. After stirring for 30 min, NEt_3 (184 μL, 1.32 mmol, 6.00 equiv) was added in one portion at -78 °C. The reaction was stirred for 20 min before removing the cooling bath and allowing it to warm to 23 °C. The reaction was quenched by filtering through Celite, rinsing with CH_2Cl_2. Volatiles were removed by rotary evaporation and the crude material was used in the next step without purification.

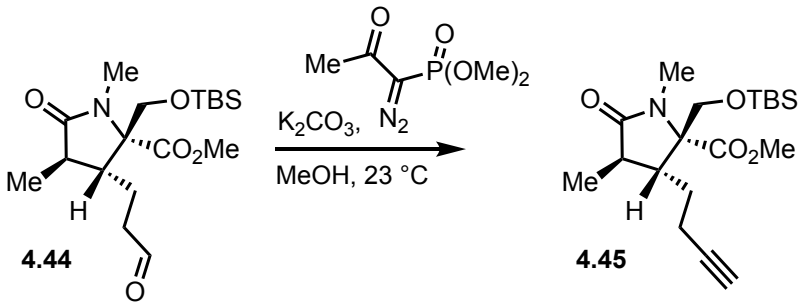

Methyl-(2R,3R,4R)-3-(but-3-yn-1-yl)-2-(((tert-butyldimethylsilyl)oxy)methyl)-1,4-dimethyl-5-oxopyrrolidine-2-carboxylate (4.45): To a single-necked, 25 mL, round-bottomed, flask containing crude aldehyde **4.44** (0.35 mmol, 1.00 equiv)was added MeOH (10 mL) followed by K_2CO_3 (967 mg, 0.70 mmol, 2.00 equiv). Ohira-Bestmann reagent was then added as a neat liquid (80.7 mg, 0.42 mmol, 1.20 equiv). The reaction was stirred at 23 °C overnight before being quenched by diluting with EtOAc, and pouring into saturated aqueous $NaHCO_3$. The layers were separated and the aqueous layer was extracted with EtOAc. The combined organic phases were dried over $MgSO_4$ and filtered through Celite. The volatiles were removed by rotary evaporation and the crude material was purified by automated flash chromatography (0 → 100%, EtOAc/hexanes, continuous gradient; product elutes at ~50% EtOAc/hexanes) affording terminal alkyne **4.45** (60.5 mg, 47% yield over three steps):

$\mathbf{R}_f$ = 0.33 (50% EtOAc/hexanes, stains faintly with I_2 on SiO_2); $[\alpha]_D^{24.5}$ +9.89 (*c* 0.89, $CHCl_3$); **IR (thin film)**: 3313, 2954, 2931, 2885, 2858, 1737, 1701 cm^{-1}; **^{1}H-NMR** (600 MHz, $CDCl_3$) δ 3.96 (d, *J* = 11.3 Hz, 1H), 3.81 (d, *J* = 11.3 Hz, 1H), 3.72 (s, 3H), 2.74 (s, 3H), 2.39-2.34 (m, 1H), 2.32-2.28 (m 1H), 2.22-2.17 (m, 1H), 1.98 (t, *J* = 2.6 Hz, 1H), 1.72-1.66 (m, 1H), 1.51-1.45 (m, 1H), 1.26 (d, *J* = 7.0 Hz, 3H), 0.87 (s, 9H), 0.09 (s, 3H), 0.07 (s, 3H); **^{13}C-NMR** (150 MHz, $CDCl_3$) δ 177.5, 171.6, 83.0, 72.8, 69.8, 61.5, 52.3, 42.9, 41.4, 29.5, 26.9, 25.8, 18.2, 17.3, 16.7, -5.4, -5.5; **HRMS (ESI+)** *m/*z calcd. for $C_{19}H_{33}NaNO_4Si$ $[M+Na]^+$: 390.2072, found: 390.2072.

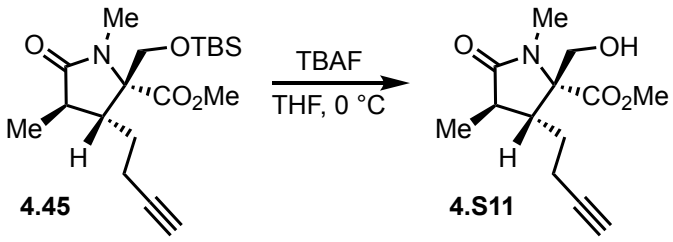

Methyl-(2R,3R,4R)-3-(but-3-yn-1-yl)-2-(hydroxymethyl)-1,4-dimethyl-5-oxopyrrolidine-2-carboxylate (4.S11): To a 25 mL, single-necked, round-bottomed flask containing silyl ether alkyne **4.45** (55 mg, 0.15 mmol, 1.00 equiv) was added THF (2 mL). The solution was stirred and cooled to 0 °C before adding a solution of TBAF (1.0 M in THF, 300 μL, 0.30 mmol, 2.00 equiv). The mixture was stirred for 1 h before removing volatiles by rotary evaporation and the crude material was purified by automated flash chromatography (0 → 100%, EtOAc/hexanes, continuous gradient; product elutes at ~100% EtOAc/hexanes) affording terminal alkyne alcohol **4.S11** (29 mg, 77%) as a colorless solid:

R_f = 0.35 (10% MeOH/CH_2Cl_2, stains with $KMnO_4$); **^{1}H-NMR** (600 MHz, $CDCl_3$) δ 4.04 (dd, *J* = 12.5, 5.0 Hz, 1H), 3.85 (dd, *J* = 12.5, 8.5 Hz, 1H), 3.76 (s, 3H), 2.81 (s, 3H), 2.44-2.31 (m, 2H), 2.30-2.21 (m, 1H), 2.18-2.10 (m, 2H), 2.03 (t, *J* = 2.6 Hz, 1H), 1.75-1.66 (m, 1H), 1.57-1.48 (m, 1H), 1.28 (d, *J* = 7.0 Hz, 3H); **^{13}C-NMR** (150 MHz, $CDCl_3$) δ 177.9, 171.9, 82.9, 72.5, 70.0, 63.8, 52.6, 43.8, 41.4, 29.5, 27.5, 17.3, 16.5.

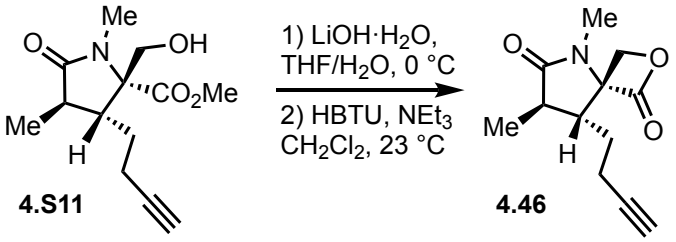

(4R,7R,8R)-8-(but-3-yn-1-yl)-5,7-dimethyl-2-oxa-5-azaspiro[3.4]octane-1,6-dione (4.46): To a flame-dried 1.5 dram vial fitted with a septum cap and charged with β-hydroxyester **4.S11** (7.0 mg, 0.028 mmol, 1.00 equiv) was added THF (0.6 mL) and H_2O (0.6 mL). The resulting solution was cooled to 0 °C and $LiOH·H_2O$ (4 mg, 0.083 mmol, 3.0 equiv) was added. The reaction was stirred overnight before diluting with EtOAc and acidifying with 1 M aqueous HCl (1 mL). NaCl solid was added to saturation and the layers were separated with a glass pipet. The aqueous layer was extracted with EtOAc and the combined organic phases were dried over $MgSO_4$ and filtered through Celite. The volatiles were removed and the crude material was used in the next step.

The crude material in a flame-dried 1.5 dram vial fitted with a septum cap was dissolved in CH_2Cl_2 (1mL) and the resulting solution was cooled to 0 °C. NEt_3 was then added (20 μL, 0.14 mmol, 5.00 equiv) followed by HBTU (16 mg, 0.042 mmol, 1.5 equiv). The reaction was stirred for 30 min before removing the cooling bath and stirring for an additional 1 h. The reaction mixture was then filtered through a plug of SiO_2, eluting with

EtOAc. The volatiles were removed and the crude material showed a β-lactone absorbance (1829 cm^{-1}). The crude material was purified with a pipette column (0 → 80%, EtOAc/hexanes, 10% increments, 2 mL each) affording the desired β-lactone along with tetramethylurea impurity. This β-lactone proved to be highly unstable and decomposed in $CDCl_3$ and would polymerize when left neat on the benchtop or in the fridge at 8 °C:

$\mathbf{R}_f$ = 0.77 (80% EtOAc/hexanes, stains with $KMnO_4$)

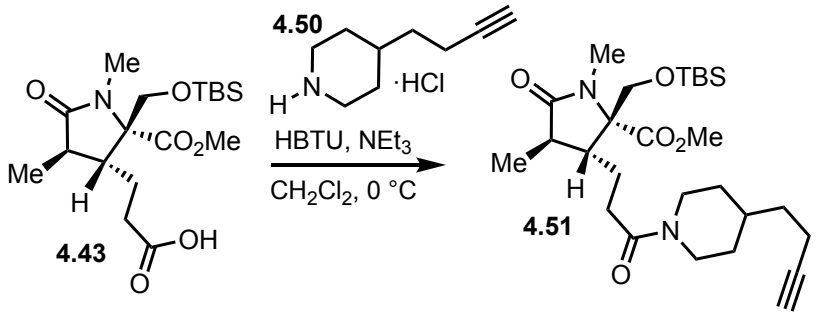

Methyl-(2R,3R,4R)-3-(3-(4-(but-3-yn-1-yl)piperidin-1-yl)-3-oxopropyl)-2-(((tert-butyldimethylsilyl)oxy)methyl)-1,4-dimethyl-5-oxopyrrolidine-2-carboxylate (4.51): To a 10 mL, single-necked, round-bottomed flask containing carboxylic acid **4.43** (52 mg, 0.13 mmol, 1.00 equiv) and butynylpiperidine **4.50** (28 mg, 0.16 mmol, 1.20 equiv) was added CH_2Cl_2 (2 mL). The resulting solution was cooled to 0 °C before adding NEt_3 (72 μL, 0.52 mmol, 4.00 equiv) followed by HBTU (64 mg, 0.17 mmol, 1.30 equiv). The reaction was allowed to stir and slowly warm to 23 °C overnight before removing the volatiles by rotary evaporation. The crude material was purified by automated flash chromatography (0 → 85%, EtOAc/hexanes, continuous gradient; product elutes at ~80% EtOAc/hexanes) affording desired amide **4.51** (43.4 mg, 66%) as a yellow foam.

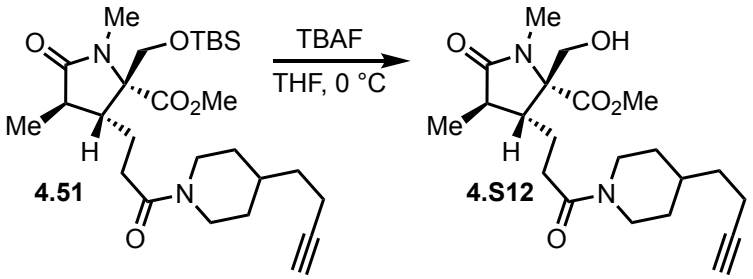

Methyl-(2*R*,3*R*,4*R*)-3-(3-(4-(but-3-yn-1-yl)piperidin-1-yl)-3-oxopropyl)-2-(hydroxymethyl)-1,4-dimethyl-5-oxopyrrolidine-2-carboxylate (4.S12): The same procedure as used above was applied here. Reagent amounts used: silyl ether **4.51** (170 mg, 0.33 mmol, 1.00 equiv), TBAF (1.0 M in THF, 660 μL, 0.66 mmol, 2.00 equiv), THF (5 mL). The desired β-hydroxyester **4.S12** was isolated as a white solid (98 mg, 75%) after purification by automated flash chromatography (20%, MeOH/EtOAc):

$\mathbf{R}_f$ = 0.20 (80% EtOAc/hexanes, stains with $KMnO_4$); $[\alpha]_D^{22.5}$ +40.08 (*c* 0.529, $CHCl_3$);

IR (thin film): 3385 br, 2926, 2854, 2361, 1734, 1683, 1624 cm^{-1}

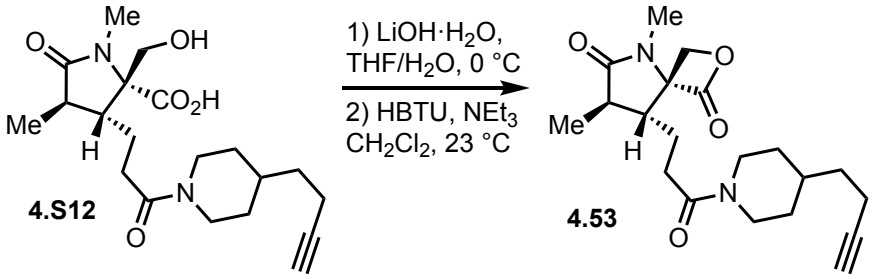

(4R,7R,8R)-8-(3-(4-(but-3-yn-1-yl)piperidin-1-yl)-3-oxopropyl)-5,7-dimethyl-2-oxa-5-azaspiro[3.4]octane-1,6-dione: The same procedure as used above was applied here. Reagent amounts used: β-hydroxyacid **4.S12** (15 mg, 0.039 mmol, 1.00 equiv), HBTU (23 mg, 0.059 mmol, 1.50 equiv), NEt_3 (27 μL, 0.195 mmol, 5.00 equiv). The desired spiro-β-

lactone was isolated along with tetramethylurea impurity and proved more stable than previous spiro-β-lactones, but still decomposed by hydrolysis and polymerization:

IR (thin film): 3646 br, 3439 br, 2939, 1829, 1699, 1633 cm^{-1}; **HRMS (ESI+)** *m/*z calcd. for $C_{20}H_{28}NaN_2O_4$ $[M+Na]^+$: 383.1942, found: 383.1943.

9. Kanzaki, H.; Wada, K.-i.; Nitoda, T.; Kawazu, K., Novel Bioactive Oxazolomycin Isomers Produced by Streptomyces albus JA3453. *Biosci., Biotechnol., Biochem.* **1998,** *62* (3), 438-442.

11. Otani, T.; Yoshida, K. I.; Kubota, H.; Kawai, S.; Ito, S.; Hori, H.; Ishiyama, T.; Oki, T., Novel Triene-β-lactone Antibiotics, Oxazolomycin Derivative and Its Isomer, Produced by *Streptomyces* sp. KSM-2690. *J. Antibiot.* **2000,** *53* (12), 1397-1400.

23. Grigorjev, P. A.; Schlegel, R.; Gräfe, U., On the Protonophoric Activity of Oxazolomycin. *Pharmazie* **1992,** *47* (9), 707-709.

32. Kende, A. S.; Kawamura, K.; Devita, R. J., Enantioselective Total Synthesis of Neooxazolomycin. *J. Am. Chem. Soc.* **1990,** *112* (10), 4070-4072.

34. Stille, J. K., The Palladium-Catalyzed Cross-Coupling Reactions of Organotin Reagents with Organic Electrophiles [New Synthetic Methods (58)]. *Angew. Chem. Int. Ed.* **1986,** *25* (6), 508-524.

35. Kende, A. S.; DeVita, R. J., A mild four-carbon homologation of aldehydes to E,E-dienamines. *Tetrahedron Lett.* **1990,** *31* (3), 307-310.

37. Eto, K.; Yoshino, M.; Takahashi, K.; Ishihara, J.; Hatakeyama, S., Total Synthesis of Oxazolomycin A. *Org. Lett.* **2011,** *13* (19), 5398-5401.

38. Ishihara, J.; Hatakeyama, S., Total Synthesis of Oxazolomycins. *Chem. Rec.* **2014,** *14* (4), 663-677.

125. Vellalath, S.; Van, K. N.; Romo, D., Direct Catalytic Asymmetric Synthesis of N-Heterocycles from Commodity Acid Chlorides by Employing α,β-Unsaturated Acylammonium Salts. *Angew. Chem. Int. Ed.* **2013,** *52* (51), 13688-13693.

128. Papillon, J. P. B.; Taylor, R. J. K., The first syntheses of the 1-oxo-2-oxa-5-azaspiro[3.4]octane ring system found in oxazolomycin. *Org. Lett.* **2000,** *2* (14), 1987-1990.

129. Donohoe, T. J.; Chiu, J. Y. K.; Thomas, R. E., Synthesis of the Pyrrolidinone Core of KSM-2690 B. *Org. Lett.* **2007,** *9* (3), 421-424.

130. Donohoe, T. J.; O'Riordan, T. J. C.; Peifer, M.; Jones, C. R.; Miles, T. J., Asymmetric Synthesis of the Fully Elaborated Pyrrolidinone Core of Oxazolomycin A. *Org. Lett.* **2012,** *14* (21), 5460-5463.

136. Abbasov, M. E.; Alvariño, R.; Chaheine, C. M.; Alonso, E.; Sánchez, J. A.; Conner, M. L.; Alfonso, A.; Jaspars, M.; Botana, L. M.; Romo, D., Simplified

immunosuppressive and neuroprotective agents based on gracilin A. *Nat. Chem.* **2019,** *11* (4), 342-350.

144. Molander, G. A., Application of lanthanide reagents in organic synthesis. *Chem. Rev.* **1992,** *92* (1), 29-68.

145. Imamoto, T.; Sugiura, Y.; Takiyama, N., Organocerium reagents. Nucleophilic addition to easily enolizable ketones. *Tetrahedron Lett.* **1984,** *25* (38), 4233-4236.

146. Liu, H. J.; Shia, K. S.; Shang, X.; Zhu, B. Y., Organocerium Compounds in Synthesis. *Tetrahedron* **1999,** *55* (13), 3803-3830.

148. Dimitrov, V.; Kostova, K.; Genov, M., Anhydrous Cerium(III) Chloride — Effect of the Drying Process on Activity and Efficiency. *Tetrahedron Lett.* **1996,** *37* (37), 6787-6790.

149. Takeda, N.; Imamoto, T., Use of Cerium (III) Chloride in the Reactions of Carbonyl Compounds with Organolithiums or Grignard Reagents for the Suppression of Abnormal Reactions: 1-butyl-1,2,3,4-tetrahydro-1-napthol. *Org. Syn.* **1999,** *76*, 228.

153. Ogasawara, M.; Okada, A.; Subbarayan, V.; Sorgel, S.; Takahashi, T., Palladium-Catalyzed Asymmetric Synthesis of Axially Chiral Allenylsilanes and Their Application to S(E)2 ' Chirality Transfer Reactions. *Org. Lett.* **2010,** *12* (24), 5736-5739.

154. Appel, R., Tertiary Phosphane/Tetrachloromethane, a Versatile Reagent for Chlorination, Dehydration, and P-N Linkage. *Angew. Chem. Int. Ed.* **1975,** *14* (12), 801-811.

155. Bailey, W. F.; Brubaker, J. D.; Jordan, K. P., Effect of solvent and temperature on the lithium-iodine exchange of primary alkyl iodides: reaction of t-butyllithium with 1-iodooctane in heptane-ether mixtures. *J. Organomet. Chem.* **2003,** *681* (1-2), 210-214.

156. Rathman, T.; Bailey, W. F., Optimization of Organolithium Reactions. *Org. Process Res. Dev.* **2009,** *13* (2), 144-151.

162. Burchat, A. F.; Chong, J. M.; Nielsen, N., Titration of alkyllithiums with a simple reagent to a blue endpoint. *J. Organomet. Chem.* **1997,** *542* (2), 281-283.

163. Beesley, R. M.; Ingold, C. K.; Thorpe, J. F., CXIX.—The formation and stability of spiro-compounds. Part I. spiro-Compounds from cyclohexane. *J. Chem. Soc., Trans.* **1915,** *107* (0), 1080-1106.

164. Carlsen, P. H. J.; Katsuki, T.; Martin, V. S.; Sharpless, K. B., A greatly improved procedure for ruthenium tetroxide catalyzed oxidations of organic compounds. *J. Org. Chem.* **1981,** *46* (19), 3936-3938.

165. Mohapatra, D. K.; Mondal, D.; Gonnade, R. G.; Chorghade, M. S.; Gurjar, M. K., Synthesis of the spiro fused beta-lactone-gamma-lactam segment of oxazolomycin. *Tetrahedron Lett.* **2006,** *47* (34), 6031-6035.

166. Mondal, D.; Bera, S., A Synthetic View of an Analogue of the Spiro-beta-lactone-gamma-lactam Ring in Oxazolomycins and Lajollamycin. *Synthesis-Stuttgart* **2010,** (19), 3301-3308.

167. Liang, X.; Andersch, J.; Bols, M., Garner's aldehyde. *J. Chem. Soc., Perkin Trans. 1* **2001,** (18), 2136-2157.

168. Adam, W.; Baeza, J.; Liu, J.-C., Stereospecific introduction of double bounds via thermolysis of .beta.-lactones. *J. Am. Chem. Soc.* **1972,** *94* (6), 2000-2006.

169. Imamoto, T.; Kusumoto, T.; Tawarayama, Y.; Sugiura, Y.; Mita, T.; Hatanaka, Y.; Yokoyama, M., Carbon-carbon bond-forming reactions using cerium metal or organocerium(III) reagents. *J. Org. Chem.* **1984,** *49* (21), 3904-3912.

170. Wright, M. H.; Sieber, S. A., Chemical proteomics approaches for identifying the cellular targets of natural products. *Nat. Prod. Rep.* **2016,** *33* (5), 681-708.

171. Guerciolini, R., Mode of action of orlistat. *Int. J. Obes. Relat. Metab. Disord.* **1997,** *21* (Suppl 3), S12-23.

172. Groll, M.; Balskus, E. P.; Jacobsen, E. N., Structural Analysis of Spiro β-Lactone Proteasome Inhibitors. *J. Am. Chem. Soc.* **2008,** *130* (45), 14981-14983.

173. Richardson, R. D.; Ma, G.; Oyola, Y.; Zancanella, M.; Knowles, L. M.; Cieplak, P.; Romo, D.; Smith, J. W., Synthesis of Novel β-Lactone Inhibitors of Fatty Acid Synthase. *J. Med. Chem.* **2008,** *51* (17), 5285-5296.

174. Zeiler, E.; Braun, N.; Böttcher, T.; Kastenmüller, A.; Weinkauf, S.; Sieber, S. A., Vibralactone as a Tool to Study the Activity and Structure of the ClpP1P2 Complex from Listeria monocytogenes. *Angew. Chem. Int. Ed.* **2011,** *50* (46), 11001-11004.

175. List, A.; Zeiler, E.; Gallastegui, N.; Rusch, M.; Hedberg, C.; Sieber, S. A.; Groll, M., Omuralide and Vibralactone: Differences in the Proteasome- β-Lactone-γ-Lactam Binding Scaffold Alter Target Preferences. *Angew. Chem. Int. Ed.* **2014,** *53* (2), 571-574.

176. Zhu, M.; Harshbarger, W. D.; Robles, O.; Krysiak, J.; Hull, K. G.; Cho, S. W.; Richardson, R. D.; Yang, Y.; Garcia, A.; Spiegelman, L.; Ramirez, B.; Wilson, C. T.; Yau, J. A.; Moore, J. T.; Walker, C. B.; Sacchettini, J. C.; Liu, W. R.; Sieber, S. A.; Smith, J. W.; Romo, D., A strategy for dual inhibition of the proteasome and fatty acid synthase with belactosin C-orlistat hybrids. *Biorg. Med. Chem.* **2017,** *25* (11), 2901-2916.

177. Truax, N. J.; Ayinde, S.; Van, K.; Liu, J. O.; Romo, D., Pharmacophore-Directed Retrosynthesis Applied to Rameswaralide: Synthesis and Bioactivity of Sinularia Natural Product Tricyclic Cores. *Org. Lett.* **2019,** *21* (18), 7394-7399.

178. Tao, Y.; Reisenauer, K. N.; Masi, M.; Evidente, A.; Taube, J. H.; Romo, D., Pharmacophore-Directed Retrosynthesis Applied to Ophiobolin A: Simplified Bicyclic Derivatives Displaying Anticancer Activity. *Org. Lett.* **2020**.

179. Truax, N. J.; Romo, D., Bridging the gap between natural product synthesis and drug discovery. *Nat. Prod. Rep.* **2020**.

180. Senapati, B. K.; Gao, L.; Lee, S. I.; Hwang, G. S.; Ryu, D. H., Highly Enantioselective Mukaiyama Aldol Reactions Catalyzed by a Chiral Oxazaborolidinium Ion: Total Synthesis of (-)-Inthomycin C. *Org. Lett.* **2010,** *12* (22), 5088-5091.

181. Balcells, S.; Haughey, M. B.; Walker, J. C. L.; Josa-Cullere, L.; Towers, C.; Donohoe, T. J., Asymmetric Total Synthesis of (-)-(3R)-Inthomycin C. *Org. Lett.* **2018,** *20* (12), 3583-3586.

182. Kumar, M.; Bromhead, L.; Anderson, Z.; Overy, A.; Burton, J. W., Short, Tin-Free Synthesis of All Three Inthomycins. *Chem. Eur. J.* **2018,** *24* (63), 16753-16756.

183. Schreiber, S. L.; Schreiber, T. S.; Smith, D. B., Reactions that proceed with a combination of enantiotopic group and diastereotopic face selectivity can deliver products with very high enantiomeric excess: experimental support of a mathematical model. *J. Am. Chem. Soc.* **1987,** *109* (5), 1525-1529.

184. Sawada, D.; Ito, Y., A new method for formacetal linkage formation: protection of alcohols, phenols and carboxylic acids. *Tetrahedron Lett.* **2001,** *42* (13), 2501-2504.

185. Roane, J.; Wippich, J.; Ramgren, S. D.; Krische, M. J., Synthesis of the C(1)–C(13) Fragment of Leiodermatolide via Hydrogen-Mediated C–C Bond Formation. *Org. Lett.* **2017,** *19* (24), 6634-6637.

186. Farina, V.; Krishnamurthy, V.; Scott, W. J., *The Stille Reaction*. 1st ed.; John Wiley & Sons, Inc.: New York, 1998; p 657.

187. Wadsworth, W. S.; Emmons, W. D., The Utility of Phosphonate Carbanions in Olefin Synthesis. *J. Am. Chem. Soc.* **1961,** *83* (7), 1733-1738.

188. Webb, M. R.; Addie, M. S.; Crawforth, C. M.; Dale, J. W.; Franci, X.; Pizzonero, M.; Donald, C.; Taylor, R. J. K., The syntheses of rac-inthomycin A, (+)-inthomycin B and (+)-inthomycin C using a unified synthetic approach. *Tetrahedron* **2008,** *64* (21), 4778-4791.

189. Omura, K.; Sharma, A. K.; Swern, D., Dimethyl sulfoxide-trifluoroacetic anhydride. New reagent for oxidation of alcohols to carbonyls. *J. Org. Chem.* **1976,** *41* (6), 957-962.

190. Müller, S.; Liepold, B.; Roth, G. J.; Bestmann, H. J., An Improved One-pot Procedure for the Synthesis of Alkynes from Aldehydes. *Synlett* **1996,** *1996* (06), 521-522.

191. Yin, J.; Bergmann, E. M.; Cherney, M. M.; Lall, M. S.; Jain, R. P.; Vederas, J. C.; James, M. N. G., Dual Modes of Modification of Hepatitis A Virus 3C Protease by a Serine-derived β-Lactone: Selective Crystallization and Formation of a Functional Catalytic Triad in the Active Site. *J. Mol. Biol.* **2005,** *354* (4), 854-871.

192. Ramer, S. E.; Moore, R. N.; Vederas, J. C., Mechanism of formation of serine β-lactones by Mitsunobu cyclization: synthesis and use of L-serine stereospecifically labelled with deuterium at C-3. *Can. J. Chem.* **1986,** *64* (4), 706-713.

193. Gaich, T.; Baran, P. S., Aiming for the Ideal Synthesis. *J. Org. Chem.* **2010,** *75* (14), 4657-4673.

194. Newhouse, T.; Baran, P. S.; Hoffmann, R. W., The economies of synthesis. *Chem. Soc. Rev.* **2009,** *38* (11), 3010-3021.

195. Gómez-Bengoa, E.; García, J. M.; Jiménez, S.; Lapuerta, I.; Mielgo, A.; Odriozola, J. M.; Otazo, I.; Razkin, J.; Urruzuno, I.; Vera, S.; Oiarbide, M.; Palomo, C., Asymmetric synthesis of propargylic alcohols via aldol reaction of aldehydes with ynals promoted by prolinol ether–transition metal–Brønsted acid cooperative catalysis. *Chem. Sci.* **2013,** *4* (8), 3198-3204.

196. Gómez-Bengoa, E.; Jiménez, J.; Lapuerta, I.; Mielgo, A.; Oiarbide, M.; Otazo, I.; Velilla, I.; Vera, S.; Palomo, C., Combined α,α-dialkylprolinol ether/Brønsted acid promotes Mannich reactions of aldehydes with unactivated imines. An entry to anti-configured propargylic amino alcohols. *Chem. Sci.* **2012,** *3* (10), 2949.

197. Protection for the Hydroxyl Group, Including 1,2- and 1,3-Diols. In *Greene's Protective Groups in Organic Synthesis*, 2006; pp 16-366.

198. Levin, J. I.; Turos, E.; Weinreb, S. M., An Alternative Procedure for the Aluminum-Mediated Conversion of Esters to Amides. *Synth. Commun.* **1982,** *12* (13), 989-993.

199. Nakatsuka, M.; Ragan, J. A.; Sammakia, T.; Smith, D. B.; Uehling, D. E.; Schreiber, S. L., Total synthesis of FK506 and an FKBP probe reagent, [C(8),C(9)-13C2]-FK506. *J. Am. Chem. Soc.* **1990,** *112* (14), 5583-5601.

CHAPTER FIVE

Pharmacophore-Directed Retrosynthesis Applied to Gracilin A: Simplified Bioactive Derivatives

This chapter was published with modifications as: Abbasov, M. E.; Alvariño, R.; Chaheine, C. M.; Alonso, E. A.; Sánchez, J. A.; Conner, M. L; Alfonso, A; Jaspars, M.; Botana, L. M.; Romo, D. Simplified Neuroprotective and Immunosuppressive Agents Based on Gracilin A. *Nature Chemistry* **2019**, *11*, 342

5.1 Introduction

The impactful and enduring role that natural products have played in improving the quality and duration of life for both humans and animals cannot be overstated. For example, rapamycin and its congeners have received Food and Drug Administration approval for various ailments, and this natural product continues to provide insights into basic cell biology.[200] Synthetic chemists are at the forefront of harvesting the full potential of natural products through synthetic efforts including classic total synthesis. Towards this goal, strategies to synthesize natural products have evolved significantly in recent years as more emphasis has been placed on biological function.[201] In Danishefsky's 'diverted total synthesis' (DTS), a synthetic sequence is developed from simple building blocks employing classical retrosynthetic analysis and then various advanced intermediates previously employed in the synthesis effort are diverted towards simplified derivatives for biological analysis (Figure 5.1A).[202] In a strategy not necessarily directed towards total synthesis, Wender's 'function-oriented synthesis' seeks to develop hypotheses regarding pharmacophores based on structural and computational analysis of distinct natural products and typically larger structure–activity relationship (SAR) data sets enabling the design and

synthesis of simplified derivatives bearing a common pharmacophore.[203] Alternatively, Schreiber's 'diversity oriented synthesis' (DOS) of natural product-like libraries[204] and the derived 'biology-oriented synthesis' (BIOS) by Waldmann[205] seeks to synthesize collections of compounds based on structural features found in natural products. Finally, Myers recently developed a convergent building block strategy for rapid access to a diverse array of structurally related scaffolds such as macrolides related to erythromycin for the discovery of novel antibiotics;[206] this was subsequently termed 'analogue-oriented synthesis' by Vanderwal.[207]

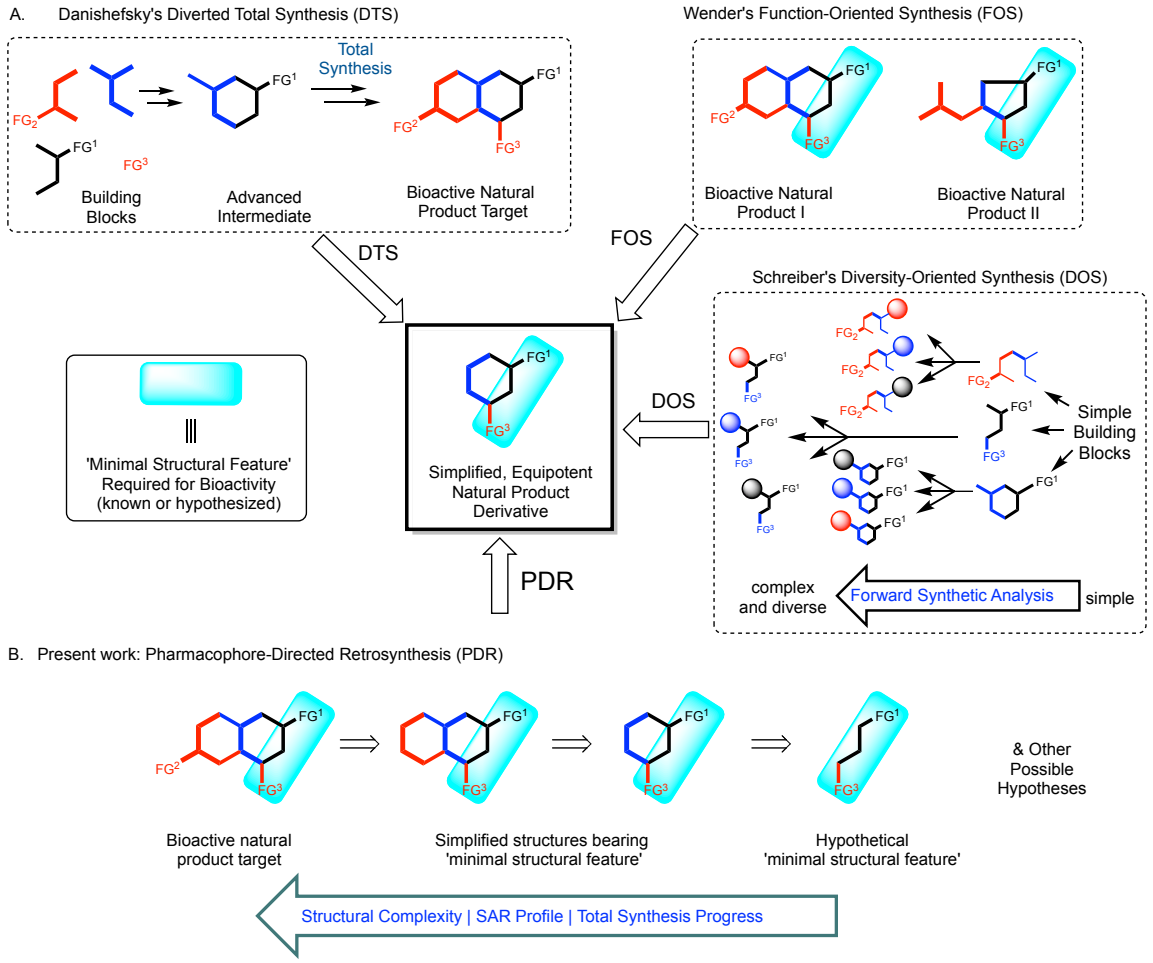

Figure 5.1. Pharmacophore-directed retrosynthesis (PDR) and comparison to other synthetic strategies that harvest the rich information content of natural products.

The simultaneous alignment of total synthesis efforts with structure-activity relationship (SAR) studies has not been fully realized to the extent possible and, in particular, with novel natural products for which minimal SAR information exists. Several truncated natural products,[208] found to possess similar bioactivity to the parent natural product, are known (for example, eribulin mesylate from halichondrin);[209] however, these derivatives were typically identified following completion of a total synthesis.[210] In an example from our laboratory, a des-methyl, des-amino variant of the protein translation initiation inhibitor pateamine A was designed and synthesized following our total synthesis and found to have nearly equipotent activity to the natural product.[211] This led to a retrospective question of whether such a derivative may have been accessed *en route* to the natural product, leading us to pose the following question. Can the total synthesis of natural products, in particular with limited SAR or unknown or unconfirmed cellular targets, be more closely aligned to proposed biological activity during the retrosynthetic planning stages?

Described here is a type of retrosynthetic analysis that seeks to more closely align total synthesis efforts with concurrent biological studies. The strategy enables the identification of simplified versions of the natural product with similar potency or potentially new functions in the course of a total synthesis effort. We term this strategy 'pharmacophore-directed retrosynthesis' (PDR) to emphasize the importance of considering hypothesized pharmacophores at the retrosynthetic planning stage of a total synthesis effort. Although this approach increases the challenges of natural product total synthesis beyond important, contemporary goals, including atom economy[212], step and redox efficiency,[194] and protecting group avoidance,[213] it has the potential to greatly

accelerate harvesting of the vast information content of natural products for basic cell biology and medicine. In PDR, we build on Wender's notion of bringing function to the forefront of a synthetic endeavor (function-oriented synthesis), but employ the logic of retrosynthesis[214] to target simplified intermediates that importantly possess the proposed minimal structural features required for bioactivity (the pharmacophore) *en route* to the natural product.[215] In applying PDR, a key first step is identification of a proposed pharmacophore. This may be based on (1) structural analysis with chemical intuition; (2) existing SAR from isolated natural product congeners; (3) the activity of structurally related compounds; (4) anticipated reactivity. A retrosynthesis is then devised that ensures that the proposed pharmacophore is present in multiple intermediates of increasing complexity, ultimately leading to the natural product. We selected a member of the spongiane diterpenoid family, gracilin A (**5.1**),[216] to initiate assessment of the utility of PDR toward exploring its recently described immunosuppressive[217] and neuroprotective activity[218] given the limited SAR information and no prior synthetic work (Figure 5.2A).[219] In the retrosynthetic analysis, as complexity is increased towards the natural product, several intermediates possessing the proposed pharmacophore are specifically targeted, thus enabling SAR to be gathered as the total synthesis progresses (for example, **5.8** → **5.7** → **5.6** → **5.1** in Figure 5.2B). It should be noted that several hypotheses regarding the pharmacophore of a particular natural product could be posited for PDR, leading to alternative retrosynthetic strategies.

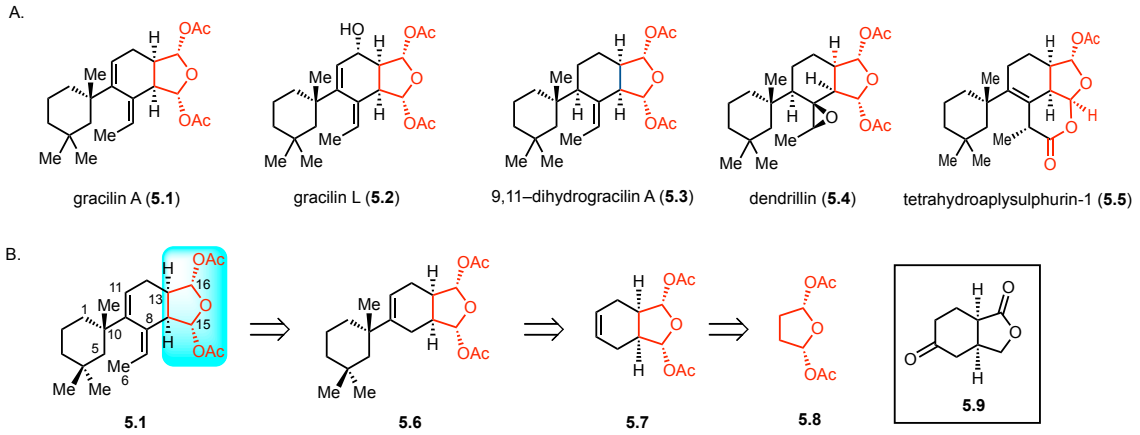

Figure 5.2. Select members of the gracilin A family and application of PDR to gracilin A.

The gracilins, including the rare nor-diterpene gracilin A,[216] were originally isolated and characterized from the Mediterranean sponge Spongionella gracilis.[220] These diterpenes are structurally unique owing to the unusual diacetoxy furanose found in most members. The cytotoxic activity of gracilins B and G–I (isolated from Spongionella pulchella) against a diverse panel of 12 human cancer cell lines has been reported, but these compounds did not progress further in preclinical evaluation.[221] The absolute configuration of gracilin A was never established, while its relative configuration was based on X-ray analysis of the keto derivative of 9,11-dihydrogracilin A (**5.3**).[222] Gracilin A was reported to be a potent inhibitor of phospholipase A2 (PLA2) with a 69% inactivation efficiency.[223] We previously reported that gracilin A was mildly cytotoxic against K562 and peripheral blood mononuclear cells (with half-maximum inhibitory concentration (IC_{50}) values of 0.6 and 0.8 μM, respectively) and inhibited the epidermal growth factor receptor by 70% at 100 μM concentration.[220] We also recently posited that gracilin A mimics the effects of cyclosporin A (CsA) through interaction with cyclophilin A (CypA)[217] and also improves the hallmarks of Alzheimer's disease *in vitro* and *in vivo*.[218, 224, 225] These results prompted

the current study to apply PDR to unravel and ideally differentiate the structural requirements for the immunosuppressive and neuroprotective effects observed with gracilin A.

The cyclophilins (Cyp) are highly conserved peptidyl–prolyl, cis–trans isomerases (PPIase) involved in protein folding and trafficking[226-228] and are found in multiple cellular compartments.[229] CypA, the cytoplasmic isoform, has several roles in cell metabolism and energy homeostasis,[230] with enhanced expression in inflammation and cancer.[231] The use of small molecules that selectively block the inflammation-related functions of CypA, is an important pharmacological strategy leading to effective immunosuppressive agents.[231] On the other hand, cyclophilin D (CypD), the mitochondrial isoform, translocates to form the mitochondrial permeability transition pore (mPTP) and its activity correlates with the mitochondrial dysfunction observed in Alzheimer's disease that leads to neuronal death.[232] CypD inhibitors devoid of immunosuppressive activity through lack of binding to CypA but possessing the desired mitochondrial effect and appropriate blood–brain barrier permeability could provide an approach to address Alzheimer's disease.

Herein, we demonstrate a proof-of-principle study of PDR through application to the spongiane diterpene, gracilin A, that has led to useful lead compounds for both immunosuppression and neuroprotection. This study revealed simplified gracilin A derivatives with high affinity for CypA and others that demonstrated significant selectivity for CypD over CypA, demonstrating their potential as neuroprotective agents devoid of immunosuppressive effects.

5.2 Results & Discussion

The bis-acetoxy furanose moiety was selected as the pharmacophore of gracilin A based on several lines of evidence. Studies of the reactivity of macfarlandin E (which possesses a 1,4-dicarbonyl masked as a bis-acyloxy furanose) with lysine derivatives provided evidence for pyrrole formation through a Paal–Knorr process,[233] and mounting evidence suggests that this is possible with a number of other bis-acetoxy furanose-containing natural products.[234] Furthermore, a computational study demonstrated the potential of the bis-acyloxy furanoses of gracilin A and aplysulphurin-1 to bind divalent cations such as Ca^{2+}, pointing to the potential importance of this moiety for bioactivity.[235] Finally, it is interesting to note that several bioactive members of the spongiane diterpenoid family possess a bis-acyloxy furanose including the structurally related gracilin L (**5.2**),[220] 9,11-dihydrogracilin A (**5.3**), dendrillin (**5.4**)[236] and tetrahydroaplysulphurin-1 (**5.5**).[237] These considerations guided application of PDR to gracilin A and imposed a requirement that multiple intermediates along the synthetic route would bear or be converted to the proposed pharmacophore, namely the bis-acetoxy furanose (for example, derivatives **5.6**–**5.8**, Figure 5.2B). In this way, SAR studies could be conducted throughout the course of the total synthesis. We recognized that keto lactone **5.9**, accessible in gram quantities through our recently described Diels–Alder lactonization organocascade,[123] would serve as a key intermediate to study the importance of the C8-exocyclic alkene (for example derivative **5.6**), the C9-appended cyclohexyl moiety (for example, derivative **5.7**). The importance of the bicyclic core of gracilin A would be ascertained by synthesis of the highly simplified monocyclic furanose **5.8** (Figure 5.2B).

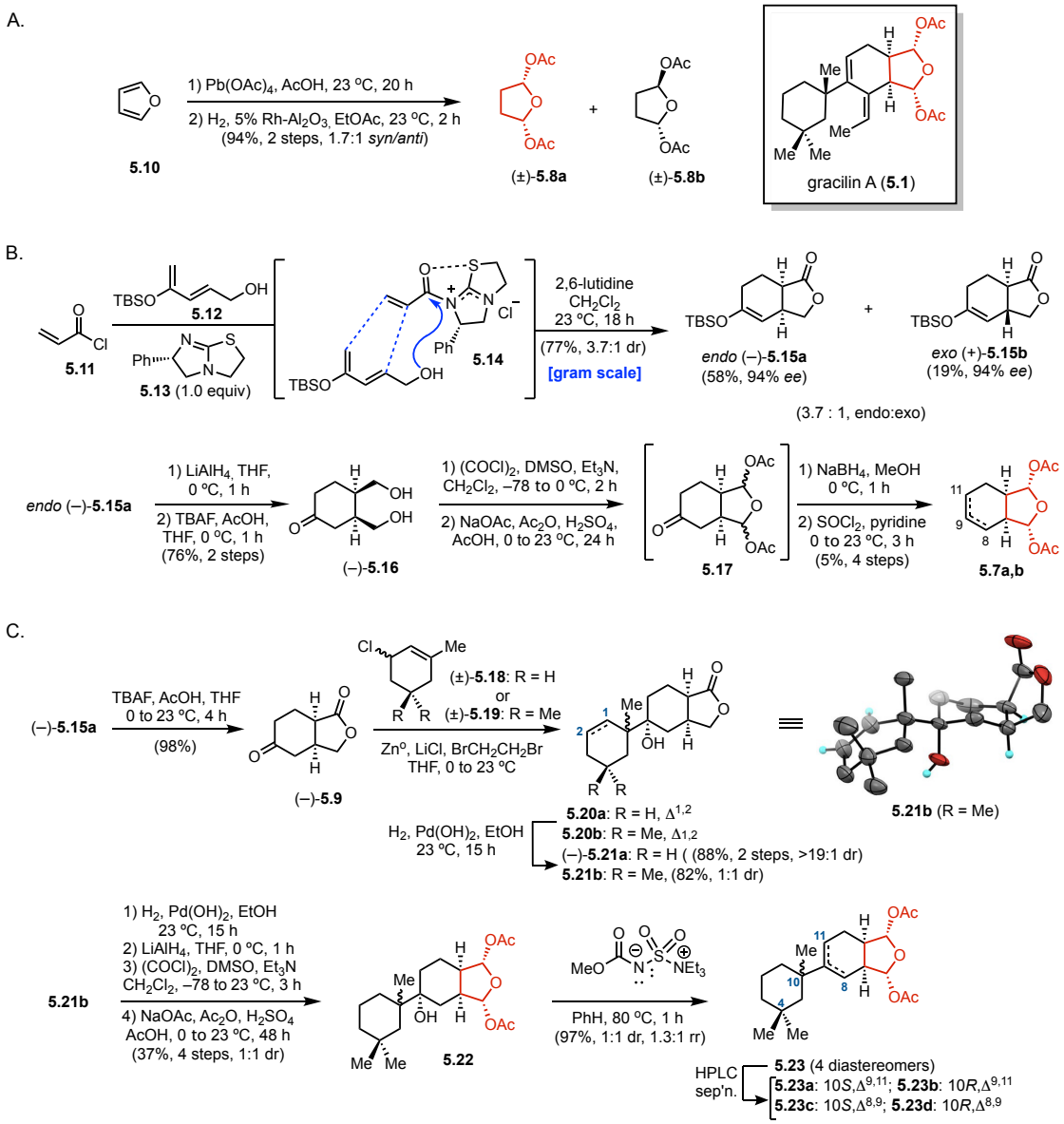

Scheme 5.1. Pharmacophore-directed retrosynthesis applied to gracilin A.

We recognized that, in applying PDR, synthetic progress with concurrent biological assays of intermediates could best be achieved in stages based on the increasing complexity of intermediates in the synthetic sequence, as outlined in Schemes 5.1A–C and 5.2A. A final stage of diverted total synthesis could enable further refinement of the SAR profile through 'gap filling' with particular targeted derivatives to answer more specific questions

building on information gathered during the initial stages. As applied to gracilin A, we first targeted the simple bis-acetoxy furanose **5.8** as the minimal pharmacophore that was readily obtained through a two-step oxidation/hydrogenation sequence to deliver the racemic *syn*-substituted acetoxy furanose (±)-**5.8a** along with the *anti*-diastereomer (±)-**5.8b** (d.r. 1.7:1). In a second stage, derivatives devoid of the cyclohexyl substituent and exocyclic alkene were targeted, namely bicyclic bis-acetoxy furanose **5.7a,b** (Scheme 5.1). The bicyclic lactone *endo*-**5.15a** (3:1 d.r., 94% e.e.) was obtained from a Diels–Alder-lactonization organocascade employing diene **5.12** and acryloyl chloride (**5.11**) with tetramisole as the Lewis base promoter. The required *endo*-diastereomer **5.15a** could be isolated in 58% yield, and subsequent reduction with $LiAlH_4$ followed by desilylation delivered ketodiol **5.16**. Swern oxidation led to a dialdehyde that was directly subjected to acid-promoted acetylation to give the unstable keto bis-acetoxy furanoses **5.17** as a mixture of syn/anti diastereomers. A subsequent reduction with $NaBH_4$ and dehydration with $SOCl_2$ delivered the bicyclic bis-acetoxy furanoses **5.7a,b** as a mixture of alkene regioisomers. The low yields obtained in this and subsequent four-step sequences leading to the bis-acetoxy furanoses were primarily a result of incomplete or non-simultaneous Swern oxidation of the diols leading to regioisomeric monoacetoxy furanoses.

We next targeted derivatives devoid of the exocyclic alkene but bearing the cyclohexyl substituent (Scheme 5.1C). Desilylation of *endo*-Diels–Alder adduct **5.15a** gave bicyclic lactone (–)-**5.9**, which was subjected to an allylzinc reagent derived from cyclohexenyl choride (±)-**5.18** employing conditions we previously used in our synthesis of spongiolactone.[238] This delivered the tricyclic adducts **5.20** as a 1:1 mixture of diastereomers at the generated quaternary carbon but with high facial selectivity, leading

to a single epimer at the tertiary alcohol center. The contra-steric addition of the allylzinc reagent to the concave face of ketone (–)-**5.9** was unexpected but likely due to stereoelectronic effects leading directly to a chair rather than a boat conformation and was verified by extensive NMR studies. In the case of addition of the *gem*-dimethyl cyclohexenyl zinc reagent derived from (±)-**5.19**, the stereochemistry was further verified by single-crystal X-ray analysis of adduct **5.20b**. However, this diastereoselectivity is inconsequential because the tertiary alcohol in **5.20b** is subsequently dehydrated. Hydrogenation reduced the cyclohexene of **5.20b** and a three-step process delivered the hydroxy bis-acetoxy furanose **5.22** as a 1:1 mixture of diastereomers. Dehydration with Burgess' reagent[239] gave alkenes **5.23** as a mixture of four diastereomers due to the alkene regioisomers produced. The four diastereomers were separable by preparative chiral HPLC, enabling biological analysis of each stereoisomer.

Gaps in the SAR profile were also back-filled following initial assays as described in the following (Scheme 5.2). This entailed application of aspects of diverted total synthesis to synthesize derivatives devoid of the cyclohexyl moiety (that is, **5.24**), variations in the oxidation state and substituents of the tetrahydrofuran and cyclohexyl moiety (that is, **5.26–5.27**), and also exploration of the enantiomeric series (that is, **5.28–5.29**).

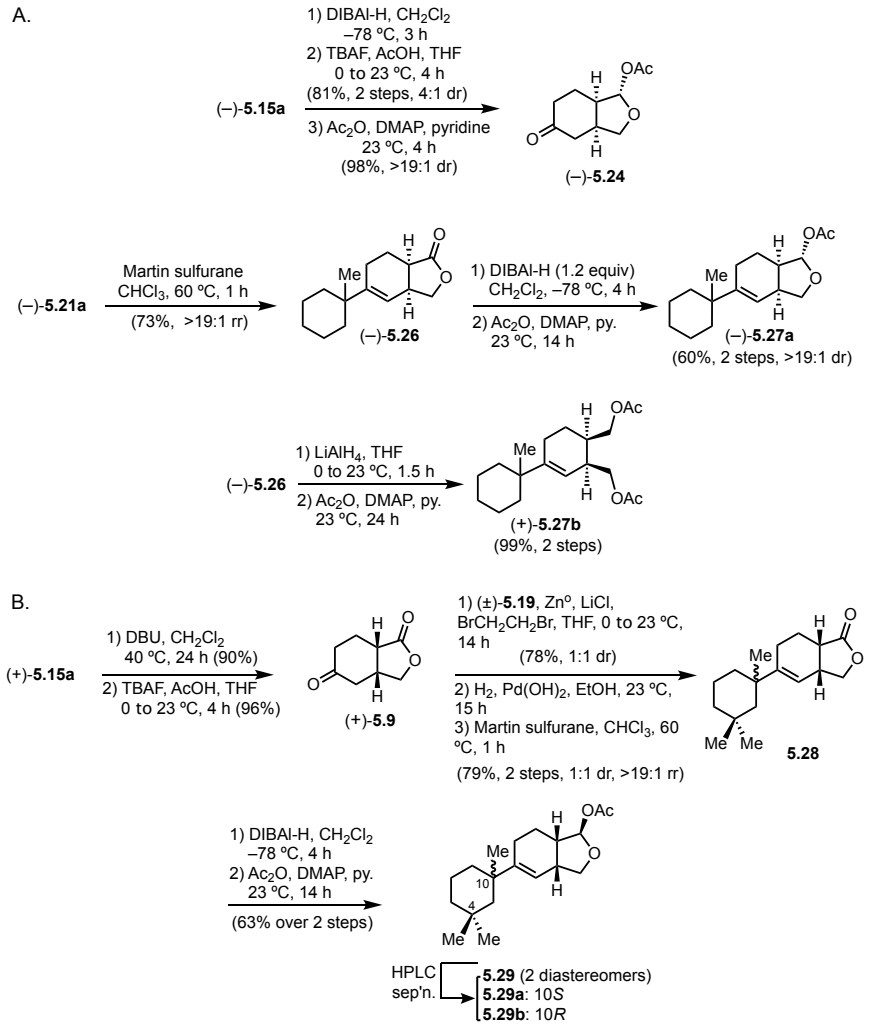

Scheme 5.2. Synthesis of gracilin A derivatives toward SAR gap filling.

As a preliminary biological screen, the initial gracilin A derivatives synthesized were analyzed by surface plasmon resonance (SPR) with immobilized CypA.[240, 241] Biological testing of gracilin A derivatives was performed in sets as the various stages of PDR were accomplished (Schemes 5.1A–C and 5.2A,B). Association curves (K_D) were measured at various concentrations in comparison to gracilin A and CsA and the initially synthesized highly simplified derivatives, monocyclic (±)-**5.8** and bicyclic **5.7** bis-acetoxy furanoses, exhibited no affinity for CypA up to 10 μM (Figure 6.3). On binding to CypA,

CsA and gracilin A modulate interleukin 2 (IL-2) release through the calcineurin pathway,[217] so the effects of these simplified derivatives on IL-2 production were also measured. Concanavalin A (ConA) was used to activate human T lymphocytes and induce IL-2 release.[242] T lymphocytes were pre-treated for 2 h with different non-toxic concentrations of compounds and then activated for 48 h in the presence of ConA (50 μg ml−1). After this time, levels of IL-2 released to the medium were measured by an enzyme-linked immunosorbent assay (ELISA) kit. As expected, the greatly simplified monocyclic (±)-**5.8a,b** and bicyclic furanoses **5.7a,b** did not inhibit IL-2 production nor exhibit T-lymphocyte toxicity at concentrations up to 10 μM (MTT assay).

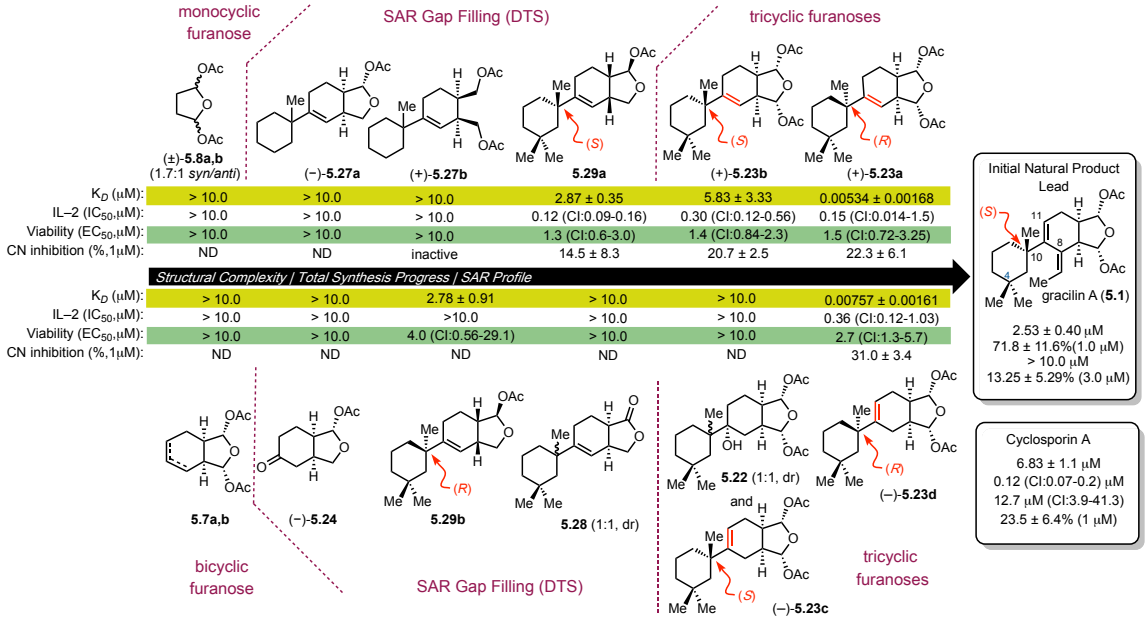

Figure 5.3. Immunosuppressive activity of gracilin A derivatives.

Gracilin A derivative **5.23** bearing the pendant cyclohexyl moiety, began to display immunosuppressive activity (Figure 6.3). The initial diastereomeric mixture of tertiary alcohols **5.22** derived from cyclohexenyl zinc addition was inactive. However, following

dehydration to introduce the tri-substituted alkenes, immunosuppressive activity was observed with only a twofold decrease in K_D relative to gracilin A (2.53 ± 0.40 μM) for alkene **5.23b** bearing the 10*S* configuration (5.83 ± 3.33 μM) with moderate IL-2 inhibition (IC_{50} 0.30 μM). The interplay between alkene regioisomers ($\Delta^{8,9}$ versus $\Delta^{9,11}$) and the C10 configuration was revealed through derivatives **5.23a** and **5.23d**, which exhibited nearly a 1,000-fold increase in K_D toward CypA compared to gracilin A (5.34 ± 1.68 nM and 7.57 ± 1.61 nM, respectively), while isomers **5.23b** and **5.23c** were either significantly less active or completely inactive, respectively. Derivatives **5.29a** and **5.23a** displayed IC_{50} values for IL-2 inhibition of 0.12 and 0.15 μM, respectively whereas the C10 epimer of **5.23a**, derivative **5.23b** and the $\Delta^{9,11}$ regioisomer **5.23d**, had higher values of 0.30 and 0.36 μM, respectively, while the epimeric, $\Delta^{9,11}$ regioisomer **5.23c** exhibited a value of >10 μM, again pointing to the interplay between the alkene regiochemistry and the C10 stereochemistry for IL-2 inhibition. The discrepancy between binding (K_D) to CypA as measured by SPR and the cellular inhibition of IL-2 expression may point to differential cell permeability or reflect differential binding to calcineurin, the presumed target of the CypA–gracilin A complex, impacted by the absence of the C8 exocyclic ethylidene. In addition, the conformation of the cyclophilins is highly dependent on the pH of the assay. This assay was performed at low pH (4.5) to demonstrate the activity of gracilin derivatives, which also lowers the K_D for CsA compared to literature values. To address this discrepancy, we also performed an enzymatic assay to measure calcineurin inhibition by gracilin A derivatives (at 1 μM) and, as expected, the most potent derivatives in the SPR assay showed comparable inhibition (22–31%) to CsA (23% at 1 μM). Despite differences in CypA binding affinity, these derivatives have comparable activity in both IL-2 and

calcineurin assays, which supports the hypothesis that these derivatives lead to differential binding to calcineurin by the respective CypA–gracilin derivative complexes. These data, taken together, suggest that conformational preferences about the C9–C10 bond play a pivotal role in the immunosuppressive activity of the gracilin family.

To fill gaps in the SAR profile regarding immunosuppressive activity, we turned to the application of diverted total synthesis and targeted additional simplified derivatives (Figure 5.3). The greatly simplified bicyclic mono-acetoxy ketone **5.24** and the bicyclic lactone **5.28**, differing from the highly active bis-acetoxy furanose **5.23a** only by the oxidation state of the tetrahydrofuran, were completely inactive. Epimerization of *exo*-**5.15b** enabled access to the enantiomeric series, leading to mono-acetoxy furanoses **5.29a,b** epimeric at the quaternary C10 center. Affinity to CypA ($K_D \approx 3$ μM) for both diastereomers **5.29a,b** was comparable to gracilin A; however, differential inhibition of IL-2 production ($IC_{50} = 0.12$ versus >10 μM) was observed for both diastereomers while remaining relatively nontoxic to T cells ($EC_{50} = 1–4$ μM). The importance of the quaternary carbon stereochemistry and alkene regisomer on IL-2 inhibition, which directly impacts the conformation about the C9–C10 bond, is again highlighted by this enantiomeric series with the natural (*S*) configuration imparting the greatest activity.

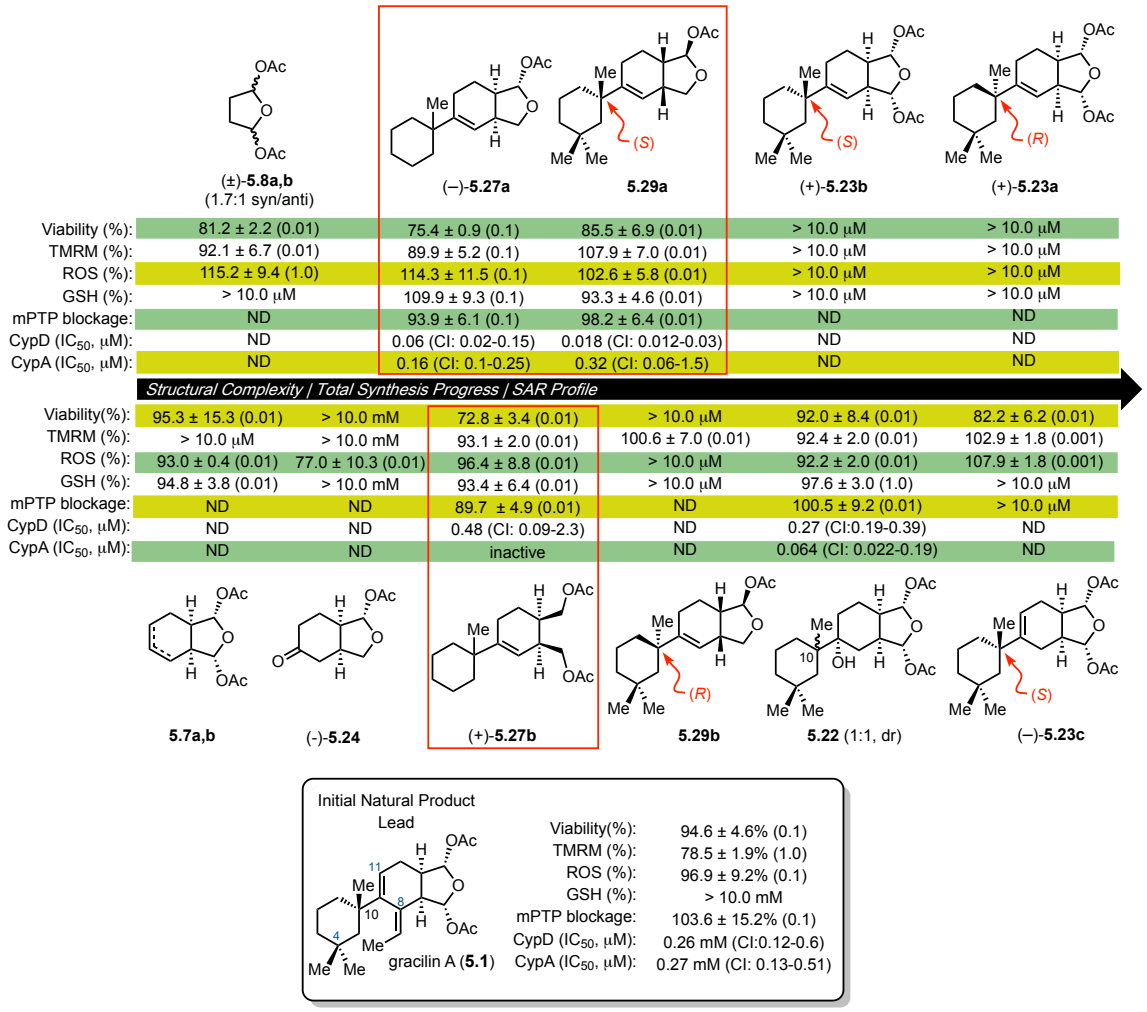

Figure 5.4. Activity of gracilin A derivatives as neuroprotective agents.

Given the neuroprotective effects previously observed for gracilin A, the derivatives synthesized through application of PDR for immunosuppressive effects were also studied for potential neuroprotective activity and of particular interest was possible selectivity for CypD versus CypA PPiase activity (Figure 5.4), a key property required for neuroprotective lead compounds devoid of immunosuppressive effects. All assays were performed at the indicated concentrations (0.001, 0.01, 0.1 or 1.0 μM) based on cytotoxicity determined with SH-SY5Y cells. In particular, compounds that displayed some toxicity against this cell line at 1 μM were tested at lower concentrations. Treatment

of SH-SY5Y cells with a known potent oxidant such as H_2O_2 produces oxidative damage with a consequent increase in reactive oxygen species (ROS) release. ROS generation provokes mitochondrial dysfunction, increases cell death and affects the cellular antioxidant systems such as the glutathione (GSH) cycle.[243] Therefore, four parameters were measured to evaluate the neuroprotective effects of the simplified gracilin A derivatives: cell viability, mitochondrial membrane potential ($\Delta\Psi_m$), ROS release and GSH levels after cellular challenge with H_2O_2. Several highly simplified gracilin A derivatives, namely monoacetoxy furanose **5.27a** and the highly simplified diacetate **5.27b** (both derived from **5.21a**), the inseparable, tertiary alcohols **5.22** (1:1, d.r.) and the enantiomeric mono-acetoxy furanose **5.29a**, but not its diastereomer **5.29b**, and even the simplest bisacetoxy furanose (±)-**5.8a,b** (1.7:1, syn/anti) displayed significant neuroprotective effects. In view of these results, the compounds with greater activity in oxidative stress assays (**5.27a**, **5.27b**, **5.29a**, **5.22** and **5.23c**) were chosen to test their ability to block the opening of the mPTP. The simplest derivatives **5.8a,b** and **5.7a,b** displayed lower activities and only at one of the concentrations tested, so these compounds were not subjected to the following assays. In PPIase activity assays, selectivity for CypD over CypA was observed for derivatives **5.27a** (~3-fold) and **5.29a** (~18-fold) with the very simple diacetate **5.27b** displaying the greatest differential CypD activity because it was inactive against CypA (up to 10 μM) but displayed activity against CypD (IC_{50} = 0.48 μM). In contrast, tertiary alcohols **5.22** had opposite selectivity for CypA over CypD (~4-fold). Our results suggest that the antioxidant effect of these gracilin A derivatives is mitochondrial-related, similar to gracilin A, mediated through interaction with CypD. These compounds protect cells from oxidative damage induced by H_2O_2 improving mitochondrial functioning measured

by MTT and TMRM assays and increased GSH levels. Moreover, they block mitochondrial pore opening and induce CypD activity inhibition. Therefore, gracilin A derivatives hold potential as neuroprotective lead compounds that are devoid of immunosuppressive effects.

5.3 Conclusion

The total synthesis of natural products continues to be an important endeavor for the discovery of novel synthetic strategies and methods in addition to the exploration of biologically relevant chemical space. The described PDR approach brings biological function into the retrosynthetic planning stages to target multiple, simplified derivatives bearing a hypothesized pharmacophore *en route* to the natural product. PDR can be considered to be a subset of Wender's function-oriented synthesis and will of course not be applicable to every natural product (that is, those where the majority of the structure is required for bioactivity). A caveat to this approach is that a balance must be found between synthetic convergency and targeting of bioactivity during the total synthesis. However, the application of PDR may only be limited by the creativity and intuition of synthetic chemists building on minimal SAR. For example, the SARs of isolated natural product congeners and other lines of evidence may direct one or more hypotheses regarding a proposed pharmacophore. Indeed, application of PDR can generate alternative strategies for a given natural product through alternative hypothesized pharmacophores in a similar way to consideration of various strategic bond disconnections in classic retrosynthesis. In the present study, the first SAR profiles of gracilin A derivatives were secured by providing proof-of-principle studies of PDR and support the notion of the bis-acetoxy furanose as a pharmacophore for immunosuppressive activity but not necessarily for neuroprotective activity (Figure 5.5).

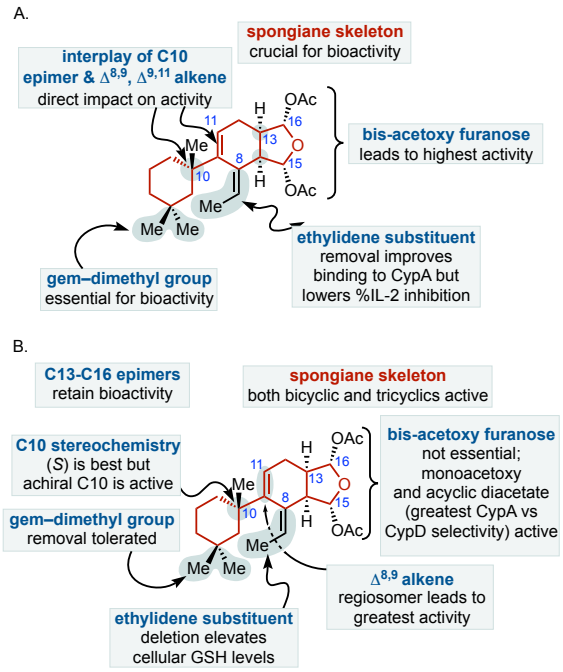

Figure 5.5. SAR profile of gracilin A for both immunosuppressive and neuroprotective activity enabled through application of PDR.

Evidence was gathered for our initial hypothesis invoking the bis-acetoxy furanose of gracilin A as the pharmacophore, as relates to immunosuppressive activity, given that derivatives with this moiety (for example, **5.23a** and **5.23d**) displayed the greatest activity ($K_D \approx 5–7$ nM), while those lacking this moiety were inactive (for example, (–)-**5.28**). Importantly, PDR disclosed that the C8-ethylidene is not required to elicit potent immunosuppressive activity and, with the availability of natural gracilin A as a comparator, it was unnecessary to complete a total synthesis.

While derivatives of CsA were previously investigated as potential neuroprotective agents through inhibition of CypD, they lacked effectiveness due to their high molecular weights and low blood–brain barrier permeability.[244-246] Several gracilin A derivatives (for example, **5.27a,b** and **5.29a**) accessed through this study, that interestingly includes the

enantiomeric series, displayed significant neuroprotective activity, importantly while also displaying selectivity for CypD versus CypA inhibition. These gracilin derivatives serve as lead compounds for neurodegenerative diseases and other CypD-mediated diseases including atherosclerosis or autoimmune diseases.[247, 248]

Although an ideal application of PDR will generally be challenging to implement, in particular when reactive functionality precludes a completely linear synthetic strategy as dictated by PDR, as in the present case of the gracilins, we expect that pharmacophore hypotheses brought into retrosynthetic planning will enable greater SAR information to be gathered *en route* to a natural product. It is also anticipated that application of PDR will provide an avenue for hypothesis-driven, natural product total synthesis efforts while simultaneously accelerating the exploration of natural product chemical space through total synthesis efforts premised on PDR.

5.5 Experimental

5.5.1 General Information

All non-aqueous reactions were performed under a nitrogen atmosphere in oven-dried glassware. Dichloromethane (CH_2Cl_2), tetrahydrofuran (THF), diethyl ether (Et_2O), acetonitrile (CH_3CN) and toluene (PhMe) were dried by filtration through activated alumina (solvent purification system). Diisopropylethylamine ($EtN(iPr)_2$) and triethylamine (Et_3N) were distilled from calcium hydride prior to use. Other solvents and reagents were used as received from commercially available sources. Deuterated solvents were purchased from Cambridge Isotopes and used as received. ^1H NMR spectra were measured at 500 MHz and referenced relative to residual chloroform (7.26 ppm) or benzene (7.16 ppm) and were reported in parts per million. Coupling constants (*J*) were reported in Hertz (Hz), with multiplicity reported following usual convention: s, singlet; d, doublet; t, triplet; q, quartet; dd, doublet of doublets; dt, doublet of triplets; dq, doublet of quartets; dq, doublet of quartets; td, triplet of doublets; tt, triplet of triplets; ddd, doublet of doublet of doublets; ddt, doublet of doublet of triplets; ddq, doublet of doublet of quartets; dddd, doublet of doublet of doublet of doublets; ddddt, doublet of doublet of doublet of doublet of triplets; ddquint, doublet of doublet of quintets; m, multiplet, br s, broad singlet. 13C NMR spectra were measured at 125 MHz and referenced relative to chloroform-d signal (77.16 ppm) or benzene (128.06 ppm) and were reported in parts per million (ppm). Flash column chromatography was performed with 60 Å Silica Gel (230-400 mesh) as stationary phase on an automated flash chromatography system (EtOAc/hexanes as eluent unless indicated otherwise). High-resolution mass spectra (ESI) were obtained through the Laboratory for Biological Mass Spectrometry (Texas A&M University). Thin Layer

Chromatography (TLC) was performed using glass-backed silica gel F254 (Silicycle, 250 μm thickness). Visualization of developed plates was performed by fluorescence quenching or by treating with Seebach's staining solution. Fourier Transform Infrared (FTIR) spectra were recorded as thin films on NaCl plates. Optical rotations were recorded on a polarimeter at 589 nm employing a 25 mm cell. High Performance Liquid Chromatography (HPLC) was performed on a chromatographic system using various chiral columns (25 cm) as noted. X-ray diffraction was obtained by the X-ray Diffraction Laboratory at Texas A&M University. (S)-(–)-TM•HCl was purchased from TCI chemicals and used as received. All other chemicals were purchased from Sigma-Aldrich or Alfa Aesar and used as received.

5.5.2 Abbreviation List

$EtN(iPr)_2$	N,N-Diisopropylethylamine
Et_3N	Triethylamine
$NaBH_4$	Sodium borohydride
(*S*)-(–)-TM·HCl	(S)-(–)-Tetramisole (levamisole) hydrochloride
$LiAlH_4$	Lithium aluminum hydride
TBAF	Tetrabutylammonium fluoride
Me_2S	Dimethyl sulfide
$(COCl)_2$	Oxalyl chloride
DMAP	4-(Dimethylamino)pyridine
Ac_2O	Acetic anhydride
DIBAl-H	Diisobutylaluminum hydride
DBU	1,8-Diazabicyclo(5.4.0)undec-7-ene

5.5.3 Synthetic Procedures

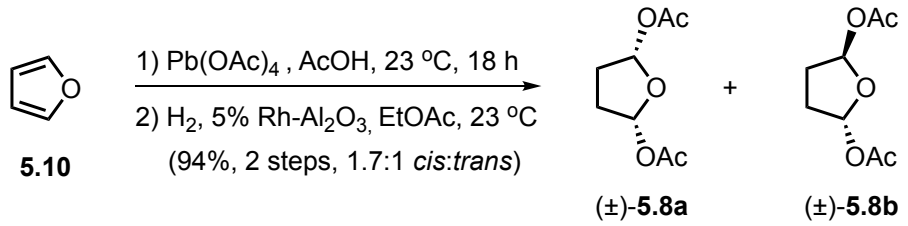

5.10 (±)-**5.8a** (±)-**5.8b**

***cis*- and *trans*-2,5-tetrahydrofuran-2,5-diyl diacetate ((±)-5.8a and (±)-5.8b):** To a suspension of $Pb(OAc)_4$ (2.00 g, 4.54 mmol, 1.10 equiv) in glacial AcOH (10.0 mL) was added furan **5.10** (0.30 mL, 4.13 mmol, 1.00 equiv) and the mixture was stirred at 23 ºC for 18 h. AcOH was evaporated and Et_2O was added to the residue. The precipitate was filtered, the filtrate was collected, evaporated and the residue was redissolved in anhydrous EtOAc (50 mL). 5% Rhodium on alumina (180 mg) was added and the hydrogenation was carried out under hydrogen atmosphere (1 atm, balloon) for 24 h. The solution was filtered through Celite, the filtrate was concentrated by rotary evaporation and purified by an automated flash chromatography system (5→50% EtOAc/hexanes) providing 721 mg (94% yield, 2 steps) of (±)-**5.8a** and (±)-**5.8b** as a clear colorless oil and as a mixture of two isomers (ratio 1.7:1 *cis:trans*, according to 500 MHz ^{1}H-NMR). **IR (thin film):** 2921, 2851, 1745 cm^{-1}; **HRMS (ESI+)** *m/z* calcd for $C_8H_{12}LiO_5$ $[M+Li]^+$: 195.0847, found: 195.0845. Spectral data matched that previously reported.

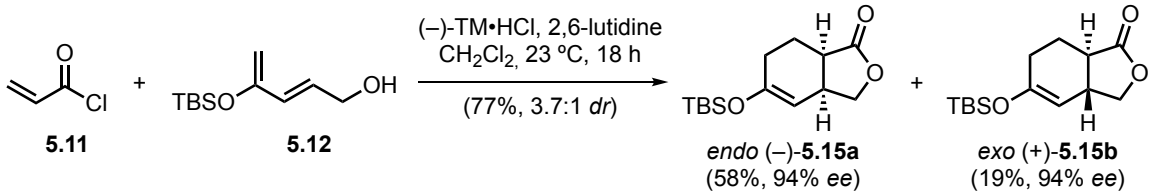

5.11 **5.12** *endo* (–)-**5.15a** (58%, 94% *ee*) *exo* (+)-**5.15b** (19%, 94% *ee*)

(3a*S*,7a*R*)-5-((*tert*-butyldimethylsilyl)oxy)-3a,6,7,7a-tetrahydroisobenzofuran-1(3*H*)-one ((–)-5.15a) and (3a*R*,7a*R*)-5-((*tert*-butyldimethylsilyl)oxy)-3a,6,7,7a-

tetrahydroisobenzofuran-1(3*H*)-one ((+)-5.15b): *The following procedure, making use of commercially available and inexpensive levamisole·HCl as stoichiometric Lewis base promoter, was adopted for scale-up to obtain multi-gram quantities of the bicyclic lactone products and gave similar results to those obtained using catalytic benzotetramizole:* To an oven-dried, 250-mL pressure reaction vessel equipped with a magnetic stir bar was added silyloxydiene alcohol **5.12** (4.00 g, 18.7 mmol, 1.00 equiv) and 150 mL of CH_2Cl_2, followed by (*S*)-(–)-TM·HCl (5.96 g, 28.9 mmol, 1.55 equiv), 2,6-lutidine (3.68 mL, 31.7 mmol, 1.70 equiv), and acryloyl chloride **5.11** (2.27 mL, 28.0 mmol, 1.50 equiv). The reaction vessel was then sealed and placed in a 40 °C oil bath and stirred for 48 h. The reaction mixture was then allowed to cool to ambient temperature (23 °C), volatiles were removed by rotary evaporation, and the residue was dissolved in a minimal amount of CH_2Cl_2 (~20 mL) and absorbed onto SiO_2, dried by rotary evaporation, and purified by automated flash column chromatography Purification by automated flash chromatography (0→50% EtOAc/hexanes) afforded bicyclic γ-lactones (–)-**5.15a** (2.90 g, 58% yield, 94% *ee*) and (+)-**5.15b** (954 mg, 19% yield, 94% *ee*).

(–)-**5.15a**: white crystalline solid; $\mathbf{R}_f$ = 0.45 (EtOAc/hexanes, 1:4 *v/v*); $[\boldsymbol{\alpha}]_D^{20.1}$ = –32.77 (*c* = 0.82, $CHCl_3$); Enantiomeric excess was determined by chiral HPLC analysis in comparison with authentic racemic material using a Chiralcel OD-H column: hexanes:^{i}PrOH = 95:05, flow rate 0.5 mL/min, λ = 210 nm: t_{major} = 13.5 min, t_{minor} = 15.2 min, 94% *ee*; **^{1}H-NMR** (500 MHz, $CDCl_3$) δ 4.76 – 4.73 (m, 1H), 4.32 (dd, *J* = 8.8, 5.9 Hz, 1H), 3.98 (dd, *J* = 8.8, 2.0 Hz, 1H), 3.17 – 3.11 (m, 1H), 2.74 (dt, *J* = 7.8, 4.3 Hz, 1H), 2.19 – 2.12 (m, 1H), 2.12 – 2.06 (m, 1H), 1.96 – 1.89 (m, 1H), 1.86 – 1.78 (m, 1H), 0.89 (s, 9H), 0.11 (s, 3H), 0.10 (s, 3H); **^{13}C-NMR** (126 MHz, $CDCl_3$) δ 178.48, 153.66, 103.01,

73.13, 37.65, 35.50, 26.12, 25.69 (3), 20.58, 18.10, -4.26, -4.44; **IR (thin film):** 2929, 2857, 1754, 1660 cm^{-1}; **HRMS (ESI+)** *m/z* calcd for $C_{14}H_{24}NaO_3Si$ $[M+Na]^+$: 291.1392, found: 291.1387. (+)-**5.15b**: clear colorless oil; $\mathbf{R}_f$ = 0.65 (EtOAc/hexanes, 1:4 *v/v*); $[\boldsymbol{\alpha}]_D^{19.8}$ = +23.84 (*c* = 1.12, $CHCl_3$); Enantiomeric excess was determined by chiral HPLC analysis; **^{1}H-NMR** (500 MHz, $CDCl_3$) δ 4.91 (d, *J* = 1.3 Hz, 1H), 4.38 (dd, *J* = 8.0, 6.6 Hz, 1H), 3.81 (dd, *J* = 11.4, 8.0 Hz, 1H), 2.91 – 2.82 (m, 1H), 2.28 – 2.17 (m, 3H), 1.70 – 1.58 (m, 2H), 0.91 (s, 9H), 0.14 (s, 3H), 0.08 (s, 3H); **^{13}C-NMR** (125 MHz, $CDCl_3$) δ 176.35, 154.19, 100.93, 71.74, 43.76, 41.00, 30.47, 25.68 (3), 20.87, 18.11, -3.46, -4.39; **IR (thin film)**: 2930, 2857, 1777, 1640 cm^{-1}; **HRMS (ESI+)** *m/z* calcd for $C_{14}H_{24}NaO_3Si$ $[M+Na]^+$: 291.1392, found: 291.1394.

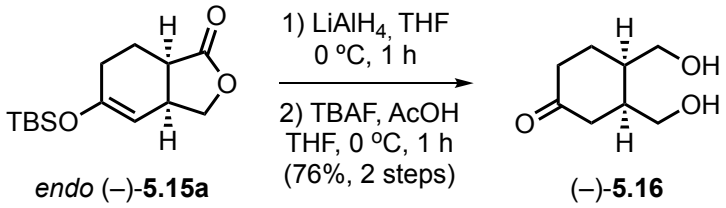

endo (–)-**5.15a** (–)-**5.16**

(3*S*,4*R*)-3,4-bis(hydroxymethyl)cyclohexan-1-one (5.16): To a 50 mL, single-necked, oven-dried, pear-shaped flask was added (–)-**5.15a** (493 mg, 1.85 mmol, 1.00 equiv) and 13.0 mL of THF. The resulting solution was cooled to 0 ºC with an ice bath and stirred for 10 min before adding $LiAlH_4$ as a solution in THF (2.40 *M*, 1.68 mL, 4.04 mmol, 2.20 equiv) dropwise via plastic syringe. After addition was complete, the mixture was allowed to stir for 1 h at 0 ºC before quenching by the method of Fieser. After quenching at 0 °C the reaction mixture is allowed to warm to ambient temperature (23 ºC) with vigorous stirring over 3 h. $MgSO_4$ is then added to the mixture and the resulting slurry is filtered

through Celite and the solvent removed by rotary evaporation, yielding an off-white oil which is used in the next step without purification.

To a 50 mL, single-necked, pear-shaped flask charged with the crude diol was added 5.0 mL of THF. The resulting solution was cooled to 0 ºC with an ice bath and AcOH was added (0.53 mL, 9.20 mmol, 5.00 equiv) followed by TBAF as a solution in THF (1.00 *M*, 9.20 mL, 9.20 mmol, 5.00 equiv). The reaction mixture was then stirred for 1 h at 0 ºC before removing the ice bath and allowing the mixture to warm to ambient temperature (23 ºC) over 1 h. The reaction mixture was then concentrated by rotary evaporation and the resulting crude oil was purified by automated flash column chromatography (0→20% MeOH/EtOAc) to afford keto diol **5.16** (220 mg, 76% yield, 2 steps) as a clear oil: $\mathbf{R}_f$ = 0.51 (MeOH/EtOAc, 1:4 *v/v*); $[\boldsymbol{\alpha}]_D^{20.0}$ -0.40 (*c* = 1.00. $CHCl_3$); **^{1}H-NMR** (600 MHz, $CDCl_3$) δ 3.83-3.86 (m, 1H), 3.72-3.75 (m, 1H), 3.60-3.66 (m, 2H), 3.57 (br s, 1H), 3.48 (br s, 1H), 2.37-2.45 (m, 3H), 2.33 (t, *J* = 7.0, 2H), 2.21-2.25 (m, 1H), 1.90-1.96 (m, 1H), 1.83-1.89 (m, 1H); **^{13}C-NMR** (150 MHz, $CDCl_3$) δ 211.8, 63.5, 63.0, 43.1, 41.5, 39.4, 39.4, 26.5; **IR (thin film)**: 3382, 2934, 2883, 1698 cm^{-1}; **HRMS (ESI+)** *m/z* calcd for $C_8H_{14}O_3Na$ $[M+Na]^+$: 181.0835, found: 181.0836.

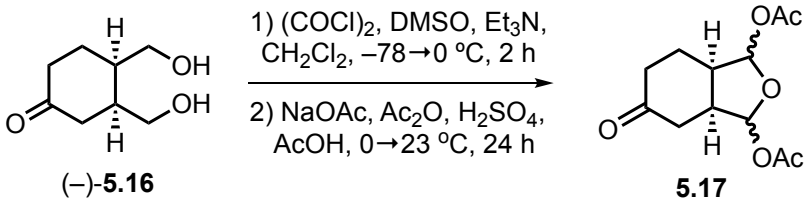

(–)-**5.16** **5.17**

(1*S*,3*R*,3a*S*,7a*R*)-5-oxooctahydroisobenzofuran-1,3-diyl diacetate (5.17): To a 50 mL, single-necked, oven-dried, pear-shaped flask was added 10 mL of CH_2Cl_2 which was cooled to –78 °C and stirred for 10 min before adding $(COCl)_2$ (596 μL, 6.95 mmol, 5.00

equiv). The solution was then stirred for another 10 min before adding DMSO as a solution in anhydrous CH_2Cl_2 (2.80 *M*, 5.00 mL, 13.9 mmol, 10.0 equiv) slowly dropwise via plastic syringe. The resulting solution was stirred for 40 min at –78 °C. Then diol **5.16** was added as a solution in CH_2Cl_2 (0.15 *M*, 220 mg, 1.39 mmol, 1.00 equiv) slowly dropwise via plastic syringe and stirred for 1 h. Et_3N (3.87 mL, 27.8 mmol, 20.0 equiv) was then added to the reaction mixture quickly along the wall of the flask via plastic syringe. The reaction mixture was then stirred for 30 min at –78 °C before replacing cooling bath with a 0 ºC ice bath and stirring for 1 h. The reaction mixture was quenched with saturated, aqueous $NaHCO_3$, extracted with CH_2Cl_2 (3 x 15 mL), dried over $MgSO_4$, filtered through Celite, and concentrated by rotary evaporation to give a crude oil which was used in the next step without purification.

To a 50 mL, single-necked, pear-shaped flask charged with crude material was added 7.0 mL of AcOH and 7.0 mL of Ac_2O, followed by NaOAc (1.14 g, 13.9 mmol, 10.0 equiv) and concentrated H_2SO_4 (74.0 μL, 1.39 mmol, 1.00 equiv). The reaction mixture was stirred at ambient temperature (23 ºC) for 48 h, poured into saturated aqueous $NaHCO_3$ solution (50 mL), and the aqueous layer was extracted with EtOAc (3 x 50 mL). The combined organic layer was washed with brine (20 mL), dried over $MgSO_4$, filtered through Celite, and concentrated under reduced pressure to give a crude oil which was filtered through a short column of silica gel to afford *bis*-acetoxy furanose **5.17** as a mixture of four diastereomers which was used in the following step without further purification: $\mathbf{R}_f$ = 0.39 (EtOAc/hexanes, 1:1 *v/v*). This bis-acetoxy furanose displayed some instability issues so was carried on directly to the following reduction/dehydration sequence without further characterization.

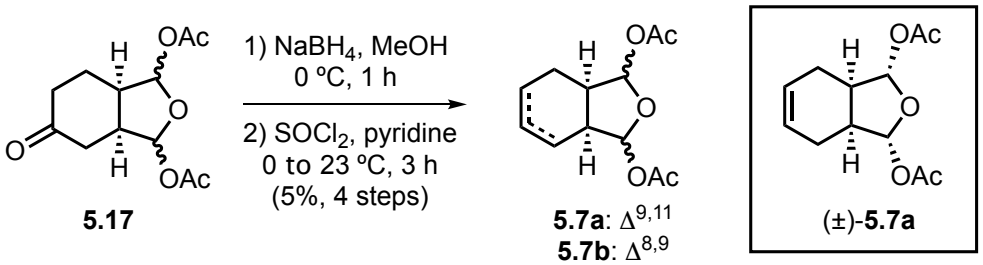

(3a*R*,7a*S*)-1,3,3a,4,5,7a-hexahydroisobenzofuran-1,3-diyl diacetate (5.7): To a 50 mL, single-necked, oven-dried, pear-shaped flask charged with **5.17** (105 mg, 0.41 mmol, 1.00 equiv) was added 12.0 mL of THF. The resulting solution was cooled to 0 ºC and stirred for 10 min before adding $NaBH_4$ (18.0 mg, 0.49 mmol, 1.20 equiv) in one portion. The resulting mixture was allowed to stir for 1 h at 0 ºC before quenching with AcOH (50.0 μL, 0.87 mmol, 2.10 equiv) and warming to ambient temperature (23 ºC). The mixture was concentrated by rotary evaporation to give a crude pale, yellow oil which was used in the next step without purification.

To a 10 mL, single-necked, oven-dried, pear-shaped flask charged with crude material was added 3.0 mL of pyridine. The resulting solution was cooled to 0 ºC and stirred for 10 min before adding $SOCl_2$ (87.0 μL, 1.20 mmol, 10.0 equiv). The cooling bath was removed and the mixture was allowed to warm to ambient temperature (23 ºC) and stir for 3 h. The reaction mixture was then concentrated by high-vacuum rotary evaporation and the crude residue was purified by flash column chromatography (0→100% EtOAc/hexanes) to afford alkene bicycle **5.7** (16.0 mg, 5% yield over 4 steps) as a clear oil and as an inseparable mixture of regioisomers and diastereomers (8 total). $\mathbf{R}_f$ = 0.39 (EtOAc/hexanes, 1:1 *v/v*). The spectral data for this mixture of 8 inseparable diastereomers and regioisomers was highly complex so full characterization is provided only for the major diastereomers, (±)-**5.7a**, which was prepared in racemic fashion through an alternative

sequence: $\mathbf{R}_f$ = 0.58 (EtOAc/hexanes, 30% *v/v*); **^{1}H-NMR** (600 MHz, C_6D_6) δ 6.19 (d, *J* = 3.1 Hz, 2H), 5.40 (m, 2H), 2.35 (m, 2H), 1.81-1.86 (m, 2H), 1.66-1.73 (m, 2H), 1.62 (s, 6H); **^{13}C-NMR** (150 MHz, C_6D_6) δ 169.36, 124.67, 102.45, 38.96, 22.30, 20.79; **IR (thin film)**: 3028, 2922, 2848, 1744 cm^{-1}; **HRMS (ESI+)** *m/z* calcd for $C_{12}H_{16}O_5Na$ $[M+Na]^+$: 263.0890, found: 263.0894.

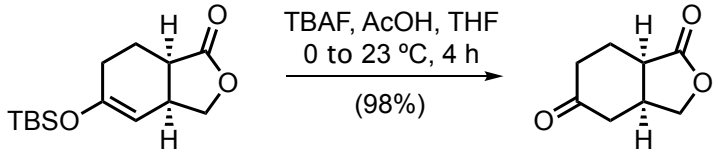

(–)-**5.15a** (*endo*) (–)-**5.9**

(3a*S*,7a*R*)-tetrahydroisobenzofuran-1,5(3*H*,4*H*)-dione ((–)-5.9): To a pre-cooled solution (0 ºC) of silylenol ether (–)-**5.15a** (495 mg, 1.84 mmol, 1.00 equiv) and glacial AcOH (0.22 mL, 3.69 mmol, 2.00 equiv) in anhydrous THF (18.0 mL) was added TBAF (1.00 M in THF, 3.70 mL, 3.69 mmol, 2.00 equiv) dropwise. The reaction mixture was allowed to warm slowly up to ambient temperature (23 ºC) over 4 h, and then concentrated by rotary evaporation. Purification by automated flash chromatography (5→80% EtOAc/hexanes) afforded keto lactone (–)-**5.9** (278 mg, 98% yield). (–)-**5.9**: clear colorless oil; $\mathbf{R}_f$ = 0.23 (EtOAc/hexanes, 1:1 *v/v*); $[\alpha]_D^{20.0}$ –57.63 (*c* = 0.38. $CHCl_3$); **^{1}H-NMR** (500 MHz, $CDCl_3$) δ 4.39 (dd, *J* = 9.4, 6.1 Hz, 1H), 3.98 (dd, *J* = 9.4, 2.3 Hz, 1H), 3.08 – 2.98 (m, 1H), 2.94 – 2.86 (m, 1H), 2.53 (dd, *J* = 15.2, 6.4 Hz, 1H), 2.38 – 2.26 (m, 4H), 2.21 – 2.10 (m, 1H); **^{13}C-NMR** (125 MHz, $CDCl_3$) δ 209.0, 177.6, 71.7, 41.2, 38.1, 37.3, 35.7, 22.7; **IR (thin film)**: 2934, 2864, 1771, 1712 cm^{-1}; **HRMS (ESI+)** *m/z* calcd for $C_8H_{11}O_3$ $[M+H]^+$: 155.0708, found: 155.0711.

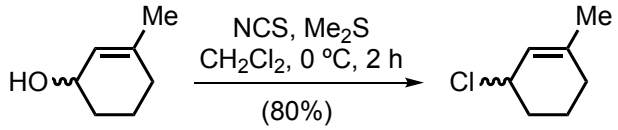

5.S1 (±)-**5.18**

3-chloro-1-methylcyclohex-1-ene ((±)-5.18): *N*-chlorosuccinimide (2.48 g, 18.6 mmol, 1.10 equiv) was weighed into an oven-dried, round-bottomed flask and suspended in CH_2Cl_2 (33.0 mL). The slurry was cooled to 0 ºC and Me_2S (1.61 mL, 21.9 mmol, 1.30 equiv) was added dropwise over ~5 min producing a white solution. 3-methylcyclohex-2-en-1-ol (**5.S1**) (2.00 mL, 16.8 mmol, 1.00 equiv) was added dropwise with vigorous stirring to provide a clear solution. Within ~10 min, a precipitate formed. The reaction was continued at 0 ºC for 2 h and concentrated under reduced pressure. Pentane (50 mL) was added leading to immediate formation a white precipitate. The flask was then placed in a freezer for 4 h and the supernatant was decanted. The remaining solid was washed with cold pentane (2 x 50 mL) and the combined organics were washed with brine (2 x 50 mL), dried over $MgSO_4$, and concentrated *in vacuo*. Allyl chloride (±)-**5.18** was isolated as a clear colorless oil, (1.76 g, 80%) and this material was of sufficient purity (>95% as judged by ^{1}H-NMR) to be carried directly to the next step without purification. $\mathbf{R}_f$ = 0.79 (EtOAc/hexanes, 3:7 *v/v*). Spectral data matched that previously reported.

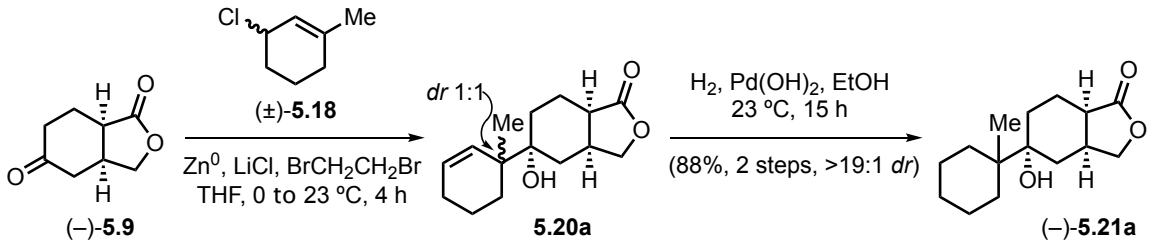

(–)-**5.9** **5.20a** (–)-**5.21a**

(3a*S*,5*R*,7a*R*)-5-hydroxy-5-(1-methylcyclohexyl)hexahydroisobenzofuran-1(3*H*)-one ((–)-5.21a): To an oven-dried round-bottomed flask was added zinc powder (2.30 g, 35.0

mmol, 25.0 equiv) and LiCl (300 mg, 7.00 mmol, 5.00 equiv) with a large bore vacuum adapter with Teflon lined seal for addition of liquids *via* syringe. The flask and solids were then carefully flame-dried under high vacuum (using a vacuum/N_2 double manifold) by repeated heating and cooling cycles with swirling of the solids to avoid the solids from clumping. After the final cycle of heating, the solids were allowed to cool for 3 min under N_2, and then anhydrous THF (20.0 mL) was slowly and carefully added with vigorous stirring. After addition of THF, 1,2-dibromoethane (0.12 mL, 1.40 mmol, 1.00 equiv) was added which sometimes led to an exotherm simultaneous with rapid gas evolution, which needs to be controlled. Pressure fluctuations generated upon addition of 1,2-dibromethane were controlled by momentarily switching the manifold from N_2 to vacuum. (Note: If gas evolution was not observed upon addition of 1,2-dibromoethane, a heat gun was employed to initiate gas evolution). The solution was allowed to cool at ambient temperature over ~5 min before being further cooled to 0 ºC. A solution of (–)-**5.9** (215 mg, 1.40 mmol, 1.00 equiv) in THF (1.00 mL) was added dropwise by syringe followed by slow addition of (±)-**5.18** (1.65 g, 12.6 mmol, 9.00 equiv) in THF (4.0 mL) *via* syringe pump at a rate of 1.0 mL/h. During this time, the reaction mixture was allowed to slowly warm to ambient temperature (23 ºC). The reaction mixture was then quenched with saturated NH_4Cl solution (100 mL). The organic phase was separated and the aqueous phase was further extracted with EtOAc (3 x 100 mL). The organic layers were combined, washed with brine (200 mL), dried with $MgSO_4$, and concentrated *in vacuo* to afford cyclohexenol lactone **5.20a** as a crude pale-yellow oil and as an inseparable mixture of two diastereomers (1:1 dr, based on ^{1}H-NMR analysis of the crude mixture) which was used in the next step without purification.

To a solution of the above crude cyclohexenol lactone **5.20a** (267 mg, 1.07 mmol, 1.00 equiv) in absolute EtOH (25.0 mL) and under an atmosphere of N_2 was added $Pd(OH)_2$ on carbon (300 mg, 20 wt%, 2.14 mmol, 2.00 equiv). A H_2 balloon was attached to the flask and after three consecutive cycles of evacuation (under high vacuum) and H_2 purge, the mixture was stirred for 15 h. An aliquot was removed for ^{1}H-NMR analysis to ensure complete hydrogenation of the cyclohexene moiety. The reaction mixture was filtered through a pad of Celite, washed with EtOAc and concentrated *in vacuo*. Purification by automated flash chromatography (5→60% EtOAc/hexanes) afforded cyclohexanol lactone **(–)-5.21a** (307 mg, 88% yield over 2 steps) as a single diastereomer (>19:1 dr, based on ^{1}H-NMR analysis of the crude mixture).

(–)-5.21a: colorless crystalline solid; $\mathbf{R}_f$ = 0.43 (EtOAc/hexanes, 1:1 *v/v*); $[\alpha]_D^{17.0}$ –34.15 (*c* = 0.41, $CHCl_3$); **^{1}H-NMR** (500 MHz, $CDCl_3$) δ 4.23 (ddd, *J* = 8.8, 4.7, 0.7 Hz, 1H), 3.91 (d, *J* = 8.9 Hz, 1H), 2.75 (dq, *J* = 11.9, 6.2 Hz, 1H), 2.63 (t, *J* = 6.4 Hz, 1H), 2.10 – 1.92 (m, 2H), 1.84 (ddd, *J* = 13.8, 6.0, 2.9 Hz, 1H), 1.66 – 1.50 (m, 4H), 1.45 – 1.19 (m, 9H), 1.07 – 0.95 (m, 1H), 0.88 (s, 3H); **^{13}C-NMR** (125 MHz, $CDCl_3$) δ 178.7, 75.5, 72.1, 40.1, 38.9, 33.2, 31.3, 30.4, 30.4, 26.4, 26.3, 22.0 (2), 18.7, 17.2; **IR (thin film)**: 3509, 2966, 2929, 2862, 1747 cm^{-1}; **HRMS (ESI+)** *m/z* calcd for $C_{15}H_{25}O_3$ $[M+H]^+$: 253.1804, found: 253.1793.

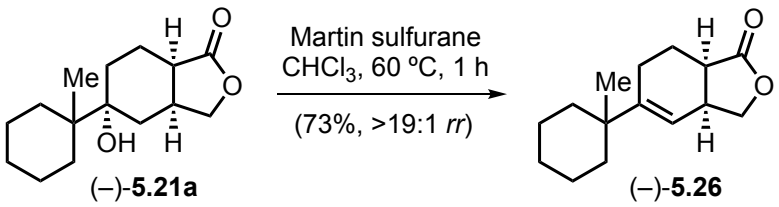

(–)-**5.21a** (–)-**5.26**

(3a*S*,7a*R*)-5-(1-methylcyclohexyl)-3a,6,7,7a-tetrahydroisobenzofuran-1(3*H*)-one ((–)-5.26): A glass tube was charged with a solution of (–)-**5.21a** (268 mg, 1.07 mmol, 1.00 equiv) in anhydrous $CHCl_3$ (35.0 mL) and Martin sulfurane dehydrating agent (1.44 g, 2.14 mmol, 2.00 equiv). The tube was sealed and placed in a 60 ºC oil bath for 1 h. The reaction mixture was cooled to ambient temperature (23 ºC), concentrated under reduced pressure and purified by automated flash chromatography (5→30% EtOAc/hexanes) to afford alkene lactone (–)-**5.26** (182 mg, 73% yield) as a single regioisomer (>19:1 *rr*, based on ^{1}H-NMR analysis of the crude mixture).

(–)-**5.26**: clear colorless oil; $\mathbf{R}_f$ = 0.40 (EtOAc/hexanes, 1:4 *v/v*); $[\alpha]_D^{16.9}$ –72.31 (*c* = 0.26, $CHCl_3$); **^{1}H-NMR** (500 MHz, $CDCl_3$) δ 5.38 (s, 1H), 4.38 (dd, *J* = 8.8, 6.7 Hz, 1H), 4.02 (dd, *J* = 8.8, 3.0 Hz, 1H), 3.10 (m, 1H), 2.76 (dt, *J* = 8.0, 4.9 Hz, 1H), 2.08 (dt, *J* = 13.3, 4.8 Hz, 1H), 2.02 – 1.88 (m, 2H), 1.73 (dddd, *J* = 13.1, 10.0, 5.4, 4.7 Hz, 1H), 1.69 – 1.58 (m, 2H), 1.48 – 1.17 (m, 8H), 0.92 (s, 3H); **^{13}C-NMR** (125 MHz, $CDCl_3$) δ 179.1, 148.0, 117.8, 72.9, 38.9, 37.9, 37.9, 36.1, 36.0, 27.0, 26.4, 22.7, 22.5, 21.4, 20.8; **IR (thin film)**: 2927, 2854, 1771 cm^{-1}; **HRMS (ESI+)** *m/z* calcd for $C_{15}H_{22}LiO_2$ $[M+Li]^+$: 241.1780, found: 241.1793.

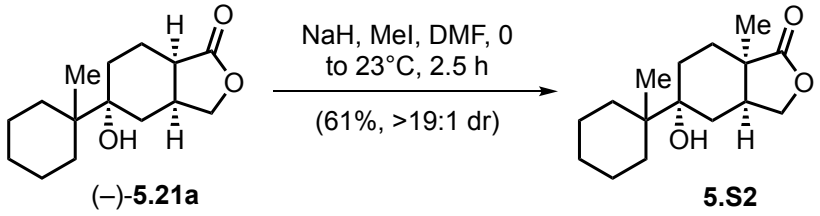

(–)-**5.21a** **5.S2**

(3aS,5R,7aR)-5-hydroxy-7a-methyl-5-(1-methylcyclohexyl)hexahydroisobenzofuran-1(3H)-one (5.S2): Alcohol (-)-**21a** (20.0 mg, 0.08 mmol, 1.00 equiv) was weighed out to a flame dried reaction vial and the atmosphere purged with N_2. The solid was dissolved in

DMF (1.00 mL, 0.08 M) and cooled to 0 ºC in an ice bath. NaH (60% w/w, 2.27 mg, 0.16 mmol, 2 equiv) was added in one portion and the reaction allowed to stir at 0 ºC for 20 minutes. MeI (6.00 mL, 0.10 mmol, 1.20 equiv) was added and the cooling bath removed. The resulting solution was stirred for 2 hours at 23 °C before quenching with H_2O (1.5 mL). The layers were separated and the aqueous phase extracted with Et_2O (3 x 1.5 mL). The combined organic extracts were washed with brine, dried over $MgSO_4$, filtered and concentrated. The crude residue was purified directly by silica gel chromatography (20% EtOAc:Hexanes) to yield 12.8 mg (61% yield) of the title compound.

5.S2: white solid, m.p. 102-104 ºC (recrystallized from pentane); **Rf** = 0.50 (EtOAc/hexanes, 1:1 v/v); $[\boldsymbol{\alpha}]_D^{23.5}$ –21.96 (*c* = 0.255, $CHCl_3$); Absolute stereochemistry was assigned based on X-ray analysis using anomalous dispersion (Figure S3). **^{1}H-NMR** (600 MHz, $CDCl_3$) δ 4.43 (dd, J = 9.0, 4.7 Hz, 1H), 3.85 (d, J = 9.0 Hz, 1H), 2.39 (ddd, J = 11.5, 6.2, 4.7 Hz, 1H), 2.05 (ddd, J = 14.0, 4.7, 2.9 Hz, 1H), 1.88 (ddd, J = 13.9, 6.3, 3.1 Hz, 1H), 1.75 (app td, J = 13.7, 4.7 Hz, 1H), 1.70 – 1.63 (m, 1H), 1.62 – 1.52 (m, 4H), 1.49 – 1.26 (m, 7H), 1.25 (s, 3H), 1.11 – 0.99 (m, 2H), 0.91 (s, 3H); **^{13}C-NMR** (150 MHz, $CDCl_3$) δ 181.1, 75.4, 71.0, 42.1, 39.9, 39.5, 32.8, 30.4, 30.3, 27.9, 27.3, 26.2, 23.5, 22.0, 21.9, 17.1; **IR (thin film)**: 3517, 2924, 2854, 1758, 1452, 1381 cm^{-1}; **HRMS (ESI+)** m/z calcd for $C_{16}H_{26}O_3Na$ $[M+Na]^+$: 289.1780, found: 289.1776.

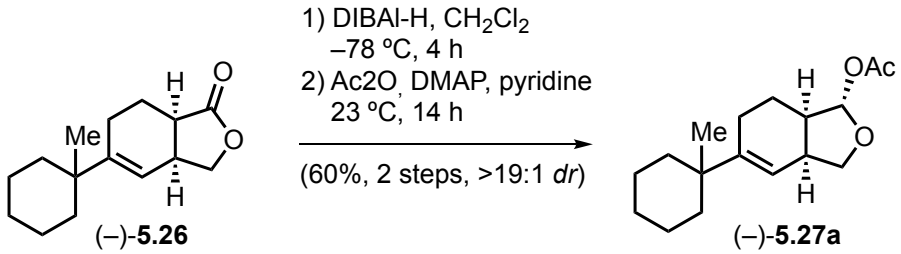

(1*S*,3a*S*,7a*R*)-5-(1-methylcyclohexyl)-1,3,3a,6,7,7a-hexahydroisobenzofuran-1-yl acetate ((–)-5.27): To a solution of (–)-**5.26** (30.0 mg, 0.128 mmol, 1.00 equiv) in CH_2Cl_2 (2.0 mL) was added DIBAl-H (1.00 M solution in CH_2Cl_2, 154 µL, 0.154 mmol, 1.20 equiv) dropwise at –78 ºC. The reaction mixture was stirred at –78 ºC for 4 h and carefully quenched in sequence with 6 µL H_2O, 11 µL 15% aqueous NaOH, and 16 µL H_2O. The dry-ice bath was removed and the mixture was allowed to warm slowly to ambient temperature (23 ºC). Subsequently, anhydrous $MgSO_4$ was added and the reaction mixture was vigorously stirred for 30 min, filtered through a pad of Celite, and concentrated by rotary evaporation. The crude lactol was of sufficient purity (>95% as judged by ^{1}H-NMR) to be carried on directly to the next step.

To a solution of the above crude lactol in anhydrous pyridine (1.00 mL) was added DMAP (2.00 mg, 12.0 µmol, 0.10 equiv) and Ac_2O (120 µL, 1.28 mmol, 10.0 equiv). The reaction mixture was stirred at ambient temperature (23 ºC) for 14 h, poured into saturated aqueous $NaHCO_3$ solution (10 mL), and the aqueous layer was extracted with CH_2Cl_2 (3 x 10 mL). The combined organic layers were washed with brine (10 mL), dried over $MgSO_4$, filtered, and concentrated under reduced pressure. Purification by automated flash chromatography (0→30% EtOAc/hexanes) afforded acetyl lactol (–)-**5.27a** (21.0 mg, 60% yield over 2 steps) as a single diastereomer (>19:1 *dr*, based on ^{1}H-NMR analysis of the crude mixture).

(–)-**5.27a**: clear colorless oil; $\mathbf{R}_f$ = 0.49 (EtOAc/hexanes, 1:4 *v/v*); $[\boldsymbol{\alpha}]_D^{19.1}$ –53.33 (*c* = 0.15, $CHCl_3$); **^{1}H-NMR** (500 MHz, $CDCl_3$) δ 6.04 (s, 1H), 5.44 (dd, *J* = 4.3, 1.6 Hz, 1H), 4.28 (t, *J* = 8.2 Hz, 1H), 3.65 (t, *J* = 7.8 Hz, 1H), 3.00 (q, *J* = 7.5 Hz, 1H), 2.30 (ddd, *J* = 11.6, 7.3, 4.4 Hz, 1H), 2.13 – 2.08 (m, 1H), 2.07 (s, 3H), 1.96 – 1.87 (m, 1H), 1.84 (m,

1H), 1.71 – 1.62 (m, 3H), 1.52 – 1.22 (m, 8H), 0.95 (s, 3H); **^{13}C-NMR** (125 MHz, $CDCl_3$) δ 170.8, 145.9, 117.6, 103.9, 74.9, 43.1, 38.7, 36.6, 36.3, 36.0, 27.1, 26.5, 22.9, 22.8, 22.7, 22.5, 21.5; **IR (thin film)**: 2931, 2857, 1746 cm^{-1}; **HRMS (ESI+)** *m/z* calcd for $C_{17}H_{26}LiO_3$ $[M+Li]^+$: 285.2042, found: 285.2052.

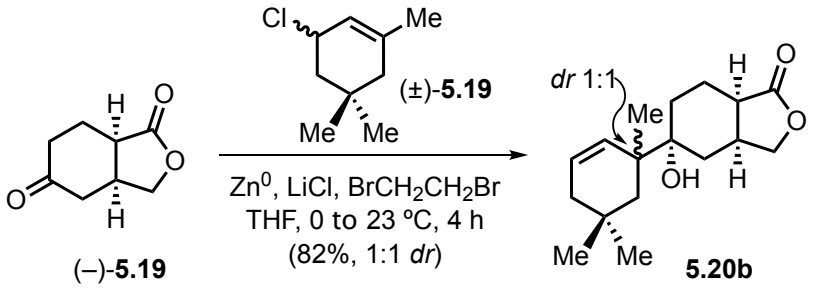

(3a*S*,5*R*,7a*R*)-5-hydroxy-5-(1,5,5-trimethylcyclohex-2-en-1-yl)hexahydroisobenzo-furan-1(3*H*)-one ((–)-5.20b): To an oven-dried round-bottomed flask was added zinc powder (2.30 g, 35.0 mmol, 25 equiv) and LiCl (300 mg, 7.00 mmol, 5.0 equiv) with a large bore vacuum adapter with Teflon lined seal for addition of liquids *via* syringe. The flask and solids were then carefully flame-dried under high vacuum (using a vacuum/N_2 double manifold) by repeated heating and cooling cycles with swirling of the solids to avoid the solids from clumping. After the final cycle of heating, the solids were allowed to cool for 3 min under N_2, and then anhydrous THF (20.0 mL) was slowly and carefully added with vigorous stirring. After addition of THF, 1,2-dibromoethane (0.12 mL, 1.40 mmol, 1.00 equiv) was added which sometimes led to an exotherm simultaneous with rapid gas evolution, which needs to be controlled. Pressure fluctuations generated upon addition of 1,2-dibromoethane were controlled by momentarily switching the manifold from N_2 to vacuum. (Note: If gas evolution was not observed upon addition of 1,2-dibromoethane, a heat gun was employed to initiate gas evolution). The solution was allowed to cool at

ambient temperature over ~5 min before being further cooled to 0 ºC. A solution of keto lactone (–)-**5.9** (215 mg, 1.40 mmol, 1.00 equiv) in THF (1.00 mL) was added dropwise by syringe followed by slow addition of allyl chloride (±)-**5.19** (2.22 g, 14.0 mmol, 10.0 equiv) in THF (4.0 mL) *via* syringe pump at a rate of 1.0 mL/h. During this time, the reaction mixture was allowed to slowly warm to ambient temperature (23 ºC). The reaction mixture was then quenched with saturated NH_4Cl solution (100 mL). The organic phase was separated and the aqueous phase was further extracted with EtOAc (3 x 100 mL). The organic layers were combined, washed with brine (200 mL), dried with $MgSO_4$, and concentrated under reduced pressure. Purification by automated flash chromatography (5→60% EtOAc/hexanes) afforded dimethyl cyclohexenol lactone **5.20b** (318 mg, 82% yield) as an inseparable mixture of two diastereomers (1:1 *dr*, based on ^{1}H-NMR analysis of the crude mixture).

5.20b: white crystalline solid, *m.p.* 161.2-163.7 ºC (recrystallized from pentane); $\mathbf{R_f}$ = 0.44 (EtOAc/hexanes, 1:1 *v/v*); Absolute stereochemistry was assigned based on X-ray analysis using anomalous dispersion; **^{1}H-NMR** (500 MHz, $CDCl_3$) δ 5.89 (ddd, *J* = 9.9, 6.3, 2.1 Hz, 1H), 5.52 (dd, *J* = 10.2, 1.8 Hz, 1H), 4.24 (dt, *J* = 9.0, 4.5 Hz, 1H), 3.93 (dd, *J* = 8.9, 4.3 Hz, 1H), 2.75 (tt, *J* = 12.0, 6.1 Hz, 1H), 2.64 (q, *J* = 5.5 Hz, 1H), 2.14 – 2.02 (m, 1H), 2.05 – 1.92 (m, 1H), 1.86 – 1.64 (m, 4H), 1.63 – 1.50 (m, 1H), 1.45 – 1.21 (m, 3H), 1.10 (dtd, *J* = 13.6, 2.7, 1.3 Hz, 1H), 1.02 (s, 3H), 0.97 (s, 3H), 0.94 (s, 3H); **^{13}C-NMR** (125 MHz, $CDCl_3$) δ 178.67, 178.63, 130.28 (2), 130.23 (2), 75.46, 75.44, 72.09, 71.97, 43.47, 43.42, 42.90, 42.85, 39.04 (2), 38.25 (2), 33.23, 33.22, 32.34, 32.33, 30.91 (2), 30.59, 30.58, 27.25, 27.19, 25.98 (2), 22.16 (2), 18.79, 18.69; **IR (thin film)**: 3518, 2951, 2867, 1766 cm^{-1}; **HRMS (ESI+)** *m/z* calcd for $C_{17}H_{27}O_3$ $[M+H]^+$: 279.1960, found: 279.1963.

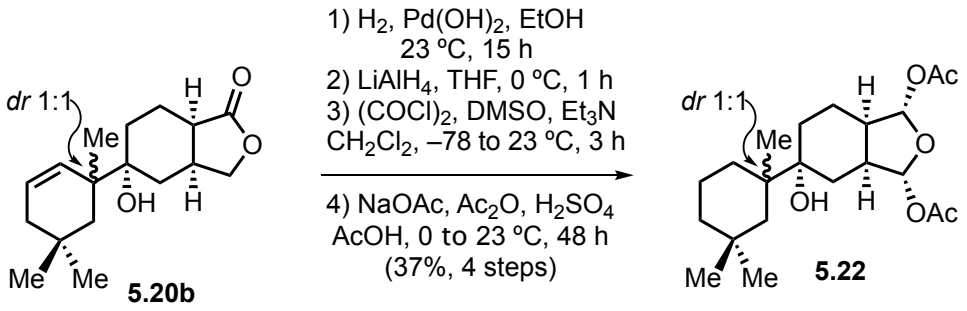

(1*S*,3*R*,3a*S*,5*R*,7a*R*)-5-hydroxy-5-(1,3,3-trimethylcyclohexyl)octahydroisobenzofuran-1,3-diyl diacetate (5.22): To a solution of cyclohexenol lactone **5.20b** (281 mg, 1.01 mmol, 1.00 equiv) in absolute EtOH (20.0 mL) and under an atmosphere of N_2 was added $Pd(OH)_2$ on carbon (284 mg, 20 wt%, 2.02 mmol, 2.00 equiv). A H_2 balloon was attached to the flask and after three consecutive cycles of evacuation (under high vacuum) and H_2 purge, the mixture was stirred for 15 h. An aliquot was removed for ^{1}H-NMR analysis to ensure complete hydrogenation of the cyclohexene moiety. The reaction mixture was filtered through a pad of Celite, washed with EtOAc, concentrated *in vacuo*, and taken on directly to the next step without purification.

To a solution of the above crude lactone in anhydrous THF (9.00 mL) was added $LiAlH_4$ (2.00 M solution in THF, 0.60 mL, 1.20 mmol, 2.7 equiv) dropwise at 0 ºC. After stirring for 20 min, the ice bath was removed and the mixture was allowed to slowly warm to ambient temperature (23 ºC) over 40 min. Upon consumption of the starting material (as judged by TLC), the reaction mixture was cooled to 0 ºC and carefully quenched in sequence with 50 µL H_2O, 85 µL 15% aqueous NaOH, and 120 µL H_2O. The ice bath was removed and the mixture was allowed to slowly warm to ambient temperature (23 ºC). Subsequently, anhydrous $MgSO_4$ was added and the reaction mixture was vigorously stirred for 30 min, filtered through a pad of Celite and concentrated by rotary evaporation.

The crude diol was of sufficient purity (>95% as judged by ^{1}H-NMR) to be carried on directly to the next step.

To a solution of $(COCl)_2$ (0.19 mL, 2.20 mmol, 10.0 equiv) in CH_2Cl_2 (15.0 mL) was added anhydrous DMSO dropwise as a solution in CH_2Cl_2 (2.50 M, 4.40 mmol, 20.0 equiv) followed by a solution of the above crude diol in CH_2Cl_2 (5.00 mL) *via* syringe pump over 1 h at –78 ºC. To the reaction mixture was added Et_3N (0.92 mL, 6.60 mmol, 30.0 equiv) quickly along the wall of the flask and the reaction mixture was stirred at –78 ºC for 1 h, and then at ambient temperature (23 ºC) for 1 h. The mixture was quenched with 2 N HCl (10 mL) and the aqueous layer was extracted with CH_2Cl_2 (3 x 50 mL). The combined organic layer was washed with brine (10 mL), dried over $MgSO_4$, filtered, and concentrated under reduced pressure. The crude dialdehyde was taken on directly to the next step without purification.

To a solution of the above crude dialdehyde in AcOH/Ac_2O (1.5:1, 4.5/3.0 mL) was added NaOAc (180 mg, 2.20 mmol, 10.0 equiv) and concentrated H_2SO_4 (11.0 µL, 0.22 mmol, 1.00 equiv) successively at 0 ºC. The reaction mixture was stirred at ambient temperature (23 ºC) for 48 h, poured carefully into saturated aqueous $NaHCO_3$ solution (10 mL), and the aqueous layer was extracted with EtOAc (3 x 50 mL). The combined organic layer was washed with brine (20 mL), dried over $MgSO_4$, filtered, and concentrated under reduced pressure. Purification by automated flash chromatography (0→50% EtOAc/hexanes) afforded cyclohexanol diacetate **5.22** (142 mg, 37% yield over 4 steps) as an inseparable mixture of two diastereomers (1:1 *dr*, based on ^{1}H-NMR analysis of the crude mixture).

5.22: white solid; R_f = 0.10 (EtOAc/hexanes, 1:4 *v/v*); Data provided for the mixture of diastereomers: **^{1}H-NMR** (500 MHz, $CDCl_3$) δ 6.17 (d, *J* = 6.6 Hz, 1H), 5.94 (d, *J* = 2.1 Hz, 1H), 2.65 – 2.57 (m, 1H), 2.59 – 2.49 (m, 1H), 2.12 (s, 3H), 2.08 (s, 3H), 2.02 – 1.77 (m, 2H), 1.70 – 1.47 (m, 5H), 1.42 – 1.21 (m, 7H), 1.15 – 1.09 (m, 1H), 1.01 (s, 3H), 1.00 (s, 3H), 0.91 (s, 3H); **^{13}C-NMR** (125 MHz, $CDCl_3$) δ 170.93 (2), 170.12 (2), 103.25, 103.22, 100.82, 100.78, 75.73, 75.72, 43.38, 43.30, 41.50, 41.48, 40.91 (2), 39.15 (2), 38.92 (2), 36.16 (2), 30.79 (4), 30.16, 30.10, 28.88, 28.82, 27.82, 27.80, 25.45, 25.39, 21.45, 21.42, 20.51 (2), 18.98 (2), 18.54 (2); **IR (thin film)**: 3527, 2948, 2865, 1748 cm^{-1}; **HRMS (ESI–)** *m/z* calcd for $C_{21}H_{34}ClO_6$ $[M+Cl]^-$: 417.2044, found: 417.2062.

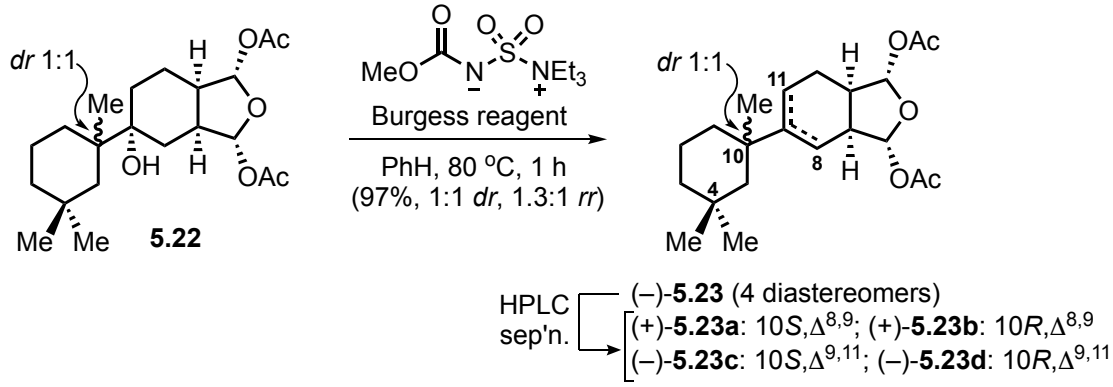

(1*S*,3*R*,3a*S*,7a*R*)-5-((*S*)-1,3,3-trimethylcyclohexyl)-1,3,3a,4,7,7a-hexahydroisobenzofuran-1,3-diyl diacetate ((+)-5.23a), (1*S*,3*R*,3a*S*,7a*R*)-5-((*R*)-1,3,3-trimethylcyclohexyl)-1,3,3a,4,7,7a-hexahydroisobenzofuran-1,3-diyl diacetate ((+)-5.23b), (1*R*,3*S*,3a*R*,7a*S*)-6-((*S*)-1,3,3-trimethylcyclohexyl)-1,3,3a,4,5,7a-hexahydroisobenzofuran-1,3-diyl diacetate ((–)-5.23c), and (1*R*,3*S*,3a*R*,7a*S*)-6-((*R*)-1,3,3-trimethyl-cyclohexyl)-1,3,3a,4,5,7a-hexahydroisobenzofuran-1,3-diyl diacetate ((–)-5.23d)): A glass tube was charged with cyclohexanol diacetate **5.22** (20.0 mg, 52.0 μmol, 1.00 equiv) and methyl *N*-

(triethylammoniosulfonyl)carbamate (Burgess reagent, 25 mg, 0.10 mmol, 2.00 equiv) in PhH (2.00 mL). The tube was sealed and placed in an 80 ºC oil bath for 1 h. The reaction mixture was cooled to ambient temperature (23 ºC) and concentrated under reduced pressure. Purification by automated flash chromatography (0→20% EtOAc/hexanes) afforded cyclohexenyl diacetates **5.23a-d** (18.0 mg, 97% yield) as a clear colorless oil and as an inseparable mixture of four diastereomers (1:1 *dr*, 1.3:1 *rr*, based on ^{1}H-NMR analysis of the crude mixture). $\mathbf{R}_f$ = 0.32 (EtOAc/hexanes, 1:4 *v/v*); **IR (thin film)**: 2924, 2864, 1750 cm^{-1}; **HRMS (ESI+)** *m/z* calcd for $C_{21}H_{32}NaO_5$ $[M+Na]^+$: 387.2147, found: 387.2151. This diastereomeric mixture was then subjected to a chiral HPLC purification using a Chiralcel OJ-H column: hexanes:^{i}PrOH = 96:04, flow rate 0.4 mL/min, λ = 210 nm: $t_{(–)\text{-}\mathbf{5.23a}}$ = 11.4–13.5 min, $t_{(–)\text{-}\mathbf{5.23b}}$ = 13.6–15.4 min, $t_{(–)\text{-}\mathbf{5.23c}}$ = 15.5–17.5 min, $t_{(–)\text{-}\mathbf{5.23d}}$ = 17.6–20.8 min.

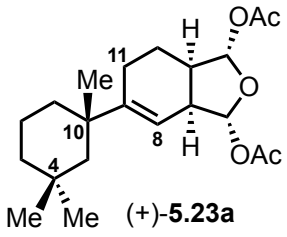

(+)-**5.23a**

(+)-**5.23a**: $[\alpha]_D^{24.1}$ = +24.80 (*c* = 0.98, $CHCl_3$); **^{1}H-NMR** (500 MHz, $CDCl_3$) δ 6.11 (d, *J* = 2.1 Hz, 1H), 6.03 (d, *J* = 3.0 Hz, 1H), 5.50 (d, *J* = 4.1 Hz, 1H), 2.96 – 2.92 (m, 1H), 2.52 (dddd, *J* = 9.4, 7.3, 4.5, 2.2 Hz, 1H), 2.11 (s, 3H), 2.09 (s, 3H), 1.98 – 1.88 (m, 2H), 1.81 – 1.70 (m, 1H), 1.67 – 1.56 (m, 3H), 1.49 – 1.38 (m, 1H), 1.33 – 1.23 (m, 2H), 1.18 – 1.08 (m, 2H), 1.06 – 0.99 (m, 1H), 0.91 (s, 3H), 0.86 (s, 3H), 0.81 (s, 3H); **^{13}C-NMR** (125 MHz, $CDCl_3$) δ 170.5, 170.3, 147.9, 114.4, 103.7, 103.1, 48.2, 44.1, 41.7, 40.4, 39.0, 36.3, 33.3, 31.6, 31.5, 26.7, 22.6, 21.8, 21.5, 21.5, 19.6; **IR (thin film)**:

2947, 2864, 1752 cm^{-1}; **HRMS (ESI+)** *m/z* calcd for $C_{21}H_{32}NaO_5$ $[M+Na]^+$: 387.2147, found: 387.2145.

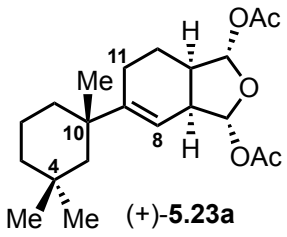

(+)-**5.23a**

(+)-**5.23b**: $[\alpha]_D^{24.4}$ = +27.30 (*c* = 1.10, $CHCl_3$); **^{1}H-NMR** (500 MHz, $CDCl_3$) δ 6.09 (d, *J* = 1.5 Hz, 1H), 6.00 (d, *J* = 3.6 Hz, 1H), 5.50 (d, *J* = 4.3 Hz, 1H), 3.01 – 2.94 (m, 1H), 2.47 (dddd, *J* = 9.7, 7.5, 4.6, 1.6 Hz, 1H), 2.11 (s, 3H), 2.09 (s, 3H), 2.00 – 1.90 (m, 2H), 1.86 – 1.80 (m, 1H), 1.66 – 1.52 (m, 2H), 1.48 – 1.36 (m, 2H), 1.33 – 1.23 (m, 2H), 1.19 – 1.08 (m, 2H), 1.04 – 0.98 (m, 1H), 0.91 (s, 3H), 0.86 (s, 3H), 0.81 (s, 3H); **^{13}C-NMR** (125 MHz, $CDCl_3$) δ 170.4, 170.2, 147.8, 114.1, 104.0, 103.1, 47.7, 43.4, 42.0, 40.3, 38.9, 36.1, 35.1, 33.2, 31.4, 26.8, 24.6, 23.0, 22.5, 21.4, 19.4; **IR (thin film)**: 2948, 2865, 1752 cm^{-1}; **HRMS (ESI+)** *m/z* calcd for $C_{21}H_{32}NaO_5$ $[M+Na]^+$: 387.2147, found: 387.2145.

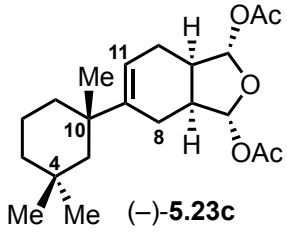

(–)-**5.23c**

(–)-**5.23c**: $[\alpha]_D^{24.4}$ = -3.46 (*c* = 1.04, $CHCl_3$);**^{1}H-NMR** (500 MHz, $CDCl_3$) δ 6.01 (d, *J* = 2.5 Hz, 1H), 5.97 (d, *J* = 2.7 Hz, 1H), 5.57 (t, *J* = 4.4 Hz, 1H), 2.65 – 2.53 (m, 2H), 2.36 – 2.22 (m, 2H), 2.10 (s, 3H), 2.09 (s, 3H), 2.07 – 1.95 (m, 2H), 1.93 – 1.87 (m, 1H), 1.63 – 1.53 (m, 2H), 1.48 – 1.38 (m, 1H), 1.31 – 1.23 (m, 1H), 1.18 – 1.10

(m, 2H), 1.03 (d, *J* = 14.0 Hz, 1H), 0.92 (s, 3H), 0.86 (s, 3H), 0.79 (s, 3H).; **^{13}C-NMR** (125 MHz, $CDCl_3$) δ 170.4, 170.3, 144.0, 116.8, 104.3, 104.1, 48.2, 42.1, 40.7, 40.4, 38.5, 36.2, 33.2, 31.4, 31.3, 27.1, 24.4, 23.7, 21.5 (2), 19.5; **IR (thin film)**: 2949, 2865, 1752 cm^{-1}; **HRMS (ESI+)** *m/z* calcd for $C_{21}H_{32}NaO_5$ $[M+Na]^+$: 387.2147, found: 387.2145.

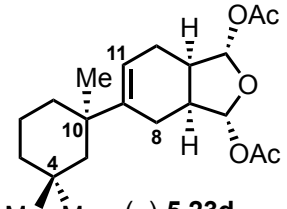

(–)-**5.23d**

(–)-**5.23d**: $[\alpha]_D^{24.7}$ = -10.71 (*c* = 0.93, $CHCl_3$); **^{1}H-NMR** (500 MHz, $CDCl_3$) δ 6.06 (d, *J* = 1.8 Hz, 1H), 6.01 (d, *J* = 3.1 Hz, 1H), 5.57 (dt, *J* = 5.5, 2.8 Hz, 1H), 2.50 (ddt, *J* = 10.2, 7.3, 3.1 Hz, 1H), 2.46 – 2.35 (m, 3H), 2.09 (s, 3H), 2.09 (s, 3H), 2.00 – 1.76 (m, 3H), 1.57 (d, *J* = 13.7 Hz, 1H), 1.49 – 1.38 (m, 1H), 1.31 – 1.22 (m, 2H), 1.14 (ddd, *J* = 13.8, 11.5, 3.6 Hz, 2H), 1.03 (d, *J* = 13.9 Hz, 1H), 0.91 (s, 3H), 0.86 (s, 3H), 0.78 (s, 3H); **^{13}C-NMR** (125 MHz, $CDCl_3$) δ 170.4, 170.3, 144.9, 116.9, 104.1, 103.7, 48.3, 43.2, 41.1, 40.3, 38.7, 36.1, 33.0, 31.4, 30.9, 27.2, 24.6, 24.5, 21.5, 21.5, 19.5; IR (thin film): 2949, 2864, 1753 cm^{-1}; **HRMS (ESI+)** *m/z* calcd for $C_{21}H_{32}NaO_5$ $[M+Na]^+$: 387.2147, found: 387.2144.

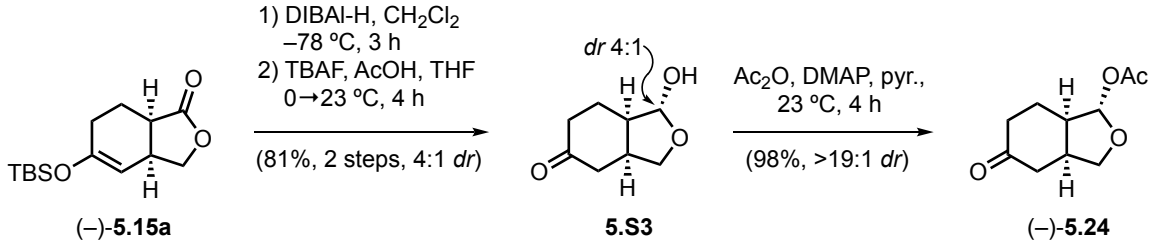

(–)-**5.15a** **5.S3** (–)-**5.24**

(1*S*,3a*S*,7a*R*)-5-oxooctahydroisobenzofuran-1-yl acetate ((–)-5.24): To a solution of lactone (–)-**5.15a** (72.0 mg, 0.27 mmol, 1.0 equiv) in CH_2Cl_2 (2.70 mL) was added DIBAl-

H (1.00 M solution in CH_2Cl_2, 321 μL, 0.32 mmol, 1.2 equiv) dropwise at –78 ºC. The reaction mixture was stirred at –78 ºC for 4 h and carefully quenched in sequence with 12 μL of H_2O, 12 μL of 20% aqueous NaOH, and 32 μL of H_2O. The dry-ice bath was removed and the mixture was allowed to slowly warm to ambient temperature (23 ºC). Subsequently, anhydrous $MgSO_4$ was added and the reaction mixture was vigorously stirred for 30 min, filtered through a pad of Celite and concentrated under reduced pressure. The crude silyl enol ether lactol was of sufficient purity (>95% as judged by ^{1}H-NMR) to be carried on directly to the next step.

To a pre-cooled solution (0 ºC) of the above crude silyl enol ether lactol and glacial AcOH (31.0 μL, 0.54 mmol, 2.00 equiv) in anhydrous THF (2.70 mL) was added TBAF (1.00 M in THF, 0.54 mL, 0.54 mmol, 2.00 equiv) dropwise. The reaction mixture was allowed to slowly warm to ambient temperature (23 ºC) over 4 h, and then concentrated under reduced pressure. Purification by automated flash chromatography (5→80% EtOAc/hexanes) afforded ketolactol **5.S3** (42.0 mg, 81% yield over 2 steps) as a mixture of two diastereomers (4:1 *dr*, based on ^{1}H-NMR analysis of the crude mixture).

5.S3: clear colorless oil; $\mathbf{R}_f$ = 0.23 (EtOAc/hexanes, 4:1 *v/v*); (NMR data is provided for the major diastereomer) **^{1}H-NMR** (500 MHz, C_6D_6) δ 5.08 (s, 1H), 3.94 (dd, *J* = 8.6, 7.4 Hz, 1H), 3.27 (dd, *J* = 8.6, 5.6 Hz, 1H), 2.40 (q, *J* = 7.0 Hz, 1H), 2.15 – 1.85 (m, 5H), 1.76 (ddd, *J* = 16.4, 11.2, 5.2 Hz, 1H), 1.50 – 1.38 (m, 1H), 1.36 – 1.23 (m, 1H); **^{13}C-NMR** (125 MHz, C_6D_6) δ 209.9, 103.4, 71.7, 44.1, 40.4, 37.8, 36.5, 23.8; **IR (thin film)**: 3383, 2924, 1710 cm^{-1}; **HRMS (ESI+)** *m/z* calcd for $C_8H_{12}LiO_3$ $[M+Li]^+$: 163.0941, found: 163.0949.

To a solution of ketolactol **5.S3** (20.0 mg, 0.12 mmol, 1.00 equiv) in anhydrous pyridine (1.00 mL) was added DMAP (2.00 mg, 12.0 μmol, 0.10 equiv) and Ac_2O (120

μL, 1.28 mmol, 10.0 equiv). The reaction mixture was stirred at ambient temperature (23 ºC) for 18 h, poured into saturated aqueous $NaHCO_3$ solution (10 mL), and the aqueous layer was extracted with CH_2Cl_2 (3 x 10 mL). The combined organic layer was washed with brine (10 mL), dried over $MgSO_4$, filtered, and concentrated under reduced pressure. Purification by automated flash chromatography (0→40% EtOAc/hexanes) afforded acetyl keto lactol (–)-**5.24** (24.0 mg, 98% yield) as a single diastereomer (>19:1 *dr*, based on ^{1}H-NMR analysis of the crude mixture).

(–)-**5.24**: clear colorless oil; $\mathbf{R}_f$ = 0.49 (EtOAc/hexanes, 4:1 *v/v*); $[\alpha]_D^{19.7}$ –21.08 (*c* = 0.13, $CHCl_3$); **^{1}H-NMR** (500 MHz, C_6D_6) δ 6.05 (s, 1H), 3.76 (dd, *J* = 8.9, 7.7 Hz, 1H), 3.23 (dd, *J* = 8.8, 5.8 Hz, 1H), 2.19 – 2.09 (m, 1H), 1.96 – 1.83 (m, 3H), 1.70 – 1.60 (m, 4H), 1.46 – 1.33 (m, 2H), 1.26 – 1.10 (m, 1H); **^{13}C-NMR** (125 MHz, C_6D_6) δ 208.1, 169.4, 103.4, 73.2, 43.3, 39.9, 37.6, 35.9, 23.4, 20.9; **IR (thin film)**: 2957, 2923, 2853, 1712 cm^{-1}; **HRMS (ESI+)** *m/z* calcd for $C_{10}H_{14}LiO_4$ $[M+Li]^+$: 205.1047, found: 205.1052.

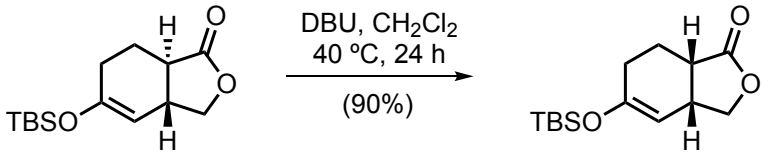

(+)-**5.15b** (+)-**5.15a**

(3a*R*,7a*S*)-5-((*tert*-butyldimethylsilyl)oxy)-3a,6,7,7a-tetrahydroisobenzofuran-1(3H)-one ((+)-5.15a): To a glass tube containing a solution of *trans*-fused bicyclic γ-lactone (+)-**5.15b** (202 mg, 0.75 mmol, 1.0 equiv) in CH_2Cl_2 (7.50 mL, 0.10 *M*) was added DBU (0.34 mL, 2.25 mmol, 3.00 equiv). The glass tube was sealed and placed in a 40 ºC oil bath for 24 h. The reaction mixture was cooled to ambient temperature (23 ºC), filtered through a short pad of SiO_2 and the filtrate was concentrated by rotary evaporation. Purification by

automated flash chromatography (5→50% EtOAc/hexanes) afforded *cis*-fused bicyclic γ-lactone (+)-**5.15a** (182 mg, 90% yield, 94% *ee*).

(+)-**5.15a**: white crystalline solid; $\mathbf{R}_f$ = 0.45 (EtOAc/hexanes, 1:4 *v/v*); $[\boldsymbol{\alpha}]_D^{19.9}$ +52.18 (*c* = 0.77, $CHCl_3$); Enantiomeric excess was determined by chiral HPLC analysis in comparison with authentic racemic material using a Chiralcel OD-H column: hexanes:^{i}PrOH = 95:05, flow rate 0.5 mL/min, λ = 210 nm: t_{minor} = 13.5 min, t_{major} = 15.0 min, 94% *ee* (Figure S1); All spectral data matched that reported for *cis*-fused bicyclic γ-lactone (–)-**5.15a**.

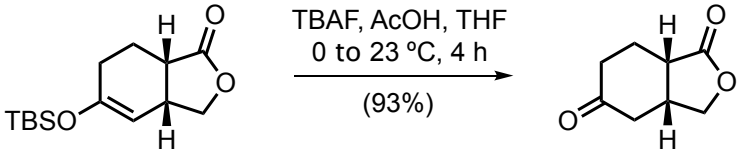

(+)-**5.15a** (+)-**5.9**

(3a*R*,7a*S*)-tetrahydroisobenzofuran-1,5(3*H*,4*H*)-dione ((+)-5.9): To a pre-cooled solution (0 ºC) of bicyclic γ-lactone (+)-**5.15a** (72.0 mg, 268 μmol, 1.00 equiv) and glacial AcOH (31.0 μL, 536 μmol, 2.0 equiv) in anhydrous THF (2.70 mL, 0.10 *M*) was added TBAF (1.00 *M* in THF, 0.54 mL, 536 μmol, 2.00 equiv) dropwise. The reaction mixture was allowed to slowly warm to ambient temperature (23 ºC) over 4 h, and then concentrated under reduced pressure. Purification by automated flash chromatography (5→80% EtOAc/hexanes) afforded ketolactone (+)-**5.9** (38 mg, 93% yield).

(+)-**5.9**: clear colorless oil; $\mathbf{R}_f$ = 0.23 (EtOAc/hexanes, 1:1 *v/v*); $[\boldsymbol{\alpha}]_D^{20.0}$ +24.35 (*c* = 0.11. $CHCl_3$); All spectral data matched that reported for ketolactone (–)-**5.9**.

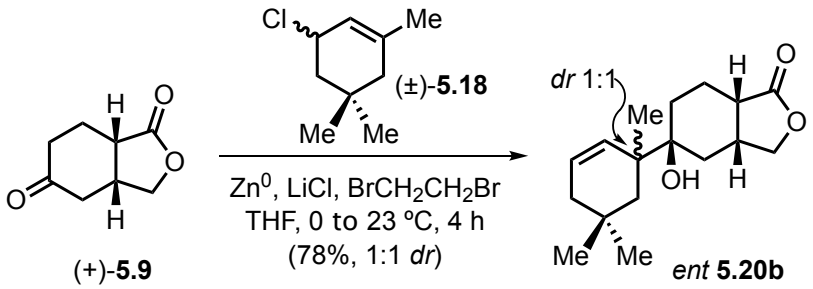

(3a*R*,5*S*,7a*S*)-5-hydroxy-5-(1,5,5-trimethylcyclohex-2-en-1-yl)hexahydroisobenzofuran-1(3*H*)-one (*ent* 5.20b): To an oven-dried round-bottomed flask was added zinc powder (766 mg, 11.6 mmol, 25.0 equiv) and LiCl (100 mg, 2.33 mmol, 5.00 equiv) with a large bore vacuum adapter with Teflon lined seal for addition of liquids *via* syringe. The flask and solids were then carefully flame-dried under high vacuum (using a vacuum/N_2 double manifold) by repeated heating and cooling cycles with swirling of the solids to avoid the solids from clumping. After the final cycle of heating, the solids were allowed to cool for 3 min under N_2, and then anhydrous THF (6.70 mL) was slowly and carefully added with vigorous stirring. After addition of THF, 1,2-dibromoethane (40.0 μL, 0.46 mmol, 1.00 equiv) was added which sometimes led to an exotherm simultaneous with rapid gas evolution, which needs to be controlled. Pressure fluctuations generated upon addition of 1,2-dibromoethane were controlled by momentarily switching the manifold from N_2 to vacuum. (Note: If gas evolution was not observed upon addition of 1,2-dibromoethane, a heat gun was employed to initiate gas evolution). The solution was allowed to cool at ambient temperature over ~5 min before being further cooled to 0 ºC. A solution of ketolactone (+)-**5.9** (71.0 mg, 0.46 mmol, 1.00 equiv) in THF (0.33 mL) was added dropwise by syringe followed by slow addition of allyl chloride (±)-**5.19** (740 mg, 4.60 mmol, 10.0 equiv) in THF (1.30 mL) *via* syringe pump at a rate of 1.0 mL/h. During this time, the reaction mixture was allowed slowly warm to ambient temperature (23 ºC). The

reaction mixture was then quenched with saturated NH_4Cl solution (30 mL). The organic phase was separated and the aqueous phase was further extracted with EtOAc (3 x 30 mL). The organic layers were combined, washed with brine (10 mL), dried with $MgSO_4$, and concentrated under reduced pressure. Purification by automated flash chromatography (5→60% EtOAc/hexanes) afforded dimethyl cyclohexenol lactone ***ent* 5.20b** (98 mg, 78% yield) as an inseparable mixture of two diastereomers (1:1 *dr*, based on ^{1}H-NMR analysis of the crude mixture).

***ent* 5.20b**: white crystalline solid; $\mathbf{R}_f$ = 0.44 (EtOAc/hexanes, 1:1 *v/v*); All spectral data matched that described for the enantiomeric dimethyl cyclohexenol lactone **5.20b** above.

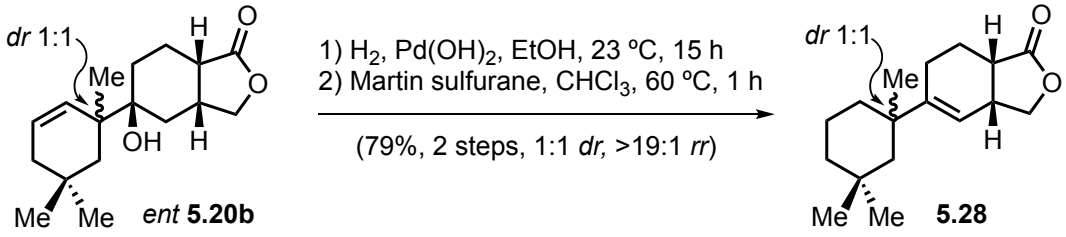

(3a*R*,7a*S*)-5-(1,3,3-trimethylcyclohexyl)-3a,6,7,7a-tetrahydroisobenzofuran-1(3*H*)-one (5.28): To a solution of dimethyl cyclohexenol lactone ***ent* 5.20b** (93.0 mg, 0.33 mmol, 1.00 equiv) in absolute EtOH (6.60 mL) and under an atmosphere of N_2 was added $Pd(OH)_2$ on carbon (94.0 mg, 20 wt%, 0.67 mmol, 2.00 equiv). A H_2 balloon was attached to the flask and after three consecutive cycles of evacuation (under high vacuum) and H_2 purge, the mixture was stirred for 15 h. An aliquot was removed for ^{1}H-NMR analysis to ensure complete hydrogenation of the cyclohexene moiety. The reaction mixture was filtered through a pad of Celite, washed with EtOAc, concentrated under reduced pressure, and taken on directly to the next step without purification.

A glass tube was charged with the above crude alcohol (89.0 mg, 0.33 mmol, 1.00 equiv) in anhydrous $CHCl_3$ (11.6 mL, 0.02 *M*) and Martin Sulfurane dehydrating agent (478 mg, 0.67 mmol, 2.00 equiv). The tube was sealed and placed in a 60 ºC oil bath for 1 h. The reaction mixture was cooled to ambient temperature (23 ºC), concentrated under reduced pressure and purified by automated flash chromatography (5→30% EtOAc/hexanes) to afford cyclohexene lactone **5.28** (69 mg, 79% yield over 2 steps) as a single regioisomer (>19:1 *rr*, based on ^{1}H-NMR analysis of the crude mixture).

5.28: clear colorless oil; $\mathbf{R}_f$ = 0.41 (EtOAc/hexanes, 1:4 *v/v*); (NMR data is provided for two diastereomers) **^{1}H-NMR** (500 MHz, $CDCl_3$) δ 5.40 (s, 2H), 4.43 – 4.33 (m, 2H), 4.08 – 3.96 (m, 2H), 3.15 – 3.02 (m, 2H), 2.82 – 2.69 (m, 2H), 2.16 – 1.85 (m, 9H), 1.80 – 1.49 (m, 7H), 1.47 – 1.38 (m, 2H), 1.31 – 1.23 (m, 2H), 1.20 – 1.05 (m, 4H), 0.91 (s, 3H), 0.88 (s, 3H), 0.86 (s, 3H), 0.82 (s, 3H), 0.79 (s, 3H), 0.77 (s, 3H); **^{13}C-NMR** (125 MHz, $CDCl_3$) δ 179.24, 179.22, 148.22, 148.03, 116.76, 116.67, 72.81, 72.79, 48.02, 47.72, 40.46, 40.37, 39.00, 38.95, 37.83, 37.82, 36.26, 36.23, 35.97, 35.93, 33.38, 33.18, 31.66, 31.64, 31.46, 31.39, 21.58, 21.57, 21.18, 20.98, 19.61, 19.46; **IR (thin film)**: 2932, 2860, 1769 cm^{-1}; **HRMS (ESI+)** *m/z* calcd for $C_{17}H_{26}LiO_2$ $[M+Li]^+$: 269.2093, found: 269.2107.

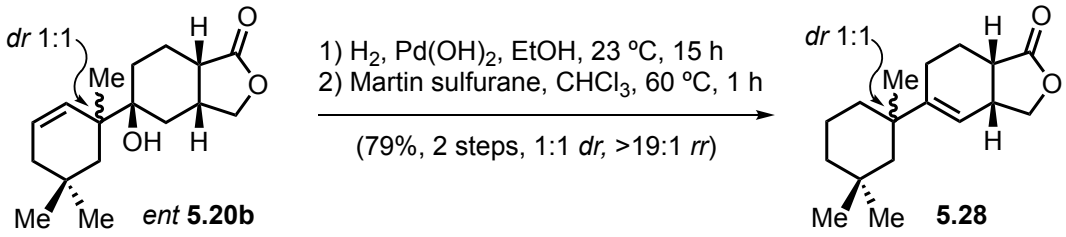

(3a*S*,7a*R*)-5-(1,3,3-trimethylcyclohexyl)-3a,6,7,7a-tetrahydroisobenzofuran-1(3*H*)-one (5.28): The title compound was prepared utilizing the same procedure as **(–)-5.26** (see

above) starting from ***ent* 5.20b**. All spectral data was in agreement with **(+)-5.28** disclosed above.

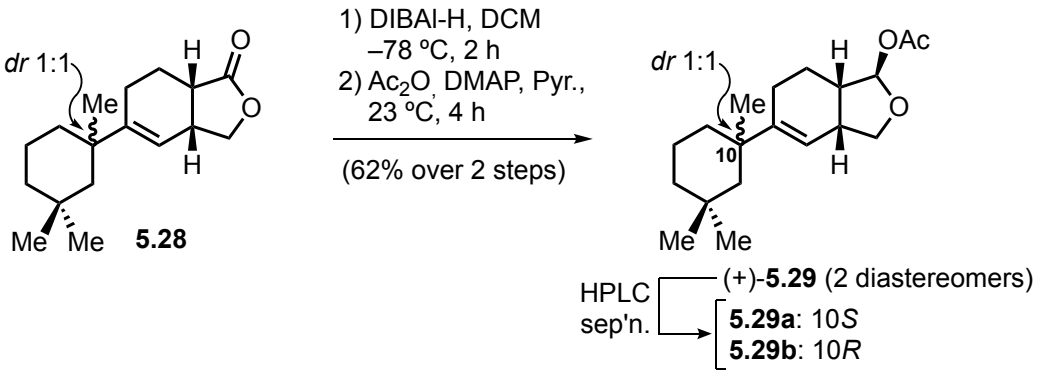

(1*R*,3a*R*,7a*S*)-5-(1,3,3-trimethylcyclohexyl)-1,3,3a,6,7,7a-hexahydroisobenzofuran-1-yl acetate ((+)-5.29): To a solution of cyclohexene lactone **5.28** (20.0 mg, 76.0 μmol, 1.00 equiv) in CH_2Cl_2 (1.30 mL, 0.06 *M*) was added DIBAl-H (1.00 *M* solution in CH_2Cl_2, 92 μL, 92.0 μmol, 1.20 equiv) dropwise at –78 ºC. The reaction mixture was stirred at –78 ºC for 4 h and carefully quenched in sequence with 92 μL MeOH and saturated aqueous Rochelle's salt (2.60 mL). The dry-ice bath was removed and the mixture was allowed to slowly warm to ambient temperature (23 ºC). Subsequently, the reaction mixture was filtered through a pad of Celite, extracted with CH_2Cl_2 (3 x 10 mL), washed with brine (10 mL), and concentrated under reduced pressure. The crude lactol was of sufficient purity (>95% as judged by ^{1}H-NMR) to be carried on directly to the next step.

To a solution of the above crude lactol in anhydrous pyridine (0.8 mL) was added DMAP (2.00 mg, 15.0 μmol, 0.20 equiv) and Ac_2O (36.0 μL, 0.38 mmol, 5.00 equiv). The reaction mixture was stirred at ambient temperature (23 ºC) for 14 h, poured into saturated aqueous $NaHCO_3$ solution (10 mL), and the aqueous layer was extracted with CH_2Cl_2 (3 x 10 mL). The combined organic layer was washed with brine (10 mL), dried over $MgSO_4$,

filtered, and concentrated under reduced pressure. Purification by automated flash chromatography (0→30% EtOAc/hexanes) afforded acetyl lactol (+)-**5.29** (14.0 mg, 62% yield over 2 steps) as a clear colorless oil and as a 1:1 mixture of diastereomers (based on ^{1}H-NMR analysis of the crude mixture). $\mathbf{R_f}$ = 0.51 (EtOAc/hexanes, 1:4 *v/v*); $[\boldsymbol{\alpha}]_D^{20.3}$ +50.91 (*c* = 0.11, $CHCl_3$); **IR (thin film)**: 2939, 2861, 1744 cm^{-1}; **HRMS (ESI+)** *m/z* calcd for $C_{19}H_{30}LiO_3$ $[M+Li]^+$: 313.2355, found: 313.2367. The diastereomeric mixture was further separated by semi-preparative reverse-phase HPLC (100 x 21.20 mm, 5 µm; linear gradient, 65% CH_3CN/H_2O, 23 mL/min) to yield **5.29a** (T_R = 20.40 min) and **5.29b** (T_R = 22.18 min).

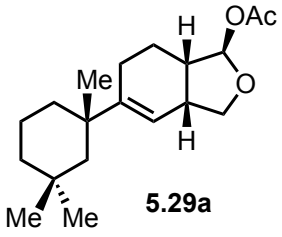

5.29a

5.29a: **^{1}H-NMR** (500 MHz, $CDCl_3$) δ 6.03 (s, 1H), 5.46 (dd, *J* = 4.6, 1.9 Hz, 1H), 4.27 (t, *J* = 8.2 Hz, 1H), 3.70 (t, *J* = 7.6 Hz, 1H), 2.96 (q, *J* = 7.3 Hz, 1H), 2.35 – 2.27 (m, 1H), 2.19 – 2.12 (m, 1H), 2.06 (s, 3H), 1.99 – 1.90 (m, 1H), 1.80 (dt, *J* = 12.9, 4.7 Hz, 1H), 1.73 – 1.67 (m, 1H), 1.66 – 1.24 (m, 5H), 1.21 – 1.07 (m, 1H), 1.03 (d, *J* = 14.0 Hz, 1H), 0.92 (s, 3H), 0.87 (s, 3H), 0.82 (s, 3H); **^{13}C-NMR** (125 MHz, $CDCl_3$) δ 170.5, 145.4, 117.4, 103.6, 74.6, 47.8, 40.2, 38.8, 37.6, 36.0, 35.7, 33.1, 31.4, 31.2, 26.8, 26.0, 21.3, 20.9, 19.4.

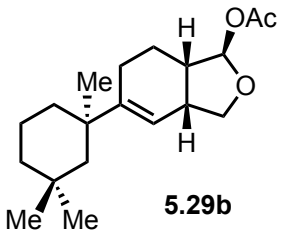

5.29b

5.29b: **^{1}H-NMR** (500 MHz, $CDCl_3$) δ 6.01 (s, 1H), 5.43 (dd, *J* = 4.5, 2.0 Hz, 1H), 4.26 (t, *J* = 8.3 Hz, 1H), 3.61 (t, *J* = 7.9 Hz, 1H), 2.98 (dt, *J* = 13.4, 7.3 Hz, 1H), 2.26 (td, *J* = 7.4, 3.7 Hz, 1H), 2.09 (dt, *J* = 16.9, 4.5 Hz, 1H), 2.05 (s, 3H), 2.01 – 1.79 (m, 2H), 1.67 – 1.52 (m, 2H), 1.46 – 1.23 (m, 4H), 1.18 – 1.06 (m, 2H), 0.99 (d, *J* = 13.9 Hz, 1H), 0.91 (s, 3H), 0.86 (s, 3H), 0.84 (s, 3H); **^{13}C-NMR** (125 MHz, $CDCl_3$) δ 170.5, 145.4, 117.4, 103.8, 74.7, 4.5, 40.1, 38.7, 37.6, 36.0, 35.7, 32.9, 31.4, 31.1, 26.8, 26.0, 21.3, 20.7, 19.2.

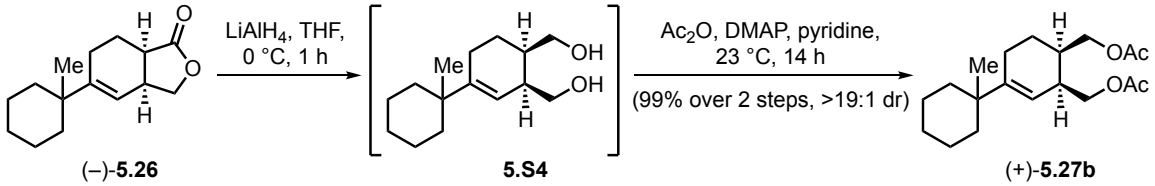

(–)-**5.26** **5.S4** (+)-**5.27b**

((3*S*,4*R*)-1'-methyl-[1,1'-bi(cyclohexan)]-1-ene-3,4-diyl)bis(methylene) diacetate ((–)-5.27b): To a solution of the cyclohexene lactone (–)-**5.26** (27.0 mg, 0.12 mmol, 1.00 equiv) in anhydrous THF (1.50 mL, 0.08 M) was added $LiAlH_4$ (2.00 M solution in THF, 0.15 mL, 0.30 mmol, 2.50 equiv) dropwise at 0 ºC. After stirring for 1 h, the ice bath was removed and the mixture was allowed to warm slowly to ambient temperature (23 ºC) over 30 min. Upon consumption of starting material (as judged by TLC), the reaction mixture was cooled to 0 ºC and carefully quenched in sequence with 12 µL H_2O, 12 µL 25% aqueous NaOH, and 30 µL H_2O. The ice bath was removed and the mixture was allowed to warm slowly to ambient temperature (23 ºC). Subsequently, anhydrous $MgSO_4$ was added and the reaction mixture was vigorously stirred for 30 min, filtered through a pad of

Celite and concentrated by rotary evaporation. The crude diol **5.S4** was of sufficient purity (>95% as judged by ^{1}H-NMR) to be carried on directly to the next step.

To a solution of the above crude diol in anhydrous pyridine (1.00 mL, 0.10 M) was added DMAP (2.00 mg, 12.0 μmol, 0.10 equiv) and Ac_2O (120 μL, 1.28 mmol, 10.0 equiv). The reaction mixture was stirred at ambient temperature (23 ºC) for 14 h, poured into saturated aqueous $NaHCO_3$ solution (10 mL), and the aqueous layer was extracted with CH_2Cl_2 (3 x 10 mL). The combined organic layer was washed with brine (10 mL), dried over $MgSO_4$, filtered, and concentrated under reduced pressure. Purification by automated flash chromatography (0→30% EtOAc/hexanes) afforded cyclohexene diacetate (+)-**5.27b** (37.0 mg, 99% yield over 2 steps) as a single diastereomer (>19:1 *dr*, based on ^{1}H-NMR analysis of the crude mixture). (+)-**5.27b**: clear colorless oil; R_f = 0.53 (EtOAc/hexanes, 1:4 *v/v*); $[\boldsymbol{\alpha}]_D^{18.5}$ +31.52 (*c* = 0.33, $CHCl_3$); **^{1}H-NMR** (500 MHz, $CDCl_3$) δ 5.34 (dt, J = 4.0, 1.6 Hz, 1H), 4.13 – 3.96 (m, 4H), 2.70 – 2.61 (m, 1H), 2.17 – 2.08 (m, 1H), 2.05 (s, 3H), 2.03 (s, 3H), 2.00 – 1.92 (m, 1H), 1.70 – 1.62 (m, 4H), 1.63 – 1.52 (m, 1H), 1.49 – 1.38 (m, 3H), 1.38 – 1.29 (m, 3H), 1.28 – 1.18 (m, 2H), 0.92 (s, 3H); **^{13}C-NMR** (125 MHz, $CDCl_3$) δ 171.3, 171.2, 146.0, 118.6, 65.5, 65.1, 38.7, 36.6, 36.4, 36.3, 34.6, 26.5, 23.3, 23.0, 22.7, 21.1, 21.1; **IR (thin film)**: 2930, 2856, 1742 cm^{-1}; **HRMS (ESI+)** *m/z* calcd for $C_{19}H_{31}O_4$ $[M+H]^+$: 323.2222, found: 323.2232.

123. Abbasov, M. E.; Hudson, B. M.; Tantillo, D. J.; Romo, D., Stereodivergent, Diels–Alder-initiated organocascades employing α,β-unsaturated acylammonium salts: scope, mechanism, and application. *Chem. Sci.* **2017,** *8* (2), 1511-1524.

194. Newhouse, T.; Baran, P. S.; Hoffmann, R. W., The economies of synthesis. *Chem. Soc. Rev.* **2009,** *38* (11), 3010-3021.

200. Li, J.; Kim, Sang G.; Blenis, J., Rapamycin: One Drug, Many Effects. *Cell Metabolism* **2014,** *19* (3), 373-379.

201. Trauner, D., Finding function and form. *Nat. Prod. Rep.* **2014,** *31* (4), 411-413.

202. Wilson, R. M.; Danishefsky, S. J., Small Molecule Natural Products in the Discovery of Therapeutic Agents: The Synthesis Connection. *J. Org. Chem.* **2006,** *71* (22), 8329-8351.

203. Wender, P. A., Toward the ideal synthesis and molecular function through synthesis-informed design. *Nat. Prod. Rep.* **2014,** *31* (4), 433-440.

204. Schreiber, S. L., Target-Oriented and Diversity-Oriented Organic Synthesis in Drug Discovery. *Science* **2000,** *287* (5460), 1964.

205. van Hattum, H.; Waldmann, H., Biology-Oriented Synthesis: Harnessing the Power of Evolution. *J. Am. Chem. Soc.* **2014,** *136* (34), 11853-11859.

206. Seiple, I. B.; Zhang, Z.; Jakubec, P.; Langlois-Mercier, A.; Wright, P. M.; Hog, D. T.; Yabu, K.; Allu, S. R.; Fukuzaki, T.; Carlsen, P. N.; Kitamura, Y.; Zhou, X.; Condakes, M. L.; Szczypiński, F. T.; Green, W. D.; Myers, A. G., A platform for the discovery of new macrolide antibiotics. *Nature* **2016,** *533* (7603), 338-345.

207. Könst, Z. A.; Szklarski, A. R.; Pellegrino, S.; Michalak, S. E.; Meyer, M.; Zanette, C.; Cencic, R.; Nam, S.; Voora, V. K.; Horne, D. A.; Pelletier, J.; Mobley, D. L.; Yusupova, G.; Yusupov, M.; Vanderwal, C. D., Synthesis facilitates an understanding of the structural basis for translation inhibition by the lissoclimides. *Nat. Chem.* **2017,** *9* (11), 1140-1149.

208. Bathula, S. R.; Akondi, S. M.; Mainkar, P. S.; Chandrasekhar, S., "Pruning of biomolecules and natural products (PBNP)": an innovative paradigm in drug discovery. *Organic & Biomolecular Chemistry* **2015,** *13* (23), 6432-6448.

209. Yu, M. J.; Zheng, W.; Seletsky, B. M., From micrograms to grams: scale-up synthesis of eribulin mesylate. *Nat. Prod. Rep.* **2013,** *30* (9), 1158-1164.

210. Crane, E. A.; Gademann, K., Capturing Biological Activity in Natural Product Fragments by Chemical Synthesis. *Angew. Chem. Int. Ed.* **2016,** *55* (12), 3882-3902.

211. Romo, D.; Choi, N. S.; Li, S.; Buchler, I.; Shi, Z.; Liu, J. O., Evidence for Separate Binding and Scaffolding Domains in the Immunosuppressive and Antitumor Marine Natural Product, Pateamine A: Design, Synthesis, and Activity Studies Leading to a Potent Simplified Derivative. *J. Am. Chem. Soc.* **2004,** *126* (34), 10582-10588.

212. Trost, B. M., The atom economy--a search for synthetic efficiency. *Science* **1991,** *254* (5037), 1471.

213. Young, I. S.; Baran, P. S., Protecting-group-free synthesis as an opportunity for invention. *Nat. Chem.* **2009,** *1* (3), 193-205.

214. Corey, E. J.; Chen, X. M., *The Logic of Chemical Synthesis*. Wiley Interscience: New York, NY, 1995.

215. Czakó, B.; Kürti, L.; Mammoto, A.; Ingber, D. E.; Corey, E. J., Discovery of Potent and Practical Antiangiogenic Agents Inspired by Cortistatin A. *J. Am. Chem. Soc.* **2009,** *131* (25), 9014-9019.

216. Mayol, L.; Piccialli, V.; Sica, D., Gracilin A, an unique: nor-diterpene metabolite from the marine sponge spongionella gracilis. *Tetrahedron Lett.* **1985,** *26* (10), 1357-1360.

217. Sánchez, J. A.; Alfonso, A.; Leirós, M.; Alonso, E.; Rateb, M. E.; Jaspars, M.; Houssen, W. E.; Ebel, R.; Tabudravu, J.; Botana, L. M., Identification of Spongionella compounds as cyclosporine A mimics. *Pharmacol. Res.* **2016,** *107*, 407-414.

218. Leirós, M.; Alonso, E.; Rateb, M. E.; Houssen, W. E.; Ebel, R.; Jaspars, M.; Alfonso, A.; Botana, L. M., Gracilins: Spongionella-derived promising compounds for Alzheimer disease. *Neuropharmacology* **2015,** *93*, 285-293.

219. Corey, E. J.; Letavic, M. A., Enantioselective Total Synthesis of Gracilins B and C Using Catalytic Asymmetric Diels-Alder Methodology. *J. Am. Chem. Soc.* **1995,** *117* (37), 9616-9617.

220. Rateb, M. E.; Houssen, W. E.; Schumacher, M.; Harrison, W. T. A.; Diederich, M.; Ebel, R.; Jaspars, M., Bioactive diterpene derivatives from the marine sponge Spongionella sp. *J. Nat. Prod.* **2009,** *72* (8), 1471-1476.

221. Ana, R.; Alejandro, L.; Rogelio, F.; Carlos, C.; Luis, F. G.-F.; Fernando, R.; Carmen, C., Gracilins G-I, Cytotoxic Bisnorditerpenes from Spongionella pulchella, and the Anti-Adhesive Properties of Gracilin B. *Letters in Drug Design & Discovery* **2006,** *3* (10), 753-760.

222. Puliti, R.; Fontana, A.; Cimino, G.; Mattia, C. A.; Mazzarella, L., Structure of a keto derivative of 9,11-dihydrogracilin A. *Acta Crystallographica Section C* **1993,** *49* (7), 1373-1376.

223. Potts, B. C. M.; Faulkner, D. J.; Jacobs, R. S., Phospholipase A2 Inhibitors from Marine Organisms. *J. Nat. Prod.* **1992,** *55* (12), 1701-1717.

224. Leirós, M.; Alonso, E.; Sanchez, J. A.; Rateb, M. E.; Ebel, R.; Houssen, W. E.; Jaspars, M.; Alfonso, A.; Botana, L. M., Mitigation of ROS Insults by Streptomyces Secondary Metabolites in Primary Cortical Neurons. *ACS Chemical Neuroscience* **2014,** *5* (1), 71-80.

225. Leirós, M.; Sánchez, J. A.; Alonso, E.; Rateb, M. E.; Houssen, W. E.; Ebel, R.; Jaspars, M.; Alfonso, A.; Botana, L. M., Spongionella Secondary Metabolites Protect Mitochondrial Function in Cortical Neurons against Oxidative Stress. *Mar. Drugs* **2014,** *12* (2).

226. Kofron, J. L.; Kuzmic, P.; Kishore, V.; Colon-Bonilla, E.; Rich, D. H., Determination of kinetic constants for peptidyl prolyl cis-trans isomerases by an improved spectrophotometric assay. *Biochemistry* **1991,** *30* (25), 6127-6134.

227. Walsh, C. T.; Zydowsky, L. D.; McKeon, F. D., Cyclosporin A, the cyclophilin class of peptidylprolyl isomerases, and blockade of T cell signal transduction. *J. Biol. Chem.* **1992,** *267* (19), 13115-8.

228. Ferreira, P. A.; Orry, A., From Drosophila to Humans: Reflections on the Roles of the Prolyl Isomerases and Chaperones, Cyclophilins, in Cell Function and Disease. *J. Neurogenet.* **2012,** *26* (2), 132-143.

229. Lee, J.; Kim, S. S., An Overview of Cyclophilins in Human Cancers. *J. Int. Med. Res.* **2010,** *38* (5), 1561-1574.

230. Hogan, P. G.; Chen, L.; Nardone, J.; Rao, A., Transcriptional regulation by calcium, calcineurin, and NFAT. *Genes Dev.* **2003,** *17* (18), 2205-2232.

231. Nigro, P.; Pompilio, G.; Capogrossi, M. C., Cyclophilin A: a key player for human disease. *Cell Death & Disease* **2013,** *4* (10), e888-e888.

232. Picone, P.; Nuzzo, D.; Caruana, L.; Scafidi, V.; Di Carlo, M., Mitochondrial Dysfunction: Different Routes to Alzheimer's Disease Therapy. *Oxidative Medicine and Cellular Longevity* **2014,** *2014*, 780179.

233. Schnermann, M. J.; Beaudry, C. M.; Egorova, A. V.; Polishchuk, R. S.; Sütterlin, C.; Overman, L. E., Golgi-modifying properties of macfarlandin E and the synthesis and evaluation of its 2,7-dioxabicyclo[3.2.1]octan-3-one core. *Proceedings of the National Academy of Sciences* **2010,** *107* (14), 6158.

234. Kornienko, A.; La Clair, J. J., Covalent modification of biological targets with natural products through Paal–Knorr pyrrole formation. *Nat. Prod. Rep.* **2017,** *34* (9), 1051-1060.

235. Nirmal, N.; Praba, G. O.; Velmurugan, D., Modeling studies on phospholipase A2-inhibitor complexes. *Indian J. Biochem. Biophys.* **2008,** *45* (4), 256-62.

236. Baker, B. J.; Kopitzke, R. W.; Yoshida, W. Y.; McClintock, J. B., Chemical and Ecological Studies of the Antarctic Sponge Dendrilla membranosa. *J. Nat. Prod.* **1995,** *58* (9), 1459-1462.

237. Buckleton, J. S.; Bergquist, P. R.; Cambie, R. C.; Clark, G. R.; Karuso, P.; Rickard, C. E. F., Structure of tetrahydroaplysulphurin-1. *Acta Crystallographica Section C* **1987,** *43* (12), 2430-2432.

238. Harvey, N. L.; Krysiak, J.; Chamni, S.; Cho, S. W.; Sieber, S. A.; Romo, D., Synthesis of (±)-Spongiolactone Enabling Discovery of a More Potent Derivative. *Chemistry – A European Journal* **2015,** *21* (4), 1425-1428.

239. Burgess, E. M.; Penton, H. R.; Taylor, E. A., Synthetic applications of N-carboalkoxysulfamate esters. *J. Am. Chem. Soc.* **1970,** *92* (17), 5224-5226.

240. Alfonso, A.; Pazos, M.-J.; Fernández-Araujo, A.; Tobio, A.; Alfonso, C.; Vieytes, M. R.; Botana, L. M., Surface Plasmon Resonance Biosensor Method for Palytoxin Detection Based on Na+,K+-ATPase Affinity. *Toxins* **2014,** *6* (1), 96-107.

241. Sánchez, J. A.; Alfonso, A.; Leirós, M.; Alonso, E.; Rateb, M. E.; Jaspars, M.; Houssen, W. E.; Ebel, R.; Botana, L. M., Spongionella Secondary Metabolites Regulate Store Operated Calcium Entry Modulating Mitochondrial Functioning in SH-SY5Y Neuroblastoma Cells. *Cell. Physiol. Biochem.* **2015,** *37* (2), 779-792.

242. Damsker, J. M.; Bukrinsky, M. I.; Constant, S. L., Preferential chemotaxis of activated human CD4+ T cells by extracellular cyclophilin A. *J. Leukocyte Biol.* **2007,** *82* (3), 613-618.

243. Moreira, P. I.; Zhu, X.; Wang, X.; Lee, H.-g.; Nunomura, A.; Petersen, R. B.; Perry, G.; Smith, M. A., Mitochondria: A therapeutic target in neurodegeneration. *Biochimica et Biophysica Acta (BBA) - Molecular Basis of Disease* **2010,** *1802* (1), 212-220.

244. Azzolin, L.; Antolini, N.; Calderan, A.; Ruzza, P.; Sciacovelli, M.; Marin, O.; Mammi, S.; Bernardi, P.; Rasola, A., Antamanide, a Derivative of Amanita phalloides, Is a Novel Inhibitor of the Mitochondrial Permeability Transition Pore. *PLOS ONE* **2011,** *6* (1), e16280.

245. Guo, H.-x.; Wang, F.; Yu, K.-q.; Chen, J.; Bai, D.-l.; Chen, K.-x.; Shen, X.; Jiang, H.-l., Novel cyclophilin D inhibitors derived from quinoxaline exhibit highly inhibitory activity against rat mitochondrial swelling and Ca2+ uptake/release. *Acta Pharmacologica Sinica* **2005,** *26* (10), 1201-1211.

246. Rao, V. K.; Carlson, E. A.; Yan, S. S., Mitochondrial permeability transition pore is a potential drug target for neurodegeneration. *Biochimica et Biophysica Acta (BBA) - Molecular Basis of Disease* **2014,** *1842* (8), 1267-1272.

247. Dawar, F. U.; Tu, J.; Khattak, M. N.; Mei, J.; Lin, L., Cyclophilin A: A Key Factor in Virus Replication and Potential Target for Anti-viral Therapy. *Curr. Issues Mol. Biol.* **2017,** *21*, 1-20.

248. Satoh, K., Cyclophilin A in Cardiovascular Homeostasis and Diseases. *The Tohoku Journal of Experimental Medicine* **2015,** *235* (1), 1-15.

APPENDICES

APPENDIX A

Chapter 2, 3 and 4 X-ray Crystal Structures and NMR Spectra

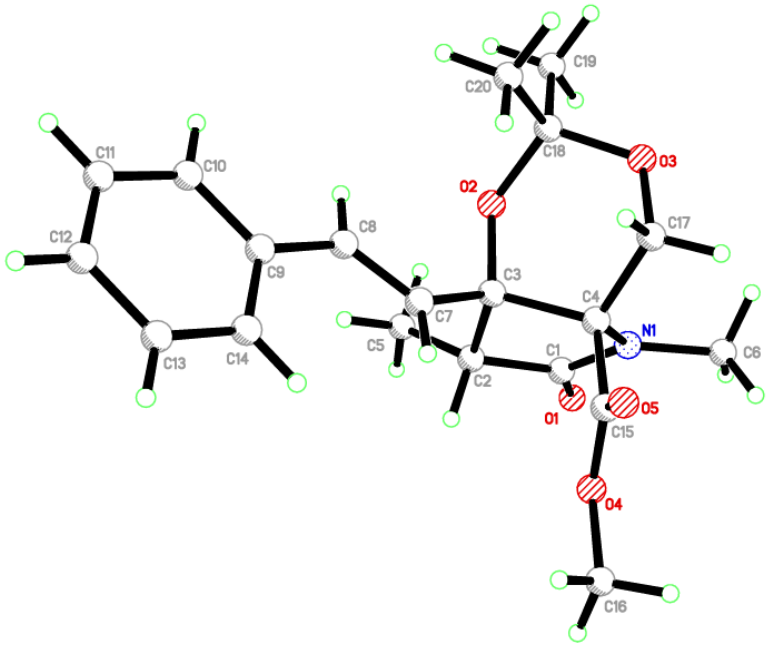

Figure A.1. Single crystal X-ray structure of compound **3.11** (ORTEP, 50% probability ellipsoid). Crystals were grown from CH_2Cl_2/hexanes by vapor diffusion. X-ray crystal data has been deposited in The Cambridge Crystallographic Data Centre database (https://www.ccdc.cam.ac.uk) under accession code CCDC 2034835.

Identification code	dr25 M	
Empirical formula	C20 H23 N O5	
Formula weight	357.39	
Temperature	150(2) K	
Wavelength	0.71073 Å	
Crystal system	Monoclinic	
Space group	$P2_1$	
Unit cell dimensions	a = 8.6616(9) Å	α= 90°.
	b = 9.8407(10) Å	β= 94.240(4)°.
	c = 11.7028(13) Å	γ = 90°.
Volume	994.77(18) $Å^3$	
Z	2	
Density (calculated)	1.193 Mg/m^3	
Absorption coefficient	0.086 mm^{-1}	
F(000)	380	
Crystal size	0.260 x 0.256 x 0.098 mm^3	
Theta range for data collection	2.358 to 26.420°.	
Index ranges	-10<=h<=10, -12<=k<=12, -14<=l<=14	
Reflections collected	19876	
Independent reflections	4052 [R(int) = 0.0708]	
Completeness to theta = 25.242°	99.9 %	
Absorption correction	Semi-empirical from equivalents	
Max. and min. transmission	0.803 and 0.792	
Refinement method	Full-matrix least-squares on F^2	
Data / restraints / parameters	4052 / 1 / 240	
Goodness-of-fit on F^2	1.070	
Final R indices [I>2sigma(I)]	R1 = 0.0432, wR2 = 0.0897	
R indices (all data)	R1 = 0.0632, wR2 = 0.0970	
Absolute structure parameter	0.9(6)	
Extinction coefficient	n/a	
Largest diff. peak and hole	0.185 and -0.189 $e.Å^{-3}$	

(x 10^4) and equivalent isotropic displacement parameters ($Å^2$x 10^3)

for dr25. U(eq) is defined as one third of the trace of the orthogonalized U^{ij} tensor.

	x	y	z	U(eq)
O(1)	6391(2)	2863(2)	6260(2)	34(1)
O(2)	2067(2)	3716(2)	6828(2)	25(1)
O(3)	1742(2)	5329(2)	5360(2)	31(1)
O(4)	6238(2)	6263(2)	7807(2)	47(1)
O(5)	4294(3)	7750(3)	7690(3)	55(1)
N(1)	4940(2)	4795(2)	6082(2)	25(1)
C(1)	5429(3)	3634(3)	6601(3)	26(1)
C(2)	4593(3)	3465(3)	7691(3)	27(1)
C(3)	3216(3)	4461(3)	7510(2)	24(1)
C(4)	3905(3)	5590(3)	6753(2)	26(1)
C(5)	4177(4)	2000(3)	7933(3)	36(1)
C(6)	5560(3)	5311(3)	5048(3)	36(1)
C(7)	2646(3)	4933(3)	8629(3)	27(1)
C(8)	1448(3)	4395(3)	9109(3)	28(1)
C(9)	868(3)	4760(3)	10218(3)	26(1)
C(10)	-477(3)	4167(4)	10545(3)	35(1)
C(11)	-1047(4)	4463(4)	11601(3)	42(1)
C(12)	-262(4)	5347(4)	12335(3)	39(1)
C(13)	1074(4)	5943(4)	12030(3)	38(1)
C(14)	1633(3)	5660(3)	10977(3)	32(1)
C(15)	4815(3)	6667(3)	7462(3)	31(1)
C(16)	7198(4)	7233(4)	8475(4)	59(1)
C(17)	2633(3)	6297(3)	6013(3)	30(1)
C(18)	961(3)	4400(3)	6043(3)	30(1)
C(19)	352(4)	3301(4)	5238(3)	41(1)
C(20)	-326(3)	5085(4)	6645(3)	37(1)

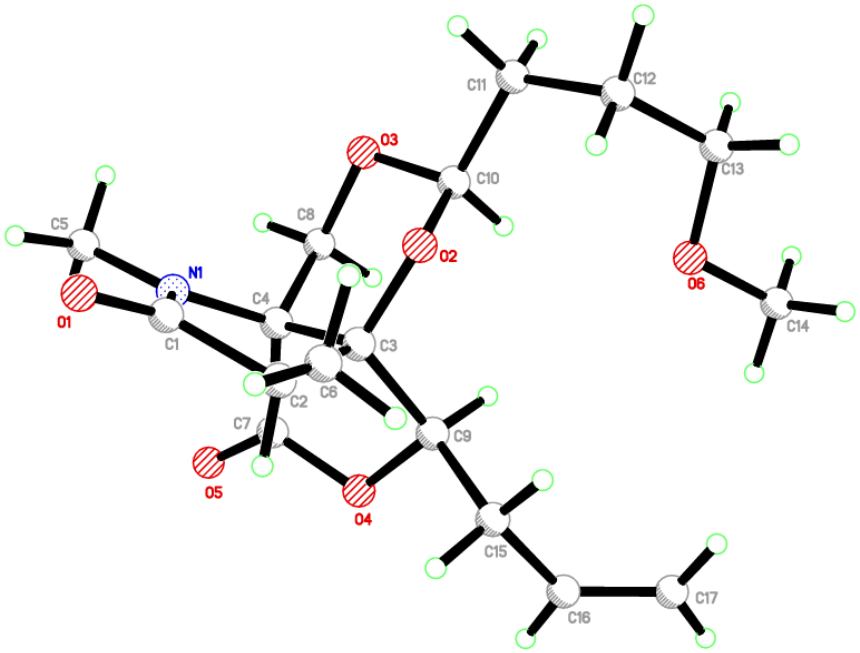

Figure A.2. Single crystal X-ray structure of compound **3.17** (ORTEP, 50% probability ellipsoid). Crystals were grown from CH_2Cl_2/hexanes by vapor diffusion. X-ray crystal data has been deposited in The Cambridge Crystallographic Data Centre database (https://www.ccdc.cam.ac.uk) under accession code CCDC 2034834

_____ Identification code	DR26	
Empirical formula	C17 H25 N O6	
Formula weight	339.38	
Temperature	150(2) K	
Wavelength	0.71073 Å	
Crystal system	Monoclinic	
Space group	$P2_1$	
Unit cell dimensions	a = 9.5426(8) Å	α= 90°.
	b = 7.5626(5) Å	β= 110.048(2)°.
	c = 12.5591(10) Å	γ = 90°.
Volume	851.43(11) $Å^3$	
Z	2	
Density (calculated)	1.324 Mg/m^3	
Absorption coefficient	0.100 mm^{-1}	
F(000)	364	
Crystal size	0.404 x 0.350 x 0.276 mm^3	
Theta range for data collection	2.335 to 28.339°.	
Index ranges	-12<=h<=12, -10<=k<=10, -16<=l<=16	
Reflections collected	19640	
Independent reflections	4231 [R(int) = 0.0262]	
Completeness to theta = 25.242°	99.9 %	
Absorption correction	Semi-empirical from equivalents	
Max. and min. transmission	0.948 and 0.936	
Refinement method	Full-matrix least-squares on F^2	
Data / restraints / parameters	4231 / 1 / 220	
Goodness-of-fit on F^2	1.450	
Final R indices [I>2sigma(I)]	R1 = 0.0312, wR2 = 0.0859	
R indices (all data)	R1 = 0.0323, wR2 = 0.0866	
Absolute structure parameter	-0.01(16)	
Extinction coefficient	n/a	
Largest diff. peak and hole	0.209 and -0.188 $e.Å^{-3}$	

(x 10^4) and equivalent isotropic displacement parameters ($Å^2$x 10^3)

for DR26. U(eq) is defined as one third of the trace of the orthogonalized U^{ij} tensor.

	x	y	z	U(eq)
O(1)	1584(2)	10108(2)	8603(1)	39(1)
O(2)	2091(1)	6159(1)	6566(1)	21(1)
O(3)	-24(1)	4648(2)	6588(1)	26(1)
O(4)	4131(1)	4167(2)	9274(1)	25(1)
O(5)	2700(1)	4335(2)	10355(1)	30(1)
O(6)	3282(1)	3143(2)	5106(1)	36(1)
N(1)	1138(2)	7136(2)	8632(1)	24(1)
C(1)	1898(2)	8576(2)	8482(1)	27(1)
C(2)	3256(2)	7947(2)	8202(1)	23(1)
C(3)	2814(2)	6066(2)	7759(1)	19(1)
C(4)	1772(2)	5493(2)	8404(1)	20(1)
C(5)	-121(2)	7238(3)	9032(2)	35(1)
C(6)	3737(2)	9208(2)	7449(1)	32(1)
C(7)	2866(2)	4618(2)	9467(1)	22(1)
C(8)	624(2)	4130(2)	7747(1)	25(1)
C(9)	4045(2)	4653(2)	8119(1)	21(1)
C(10)	1095(2)	4731(2)	6091(1)	23(1)
C(11)	363(2)	5079(2)	4830(1)	28(1)
C(12)	1443(2)	5356(2)	4186(1)	32(1)
C(13)	2266(2)	3712(2)	4040(1)	33(1)
C(14)	4072(3)	1607(3)	4988(2)	46(1)
C(15)	5595(2)	5154(2)	8143(1)	26(1)
C(16)	6618(2)	3581(2)	8445(1)	30(1)
C(17)	7160(2)	2742(3)	7758(2)	36(1)

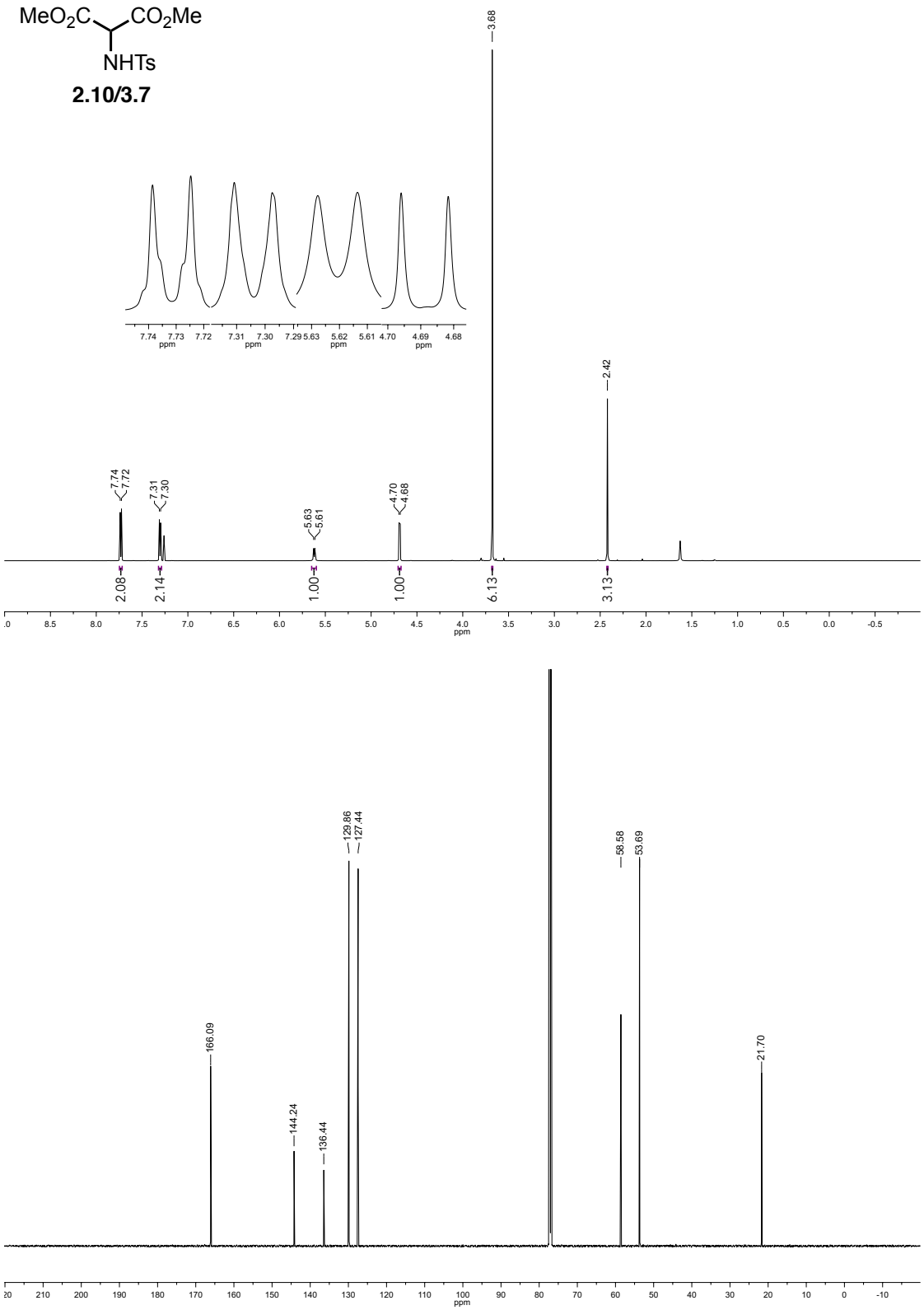

Figure A.3. ^{1}H-NMR (600 MHz) and ^{13}C-NMR (150 MHz) of compound **2.10**/**3.7** in $CDCl_3$

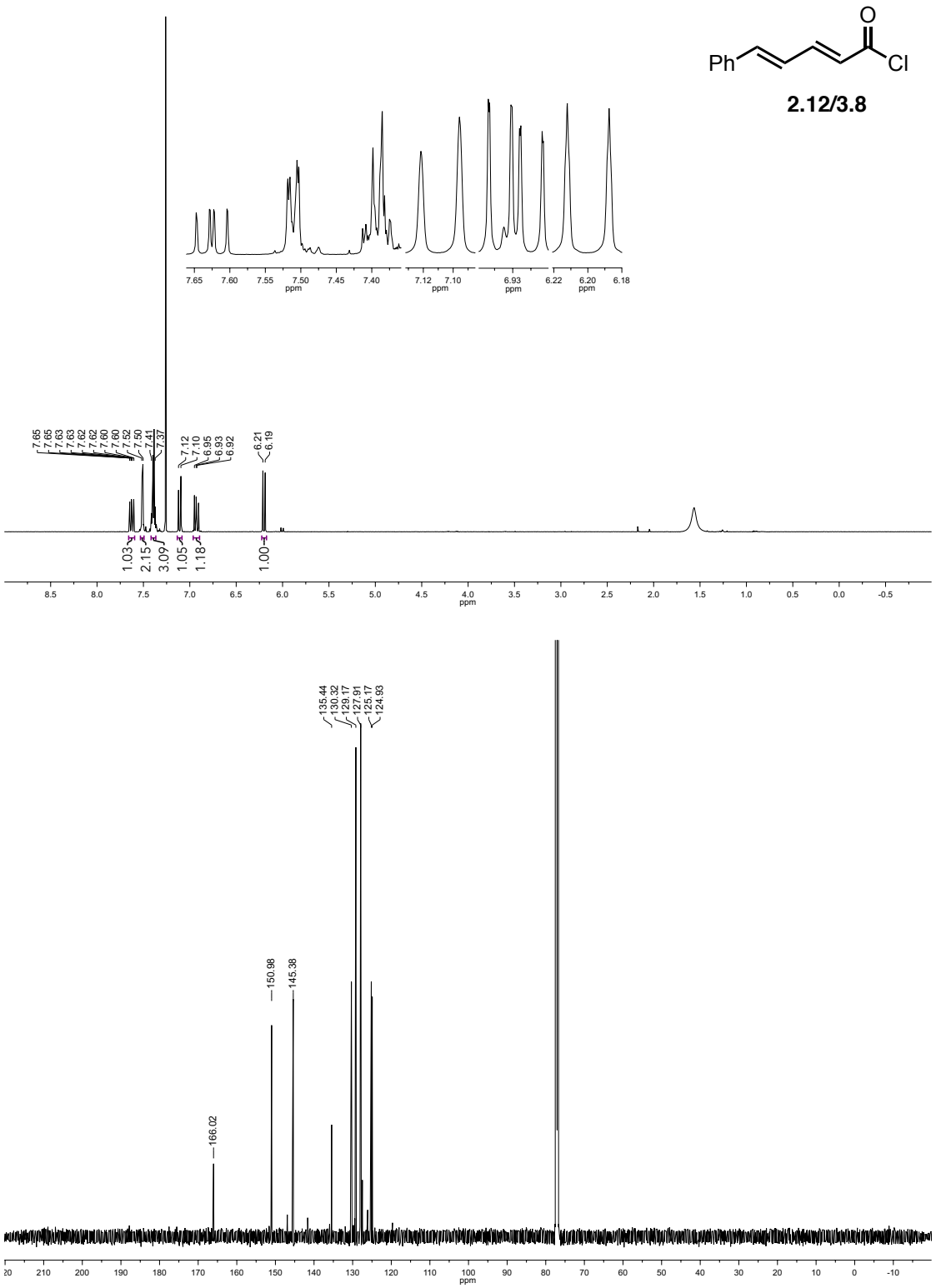

Figure A.4. ^{1}H-NMR (600 MHz) and ^{13}C-NMR (150 MHz) of compound **2.12**/**3.8** in $CDCl_3$

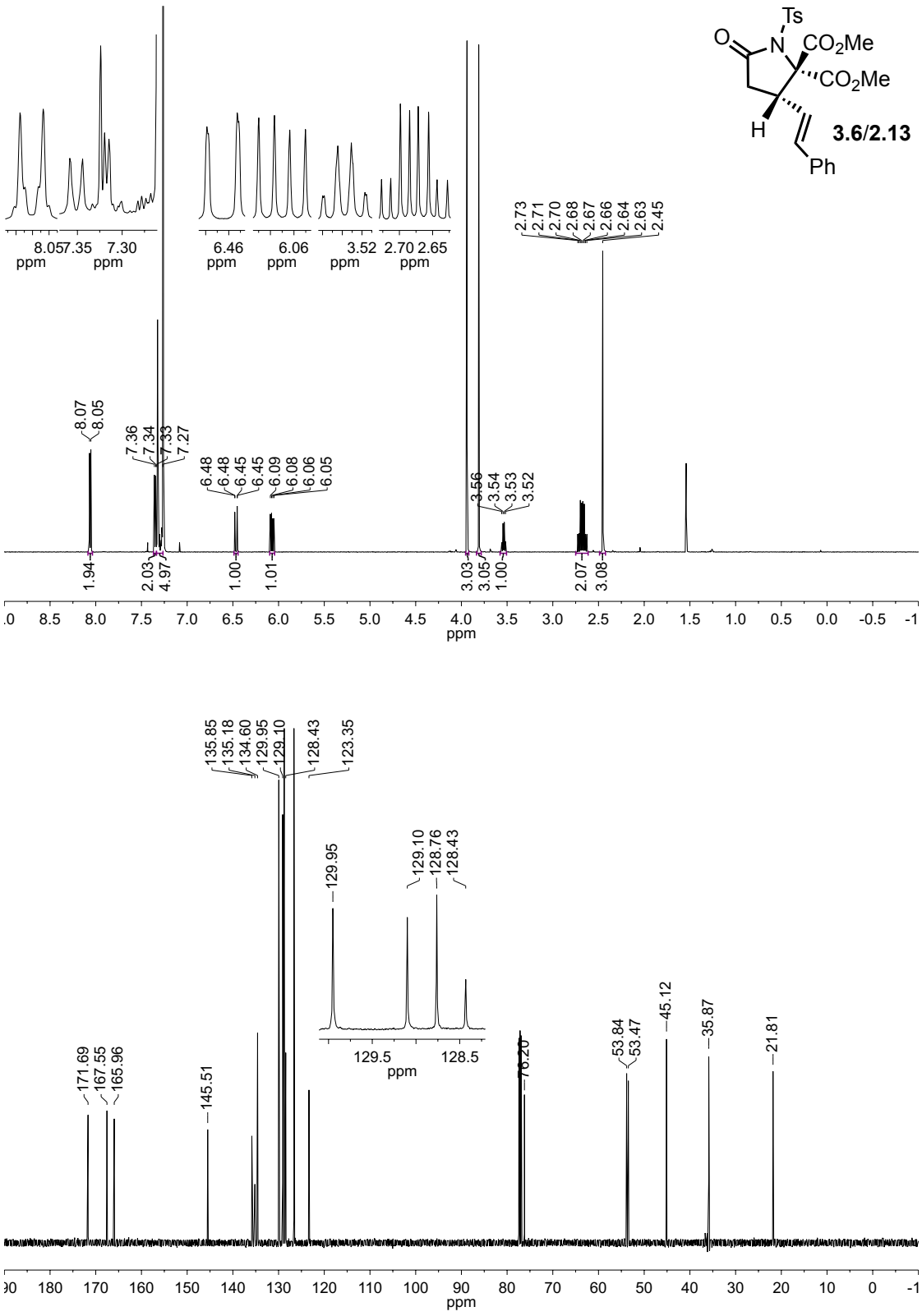

Figure A.5. ^{1}H-NMR (600 MHz) and ^{13}C-NMR (125 MHz) of compound **2.13**/**3.6** in $CDCl_3$

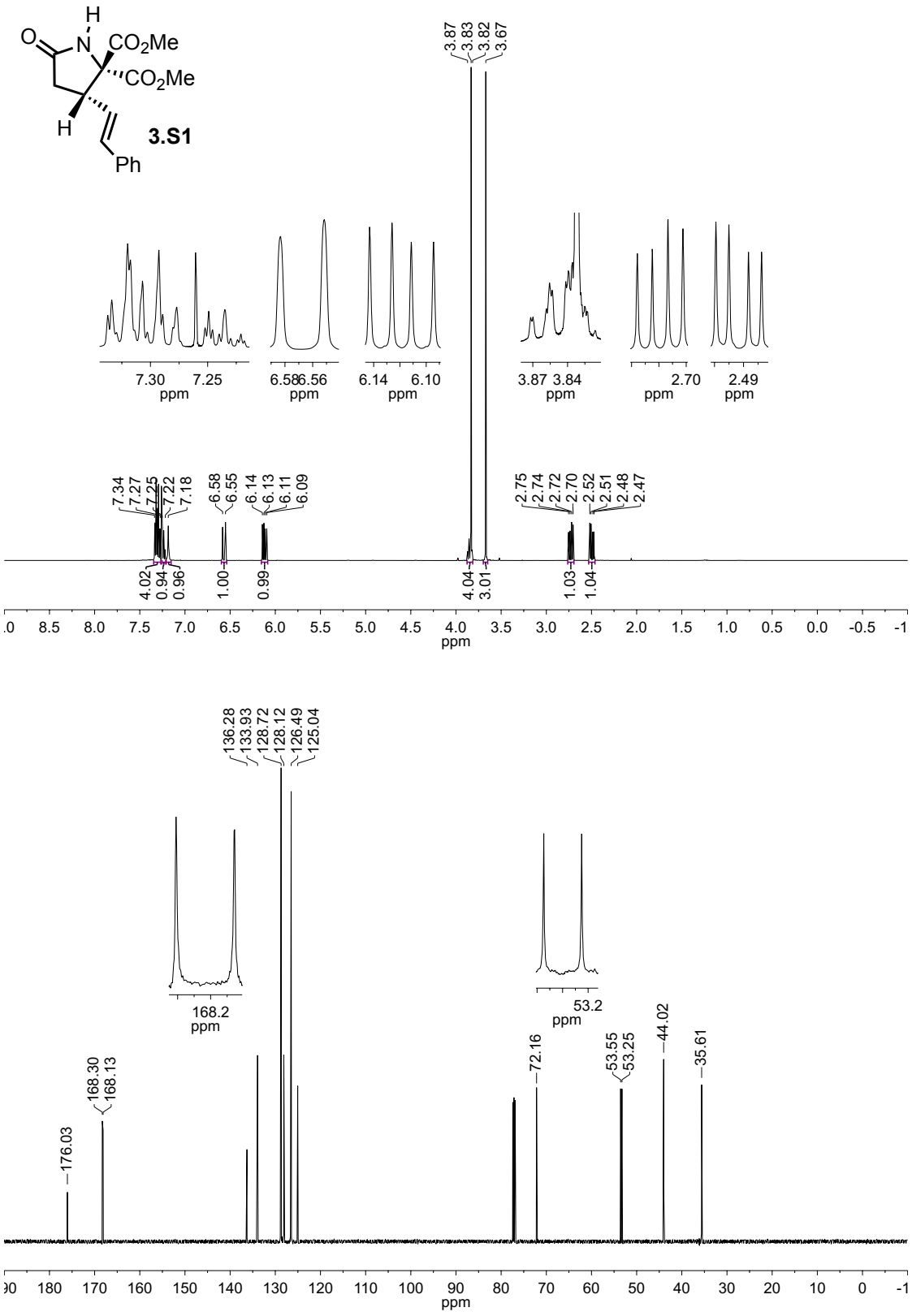

Figure A.6. ^{1}H-NMR (500 MHz) and ^{13}C-NMR (125 MHz) of compound **3.S1** in $CDCl_3$

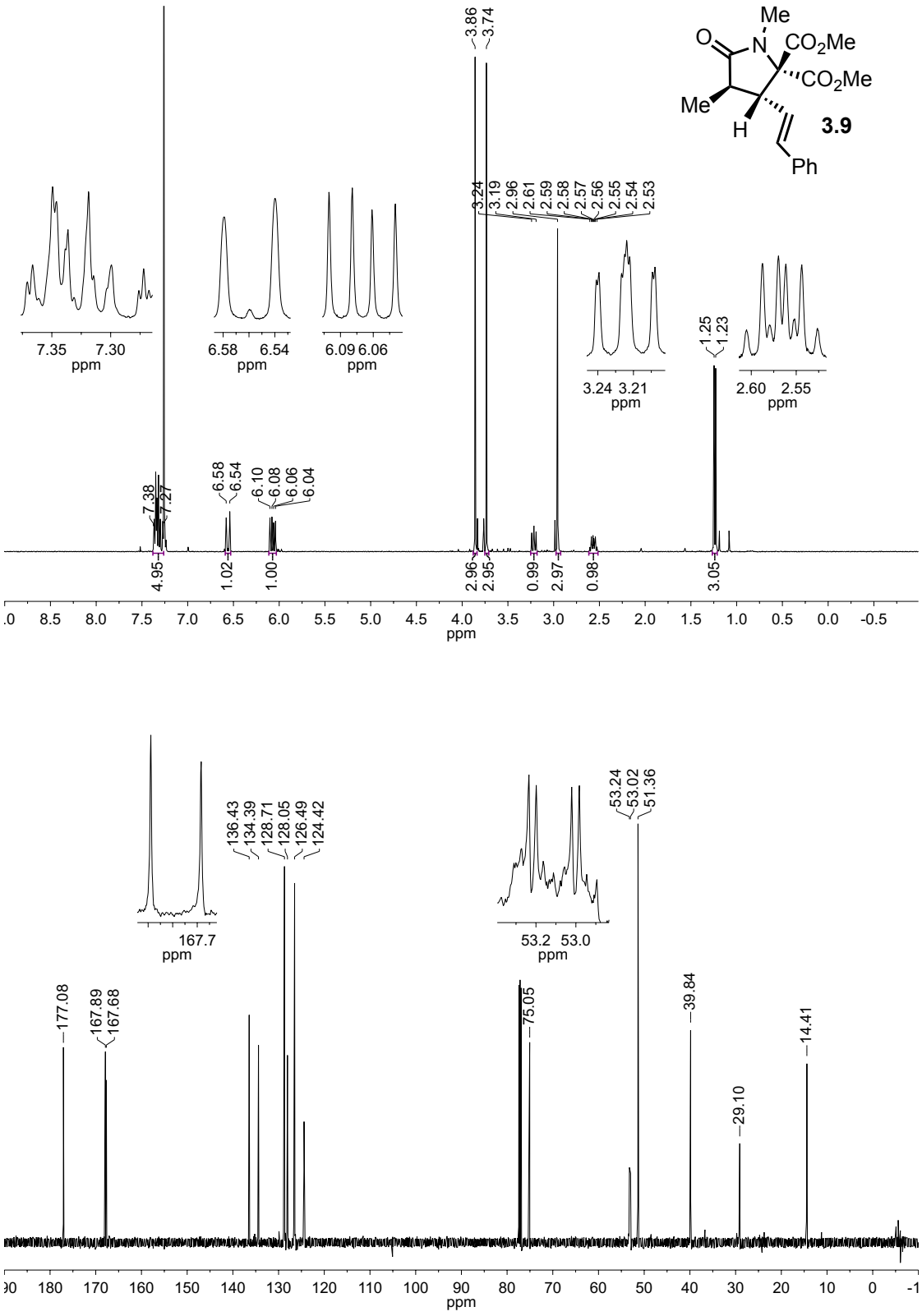

Figure A.7. ^{1}H-NMR (600 MHz) and ^{13}C-NMR (125 MHz) of compound **3.9** in $CDCl_3$

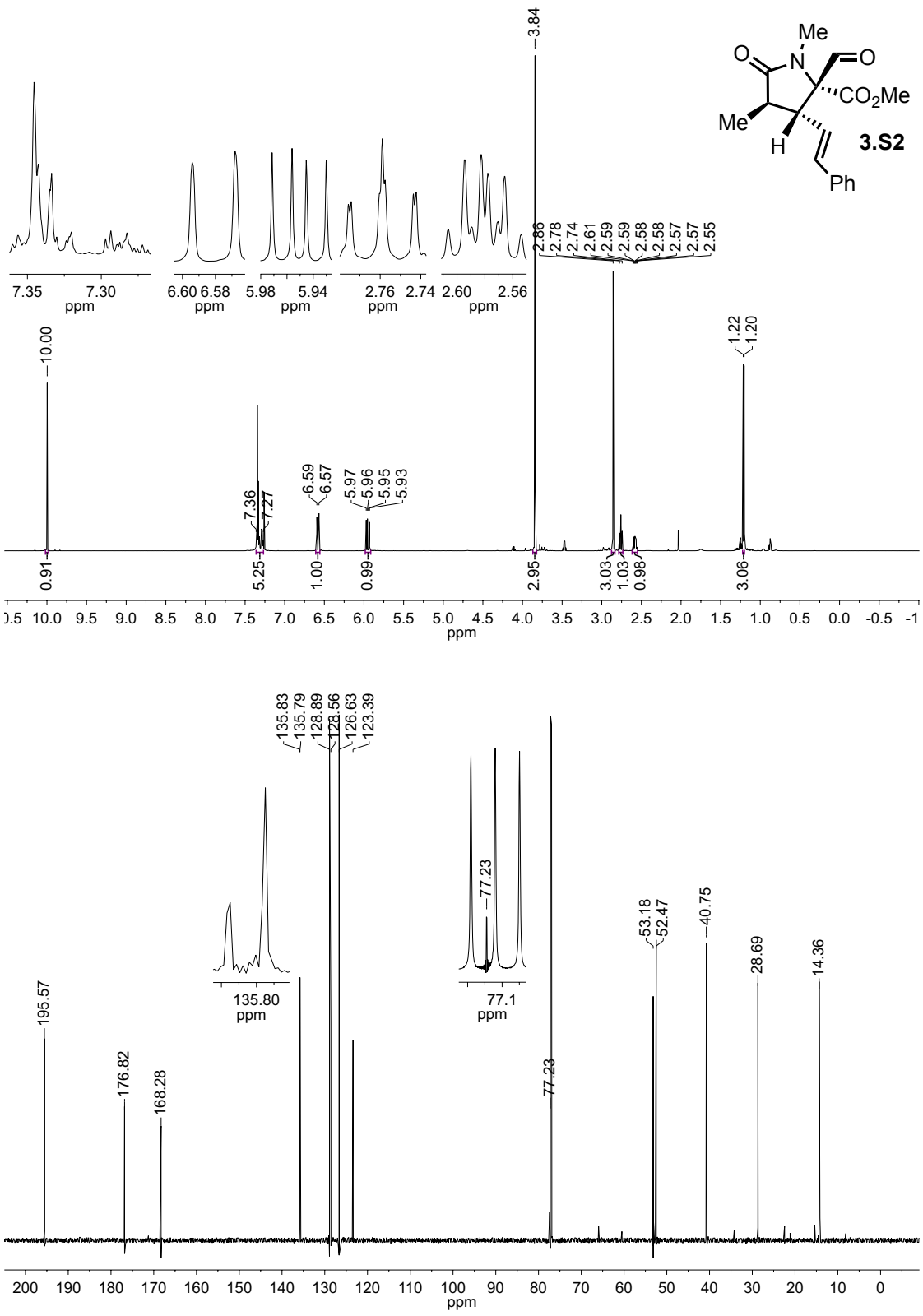

Figure A.8. ^{1}H-NMR (600 MHz) and ^{13}C-NMR (150 MHz) of compound **3.S2** in $CDCl_3$

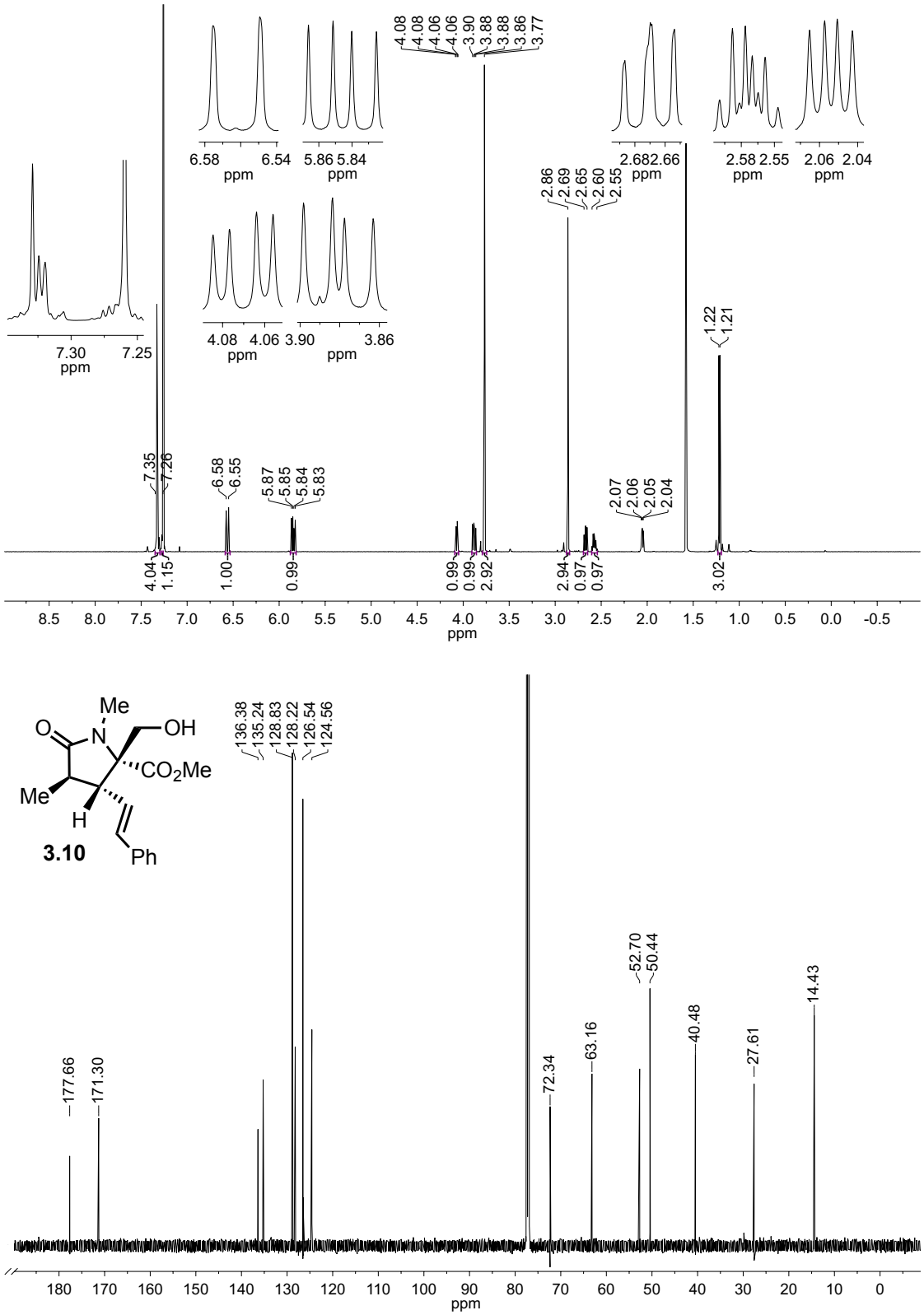

Figure A.9. ^{1}H-NMR (600 MHz) and ^{13}C-NMR (150 MHz) of compound **3.10** in $CDCl_3$

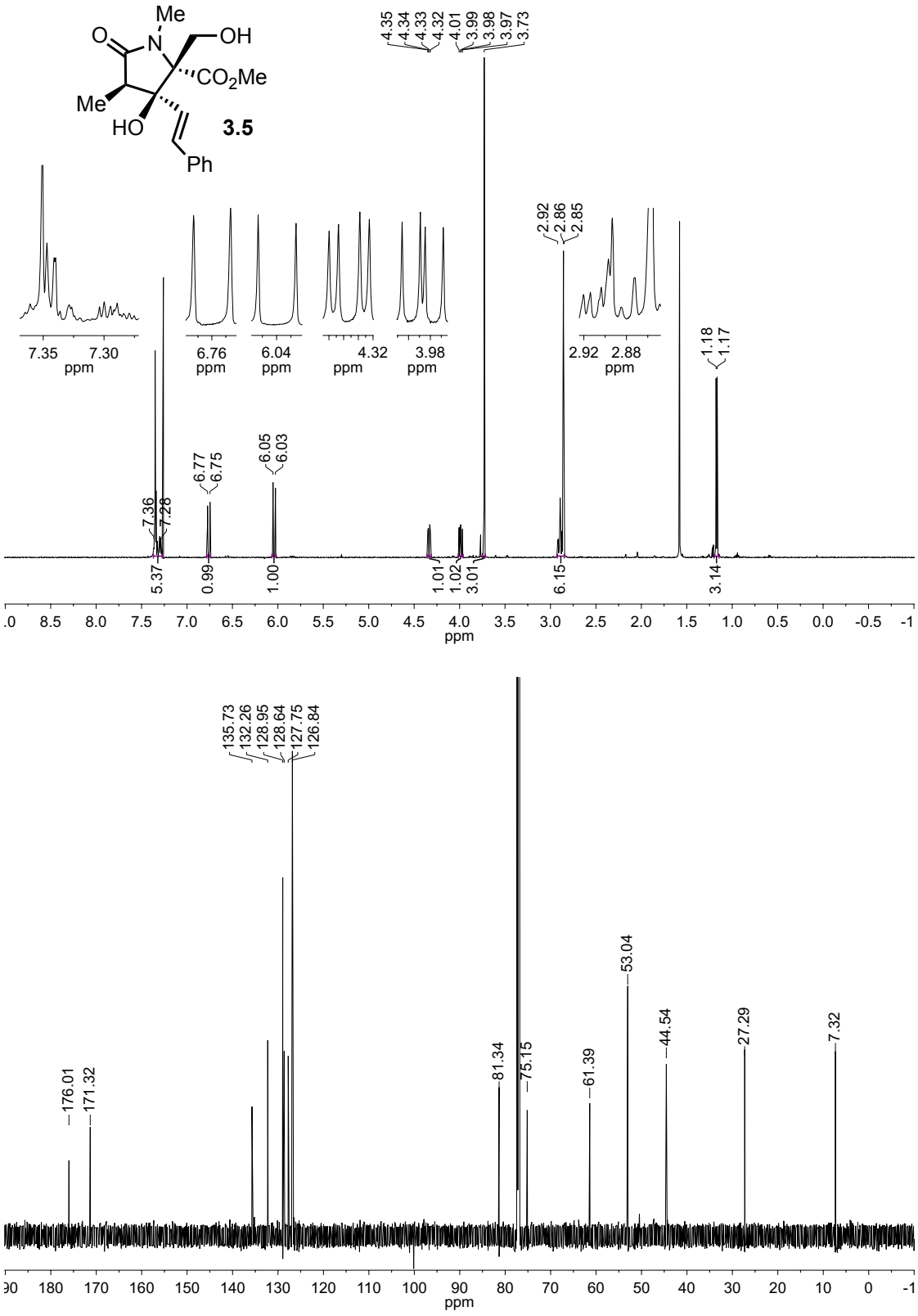

Figure A.10. ^{1}H-NMR (600 MHz) and ^{13}C-NMR (150 MHz) of compound **3.5** in $CDCl_3$

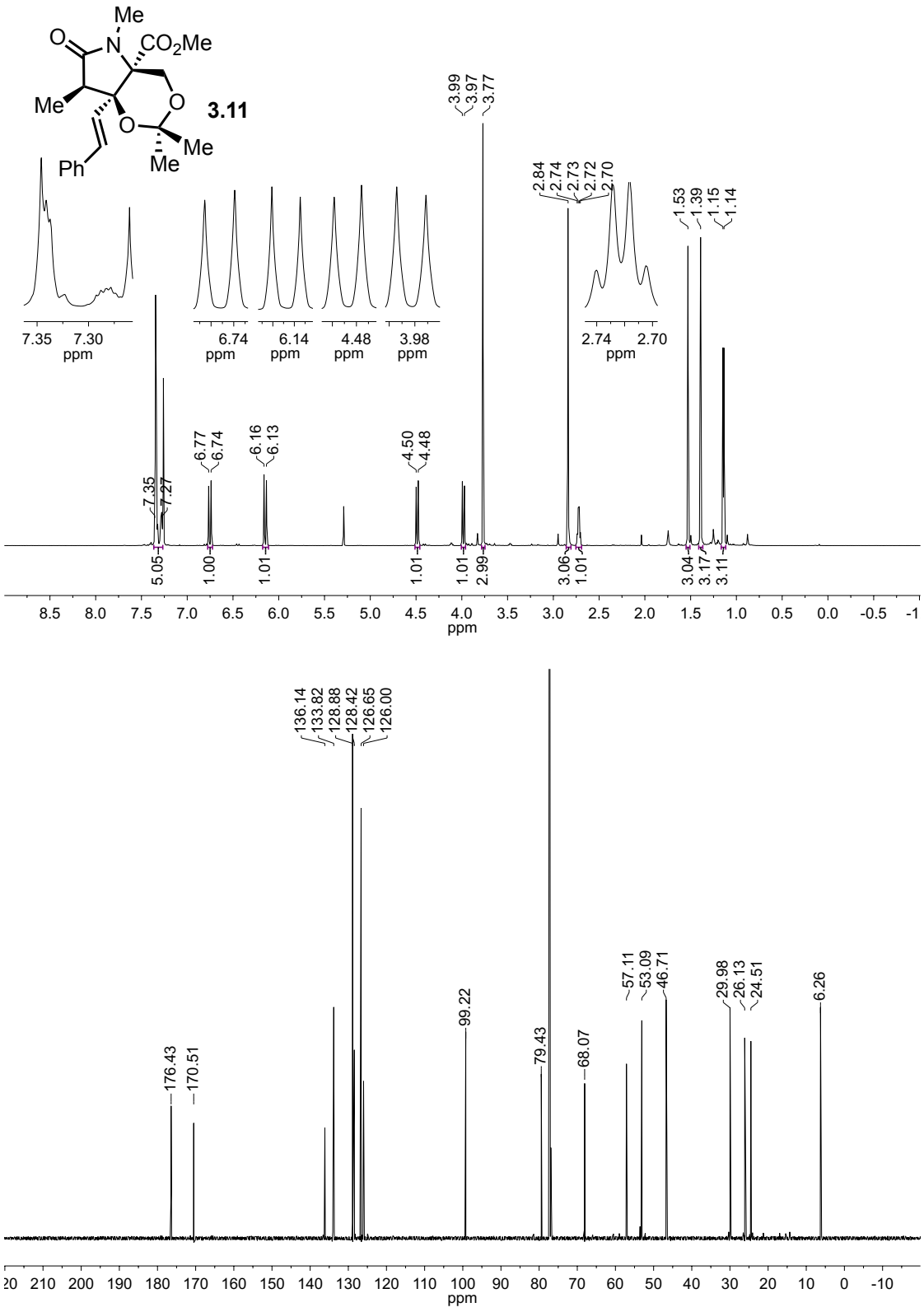

Figure A.11. ^{1}H-NMR (600 MHz) and ^{13}C-NMR (150 MHz) of compound **3.11** in $CDCl_3$

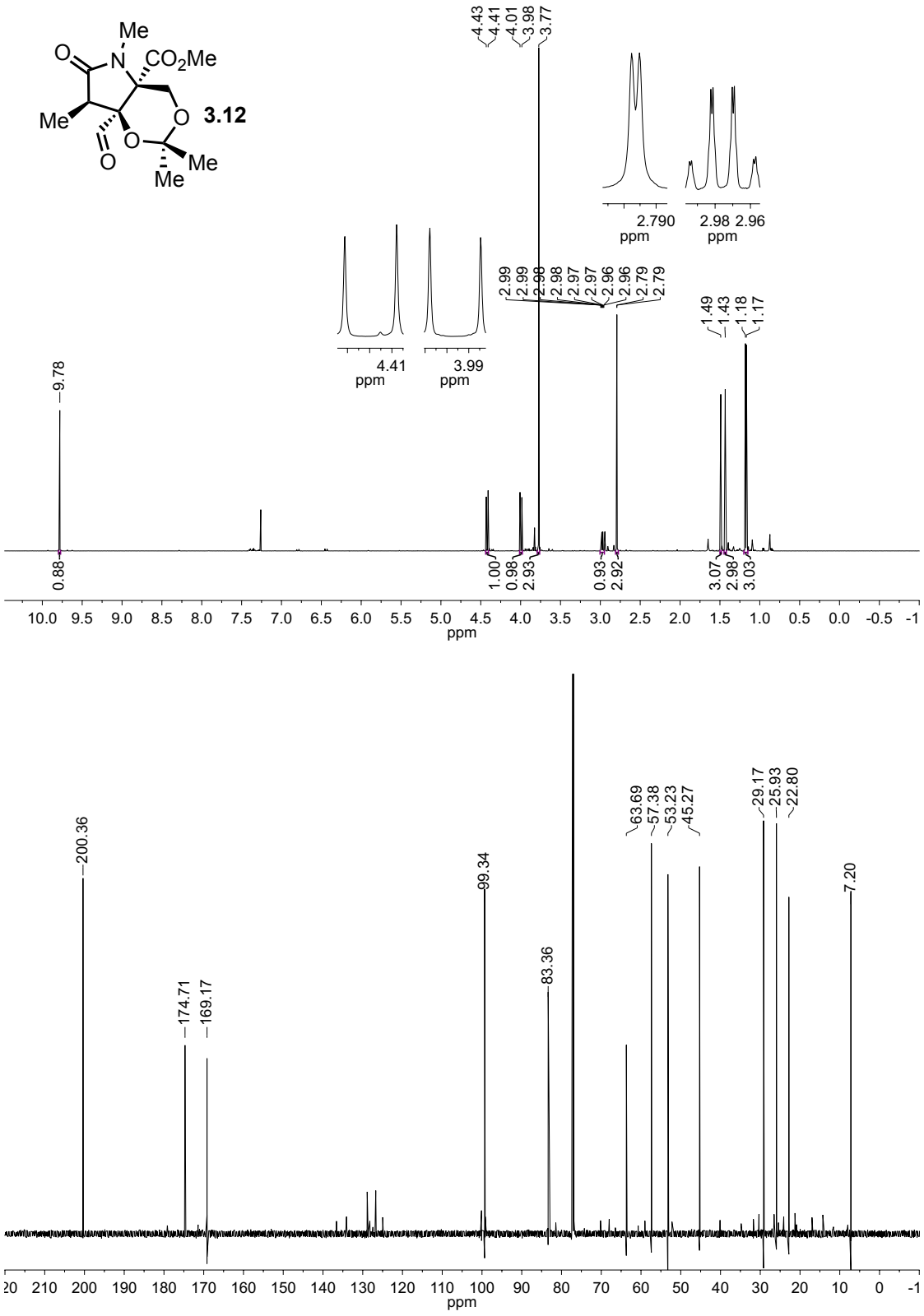

Figure A.12. ^{1}H-NMR (600 MHz) and ^{13}C-NMR (150 MHz) of compound **3.12** in $CDCl_3$

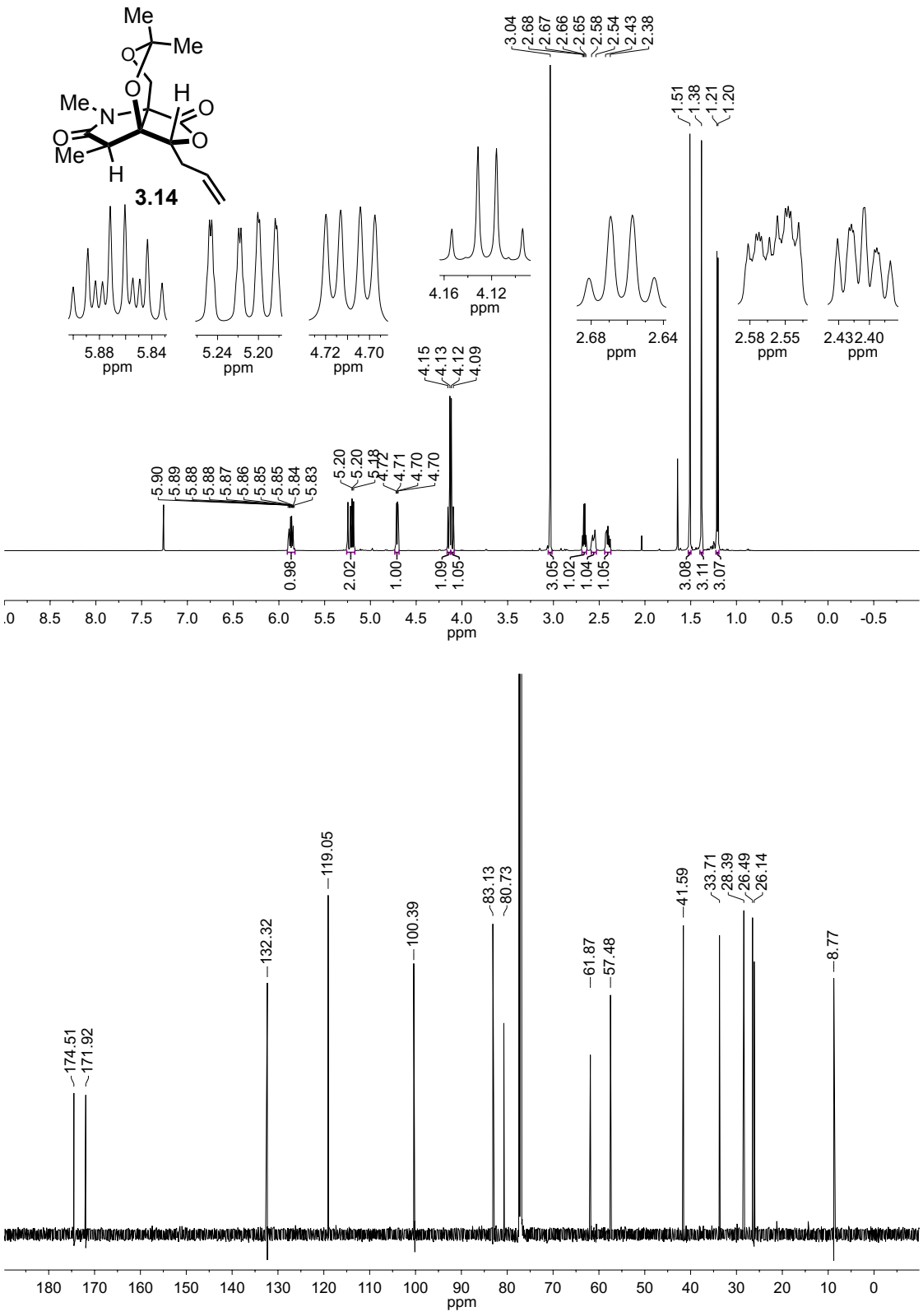

Figure A.13. ^{1}H-NMR (600 MHz) and ^{13}C-NMR (150 MHz) of compound **3.14** in $CDCl_3$

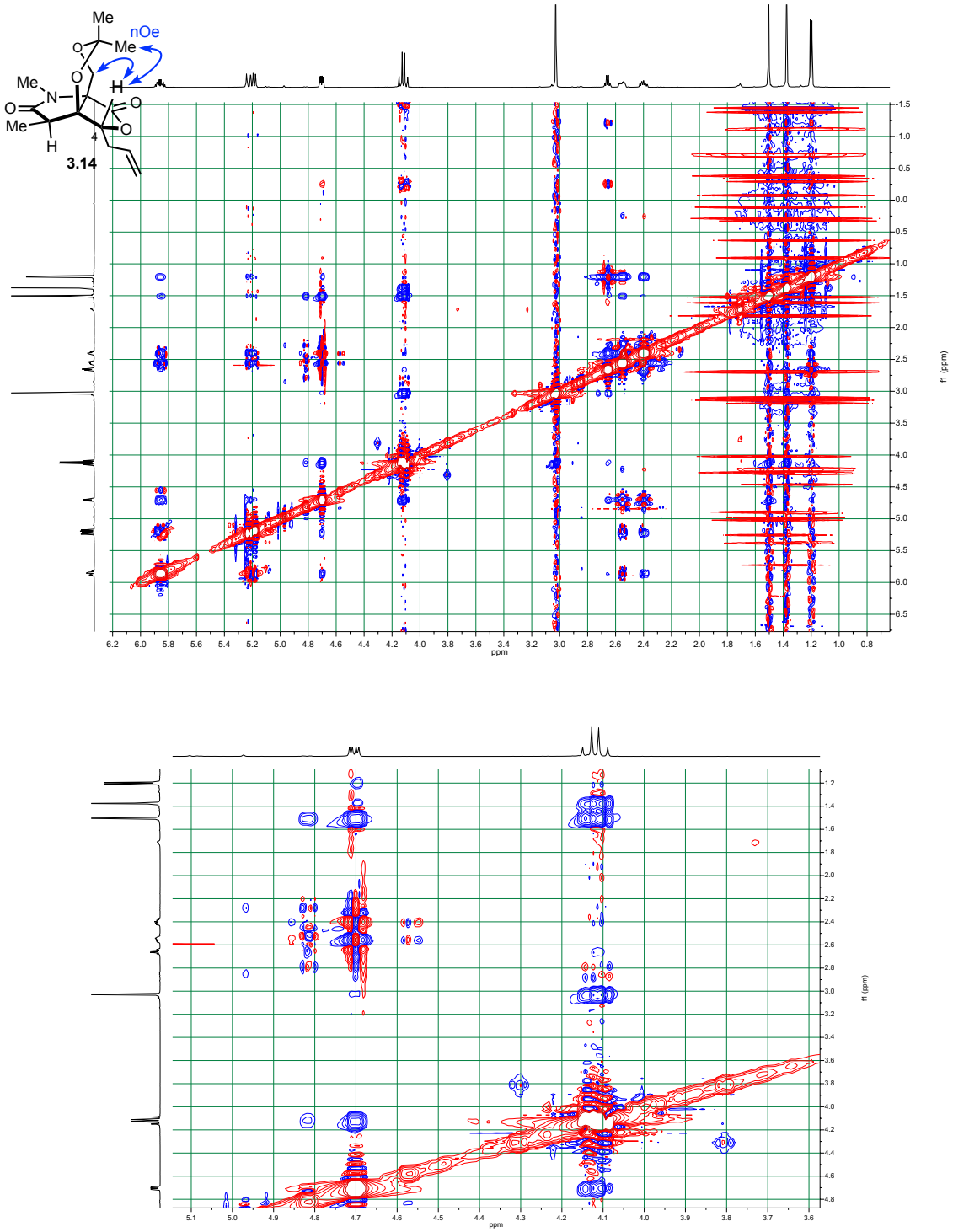

Figure A.14. ^{1}H-^{1}H NOESY 2D-NMR (600 MHz) of compound **3.14** in $CDCl_3$

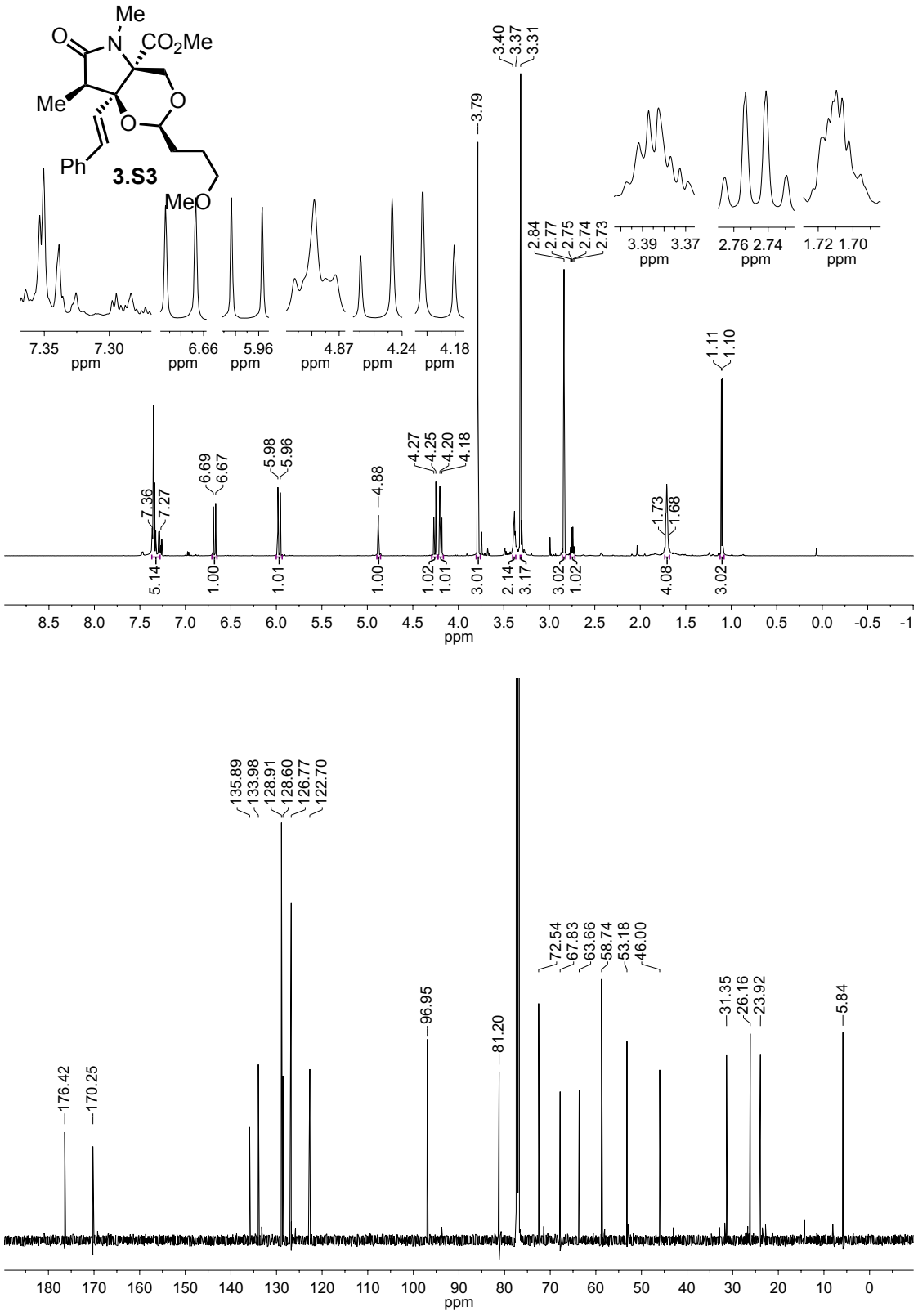

Figure A.15. ^{1}H-NMR (600 MHz) and ^{13}C-NMR (150 MHz) of compound **3.S3** in $CDCl_3$

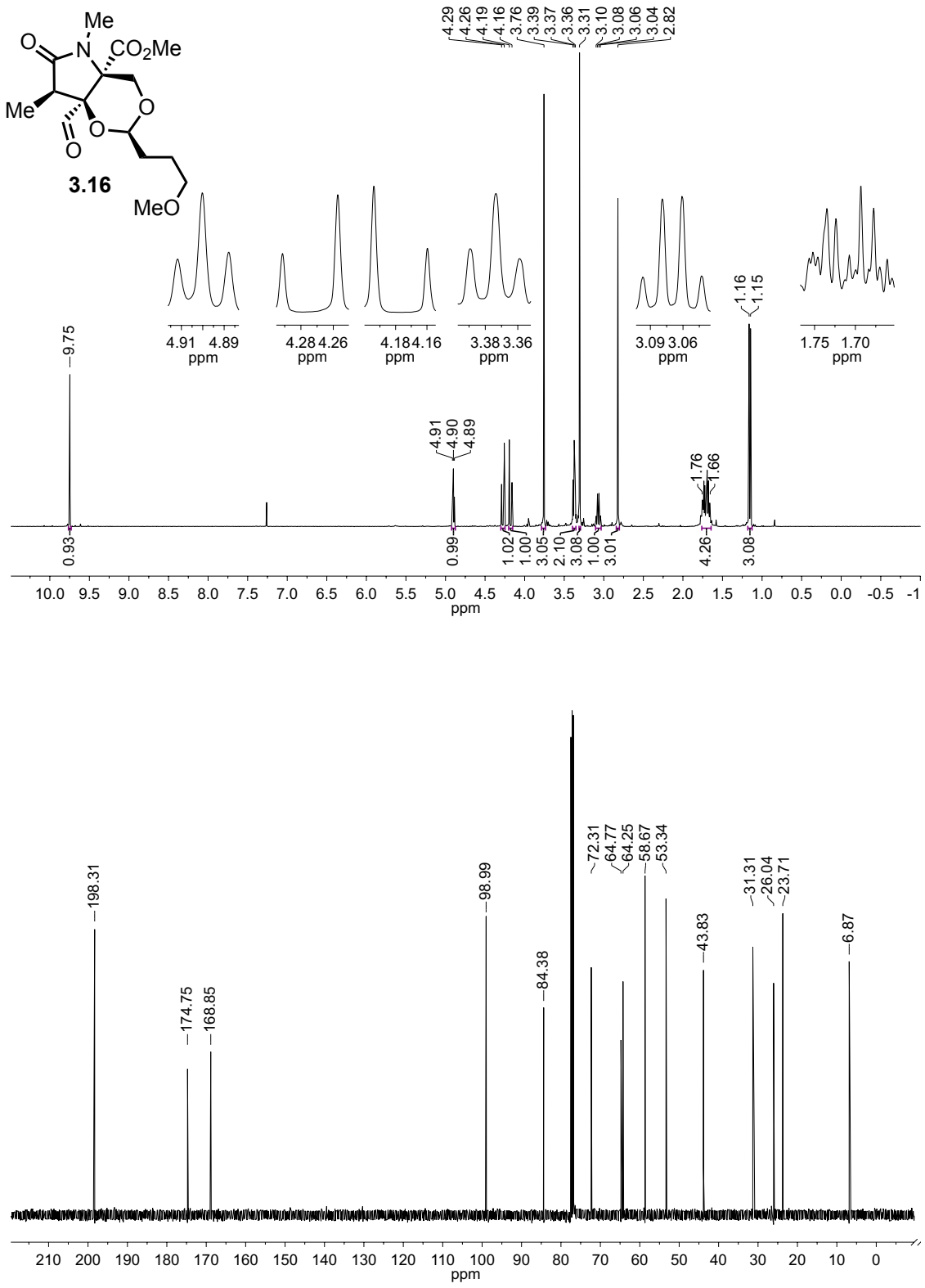

Figure A.16. ^{1}H-NMR (600 MHz) and ^{13}C-NMR (150 MHz) of compound **3.16** in $CDCl_3$

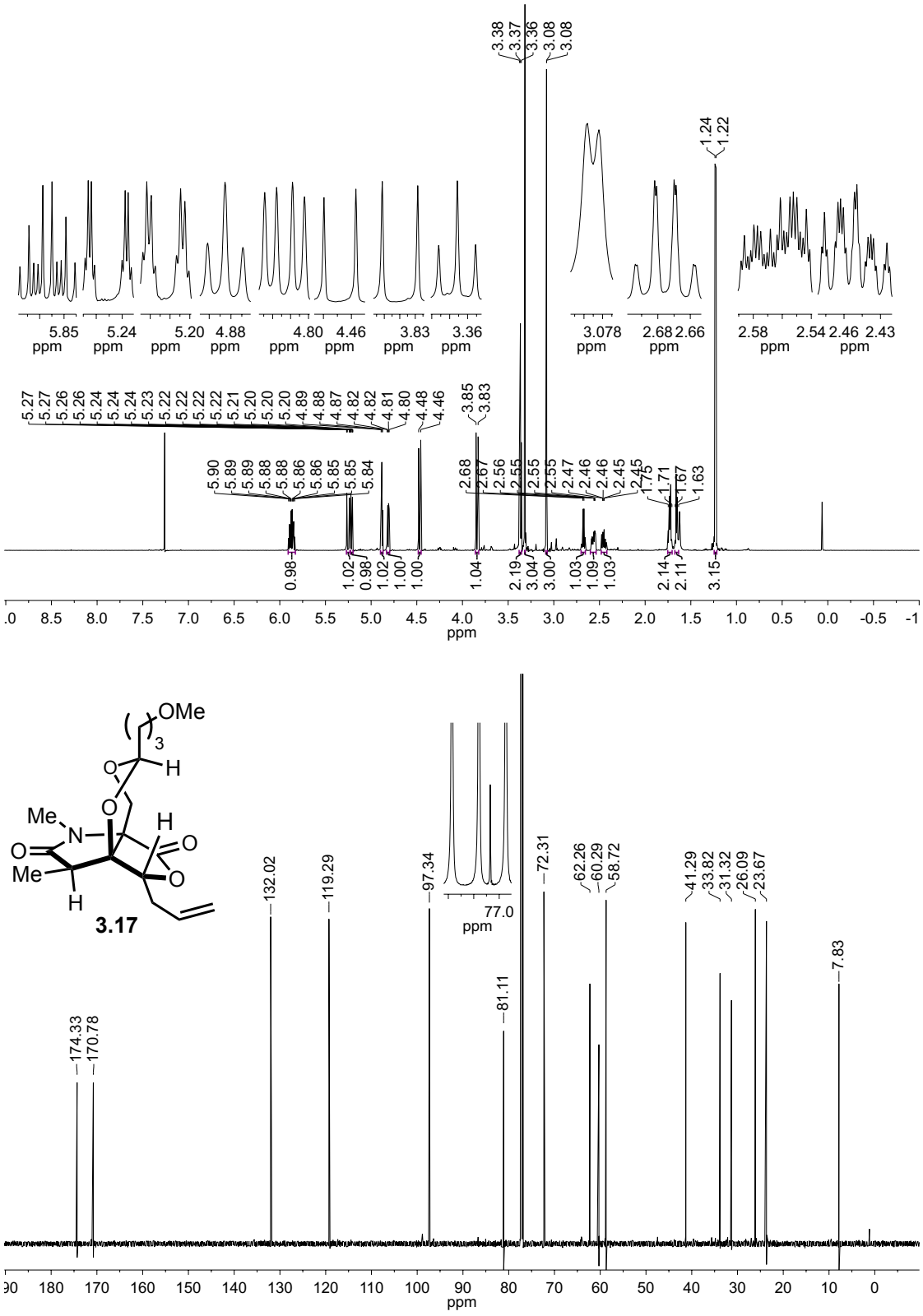

Figure A.17. ^{1}H-NMR (600 MHz) and ^{13}C-NMR (150 MHz) of compound **3.17** in $CDCl_3$

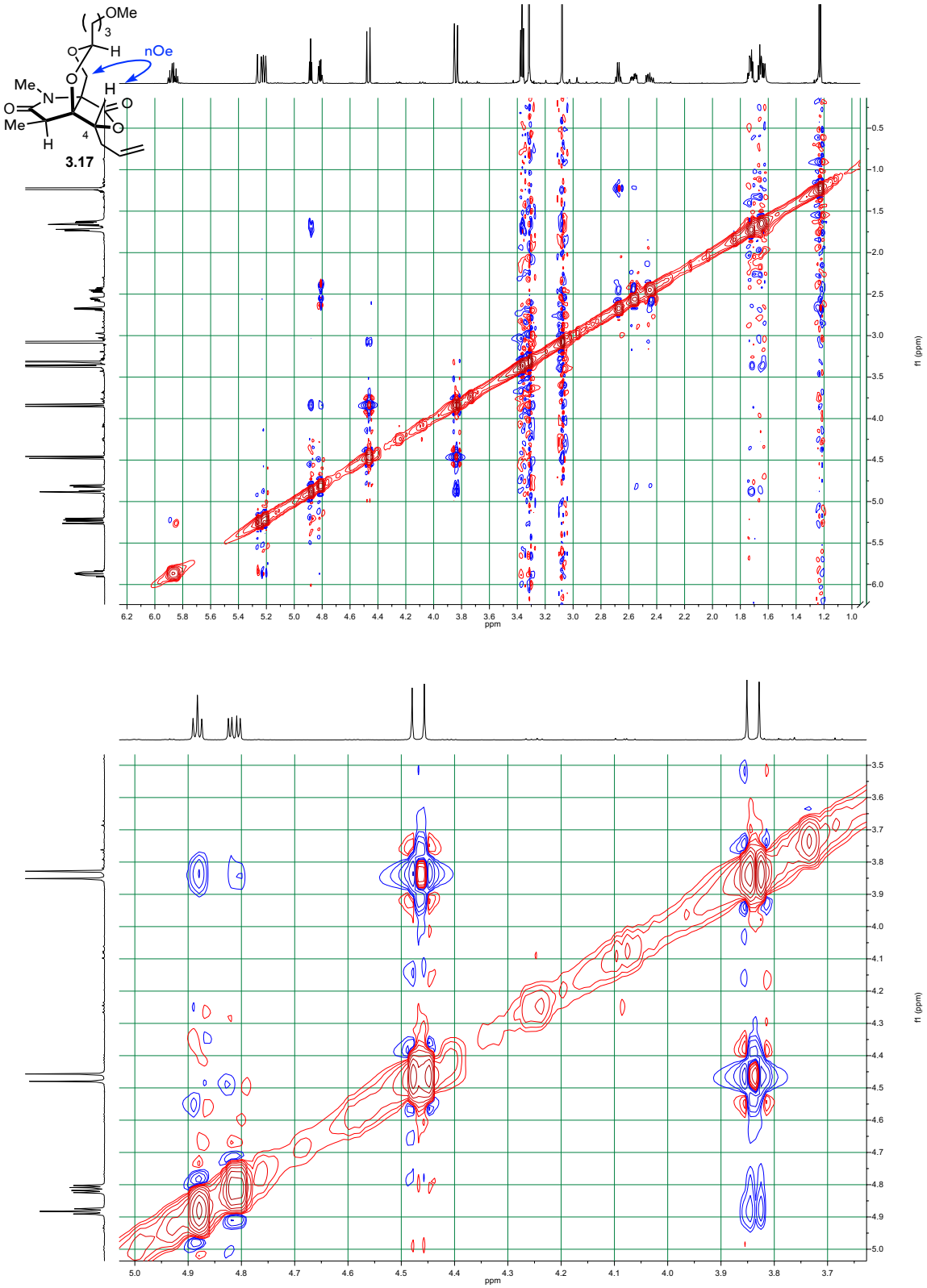

Figure A.18. ^{1}H-^{1}H NOESY 2D-NMR (600 MHz) of compound **3.17** in $CDCl_3$

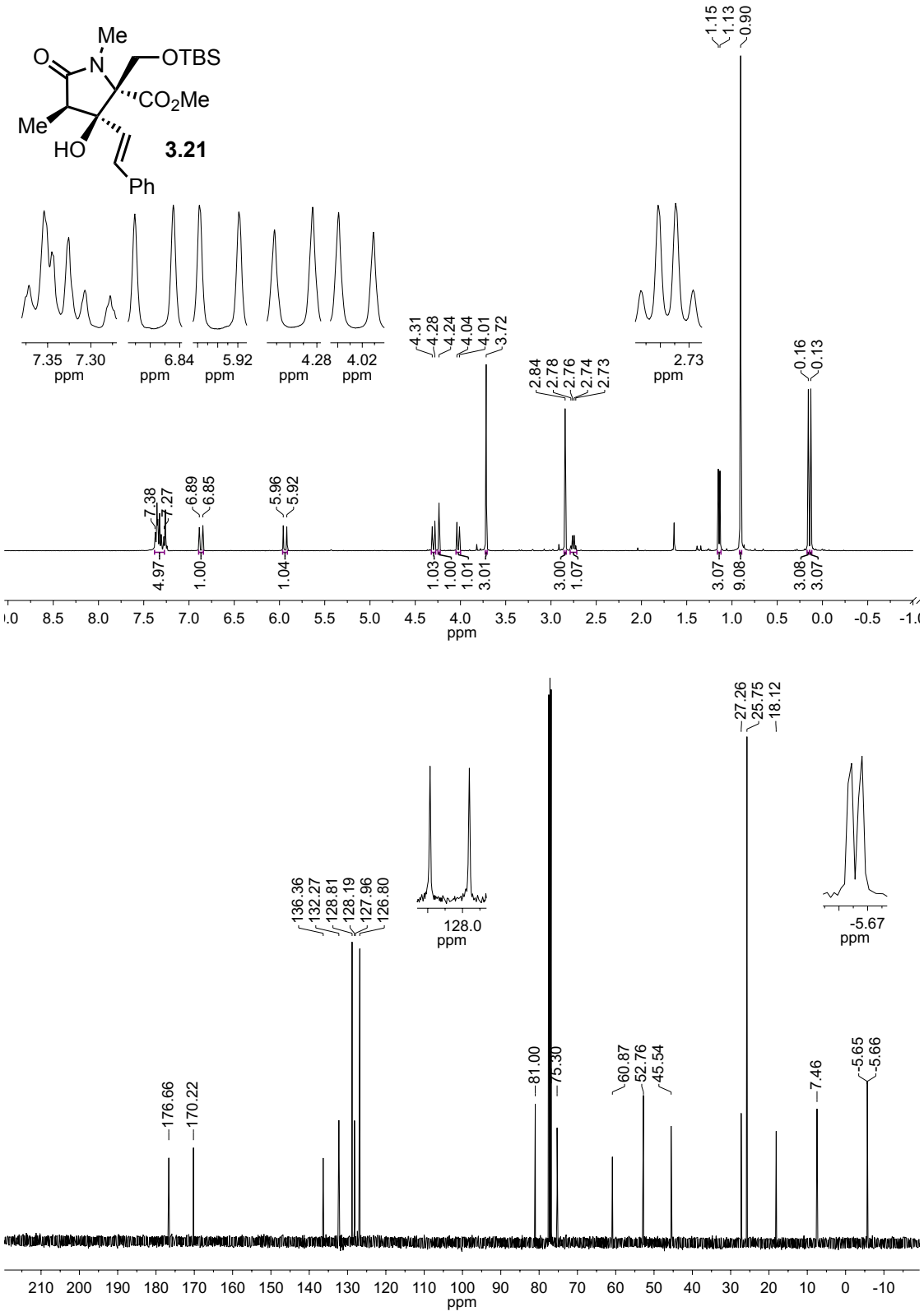

Figure A.19. ^{1}H-NMR (400 MHz) and ^{13}C-NMR (100 MHz) of compound **3.21** in $CDCl_3$

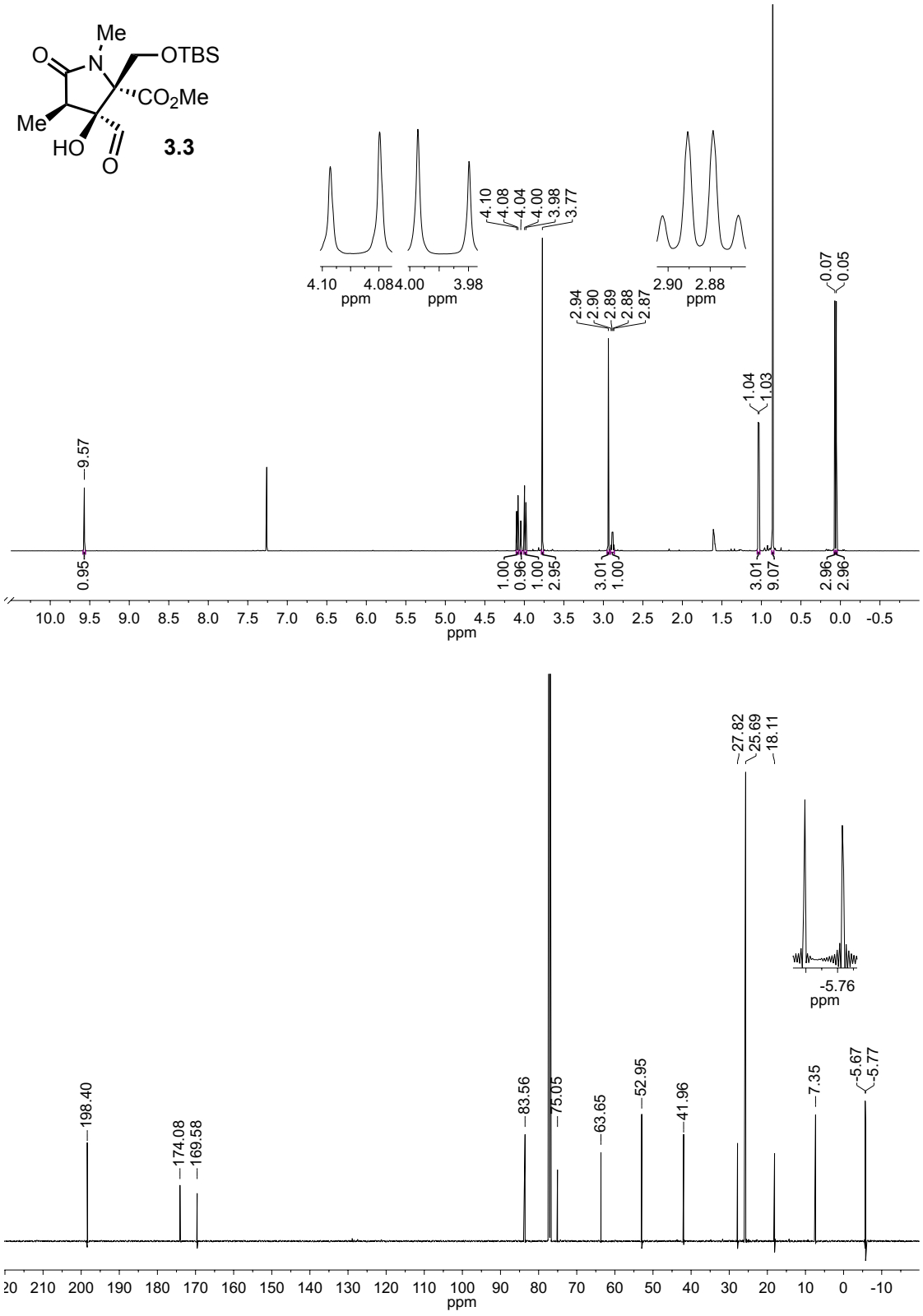

Figure A.20. ^{1}H-NMR (600 MHz) and ^{13}C-NMR (150 MHz) of compound **3.3** in $CDCl_3$

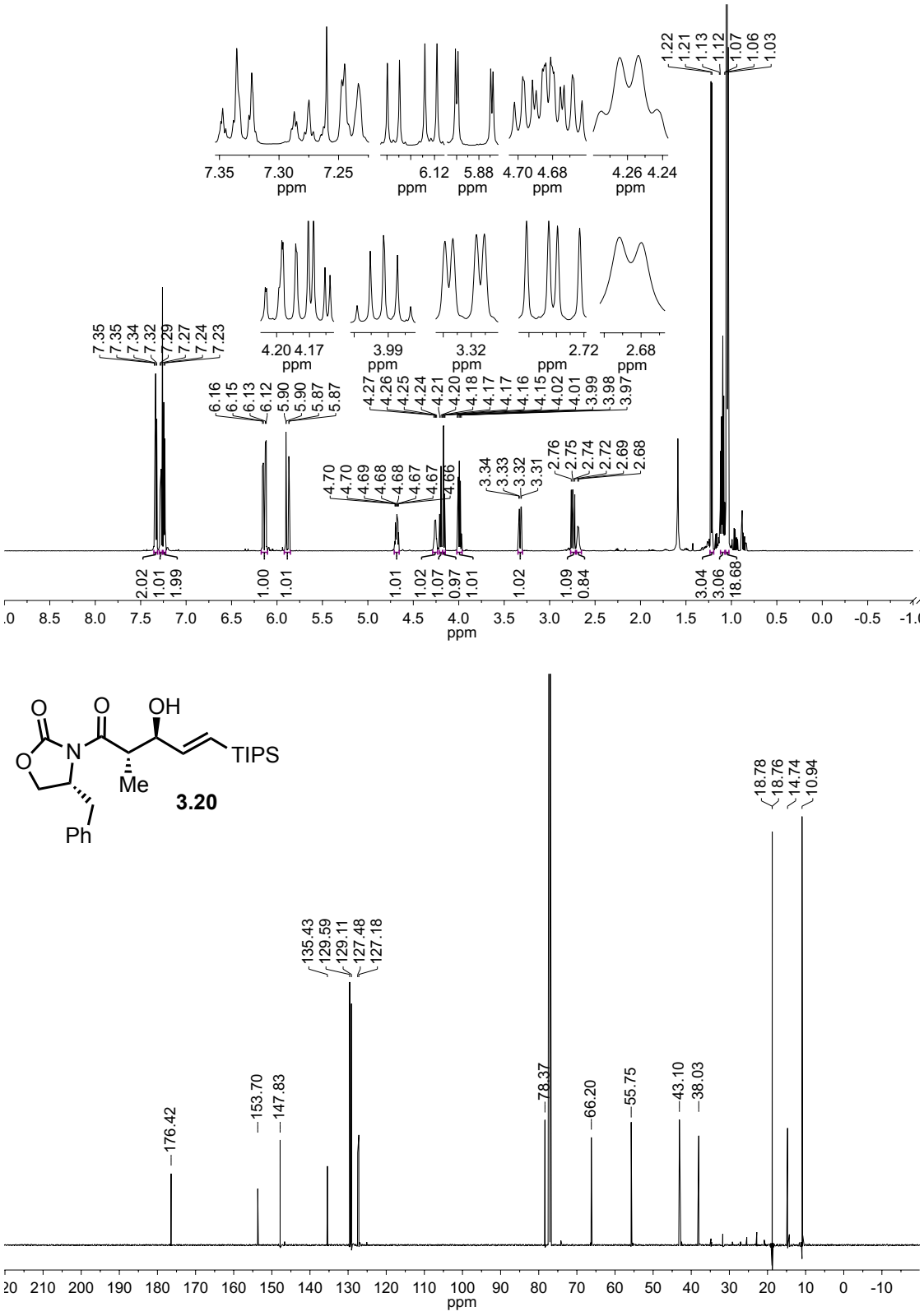

Figure A.21. ^{1}H-NMR (600 MHz) and ^{13}C-NMR (150 MHz) of compound **3.20** in $CDCl_3$

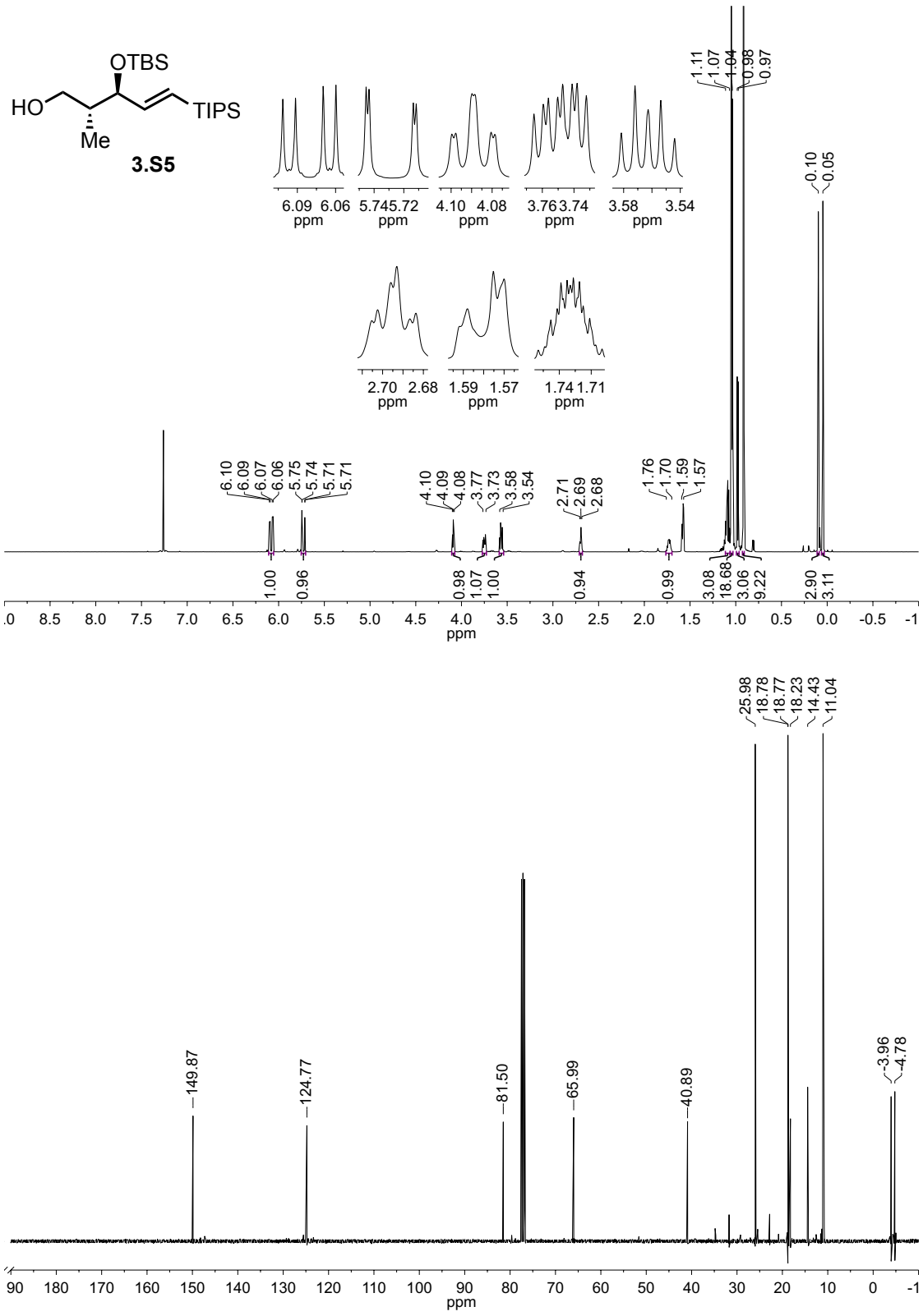

Figure A.22. ^{1}H-NMR (600 MHz) and ^{13}C-NMR (100 MHz) of compound **3.S5** in $CDCl_3$

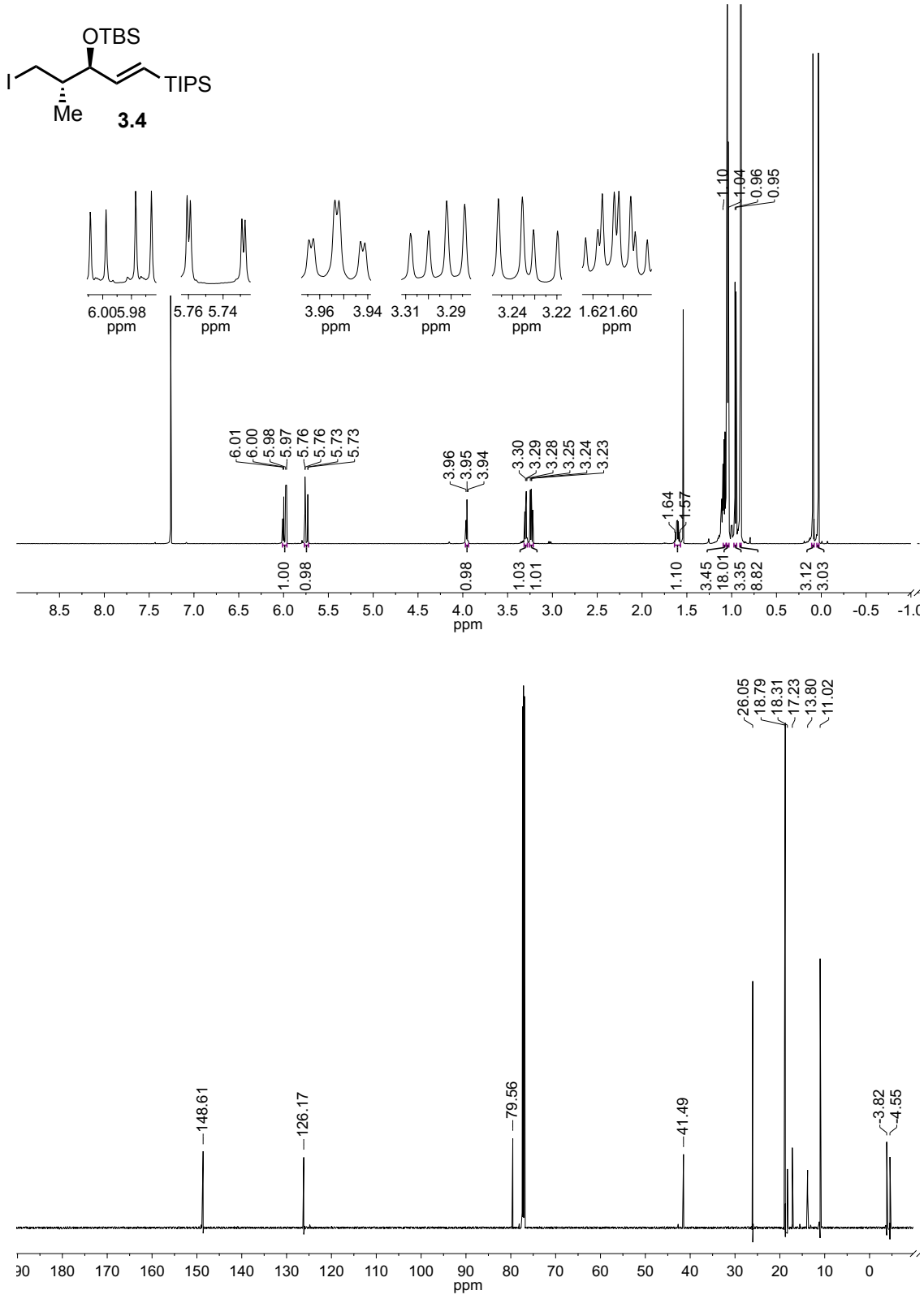

Figure A.23. ^{1}H-NMR (600 MHz) and ^{13}C-NMR (150 MHz) of compound **3.4** in $CDCl_3$

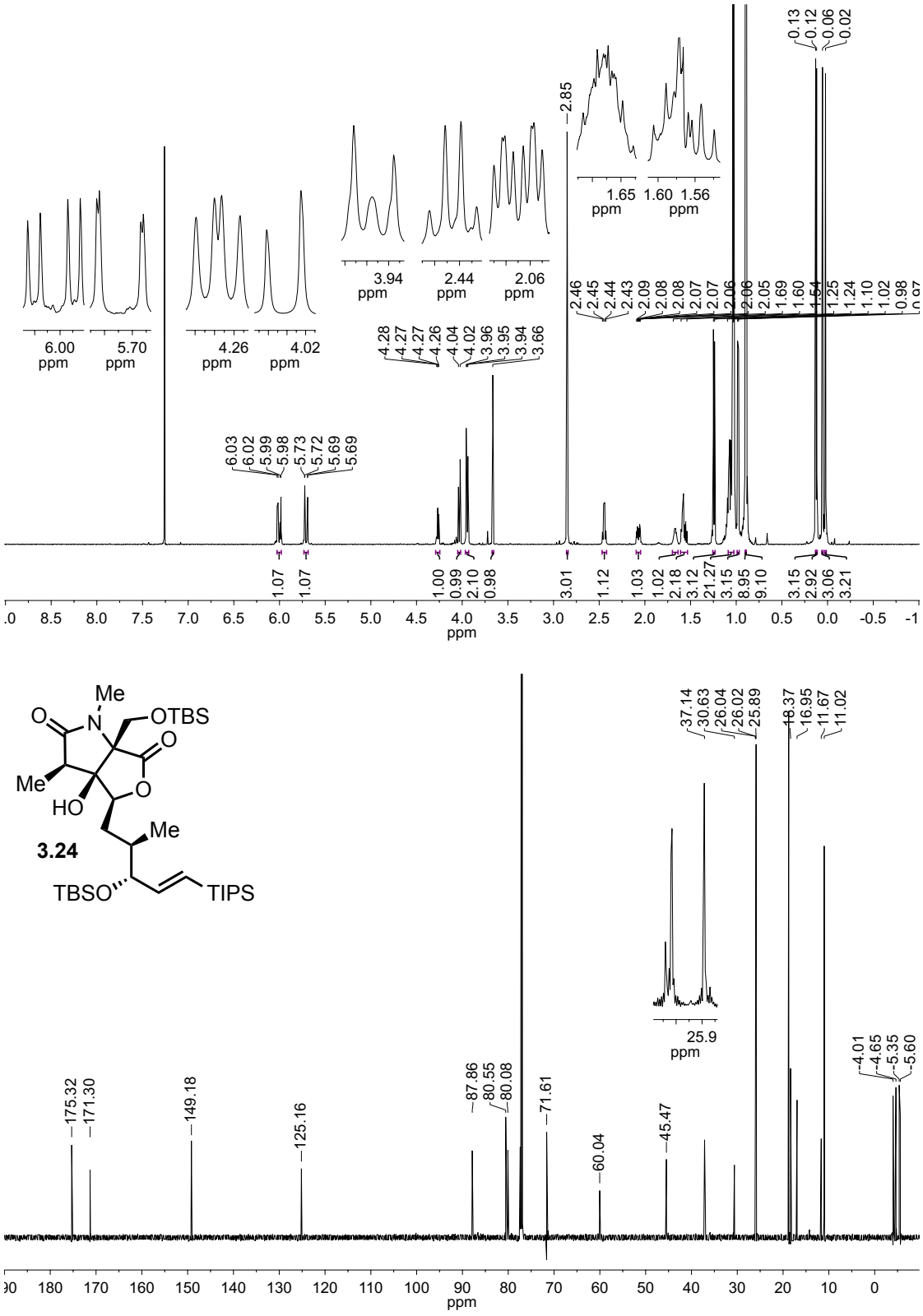

Figure A.24. ^{1}H-NMR (600 MHz) and ^{13}C-NMR (150 MHz) of compound **3.24** in $CDCl_3$

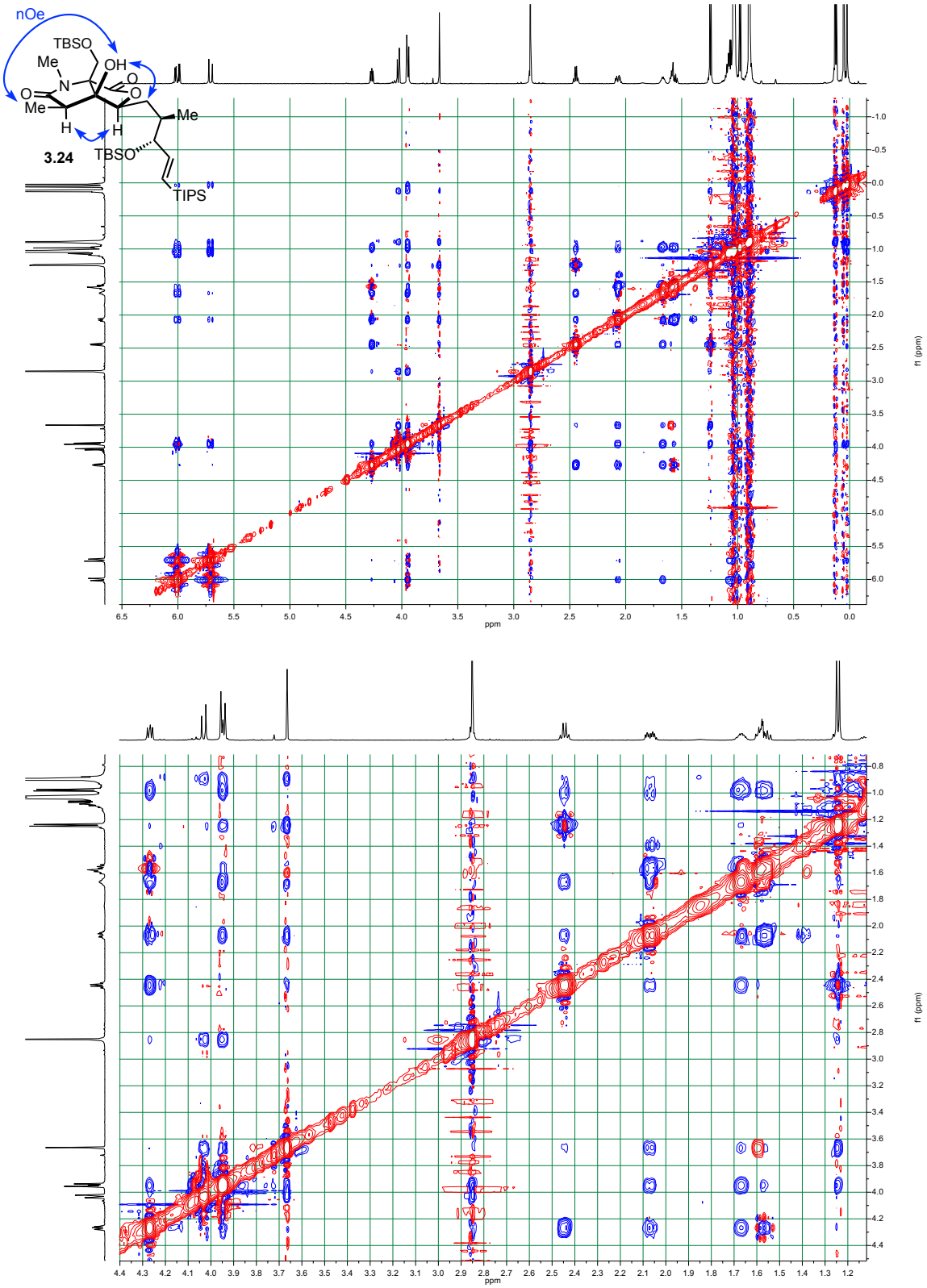

Figure A.25. ^{1}H-^{1}H NOESY 2D-NMR (600 MHz) of compound **3.24** in $CDCl_3$

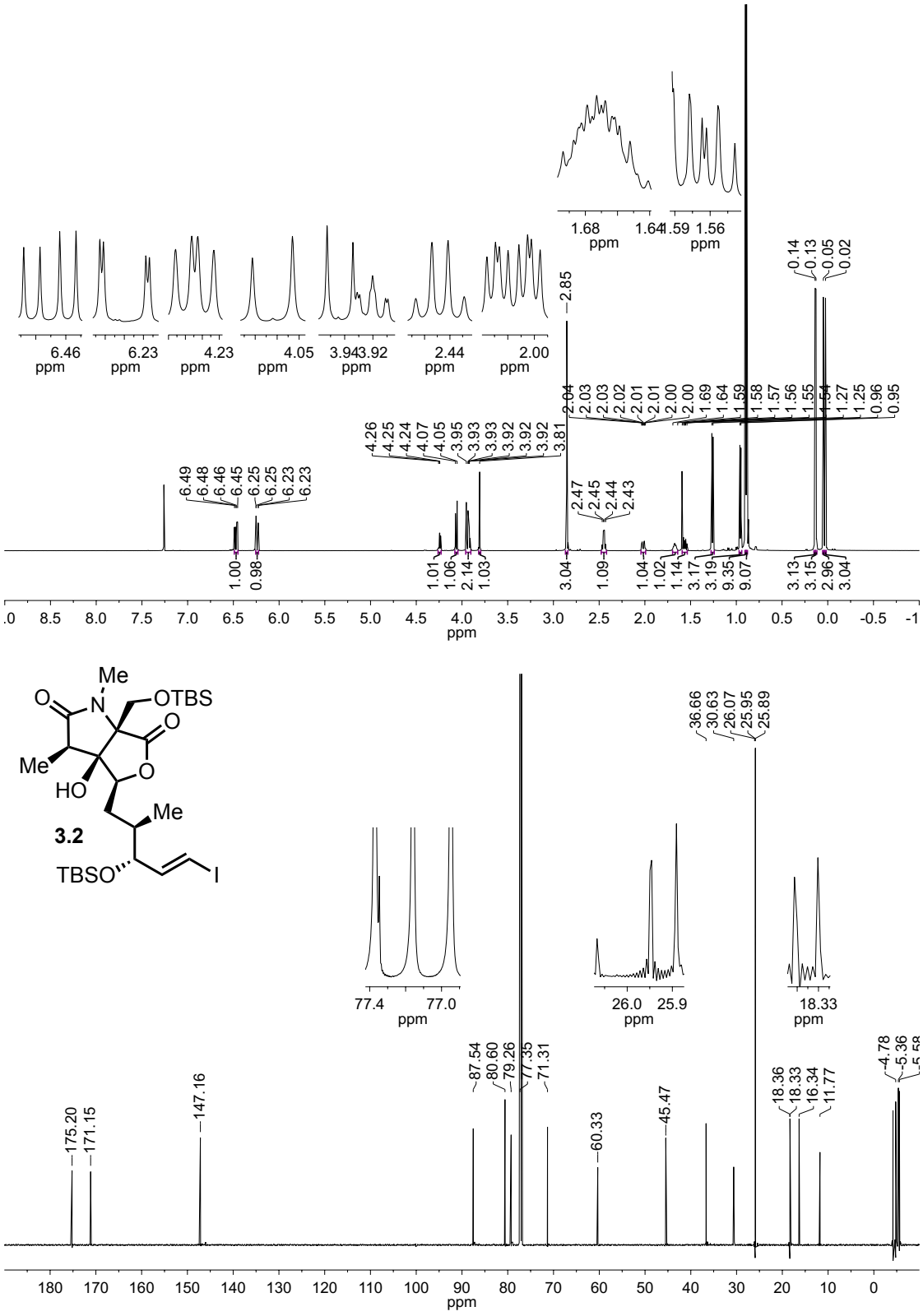

Figure A.26. ^{1}H-NMR (600 MHz) and ^{13}C-NMR (150 MHz) of compound **3.2** in $CDCl_3$

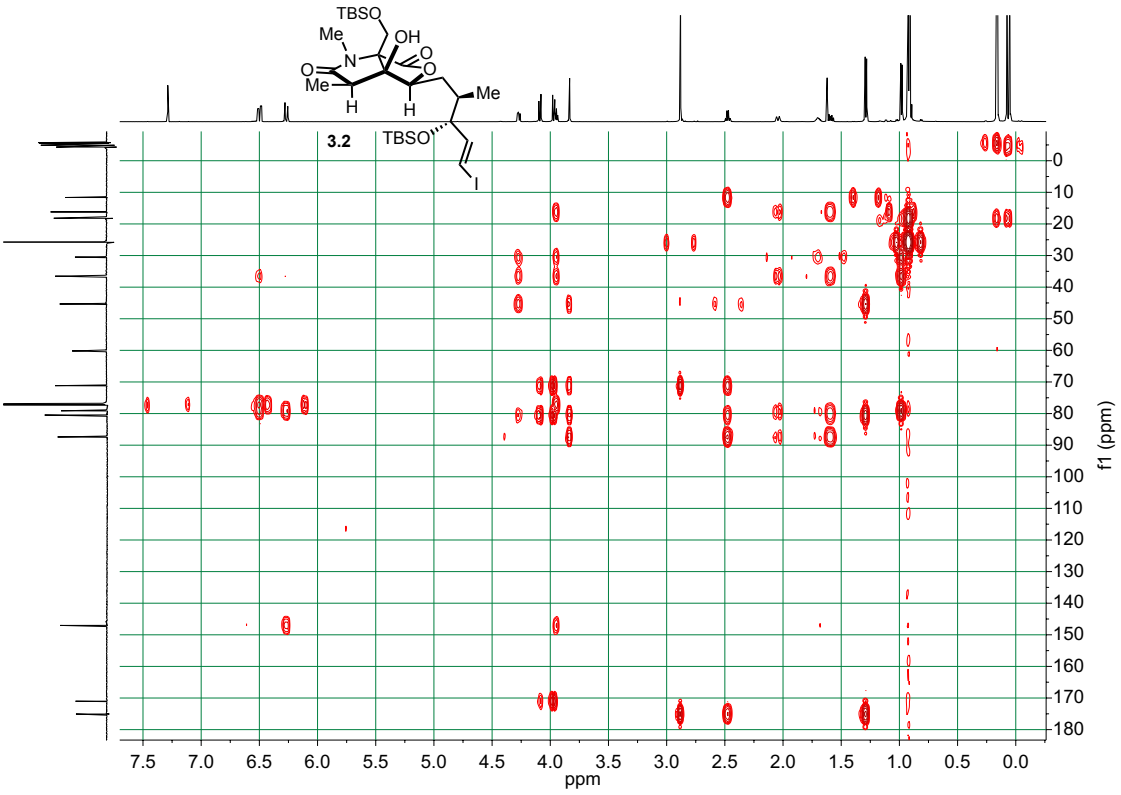

Figure A.27. ^{1}H-^{13}C HMBC 2D-NMR (150 MHz) of compound **3.2** in $CDCl_3$

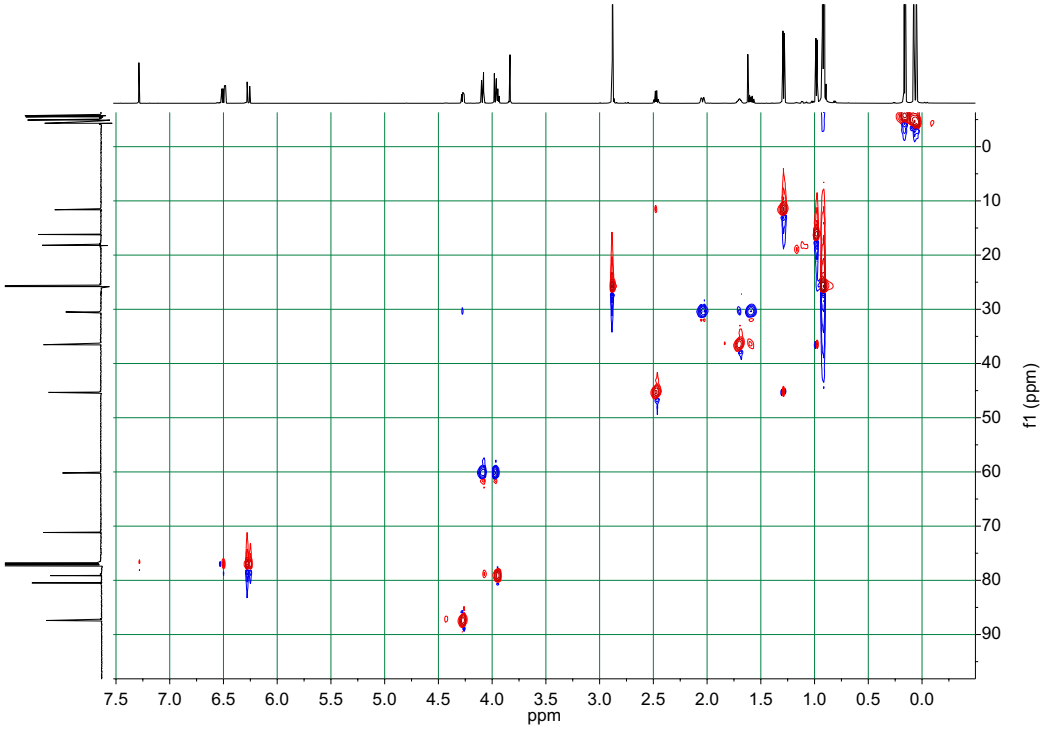

Figure A.28. ^{1}H-^{13}C HSQC 2D-NMR (150 MHz) of compound **3.2** in $CDCl_3$

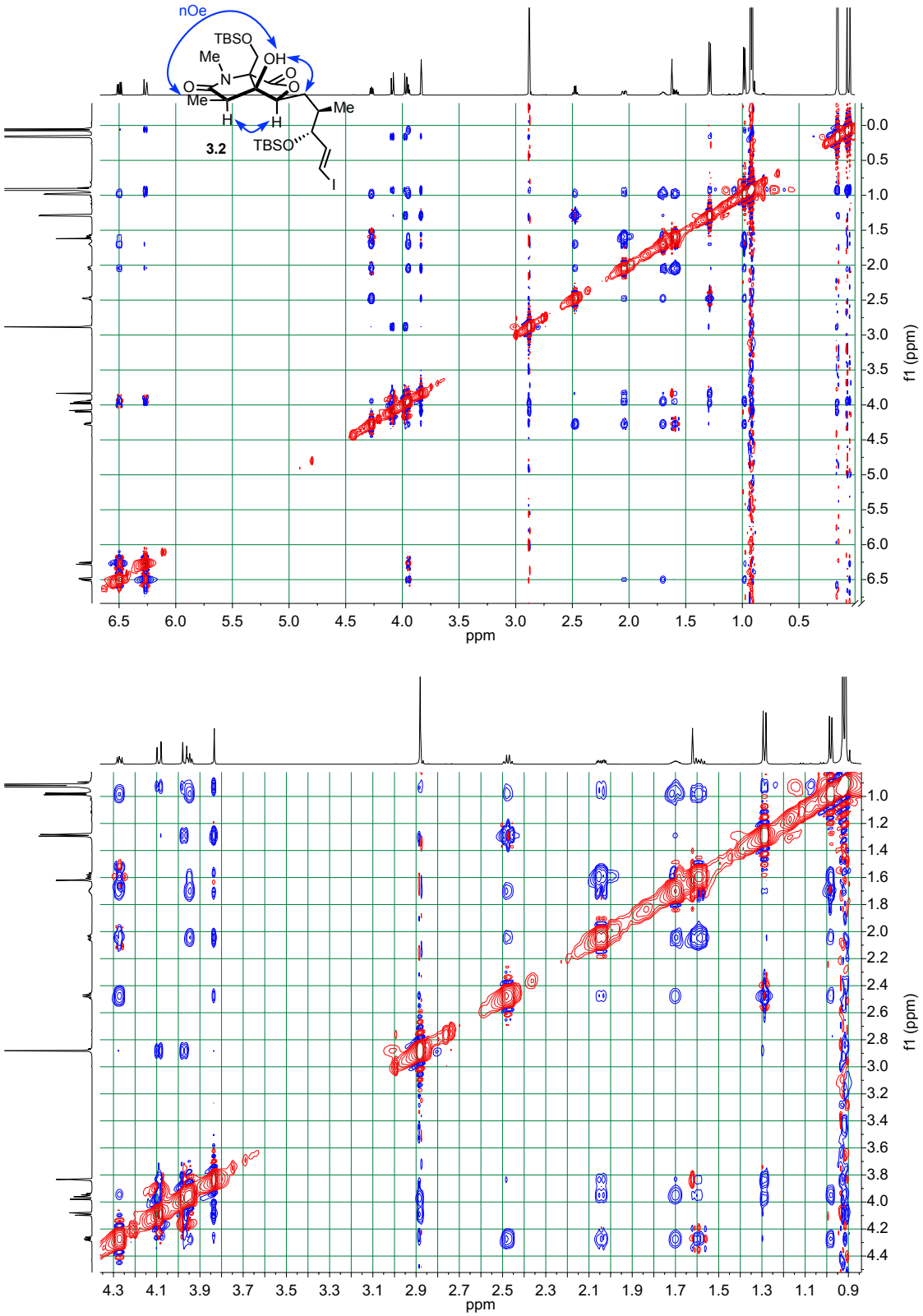

Figure A.29. ^{1}H-^{1}H NOESY 2D-NMR (600 MHz) of compound **3.2** in $CDCl_3$

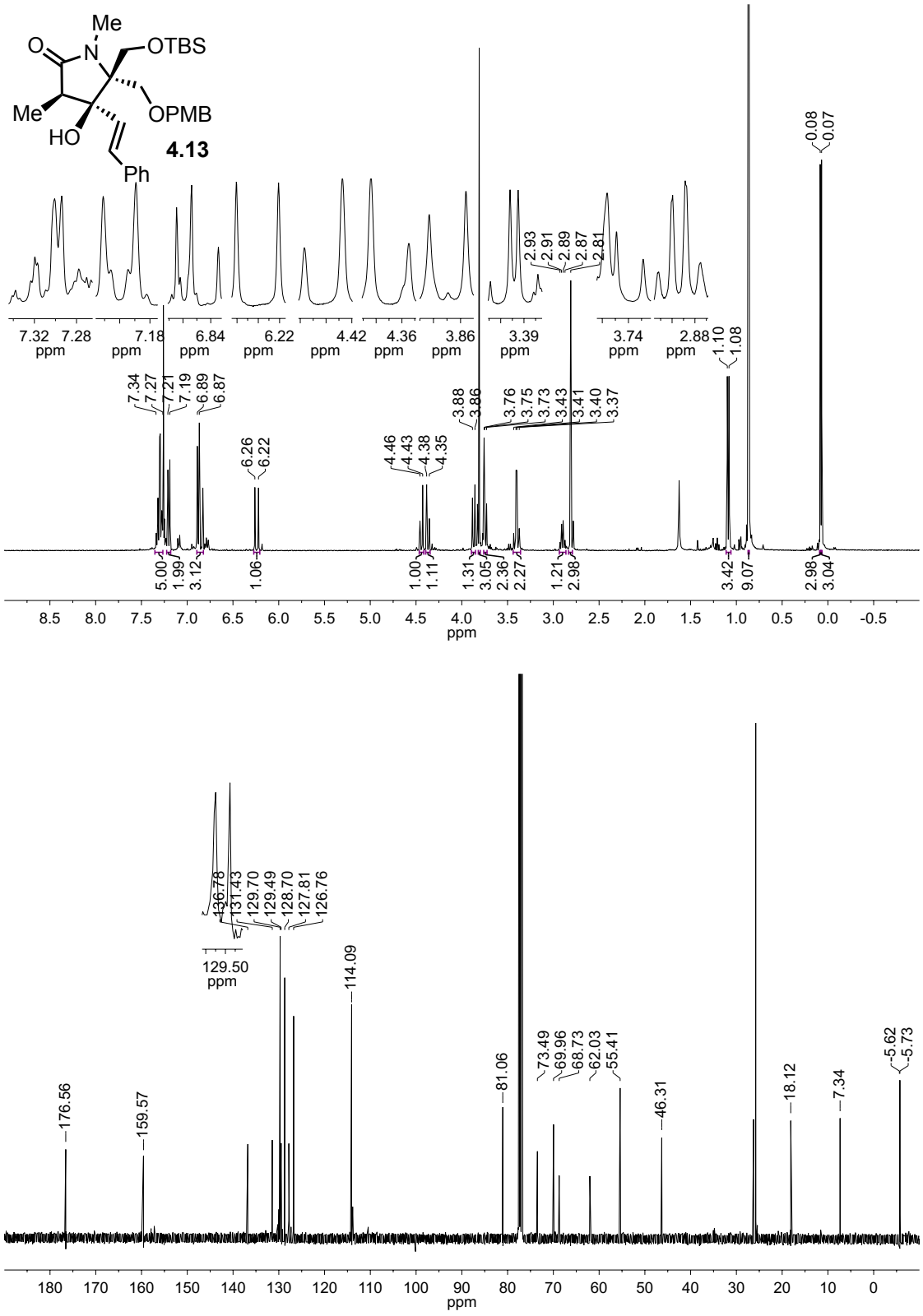

Figure A.30. ^{1}H-NMR (400 MHz) and ^{13}C-NMR (100 MHz) of compound **4.13** in $CDCl_3$

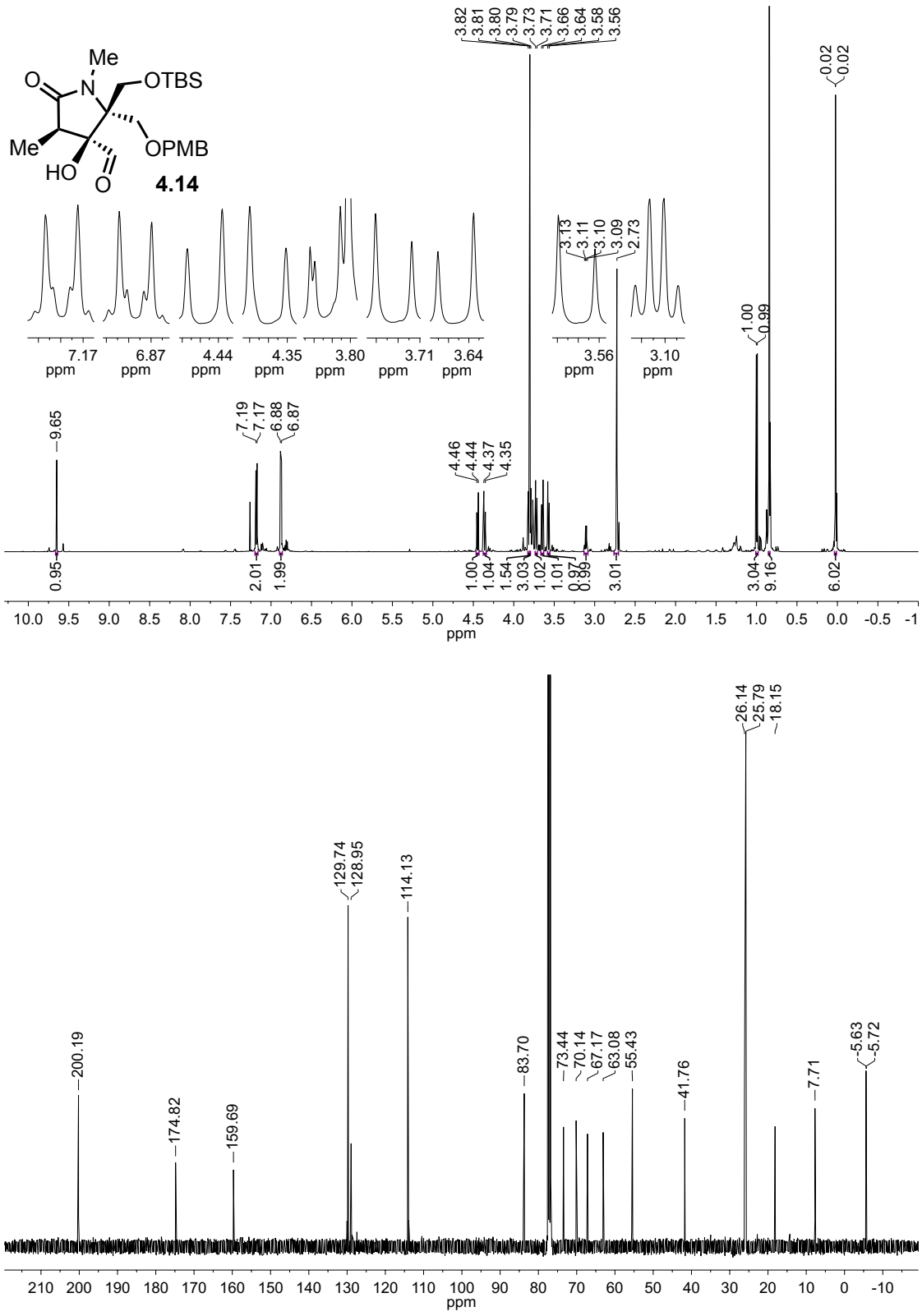

Figure A.31. ^{1}H-NMR (600 MHz) and ^{13}C-NMR (100 MHz) of compound **4.14** in $CDCl_3$

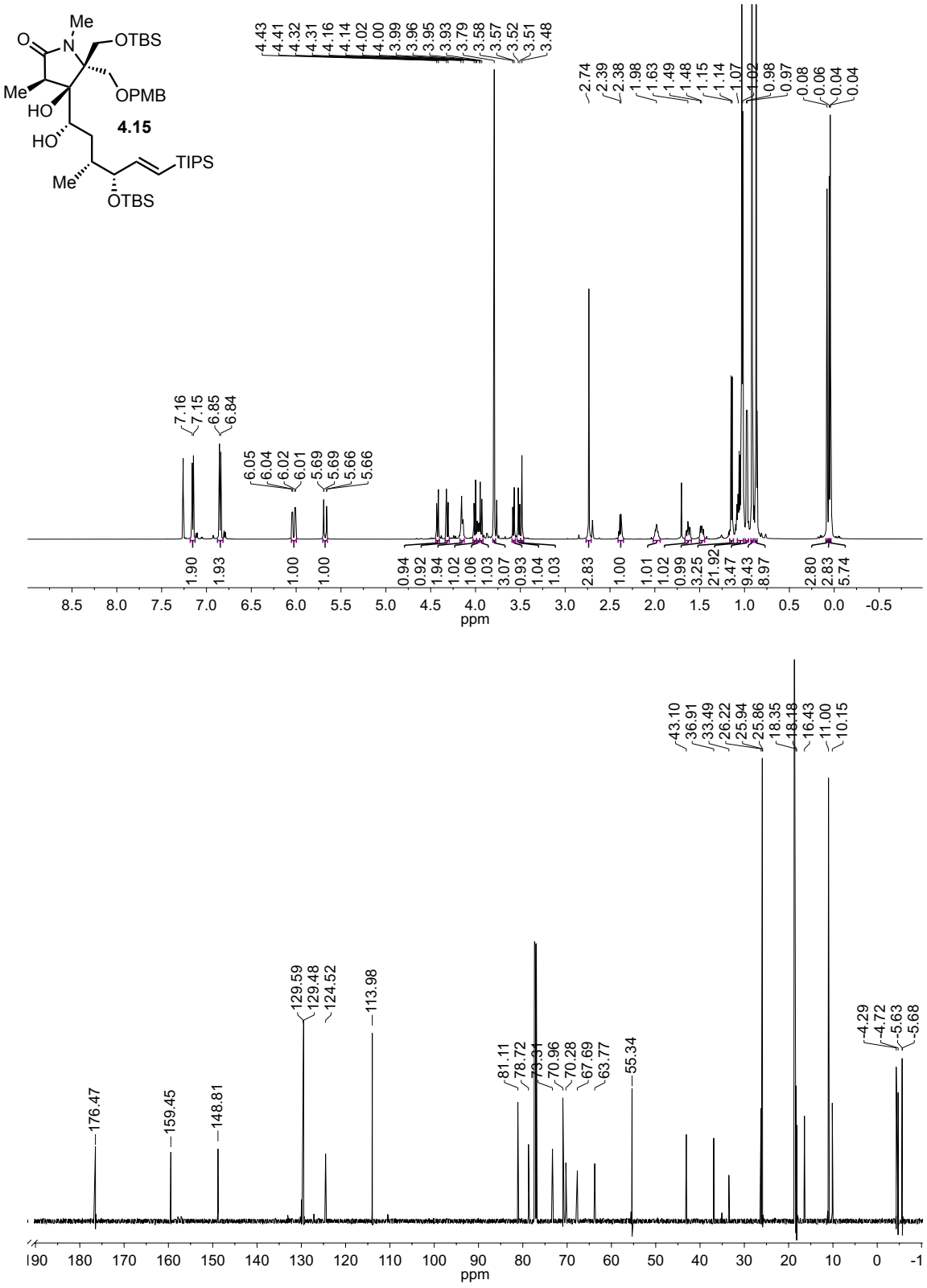

Figure A.32. ^{1}H-NMR (600 MHz) and ^{13}C-NMR (150 MHz) of compound **4.15** in $CDCl_3$

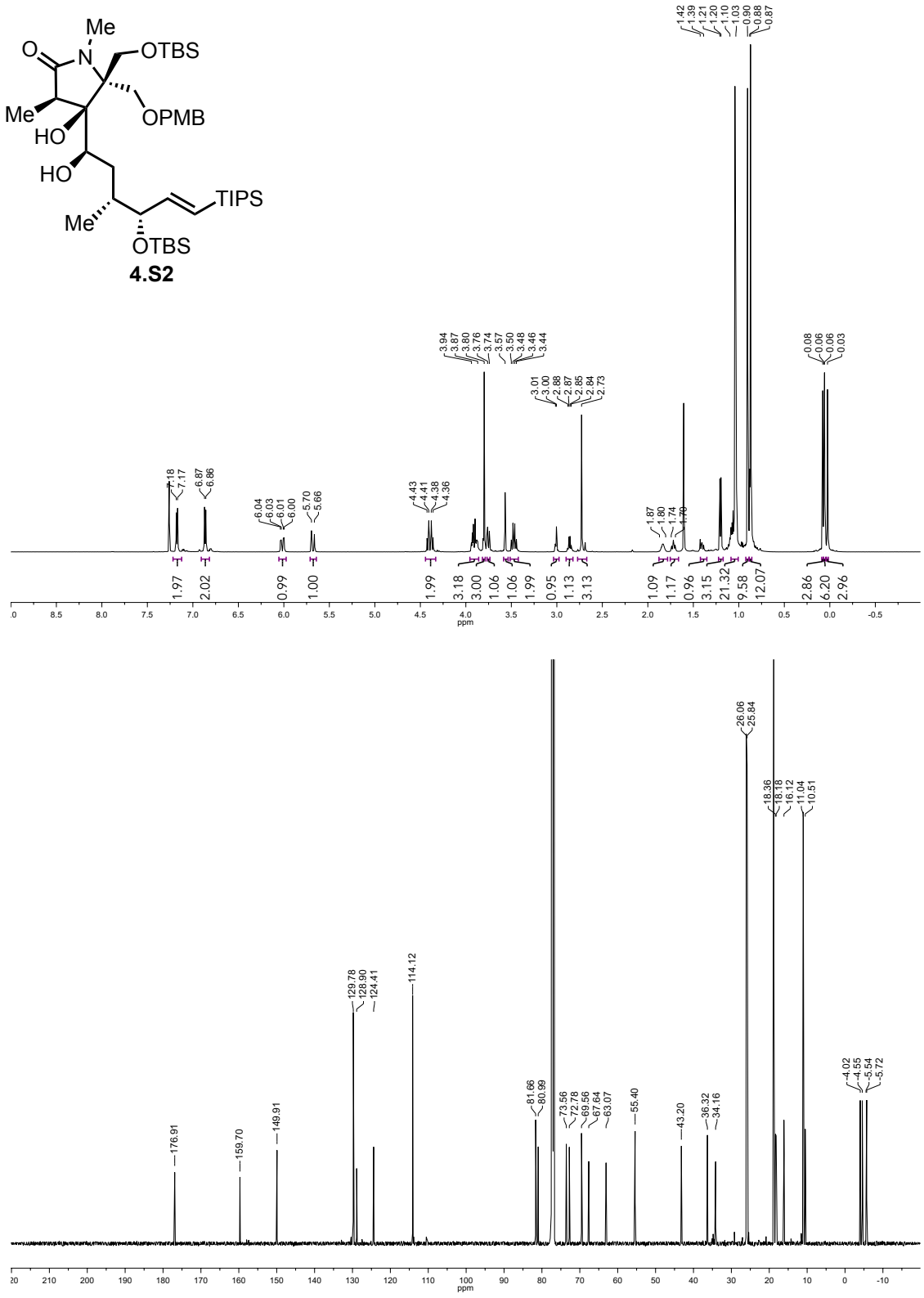

Figure A.33. ^{1}H-NMR (600 MHz) and ^{13}C-NMR (150 MHz) of compound **4.S2** in $CDCl_3$

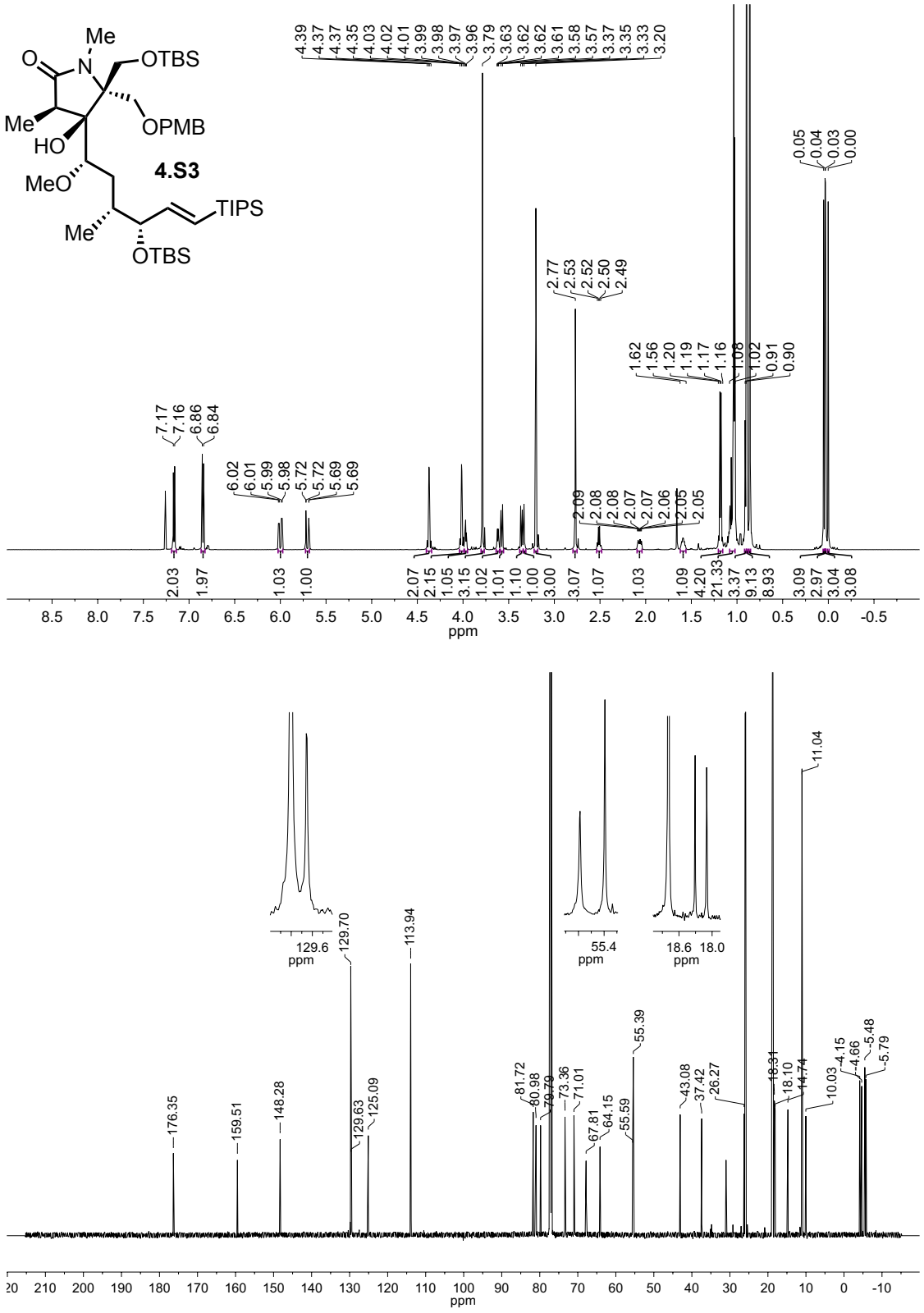

Figure A.34. ^{1}H-NMR (600 MHz) and ^{13}C-NMR (150 MHz) of compound **4.S3** in $CDCl_3$

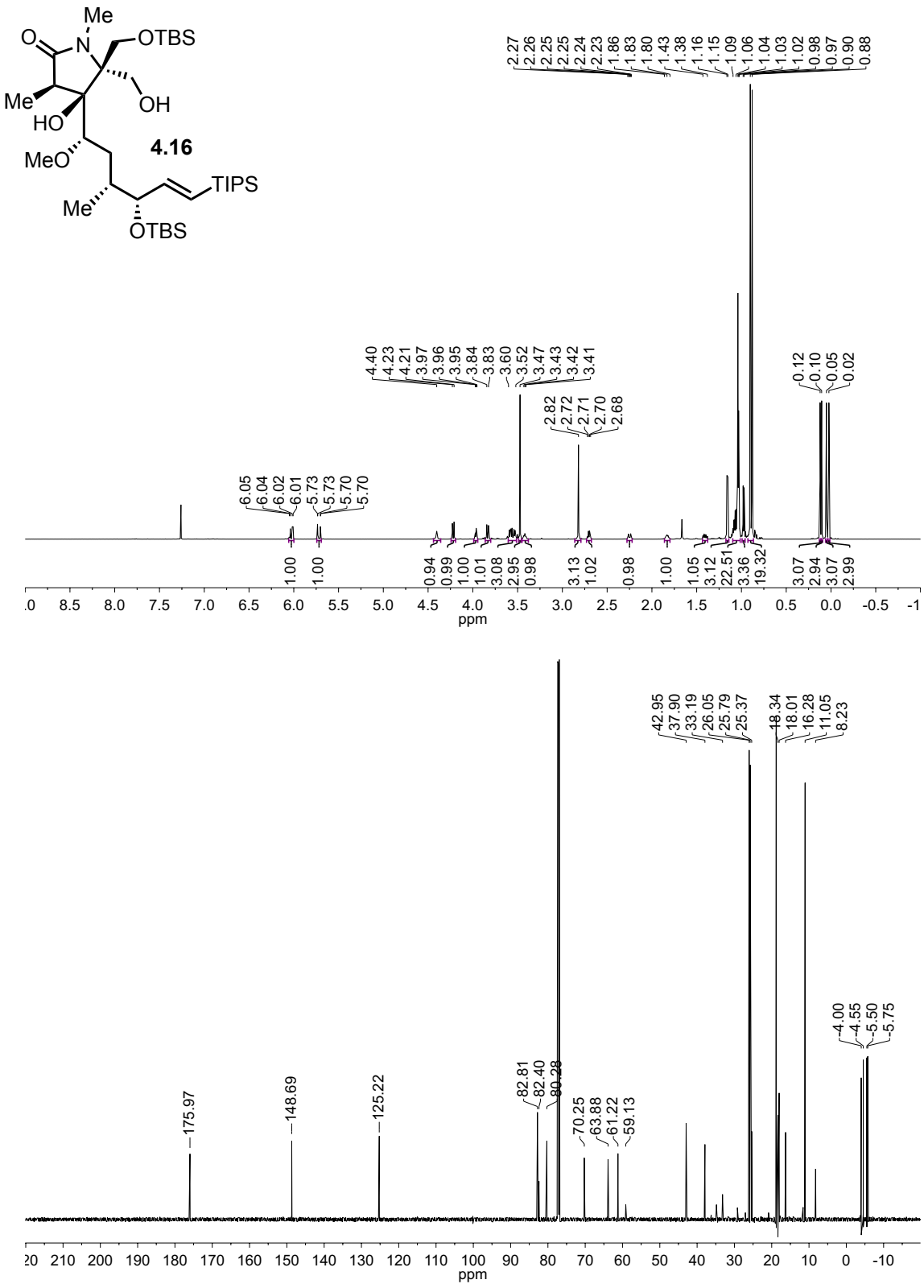

Figure A.35. ^{1}H-NMR (600 MHz) and ^{13}C-NMR (150 MHz) of compound **4.16** in $CDCl_3$

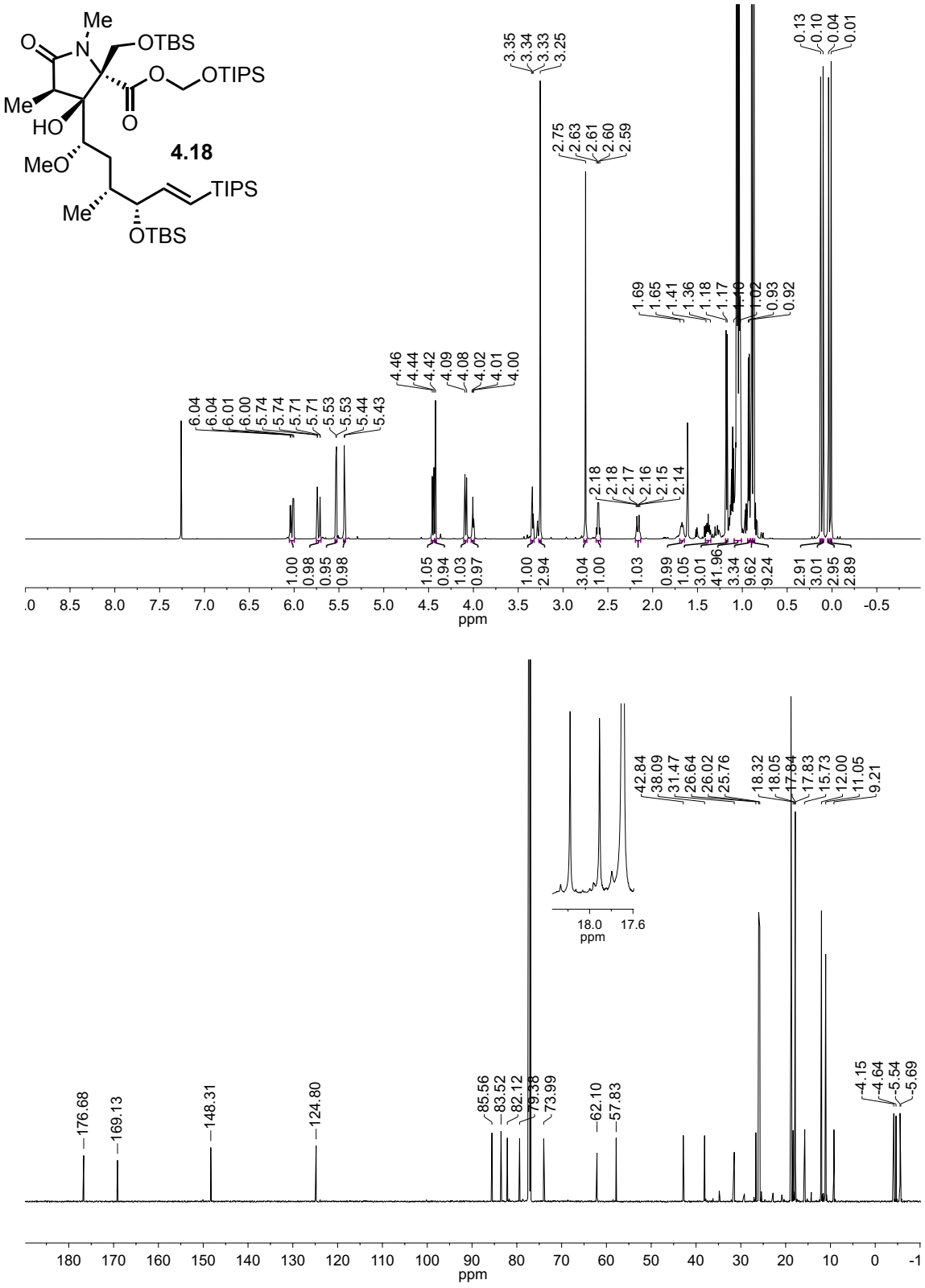

Figure A.36. ^{1}H-NMR (600 MHz) and ^{13}C-NMR (150 MHz) of compound **4.18** in $CDCl_3$

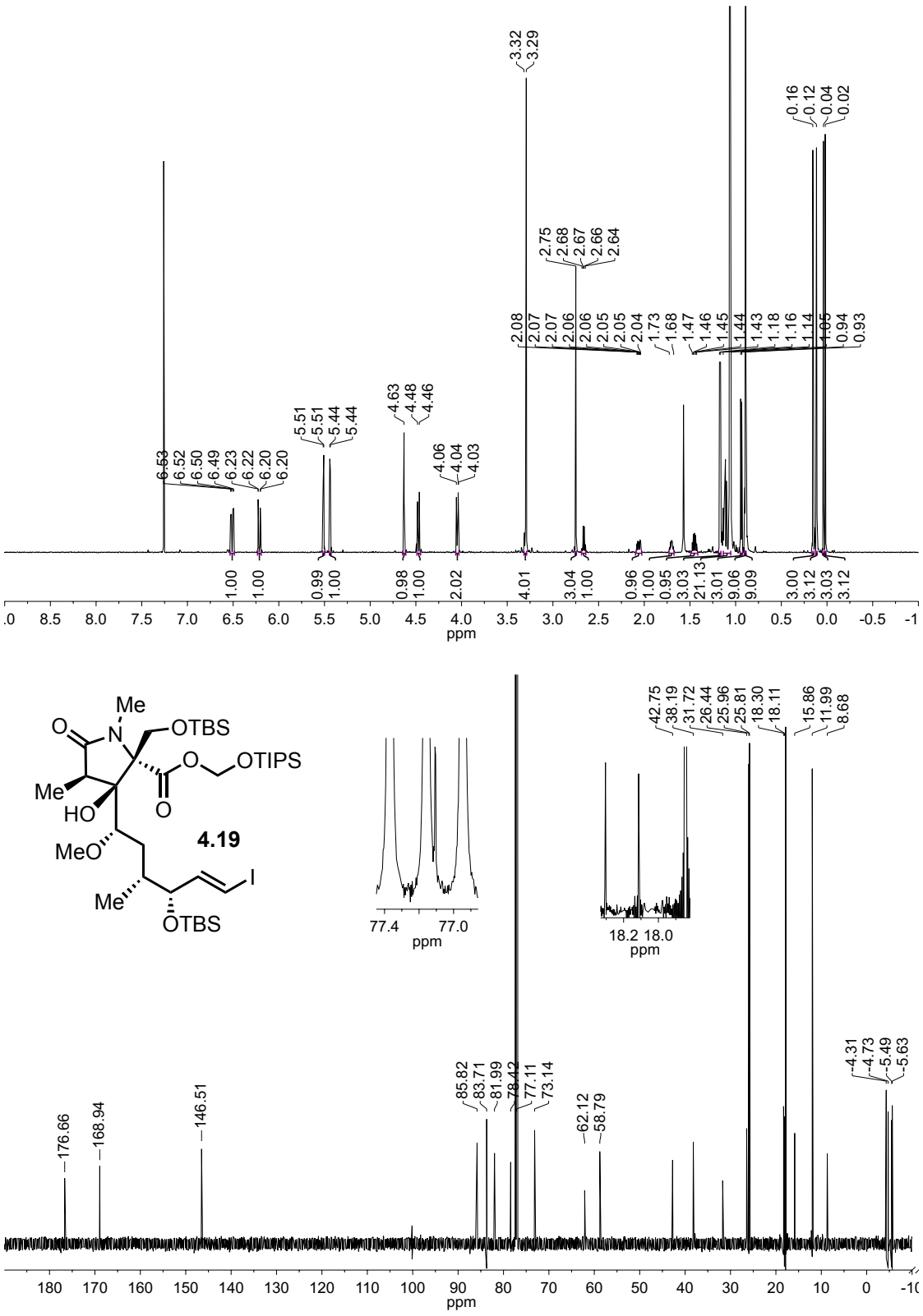

Figure A.37. ^{1}H-NMR (600 MHz) and ^{13}C-NMR (150 MHz) of compound **4.19** in $CDCl_3$

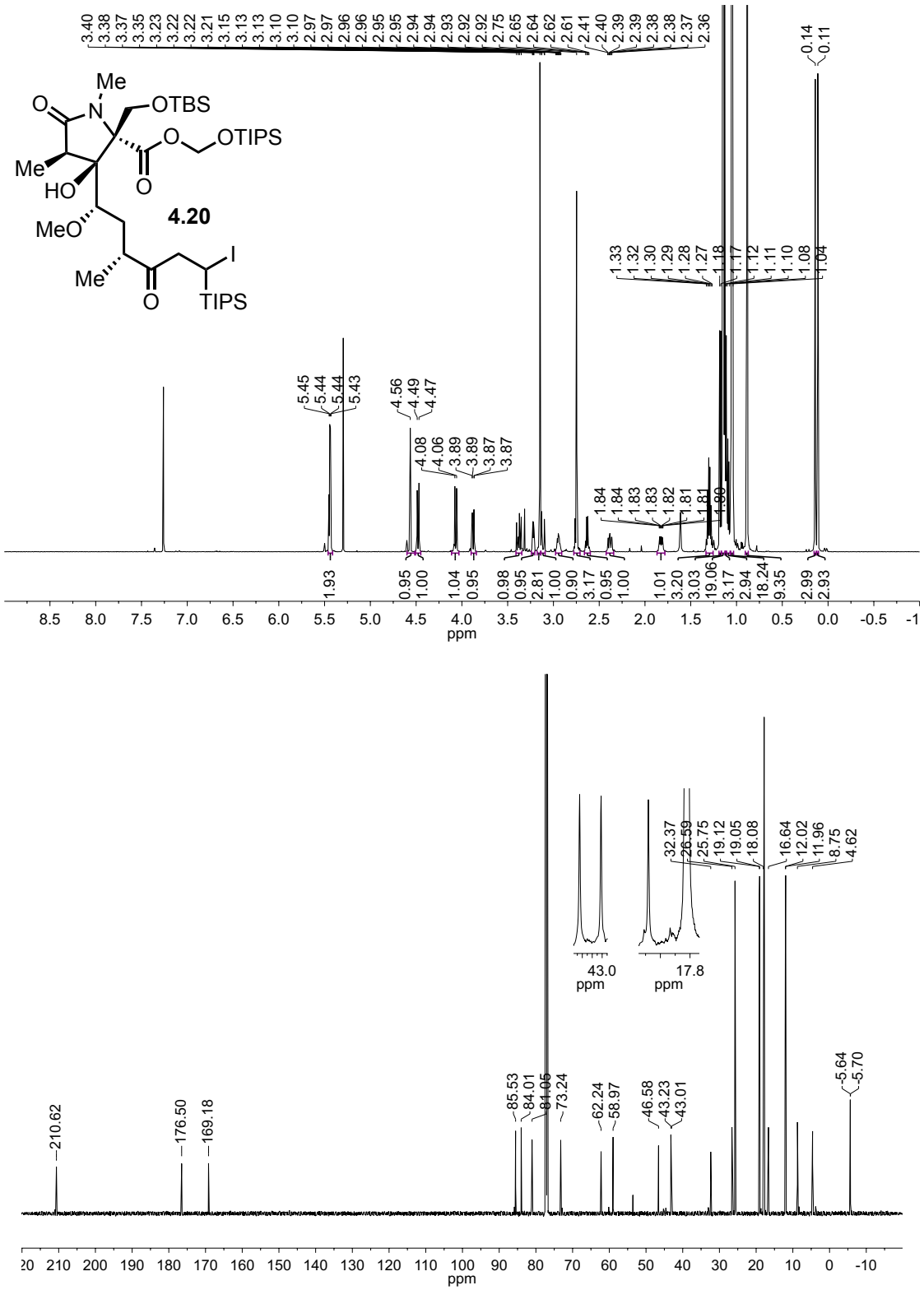

Figure A.38. ^{1}H-NMR (600 MHz) and ^{13}C-NMR (150 MHz) of compound **4.20** in $CDCl_3$

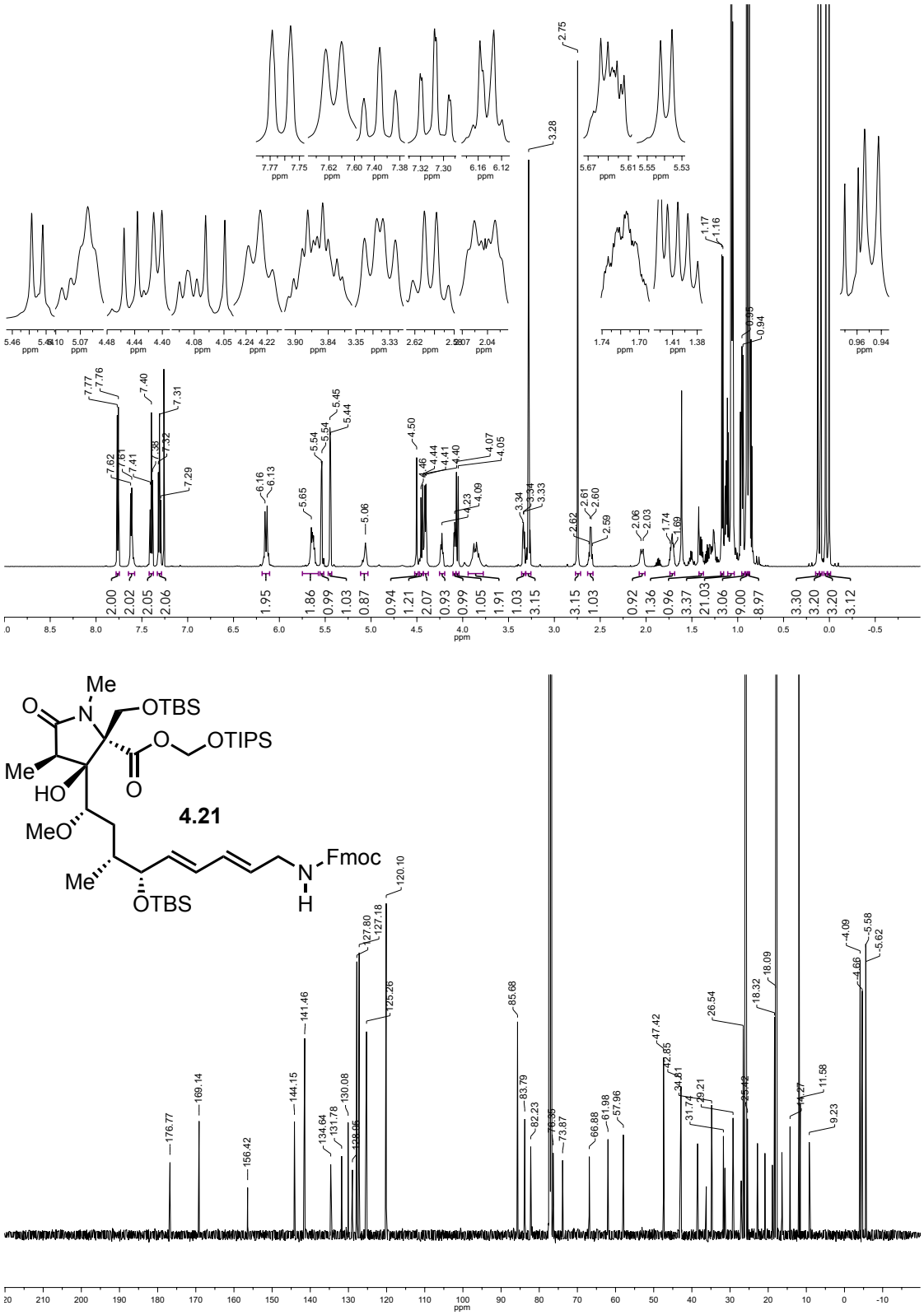

Figure A.39. ^{1}H-NMR (600 MHz) and ^{13}C-NMR (150 MHz) of compound **4.21** in $CDCl_3$

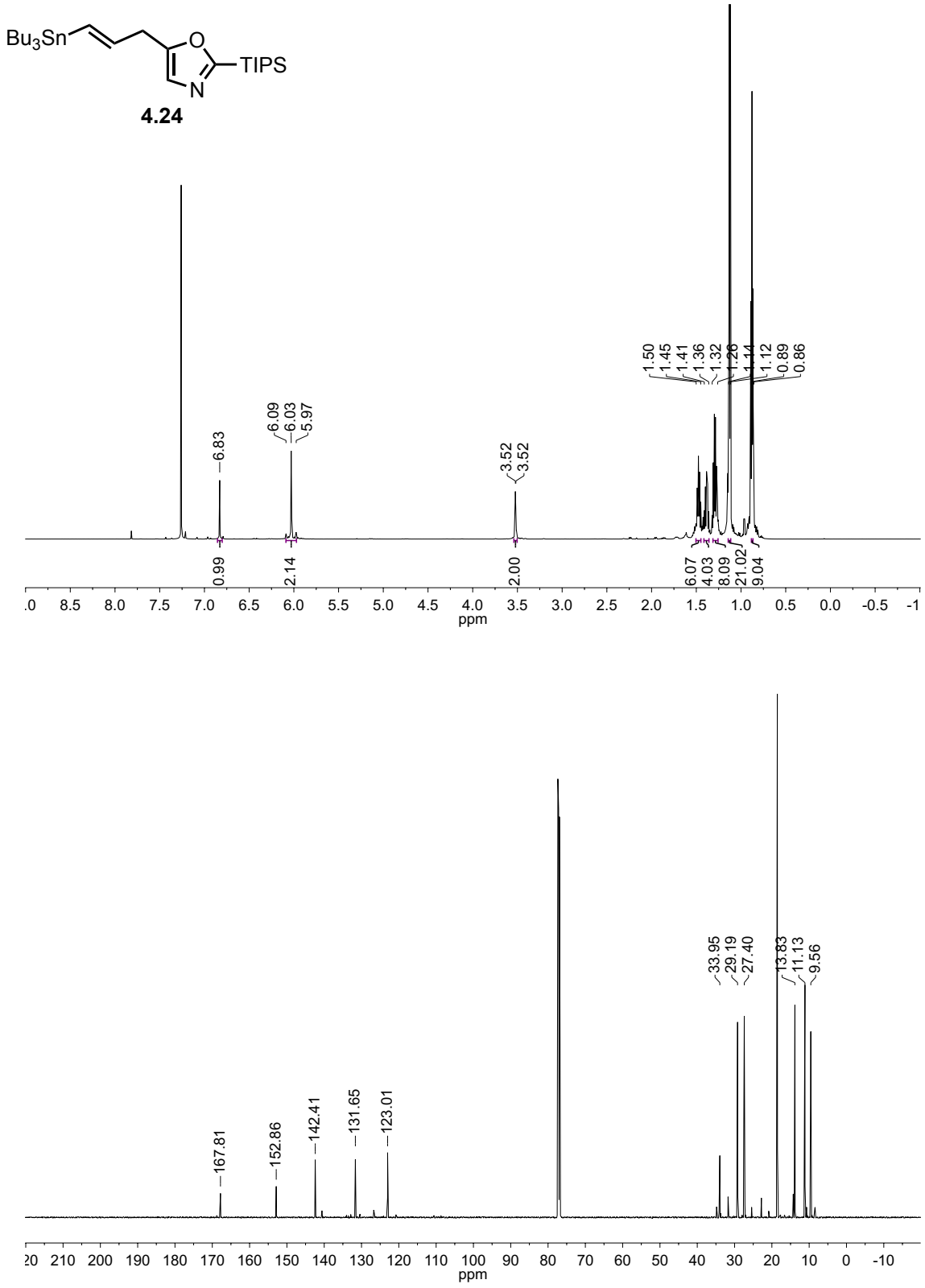

Figure A.40. ^{1}H-NMR (600 MHz) and ^{13}C-NMR (150 MHz) of compound **4.24** in $CDCl_3$

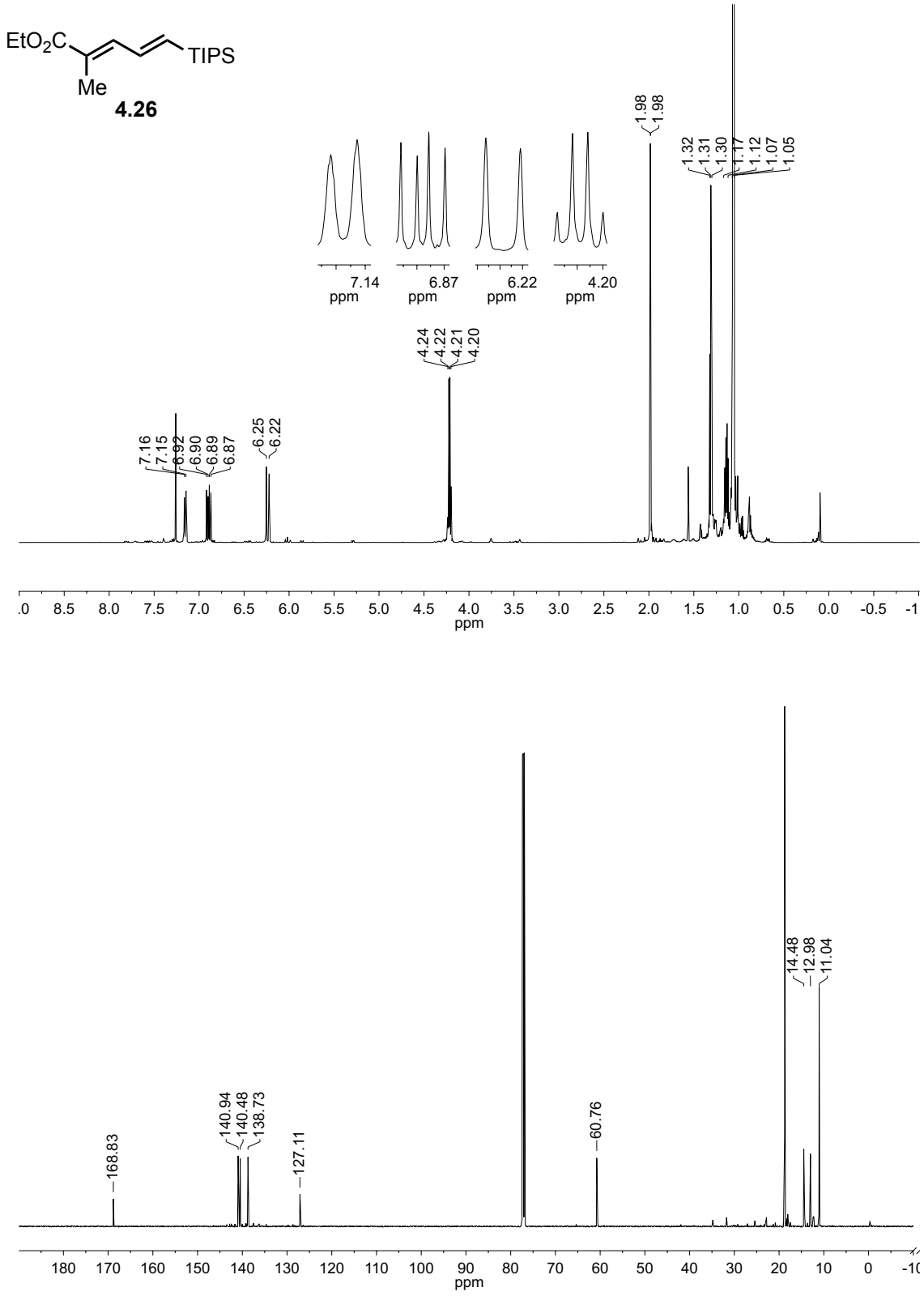

Figure A.41. ^{1}H-NMR (600 MHz) and ^{13}C-NMR (150 MHz) of compound **4.26** in $CDCl_3$

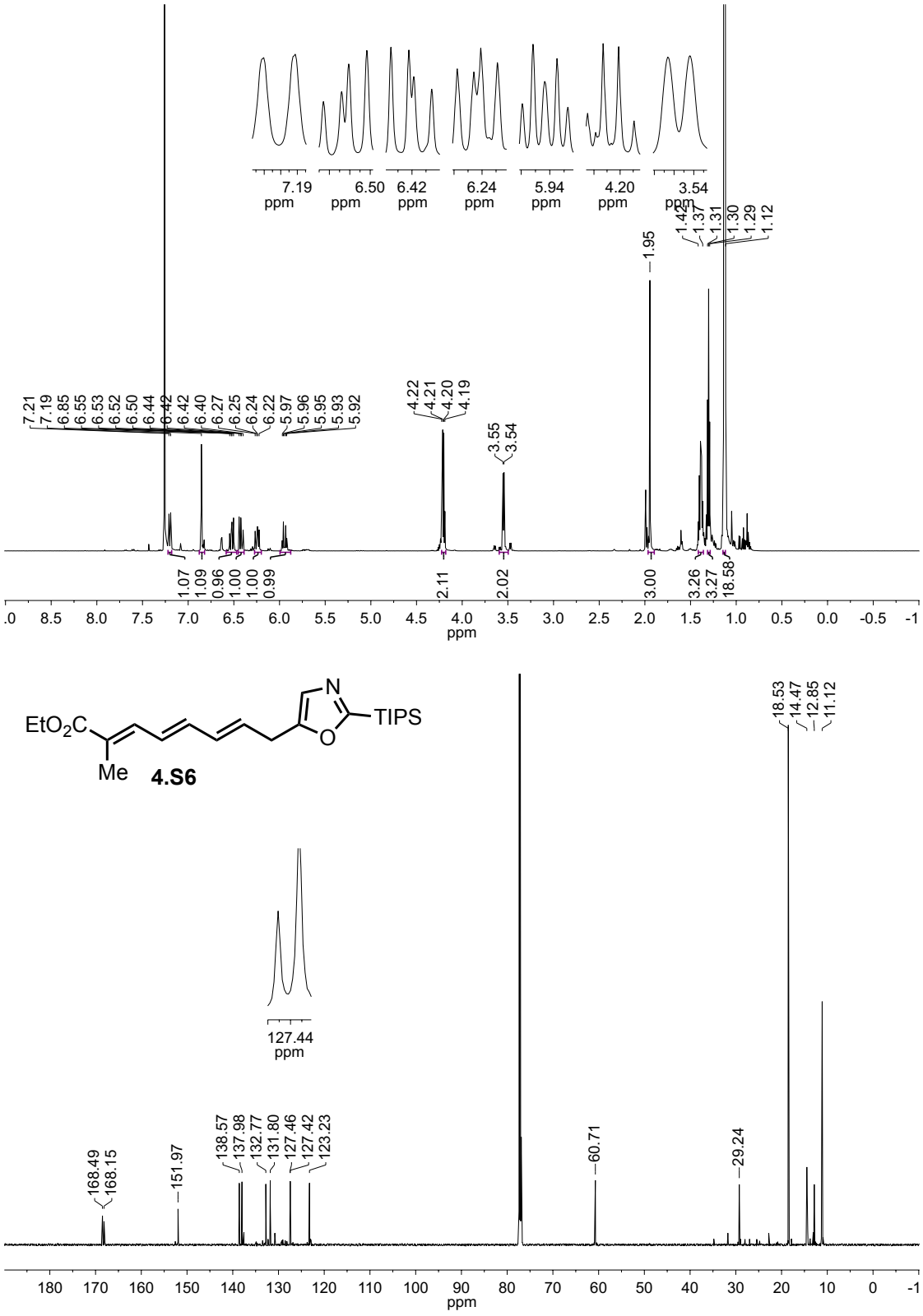

Figure A.42. ^{1}H-NMR (600 MHz) and ^{13}C-NMR (150 MHz) of compound **4.S6** in $CDCl_3$

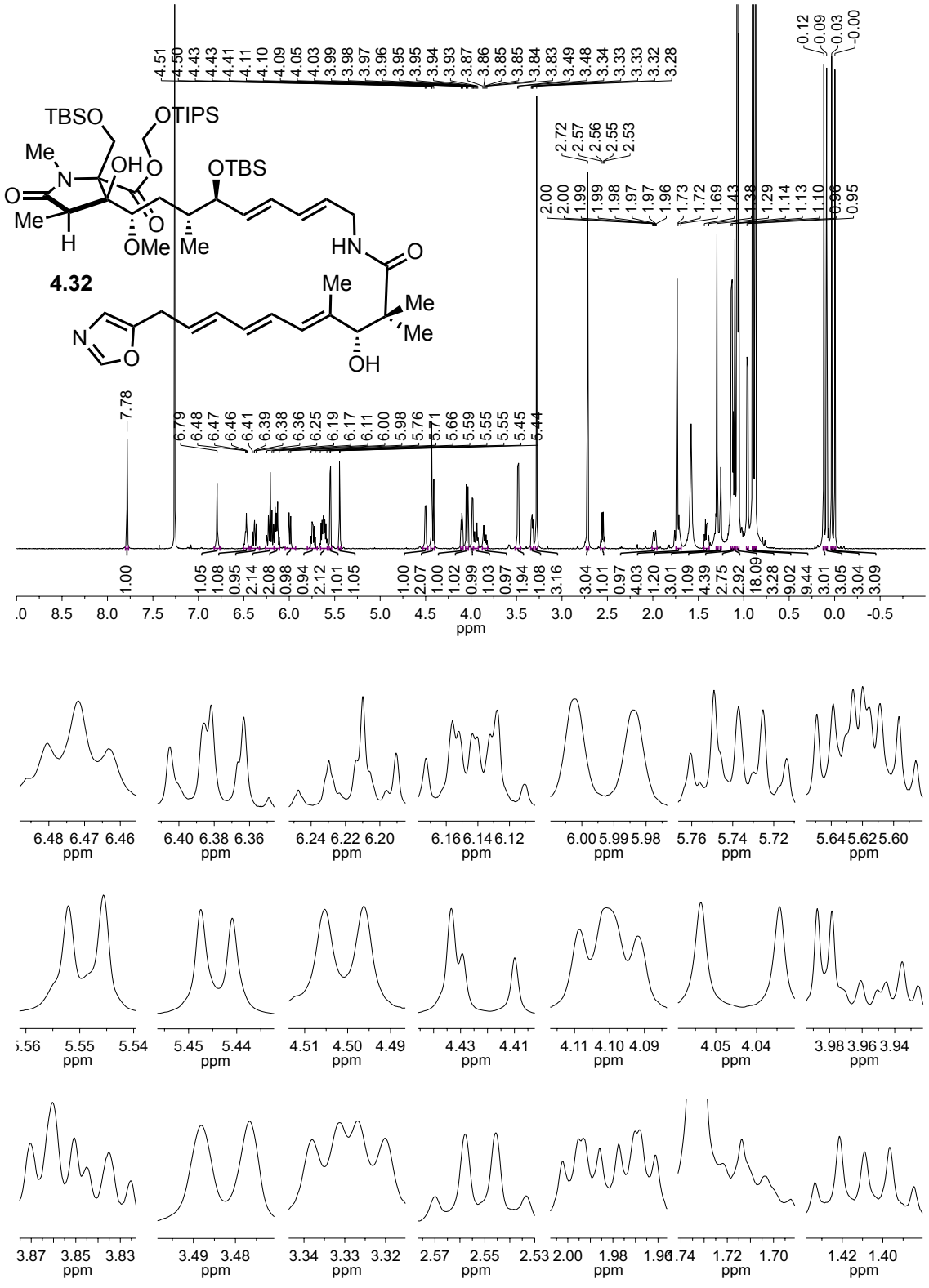

Figure A.43. ^{1}H-NMR (600 MHz) of compound **4.32** in $CDCl_3$ with expansions

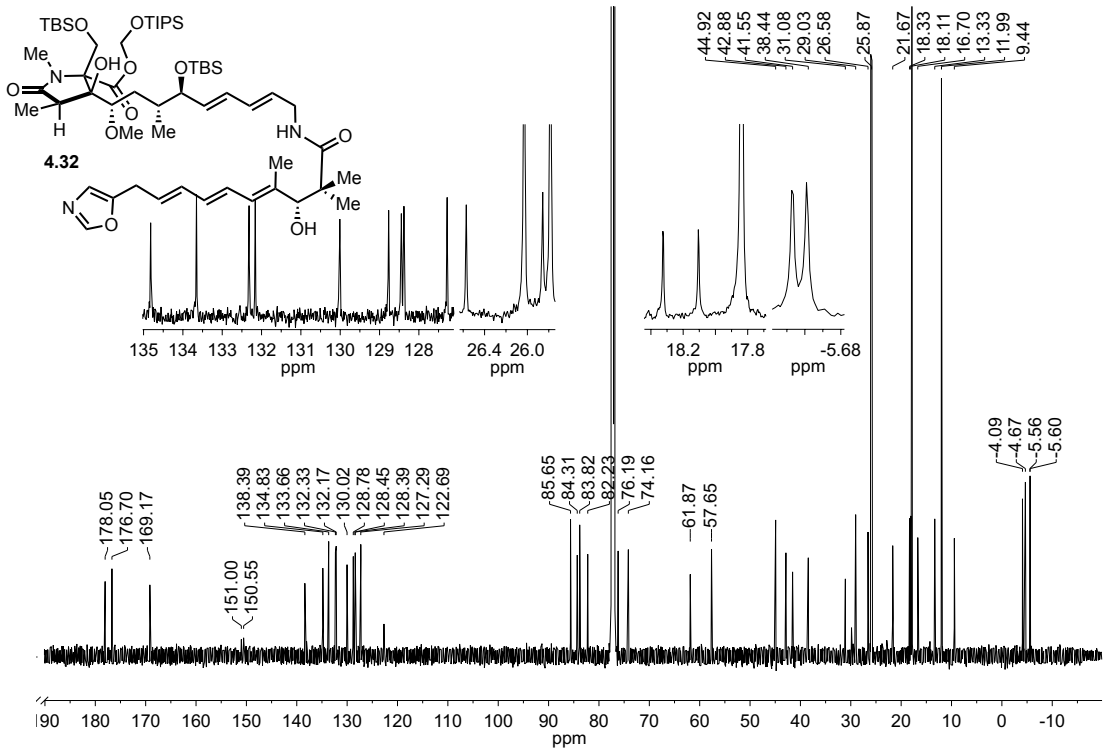

Figure A.44. ^{13}C-NMR (150 MHz) of compound **4.32** in $CDCl_3$

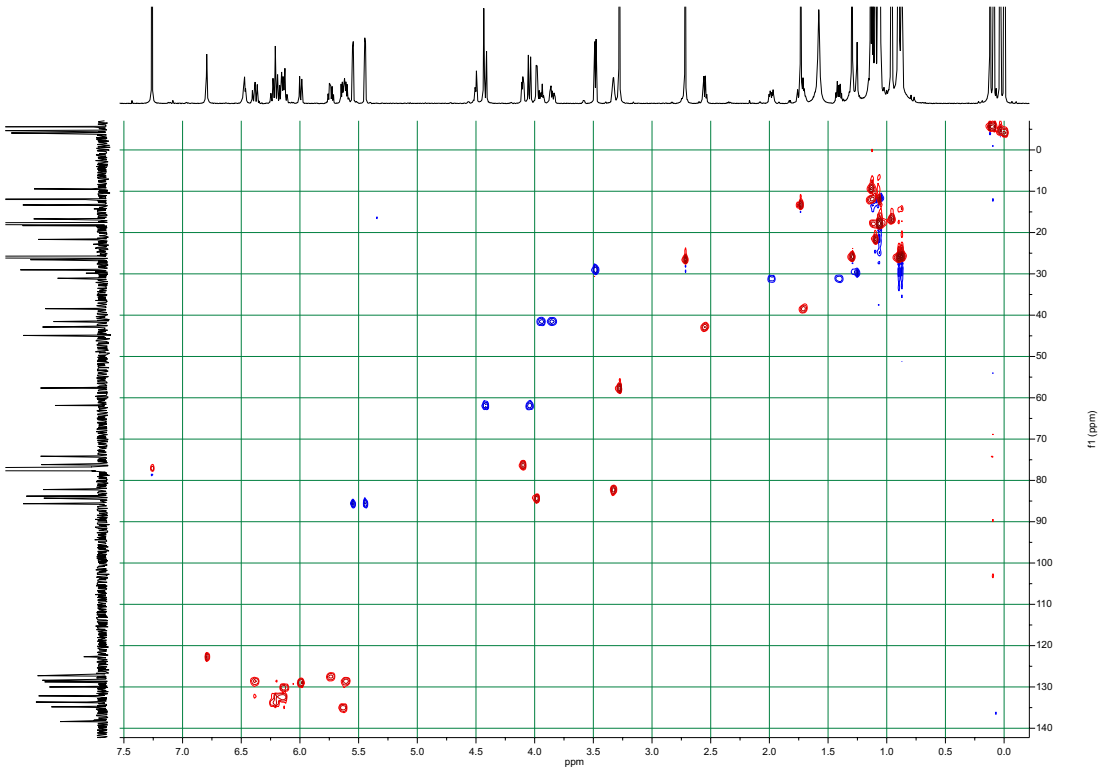

Figure A.45. ^{1}H-^{13}C HSQC 2D-NMR (150 MHz) of compound **4.32** in $CDCl_3$

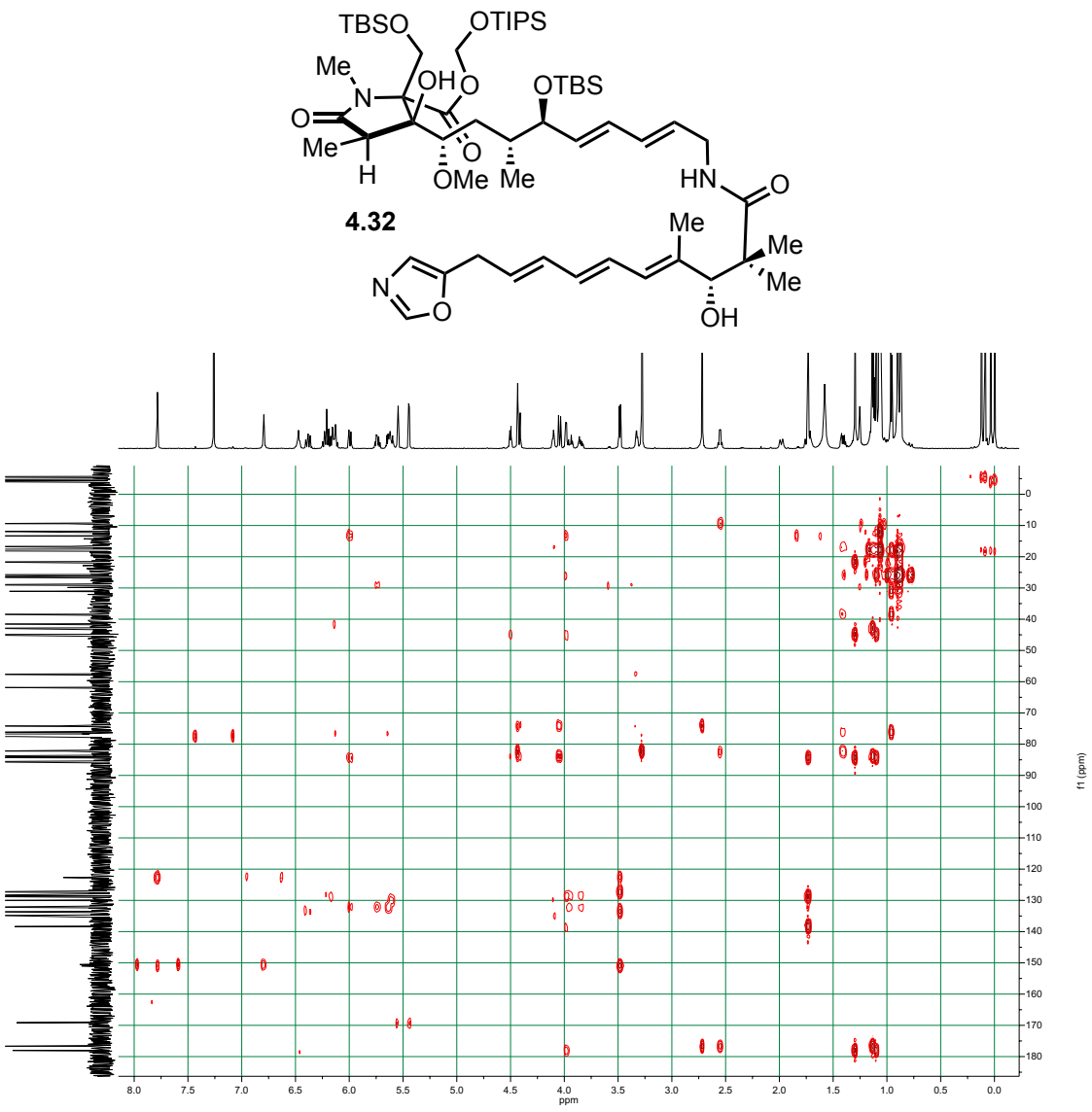

Figure A.46. ^{1}H-^{13}C HMBC 2D-NMR (150 MHz) of compound **4.32** in $CDCl_3$

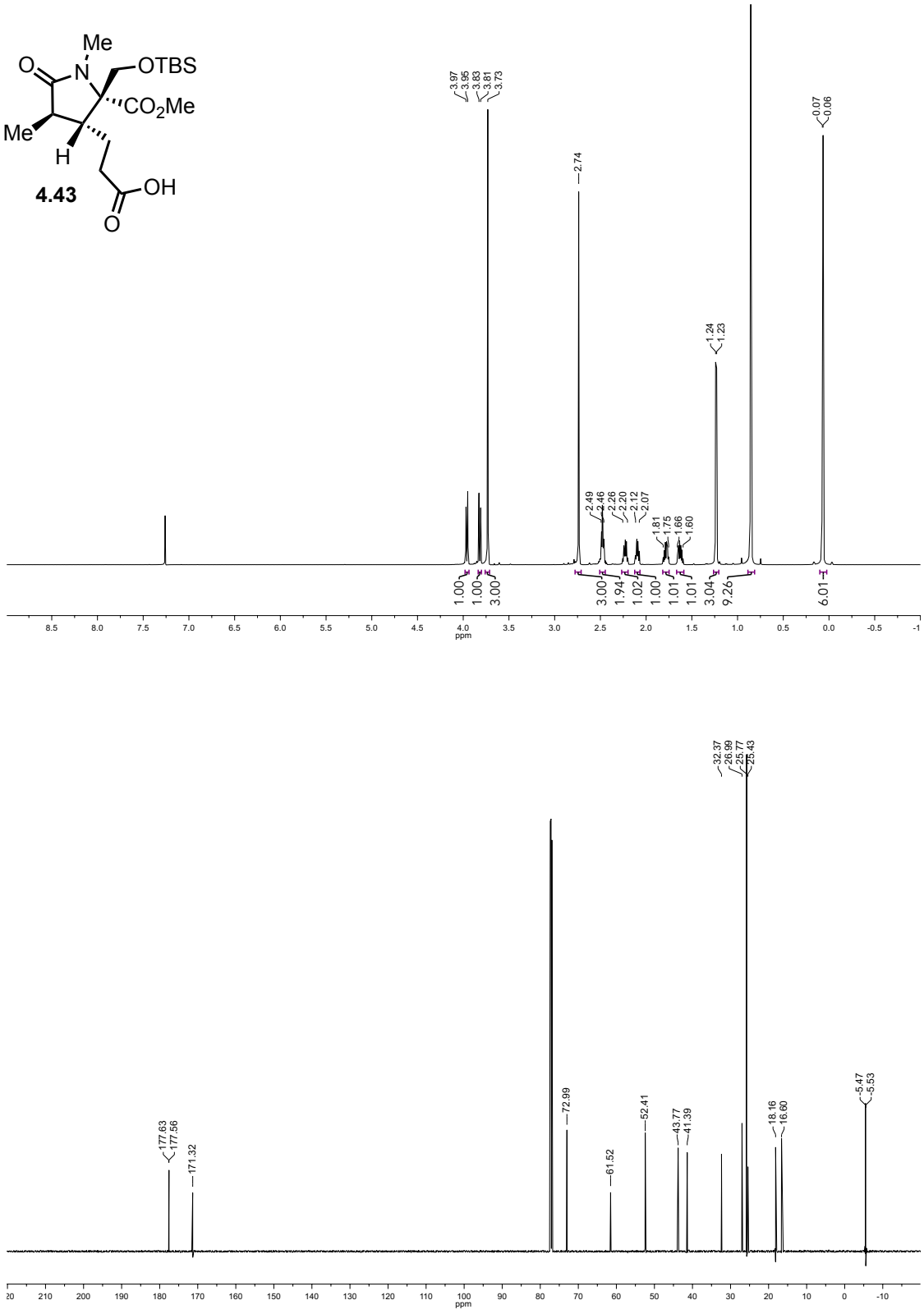

Figure A.47. ^{1}H-NMR (600 MHz) and ^{13}C-NMR (150 MHz) of compound **4.43** in $CDCl_3$

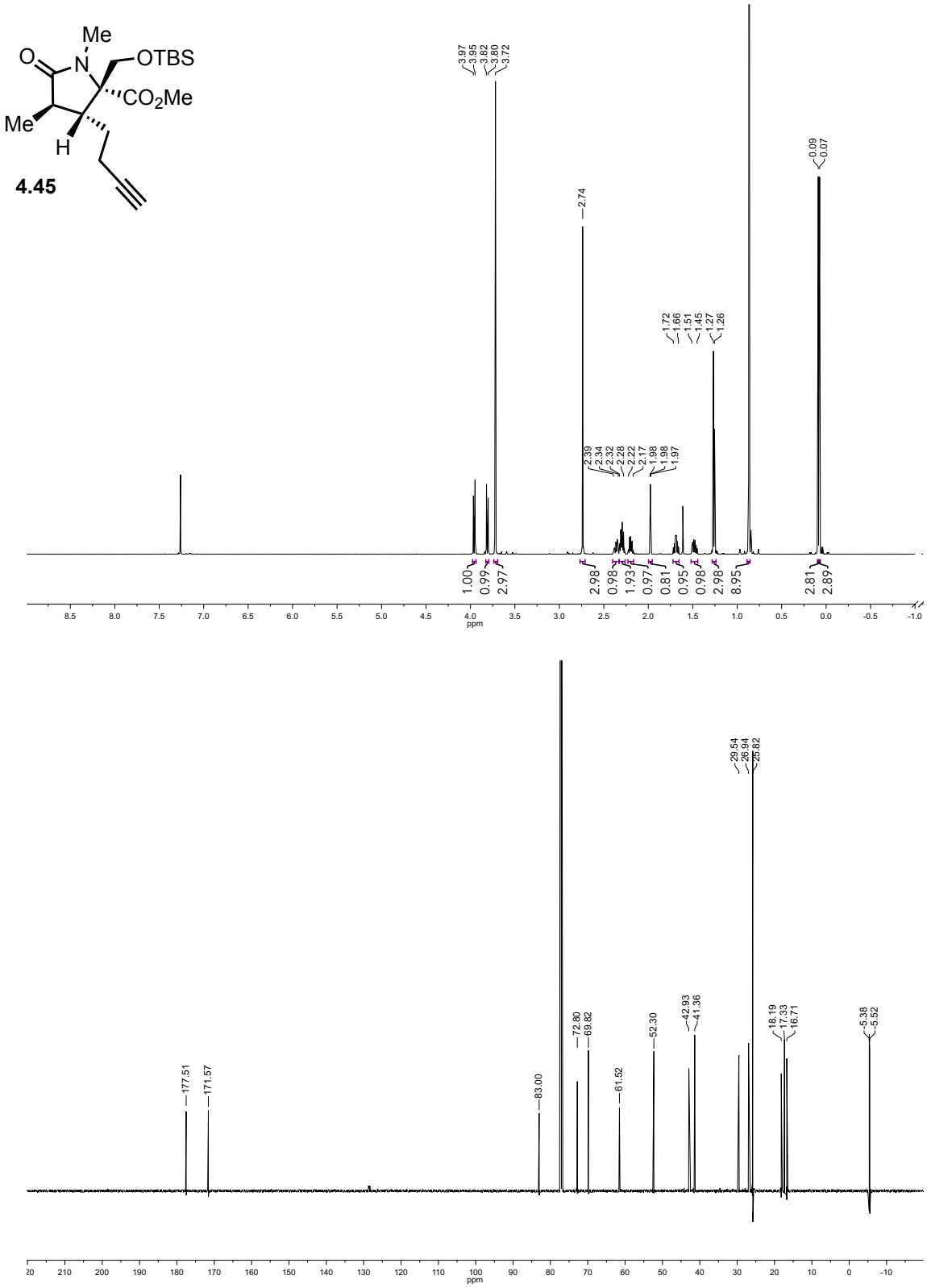

Figure A.48. ^{1}H-NMR (600 MHz) and ^{13}C-NMR (150 MHz) of compound **4.45** in $CDCl_3$

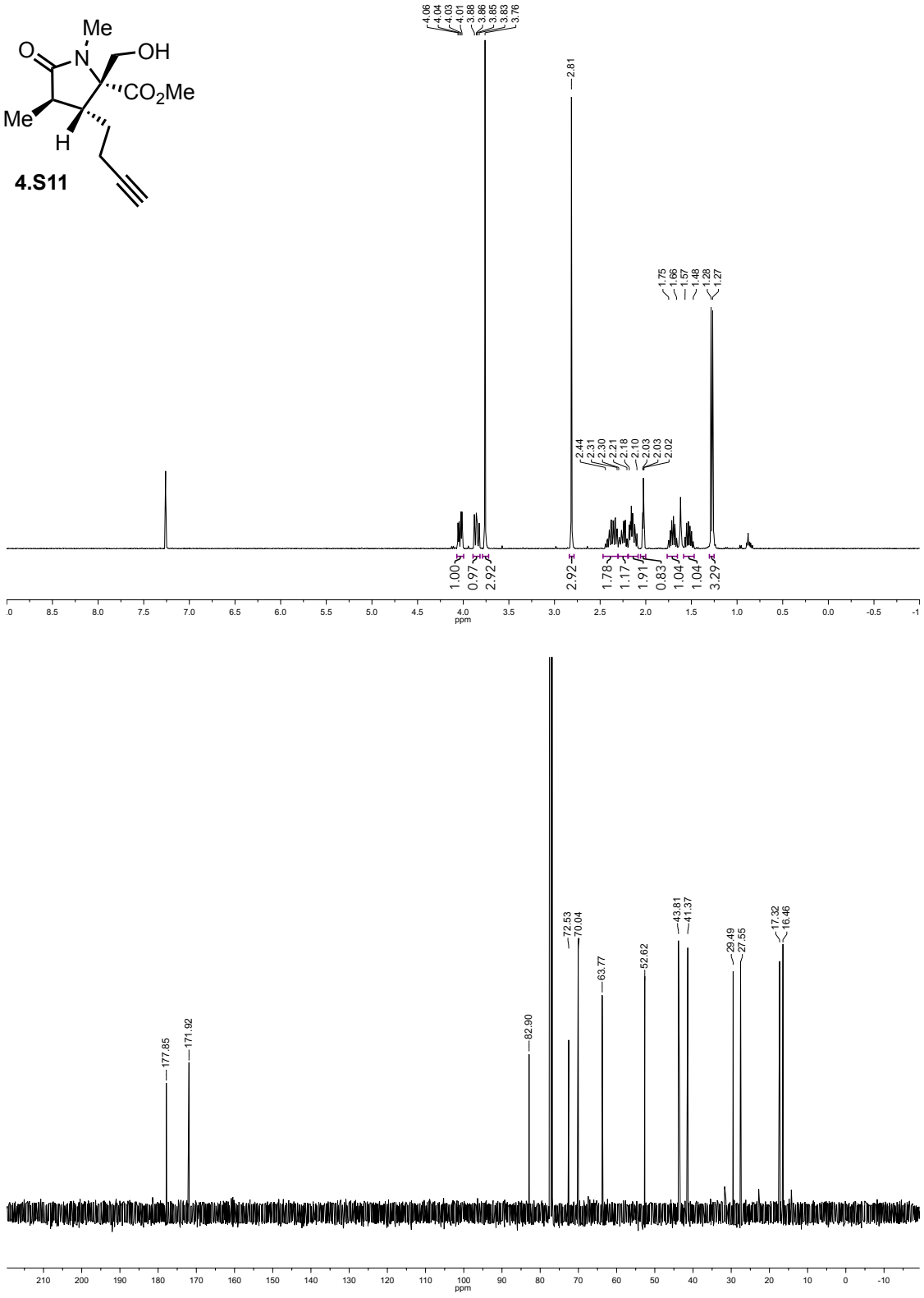

Figure A.49. ^{1}H-NMR (600 MHz) and ^{13}C-NMR (150 MHz) of compound **4.S11** in $CDCl_3$

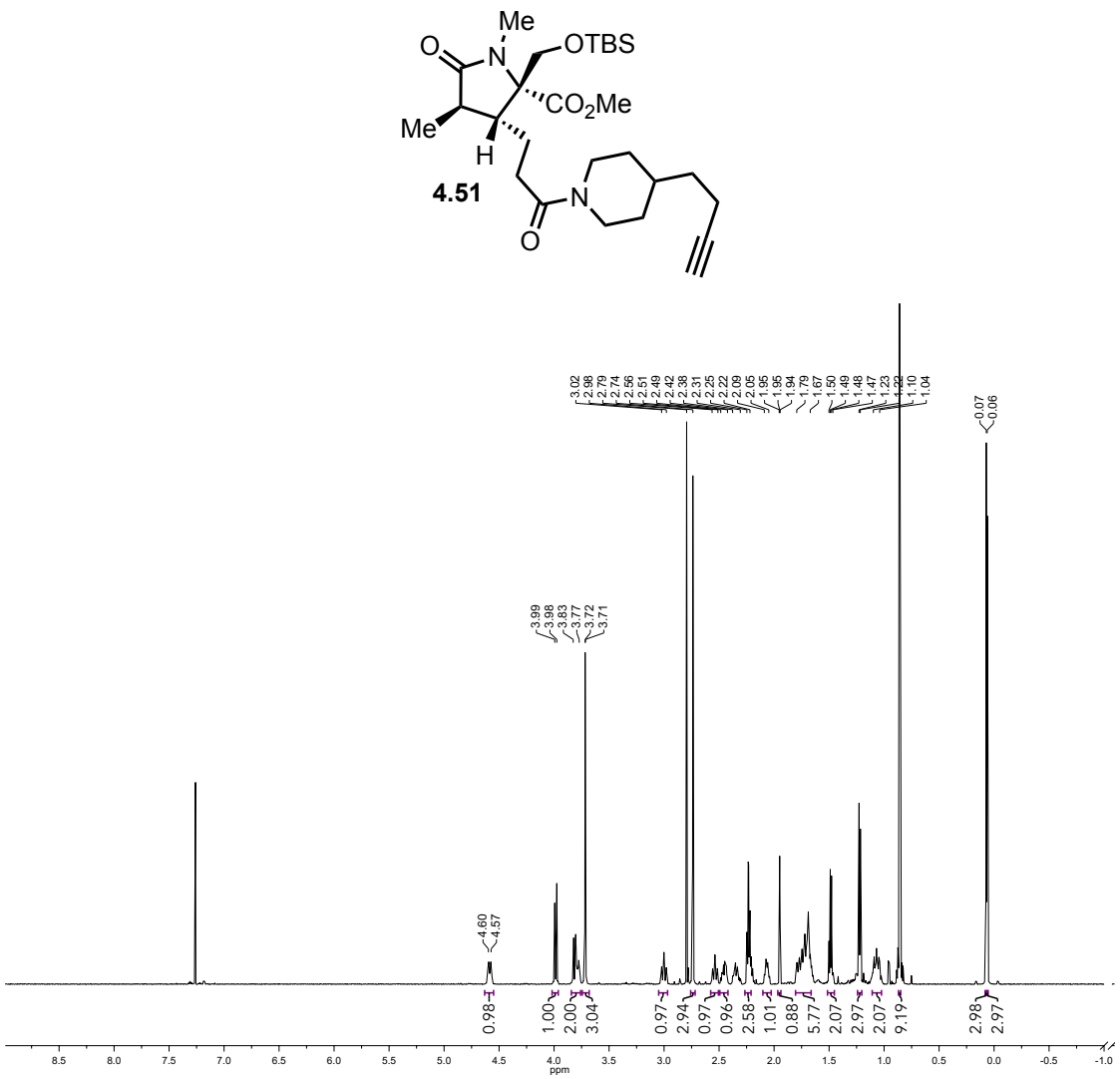

Figure A.50. ^{1}H-NMR (600 MHz) of compound **4.51** in $CDCl_3$

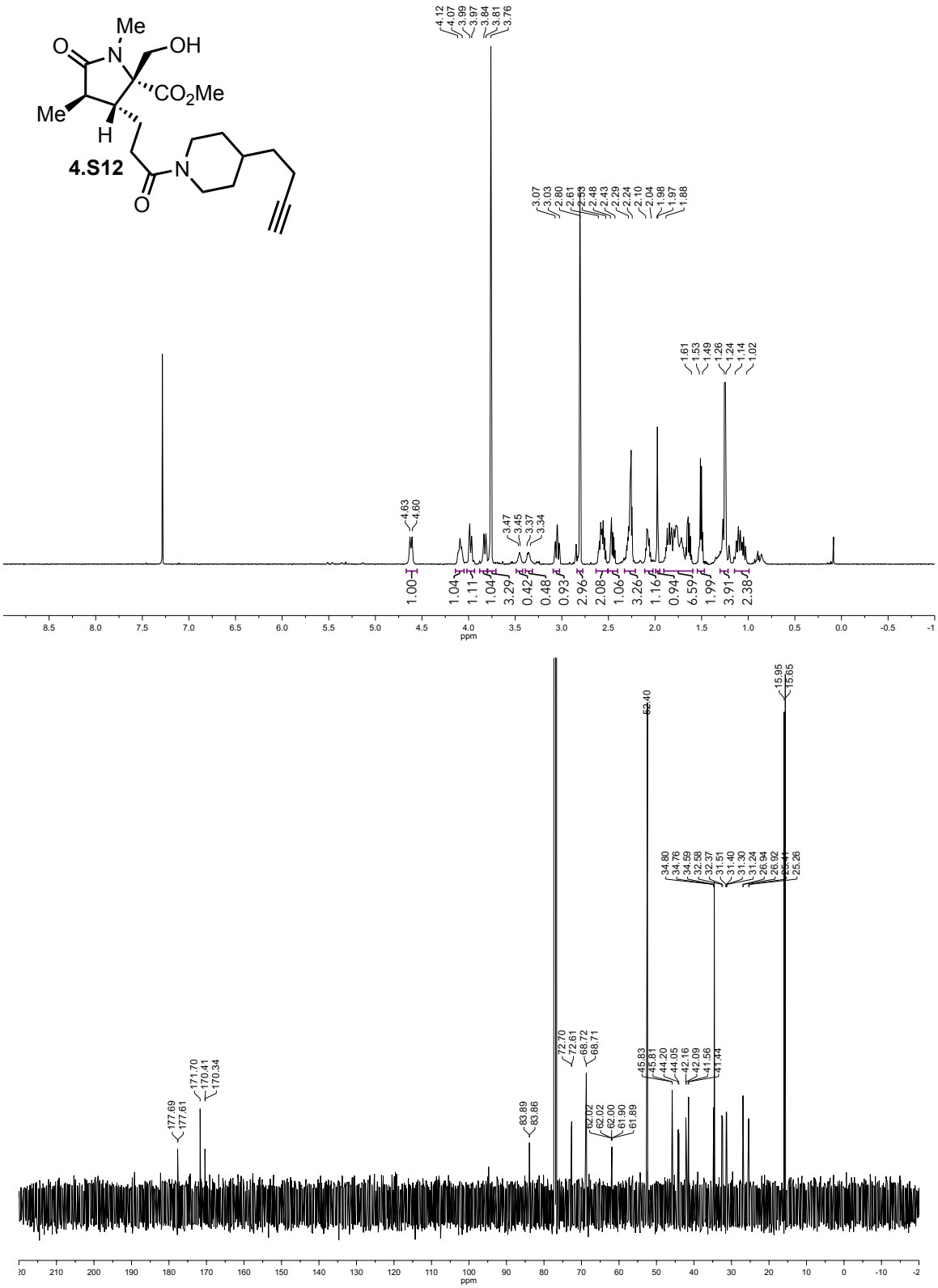

Figure A.51. ^{1}H-NMR (600 MHz) and ^{13}C-NMR (150 MHz) of compound **4.S12** in $CDCl_3$

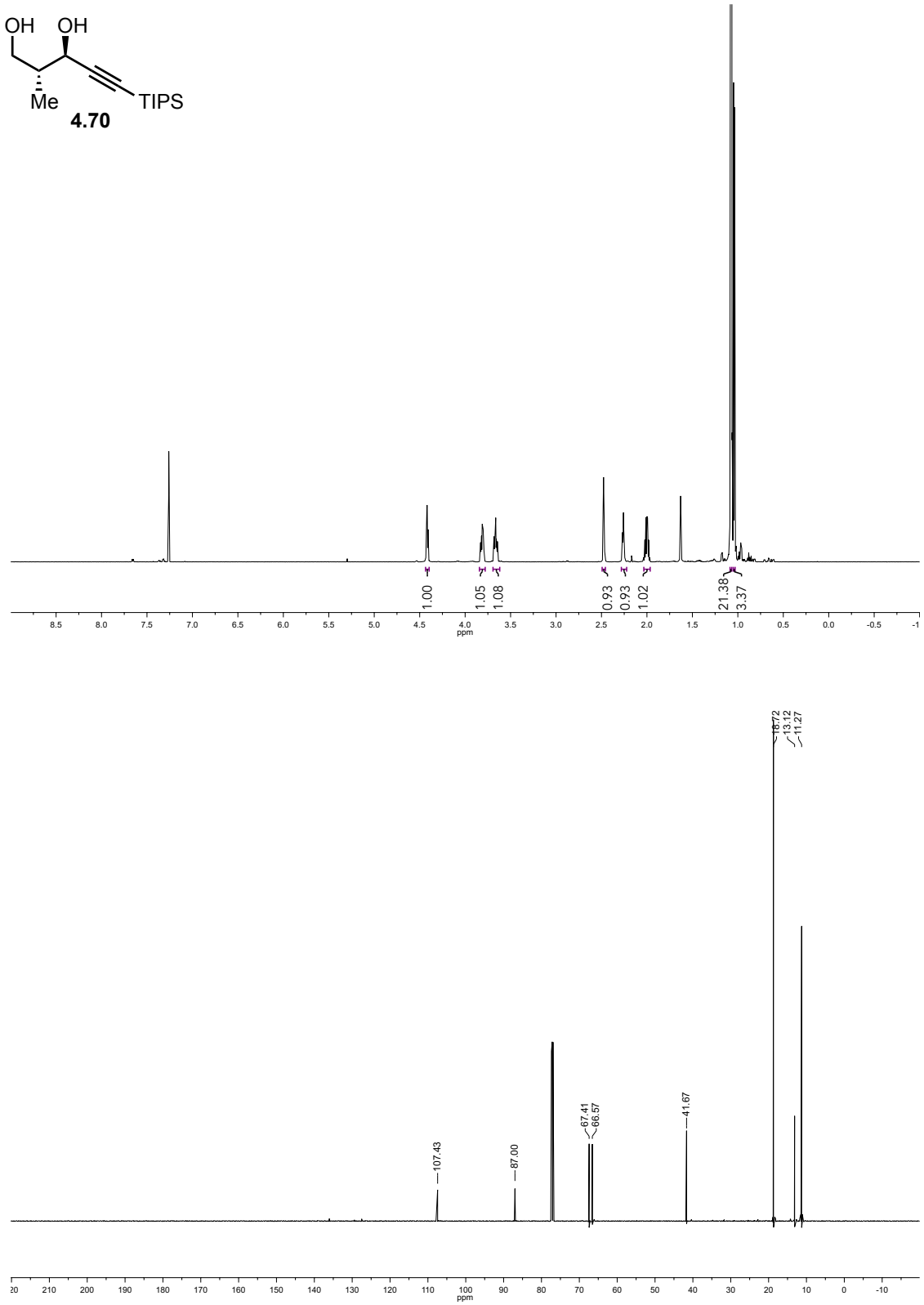

Figure A.52. ^{1}H-NMR (600 MHz) and ^{13}C-NMR (150 MHz) of compound **4.70** in $CDCl_3$

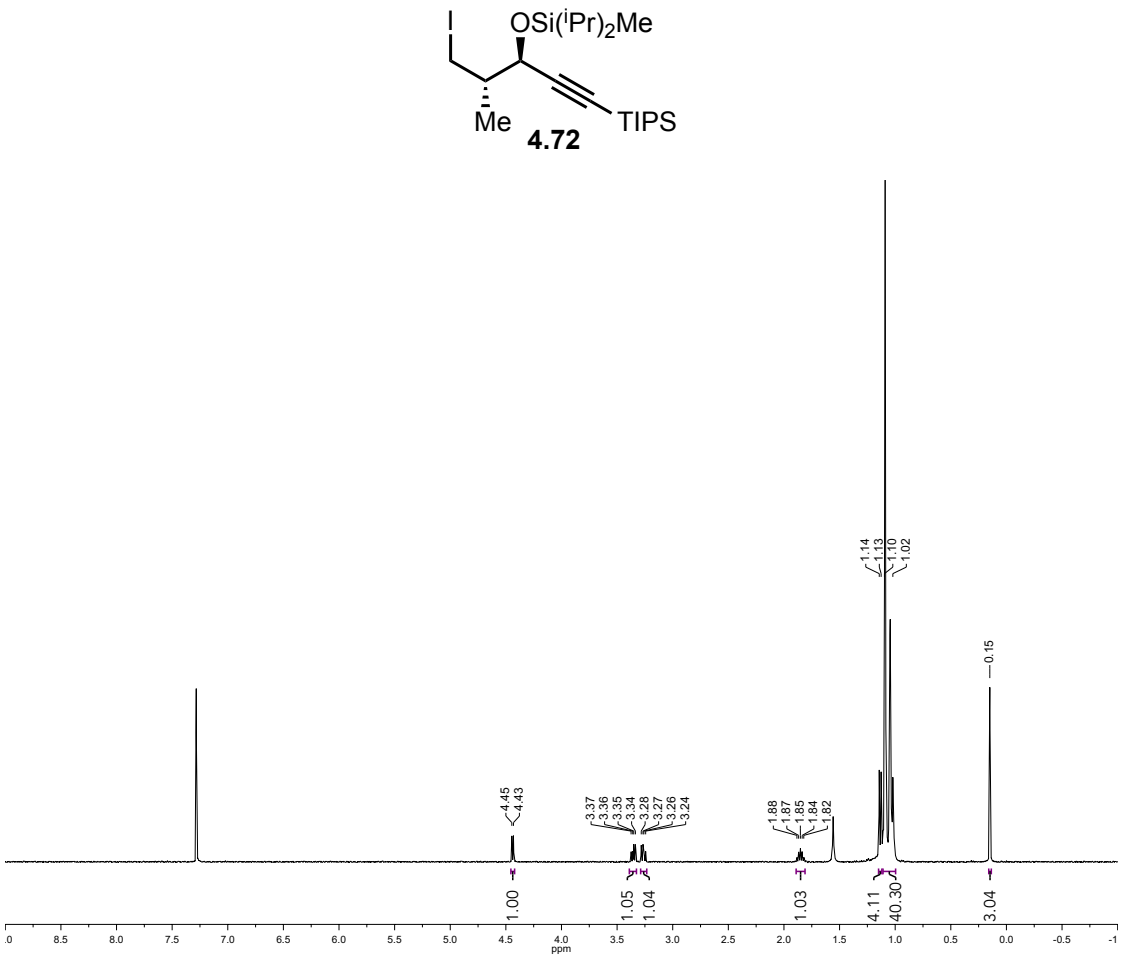

Figure A.53. ^{1}H-NMR (600 MHz) of compound **4.72** in $CDCl_3$

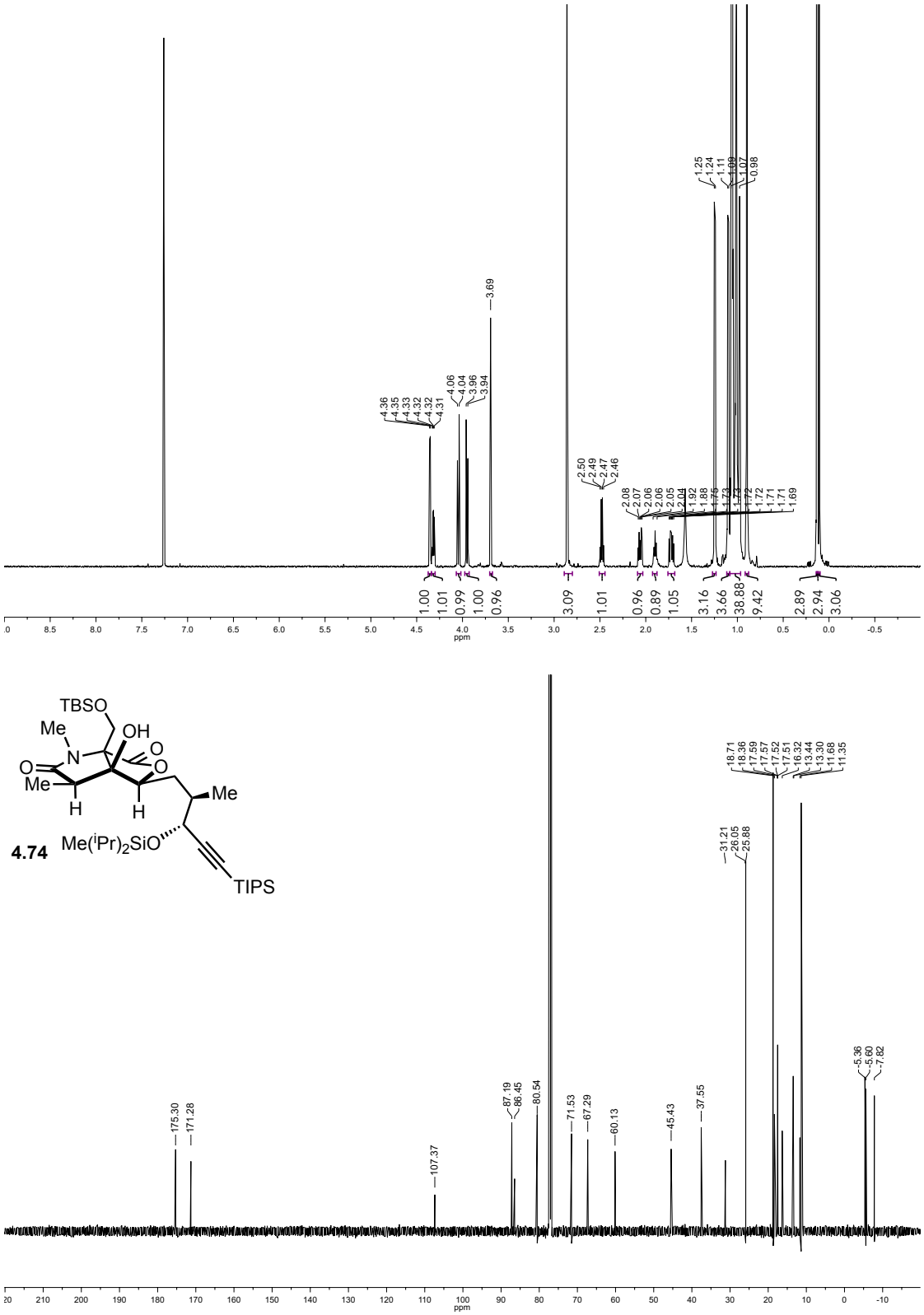

Figure A.54. ^{1}H-NMR (600 MHz) and ^{13}C-NMR (150 MHz) of compound **4.74** in $CDCl_3$

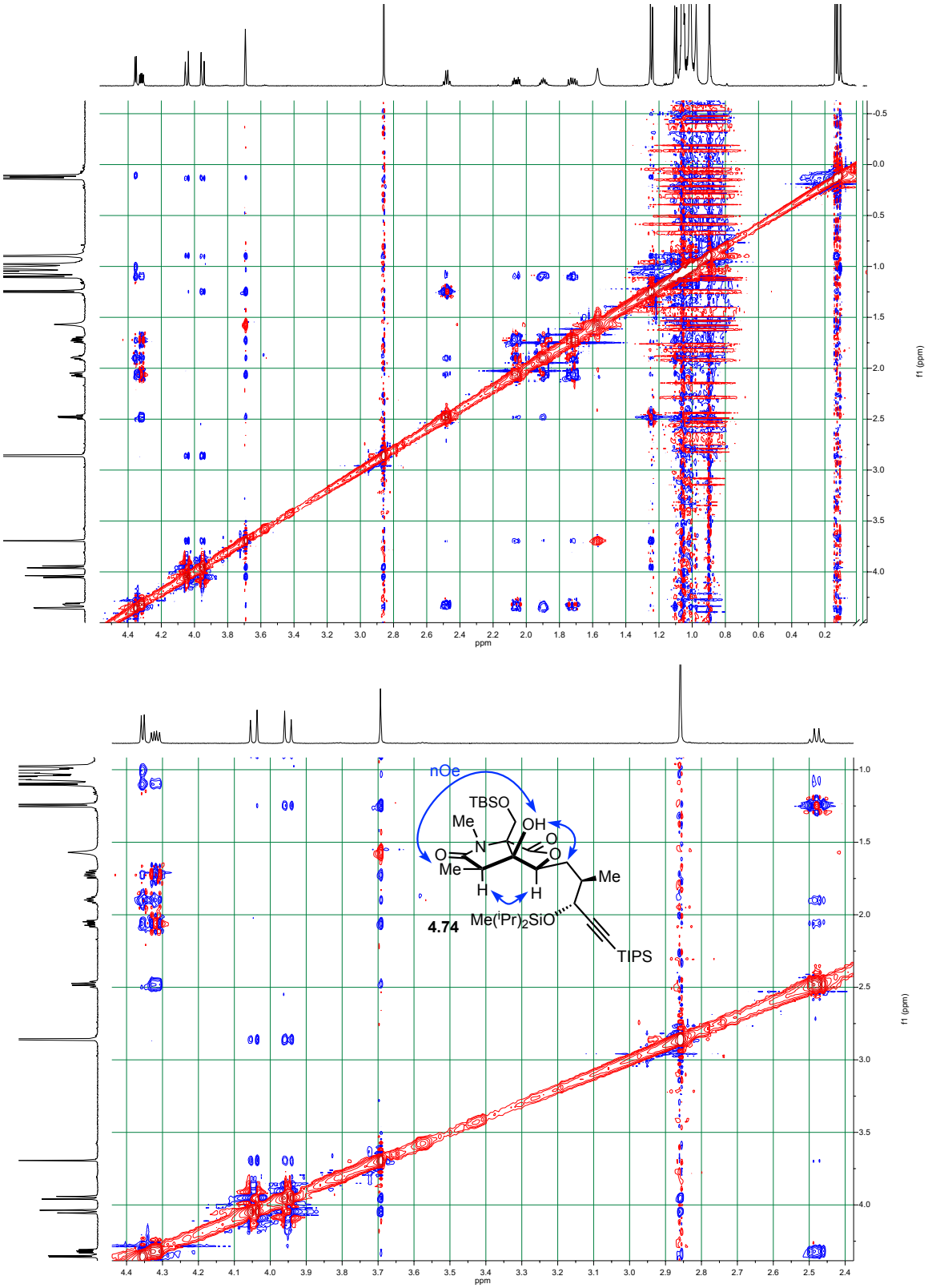

Figure A.55. ^{1}H-^{1}H NOESY 2D-NMR (600 MHz) of compound **4.74** in $CDCl_3$

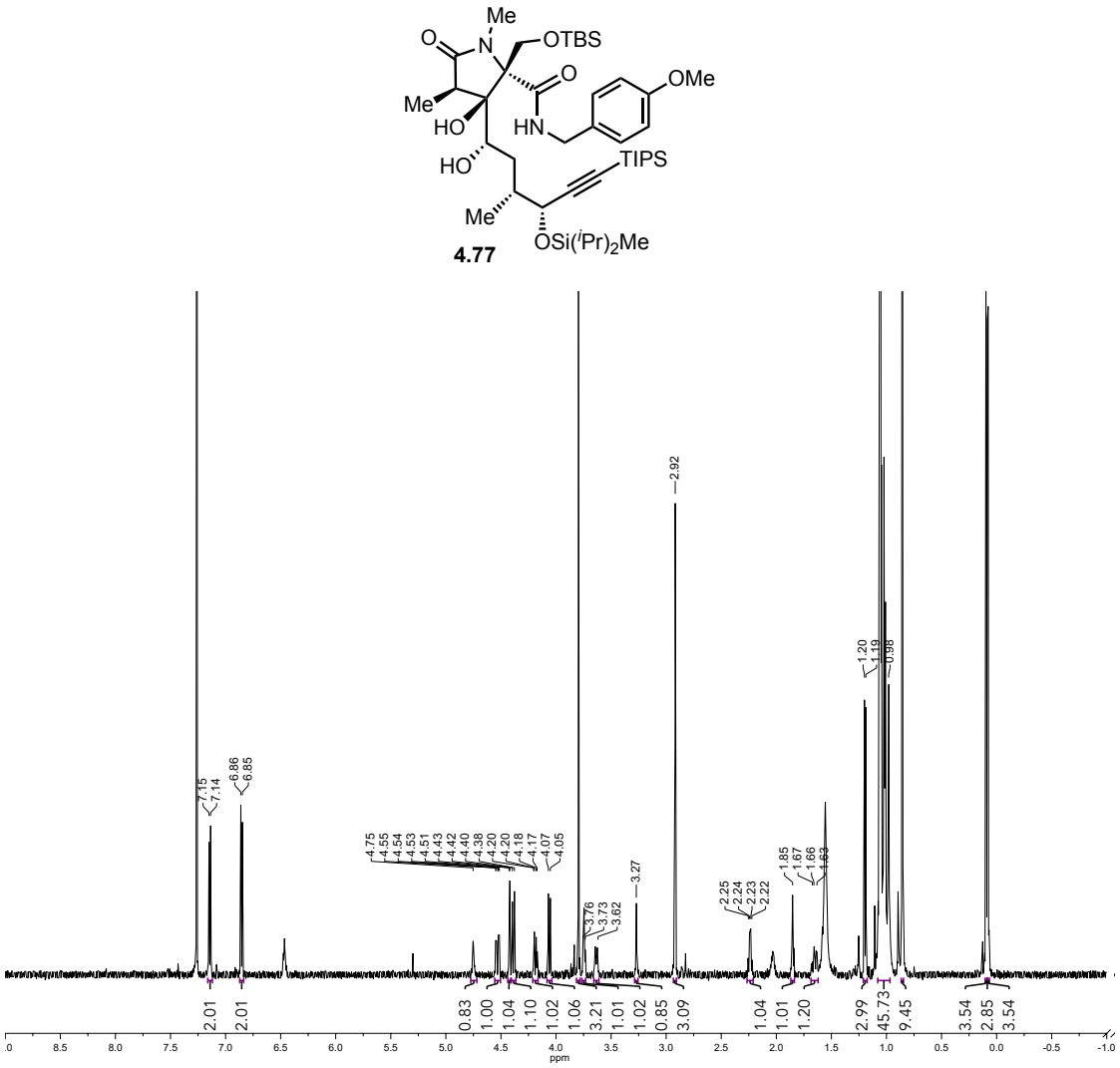

Figure A.56. ^{1}H-NMR (600 MHz) of compound **4.77** in $CDCl_3$

APPENDIX B

Chapter 5 NMR Spectra

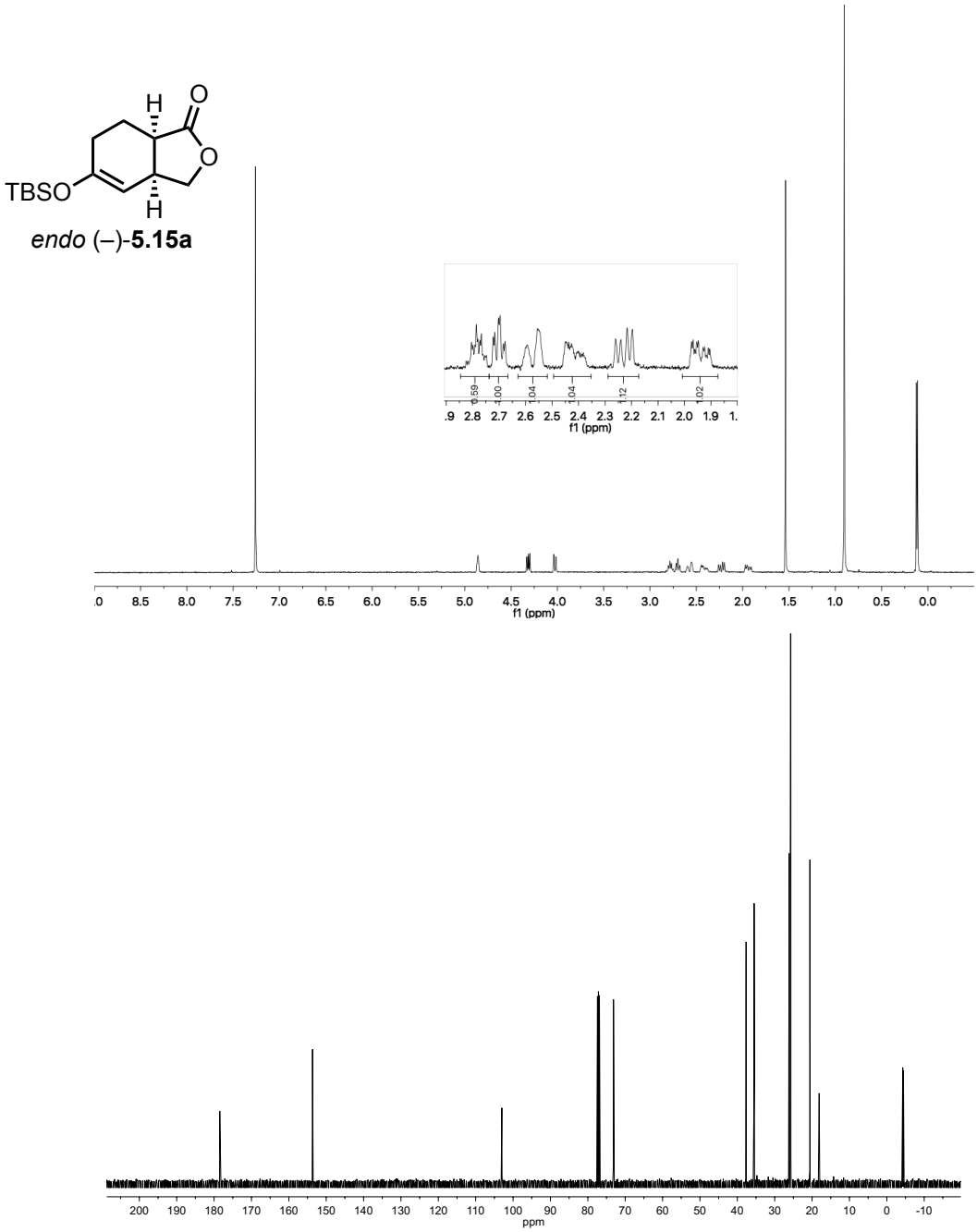

Figure B.1. ^{1}H-NMR (400 MHz) and ^{13}C-NMR (125 MHz) of compound **5.15a** in $CDCl_3$

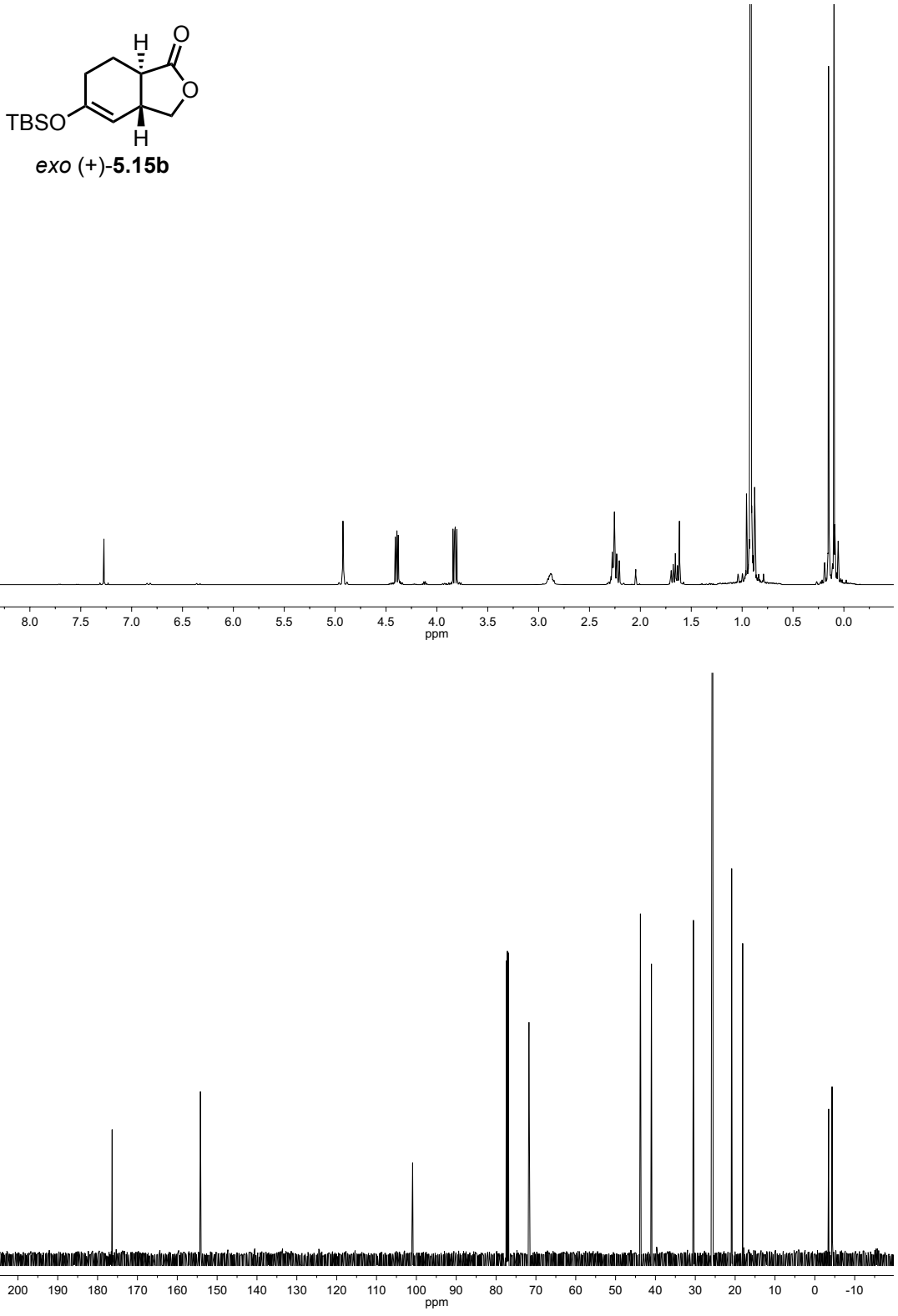

exo (+)-**5.15b**

Figure B.2. ^{1}H-NMR (500 MHz) and ^{13}C-NMR (125 MHz) of compound **5.15b** in $CDCl_3$

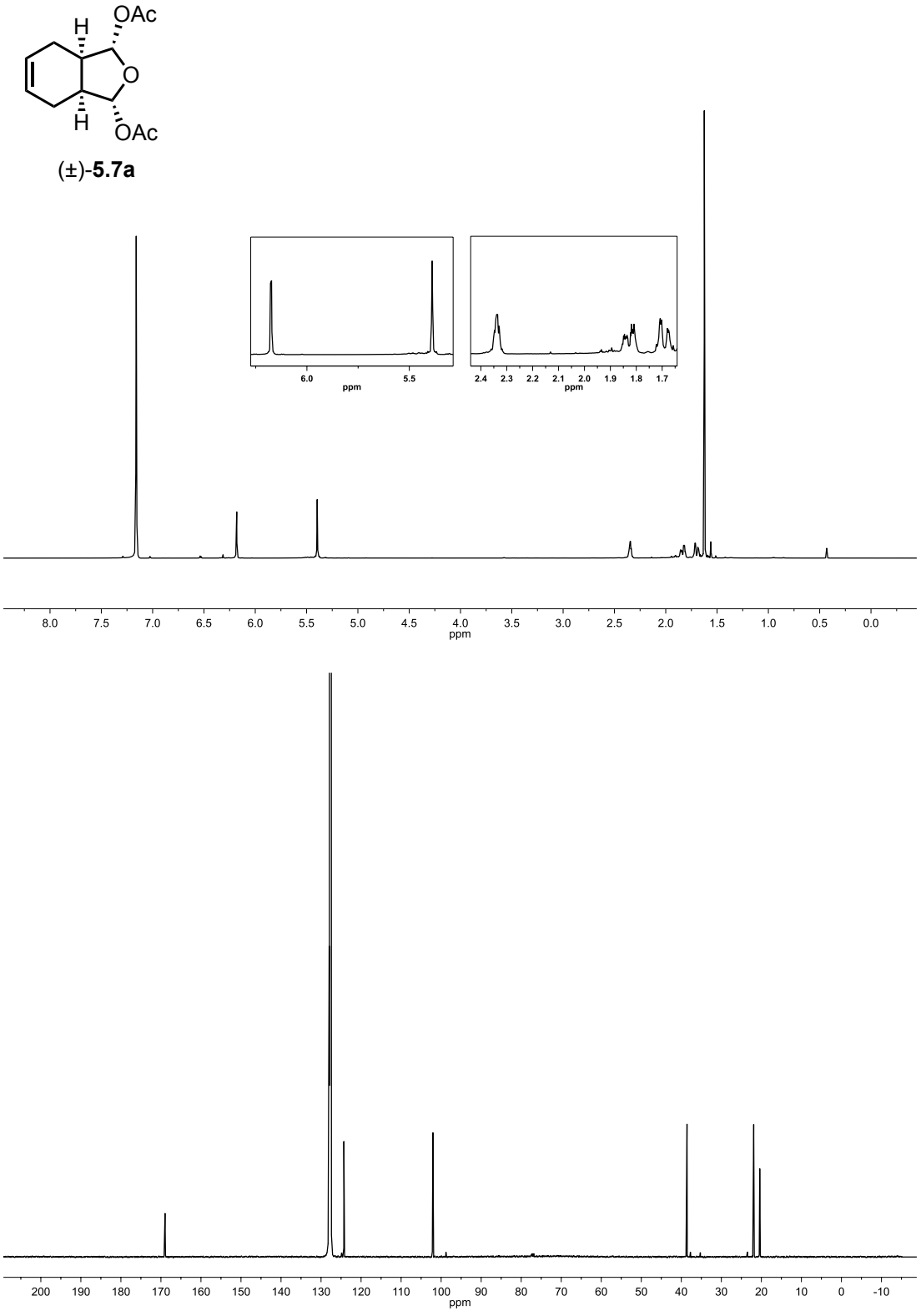

Figure B.3. ^{1}H-NMR (600 MHz) and ^{13}C-NMR (150 MHz) of compound **5.7a** in $CDCl_3$

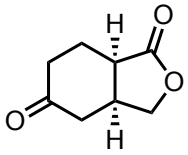

(–)-**5.9**

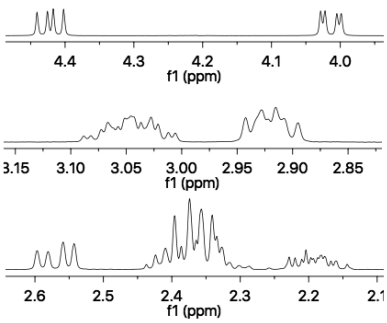

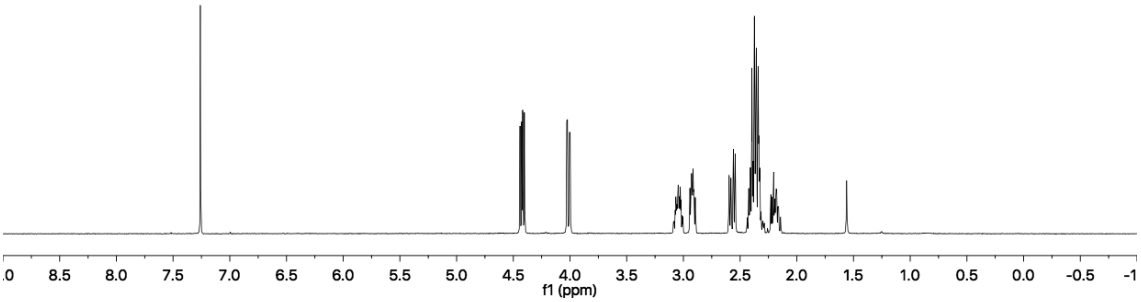

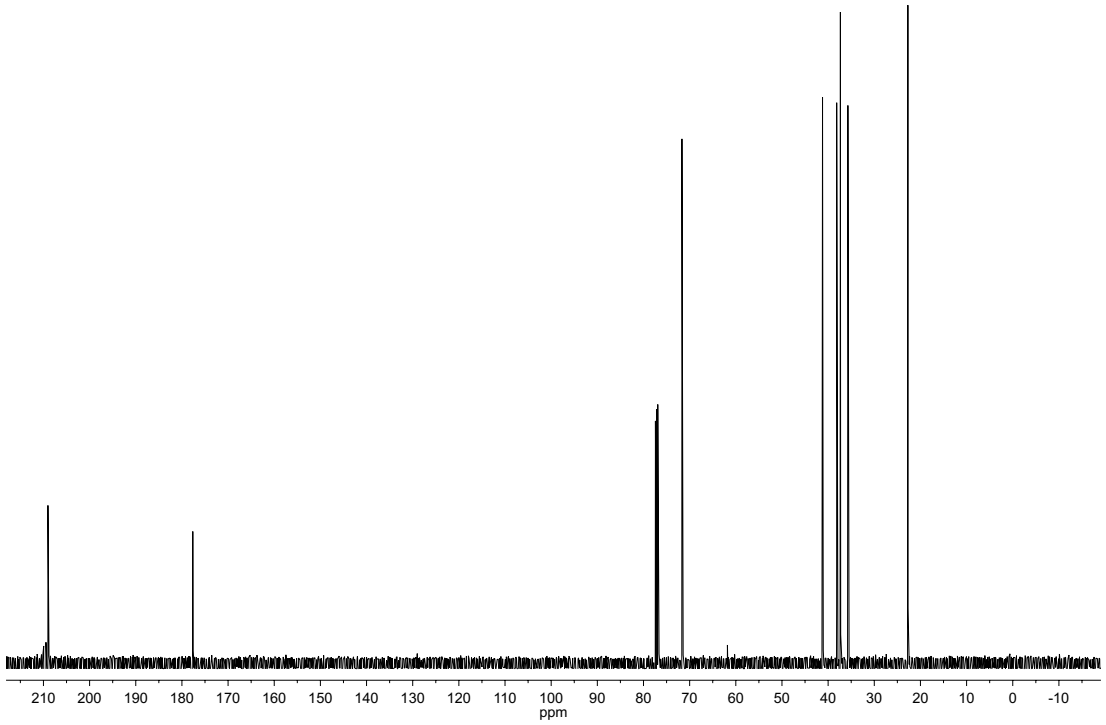

Figure B.4. ^{1}H-NMR (400 MHz) and ^{13}C-NMR (125 MHz) of compound **5.9** in $CDCl_3$

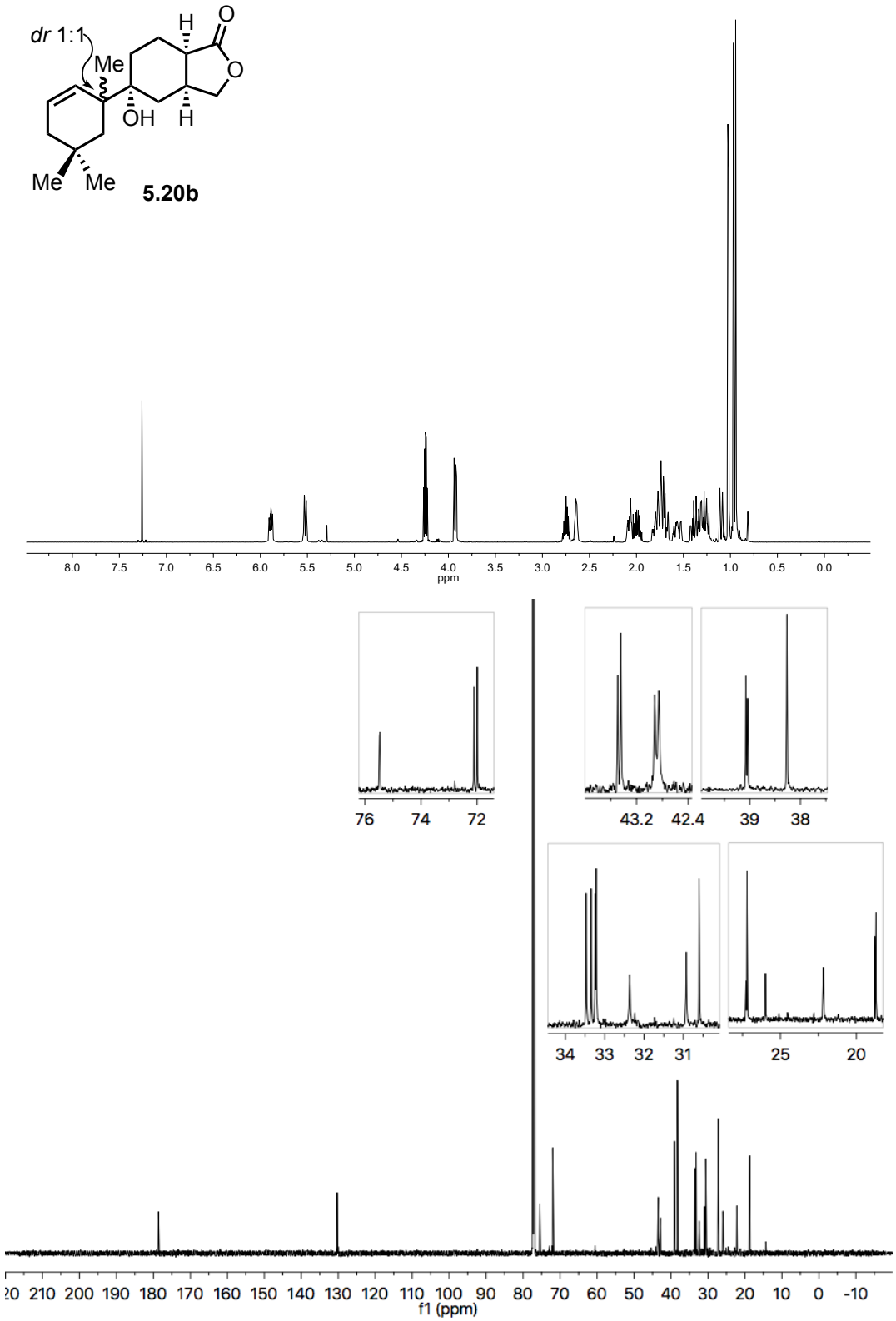

Figure B.5. ^{1}H-NMR (500 MHz) and ^{13}C-NMR (150 MHz) of compound **5.20b** in $CDCl_3$

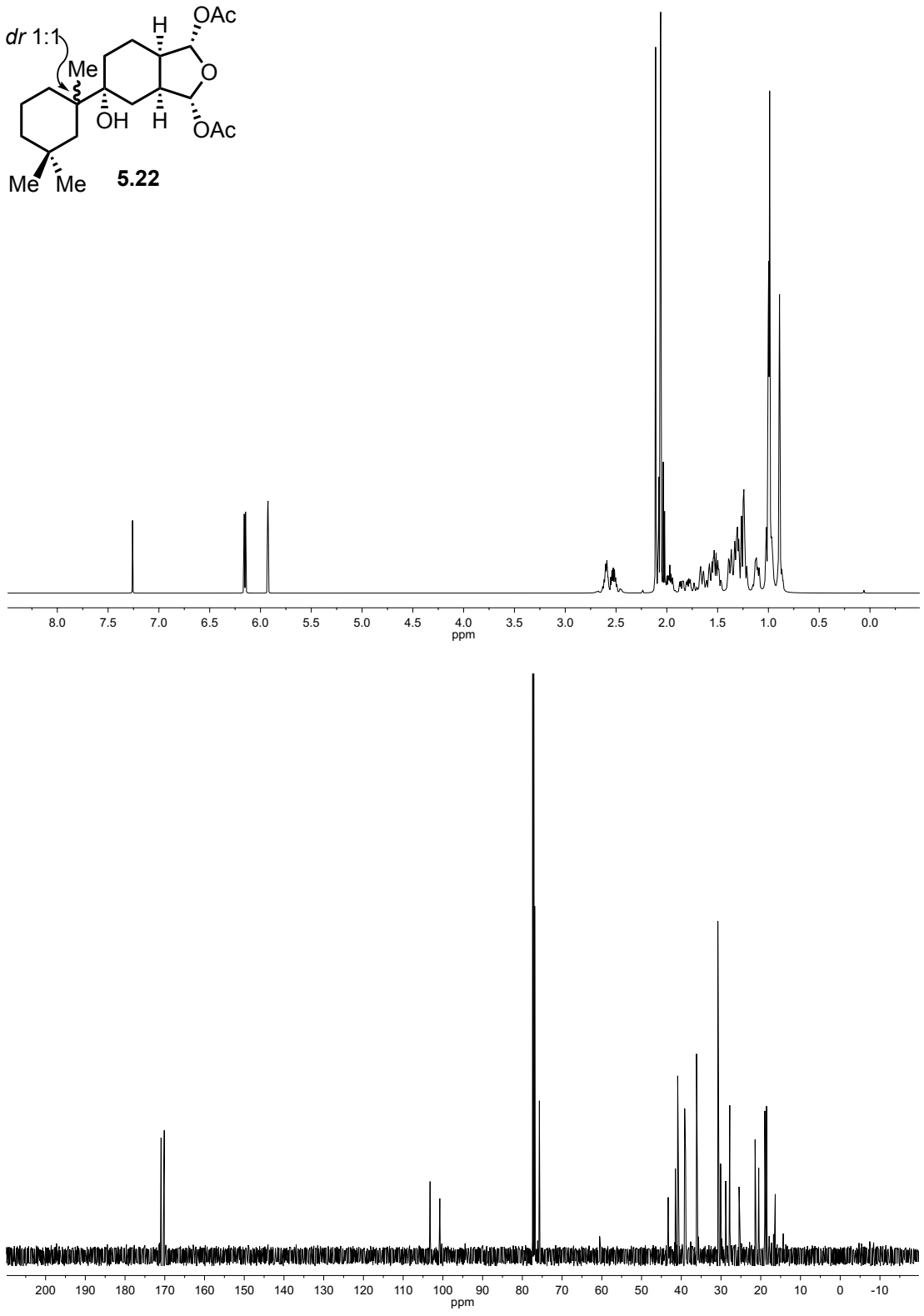

Figure B.6. ^{1}H-NMR (500 MHz) and ^{13}C-NMR (125 MHz) of compound **5.22** in $CDCl_3$

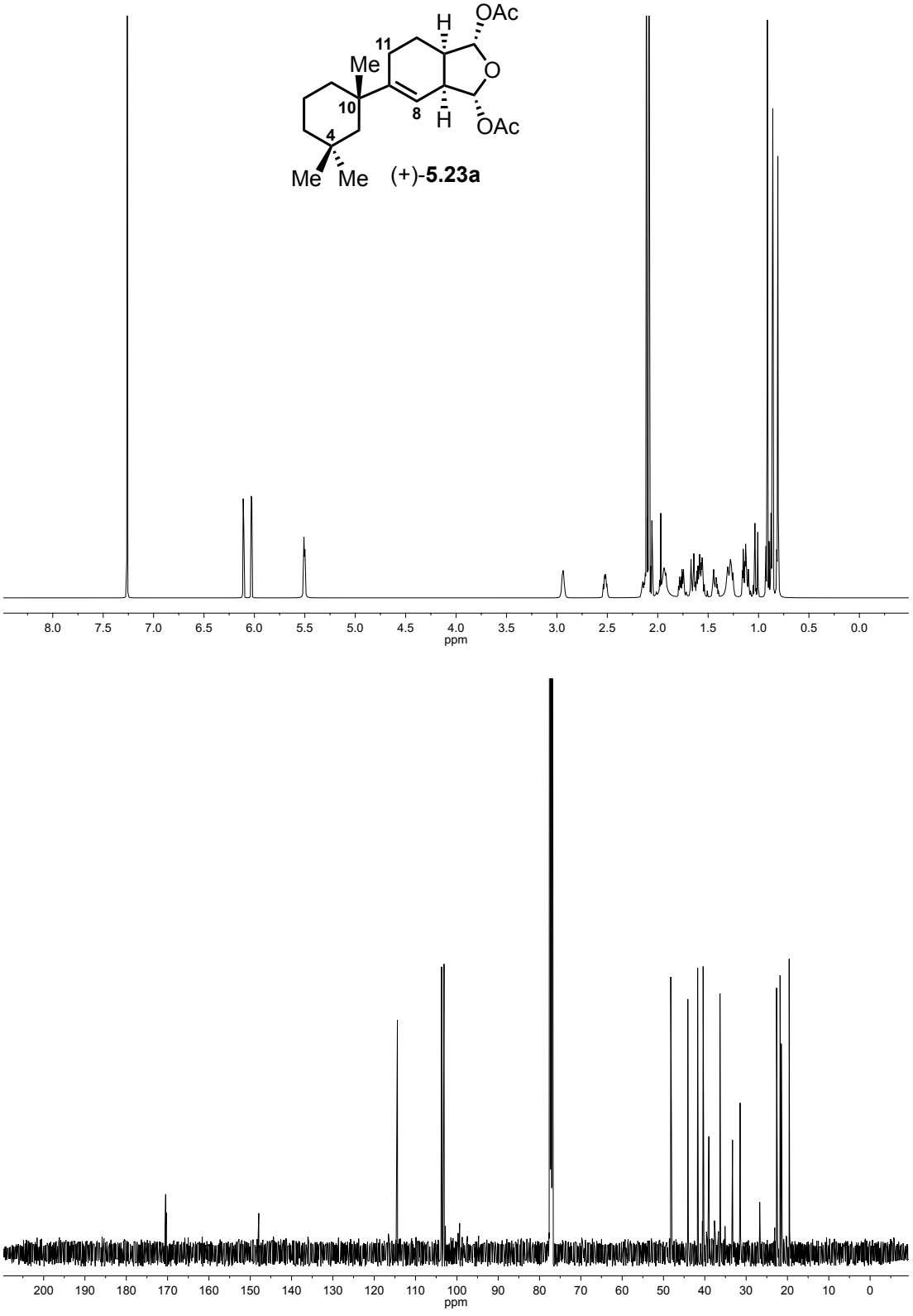

Figure B.7. ^{1}H-NMR (500 MHz) and ^{13}C-NMR (125 MHz) of compound **5.23a** in $CDCl_3$

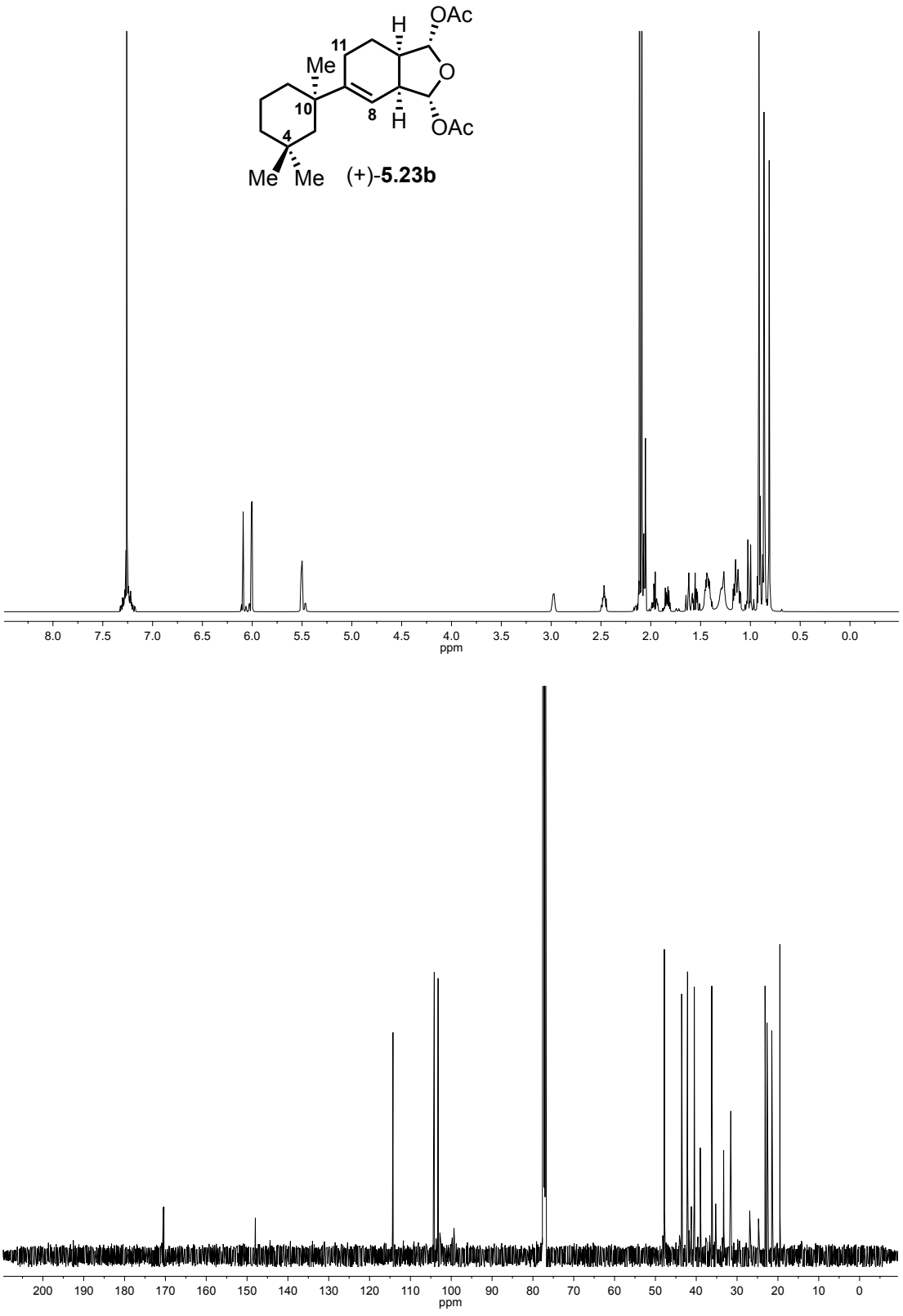

Figure B.8. ^{1}H-NMR (500 MHz) and ^{13}C-NMR (125 MHz) of compound **5.23b** in $CDCl_3$

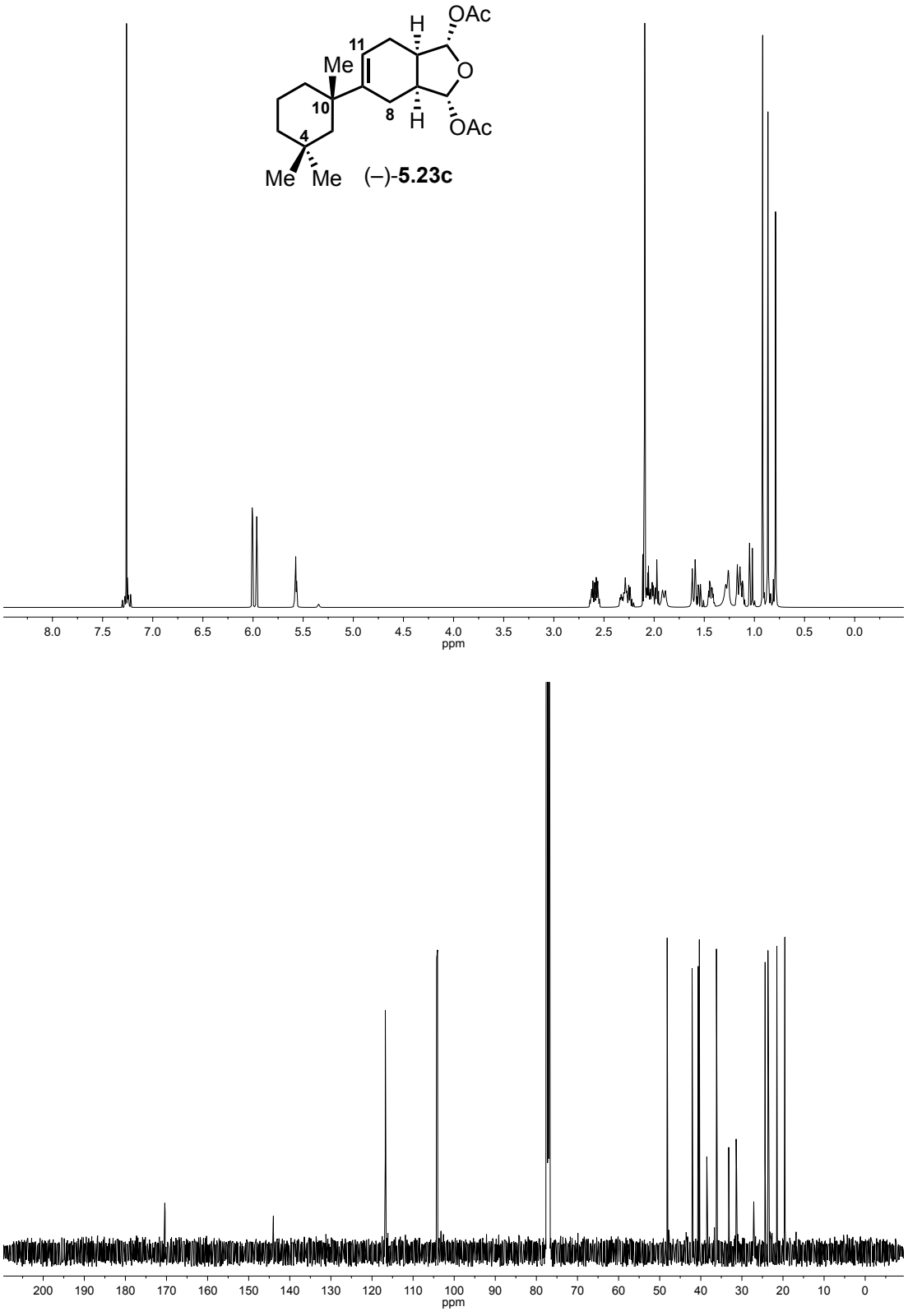

Figure B.9. ^{1}H-NMR (500 MHz) and ^{13}C-NMR (125 MHz) of compound **5.23c** in $CDCl_3$

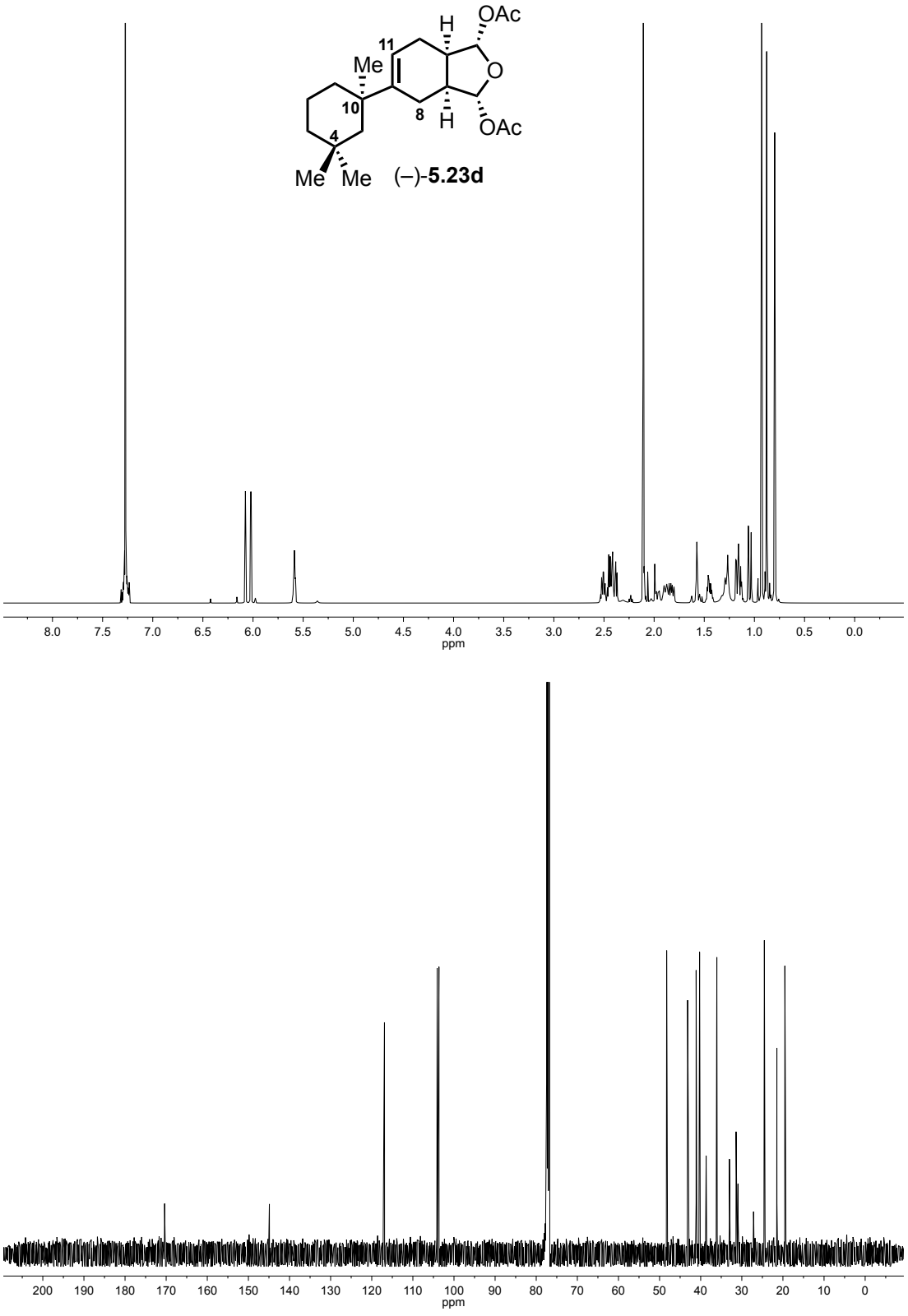

Figure B.10. ^{1}H-NMR (500 MHz) and ^{13}C-NMR (125 MHz) of compound **5.23d** in $CDCl_3$

BIBLIOGRAPHY

1. Moloney, M. G.; Trippier, P., C.; Yaqoob, M.; Wang, Z., The Oxazolomycins: A Structurally Novel Class of Bioactive Compounds. *Curr. Drug Disc. Technol.* **2004,** *1* (3), 181-199.

2. Aizawa, S.; Shibuya, M.; Shirato, S., Resistaphilin, A New Antibiotic. I, Production, Isolation and Properties. *J. Antibiot.* **1971,** *24* (6), 393-396.

3. Mori, T.; Takahashi, K.; Kashiwabara, M.; Uemura, D.; Katayama, C.; Iwadare, S.; Shizuri, Y.; Mitomo, R.; Nakano, F.; Matsuzaki, A., Structure of Oxazolomycin, a Novel Beta-Lactone Antibiotic. *Tetrahedron Lett.* **1985,** *26* (8), 1073-1076.

4. Ogura, M.; Nakayama, H.; Furihata, K.; Shimazu, A.; Seto, H.; Otake, N., Structure of a New Antibiotic Curromycin A Produced by a Genetically Modified Strain of *Streptomyces Hygroscopicus* a Polyether Antibiotic Producing Organism. *J. Antibiot.* **1985,** *38* (5), 669-673.

5. Ogura, M.; Nakayama, H.; Furihata, K.; Shimazu, A.; Seto, H.; Otake, N., Isolation and Structural Determination of a New Antibiotic Curromycin-B. *Agric. Biol. Chem.* **1985,** *49* (6), 1909-1910.

6. Takahashi, K.; Kawabata, M.; Uemura, D.; Iwadare, S.; Mitomo, R.; Nakano, F.; Matsuzaki, A., Structure of Neooxazolomycin, an Antitumor Antibiotic. *Tetrahedron Lett.* **1985,** *26* (8), 1077-1078.

7. Ikeda, Y.; Kondo, S.; Naganawa, H.; Hattori, S.; Hamada, M.; Takeuchi, T., New Triene-β-lactone Antibiotics, Triedimycins A and B. *J. Antibiot.* **1991,** *44* (4), 453-455.

8. Ryu, G.; Hwang, S.; Kim, S. K., 16-methyloxazolomycin, a new antimicrobial and cytotoxic substance produced by a Streptomyces sp. *J. Antibiot.* **1997,** *50* (12), 1064-1066.

9. Kanzaki, H.; Wada, K.-i.; Nitoda, T.; Kawazu, K., Novel Bioactive Oxazolomycin Isomers Produced by Streptomyces albus JA3453. *Biosci., Biotechnol., Biochem.* **1998,** *62* (3), 438-442.

10. Ryu, G. S.; Kim, S. K., Absolute stereochemistry determination of 16-methyloxazolomycin produced by a Streptomyces sp. *J. Antibiot.* **1999,** *52* (2), 193-197.

11. Otani, T.; Yoshida, K. I.; Kubota, H.; Kawai, S.; Ito, S.; Hori, H.; Ishiyama, T.; Oki, T., Novel Triene-β-lactone Antibiotics, Oxazolomycin Derivative and Its Isomer, Produced by *Streptomyces* sp. KSM-2690. *J. Antibiot.* **2000,** *53* (12), 1397-1400.

12. Manam, R. R.; Teisan, S.; White, D. J.; Nicholson, B.; Grodberg, J.; Neuteboom, S. T. C.; Lam, K. S.; Mosca, D. A.; Lloyd, G. K.; Potts, B. C. M., Lajollamycin, a nitro-tetraene spiro-beta-lactone-gamma-iactam antibiotic from the marine actinomycete Streptomyces nodosus. *J. Nat. Prod.* **2005,** *68* (2), 240-243.

13. Ko, K.; Lee, S. H.; Kim, S. H.; Kim, E. H.; Oh, K. B.; Shin, J.; Oh, D. C., Lajollamycins, Nitro Group-Bearing Spiro-β-lactone-γ-lactams Obtained from a Marine-Derived Streptomyces sp. *J. Nat. Prod.* **2014,** *77* (9), 2099-2104.

14. Shiomi, K.; Arai, N.; Shinose, M.; Takahashi, Y.; Yoshida, H.; Iwabuchi, J.; Tanaka, Y.; Omura, S., New Antibiotics Phthoxazolins B, C and D Produced by *Streptomyces* sp. KO-7888. *J. Antibiot.* **1995,** *48* (7), 714-719.

15. Tanaka, Y.; Kanaya, I.; Takahashi, Y.; Shinose, M.; Tanaka, H.; Omura, S., Phthoxazolin A, A Specific Inhibitor of Cellulose Biosynthesis from Microbial Origin, II. Isolation, Physio-chemical Properties, and Structural Elucidation. *J. Antibiot.* **1993,** *46* (8), 1208-1213.

16. Tanaka, Y.; Kanaya, I.; Shiomi, K.; Tanaka, H.; Omura, S., Phthoxazolin A, A Specific Inhibitor of Cellulose Biosynthesis from Microbial Origin, I. Discovery, Taxonomy of Producing Microorganism, Fermentation, and Biological Activity. *J. Antibiot.* **1993,** *46* (8), 1214-1218.

17. Henkel, T.; Zeeck, A., Secondary Metabolites by Chemical-Screening .16. Inthomycins, New Oxazole-Trienes from Streptomyces-Sp. *Liebigs Ann. Chem.* **1991,** (4), 367-373.

18. Omura, S.; Tanaka, Y.; Kanaya, I.; Shinose, M.; Takahashi, Y., Phthoxazolin, A Specific Inhibitor of Cellulose Biosynthesis, Produced by a Strain of *Sreptomyces* sp. *J. Antibiot.* **1990,** *43* (8), 1034-1036.

19. Kawada, M.; Inoue, H.; Usami, I.; Ikeda, D., Phthoxazolin A inhibits prostate cancer growth by modulating tumor-stromal cell interactions. *Cancer Sci.* **2009,** *100* (1), 150-157.

20. Kreiss, W.; Frode, R.; Mohrle, V.; Eberz, G., Chromatography-bioluminescence coupling reveals surprising bioactivity of inthomycin A. *Anal. Bioanal. Chem.* **2010,** *398* (5), 2081-2088.

21. Koomsiri, W.; Inahashi, Y.; Kimura, T.; Shiomi, K.; Takahashi, Y.; Ōmura, S.; Thamchaipenet, A.; Nakashima, T., Bisoxazolomycin A: a new natural product from 'Streptomyces subflavus subsp. irumaensis' AM-3603. *J. Antibiot.* **2017,** *70* (12), 1142-1145.

22. Kawai, S.; Kawabata, G.; Kobayashi, A.; Kawazu, K., Inhibitory Effect of Oxazolomycin on Crown Gall Formation. *Agric. Biol. Chem.* **1989,** *53* (4), 1127-1133.

23. Grigorjev, P. A.; Schlegel, R.; Gräfe, U., On the Protonophoric Activity of Oxazolomycin. *Pharmazie* **1992,** *47* (9), 707-709.

24. Kawazu, K.; Kanzaki, H.; Kawabata, G.; Kawai, S.; Kobayashi, A., Oxazolomycin Esters, Specific Inhibitors of Plant Transformation. *Biosci., Biotechnol., Biochem.* **1992,** *56* (9), 1382-1385.

25. Tonew, E.; Tonew, M.; Grafe, U.; Zopel, P., On the Antiviral Activity of Diffusomycin (Oxazolomycin). *Acta Virol.* **1992,** *36* (2), 166-172.

26. Nakamura, M.; Honma, H.; Kamada, M.; Ohno, T.; Kunimoto, S.; Ikeda, Y.; Kondo, S.; Takeuchi, T., Inhibitory Effect of Curromycin-a and Curromycin-B on Human-Immunodeficiency-Virus Replication. *J. Antibiot.* **1994,** *47* (5), 616-618.

27. Grafe, U.; Kluge, H.; Thiericke, R., Biogenetic Studies on Oxazolomycin, a Metabolite of Streptomyces-Albus (Strain Ja-3453). *Liebigs Ann. Chem.* **1992,** (5), 429-432.

28. Zhao, C. H.; Ju, J. H.; Christenson, S. D.; Smith, W. C.; Song, D. F.; Zhou, X. F.; Shen, B.; Deng, Z. X., Utilization of the methoxymalonyl-acyl carrier protein biosynthesis locus for cloning the oxazolomycin biosynthetic gene cluster from Streptomyces albus JA3453. *J. Bacteriol.* **2006,** *188* (11), 4142-4147.

29. Song, D. F.; Coughlin, J.; Ju, J. H.; Zhou, X. F.; Shen, B.; Zhao, C. H.; Deng, Z. X., Alternative method for site-directed mutagenesis of complex polyketide synthase in Streptomyces albus JA3453. *Acta Biochim. Biophys. Sin.* **2008,** *40* (4), 319-326.

30. Zhao, C. H.; Coughlin, J. M.; Ju, J. H.; Zhu, D. Q.; Wendt-Pienkowski, E.; Zhou, X. F.; Wang, Z. J.; Shen, B.; Deng, Z. X., Oxazolomycin Biosynthesis in Streptomyces albus JA3453 Featuring an "Acyltransferase-less" Type I Polyketide Synthase That Incorporates Two Distinct Extender Units. *J. Biol. Chem.* **2010,** *285* (26), 20097-20108.

31. Xie, X.; Cane, D. E., Stereospecific Formation of Z-Trisubstituted Double Bonds by the Successive Action of Ketoreductase and Dehydratase Domains from trans-AT Polyketide Synthases. *Biochemistry* **2018,** *57* (22), 3126-3129.

32. Kende, A. S.; Kawamura, K.; Devita, R. J., Enantioselective Total Synthesis of Neooxazolomycin. *J. Am. Chem. Soc.* **1990,** *112* (10), 4070-4072.

33. Kende, A. S.; Devita, R. J., Synthesis of the Fused Bicyclic Lactam-Lactone Terminus of Neooxazolomycin by a Novel Dianion Cyclocondensation. *Tetrahedron Lett.* **1988,** *29* (21), 2521-2524.

34. Stille, J. K., The Palladium-Catalyzed Cross-Coupling Reactions of Organotin Reagents with Organic Electrophiles [New Synthetic Methods (58)]. *Angew. Chem. Int. Ed.* **1986,** *25* (6), 508-524.

35. Kende, A. S.; DeVita, R. J., A mild four-carbon homologation of aldehydes to E,E-dienamines. *Tetrahedron Lett.* **1990,** *31* (3), 307-310.

36. Onyango, E. O.; Tsurumoto, J.; Imai, N.; Takahashi, K.; Ishihara, J.; Hatakeyama, S., Total synthesis of neooxazolomycin. *Angew. Chem. Int. Ed.* **2007,** *46* (35), 6703-6705.

37. Eto, K.; Yoshino, M.; Takahashi, K.; Ishihara, J.; Hatakeyama, S., Total Synthesis of Oxazolomycin A. *Org. Lett.* **2011,** *13* (19), 5398-5401.

38. Ishihara, J.; Hatakeyama, S., Total Synthesis of Oxazolomycins. *Chem. Rec.* **2014,** *14* (4), 663-677.

39. Nishimaru, T.; Eto, K.; Komine, K.; Ishihara, J.; Hatakeyama, S., Total Synthesis of Lajollamycin B. *Chem. Eur. J.* **2019,** *25* (33), 7927-7934.

40. Andrews, M. D.; Brewster, A. G.; Moloney, M. G., Highly functionalised pyroglutamates by intramolecular aldol reactions: Towards the pyroglutamate skeleton of oxazolomycin. *Synlett* **1996,** (7), 612-&.

41. Panday, S. K.; Prasad, J.; Dikshit, D. K., Pyroglutamic acid: a unique chiral synthon. *Tetrahedron: Asymmetry* **2009,** *20* (14), 1581-1632.

42. Nájera, C.; Yus, M., Pyroglutamic acid: a versatile building block in asymmetric synthesis. *Tetrahedron: Asymmetry* **1999,** *10* (12), 2245-2303.

43. Saldívar-González, F. I.; Lenci, E.; Trabocchi, A.; Medina-Franco, J. L., Exploring the chemical space and the bioactivity profile of lactams: A chemoinformatic study. *RSC Advances* **2019,** *9* (46), 27105-27116.

44. Khan, M. K.; Wang, D.; Moloney, M. G., Functionalised Nitrogen Heterocycles and the Search for New Antibacterials and Bioactives. *Synthesis (Germany)* **2020,** *52* (11), 1602-1616.

45. Nay, B.; Riache, N.; Evanno, L., Chemistry and biology of non-tetramic γ-hydroxy-γ-lactams and γ-alkylidene-γ-lactams from natural sources. *Nat. Prod. Rep.* **2009,** *26* (8), 1044-1062.

46. Kim, J. H.; Kim, I.; Song, Y.; Kim, M. J.; Kim, S., Asymmetric Total Synthesis of (+)-Neooxazolomycin Using a Chirality-Transfer Strategy. *Angew. Chem. Int. Ed.* **2019,** *58* (32), 11018-11022.

47. Mahashur, A.; Thomas, P. K.; Mehta, P.; Nivangune, K.; Muchhala, S.; Jain, R., Pidotimod: In-depth review of current evidence. *Lung India : official organ of Indian Chest Society* **2019,** *36* (5), 422-433.

48. Gulder, T. A. M.; Moore, B. S., Salinosporamide Natural Products: Potent 20 S Proteasome Inhibitors as Promising Cancer Chemotherapeutics. *Angew. Chem. Int. Ed.* **2010,** *49* (49), 9346-9367.

49. Shibasaki, M.; Kanai, M.; Fukuda, N., Total Synthesis of Lactacystin and Salinosporamide A. *Chemistry – An Asian Journal* **2007,** *2* (1), 20-38.

50. Uesugi, S.; Fujisawa, N.; Yoshida, J.; Watanabe, M.; Dan, S.; Yamori, T.; Shiono, Y.; Kimura, K.-i., Pyrrocidine A, a metabolite of endophytic fungi, has a potent apoptosis-inducing activity against HL60 cells through caspase activation via the Michael addition. *The Journal of Antibiotics* **2016,** *69* (3), 133-140.

51. Chu, S.; Liu, S.; Duan, W.; Cheng, Y.; Jiang, X.; Zhu, C.; Tang, K.; Wang, R.; Xu, L.; Wang, X.; Yu, X.; Wu, K.; Wang, Y.; Wang, M.; Huang, H.; Zhang, J., The anti-dementia drug candidate, (−)-clausenamide, improves memory impairment through its multi-target effect. *Pharmacol. Ther.* **2016,** *162*, 179-187.

52. Chu, S.-f.; Zhang, J.-t., Recent advances in the study of (–)clausenamide: chemistry, biological activities and mechanism of action. *Acta Pharmaceutica Sinica B* **2014,** *4* (6), 417-423.

53. He, H.; Yang, H. Y.; Bigelis, R.; Solum, E. H.; Greenstein, M.; Carter, G. T., Pyrrocidines A and B, new antibiotics produced by a filamentous fungus. *Tetrahedron Lett.* **2002,** *43* (9), 1633-1636.

54. Caruano, J.; Muccioli, G. G.; Robiette, R., Biologically active γ-lactams: synthesis and natural sources. *Org. Biomol. Chem.* **2016,** *14* (43), 10134-10156.

55. Shorvon, S., Pyrrolidone derivatives. *The Lancet* **2001,** *358* (9296), 1885-1892.

56. Varvounis, G.; Gerontitis, I. E.; Gkalpinos, V., Metal-catalyzed synthesis of five-membered ring N-heterocycles. A recent update. *Chemistry of Heterocyclic Compounds* **2018,** *54* (3), 249-268.

57. Rivas, F.; Ling, T., Advances toward the Synthesis of Functionalized γ-Lactams. *Org. Prep. Proced. Int.* **2016,** *48* (3), 254-295.

58. Ye, L.-W.; Shu, C.; Gagosz, F., Recent progress towards transition metal-catalyzed synthesis of γ-lactams. *Org. Biomol. Chem.* **2014,** *12* (12), 1833-1845.

59. Ordóñez, M.; Cativiela, C., Stereoselective synthesis of γ-amino acids. *Tetrahedron: Asymmetry* **2007,** *18* (1), 3-99.

60. Soleimani-Amiri, S.; Vessally, E.; Babazadeh, M.; Hosseinian, A.; Edjlali, L., Intramolecular cyclization of: N-allyl propiolamides: A facile synthetic route to highly substituted γ-lactams (a review). *RSC Advances* **2017,** *7* (45), 28407-28418.

61. Deng, B.; Rao, C. B.; Zhang, R.; Li, J.; Liang, Y.; Zhao, Y.; Gao, M.; Dong, D., A Formal [3+2] Annulation of β-Oxoamides and 3-Alkyl- or 3-Aryl-Substituted Prop-2-Ynyl Sulfonium Salts: Substrate-Controlled Chemoselective Synthesis of Substituted γ-Lactams and Furans. *Adv. Synth. Catal.* **2019,** *361* (19), 4549-4557.

62. Zhu, X. Q.; Yuan, H.; Sun, Q.; Zhou, B.; Han, X. Q.; Zhang, Z. X.; Lu, X.; Ye, L. W., Benign catalysis with zinc: Atom-economical and divergent synthesis of nitrogen heterocycles by formal [3 + 2] annulation of isoxazoles with ynol ethers. *Green Chem.* **2018,** *20* (18), 4287-4291.

63. Zhmurov, P. A.; Ushakov, P. Y.; Novikov, R. A.; Sukhorukov, A. Y.; Ioffe, S. L., A Novel Entry to 3,4,5-Trisubstituted 2-Pyrrolidones from Isoxazoline-N-oxides. *Synlett* **2018,** *29* (14), 1871-1874.

64. Çinar, S.; Ünaleroglu, C., Facile synthesis of heteroaryl substituted γ-lactams from nitrovinyl arenes. *Turkish Journal of Chemistry* **2018,** *42* (1), 29-35.

65. Mardjan, M. I. D.; Mayooufi, A.; Parrain, J.-L.; Thibonnet, J.; Commeiras, L., Straightforward Access to a Great Diversity of Complex Biorelevant γ-Lactams Thanks to a Tunable Cascade Multicomponent Process. *Org. Process Res. Dev.* **2020,** *24* (5), 606-614.

66. Borja-Miranda, A.; Sánchez-Chávez, A. C.; Polindara-García, L. A., Ammonium Persulfate Promotes Radical Cyclization of 1,3-Dicarbonyl-Ugi 4-CR Adducts: Synthesis of Polysubstituted γ-Lactams in Aqueous Media. *Eur. J. Org. Chem.* **2019,** *2019* (14), 2453-2471.

67. Gockel, S. N.; Buchanan, T. L.; Hull, K. L., Cu-Catalyzed Three-Component Carboamination of Alkenes. *J. Am. Chem. Soc.* **2018,** *140* (1), 58-61.

68. De Marigorta, E. M.; De Los Santos, J. M.; De Retana, A. M. O.; Vicario, J.; Palacios, F., Multicomponent reactions in the synthesis of γ-Lactams. *Synthesis (Germany)* **2018,** *50* (23), 4539-4554.

69. Audic, B.; Cramer, N., Rhodium(III)-Catalyzed Cyclopropane C-H/C-C Activation Sequence Provides Diastereoselective Access to α-Alkoxylated γ-Lactams. *Org. Lett.* **2020**.

70. Jung, H.; Schrader, M.; Kim, D.; Baik, M. H.; Park, Y.; Chang, S., Harnessing Secondary Coordination Sphere Interactions That Enable the Selective Amidation of Benzylic C-H Bonds. *J. Am. Chem. Soc.* **2019,** *141* (38), 15356-15366.

71. Huh, S.; Hong, S. Y.; Chang, S., Synthetic Utility of N-Benzoyloxyamides as an Alternative Precursor of Acylnitrenoids for γ-Lactam Formation. *Org. Lett.* **2019,** *21* (8), 2808-2812.

72. Zhou, D.; Wang, C.; Li, M.; Long, Z.; Lan, J., Palladium-catalyzed 2-pyridylmethyl-directed β-C(sp3)–H activation and cyclization of aliphatic amides with gem-dibromoolefins: A rapid access to γ-lactams. *Chin. Chem. Lett.* **2018,** *29* (1), 191-193.

73. Png, Z. M.; Cabrera-Pardo, J. R.; Peiró Cadahía, J.; Gaunt, M. J., Diastereoselective C-H carbonylative annulation of aliphatic amines: A rapid route to functionalized γ-lactams. *Chemical Science* **2018,** *9* (39), 7628-7633.

74. Zheng, S.; Gutiérrez-Bonet, Á.; Molander, G. A., Merging Photoredox PCET with Ni-Catalyzed Cross-Coupling: Cascade Amidoarylation of Unactivated Olefins. *Chem* **2019,** *5* (2), 339-352.

75. Koleoso, O. K.; Elsegood, M. R. J.; Teat, S. J.; Kimber, M. C., Photoredox Approach to N-Acyl-N′-aryl-N,N′-aminals Using Enamides and Their Conversion to γ-Lactams. *Org. Lett.* **2018,** *20* (4), 1003-1006.

76. Jia, J.; Ho, Y. A.; Bülow, R. F.; Rueping, M., Brønsted Base Assisted Photoredox Catalysis: Proton Coupled Electron Transfer for Remote C−C Bond Formation via Amidyl Radicals. *Chem. Eur. J.* **2018,** *24* (53), 14054-14058.

77. Rao, W. H.; Jiang, L. L.; Liu, X. M.; Chen, M. J.; Chen, F. Y.; Jiang, X.; Zhao, J. X.; Zou, G. D.; Zhou, Y. Q.; Tang, L., Copper(II)-Catalyzed Alkene Aminosulfonylation with Sodium Sulfinates for the Synthesis of Sulfonylated Pyrrolidones. *Org. Lett.* **2019,** *21* (8), 2890-2893.

78. Fukuyama, T.; Okada, T.; Nakashima, N.; Ryu, I., Radical Mediated Aza-Pauson-Khand Reaction of Acetylenes, Imines, and CO Leading to Five-Membered Unsaturated Lactams. *Helv. Chim. Acta* **2019,** *102* (10).

79. Ganesh Kumar, M.; Veeresh, K.; Nalawade, S. A.; Nithun, R. V.; Gopi, H. N., Direct Transformation of N-Protected α,β-Unsaturated γ-Amino Amides into γ-Lactams through a Base-Mediated Molecular Rearrangement. *J. Org. Chem.* **2019,** *84* (23), 15145-15153.

80. Ye, J.; Kalvet, I.; Schoenebeck, F.; Rovis, T., Direct α-alkylation of primary aliphatic amines enabled by CO<inf>2</inf> and electrostatics. *Nat. Chem.* **2018,** *10* (10), 1037-1041.

81. Wang, F.; Zhang, X.; He, Y.; Fan, X., Selective synthesis of pyrrolidin-2-ones and 3-iodopyrroles: Via the ring contraction and deformylative functionalization of piperidine derivatives. *Organic and Biomolecular Chemistry* **2019,** *17* (1), 156-164.

82. Dražić, T.; Roje, M., β-Lactam rearrangements into five-membered heterocycles. *Chemistry of Heterocyclic Compounds* **2017,** *53* (9), 953-962.

83. Schröder, F.; Erdmann, N.; Noël, T.; Luque, R.; Van der Eycken, E. V., Leaching-Free Supported Gold Nanoparticles Catalyzing Cycloisomerizations under Microflow Conditions. *Adv. Synth. Catal.* **2015,** *357* (14-15), 3141-3147.

84. Mourelle-Insua, Á.; Zampieri, L. A.; Lavandera, I.; Gotor-Fernández, V., Conversion of γ- and δ-Keto Esters into Optically Active Lactams. Transaminases in Cascade Processes. *Adv. Synth. Catal.* **2018,** *360* (4), 686-695.

85. Su, Y.; Gao, S.; Li, H.; Zheng, G., Enantioselective resolution of γ-lactam utilizing a novel (+)-γ-lactamase from Bacillus thuringiensis. *Process Biochem.* **2018,** *72*, 96-104.

86. Bagum, H.; Christensen, K. E.; Genov, M.; Pretsch, A.; Pretsch, D.; Moloney, M. G., Synthetic access to 3,4-disubstituted pyroglutamates from tetramate derivatives from serine, allo-threonine and cysteine. *Tetrahedron* **2019,** *75* (40).

87. Verho, O.; Maetani, M.; Melillo, B.; Zoller, J.; Schreiber, S. L., Stereospecific Palladium-Catalyzed C–H Arylation of Pyroglutamic Acid Derivatives at the C3 Position Enabled by 8-Aminoquinoline as a Directing Group. *Org. Lett.* **2017,** *19* (17), 4424-4427.

88. Enders, D.; Niemeier, O.; Henseler, A., Organocatalysis by N-Heterocyclic Carbenes. *Chem. Rev.* **2007,** *107* (12), 5606-5655.

89. del Corte, X.; Maestro, A.; Vicario, J.; Martinez de Marigorta, E.; Palacios, F., Brönsted-Acid-Catalyzed Asymmetric Three-Component Reaction of Amines, Aldehydes, and Pyruvate Derivatives. Enantioselective Synthesis of Highly Functionalized γ-Lactam Derivatives. *Org. Lett.* **2018,** *20* (2), 317-320.

90. Hu, B.; Deng, L., Catalytic Asymmetric Synthesis of Trifluoromethylated γ-Amino Acids through the Umpolung Addition of Trifluoromethyl Imines to Carboxylic Acid Derivatives. *Angewandte Chemie - International Edition* **2018,** *57* (8), 2233-2237.

91. Collar, A. G.; Trujillo, C.; Lockett-Walters, B.; Twamley, B.; Connon, S. J., Catalytic Asymmetric γ-Lactam Synthesis from Enolisable Anhydrides and Imines. *Chem. Eur. J.* **2019,** *25* (30), 7275-7279.

92. Sućˊ Sajko, J.; Ljoljić Bilić, V.; Kosalec, I.; Jerić, I., Multicomponent Approach to a Library of N-Substituted γ-Lactams. *ACS Combinatorial Science* **2019,** *21* (1), 28-34.

93. de Gracia Retamosa, M.; Ruiz-Olalla, A.; Bello, T.; de Cozar, A.; Cossio, F. P., A Three-Component Enantioselective Cyclization Reaction Catalyzed by an Unnatural Amino Acid Derivative. *Angew Chem Int Ed Engl* **2018,** *57* (3), 668-672.

94. Hu, Z.; Zhu, Y.; Fu, Z.; Huang, W., Asymmetric Synthesis of Enantioenriched 6-Hydroxyl Butyrolactams Promoted by N-Heterocyclic Carbene. *J. Org. Chem.* **2019,** *84* (16), 10328-10337.

95. Li, X. S.; Zhao, L. L.; Wang, X. K.; Cao, L. L.; Shi, X. Q.; Zhang, R.; Qi, J., Enantioselective [3 + 2] Annulation of Enals with 2-Aminoacrylates Catalyzed by N-Heterocyclic Carbene. *Org. Lett.* **2017,** *19* (14), 3943-3946.

96. Zhang, K.; Deiana, L.; Grape, E. S.; Inge, A. K.; Córdova, A., Catalytic Enantioselective Synthesis of Bicyclic Lactam N,S-Acetals in One Pot by Cascade Transformations. *Eur. J. Org. Chem.* **2019,** *2019* (29), 4649-4657.

97. Shi, Y.; Tan, X.; Gao, S.; Zhang, Y.; Wang, J.; Zhang, X.; Yin, Q., Direct Synthesis of Chiral NH Lactams via Ru-Catalyzed Asymmetric Reductive Amination/Cyclization Cascade of Keto Acids/Esters. *Org. Lett.* **2020,** *22* (7), 2707-2713.

98. Wang, C.; Ge, S., Versatile Cobalt-Catalyzed Enantioselective Entry to Boryl-Functionalized All-Carbon Quaternary Stereogenic Centers. *J. Am. Chem. Soc.* **2018,** *140* (34), 10687-10690.

99. Zhou, Z.; Chen, S.; Hong, Y.; Winterling, E.; Tan, Y.; Hemming, M.; Harms, K.; Houk, K. N.; Meggers, E., Non-C2-Symmetric Chiral-at-Ruthenium Catalyst for Highly Efficient Enantioselective Intramolecular C(sp3)–H Amidation. *J. Am. Chem. Soc.* **2019,** *141* (48), 19048-19057.

100. Xing, Q.; Chan, C. M.; Yeung, Y. W.; Yu, W. Y., Ruthenium(II)-Catalyzed Enantioselective gamma-Lactams Formation by Intramolecular C-H Amidation of 1,4,2-Dioxazol-5-ones. *J. Am. Chem. Soc.* **2019,** *141* (9), 3849-3853.

101. Wang, H.; Park, Y.; Bai, Z.; Chang, S.; He, G.; Chen, G., Iridium-Catalyzed Enantioselective C(sp(3))-H Amidation Controlled by Attractive Noncovalent Interactions. *J. Am. Chem. Soc.* **2019,** *141* (17), 7194-7201.

102. Park, Y.; Chang, S., Asymmetric formation of γ-lactams via C–H amidation enabled by chiral hydrogen-bond-donor catalysts. *Nature Catalysis* **2019,** *2* (3), 219-227.

103. Wang, S. G.; Liu, Y.; Cramer, N., Asymmetric Alkenyl C−H Functionalization by CpxRhIII forms 2H-Pyrrol-2-ones through [4+1]-Annulation of Acryl Amides and Allenes. *Angewandte Chemie - International Edition* **2019,** *58* (50), 18136-18140.

104. Lang, Q.; Gu, G.; Cheng, Y.; Yin, Q.; Zhang, X., Highly Enantioselective Synthesis of Chiral γ-Lactams by Rh-Catalyzed Asymmetric Hydrogenation. *ACS Catalysis* **2018,** *8* (6), 4824-4828.

105. Yuan, Q.; Liu, D.; Zhang, W., Iridium-Catalyzed Asymmetric Hydrogenation of β,γ-Unsaturated γ-Lactams: Scope and Mechanistic Studies. *Org. Lett.* **2017,** *19* (5), 1144-1147.

106. Jette, C. I.; Geibel, I.; Bachman, S.; Hayashi, M.; Sakurai, S.; Shimizu, H.; Morgan, J. B.; Stoltz, B. M., Palladium-Catalyzed Construction of Quaternary Stereocenters by Enantioselective Arylation of γ-Lactams with Aryl Chlorides and Bromides. *Angewandte Chemie - International Edition* **2019,** *58* (13), 4297-4301.

107. Nanjo, T.; De Lucca, E. C.; White, M. C., Remote, Late-Stage Oxidation of Aliphatic C-H Bonds in Amide-Containing Molecules. *J. Am. Chem. Soc.* **2017,** *139* (41), 14586-14591.

108. Chen, M.; Dong, G., Direct Catalytic Desaturation of Lactams Enabled by Soft Enolization. *J. Am. Chem. Soc.* **2017,** *139* (23), 7757-7760.

109. Harris, L.; Gilpin, M.; Thompson, A. L.; Cowley, A. R.; Moloney, M. G., Uncatalysed diaryldiazo cyclopropanations on bicyclic lactams: access to annulated prolines. *Org. Biomol. Chem.* **2015,** *13* (23), 6522-6550.

110. Wegler, R., Über die mit verschiedener Reaktionsgeschwindigkeit erfolgende Veresterung der optischen Antipoden eines Racemates durch opt. akt. Katalysatoren. *Justus Liebigs Ann. Chem.* **1932,** *498* (1), 62-76.

111. Vellalath, S.; Romo, D., Asymmetric Organocatalysis: The Emerging Utility of α,β-Unsaturated Acylammonium Salts. *Angew Chem Int Ed Engl* **2016,** *55* (45), 13934-13943.

112. Biswas, A.; Mondal, H.; Maji, M. S., Synthesis of Heterocycles by Isothiourea Organocatalysis. *J. Heterocycl. Chem.* **2020**.

113. Ahlemeyer, N. A.; Streff, E. V.; Muthupandi, P.; Birman, V. B., Dramatic Acceleration of an Acyl Transfer-Initiated Cascade by Using Electron-Rich Amidine-Based Catalysts. *Org. Lett.* **2017,** *19* (24), 6486-6489.

114. Birman, V. B.; Li, X., Homobenzotetramisole: An Effective Catalyst for Kinetic Resolution of Aryl-Cycloalkanols. *Org. Lett.* **2008,** *10* (6), 1115-1118.

115. Birman, V. B.; Uffman, E. W.; Jiang, H.; Li, X.; Kilbane, C. J., 2,3-Dihydroimidazo[1,2-a]pyridines: A New Class of Enantioselective Acyl Transfer Catalysts and Their Use in Kinetic Resolution of Alcohols. *J. Am. Chem. Soc.* **2004,** *126* (39), 12226-12227.

116. Robinson, E. R. T.; Walden, D. M.; Fallan, C.; Greenhalgh, M. D.; Cheong, P. H.-Y.; Smith, A. D., Non-bonding 1,5-S···O interactions govern chemo- and enantioselectivity in isothiourea-catalyzed annulations of benzazoles. *Chemical Science* **2016,** *7* (12), 6919-6927.

117. Matviitsuk, A.; Greenhalgh, M. D.; Antúnez, D.-J. B.; Slawin, A. M. Z.; Smith, A. D., Aryloxide-Facilitated Catalyst Turnover in Enantioselective α,β-Unsaturated Acyl Ammonium Catalysis. *Angew. Chem. Int. Ed.* **2017,** *56* (40), 12282-12287.

118. Shu, C.; Liu, H.; Slawin, A. M. Z.; Carpenter-Warren, C.; Smith, A. D., Isothiourea-catalysed enantioselective Michael addition of N-heterocyclic pronucleophiles to α,β-unsaturated aryl esters. *Chemical Science* **2020,** *11* (1), 241-247.

119. Matviitsuk, A.; Greenhalgh, M. D.; Taylor, J. E.; Nguyen, X. B.; Cordes, D. B.; Slawin, A. M. Z.; Lupton, D. W.; Smith, A. D., Unanticipated Silyl Transfer in Enantioselective α,β-Unsaturated Acyl Ammonium Catalysis Using Silyl Nitronates. *Org. Lett.* **2020,** *22* (1), 335-339.

120. Morris, K. A.; Arendt, K. M.; Oh, S. H.; Romo, D., Double Diastereoselective, Nucleophile-Catalyzed Aldol Lactonizations (NCAL) Leading to β-Lactone Fused Carbocycles and Extensions to β-Lactone Fused Tetrahydrofurans. *Org. Lett.* **2010,** *12* (17), 3764-3767.

121. Cortez, G. S.; Tennyson, R. L.; Romo, D., Intramolecular, nucleophile-catalyzed aldol-lactonization (NCAL) reactions: catalytic, asymmetric synthesis of bicyclic beta-lactones. *J. Am. Chem. Soc.* **2001,** *123* (32), 7945-7946.

122. Liu, G.; Shirley, M. E.; Van, K. N.; McFarlin, R. L.; Romo, D., Rapid assembly of complex cyclopentanes employing chiral, α,β-unsaturated acylammonium intermediates. *Nat. Chem.* **2013,** *5* (12), 1049-1057.

123. Abbasov, M. E.; Hudson, B. M.; Tantillo, D. J.; Romo, D., Stereodivergent, Diels–Alder-initiated organocascades employing α,β-unsaturated acylammonium salts: scope, mechanism, and application. *Chem. Sci.* **2017,** *8* (2), 1511-1524.

124. Abbasov, M. E.; Hudson, B. M.; Tantillo, D. J.; Romo, D., Acylammonium salts as dienophiles in Diels-Alder/lactonization organocascades. *J. Am. Chem. Soc.* **2014,** *136* (12), 4492-5.

125. Vellalath, S.; Van, K. N.; Romo, D., Direct Catalytic Asymmetric Synthesis of N-Heterocycles from Commodity Acid Chlorides by Employing α,β-Unsaturated Acylammonium Salts. *Angew. Chem. Int. Ed.* **2013,** *52* (51), 13688-13693.

126. Kang, G.; Yamagami, M.; Vellalath, S.; Romo, D., Enantioselective Synthesis of Medium-Sized Lactams via Chiral α,β-Unsaturated Acylammonium Salts. *Angew. Chem. Int. Ed.* **2018,** *57* (22), 6527-6531.

127. Nguyen, H.; Oh, S.; Henry-Riyad, H.; Sepulveda, D.; Romo, D., Organocatalytic enantioselective synthesis of bicyclic β-lactones from aldehyde acids via nucleophile-catalyzed aldollactonization (NCAL). In *Org. Syn.*, **2011**; Vol. 88, pp 121-137.

128. Papillon, J. P. B.; Taylor, R. J. K., The first syntheses of the 1-oxo-2-oxa-5-azaspiro[3.4]octane ring system found in oxazolomycin. *Org. Lett.* **2000,** *2* (14), 1987-1990.

129. Donohoe, T. J.; Chiu, J. Y. K.; Thomas, R. E., Synthesis of the Pyrrolidinone Core of KSM-2690 B. *Org. Lett.* **2007,** *9* (3), 421-424.

130. Donohoe, T. J.; O'Riordan, T. J. C.; Peifer, M.; Jones, C. R.; Miles, T. J., Asymmetric Synthesis of the Fully Elaborated Pyrrolidinone Core of Oxazolomycin A. *Org. Lett.* **2012,** *14* (21), 5460-5463.

131. Heaviside, E. A.; Moloney, M. G.; Thompson, A. L., Diastereoselective intramolecular aldol ring closures of threonine derivatives leading to densely functionalised pyroglutamates related to oxazolomycin. *RSC Adv.* **2014,** *4* (31), 16233-16249.

132. Josa-Culleré, L.; Towers, C.; Willenbrock, F.; Macaulay, V. M.; Christensen, K. E.; Moloney, M. G., Synthesis and bioactivity of fused- and spiro-β-lactone-lactam systems. *Org. Biomol. Chem.* **2017,** *15* (25), 5373-5379.

133. Eto, K.; Ishihara, J.; Hatakeyama, S., Stereoselective synthesis of the right-hand cores of 16-methylated oxazolomycins. *Tetrahedron* **2018,** *74* (7), 711-719.

134. Bastin, R.; Dale, J. W.; Edwards, M. G.; Papillon, J. P. N.; Webb, M. R.; Taylor, R. J. K., Formal synthesis of (+)-neooxazolomycin via a Stille cross-coupling/deconjugation route. *Tetrahedron* **2011,** *67* (51), 10026-10044.

135. Fritz, S. P.; Moya, J. F.; Unthank, M. G.; McGarrigle, E. M.; Aggarwal, V. K., An Efficient Synthesis of Azetidines with (2-Bromoethyl)sulfonium Triflate. *Synthesis* **2012,** *44* (10), 1584-1590.

136. Abbasov, M. E.; Alvariño, R.; Chaheine, C. M.; Alonso, E.; Sánchez, J. A.; Conner, M. L.; Alfonso, A.; Jaspars, M.; Botana, L. M.; Romo, D., Simplified immunosuppressive and neuroprotective agents based on gracilin A. *Nat. Chem.* **2019,** *11* (4), 342-350.

137. Tao, Y.; Reisenauer, K. N.; Masi, M.; Evidente, A.; Taube, J. H.; Romo, D., Pharmacophore-Directed Retrosynthesis Applied to Ophiobolin A: Simplified Bicyclic Derivatives Displaying Anticancer Activity. *Org. Lett.* **2020**, **Article ASAP**.

138. Truax, N. J. R., D., Bridging the Gap Between Natural Product Synthesis and Drug Discovery. *Nat. Prod. Rep.* **2020**, *accepted*.

139. Chaheine, C. M. S., Conner J.; Gladen, P. T.; Romo, D., Enantioselective Michael-Proton Transfer-Lactamization for Pyroglutamic Acid Derivatives: Synthesis of dimethyl-(S,E)-5-oxo-3-styryl-1-tosylpyrrolidine-2,2-dicarboxylate. *Org. Syn.* **2020**, submitted.

140. Horwitz, M. A.; Johnson, J. S., Local Desymmetrization through Diastereotopic Group Selection: An Enabling Strategy for Natural Product Synthesis. *Eur. J. Org. Chem.* **2017,** *2017* (11), 1381-1390.

141. Lee, G. H.; Youn, I. K.; Choi, E. B.; Lee, H. K.; Yon, G. H.; Yang, H. C.; Pak, C. S., Magnesium in Methanol (Mg / MeOH) in Organic Syntheses. *Curr. Org. Chem.* **2004,** *8* (13), 1263-1287.

142. Leduc, A. B.; Kerr, M. A., Total Synthesis of (±)-Decursivine. *Eur. J. Org. Chem.* **2007,** *2007* (2), 237-240.

143. Hoveyda, A. H.; Evans, D. A.; Fu, G. C., Substrate-directable chemical reactions. *Chem. Rev.* **1993,** *93* (4), 1307-1370.

144. Molander, G. A., Application of lanthanide reagents in organic synthesis. *Chem. Rev.* **1992,** *92* (1), 29-68.

145. Imamoto, T.; Sugiura, Y.; Takiyama, N., Organocerium reagents. Nucleophilic addition to easily enolizable ketones. *Tetrahedron Lett.* **1984,** *25* (38), 4233-4236.

146. Liu, H. J.; Shia, K. S.; Shang, X.; Zhu, B. Y., Organocerium Compounds in Synthesis. *Tetrahedron* **1999,** *55* (13), 3803-3830.

147. Duttwyler, S.; Chen, S.; Takase, M. K.; Wiberg, K. B.; Bergman, R. G.; Ellman, J. A., Proton Donor Acidity Controls Selectivity in Nonaromatic Nitrogen Heterocycle Synthesis. *Science* **2013,** *339* (6120), 678.

148. Dimitrov, V.; Kostova, K.; Genov, M., Anhydrous Cerium(III) Chloride — Effect of the Drying Process on Activity and Efficiency. *Tetrahedron Lett.* **1996,** *37* (37), 6787-6790.

149. Takeda, N.; Imamoto, T., Use of Cerium (III) Chloride in the Reactions of Carbonyl Compounds with Organolithiums or Grignard Reagents for the Suppression of Abnormal Reactions: 1-butyl-1,2,3,4-tetrahydro-1-napthol. *Org. Syn.* **1999,** *76*, 228.

150. Evans, D. A.; Downey, C. W.; Shaw, J. T.; Tedrow, J. S., Magnesium Halide-Catalyzed Anti-Aldol Reactions of Chiral N-Acylthiazolidinethiones. *Org. Lett.* **2002,** *4* (7), 1127-1130.

151. Evans, D. A.; Tedrow, J. S.; Shaw, J. T.; Downey, C. W., Diastereoselective Magnesium Halide-Catalyzed anti-Aldol Reactions of Chiral N-Acyloxazolidinones. *J. Am. Chem. Soc.* **2002,** *124* (3), 392-393.

152. Gage, J. R.; Evans, D. A., Diastereoselective Aldol Condensaiton Using a Chiral Oxazolidinone Auxiliary: (*2S,3S*)-3-hydroxy-3-phenyl-2methylpropanoic Acid. *Org. Syn.* **1990,** *68*, 83.

153. Ogasawara, M.; Okada, A.; Subbarayan, V.; Sorgel, S.; Takahashi, T., Palladium-Catalyzed Asymmetric Synthesis of Axially Chiral Allenylsilanes and Their Application to S(E)2 ' Chirality Transfer Reactions. *Org. Lett.* **2010,** *12* (24), 5736-5739.

154. Appel, R., Tertiary Phosphane/Tetrachloromethane, a Versatile Reagent for Chlorination, Dehydration, and P-N Linkage. *Angew. Chem. Int. Ed.* **1975,** *14* (12), 801-811.

155. Bailey, W. F.; Brubaker, J. D.; Jordan, K. P., Effect of solvent and temperature on the lithium-iodine exchange of primary alkyl iodides: reaction of t-butyllithium with 1-iodooctane in heptane-ether mixtures. *J. Organomet. Chem.* **2003,** *681* (1-2), 210-214.

156. Rathman, T.; Bailey, W. F., Optimization of Organolithium Reactions. *Org. Process Res. Dev.* **2009,** *13* (2), 144-151.

157. Krasovskiy, A.; Kopp, F.; Knochel, P., Soluble Lanthanide Salts (LnCl3·2 LiCl) for the Improved Addition of Organomagnesium Reagents to Carbonyl Compounds. *Angew. Chem. Int. Ed.* **2006,** *45* (3), 497-500.

158. Ilardi, E. A.; Stivala, C. E.; Zakarian, A., Hexafluoroisopropanol as a Unique Solvent for Stereoselective Iododesilylation of Vinylsilanes. *Org. Lett.* **2008,** *10* (9), 1727-1730.

159. Sidera, M.; Costa, A. M.; Vilarrasa, J., Iododesilylation of TIPS-, TBDPS-, and TBS-Substituted Alkenes in Connection with the Synthesis of Amphidinolides B/D. *Org. Lett.* **2011,** *13* (18), 4934-4937.

160. King, S. A., Orthoester-Dependent Alcoholysis of Lactones. Facile Preparation of 4-Alkoxybutanoates and 5-Alkoxypentanoates. *J. Org. Chem.* **1994,** *59* (8), 2253-2256.

161. Chau, S. T.; Hayakawa, Y.; Sulikowski, G. A., 18O Assisted Analysis of a γ,δ-Epoxyketone Cyclization: Synthesis of the C16−C28 Fragment of Ammocidin D. *Org. Lett.* **2011,** *13* (4), 756-759.

162. Burchat, A. F.; Chong, J. M.; Nielsen, N., Titration of alkyllithiums with a simple reagent to a blue endpoint. *J. Organomet. Chem.* **1997,** *542* (2), 281-283.

163. Beesley, R. M.; Ingold, C. K.; Thorpe, J. F., CXIX.—The formation and stability of spiro-compounds. Part I. spiro-Compounds from cyclohexane. *J. Chem. Soc., Trans.* **1915,** *107* (0), 1080-1106.

164. Carlsen, P. H. J.; Katsuki, T.; Martin, V. S.; Sharpless, K. B., A greatly improved procedure for ruthenium tetroxide catalyzed oxidations of organic compounds. *J. Org. Chem.* **1981,** *46* (19), 3936-3938.

165. Mohapatra, D. K.; Mondal, D.; Gonnade, R. G.; Chorghade, M. S.; Gurjar, M. K., Synthesis of the spiro fused beta-lactone-gamma-lactam segment of oxazolomycin. *Tetrahedron Lett.* **2006,** *47* (34), 6031-6035.

166. Mondal, D.; Bera, S., A Synthetic View of an Analogue of the Spiro-beta-lactone-gamma-lactam Ring in Oxazolomycins and Lajollamycin. *Synthesis-Stuttgart* **2010,** (19), 3301-3308.

167. Liang, X.; Andersch, J.; Bols, M., Garner's aldehyde. *J. Chem. Soc., Perkin Trans. 1* **2001,** (18), 2136-2157.

168. Adam, W.; Baeza, J.; Liu, J.-C., Stereospecific introduction of double bounds via thermolysis of .beta.-lactones. *J. Am. Chem. Soc.* **1972,** *94* (6), 2000-2006.

169. Imamoto, T.; Kusumoto, T.; Tawarayama, Y.; Sugiura, Y.; Mita, T.; Hatanaka, Y.; Yokoyama, M., Carbon-carbon bond-forming reactions using cerium metal or organocerium(III) reagents. *J. Org. Chem.* **1984,** *49* (21), 3904-3912.

170. Wright, M. H.; Sieber, S. A., Chemical proteomics approaches for identifying the cellular targets of natural products. *Nat. Prod. Rep.* **2016,** *33* (5), 681-708.

171. Guerciolini, R., Mode of action of orlistat. *Int. J. Obes. Relat. Metab. Disord.* **1997,** *21* (Suppl 3), S12-23.

172. Groll, M.; Balskus, E. P.; Jacobsen, E. N., Structural Analysis of Spiro β-Lactone Proteasome Inhibitors. *J. Am. Chem. Soc.* **2008,** *130* (45), 14981-14983.

173. Richardson, R. D.; Ma, G.; Oyola, Y.; Zancanella, M.; Knowles, L. M.; Cieplak, P.; Romo, D.; Smith, J. W., Synthesis of Novel β-Lactone Inhibitors of Fatty Acid Synthase. *J. Med. Chem.* **2008,** *51* (17), 5285-5296.

174. Zeiler, E.; Braun, N.; Böttcher, T.; Kastenmüller, A.; Weinkauf, S.; Sieber, S. A., Vibralactone as a Tool to Study the Activity and Structure of the ClpP1P2 Complex from Listeria monocytogenes. *Angew. Chem. Int. Ed.* **2011,** *50* (46), 11001-11004.

175. List, A.; Zeiler, E.; Gallastegui, N.; Rusch, M.; Hedberg, C.; Sieber, S. A.; Groll, M., Omuralide and Vibralactone: Differences in the Proteasome- β-Lactone-γ-Lactam Binding Scaffold Alter Target Preferences. *Angew. Chem. Int. Ed.* **2014,** *53* (2), 571-574.

176. Zhu, M.; Harshbarger, W. D.; Robles, O.; Krysiak, J.; Hull, K. G.; Cho, S. W.; Richardson, R. D.; Yang, Y.; Garcia, A.; Spiegelman, L.; Ramirez, B.; Wilson, C. T.; Yau, J. A.; Moore, J. T.; Walker, C. B.; Sacchettini, J. C.; Liu, W. R.; Sieber, S. A.; Smith, J. W.; Romo, D., A strategy for dual inhibition of the proteasome and fatty acid synthase with belactosin C-orlistat hybrids. *Biorg. Med. Chem.* **2017,** *25* (11), 2901-2916.

177. Truax, N. J.; Ayinde, S.; Van, K.; Liu, J. O.; Romo, D., Pharmacophore-Directed Retrosynthesis Applied to Rameswaralide: Synthesis and Bioactivity of Sinularia Natural Product Tricyclic Cores. *Org. Lett.* **2019,** *21* (18), 7394-7399.

178. Tao, Y.; Reisenauer, K. N.; Masi, M.; Evidente, A.; Taube, J. H.; Romo, D., Pharmacophore-Directed Retrosynthesis Applied to Ophiobolin A: Simplified Bicyclic Derivatives Displaying Anticancer Activity. *Org. Lett.* **2020**.

179. Truax, N. J.; Romo, D., Bridging the gap between natural product synthesis and drug discovery. *Nat. Prod. Rep.* **2020**.

180. Senapati, B. K.; Gao, L.; Lee, S. I.; Hwang, G. S.; Ryu, D. H., Highly Enantioselective Mukaiyama Aldol Reactions Catalyzed by a Chiral Oxazaborolidinium Ion: Total Synthesis of (-)-Inthomycin C. *Org. Lett.* **2010,** *12* (22), 5088-5091.

181. Balcells, S.; Haughey, M. B.; Walker, J. C. L.; Josa-Cullere, L.; Towers, C.; Donohoe, T. J., Asymmetric Total Synthesis of (-)-(3R)-Inthomycin C. *Org. Lett.* **2018,** *20* (12), 3583-3586.

182. Kumar, M.; Bromhead, L.; Anderson, Z.; Overy, A.; Burton, J. W., Short, Tin-Free Synthesis of All Three Inthomycins. *Chem. Eur. J.* **2018,** *24* (63), 16753-16756.

183. Schreiber, S. L.; Schreiber, T. S.; Smith, D. B., Reactions that proceed with a combination of enantiotopic group and diastereotopic face selectivity can deliver products with very high enantiomeric excess: experimental support of a mathematical model. *J. Am. Chem. Soc.* **1987,** *109* (5), 1525-1529.

184. Sawada, D.; Ito, Y., A new method for formacetal linkage formation: protection of alcohols, phenols and carboxylic acids. *Tetrahedron Lett.* **2001,** *42* (13), 2501-2504.

185. Roane, J.; Wippich, J.; Ramgren, S. D.; Krische, M. J., Synthesis of the C(1)–C(13) Fragment of Leiodermatolide via Hydrogen-Mediated C–C Bond Formation. *Org. Lett.* **2017,** *19* (24), 6634-6637.

186. Farina, V.; Krishnamurthy, V.; Scott, W. J., *The Stille Reaction*. 1st ed.; John Wiley & Sons, Inc.: New York, 1998; p 657.

187. Wadsworth, W. S.; Emmons, W. D., The Utility of Phosphonate Carbanions in Olefin Synthesis. *J. Am. Chem. Soc.* **1961,** *83* (7), 1733-1738.

188. Webb, M. R.; Addie, M. S.; Crawforth, C. M.; Dale, J. W.; Franci, X.; Pizzonero, M.; Donald, C.; Taylor, R. J. K., The syntheses of rac-inthomycin A, (+)-inthomycin B and (+)-inthomycin C using a unified synthetic approach. *Tetrahedron* **2008,** *64* (21), 4778-4791.

189. Omura, K.; Sharma, A. K.; Swern, D., Dimethyl sulfoxide-trifluoroacetic anhydride. New reagent for oxidation of alcohols to carbonyls. *J. Org. Chem.* **1976,** *41* (6), 957-962.

190. Müller, S.; Liepold, B.; Roth, G. J.; Bestmann, H. J., An Improved One-pot Procedure for the Synthesis of Alkynes from Aldehydes. *Synlett* **1996,** *1996* (06), 521-522.

191. Yin, J.; Bergmann, E. M.; Cherney, M. M.; Lall, M. S.; Jain, R. P.; Vederas, J. C.; James, M. N. G., Dual Modes of Modification of Hepatitis A Virus 3C Protease by a Serine-derived β-Lactone: Selective Crystallization and Formation of a Functional Catalytic Triad in the Active Site. *J. Mol. Biol.* **2005,** *354* (4), 854-871.

192. Ramer, S. E.; Moore, R. N.; Vederas, J. C., Mechanism of formation of serine β-lactones by Mitsunobu cyclization: synthesis and use of L-serine stereospecifically labelled with deuterium at C-3. *Can. J. Chem.* **1986,** *64* (4), 706-713.

193. Gaich, T.; Baran, P. S., Aiming for the Ideal Synthesis. *J. Org. Chem.* **2010,** *75* (14), 4657-4673.

194. Newhouse, T.; Baran, P. S.; Hoffmann, R. W., The economies of synthesis. *Chem. Soc. Rev.* **2009,** *38* (11), 3010-3021.

195. Gómez-Bengoa, E.; García, J. M.; Jiménez, S.; Lapuerta, I.; Mielgo, A.; Odriozola, J. M.; Otazo, I.; Razkin, J.; Urruzuno, I.; Vera, S.; Oiarbide, M.; Palomo, C., Asymmetric synthesis of propargylic alcohols via aldol reaction of aldehydes with ynals promoted by prolinol ether–transition metal–Brønsted acid cooperative catalysis. *Chem. Sci.* **2013,** *4* (8), 3198-3204.

196. Gómez-Bengoa, E.; Jiménez, J.; Lapuerta, I.; Mielgo, A.; Oiarbide, M.; Otazo, I.; Velilla, I.; Vera, S.; Palomo, C., Combined α,α-dialkylprolinol ether/Brønsted acid promotes Mannich reactions of aldehydes with unactivated imines. An entry to anti-configured propargylic amino alcohols. *Chem. Sci.* **2012,** *3* (10), 2949.

197. Protection for the Hydroxyl Group, Including 1,2- and 1,3-Diols. In *Greene's Protective Groups in Organic Synthesis*, 2006; pp 16-366.

198. Levin, J. I.; Turos, E.; Weinreb, S. M., An Alternative Procedure for the Aluminum-Mediated Conversion of Esters to Amides. *Synth. Commun.* **1982,** *12* (13), 989-993.

199. Nakatsuka, M.; Ragan, J. A.; Sammakia, T.; Smith, D. B.; Uehling, D. E.; Schreiber, S. L., Total synthesis of FK506 and an FKBP probe reagent, [C(8),C(9)-13C2]-FK506. *J. Am. Chem. Soc.* **1990,** *112* (14), 5583-5601.

200. Li, J.; Kim, Sang G.; Blenis, J., Rapamycin: One Drug, Many Effects. *Cell Metabolism* **2014,** *19* (3), 373-379.

201. Trauner, D., Finding function and form. *Nat. Prod. Rep.* **2014,** *31* (4), 411-413.

202. Wilson, R. M.; Danishefsky, S. J., Small Molecule Natural Products in the Discovery of Therapeutic Agents: The Synthesis Connection. *J. Org. Chem.* **2006,** *71* (22), 8329-8351.

203. Wender, P. A., Toward the ideal synthesis and molecular function through synthesis-informed design. *Nat. Prod. Rep.* **2014,** *31* (4), 433-440.

204. Schreiber, S. L., Target-Oriented and Diversity-Oriented Organic Synthesis in Drug Discovery. *Science* **2000,** *287* (5460), 1964.

205. van Hattum, H.; Waldmann, H., Biology-Oriented Synthesis: Harnessing the Power of Evolution. *J. Am. Chem. Soc.* **2014,** *136* (34), 11853-11859.

206. Seiple, I. B.; Zhang, Z.; Jakubec, P.; Langlois-Mercier, A.; Wright, P. M.; Hog, D. T.; Yabu, K.; Allu, S. R.; Fukuzaki, T.; Carlsen, P. N.; Kitamura, Y.; Zhou, X.; Condakes, M. L.; Szczypiński, F. T.; Green, W. D.; Myers, A. G., A platform for the discovery of new macrolide antibiotics. *Nature* **2016,** *533* (7603), 338-345.

207. Könst, Z. A.; Szklarski, A. R.; Pellegrino, S.; Michalak, S. E.; Meyer, M.; Zanette, C.; Cencic, R.; Nam, S.; Voora, V. K.; Horne, D. A.; Pelletier, J.; Mobley, D. L.; Yusupova, G.; Yusupov, M.; Vanderwal, C. D., Synthesis facilitates an understanding of the structural basis for translation inhibition by the lissoclimides. *Nat. Chem.* **2017,** *9* (11), 1140-1149.

208. Bathula, S. R.; Akondi, S. M.; Mainkar, P. S.; Chandrasekhar, S., "Pruning of biomolecules and natural products (PBNP)": an innovative paradigm in drug discovery. *Organic & Biomolecular Chemistry* **2015,** *13* (23), 6432-6448.

209. Yu, M. J.; Zheng, W.; Seletsky, B. M., From micrograms to grams: scale-up synthesis of eribulin mesylate. *Nat. Prod. Rep.* **2013,** *30* (9), 1158-1164.

210. Crane, E. A.; Gademann, K., Capturing Biological Activity in Natural Product Fragments by Chemical Synthesis. *Angew. Chem. Int. Ed.* **2016,** *55* (12), 3882-3902.

211. Romo, D.; Choi, N. S.; Li, S.; Buchler, I.; Shi, Z.; Liu, J. O., Evidence for Separate Binding and Scaffolding Domains in the Immunosuppressive and Antitumor Marine Natural Product, Pateamine A: Design, Synthesis, and Activity Studies Leading to a Potent Simplified Derivative. *J. Am. Chem. Soc.* **2004,** *126* (34), 10582-10588.

212. Trost, B. M., The atom economy--a search for synthetic efficiency. *Science* **1991,** *254* (5037), 1471.

213. Young, I. S.; Baran, P. S., Protecting-group-free synthesis as an opportunity for invention. *Nat. Chem.* **2009,** *1* (3), 193-205.

214. Corey, E. J.; Chen, X. M., *The Logic of Chemical Synthesis*. Wiley Interscience: New York, NY, 1995.

215. Czakó, B.; Kürti, L.; Mammoto, A.; Ingber, D. E.; Corey, E. J., Discovery of Potent and Practical Antiangiogenic Agents Inspired by Cortistatin A. *J. Am. Chem. Soc.* **2009,** *131* (25), 9014-9019.

216. Mayol, L.; Piccialli, V.; Sica, D., Gracilin A, an unique: nor-diterpene metabolite from the marine sponge spongionella gracilis. *Tetrahedron Lett.* **1985,** *26* (10), 1357-1360.

217. Sánchez, J. A.; Alfonso, A.; Leirós, M.; Alonso, E.; Rateb, M. E.; Jaspars, M.; Houssen, W. E.; Ebel, R.; Tabudravu, J.; Botana, L. M., Identification of Spongionella compounds as cyclosporine A mimics. *Pharmacol. Res.* **2016,** *107*, 407-414.

218. Leirós, M.; Alonso, E.; Rateb, M. E.; Houssen, W. E.; Ebel, R.; Jaspars, M.; Alfonso, A.; Botana, L. M., Gracilins: Spongionella-derived promising compounds for Alzheimer disease. *Neuropharmacology* **2015,** *93*, 285-293.

219. Corey, E. J.; Letavic, M. A., Enantioselective Total Synthesis of Gracilins B and C Using Catalytic Asymmetric Diels-Alder Methodology. *J. Am. Chem. Soc.* **1995,** *117* (37), 9616-9617.

220. Rateb, M. E.; Houssen, W. E.; Schumacher, M.; Harrison, W. T. A.; Diederich, M.; Ebel, R.; Jaspars, M., Bioactive diterpene derivatives from the marine sponge Spongionella sp. *J. Nat. Prod.* **2009,** *72* (8), 1471-1476.

221. Ana, R.; Alejandro, L.; Rogelio, F.; Carlos, C.; Luis, F. G.-F.; Fernando, R.; Carmen, C., Gracilins G-I, Cytotoxic Bisnorditerpenes from Spongionella pulchella, and the Anti-Adhesive Properties of Gracilin B. *Letters in Drug Design & Discovery* **2006,** *3* (10), 753-760.

222. Puliti, R.; Fontana, A.; Cimino, G.; Mattia, C. A.; Mazzarella, L., Structure of a keto derivative of 9,11-dihydrogracilin A. *Acta Crystallographica Section C* **1993,** *49* (7), 1373-1376.

223. Potts, B. C. M.; Faulkner, D. J.; Jacobs, R. S., Phospholipase A2 Inhibitors from Marine Organisms. *J. Nat. Prod.* **1992,** *55* (12), 1701-1717.

224. Leirós, M.; Alonso, E.; Sanchez, J. A.; Rateb, M. E.; Ebel, R.; Houssen, W. E.; Jaspars, M.; Alfonso, A.; Botana, L. M., Mitigation of ROS Insults by Streptomyces Secondary Metabolites in Primary Cortical Neurons. *ACS Chemical Neuroscience* **2014,** *5* (1), 71-80.

225. Leirós, M.; Sánchez, J. A.; Alonso, E.; Rateb, M. E.; Houssen, W. E.; Ebel, R.; Jaspars, M.; Alfonso, A.; Botana, L. M., Spongionella Secondary Metabolites Protect Mitochondrial Function in Cortical Neurons against Oxidative Stress. *Mar. Drugs* **2014,** *12* (2).

226. Kofron, J. L.; Kuzmic, P.; Kishore, V.; Colon-Bonilla, E.; Rich, D. H., Determination of kinetic constants for peptidyl prolyl cis-trans isomerases by an improved spectrophotometric assay. *Biochemistry* **1991,** *30* (25), 6127-6134.

227. Walsh, C. T.; Zydowsky, L. D.; McKeon, F. D., Cyclosporin A, the cyclophilin class of peptidylprolyl isomerases, and blockade of T cell signal transduction. *J. Biol. Chem.* **1992,** *267* (19), 13115-8.

228. Ferreira, P. A.; Orry, A., From Drosophila to Humans: Reflections on the Roles of the Prolyl Isomerases and Chaperones, Cyclophilins, in Cell Function and Disease. *J. Neurogenet.* **2012,** *26* (2), 132-143.

229. Lee, J.; Kim, S. S., An Overview of Cyclophilins in Human Cancers. *J. Int. Med. Res.* **2010,** *38* (5), 1561-1574.

230. Hogan, P. G.; Chen, L.; Nardone, J.; Rao, A., Transcriptional regulation by calcium, calcineurin, and NFAT. *Genes Dev.* **2003,** *17* (18), 2205-2232.

231. Nigro, P.; Pompilio, G.; Capogrossi, M. C., Cyclophilin A: a key player for human disease. *Cell Death & Disease* **2013,** *4* (10), e888-e888.

232. Picone, P.; Nuzzo, D.; Caruana, L.; Scafidi, V.; Di Carlo, M., Mitochondrial Dysfunction: Different Routes to Alzheimer's Disease Therapy. *Oxidative Medicine and Cellular Longevity* **2014,** *2014*, 780179.

233. Schnermann, M. J.; Beaudry, C. M.; Egorova, A. V.; Polishchuk, R. S.; Sütterlin, C.; Overman, L. E., Golgi-modifying properties of macfarlandin E and the synthesis and evaluation of its 2,7-dioxabicyclo[3.2.1]octan-3-one core. *Proceedings of the National Academy of Sciences* **2010,** *107* (14), 6158.

234. Kornienko, A.; La Clair, J. J., Covalent modification of biological targets with natural products through Paal–Knorr pyrrole formation. *Nat. Prod. Rep.* **2017,** *34* (9), 1051-1060.

235. Nirmal, N.; Praba, G. O.; Velmurugan, D., Modeling studies on phospholipase A2-inhibitor complexes. *Indian J. Biochem. Biophys.* **2008,** *45* (4), 256-62.

236. Baker, B. J.; Kopitzke, R. W.; Yoshida, W. Y.; McClintock, J. B., Chemical and Ecological Studies of the Antarctic Sponge Dendrilla membranosa. *J. Nat. Prod.* **1995,** *58* (9), 1459-1462.

237. Buckleton, J. S.; Bergquist, P. R.; Cambie, R. C.; Clark, G. R.; Karuso, P.; Rickard, C. E. F., Structure of tetrahydroaplysulphurin-1. *Acta Crystallographica Section C* **1987,** *43* (12), 2430-2432.

238. Harvey, N. L.; Krysiak, J.; Chamni, S.; Cho, S. W.; Sieber, S. A.; Romo, D., Synthesis of (±)-Spongiolactone Enabling Discovery of a More Potent Derivative. *Chemistry – A European Journal* **2015,** *21* (4), 1425-1428.

239. Burgess, E. M.; Penton, H. R.; Taylor, E. A., Synthetic applications of N-carboalkoxysulfamate esters. *J. Am. Chem. Soc.* **1970,** *92* (17), 5224-5226.

240. Alfonso, A.; Pazos, M.-J.; Fernández-Araujo, A.; Tobio, A.; Alfonso, C.; Vieytes, M. R.; Botana, L. M., Surface Plasmon Resonance Biosensor Method for Palytoxin Detection Based on Na+,K+-ATPase Affinity. *Toxins* **2014,** *6* (1), 96-107.

241. Sánchez, J. A.; Alfonso, A.; Leirós, M.; Alonso, E.; Rateb, M. E.; Jaspars, M.; Houssen, W. E.; Ebel, R.; Botana, L. M., Spongionella Secondary Metabolites Regulate Store Operated Calcium Entry Modulating Mitochondrial Functioning in SH-SY5Y Neuroblastoma Cells. *Cell. Physiol. Biochem.* **2015,** *37* (2), 779-792.

242. Damsker, J. M.; Bukrinsky, M. I.; Constant, S. L., Preferential chemotaxis of activated human CD4+ T cells by extracellular cyclophilin A. *J. Leukocyte Biol.* **2007,** *82* (3), 613-618.

243. Moreira, P. I.; Zhu, X.; Wang, X.; Lee, H.-g.; Nunomura, A.; Petersen, R. B.; Perry, G.; Smith, M. A., Mitochondria: A therapeutic target in neurodegeneration. *Biochimica et Biophysica Acta (BBA) - Molecular Basis of Disease* **2010,** *1802* (1), 212-220.

244. Azzolin, L.; Antolini, N.; Calderan, A.; Ruzza, P.; Sciacovelli, M.; Marin, O.; Mammi, S.; Bernardi, P.; Rasola, A., Antamanide, a Derivative of Amanita phalloides, Is a Novel Inhibitor of the Mitochondrial Permeability Transition Pore. *PLOS ONE* **2011,** *6* (1), e16280.

245. Guo, H.-x.; Wang, F.; Yu, K.-q.; Chen, J.; Bai, D.-l.; Chen, K.-x.; Shen, X.; Jiang, H.-l., Novel cyclophilin D inhibitors derived from quinoxaline exhibit highly inhibitory activity against rat mitochondrial swelling and Ca2+ uptake/release. *Acta Pharmacologica Sinica* **2005,** *26* (10), 1201-1211.

246. Rao, V. K.; Carlson, E. A.; Yan, S. S., Mitochondrial permeability transition pore is a potential drug target for neurodegeneration. *Biochimica et Biophysica Acta (BBA) - Molecular Basis of Disease* **2014,** *1842* (8), 1267-1272.

247. Dawar, F. U.; Tu, J.; Khattak, M. N.; Mei, J.; Lin, L., Cyclophilin A: A Key Factor in Virus Replication and Potential Target for Anti-viral Therapy. *Curr. Issues Mol. Biol.* **2017,** *21*, 1-20.

248. Satoh, K., Cyclophilin A in Cardiovascular Homeostasis and Diseases. *The Tohoku Journal of Experimental Medicine* **2015,** *235* (1), 1-15.